Synthesis, Modification and Biological Activity of Hexacoordinate Silicon(IV) Complexes

Dissertation

zur Erlangung

des Doktorgrades

der Naturwissenschaften

(Dr. rer. nat.)

dem Fachbereich Chemie

der Philipps-Universität Marburg

vorgelegt von

Jens Henker

aus
Halle/Saale

Marburg/Lahn, 2016

Die vorliegende Dissertation entstand in der Zeit von März 2012 bis Oktober 2016 am Fachbereich Chemie der Philipps-Universität Marburg in der Arbeitsgruppe und unter der Betreuung von Herrn Prof. Dr. Eric Meggers.

Vom Fachbereich Chemie der Philipps-Universität Marburg (Hochschulkennziffer 1180) als Dissertation am _____ angenommen.

Abgabedatum:
Erstgutachter: Prof. Dr. Eric L. Meggers
Zweitgutachter: Prof. Dr. Paultheo von Zezschwitz

"Der Mensch muß bei dem Glauben verharren,
daß das Unbegreifliche begreiflich sei:
Er würde sonst nicht forschen."
(Johann Wolfgang von Goethe, 1749 – 1832)

Für meine Eltern, Großeltern
und meine Schwester

Many thanks to...

...Prof. Dr. Eric Meggers for the opportunity to work in his research group for several years covering the interesting field of bioinorganic coordination chemistry. Starting with metal based enzyme inhibitors during a research internship in 2012, over highly charged multinuclear metal complexes in my master thesis in 2012/13, the research focus was finally laid on higher coordinate silicon complexes. During all these years, the working conditions were excellent. Thanks for granting that much freedom to finish the thesis but also being open to discussions and new directions to deal with problems associated with higher coordinate silicon complexes. I am also very thankful for the opportunities to present my research progress to the scientific community during the ICBIC 16 and the ISOS XVII. Finally, I would like to thank Prof. Meggers for affording me a two month research internship at the Xiamen University in China.

...Prof. Dr. Paultheo von Zezschwitz for taking over the second export report.

...my supervisor at Xiamen university, Assoc. Prof. Dr. Lei Gong for inviting me in his lab as well as for the interesting and helpful but also funny discussions.

...Junior Prof. Dr. Ollala Vázquez for the ideas concerning the Bodipy project, the scientific and non-scientific discussions, and the fun activities outside the laboratory. I hope your working group will grow and that you will have great success in your academic career.

...the members of the analytical service departments of the chemistry department of Philipps-Universität Marburg for the quick and reliable processing of the analytical measurements. The members of the NMR department around Dr. Xie should be mentioned particularly for their afford to solve the problems arising during the measurements of ^{29}Si-NMR spectra.

...all present and former members of the Meggers, Höbenreich and Vázquez group for the nice working atmosphere and several good suggestions for this thesis. It was always enjoyable to work and share my lifespan with you. A special thanks go to Dr. Tom Breiding, Dr. Chen Fu and Dr. Yonggang Xiang for the great teamwork handling the problems of the silicon project and the two papers. In addition, I would like to thank Thomas Mietke and Melanie Helms for proofreading this thesis. In particular, I would like to thank Katja Körner, Dr. Anja Ludewig, Dr. Kathrin Wähler, Dr. Cornelia Ritter, Dr. Sandra Dieckmann, Elisabeth Martin, Nathalie Nett, Dr. Manuel Streib, Dr. Florian Ritterbusch, Dr. Sebastian Blanck, Rajathees Rajaratnam and Markus Dörr for the nice time in and outside the laboratory, like our regular trips to the beautiful city Lich or the hibernal snow activities.

...my Bachelor and Vertiefungsstudents Saskia Döhring, Steffen Glöckner, Malte Hoffarth, Alexandra Gruber, Christoph Middel, Sebastian Ullrich, Andreas Schrimpf, Tobias Vollgraff and Sebastian Weber for their contribution to this thesis. Although not everything worked as planned, I hope you learned a lot including new techniques pure organic chemistry does not utilize.

...the complete Xiamen University research group for their kind welcome and the interesting introduction into the Chinese culture. I had a really nice time in Xiamen because of all of you. A special thank goes to my friend and "Chinese guide" Kaifang Huang for all the help during the stay, the discussions about chemistry and Chinese culture (Monkey King, anyone?), funny moments and culinary experiences.

...Julia Wirmer-Bartoschek and Prof. Harald Schwalbe for the cooperation in the context of the Löwe research cluster. Moreover, I thank Sumaira Ashaf of the research group of Wolfgang Parak for the measurements using the confocal laser scanning microscope.

...Lilu Zhang, Ina Pinnschmidt and Andrea Tschirch for the ordering of chemicals and the help concerning organizational questions.

Last but not least, I would like to thank my parents, my sister, my grandparents and especially my girl friend Melanie Helms. Without your support, experiences and pressure at the right time, neither my studies of chemistry nor this thesis could have been accomplished.

Publications and Conference Contributions

Articles with Peer-Review

- **J. Henker**, Julia Wirmer-Bartoschek, Lars Erik Bendel, Yonggang Xiang, Chen Fu, Klaus Harms, Harald Schwalbe, Eric Meggers, *Progress on the Synthesis and Bioactivity of Hexacoordinate Silicon(IV) Complexes*, *Eur. J. Inorg. Chem.* **2016**, Manuscript accepted (DOI: 10.1002/ejic.201600953).

- T. Breiding, **J. Henker**, C. Fu, Y. Xiang, S. Glöckner, P. Hofmann, K. Harms, E. Meggers, *Synthesis and Functionalization of Hexacoordinate (Arenediolato)bis(polypyridyl)silicon(IV) Complexes*, *Eur. J. Inorg. Chem.* **2014**, 2924–2933.

Conference Contributions

- International Symposium on Silicon Chemistry (ISOS) XVII, 03.–08.08.2014 in Berlin, Germany, Poster presentation and short presentation (Silicon Slam) with the title: *Synthesis, Modification and Biological Activity of Hexacoordinate Silicon Complexes*.

- International Conference on Bioinorganic Chemistry (ICBIC) 16, 22.–26.07.2013 in Grenoble, France, Poster presentation with the title: *Dinuclear Ruthenium-Silicon Complexes as DNA and G4 DNA Binding Agents*.

Articles about Conference Contributions

- **J. Henker**, S. Glöckner, E. Meggers, *Dinuclear Ruthenium-Silicon Complexes as DNA and G4 DNA Binding Agents*, *J. Biol. Inorg. Chem.* **2014**, *19 (Suppl. 1)*, S367.

Abstract

The metalloid silicon is one of the most versatile elements of the world. Besides its widespread occurrence in the lithosphere, silicon containing compounds, for example the polymeric silicones, are used in numerous applications of the modern world. Moreover, the digital revolution and the progress in the photovoltaic industry is relying on silicon and its semiconductor properties. In contrast to its lower homologue, the carbon, silicon is capable of expanding its coordination geometry forming penta-, hexa- and even heptacoordinate complexes. Several of these structures have been examined over the last decades. However, most of these higher coordinate silicon complexes have been found to be hydrolytically unstable limiting their wider use, for instance in biological applications. The present thesis is addressing these limitations by investigating hexacoordinate (arenediolato)bis(polypyridyl)silicon(IV) complexes.

The first part of the thesis deals with the synthesis and synthetic modification of higher coordinate silicon(IV) complexes. A successful post-coordination functionalization of silicon(IV) complexes is demonstrated. Besides halogenation, oxidation, and nitration reactions, a convenient nitration-reduction-condensation strategy tolerating various functional groups is discussed. Moreover, a synthetic approach to tris-heteroleptic complexes coordinating the DNA-intercalating ligand dppz is shown. In a prove of principal study, the results of the binding affinity of some silicon(IV) complexes to *calf thymus* DNA are presented.

In a second project, the syntheses and biological properties of dinuclear metal-silicon(IV) complexes are studied. In order to constitute a small library of dinuclear complexes, different synthetic strategies including the previously presented nitration-reduction-condensation strategy, are discussed. With the library in hand, the biological activities of these complexes are investigated through binding studies to *calf thymus* DNA and G-quadruplex DNA. Moreover, the outcome of a cytotoxicity study using the MTT test for some dinuclear complexes is presented.

In a third project, a Bodipy fluorophor is attached to the silicon(IV) complexes using various synthetic routes including the nitration-reduction-condensation strategy as well as a post-coordination click-chemistry approach. The photochemical and biological properties, namely the binding to *calf thymus* DNA and the light-switch behavior, of the obtained complexes are examined. Finally, the results of *in-vitro* confocal laser scanning microscope tests studying the ability of the complexes to enter the cell nucleus are shown.

Contents

1. Introduction

1.1. Silicon: Like Sand on the Beach

Silicon was found to be one of the most abundant elements in the universe.[1] Moreover, it is the third most common element, after oxygen and iron, on the whole earth.[2] Nevertheless, the metalloid appears very rarely as isolated element,[3] instead it is mainly bond to oxygen forming silicon dioxide or silicate containing minerals that are building up most of the Earth's crust.[3,4] Nearly all silicon based minerals are composed of $[SiO_4]$-tetraeders capable of forming various inorganic structures, for example *Quartz*, *Olivine*, *Muscovite* or *Zeolites*.[3,4] In addition, some minerals are known in which the silicon is incorporated into an octahedral geometry, for example in *Thaumasite*[5,6] or *Stishovite*.[3] In contrast to the widespread natural abundance in the lithosphere, silicon exist only rarely in the hydrosphere,[4] mainly as non dissociate *ortho*-silic acid.[7] Silicon can also be found in the biosphere, where it is used for building up the exoskeleton of lower-order organisms like *Dictyochales*, *Datomes*, *Demospongiae Heliozoa*, or *Radiolaria* by an enzymatic condensation of silic acid.[4,7] Moreover, silicon is an essential part of plants with a notably high amount in *Equisetum* or fern, by way of example.[4] In higher-order animals or humans, silicon is a major trace element that is assumed to play an important role for the bone health[8] as well as in physiological processes[4] within the human body.

Most silica is commonly used as obtained from natural sources without huge processing, for example as building and isolation materials (e.g. clay, mortar, mica), filtering agents (*Celite*), gemstones, ion exchange (zeolites), or as basis for powder and make-up in the cosmetic industry (talc).[3,9] However, the first technical processing of silica dates back to the old Egyptians and Eastern Mesopotamia, the time when the first glass, amorphous solidified silica melt, was prepared. Since then, the technical development of preparing silicon containing materials has been increased dramatically. For example, various types of glass or ceramics, especially the high-performance ceramics like silicon carbide (SiC) or silicon nitride (Si_3N_4) are of great interest, with different properties have been developed.[3] Recently, silica aerogel has received huge interest both in science and industrial research as it shows high versatility due to its unique properties.[10] For example, it is used as composite, catalyst, thermal insulator, or space dust particle trap. Fine-particle of synthetic manufactured silica plays also a very important role in the cosmetic and pharmaceutical industry, for example as tableting aid, adsorbent, or drying agent.[9] Further biological applications for silicon were studied in the context of carbon-silicon-bioisosterism, at which a carbon atom of a drug molecule is replaced with a silicon atom and the change of the bioactivity is investigated.[11–13]

Besides the above mentioned applications, silicon containing compounds were studied throughout over the last decades revealing interesting catalytic properties, structures, reactivity and applications.[14–22] Although basic research on the topic of organosilicon chemistry was done by Kipping in the early 20th Century,[23,24] the great breakthrough in this field came in the 1940s after Rochow and Müller developed an economically industrial procedure to synthesize organohalogen silanes $R_nSiCl_{(4-n)}$. This so called Müller-Rochow-sythesis laid the ground stone for silicon based polymers, the silicones or poly(organo)siloxanes. Possessing very stable and conformational flexible Si−O−Si and R−Si bonds, silicones show superior properties compared to organic polymers. For example, the chemical aging of

silicones is slower due to a higher stability towards temperature, UV- and weather. This chemical inertness in combination with a low toxicity explains, why silicones are widely used in medical and cosmetic applications (catheter, implants, contact lens, additives in shampoos and creams), in the automotive and construction field (lubricants, sealing agents), or as article of daily use (cookware), by way of example.[3,23]

Over the last decades, the semiconductor properties of silicon were getting increased attention with the proceeding development of electric devices. Upon doping a silicon grid with foreign atoms like phosphorous (n-type semiconductor, mobile electrons) or indium (p-type semiconductor, electron holes), the electric conductivity can be increased.[3,25] Combining both semiconductor types creates a p-n junction in which the electricity is transported in only one direction and that is used in most semiconductor devices.[25] However, the concentration of the impurities in the silicon grid is very low.[23] Therefore, the silicon used has to be extremely pure what is achieved upon several chemical conversions, purification, and recrystallization steps starting from silicon dioxide and silicates.[3,26,27] The photovoltaic is another huge field of application for high-purity silicon.[26,27] It relies on the photovoltaic effect in which electricity is produced by separating charges that are generated upon irradiation of the semiconductor silicon with light. This leads to an excitation of charge carriers in form of electrons and holes.[28,29]

1.2. Higher Coordinate Silicon

1.2.1. The missing "Hypervalent Carbon"?

Silicon and carbon belong both to the 14th group of the periodic table, indicating similar properties and reactivity. However, there are main differences in their reactivity and structural properties. In contrast to carbon, silicon has only a limited capability of forming multiple bonds but readily establishes stable coordination geometries of higher order.[30] A sp^3 hybridized silicon center forming a tetrahedral coordination geometry readily reacts with a further ligand to a pentacoordinate silicon center (Scheme 1). Due to a Berry pseudorotation mechanism, pentacoordinate silicon complexes were found to show stereoisomerization between a trigonal bipyramidal and square pyramidal geometry.[23,31–33] Addition of a further ligand leads to a more or less distorted octahedral[30–33] or trigonal antiprismatic[34] coordination sphere of the silicon center. Although a further extension of the coordination geometry is very unlikely,[30] heptacoordinate silicon complexes were described in the literature.[32,35,36] Due to these structural diversity, higher coordinate silicon can be considered as an excellent substitute for the missing "hypervalent carbon".[37,38]

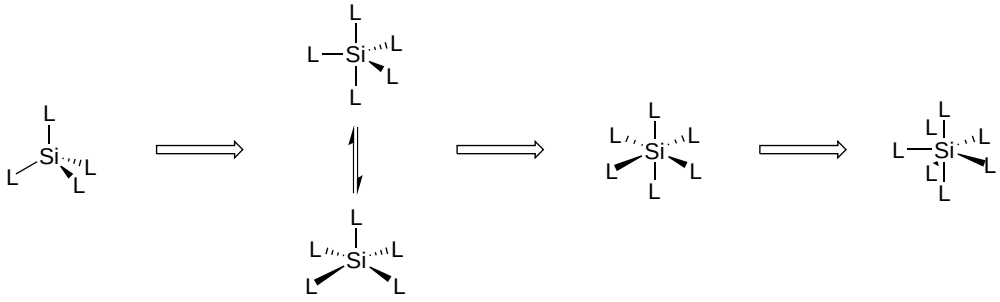

Scheme 1: Possible coordination geometries of silicon coordinating four to seven ligands.

Upon increased coordination, the electron density at the silicon center is decreased leading to an enhancement of its *Lewis* acidity. Nevertheless, it is worth mentioning that the octahedral coordinate silicon center is not acting as LEWIS acid because the enlargement of the coordination sphere is very unlikely.[30] However, the electron density at the ligands, and hence their nucleophilicity, is increased upon expanding the coordination geometry, explaining the fact that higher coordinate silicon complexes are very potent donors for carbon or hydride nucleophiles.[30,39–41]

Synthetically, higher coordinate silicon complexes are accessible by various routes including coordination of an anionic or neutral mono- or polydentate ligand to tetrahedral coordinate silicon. However, providing an additional intramolecular coordination site, a tetra(organo)silicon center was also used for the preparation of pentacoordinate silicon complexes. Another method described in the literature relies on the substitution of halogen or alkoxy ligands by polydentate ligands, like for example 1,2-benzenedio or triethanolamine.[33]

1.2.2. Binding Situation

Over the last decades, the description of the binding situation of "hypervalent" main group molecules was discussed controversially.[42–44] In doing so, the terms hypercoordination and hypervalency were often poorly defined or even used equivalent although the meanings are different.[23,44] In general, the coordination number is the amount of neighbors in the primary coordination sphere of a central atom.[23,44] The term valency was commonly used in the 1870s, when the first structural formula of molecules were drawn, and back then, it was equal to the amount of bonds an atom formed in such chemical structures.[23,44] Later, LEWIS and LANGMUIR recognized that most stable molecules have an even number of electrons, assuming that each bond corresponds to a pair of electrons (*rule of two*), and that a central atom of a AX_n molecule or an ion has eight electrons which corresponds to four electron pairs in its valence shell (*rule of eight* or *octet rule*).[45–47] However, it was not before 1969 that the concept of hypervalency was introduced by MUSHER for molecules violating the *octet rule* by exceeding the amounts of valences allowed.[42–45,48] For example, the phosphor atom of PF_5 is hyper- or higher coordinate since is is surrounded by five fluorine atoms. Moreover, if the valence shell of the phosphor atom is exceeded by forming five electron pair bonds (Scheme 2a), the molecule is hypervalent according to the definition of MUSHER. However, the P−F bonds are strongly polarized allowing a non hypervalent description of the molecule using ionic resonance structures introduced by PAULING[43] which do not exceed the *octet rule* (Scheme 2b).[23]

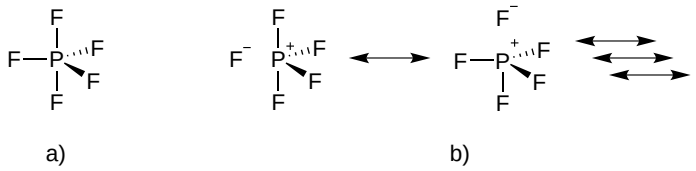

Scheme 2: LEWIS structures of PF_5. a) Hypervalent LEWIS structure in which the valence shell of the phosphor atom is exceeded. b) Resonance structures proposed by PAULING obeying the *octet rule*.

For many years, it was assumed that the d orbitals play an important role in the bonding of higher coordinate main group elements. For example, a sp^3d or a sp^3d^2 hybridization on the coordination center

was proposed for penta-, respectively hexavalent atoms.[30,37,49] However, recent quantum chemical *ab initio* calculations proved this theory wrong but admit that the d orbitals are still involved in the binding process by polarizing the p orbitals.[43,45,49–54] Moreover, the calculations support the concept of a 3-center-4-electron (3c-4e) bond which was introduced by PIMENTEL[55] and RUNDLE[56,57] in 1951 to describe the bonding situation in XeF_2 or I_3^-.[43,52] These inital works were further developed by RUNDLE and MUSHER leading to the general theory of hypervalency.[48,52] Using a qualitative molecular orbital model, the 3c-4e bond can be described by linear combination of the central atoms p orbital and a σ-bonding orbital from each of two opposing ligands surrounding the center. This leads to set of three molecule orbitals, a bonding σ, a nonbonding n, and an antibonding σ^* orbital (Figure 1). The four electrons of the bond are populated in the bonding σ orbital as well as in the nonbonding n orbital. The n orbitals are located exclusively on the ligands, explaining why the 3c-4e bond is preferred by electronegative ligands or atoms. Therefore, it can also be interpret as an ionic bond, which would be in accordance with the PAULINGs ionic resonance structures. Moreover, the resulting bonding order for the central atom to each ligand is 0.5.[43,45,54]

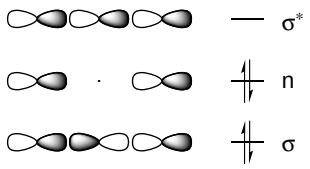

Figure 1: Molecul orbitals of the 3-ceter-4-electron (3c-4e) bond. It is composed of a bonding σ (populated), a nonbonding n (populated), and an antibonding σ^* orbital. The electrons in the n orbital are located entirely on the ligands.[43]

In the following, the concept of the 3c-4e bond is adopted to higher coordinate silicon(IV) complexes. In pentacoordinate complexes, the binding situation can be described using a sp^2p hybridization of the silicon (Figure 2a). The three equatorial ligands bound the three sp^2 hybrid orbitals via normal 2-center-2-electron (2c-2e) bonds. The axial ligands are bound by a 3c-4e bond utilizing the remaining p_z orbital of the silicon center. As a result, bonding orders of 1 and 0.5 were obtained for the equatorial and axial ligands, respectively.[43,45,54] These theoretical data were supported by crystal structure analysis as the bonding lengths of the axial ligands is longer compared to the equatorial ones.[58] Besides the theory mentioned, further multicenter bonding models for pentacoordinate main group elements, like a 4-center-6-electrons (4c-6e) bond, were proposed.[43]

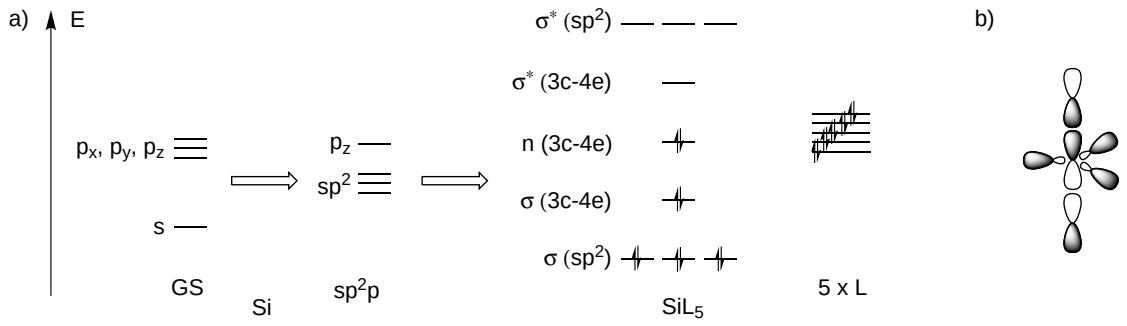

Figure 2: a) Schematic molecular orbital diagram for a pentacoordinate silicon center using a 3c-4e bond. b) Scheme of the orbitals at the silicon center.

Using the schematic molecular orbital diagram of hexacoordinate silicon (Figure 3a), two bonding motives can be discussed. Expanding the concept of the pentacoordination, the bonding of hexacoordinate silicon may be described using two 3c-4e bonds. Therefore, the silicon orbitals are sp hybridized forming two normal 2c-2e bonds and the residual p orbitals are involved in the formation of two linear multicenter bonds. In this case, the bonding situation can alternatively specified as four "covalent" ($a_{1\,g}$, $t_{1\,u}$) and two "ionic" (e_g) bonds. On the other hand, the bonding can be described as a combination of three 3c-4e bonds ($t_{1\,u}$) in combination with a bonding orbital "formed from the 3s orbital on [silicon] and the fully symmetric nonbonding combination of the 3c-4e nonbonding orbitals"[43] (Figure 3c). This interpretation can be seen as four bonds distributed over six silicon-ligand pairs. In any case, the *octet rule* is obeyed as all electrons associated with the silicon are located in the $a_{1\,g}$ and $t_{1\,u}$ orbitals. Moreover, the bonding order of a single bond is 2/3.[43,54]

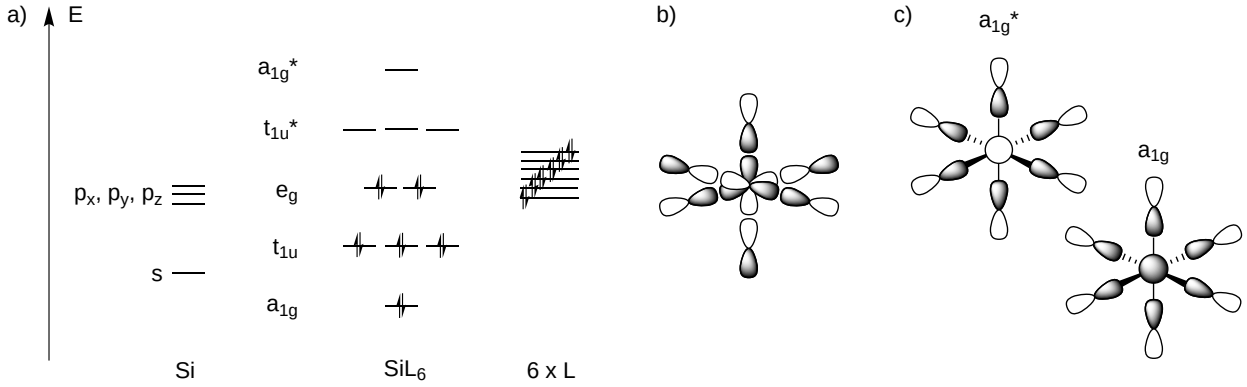

Figure 3: a) Schematic molecular orbital diagram used for the description of a hexacoordinate silicon center. b) Scheme of the orbitals at the silicon center if two 3c-4e bonds are used. c) Representation of the $a_{1\,g}$ and $a_{1\,g}{}^*$ orbitals if three 3c-4e bonds are used.

1.3. Hexacoordinate Silicon Complexes

The presence of silicon compounds with a coordination number greater than four are already known for more than 200 years.[33] At the beginning of the 19th Century, Gay-Lussac[59] and Davy[60] independently observed the formation of the anion $[SiF_6]^{2-}$ (**1**) upon studying reactions of silicon tetraiodide (**2**) and silicon dioxide with hydrogen fluoride or water. Further investigations of silicon tetraiodide (**2**) resulted *inter alia* in the formation of the diammintetrafluoridosilicon(IV) complex **3**[60] and the first isolation of the amorphous, elementary silicon by Berzelius in 1824.[61,62]

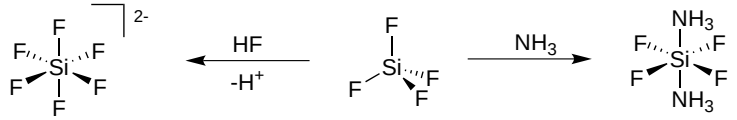

Scheme 3: Examples for the first higher coordinate silicon complexes synthesized at the beginning of the 19th Century by Gay-Lussac[59] and Davy.[60]

Due to the topic of the present Thesis, only examples for hexacoordinate silicon(IV) complexes will be discussed in the following. Moreover, according to their charge, they are grouped as neutral, anionic and cationic complexes.

1.3.1. Neutral Silicon Complexes

The previously mentioned complex **3** was one of the first neutral octahedral silicon complexes that has been discovered. Later on, it was demonstrated that silicon tetrachloride readily reacts with polypyridyl ligands,[33] for example 2,2'-bipyridine or 1,10-phenanthroline, giving the neutral hexacoordinate silicon complexes **4** (Scheme 4) as demonstrated by Wannagat in 1957.[63] Conversion of of 2,2'-bipyridine derivative with Li_2bpy afforded the neutral complexes **5** and **6** in which the silicon center has a formal charge of +2 and 0, respectively.[33]

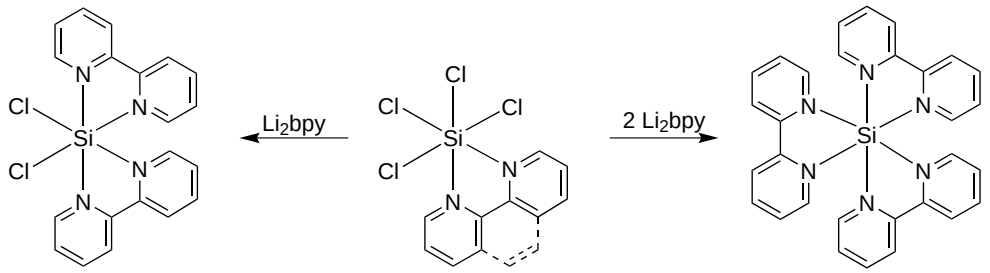

5 **4** **6**

Scheme 4: Syntheses of neutral hexacoordinate silicon complexes with a Si^{+2} (**5**), respectively Si^0 (**6**) center.[33]

In 1966, Pike *et al.* reported the synthesis and isolation of complex **7** (Figure 4).[64] The choice of the silicon precursor proved to be crucial for this reaction as the neutral complex was obtained using silicon tetraacetate whereas silicon tetrachloride afforded a trishomoleptic cationic derivative as descirbed later on. Reacting a spirosilane and 1,10-phenanthroline, Farnham and co-workers obtained complex **8** which showed enantio- and diastereoisomerization via dissociation of the polypyridyl ligand.[65] The structural similar complexes **9** and **10** showed very different reactivities towards nucleophiles.[66,67] While the chlorido ligands of complex **9** were substituted easily by various nucleophiles, complex **10** showed no conversion at all. A possible explanation for this behavior might be that the chlorine atom has a higher polarizability compared to fluorine leading to a longer Si−Cl bond in a "semi-ionic" state.[66]

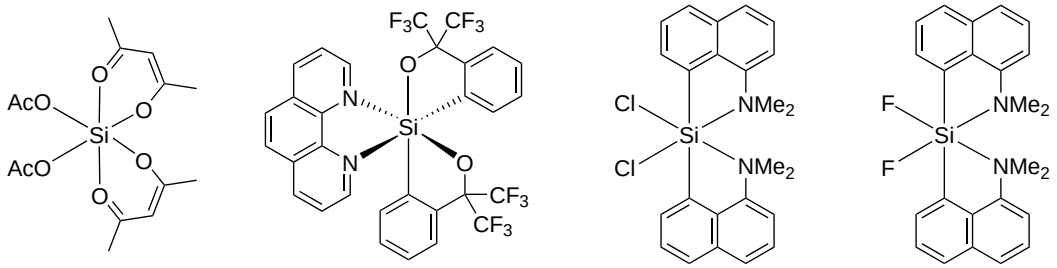

7 **8** **9** **10**

Figure 4: Examples for neutral hexacoordinate silicon complexes.[64–67]

Over the last decades, Tacke and co-workers synthesized and structurally characterized numerous octahedral silicon complexes coordinate by various mono- and polydentate ligands (Figure 5).[68–76] In doing so, different silicon sources like tetra(cyanato-*N*)silane (**11**),[76] tetra(thiocyanato-*N*)silane (**12**),[70] or silicon tetrahalides were utilized. Interestingly, the stereochemistry of the complexes has

no influence on the ^{29}Si chemical shift as demonstrated by theoretical studies for complex **12**.[70] The benzamidinato ligand proved to be a very versatile ligand for the synthesis of higher coordinate complexes like the tris-heteroleptic complex **13**.[68] Another example is complex **14** that was obtained upon activation of sulfur dioxide by a bis(benzamidinato) silylene, which has been demonstrated to activate also other small molecules like carbon dioxide or nitrous oxide.[71–73] More recently, some other nice hexacoordinate silicon structures were reported by the research groups of Kroke[77–79] and Kotali.[80]

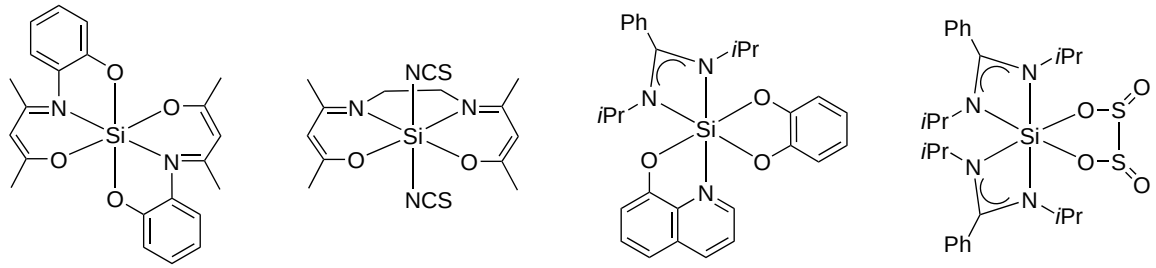

11 **12** **13** **14**

Figure 5: Examples for neutral hexacoordinate silicon complexes synthesized in the Tacke group.

The complexes discussed so far are use to study the synthesis, structure and chemical reactivity of hexacoordinate silicon complexes. However, there are also some examples of neutral complexes showing biological activity. For example, complex **15** (Figure 5) was found to exhibit strong fungicidal and bactericidal activity.[81] Later Singh and co-workers showed for a structural similar silicon complex *in-vitro* antimicrobial activity.[82] In many cases, neutral hexacoordinate silicon complexes do not posses any photochemical properties. However, if coordinate to a phthalocyanine, the photochemical properties are dramatically changed allowing the complexes to be used as photosensitzer in the photodynamic therapy (PDT).[83–85] Upon variation of the helical ligands, the characteristics of the complexes like quantum yield, solubility or cellular uptake can be altered in order to influence their biological and photophysical activity. Therefore, silicon phthalocyanine complexes are interesting lead structures for the development of novel agents for treating cancer as demonstrated by *in-vitro* and *in-vivo* studies for complexes **17**,[83] respectively **18**,[84] by way of example.

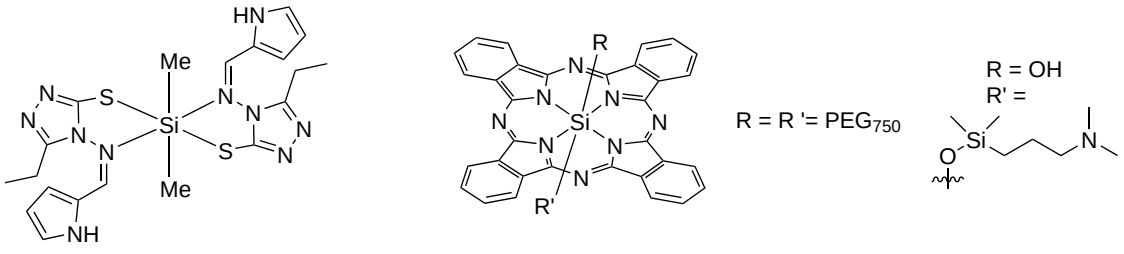

15 **16** **17** **18**

Figure 6: Examples for biological active silicon complexes.[81,83–85]

1.3.2. Anionic Silicon Complexes

After the discovery of the anion $[SiF_6]^{2-}$ (**1**), the synthesis and chemical properties of organopentafluoridosilcate ($[F_5RSi]^{-2}$ were investigated by Tansjoe, Müller *et al.* as well as by Kumada and co-

workers.[33,86,87] These complexes were found to be applicable versatilely in organic synthesis, including for example fluorination or carbon-carbon bond-forming reactions catalyzed either by palladium, copper(I), or silver(I). However, the reaction of a tetraalkoxysiliane with 1,2-dihydroxybenzene under basic conditions afforded another class of dianionic hexacoordinate silicon complexes, tris(benzene-1,2-diolato)silicate **19**. 1,2-dihydroxybenzene proved to be an excellent ligand for the synthesis of higher coordinate silicon complexes, since it allows the synthesis of complex **19** using other silicon sources like silicon dioxide or even $[SiF_6]^{2-}$ (Scheme 5).[33] Moreover, Laine and co-workers demonstrated that silicon dioxide readily reacts with aliphatic 1,2-diols in the presence of barium oxide yielding tris-homoleptic complexes, for example complex **20**.[33]

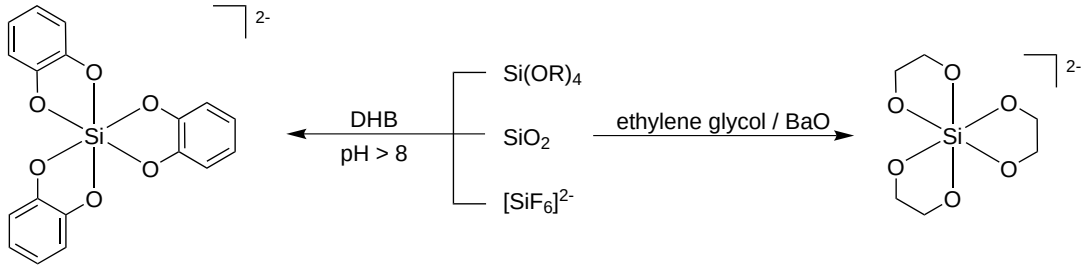

19 **20**

Scheme 5: Synthesis of two tris-homoleptic, dianionic silicon complexes starting with various silicon sources.[33] Complex **20** was obtained upon reaction of silicon dioxide with aliphatic 1,2-diols in the presence of bariumoxide. Complex cations are not shown.

Complex **19** was found to be an excellent building block for the synthesis of organosilanes as it reacts rapidly with aluminium hydride, Grignard or organolithium reagents.[33] Depending on the chemical structure of the Grignard reagent, different substitution patters can be obtained. For example, the conversion with a di-Grignard reagent, a spirosilane (**21**) is obtained (Scheme 6).[33] In contrast, the reaction with ethylmagnesium bromide (EtMgBr) and subsequent conversion with hydrogen chloride yields chlorosilane **22**.[88,89]

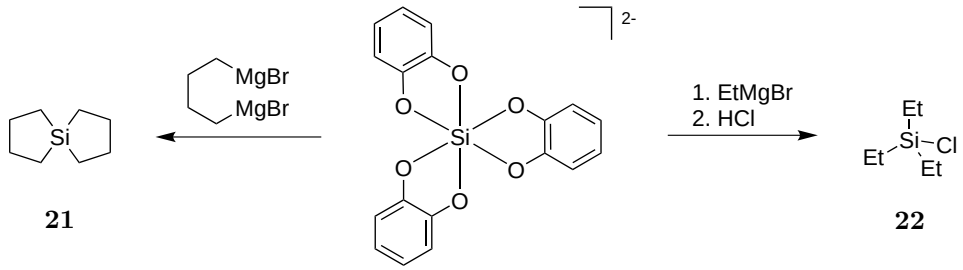

21 **19** **22**

Scheme 6: Examples for the reaction of complex **19** with Grignard reagents.[33] Complex cations are not shown.

Over the last decades, the synthesis and characterization of anionic hexacoordinate silicon(IV) complexes was driven *inter alia* by the research groups around Tacke[90,91] or Klüfers.[92,93] For the coordination, structurally diverse ligands like carbohydrates, nucleosides or oxalates were used. Some examples complexes are given in Figure 7, by way of example.

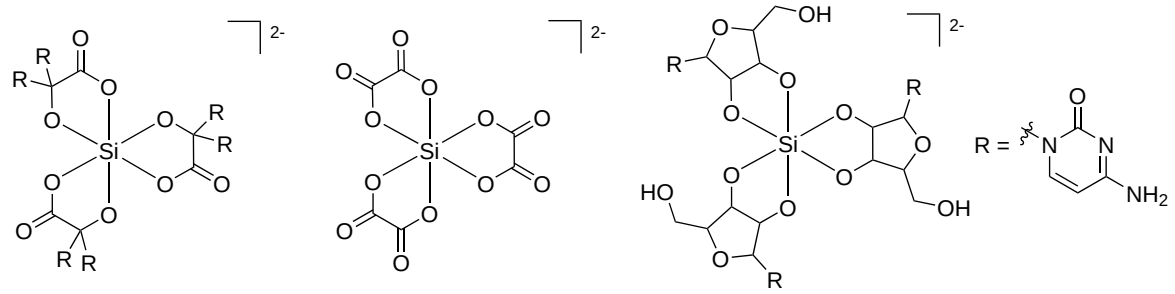

Figure 7: Examples for dianionic, hexacoordinate silicon complexes coordinate to various ligands.[90–92] Complex cations are not shown.

As discussed earlier, silicon is a crucial biological trace element for most humans and plants. However, nearly nothing is known about silicon biochemistry since no evidence of organosilicon compounds in living systems have been observed for a very long time. Anyhow, it was expected that higher coordinate silicon geometries play an important role in its interaction with biological systems and its biomineralization.[90,94] A first evidence proving this hypothesis true was reported by Kinrade *et al.* in 2002. Using ^{29}Si-NMR spectroscopy, a transient hexacoordinate silicon species formed *in vivo* by the diatom *Navicula pelliculosa* was identified.[94] More recently, it was found that the naturally occurring iron-chelating siderophors enterobactin (**26**) and salmochelin (**27**) are binding silicon in a hexacoordinate geometry using three 1,2-benzenediolate moieties (Figure 8).[95,96] In addition, these complexes were found to be stable under physiological conditions. Hence, it was assumed that siderophores play an important role in the cellular uptake of silicon in addition to the well-established pathway for iron(III).[95–97]

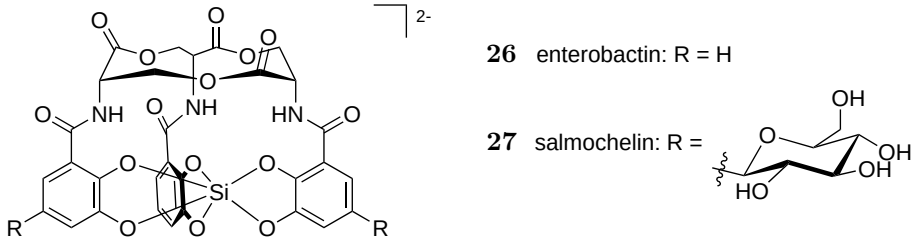

Figure 8: Hexacoordinate silicon bound to the naturally occurring siderophors enterobactin (**26**) and salmochelin (**27**).[95,96] The counterions are omitted.

1.3.3. Cationic Silicon Complexes

The chemistry of cationic hexacoordinate silicon complexes is mainly derived from the work of Dilthey in 1903.[28,98] Upon the reaction of silicon tetrachloride with the bidentate ligand acetyl acetone, a cationic complex of the formula $[Si(acac)_3]Cl \cdot HCl$ was obtained. Dilthey and co-workers proposed an octahedral geometry of the cation in 1906,[99] which was verified about 50 years later by West[100] using IR-spectroscopy and Kirschner *et al.* using optical resolution studies.[101,102] In 1964, Muetterties and Wright used α-tropolone and α-aminotroponimine, widespread ring structures in natural products,[103] for building up monocationic hexacoordinate silicon complexes.[104]

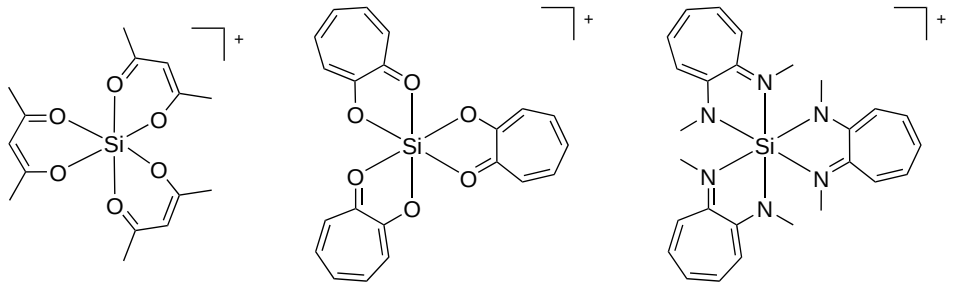

28 **29** **30**

Figure 9: Structures of the cationic hexacoordinate silicon complexes coordinate to acetyl acetonat (**28**),[98,99] α-tropolonat (**29**), and its amino derivative (**30**).[104] The counterions are omitted.

In the 1950s, (polypyridyl)silicon(IV) complexes were investigated thoroughly. In doing so, neutral hexacoordinate silicon complexes, like for example **4**, were isolated. However, using other silicon sources, cationic hexacoordinate silicon complexes could be obtained as demonstrated by KUMMER and co-workers for several complexes.[105–110] For example, the reaction with Si_2Br_6 yielded the tris-homoleptic complex **31**[108] whereas the silicon precursor SiI_2XY (with X, Y = H, Cl, I, OH, OCH_3, CH_3, C_6H_5) afforded the corresponding bis-homoleptic complexes (Figure 10).[105,106] It is worth mentioning that only the iodine substituents were replaced during the reaction with SiI_2XY. The octahedral geometry of the silicon cations were verified using IR- and NMR-spectroscopy.

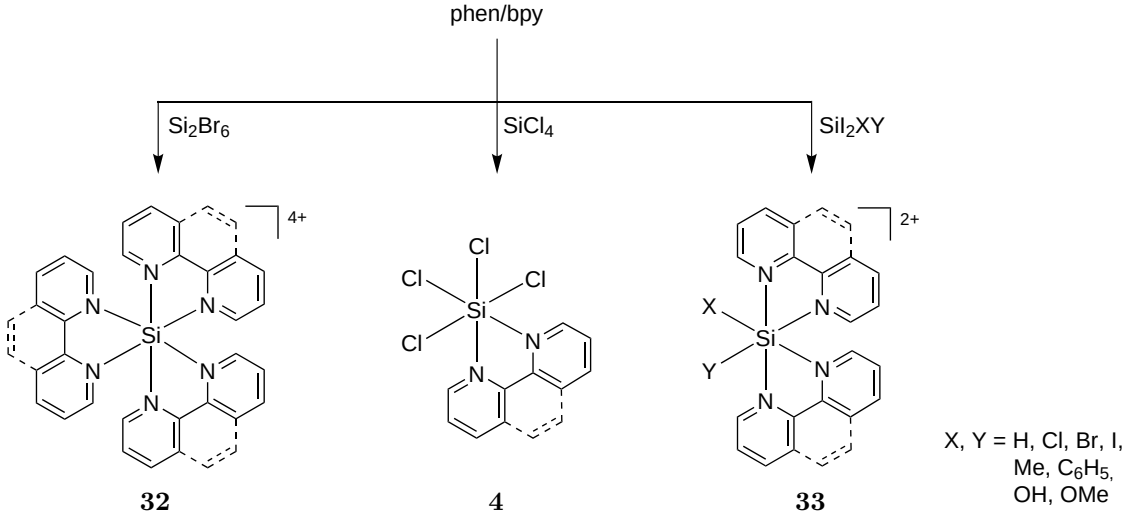

32 **4** **33**

Figure 10: The conversion of polypyridyl ligands with different silicon sources allows the synthesis of neutral or cationic hexacoordinate silicon(IV) complexes.[63,105–107] The counterions are not shown.

Surprisingly, the tris-homoleptic complexes showed remarkable stability towards solvolysis in water and methanol.[108] Both complexes could be stored in an aqueous medium for months. Moreover, acidic conditions as well as heating under reflux conditions had no influence on the complexes. However, the stability towards bases **32** proved to be less pronounced as the presence of hydroxide led to a fast degradation of the complexes. Similar results were obtained for the bis-homoleptic complexes **33** if at least one substituent (X, Y) is a chlorine or an oxygen bound ligand.[105–107] Otherwise and depending on the solvent used, a substitution of the monodentate ligands with two hydroxy, respectively methoxy groups can be observed. The unexpected stability may be explained by

electronic (acceptor strength of the corresponding silanes) rather steric factors.[105] Due to the high stability towards hydrolysis, YOSHIKAWA and co-workers were successful to resolve the enantiomers of the tris-homoleptic cations **32** after exchanging the counterion to the chiral antimonyl tartrate ($[Sb_2((^+)-tartrate)_2]^{2-}$).[111] In doing so, the remarkable stability towards hydrolysis could be demonstrated once more since a racemization of the isolated enantiomers was not observed.

Following the work of KUMMER *et al.*, the working groups around MEGGERS and SCHMEDAKE were recently able to synthesize (arenediolato)bis(polypyrdidyl)silicon(IV) complexes[37,112,113] as well as the octahedral complex bis(2,2':6',2"-terpyridine)silicon(IV)[114] (Figure 11). Complex **34** was demonstrated to be stable towards hydrolysis and to bind *calf thymus* DNA via intercalation.[37] Complex **35** is an interesting structure as it possesses another binding site for transition metals and could therefore be used for the synthesis of dinuclear metal-silicon complexes. The terpyridine complex **36** showed interesting fluorescence properties demonstrating that silicon complexes may be used as molecular dyes or as mediators in photovoltaic applications.[114]

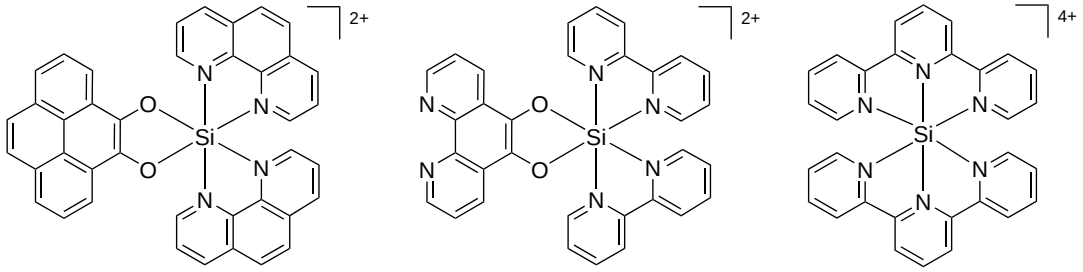

34 **35** **36**

Figure 11: Some examples for hexacoordinate (arenediolato)bis(polypyrdidyl)silicon(IV) and bis(2,2':6',2"-terpyridine)silicon(IV) complexes synthesized by the groups of MEGGERS[37] and SCHMEDAKE.[113,114] The counterions are omitted.

Over the last decade, various cationic hexacoordinate silicon structures have been prepared. In doing so, different ligands were used. A few recent examples with NO-chelating ligands are given in Figure 12.[77]

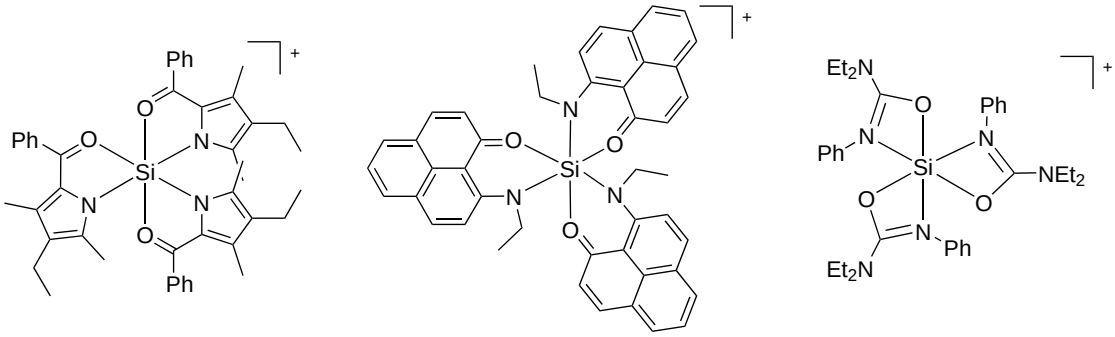

37 **38** **39**

Figure 12: Some recent examples for hexacoordinate silicon(IV) complexes bound to NO-chelating ligands.[77] The counterions are omitted.

1.4. Duplex DNA

1.4.1. Interaction of Metal Complexes with Duplex DNA

There are various different possibilities for the interaction of metal complexes with double stranded DNA known. For example, the well-know and commonly used anti-cancer agents Cisplatin (**40**, Figure 13) and its derivatives, like Carboplatin (**41**),[115,116] are capable of forming an irreversible bond between the platinum center and the N7 atom of purine bases.[117–120] The major DNA adducts formed by Cisplatin are 1,2-intrastrand cross-links involving mainly two guanine bases (*cis*-[$Pt(NH_3)_2d(GpG)$]) or, to a lesser amount, a guanine and an adenine base (*cis*-[$Pt(NH_3)_2d(ApG)$]).[117–119,121] In addition, 1,3-intrastrand as well as interstrand adducts are observed at low percentage.[118,119,121] As a matter of fact, the platinum induced cross-link of the DNA leads to an unwinding and bending of the DNA causing a destacking of the bases, and with this change in the secondary DNA structure, the helix is destabilized.[117,118,122,123] In 1979, Köpf and Köpf-Maier showed that the structural similar complex titanocene dichloride (**42**) possesses antitumor activity[124] which might also be due to an interaction with DNA.[117,125] Studies with various titaoncen derivatives binding to DNA showed a strong binding to DNA at the N1 or N7 atoms of the nucleotide or the phosphate backbone.[117,125,126] In addition, $TiCl_2Cp_2$ was demonstrated to disrupts the Watson-Crick pairing of the hydrogen bond of A-T base pairs.[125,127] Interestingly, $TiCl_2Cp_2$ showed a pH-dependency of the binding since the complex is unstable at pH > 5.[117,125] However, due to this fact and other possible biological targets for titanocen dichloride, like for example protein kinase C, the exact mode of its anti tumor activity is still unclear.[117,125]

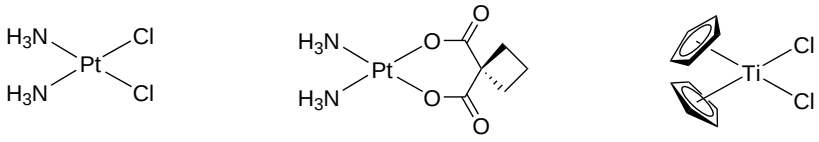

40 **41** **42**

Figure 13: Structure of the DNA-binding agents Cisplatin (**40**),[120] Carboplatin (**41**),[115] and titanocene dichloride (**42**).

In addition to reactive metal complexes binding to DNA, there are mainly three possible interactions of nonreactive metal complexes with double stranded DNA known (Figure 14).[128] These are either groove binding (Figure 14a), metallo intercalation (Figure 14b) or metallo insertion (Figure 14c). In comparison to reactive metal complexes, like for example the platinum derivatives discussed earlier, nonreactive complexes do not form covalent bonds to DNA but bind reversibly through electrostatic or van-der-Waals interactions.[118,128,129]

Figure 14: Binding motives of nonreactive metal complexes with double stranded DNA which are mainly groove binding (a), intercalation (b), and insertion (c).[128]

One of the first octahedral metal complexes studied for their interaction with DNA have been tris(phenanthroline) complexes of the metals ruthenium, chromium, nickel, zinc, osmium and cobalt.[128,130] Investigating their nature of DNA interaction, two different binding modes were found. On the on hand, the interaction with DNA resulted from a partial intercalation of one 1,10-phenanthroline ligand into the helix in the major groove, like for example complex Δ-$[Ru(phen)_3]^{2+}$ (Δ-**43**, Figure 15).[128,129] On the other hand, hydrophobic interactions with the minor groove also result in a strong binding to DNA as demonstrated for the Λ-enantiomer of $[Ru(phen)_3]^{2+}$ (Λ-**43**).[128,129] However, this example for octahedral metal complexes binding DNA revealed, how important chirality is for the design of DNA binding complexes.[128,129,131] The chiral discrimination could be enhanced further by using sterically more demanding ligands.[128,129] A nice example for this behavior is tris(4,7-diphenyl-1,10-penanthroline)ruthenium(II) complex **44** (Figure 15) since the Δ-isomer binds right-handed B-DNA whereas the Λ-isomer binds only left-handed Z-DNA as demonstrated by Barton and co-workers in 1984.[132]

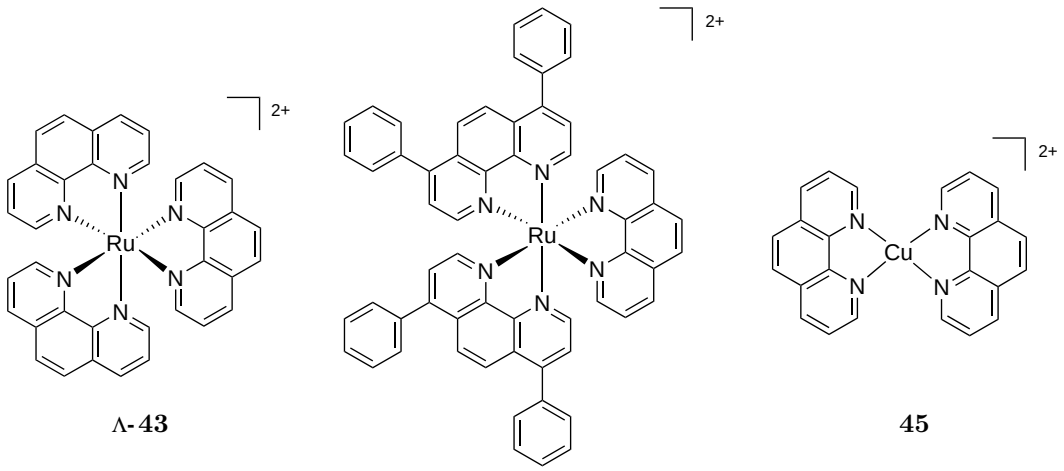

Λ-**43** Λ-**44** **45**

Figure 15: Metal complexes capable of binding DNA. Complexes Λ-**46** and **45** interact with DNA through groove binding in the minor groove of the helix whereas λ-**44** binds only left-handed Z-DNA.[128,129,132] The counterions are omitted.

Besides octahedral ruthenium complexes, the work of Sigman *et al.* laid the ground stone for the rich chemistry of groove binding complexes by using the copper(I) bound 1,10-phenanthroline complex $[Cu(phen)_2]^+$ (**45**, Figure 15) starting in the late 1970's.[128,133,134] In addition to binding DNA through the minor groove, this complex was also found to be able of cleaving DNA macromolecules in the presence of hydrogen peroxide.[128,133,134]

The intercalation is the second and most extensively studied way for metal complexes to bind double stranded DNA.[128–130,132,135–145] The mode of action is an unwinding of the DNA by the metal complex followed by a π-stacking between two base pairs of the helix.[128,129] Hence, metallointercalators are composed of two important building blocks, a planar intercalating ligand and a ancillary moiety as demonstrated for the two well-known ruthenium complexes in Figure 16.[128,146] In order to easily slip between the base pair layers of the DNA double helix, the intercalating ligand itself is oriented parallel to the base pairs and away from the metal center.[117,128] The metal center itself together with the remaining ligands act as a stable anchor ascertain that the complex has the correct stereo chemistry for binding DNA double helix.[128,132] In addition, the positive charge of the metal center increases the binding affinity even more due o electrostatic interaction with the negatively charged phosphate backbone of the DNA.[117,146] Although intercalation is preferred to occur through the major groove of the helix, there are also complexes known to intercalate via the minor groove, like for example complex **48**.[128]

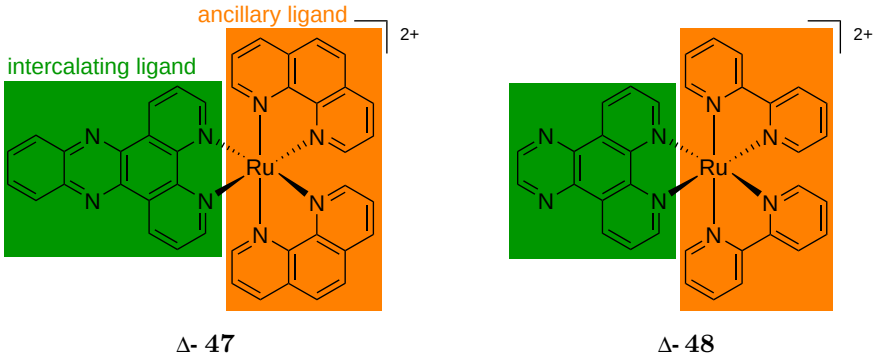

Figure 16: Examples of two ruthenium based DNA intercalating metal complexes. The intercalating ligands are highlighted in green and the ancillary mojiety in orange.[128,129,135,136]

Finally, the class of metalloinsertors should be discussed briefly. Similar to metallointercalators, inserting metal complexes are coordinate to planar ligand that is capable of extending the base-stack of the DNA by inserting into the helix.[128] In doing so, the metalloinsertor is ejecting a single base pair of the base stack with the inserting ligandin order to adopt the role of the replaced base pair in the π-stacking.[128] Two of the few examples of metalloinsertors reported are rhodium complexes **Δ-49/50**(Figure 17), which insert into the DNA helix using its diimine ligands.[147,148] Although only few DNA insertors, no matter whether organic or inorganic, are reported until now, they show a strong potential for biological applications as they can be used to recognize mismatched DNA base pairs.[128,147,148] Moreover, the hexacoordinate silicon complex **51**, synthesized by Yonggang Xiang during his Ph.D. in the Meggers group was also believed to act as a DNA insertor detecting mismatched DNA base pairs.[149,150]

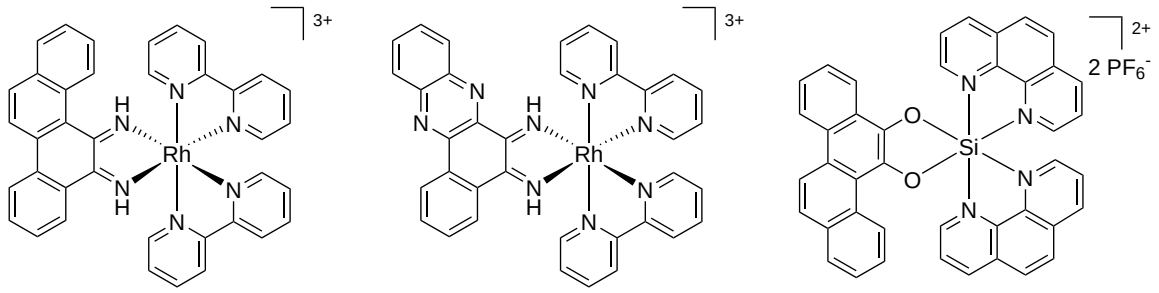

Δ-**49** Δ-**50** **51**

Figure 17: Metal complexes acting as metalloinsertors.[147–149] The counterions are not shown.

Besides mononuclear metal complexes, there are also an increasing number of polynuclear metal complexes know to interact with double stranded DNA. Two of the most prominent and extensively studied examples are the tetrakis(polypyridine)diruthenium complexes **52** and **53** (Figure 18).[140,144,151,152] Although it was shown that these complexes bind DNA very strongly, the binding motive is discussed controversially in the literature.[140,144,152] Hence, in 2006 Thomas and co-workers postulated an intercalative binding of these complexes due to viscosity studies.[140] On the other hand, in 2008 Turro *et al.* demonstrated by viscosity studies, ionic strength dependency of the DNA binding constant, reverse salt titrations and comparison of thermodynamic parameters that complex **52** is no DNA intercalator but binds DNA via electrostatic surface binding.[144] However, one year later, Thomas and co-workers used complexes **52** and **53** as biological imaging agents to stain eukaryotic and prokarytotc DNA in living cells.[152] Structural similar (polypyridyl)diruthenium complexes were studied for example by Kumbhar[151] *et al.* or Wang[153] and co-workers.

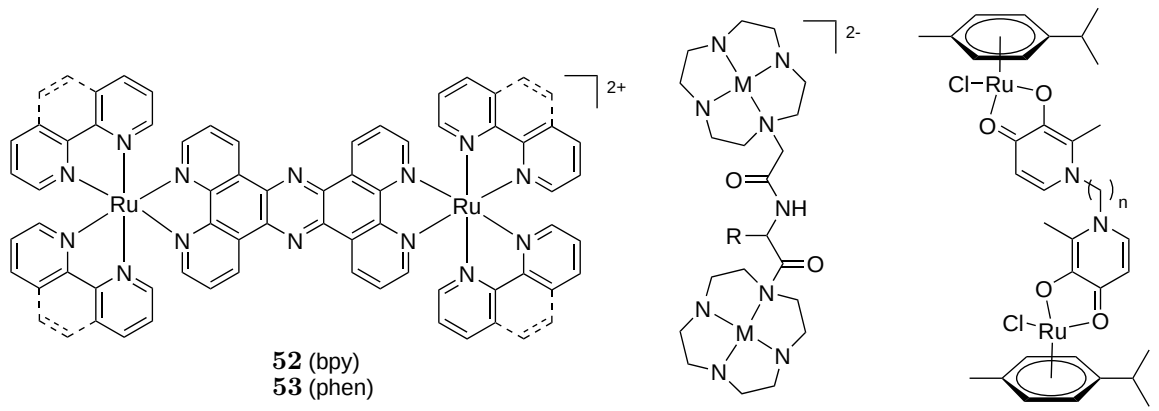

54 **55**

Figure 18: Examples for polynuclear metal complexes known to interact with double stranded DNA. Possible counterions are omitted.

A structural more sophisticated complex based on a copper porphyrin structure substituted with three bis(bipyridine)ruthenium fragments was introduced by Swavey *et al.* in 2010.[154] It was shown that the complex favors DNA groove binding over DNA intercalation.[154] Moreover, it was shown to cleave single stranded supercoiled plasmid DNA upon irradiation with low energy light due to a formation of singlet oxygen.[154] Another polynuclear complex capable of cleaving plasmid DNA is the macrocylic polyamine complex **54** (Figure 18).[155] In addition, the dinuclear half sandwich ruthenium complexes

55, introduced by Maruszak and Nazarov *et al.* in 2009, reacts rapidly with DNA forming DNA-protein and DNA interduplex crosslinks.[156] Moreover, these complexes showed antitumor activity, also inhibiting oxoplatin resistent cell lines.

1.4.2. DNA light-switch

In the late 1980's, it was discovered that DNA intercalation of (polypyridyl)metal complexes, like for example $[Ru(dppz)(phen)]^{2+}$ (**47**), results in an enhancement of its fluorescence.[128,129,141,142,144,157,158] This phenomena, commonly known as DNA *light-switch*, was first described by Barton *et al.*[142] in 1990 for $[Ru(dppz)(phen)]^{2+}$ and was getting increasingly more attention thereafter.[128–130,140–144,152,157–160] It is based on a luminescence of a metal complex in an organic solvent or in the presence of DNA which is quenched completely in an aqueous surrounding.[128,142,144,146] Although it was common sense for a long period of time that DNA intercalation is needed for light-switch behavior, Turro and co-workers proved this hypothesis wrong for the dinuclear metal complex $[Ru_2(bpy)_4(\mu\text{-tpphz})]^{4+}$ (**52**) in 2008.[144] They found that complex **52** is acting as molecular light-switch but is binding DNA through electrostatic surface binding.[144] Hence, "intercalation is not required for DNA light-switch behavior".[144]

In order to understand the light-switch mechanism, the model system $[Ru(dppz)(bpy)]^{2+}$ was studied thoroughly. It was found that the luminescence of the complex arises from a metal-to-ligand charge transfer (MLCT) excited state from the ruthenium(II) center to the dppz ligand.[144,159,160] However, the emission lifetime is temperature depending as it decreases upon heating in the range of 254–350 K as well as below 254 K.[144,159,160] Trying to explain this observations, a three staged energy level diagram was proposed to describe the luminescence behavior (Figure 19). In the model system, the lowest energy level is the nonluminescent dark state (D) arising from a ^{3}MLCT transition from the ruthenium(II) to the phenazine part of the dppz ligand.[144,159,160] Since this state is enthalpically favored, it is populated at lower temperatures.[159,160] In an energetically close region, the luminescent bright state (B) arising from a ^{3}MLCT transition from the ruthenium(II) to the bipyridine part of the intercalating ligand comes next, followed by an incredibly higher lying, nonluminescent ^{3}dd state that is getting more and more populated at higher temperatures.[144,159,160] In contrast to the dark state, the entropically favored bright state is populated at higher temperatures.[159,160]

The light-switch behavior now originates from a dynamic, thermal equilibrium between the dark and bright state meaning that the excited state population is shared between different fragments of the dppz ligand.[144,159,160] On the one hand, lowering the temperature leads to a decrease of the entropically contribution to the free energy shifting equilibrium to the dark state and hence decreasing the emission.[159,160] On the other hand, the energetic level of the dark state can be can be modified by the polarity of solvent. In aqueous solutions at 298 K, the energy gap between the dark and the bright state is too large for a thermal equilibrium of both states turning off the emission.[144] The reason for the huge energy gap in water and thus the deactivation of the excited state are hydrogen bonds formed between the water molecules and endocyclic nitrogen atoms of the complex lowering the dark state.[128,146,159] Upon DNA intercalation or in aprotic solvents, these hydrogen bonds are destroyed or non existent leading to a rise of the dark state energy level. This allows an equilib-

rium between the dark and the now thermally accessible bright state turning on the characteristic luminescence.[128,144,146,158–160]

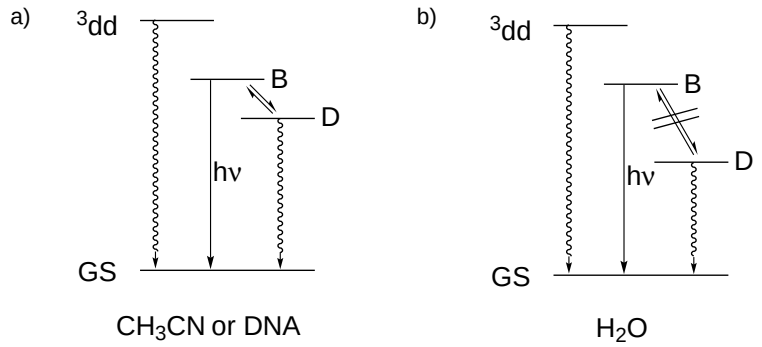

Figure 19: Proposed energy level diagram of $[Ru(dppz)(bpy)]^{2+}$ in a) aprotic solvents or in the presence of DNA and b) in water. The luminescent bright state (B) and the nonluminescent dark state (D) arise from a MLCT transition from the ruthenium to different fragments of the dppz ligand. The energetic level of the dark state can be altered by the polarity of the solvent. The light switch behavior arises from a dynamic, thermal equilibrium between both states. For example, the energy gap between both states in water at 298 K is to huge to overcome thermally explaining the non luminescence of the complex in aqueous surrounding. Upon coordination to DNA, the state is genetically raised turning on the emission.[144,159,160]

1.5. G-Quadruplex DNA

1.5.1. Structure of G-quadruplex DNA

Since the discovery of the DNA double helix structure by Watson and Crick in 1953,[161] a variety of different DNA and RNA structures were found.[162–164] One of the most interesting, both structurally and biological, among them is the G-Quadruplex.

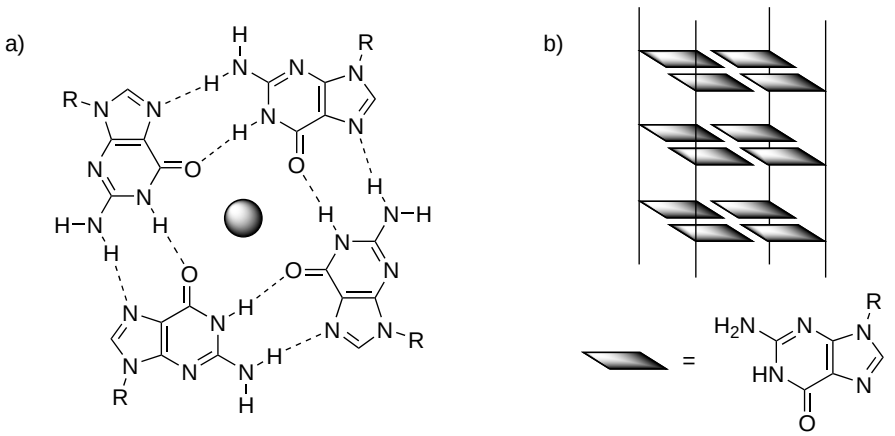

Figure 20: a) A G-quartet formed by four guanine bases bound to each other by Hoogsteen like hydrogen bonding. The gray sphere represents the monovalent cation stabilizing the structure. b) The G-quartets can stack on top of each other, hold together by π-stacking and the sugar-phosphate backbone, building up the G-quadruplex structure. Although the G-quadruplex is helical in nature,[163,165] it is shown without the helix for simplicity.

The structural groundwork for the G-quadruplex was report in 1962 by Gellert and co-workers describing the ability of four guanine residues to self-assembly into planar molecular squares.[164,166] This highly symmetric structure, called G-quartet, is formed by hydrogen bonds between the Watson-Crick edge of each guanine to the Hoogsteen edge of the adjacent bases and is further stabilized by monovalent cations, like for example K^+, Na^+ or $NH_4{}^+$, binding the oxygen atoms surrounding the central core (Figure 20a).[162–164,166,167]

Due to its planar nature, multiple G-quartets can stack on top of each other forming a helical[165] G-quadruplex structure which is stabilized by $\pi\pi$-interactions and linked by the sugar phosphate backbone (Figure 20b).[162–164] In addition, further stabilization occurs through binding of monovalent cations in the central channel of the G-quadruplex formed.[162–164] Unlike to the double helix structure, the G-quadruplexes structure can be formed by one (intramoleculacre), two (bimolecular) or four (tetramolecular) gunaine rich strands of various nucleic acids like for example DNA, RNA or PNA.[162–164] This results in numerous folding patters of G-quadruplex, in which the neighboring strands may be parallel or antiparallel orientated (from 5' to 3' end) in respect to the conformational direction of the glycosidic bond that is either *syn* or *anti*.[162,163] In Figure 21, a few examples for different G-quadruplex topologies are demonstrated.

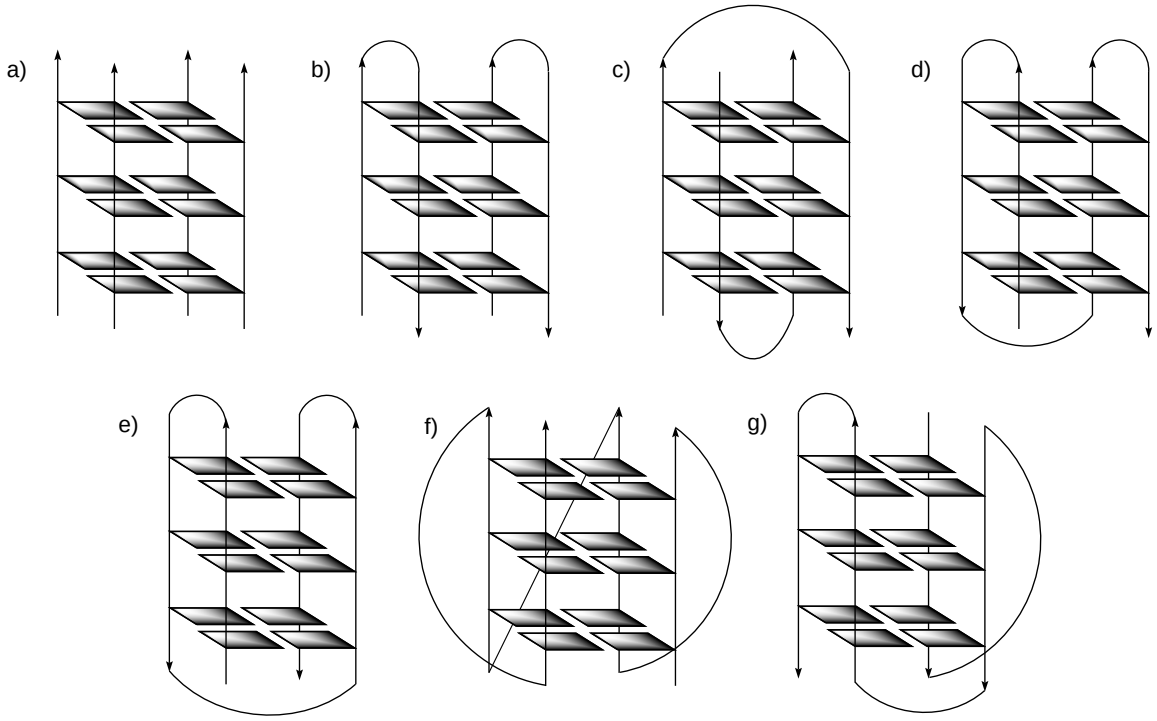

Figure 21: A few examples of G-quadruplex structures. a) Tetramolecular with all strands parallel, b) bimolecular with lateral loops, c) bimolecular with diagonal loops, d) monomolecular/intrastrand with lateral loops, e) monomolecular/intrastrand with two lateral and one diaogonal loops,[168] f) monomolecular/intrastrand with three external (propeller) loops,[169] and g) monomolecular/intrastrand with two lateral loops and one propeller loops. Although the structures e-g feel strange, all have been observed for the human telomers.[162,168,169]

If the quadruplex is formed by four single strands, an all-parallel orientation with *anti* conformation of the bases is preferred as shown in a.[162,163,165] G-quadruplexes formed by two (Figure 21b,c) or even

one strand (Figure 21d-g) are capable of building up various sophisticated structures including lateral (along the side linking nearby antiparallel strands), diagonal (linking diagonally faced antiparallel strands) as well as external, also propeller called (linking nearby parallel strands outside the structure), loops.[162,163,168,169] These loops normally consists of one to seven bases and determine the structural complexity of the four grooves arising from the G-quadruplex structure.[162,163] Crystallographic analysis and NMR-experiments support the broad variety of G-quadruplex structures.[162–165,168–175]

1.5.2. Biological Role of G-quadruplex DNA

During the last decade, numerous sequences capable of forming G-quadruplex structures were discovered in the human genomes and thus expected to play an important role in biological processes.[162–164] In detail, about 350 000–370 000 of those sequences were identified.[162,164] Surprisingly, the G-quadruplex sequences are accumulated at the chromosomal ends, the telomeres which will be discussed in more detail in Chapter 1.5.3, as well as at intra-chromosomal, oncogenic promoter regions (for example *c-myc* and *c-kit*).[162–164] Especially the oncogene *c-myc*, an important transcription factor involved in the regulation of about 15 % of all human genes that is overexpressed in many cancer cells,[163] was studied extensively by Hurley *et al.* demonstrating that G-quadruplex assembling may play an important role in regulating the oncogene transcription.[162,164,176] As a further prove for this assumption, Hurley and co-workers demonstrated in 2002 that the *c-myc* expression is downregulated due to a binding of the porphyrine TMPyP4 to the G-quadruplex structure.[177] Hence, it is assumed that G-quadruplex is somehow involved in the gene expression and its regulation. Moreover, it has been demonstrated that a G-quadruplex structures at the 5'-end of untranslated mRNA of the signal transduction gene *NRAS* decreases its translation efficiency.[163] This influence of G-quadruplex structures on the protein synthesis seems to be general for thousands of genes due to the high stability of RNA G-quadruplexes and as revealed by genomic searching.[163]

1.5.3. Telomeres and *Telomerase*

In eukaryotic cells, the ends of the linear chromosomes are called telomeres. These regions are encoded with a repeated specific sequence of guanine rich DNA.[163,168,175,178–180] In general, these repeated patterns, for example $(TTAGGG)_n$ in human cells,[163,168,180] consists of a GGG-moieties capable of building up G-quadruplex structures that are separated by other bases forming the loops.[163] Structural investigations of this telomeric sequence revealed a spontaneously intramolecular formation of a physiological stable G-quadruplex structure with various structural motives that seem to be in an equilibrium with each other.[163,168,169,173,175,181] For example, telomeres sequences with the structure Figure 21f were found by Wang and Patel by NMR experiments in 1993.[169] However, in 2002, Parkinson *et al.* found structure Figure 21e for the same telomeric sequence Wang and Patel used via X-ray crystallography.[168] These findings indicate the structural variety that telomeric G-quadruplex strands are able to form.

Especially in human cells, telomeres are often build of two structurally different regions, a double stranded region with about 1000 repeats of the T_2AG_3 sequence followed by a single stranded 3'-overhang region with 1–200 repetitions.[163,168,172,175] The reason for this single strand overhang is the so called *end replication problem* - the enzymes responsible for the DNA replication, the

polymerases, are unable to replicate the far 5'-end of the DNA due to a RNA primer needed for the replication at this position.[163,182] Since the *polymerases* synthesize the DNA in 5'→3' direction, the RNA primer region cannot be duplicated leading to a shortening of double stranded section of the telomeres 5'-end with each replication step.[163,182] As a consequence, the telomeres determine the lifetime of a normal cell because after reaching a critical minimum length, the DNA cannot be duplicated any more leading to chromosome fusion and ultimately to apoptosis.[163,168,172,175]

By this process, the restricted lifetime of normal cells is determined. However, stem cells and cancer cells show an infite lifetime leading to the assumption that there has to be a way circumventing the telomere reduction. And in fact, in 1985, Greider and Blackburn discovered the telomere prolonging enzyme *telomerase* in the ciliate *tetrahymena*.[163,180,183] This enzyme uses an internal RNA template to elongate the telomeres and hence increase the lifespan of a cell dramatically.[163] Although in nearly all cells no *telomerase* activity is observed, the enzyme is overexpressed and active in around 85 % of cancer cells.[163,164] Hence, the enzyme *telomerase* plays an important role in immortalizing cancer cells and, therefore, is a very interesting target for interesting target for the development of novel anticancer therapies and drugs.[163,164,178,184] Since the discovery that the formation of singlestranded telomeric G-quadruplex or a molecule binding and thus stabilizing the G-quadruplex structure inhibit *telomerase* activity,[178] telomeres became an essential target for novel drug discovery.[163,164,171,184] For this reason, various research groups focused on the synthesis and investigation of compounds binding strongly to or inducing a G-quadruplex structure in order to inhibit *telomerase* activity or to regulate the transcription of oncogenes in cancer cells.[162–164,171,178,184–190]

1.5.4. Interaction of Metal Complexes with G-quadruplex DNA

Due to the structure of G-quadruplex, there are four binding motives of metal complexes or pure organic compounds possible - direct coordination, central channel binding, $\pi\pi$ interactions and groove binding.[162,164] In analogy to the binding of metal complexes to duplex DNA, a covalent coordination of platinum complexes to the guanine-N7 atom has been observed.[164] Some examples of such complexes are given in Figure 22.

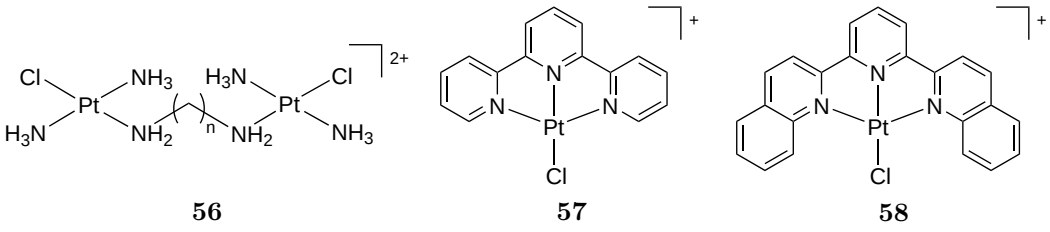

56 **57** **58**

Figure 22: Examples for platinium(II) complexes used for direct coordination to G-quadruplex structures. Complexes **56** crosslinks guanine bases,[191] **57** binds to adenine bases in the loops and **58** does not bind G4-DNA at all.[192]

It is worth mentioning that, in contrast to duplex DNA, the crosslinking pattern depends on the actual structure of the G-quadruplex (accessibility of the bases) as well as the characteristics of the metal complex.[163] For example, the dinuclear platinum(II) complex **56** was shown to crosslink two guanine bases in a G-quadruplex.[191] In contrast, the (terpy)platinum(II) complex **57** prefers binding

adenin-N7 over guanine-N7 and hence selectively binds at the loop of the G-quadruplex structure.[192] Moreover, if the planar system is increased by two ring systems yielding complex **58**, no binding was observed due to the sterically demanding ligand.[192]

The first noncovalent interaction of metal ions with G-quadruplex structures is already achieved upon its formation. In the central channel of the G-quadruplex, metal ions are incorporated stabilizing its structure. However, there are also organic molecules known mimicking the function of the alkali ions.[162] A nice example for such a threading binder is compound **59** (Figure 23) that has been introduced by Balasubramanian and co-workers in 2007.[193] Moreover, **59** was the first molecule inducing G-quadruplex assembling in the absence of any cations.[193] The mode of action is proposed as a π-stacking of the anthracene moiety on top of the structure while the amines of the aliphatic side chain form hydrogen bonds to the guanine-N7 atoms.[162,193]

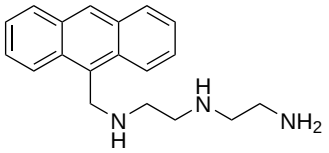

59

Figure 23: The first example of an organic molecule inducing G-quadruplex formation in the absence of cations.[193]

In comparison to duplex DNA, a $\pi\pi$ interaction of molecules to a G-quadruplex structure is not achieved by intercalation between the base pairs but by π-stacking onto the end of the G-quadruplex structure as revealed by binding studies with duplex DNA intercalating agents.[162,163,194] With this knowledge in hand, it is straight forward to design molecules capable of binding G-quadruplex DNA. The binding could be improved by a large π-surface of the binding agent - much larger compared to duplex DNA intercalators - to increase the van-der-Waals interactions with the G4-DNA structure.[162–164,195] Moreover, a cationic charge at side chains of the binding agent would increase both, the water solubility as well as the binding itself through electrostatic interactions with the negatively charged phosphate backbone.[162–164,195] For this reason, various G-quadruplex $\pi\pi$ binding compounds with different structural motives have been introduced during the last decade,[162,163,193,195] for example the throughoutly investigated cationic porphyrin **60**,[186,194] the anthraquinone derivative **61**,[196] or the macrocycle telomestatin[185] (**62**) which was isolated from the bacterium *Streptomyces anulatus* (Figure 24). However, the main problem in the development of potent G-quadruplex binders, the selectivity over duplex-DNA structures, is much harder to achieve and of great interest to the scientific community nowadays.

One of the first metal complexes studied towards their interaction with G-quadruplex structures have been metalloporphyrin systems[197–200] as well as metallophthalocyanines,[201–203] which exhibit an even larger aromatic surface.[164] A few examples are given in Figure 25. Although the key binding motives of these complexes are similar to the free ligands, the metal center is proposed to enhance the binding further by electrostatic interactions.[164] Due to the mainly symmetrically composition of the complexes, the metal ion may interact with the central channel of the G-quadruplex structure or

interact with the aromatic ring system via cation-π-interactions. Increasing this interactions, metal ions forming square planar or square pyramidal complexes, like zinc(II), copper(II) or palladium(II), were preferably used for such complexes as it was assumed that a planar face of the complexes needs to be accessible for π-stacking with rigid G-quadruplex structures.[164,198,199,201–203] This assumption was proved true by the strong binding various metal complexes (**63**) derived from porphyrin ligand **60** (Figure 25).[164,197–199]

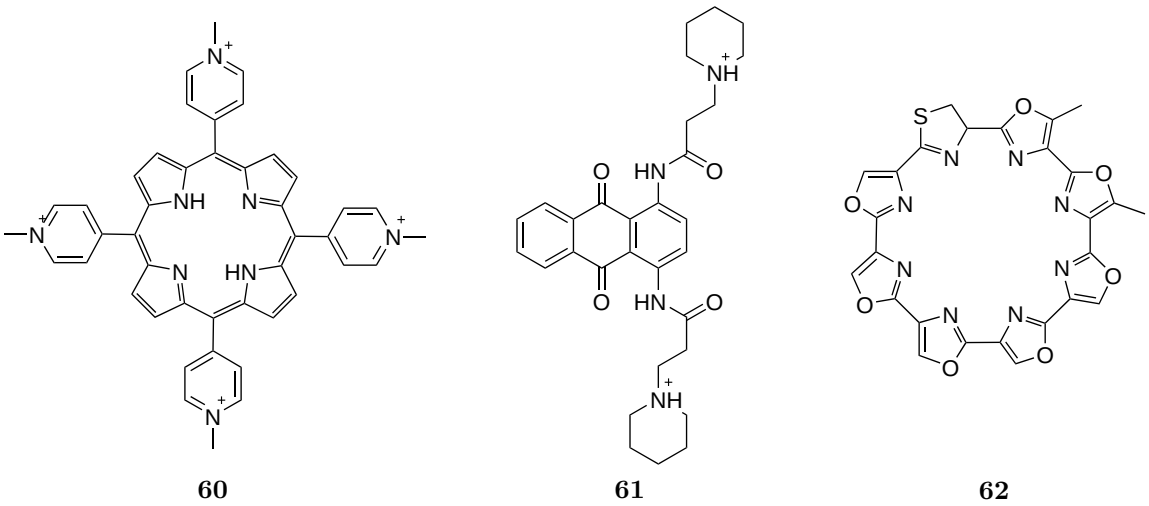

60 **61** **62**

Figure 24: Examples for organic molecules capable of π-stacking onto a G-quadruplex structure.[185,186,196]

Moreover, a certain discrimination between G-quadruplex and double stranded DNA structures could be achieved upon addition of the metal center as demonstrated for (phtalocyanine)zinc(II) complex **65** by Luedtke and co-workers in 2009.[201] This complex showed a very high selectivity of G-rich DNA sequences, such as H-telo or the *c-myc* and *KRAS* oncogene promoter, over their complementary C-rich-DNA sequences H-telo-C, *c-myc-C* or *calf thymus* DNA.[201] These results were further confirmed by *in-vitro* tests as cells over-expressing either *c-myc* or *KRAS* decrease the expression of the oncogenes after treatment with **65**.[164,201]

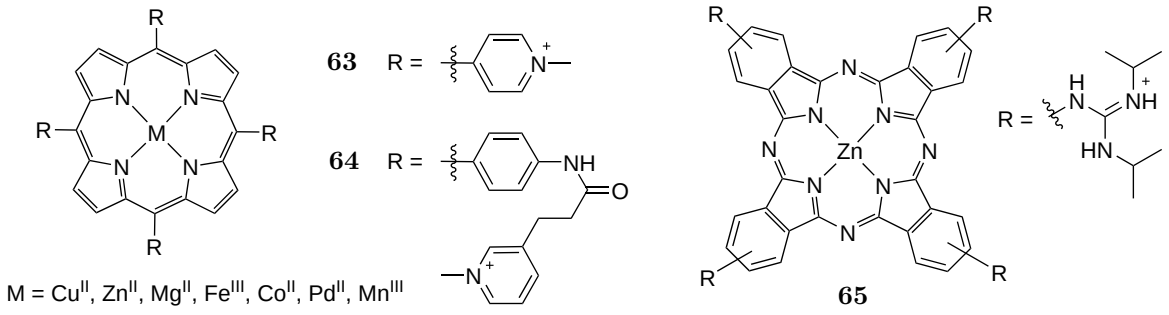

Figure 25: Examples for metalloporphyrin (**63** and **64**) and -phthalocyanine (**65**) systems capable of π-stacking onto a G-quuadruplex structure.[197–201]

However, some metalloporphyrins with an octahedral metal center show surprisingly strong binding to human telomerase.[164] This observation implicates that this G-DNA is not a rigid structure but seems to be in a dynamic equilibrium providing various alternative binding modes or that one axial

ligand gets labile in the presence of G-quadruplex and is easily replaced.[164] In 2007, Pratviel *et al.* introduced such a complex (**64**).[200] In addition, this manganese(III) complexes showed a very strong binding to G-quadruplex DNA of about $10^8\,\mathrm{M}^{-1}$ together with a very high selectivity of four orders of magnitude towards duplex DNA.[164,200]

Besides the above mentioned structures, complexes coordinate to nonmacrocyclic ligands, like for example salphen or salphene derivatives (Figure 26),[204–206] were also studied extensively. These ligands possess an extended π-system and can be modified with an amine based side arm that can be easily protonated under physiological conditions leading to favorable electrostatic interactions with the negatively charged phosphate backbone of either the loop or the groves of the G-quadruplex.[164] However, the ligands itself are often very poor G-quadruplex binder due to their flexibility which inhibits strong *van-der Waals* interactions with the DNA.[164] Therefore, the metal atom plays an important structural role for these complexes since it induces a rigid structure and thus the biological active form. The coordination geometry of the central ion is also playing an important role for the binding since square planar metal ions show far better results compared to square pyramidal geometries as demonstrated by Vilar and co-workers in 2008.[205] Moreover, it is assumed that the metal center can replace a metal ion that is normally located at the end of the central channel with the result of further increasing the binding.[204] For example, nickel(II) and platinum(II) complexes coordinate to salphen derivatives with cyclic *tert*-amine side arms (**66**, Figure 26) displayed a very high stabilization of G-quadruplex structures together with a certain selectivity for human telomerase towards duplex DNA.[164,204,206] Moreover, some of these complexes show *in-vitro* inhibition of *human telomerase*[204] as well as expression suppression of the oncogene *c-myc*[206] in cultured cells.

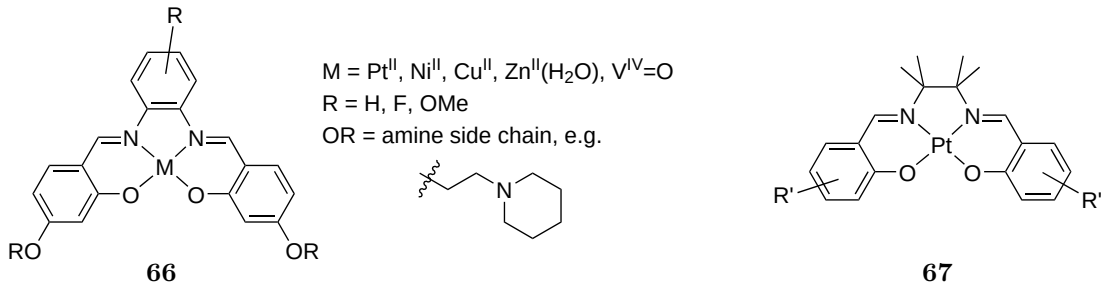

Figure 26: Examples for metallosalphen (**66**) and -salene (**67**) complexes capable of π-stacking onto a G-quuadruplex structure.[204–206]

Instead of using a poor binding ligand and increase the affinity upon metal coordination, Mergny and co-workers presented a reverse concept in 2008.[207] Using the bisquinolinium ligand **68** they described a metal-mediated conformational switch controlling the structure of the G-quadruplex. Compound **68** is one of the most selective and strongest binder for G-quadruplex DNA[207] which is associated with its structure forming a V-shape due to intramolecular hydrogen bonds. However, upon addition of copper(II), a conformational change to a linear system (**69**, Scheme 7) occurs reducing the affinity to G-quadruplex dramatically. Hence, addition of copper(II) ions to a adduct of G-quadruplex and the free bisquinolinium **68** triggers an unfolding of the DNA structure to the single-stranded form.[164,207]

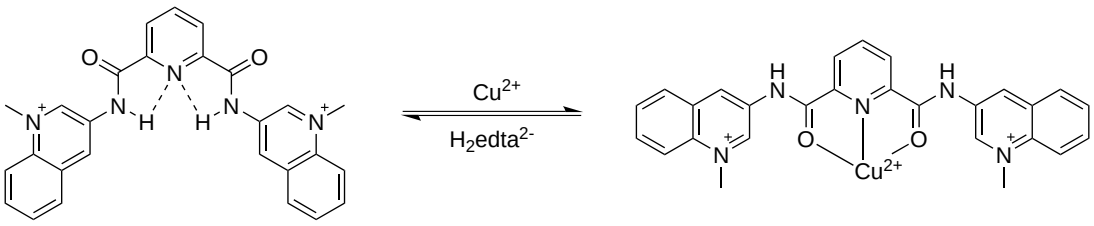

68 **69**

Scheme 7: In the presence of copper(II), the strong G-quadruplex binder **68** undergoes a conformational change to the linear form **69** leading to a significant weakening of the binding and hence to an unfolding of the G-quadruplex.[207]

In the context of duplex DNA binding, (polypyridyl)metal complexes play an important role (see Chapter 1.4). Hence, these structures were also investigated towards their affinity to G-quadruplex structures.[164,208–212] For example, in 2007 Teulade-Fichou and co-workers explored the versatility of metalloterpyridine complexes (**70**, Figure 27) towards their binding affinity to G-quadruplex DNA.[209]

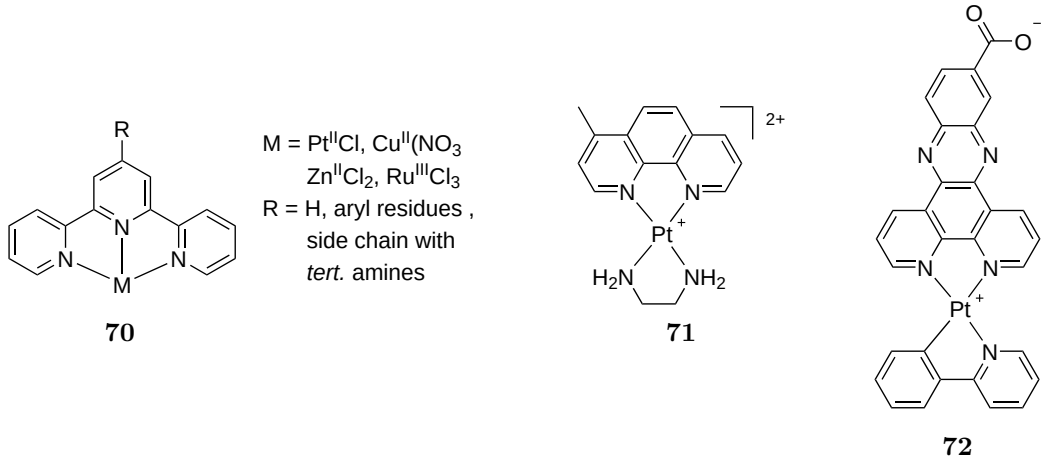

70 **71** **72**

Figure 27: Examples for G-quadruplex binding polypyridyl complexes. Terpyridine derivatives (**70**),[208,209] square planar (phenathroline)platinum(II) complex **71**,[210] and the (dppz)platinum complex **72** that exhibit light-switch behavior.[212]

Using square planar (platinum(II)), square pyramidal (copper(II)), trigonal bipyramidal (zinc(II)) and octahedral (ruthenium(III)) coordination geometries of the metal center, it was found that only the platinum(II) and copper(II) complexes exhibit a strong binding towards G-quadruplex DNA. Again, these findings can be explained by the accessible planer π-surface that these coordination spheres offer.[209] However, the square pyramidal coordination geometry was demonstrated to be superior to the square planar one in the context of selectivity since the axial ligand is suspected to sterically interfere DNA intercalation.[209] Square planer (1,10-phenanthroline)platinum(II) complexes (for example **71**, Figure 27) were studied by Ralph and co-workers in 2008 but were found to exhibit significantly less affinity to G-quadruplex DNA compared to duplex DNA.[210] Anyhow, the binding selectivity of these complexes could be inverted upon modification of the ligand system with a cyclic amine side chain.[211] In 2009, Che and co-workers introduced the square planer platinum(II) complex **72** coordinate to a carbonic acid modified dppz ligand (Figure 27).[212] Besides its high selectivity

and affinity towards G-quadruplex DNA, this nanomolar *telomerase* inhibitor was found to act as a potent molecular light-switch for G-quadruplex DNA as it showed only very weak luminescence in the the presence of double stranded DNA.[212]

The huge π-surface of G-quadruplex structures allows the development of large structures interacting with it. Hence, Sleiman and co-workers used a supramolecular platinum(II) based square to bind G-quadruplex DNA and to inhibit the enzyme *telomerase* in 2008 (Figure 28).[213] Molecular modeling studies revealed that the square has the ideal size and shape to sit on top of the terminal G-quartet with the amine groups forming hydrogen bonds to the phosphate backbone.[164,213] Further supramolecular structures, like for example chiral cylinders of cubes, were also investigated showing promissing results.[164]

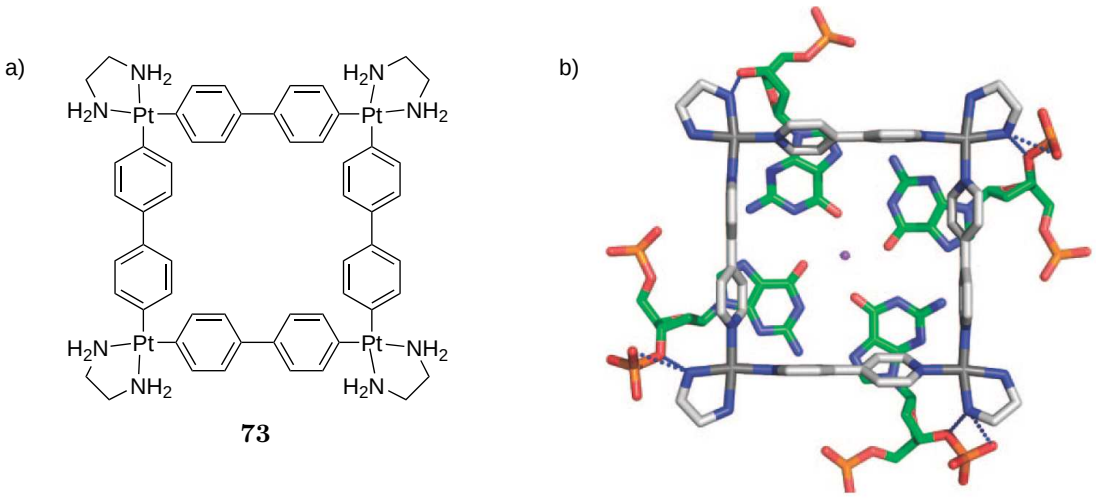

Figure 28: a) Supramolecular platinum(II) based square synthesized and investigated by Sleiman and co-workers.[212] b) Binding model of **73** stacked on top of a 22-mer G-quadruplex.[212] (Picture is taken from Ref.[212])

Over the last decade, several octahedral metal complexes with planar intercalating ligands, mainly ruthenium(II) based like for example the dppz complex **47** (Figure 16), were studied towards their interaction with G-quadruplex DNA.[140,164,210,212,214] Lacking an accessible planar π-surface, the octahedral metal itself is very unlikely to stack on a G-quartet whereas the planar ligands of the complexes are qualified to partially intercalate between or stack on the final the G-quartets, in analogy to the intercalative binding mode observed for duplex DNA.[162,164] However, the binding mode of the whole complex is proposed to be an interaction with the groove and loops in the negatively charged sugar-phosphate backbone of the G-quadruplex.[162,164] Showing very interesting light-switch behavior in the presence of and high affinities to duplex DNA, ruthenium(II) and nickel(II) complexes coordinate to a dppz or dpq ligand (Figure 16, **48** and **47**) were studied towards their interactions with G-quadruplex DNA. Despite the expectations, all complexes tested showed only weak and, in contrast to double stranded DNA, a ligand independent binding to G4-DNA.[164,210,212] The same is true for tris(phen)ruthenium(II) (**43**, Figure 15).[210] However, the dinuclear derivatives, ruthenium complexes **52** and **53** with the bridging ligand tpphz (Figure 18) as well as the prolonged complex **74** (Figure 29), were found to have similar or even higher affinity to G-quadruplex DNA compared to double stranded

DNA.[140] Moreover, these complexes showed a characteristic quadruplex light-switch behavior upon binding that was even more pronounced compared to the observations made for ds-DNA.[140,162]

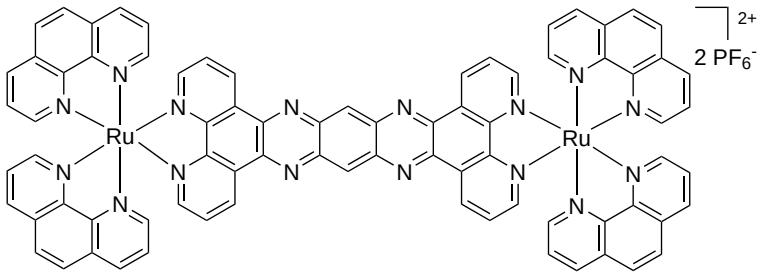

74

Figure 29: Dinuclear ruthenium complex introduced by Thomas *et al.* as G-quadruplex binder.[140]

In 2008, Liu and co-workers introduced another dinuclear and luminescent ruthenium complex bridged by 2-(2-pyridyl)imidazo[4,5-*f*][1,10]-phenanthroline (Figure 30).[215] This complex was found to induce the formation of an antiparallel G-quadruplex structure of the human telomeric repeat in the absence of metal cations. In addition, its affinity to G4-DNA is about one order of magnitude higher compared to duplex DNA.

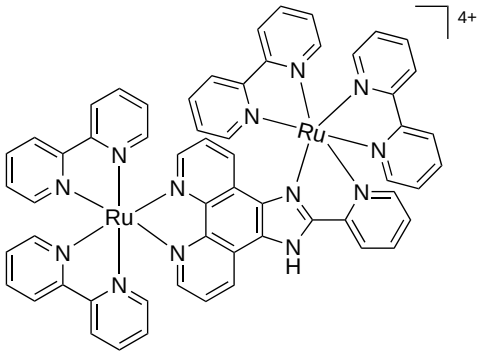

75

Figure 30: Dinuclear ruthenium complex introduced by Liu *et al.* as G-quadruplex binder.[215]

2. Aim of the Work

Over the last decades, the development of novel metal based pharmaceuticals was getting more and more interest from university as well as industrial research all over the world due to their unique geometries and photochemical properties. Especially in context of potential anti tumor activities, metal complexes showed to be promising and selective lead structures as demonstrated by the MEGGERS group.[216–222] Using a pharmaceutical active ligand coordinate to a non reactive, structure-bearing metal center, selective inhibition of various *protein kinases* was achieved. However, another promising and well-established target for metal based pharmaceuticals was shown to be DNA, either in its double stranded form or as a G-quadruplex, as demonstrated by the research groups of BARTON,[128,129,141,142,223] THOMAS,[140,152] or VILAR,[204,205,208,211] to name a few examples.

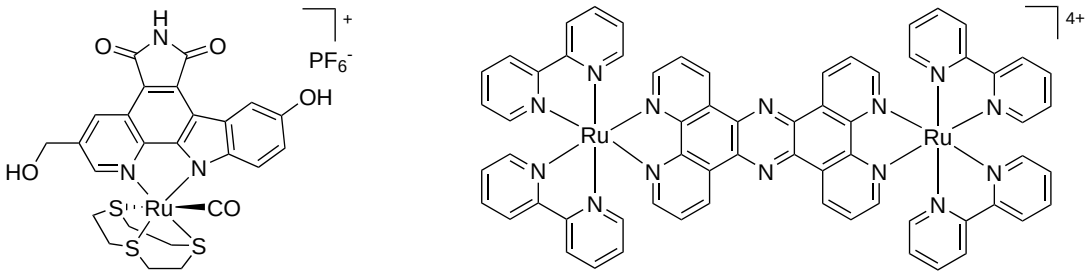

76 **52**

Figure 31: In the MEGGERS group metal complexes coordinate to a pyridocarbazole ligand like for example **76**, were shown to be highly selective *protein kinase* inhibitors.[216] The dinuclear ruthenium complex **52** was shown to bind double stranded DNA as well as G-quadruplex structures and to act as a staining agent for DNA in living cells.[140,152]

Besides the advantages of the metal complexes over purely organic structures, there are also some major disadvantages. For example, the metals used are often very expensive and despite their kinetic inertness, a certain cytotoxicity of the complexes cannot be excluded. Silicon is a suitable substitute for the metal center as it is easily available in larger amounts, possess only a low cytotoxcicity and is capable of forming penta- and hexacoordinate coordination geometries. Unfortunately, most of these higher coordinate silicon complexes are hydrolytically unstable which limits their use in biological applications. Addressing this problem, this Ph.D. thesis was dealing with the synthesis and modification of hydrolytically stable, hexacoordinate silicon(IV) complexes and their biological applications. In doing so, both, mononuclear and dinuclear silicon(IV) complexes, should be synthesized, characterized and studied towards their biological behavior.

First, a synthesis route to obtain kinetically inert, hydrolytically stable silicon(IV) complexes coordinate to two bidentate polypyridine ligands and one bidentate arenediolato ligand starting from silicon tetraiodide should be established. The main focus on this project should be directed on the introduction of functionalized benzen-1,2-diolato ligands and the synthesis of dinuclear silicon(IV) complexes. Having suitable methods in hand, post-coordination modification of the higher coordinate silicon(IV) complexes should be studied more detailed using standard organic reactions like for example halogenations or condensations. Finally, the complexes should be studied towards their biological behavior. Due to the high charge of the silicon(IV) complexes, ds-DNA and G4-DNA was chosen as the target

system. Therefore, silicon(IV) complexes that are structural similar to the well-established ruthenium based DNA inhibitors, like for example Ru(dppz)(phen)$_2^{2+}$ (**47**) or the dinuclear complex **52**, should be synthesized first. As silicon(IV) complexes would posses different physicochemical properties, for example luminescence behavior, compared to metal complexes, multinuclear complexes with at least one silicon(IV) center should be investigated too, in order to combine the properties of both centers. In doing so, it should be tried to obtain luminescence silicon(IV) complexes that could potentially be used as DNA imaging agents. As an alternative to the dinuclear complexes, it should be tried to attach a fluorophor to the silicon(IV) complexes.

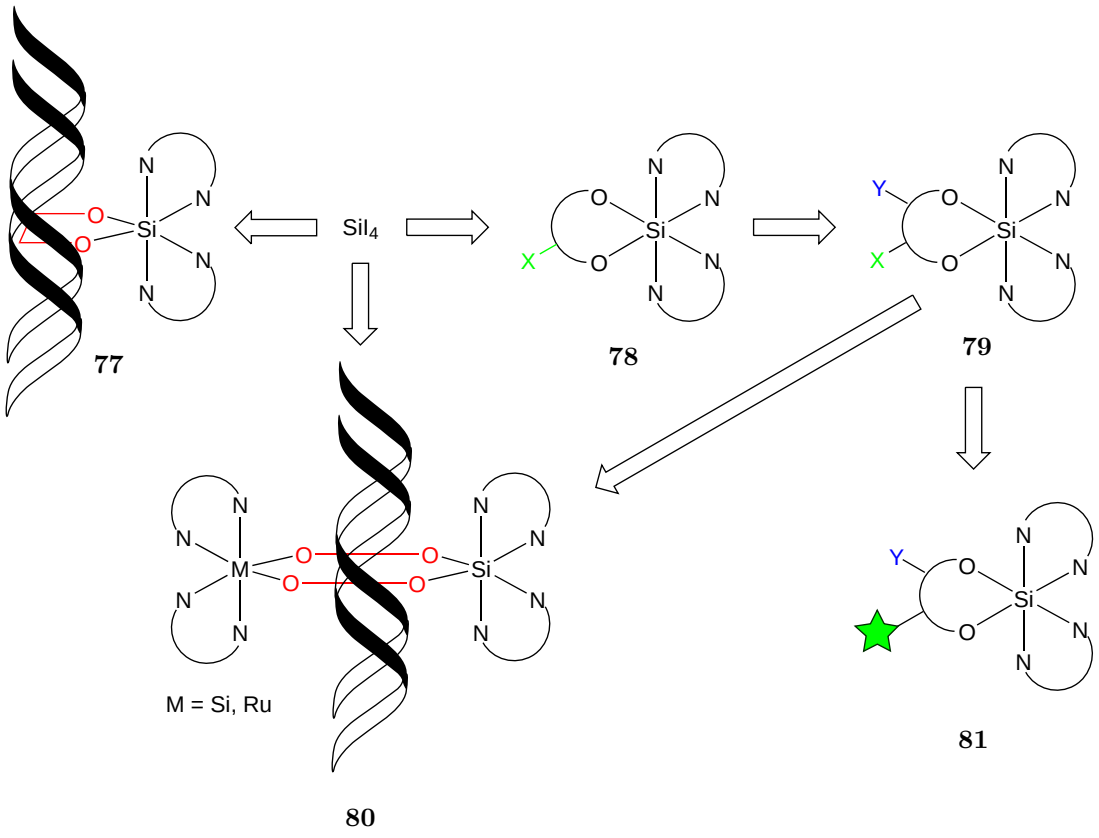

Scheme 8: The aim of this work is the synthesis of mono- and dinuclear hexacoordinate silicon(IV) complexes starting from silicon tetraiodide and to study their interaction with DNA (**82** and **83**, a planar intercalating ligand). Furthermore, a post-coordination modification of the silicon(IV) complexes should be investigated (**84**, X, Y = different functional groups). Having synthesis and modifications methods in hand, it should be tried to obtain fluorescent silicon(IV) complexes, for example by coordination to a metal center (**80**) or by attaching a fluorophor (**81**, fluorophor) to the complex.

3. Results and Discussion

3.1. Synthesis of Octahedral Silicon(IV) Complexes

Bis-heteroleptic, hexacoordinate (benzene-1,2-diolato)silicon(IV) complexes containing two additional polypyryridyl ligands (2,2'-bipyridine, 1,10-phenathroline) were synthesized according to a procedure introduced by Kummer *et al.*[105–107] that was modified in our working group.[28,37,149,150,224] Therefore, silicon tetraiodide was first reacted with the polypyridyl ligand in anhydrous chloroform at 55 °C over night under an atmosphere of nitrogen affording crude octahedral diiodosilicon(IV) complexes $[SiI_2(pp)_2]I_2$ (**85**, **86**) as moisture sensitive solids in good yields (Scheme 9). The usage of a non-coordinative and non-protonic solvent is crucial as silicon tetraiodide as well as the synthesized hexacoordinate diiodosilicon(IV) species **85** and **86** readily react with protic or coordinative solvents like ethanol, water or *N,N*-dimethyformamide. The brown solids (**85** and **86**) can be stored under nitrogen at room temperature but decompose upon contact with moisture yielding a yellow solid. However, bis(1,10-phenanthroline)silicon(IV) complex **86** seems to be more stable towards hydrolysis than bis(2,2'-bipyridine)silicon(IV)complex **85**. Further reaction with anhydrous catechol in anhydrous chloroform under reflux conditions over night under an atmosphere of nitrogen, followed by anion metathesis with ammonium hexafluorophosphate gave the yellow octahedral silicon complexes **87** and **88** in yields of 39 % and 41 %, respectively. Crude (benzene-1,2-diolato)silicon(IV) complexes were purified by salt column chromatography on silica gel using $MeCN/H_2O$/satd. aq. KNO_3 as eluent, followed by an anion exchange. Anyhow, the complexation reaction could also be performed in a one pot synthesis without isolating the diiodo species. In this case, complex **88** was obtained in a yield of 36 % over two steps.

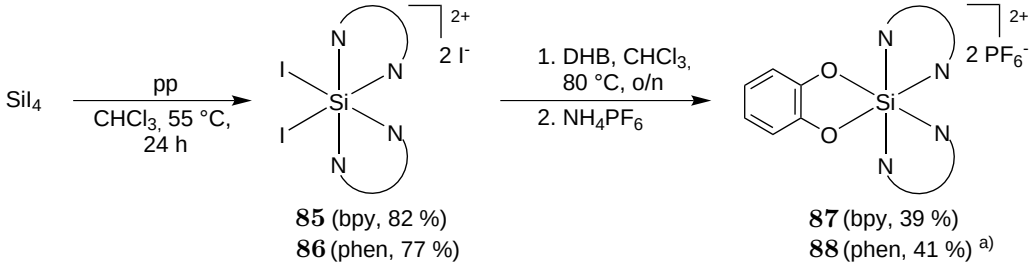

Scheme 9: Synthesis of hexacoordinate (benzene-1,2-diolato)silicon(IV) complexes **87** and **88** according to a modified literature procedure of Kummer and co-workers.[105–107] ([a] In a one pot synthesis without isolating **86**, complex **88** was obtained in a yield of 36 % over two steps.)

The quite low yields can be explained by a side reaction forming the monopolypyridyl complex, which cannot be converted into the biscoordinate derivative even upon addition of excess ligand.[106] This observation was examined by ^{1}H-NMR. During flash column chromatography, a red band eluting before the yellow product fraction was isolated. The ^{1}H-NMR shows only the signals of the polypyridine ligand leading to the conclusion that only the monocoordinated species was isolated. To prevent the formation of monocoordinate complexes, Kummer *et al.* proposed to add a solution of silicon tetraiodide in chloroform very slowly to a chloroformic solution of the ligands.[106] This procedure was also tried but, unfortunately, did not lead to higher yields. Therefore, this method was not considered any further.

The octahedral structure of silicon(IV) complex **88** was verified by crystal structure analysis (Figure 32). Single crystals suitable for crystal structure analysis were obtained upon slow diffusion of diethylether into a concentrated solution of the complex in acetonitrile at 4 °C. Complex **88** crystallized as orange block in the monoclinic space group C 2/c with eight formula units per unit cell. Together with the complex, two formula units of the counter ion PF_6^- and two formula units of acetonitrile as crystal solvent were incorporated in the crystal structure. A crystal structure of complex **87** confirming the octahedral structure of the complex was obtained by Steffen Glöckner during his bachelor thesis and has been published recently.[224,225]

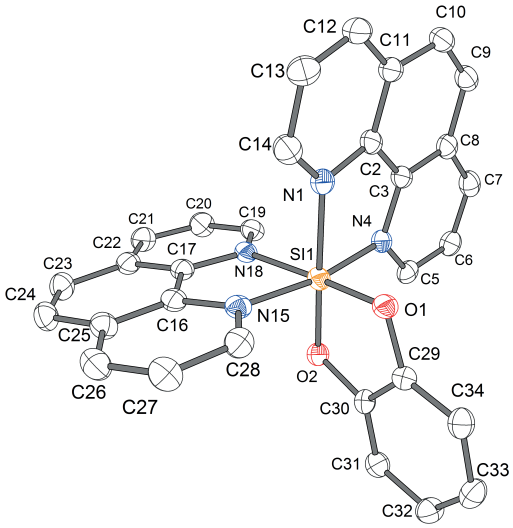

Figure 32: Crystal structure of complex **88**. ORTEP drawing with 50 % probability thermal ellipsoids. The PF_6^- counterions and solvent molecules are omitted for clarity. Selected bond lengths [Å] and angles [°]: N1–Si1 1.9538(18), N4–Si1 1.9238(16), N15–Si1 1.9377(17), N18–Si1 1.9557(18), O1–Si1 1.7073(15), O2–Si1 1.7030(15), O2–Si1–O1 93.54(7), O2–Si1–N4 93.11(7), O1–Si1–N4 94.06(7), O2–Si1–N15 92.97(7), O1–Si1–N15 92.66(7), N4–Si1–N15 170.64(8), O2–Si1–N1 175.74(7), O1–Si1–N1 88.48(7), N4–Si1–N1 83.00(7), N15–Si1–N1 90.68(7), O2–Si1–N18 87.30(7), O1–Si1–N18 175.11(7), N4–Si1–N18 90.70(7), N15–Si1–N18 82.49(7), N1–Si1–N18 91.01(7).

The reaction of silicon tetraiodide with 3,4,7,8-tetramethyl-1,10-phenanthroline and subsequent conversion with catechol gave complex **89** in a yield of 11 % over two steps (Scheme 10). The reaction was performed in anhydrous chloroform under an atmosphere of nitrogen in a one pot synthesis without isolating the intermediate formed diiodosilicon(IV) complex. The yield is low due to the short reaction time of the second reaction step, and can be improved up to 40 % as demonstrated by Chen Fu during his Ph.D. studies in the Meggers group.[150,224]

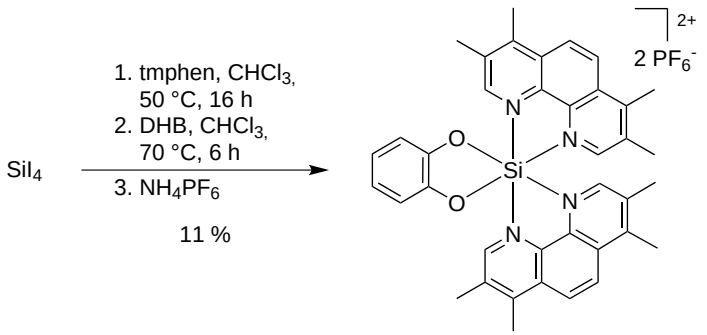

89

Scheme 10: Synthesis of hexacoordinate (benzene-1,2-diolato)bis(3,4,7,8-tetramethyl-1,10-phenanthroline) silicon(IV) complex **89**. The yield is given over two steps.

Upon slow diffusion of diethylether into a concentrated solution of the complex **89** in acetonitrile at 4 °C, single crystals suitable for crystal structure analysis were obtained. It crystallized as yellow block in the triclinic space group P −1 with four formula units per unit cell. Together with the complex, two formula units of the counter ion PF_6^- were incorporated in the crystal structure. The structure verifies the hexacoordinate geometry of the silicon center, which is coordinate by one catechol and two 3,4,7,8-tetrametyhl-1,10-phenantroline ligands (Figure 33).

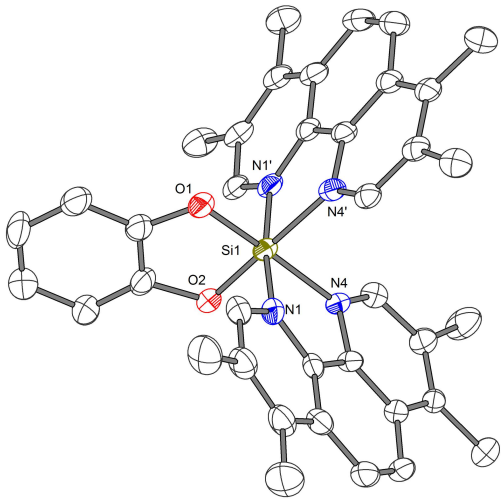

Figure 33: Crystal structure of complex **89**. ORTEP drawing with 50 % probability thermal ellipsoids. The PF_6^- counterions are omitted for clarity. Selected bond lengths [Angstrom] and angles [°]: Si1–O1 1.709(3), Si1–O2 1.719(3), Si1–N1 1.901(3), Si1–N1' 1.922(3), Si1–N4 1.929(3), Si1–N4' 1.934(3), O1–Si1–O2 92.63(13), O1–Si1–N1 92.56(13), O2–Si1–N1 93.07(13), O1–Si1–N1' 92.21(13), O2–Si1–N1' 92.44(13), N1–Si1–N1' 172.54(14), O1–Si1–N4 175.68(14), O2–Si1–N4 88.04(13), N1–Si1–N4 83.14(13), N1'–Si1–N4 92.03(13), O1–Si1–N4' 90.65(13), O2–Si1–N4' 174.30(14), N1–Si1–N4' 91.43(13), N1'–Si1–N4' 82.77(13), N4–Si1–N4' 89.03(13).

Next, diiodobis(1,10-phenanthroline)silicon(IV)-diiodide (**86**) was reacted with different substituted catechols in chloroform at reflux overnight under an atmosphere of nitrogen to investigate the scope of the complexation reaction. Using 3,4-dihydroxytoluene, complex **90** was obtained in a yield of

41 %. The reaction also tolerates free hydroxy groups as conversion with 1,2,4-trihydroxybenzene gave silicon(IV) complex **91** in a yield of 34 %. The introduction of an aldehyde was investigated next because this functional group easily allows further modification of the complex. Unfortunately, complex **92** was obtained in a very low yield of only 4 %. In addition, trying to improve the yield by modifying the reaction conditions, for example using the solvent *ortho*-xylene or changing the reaction temperature and time, was not successful. In all cases, the main product was the yellow decomposition product eluting with acetonitrile during flash column chromatography. The structure of this product was not determined but it is very likely formed upon the contact of complex **86** with water as a little bit of this side product is formed in every complexation reaction. An explanation for the formation of the decomposition product may be a hydrate formation of the 3,4-dihydroxybenzaldehyde used. A similar result was obtained by using 3,4-dihydroxybenzoic acid to yield complex **93** bearing a carboxylic acid. However, complex **93** could not be obtained using various complexation conditions and solvents.

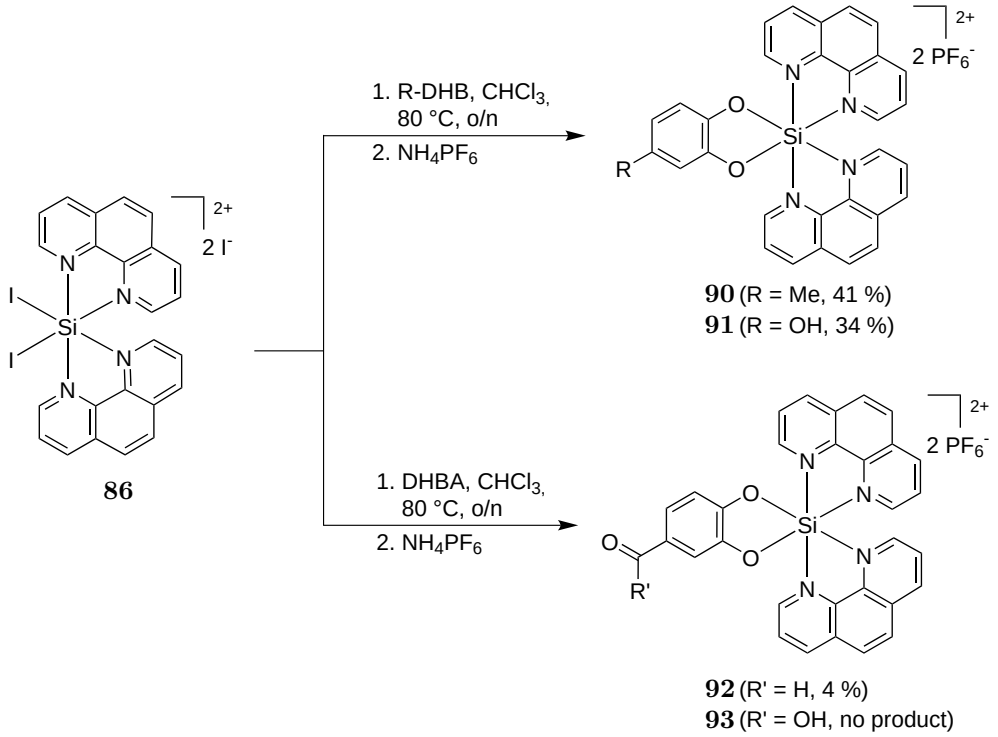

Scheme 11: Synthesis of substituted hexacoordinate (benzene-1,2-diolato)silicon(IV) complexes **90**-**93**.

For a post-coordinative derivatization of the hexacoordinate silicon(IV) complexes, a dione functionality may be very helpful as it should allow the enlargement of the ligand utilizing a condensation reaction. For this reason, silicon precursor **86** was reacted with 2,5-dihydroxy-*p*-benzoquinone (**94**) in anhydrous chloroform at 70 °C for two days (Scheme 12). Although an orange solid was isolated during flash column chromatography on silica gel, the desired product **95** was not obtained. Unfortunately, the isolated compound could not be identified by mass spectrometry and ^{1}H-NMR spectroscopy preventing a deeper insight of the reaction. Similar results for this complexation reaction were obtained by Yongang Xiang during his PhD Thesis in the Meggers group.

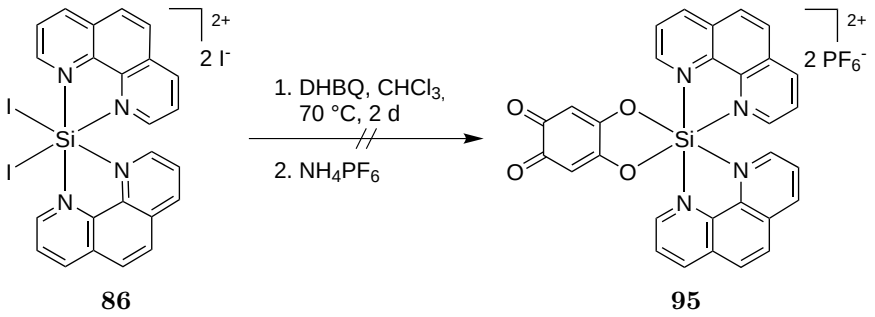

86 **95**

Scheme 12: Attempt to synthesize silicon(IV) complex **95**.

The attempt to synthesize bromine substituted silicon(IV) complex **96** started with a two-step preparation of 4-bromocatechol (**97**) (Scheme 13). First, veratrole (**98**) was brominated according to a literature procedure of Yang *et al.* by reacting **98** with ammonium bromide and hydrogen peroxide in acetic acid at room temperature for 20 hours.[226] After distillation, 4-bromoveratrole (**99**) was obtained in a yield of 84 %. According to Sharma *et al.*, subsequent deprotection of the methoxy groups using boron tribromide in dichloromethane gave **97** in almost quantitative yield.[227] Finally, **97** was reacted with $[SiI_2(phen)_2]I_2$ (**86**) in chloroform using the previously discussed conditions.

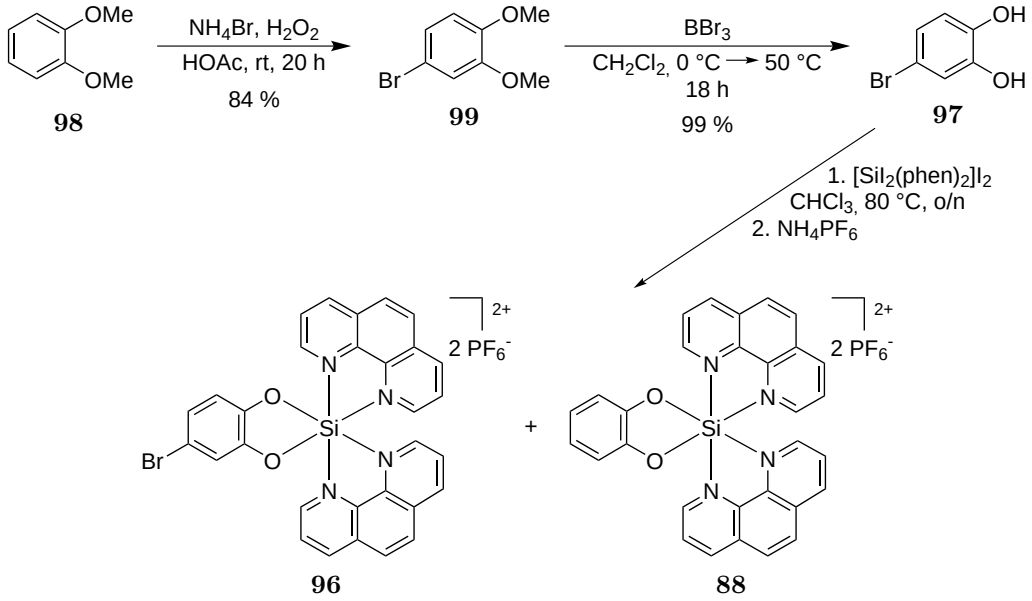

98 **99** **97**

96 **88**

Scheme 13: Synthesis of 4-bromocatechol (**97**) and attempt to synthesize silicon(IV) complex **96**.

Interestingly, the reaction led to an inseparable mixture of the desired monobrominated product **96** together with the unsubsituted (benzene-1,2-diolato)silicon(IV) complex **88** in a ratio of around 1:0.5 (Scheme 13) as determined by ^{1}H-NMR spectroscopy (Figure 34). The same observation was also made using newly bought 4-bromocatechol (**97**) and can be explained by the harsh reaction conditions. In the course of the complexation, the acid hydrogen iodide is formed which can initiate a partial *ipso* substitution of the bromo substituent with a proton leading to the two products.[224] In conclusion, the reaction of functionalized catechols with the diiodosilicon(IV) complex **86** seems to tolerate only very few functional groups which is possibly associated with an incompatibility to the strong acid hydrogen iodide generated during the complexation.[224] Unfortunately, attempts to snatch the acid

away using different bases like potassium carbonate or proton sponge did not show the desired results but lowered only the yield of the complexation reaction of unsubstituted catechols. Therefore, this strategy of introducing functionalized catechols was not followed any further.

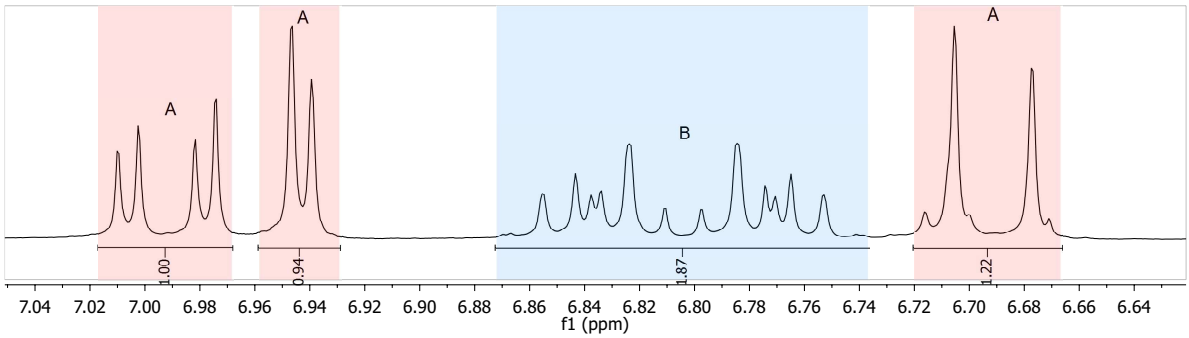

Figure 34: ^{1}H-NMR of the product obtained after the reaction of **86** with 4-bromobenzene-1,2-diol in acetonitrile-d_3. Shown is the aromatic region of the ^{1}H-NMR in which the catechol signals appear. Signals marked with A and B belong to the product **96** and the side product **88**, respectively. **96** and **88** were obtained in a ratio of around 1:0.5.

Next, it was investigated whether the two iodo ligands of **86** can be replaced by analogous double deprotonated arenediols with more extended aromatic systems like 2,3-dihydroxynaphtalene or pyrene-4,5-diol (Scheme 14). Therefore, the arenediols were reacted with $[SiI_2(phen)_2]I_2$ (**86**) in anhydrous chloroform or *ortho*-xylene using the previously discussed conditions and work-up. Hereby, the octahedral silicon complexes **100**–**103** were obtained in moderate yields.[37,224] Complexes **101**–**103** were synthesized by Chen Fu[150] and Yonggang Xiang.[149]

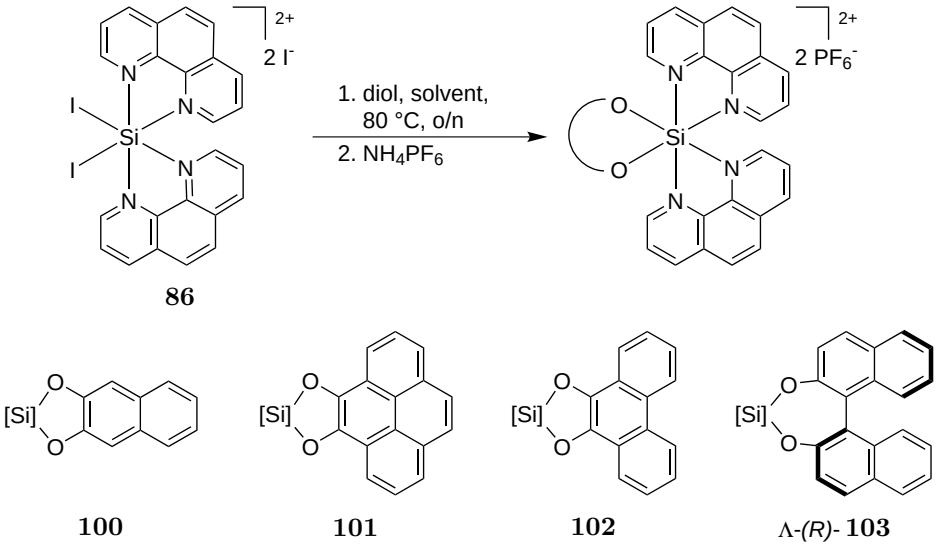

Scheme 14: Synthesis of octahedral (arenediolato)silicon(IV) complexes. Examples **101**–**103** were synthesized by Chen Fu[150] and Yonggang Xiang.[149]

One aim of this work was the synthesis of dinuclear silicon(IV) complexes. For this reason, ligand 7,8-dimethoxyphenazine-2,3-diol **104** was synthesized in a three step synthesis starting from veratrole (**98**). According to a modified literature procedure of Alcalde and co-workers,[228] **98** was nitrated with potassium nitrate in concentrated sulphuric acid obtaining 4,5-dinitroveratrole (**105**) in a yield

of 39 %. Under an atmosphere of hydrogen and in the presence of palladium on charcoal, the nitro groups of **105** were reduced to the amino groups in accordance with a procedure published by Baudy *et al.*[229] Compound **106** was obtained in a yield of 97 %. Finally, **106** was reacted with 2,5-dihydroxy-*p*-benzoquinone (**94**) in water at 100 °C over night. After this condensation reaction, ligand **104** was isolated by filtration in a yield of 88 %. Having the ligand in hand, the next step was to coordinate the ligand to the silicon(IV). Hence, ligand **104** was reacted with diiodosilicon(IV) precursors **85** and **86** in anhydrous chloroform under an atmosphere of nitrogen and reflux conditions over night. Unfortunately, no product could be isolated during flash column chromatography for both precursors. Changing the solvent to anhydrous *ortho*-xylene and hence increasing the reaction temperature was unsuccessful too. Moreover, the crude reaction mixture was investigated by mass spectrometry but the desired complex was not found. An explanation may be a possible interaction of the ligand with the Lewis acid $[SiI_2(pp)_2]I_2$ which could interfere the complexation reaction. For example, the nitrogen atoms of the phenazine structure can coordinate the silicon(IV) and thus prevent the complexation of the diolates. As the direct complexation of the ligand did not work, another synthesis strategy including a post-coordination derivatization was examined.

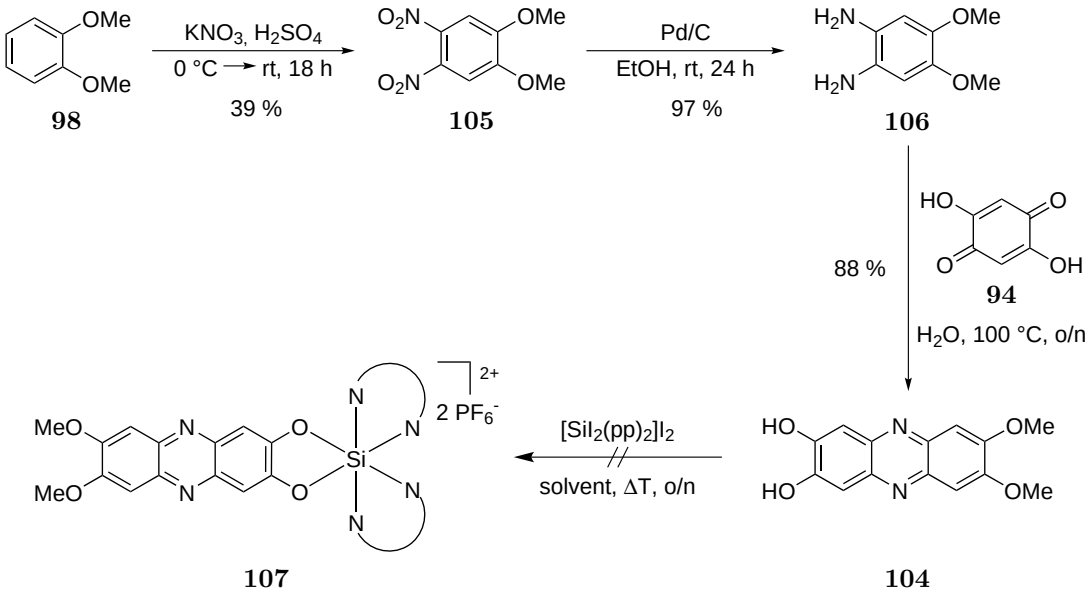

Scheme 15: Synthesis of 7,8-Dimethoxyphenazine-2,3-diol (**104**) and attempt to obtain complexes **107**.

The hydrolytical stability of the hexacoordinate silicon(IV) complexes synthesized was studied exemplary for complex **90** (Figure 35). For this reason, a solution of complex **90** in CD_3CN/D_2O (1:1) at room temperature under daylight was monitored by ^{1}H-NMR spectroscopy over nine days. As a result, complex **90** did not show any sign of decomposition, which is in accordance with previously reported studies.[37,224] Hence, the synthesized octahedral silicon complexes are hydrolytically completely stable for at least nine days. The kinetic inertness matches with the preparative observations since all higher-coordinate silicon(IV) complexes synthesized in this work can be purified by column chromatography with water as part of the eluent.

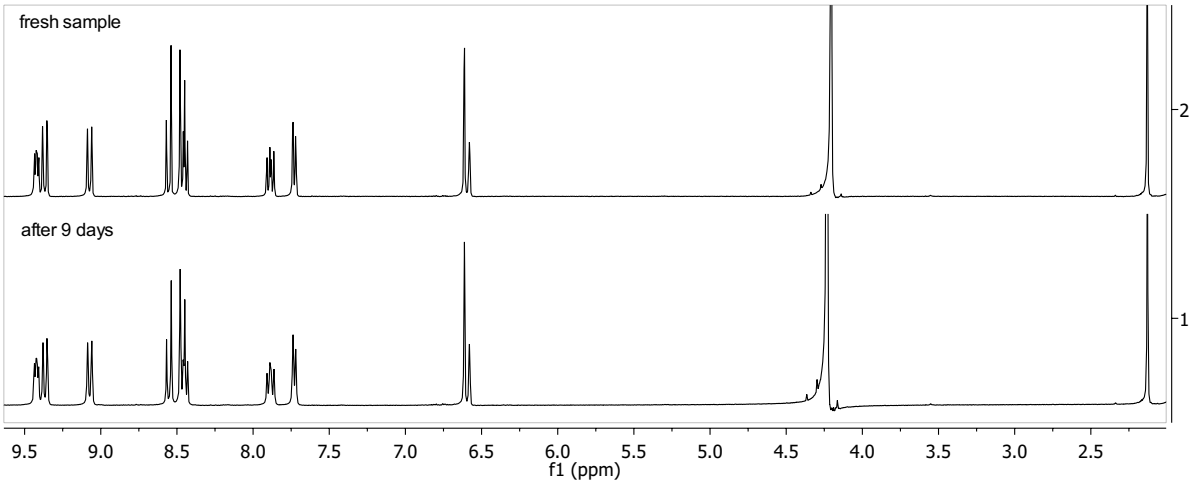

Figure 35: Hydrolytical stability of the hexacoordinate silicon(IV) complex **90** (9 mM) in CD_3CN/D_2O (1:1) at room temperature under daylight. Shown are the ^{1}H-NMR spectra right after the addition of D_2O(peak at $\delta = 4.23$ ppm) and after nine days. No decomposition can be observed.

The stability of the synthesized higher-coordinate silicon(IV) complexes towards fluoride was studied for complex **100** by way of example. Figure 36 shows the change of the ^{1}H-NMR spectra of complex **100** in CD_3CN upon addition of one and two equivalents of a solution of tetra-*n*-butylammonium fluoride in tetrahydrofuran (TBAF, 1 M). As expected, upon addition of only one equivalent TBAF complex, **100** showed very strong decomposition and after addition of the second equivalent, **100** was completely decomposed confirming the tendency of silicon to react readily with fluoride. The disintegration of the silicon(IV) complex upon addition of fluoride can also be monitored visibly as the yellow solution of **100** turned into a red suspension upon addition of tetra-*n*-butylammonium fluoride.

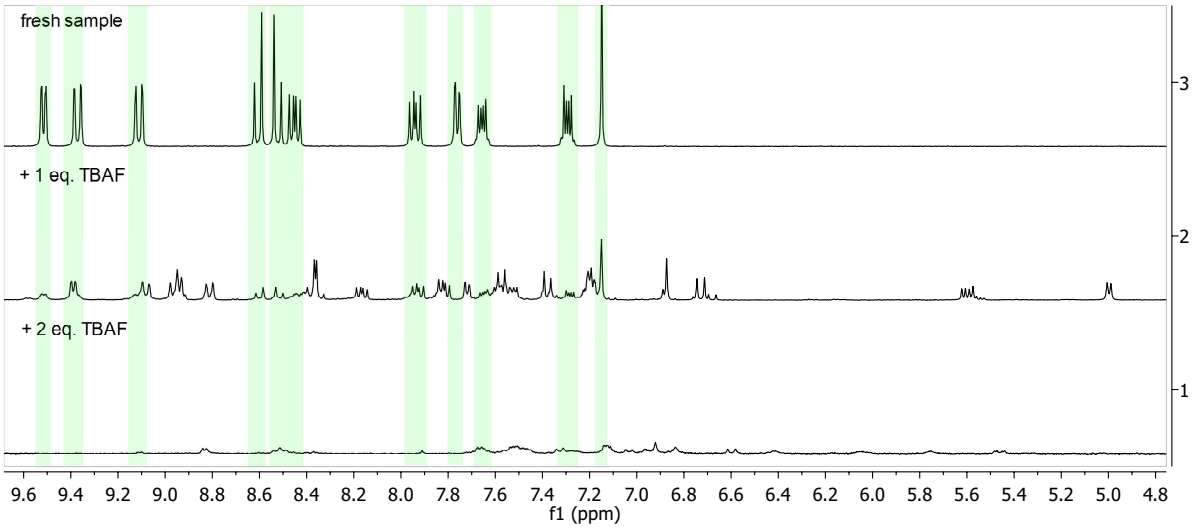

Figure 36: Stability against fluoride of the hexacoordinate silicon(IV) complex **100** (20 mM) in acetonitrile-d_3 at room temperature. Shown are the aromatic regions of the ^{1}H-NMR spectra of a fresh sample as well as after the addition of one and two equivalents of a tetra-*n*-butylammonium fluoride solution in tetrahydrofuran (1 M). The spectra are scaled to the solvent signal.

Having the results of the stability against fluoride in hand, the next step was to study the the stability of the octahedral silicon complexes towards bases. This trial was performed by Andreas

Schrimpf during his research project.[230] He first investigated the stability of (4-hydroxybenzene-1,2-diolato)silicon(IV) complex **91** towards cesium carbonate in acetonitrile at room temperature under daylight over a certain period of time. As a result, he found out that the hexacoordinate silicon(IV) complexes are not stable towards strong bases as **91** decomposes quite rapidly upon contact with the cesium carbonate. After already 16 hours, complex **91** was nearly completely decomposed as demonstrated in Figure 37.

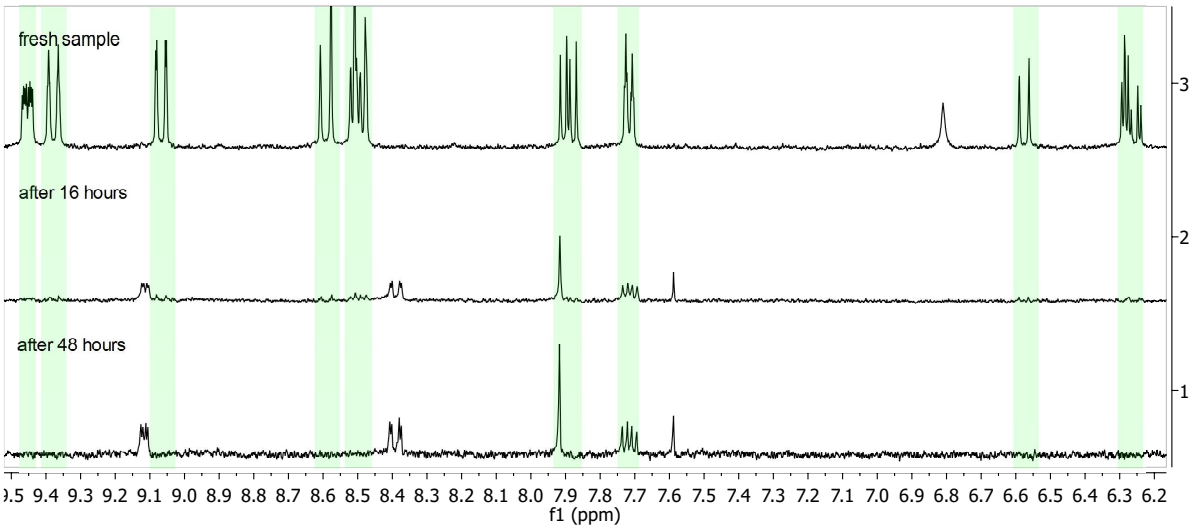

Figure 37: Stability of the hexacoordinate silicon(IV) complex **91** against cesium carbonate in acetonitrile-d_3 at room temperature. Shown are the aromatic regions of the ^{1}H-NMR spectra of a fresh sample as well as after 16 and 48 hours. The spectra are scaled to the solvent signal.[230]

The stability of complex **88** towards the in organic chemistry commonly used base *N,N*-diisopropylethylamine was studied next. The presence of the amine base also leads to a disintegration of the silicon(IV) complex but, in contrast to cesium carbonate, the rate of decomposition is much slower as monitored by ^{1}H-NMR spectroscopy (Figure 38).

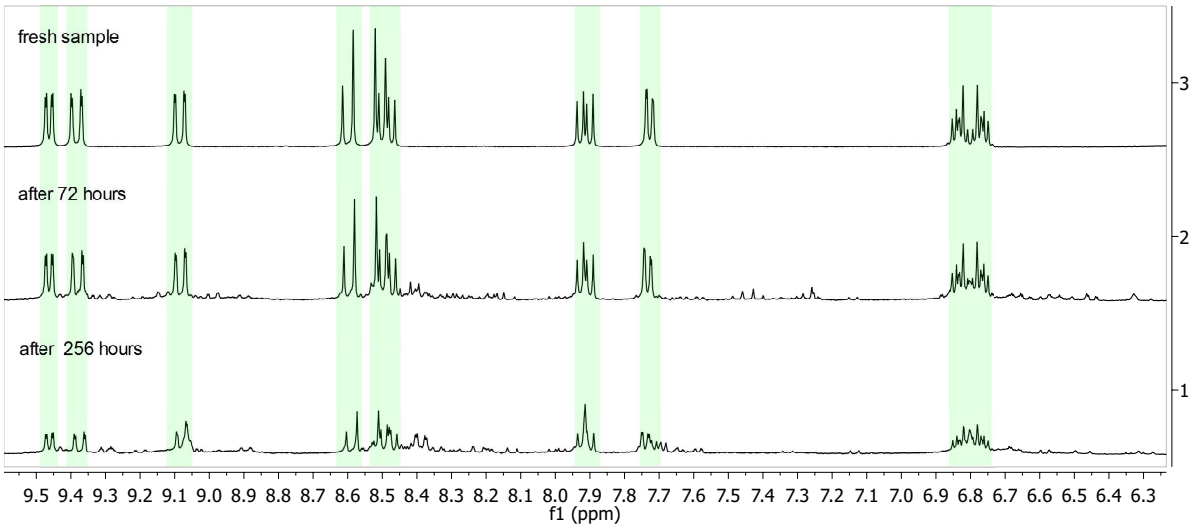

Figure 38: Stability of the hexacoordinate silicon(IV) complex **88** (20 mM) against one equivalent *N,N*-diisopropylethylamine in acetonitrile-d_3 at room temperature. Shown are the aromatic regions of the ^{1}H-NMR spectra of a fresh sample as well as after 72 and 256 hours. The spectra are scaled to the solvent signal.[230]

Even after 256 hours, the starting complex is still there leading to the assumption that silicon(IV) complexes can tolerate small amounts of amine bases for a short period of time. More surprisingly, the complex **88** showed no decomposition after treatment with two equivalents pyridine and is stable under this conditions for at least 31 hours at room temperature (Figure 39). Hence, if a reaction has be performed under basic conditions, pyridine is the base of choice.

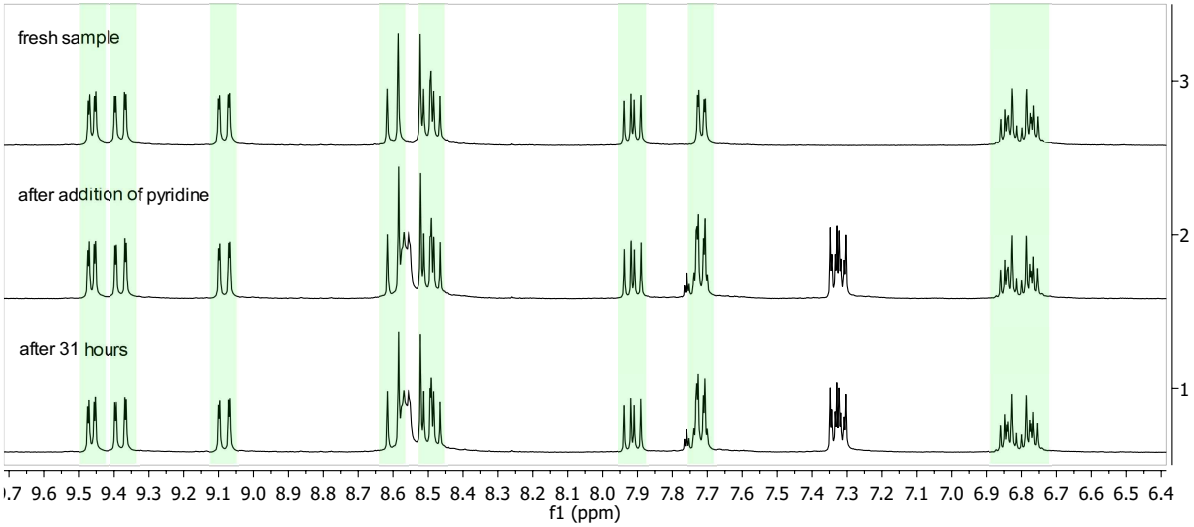

Figure 39: Stability of the hexacoordinate silicon(IV) complex **88** (21 mM) against two equivalents pyridine in acetonitrile-d_3 at room temperature. Shown are the aromatic regions of the ^{1}H-NMR spectra of a fresh sample as well as after 31 hours. The spectra are scaled to the solvent signal.

3.2. Post-Coordination Modification of Octahedral Silicon(IV) Complexes

3.2.1. Halogenation

As the direct coordination of brominated catechols to the hexacoordinate silicon complexes led to a partial *ipso*-substitution of the bromine residue and thus to a mixture of mono-brominated (**96**) and unsubstituted complex (**88**), a post-coordination halogenation of (benzene-1,2-diolato)silicon(IV) complexes (**87**, **88** and **90**) was investigated next. The introduction of only one bromine substituent was studied, using an oxidative bromination approach introduced by Roy and co-workers in 2001, for complex **88** by way of example.[231] Therefore, complex **88** was reacted with the bromine source lithium bromide and the oxidant ceric ammonium nitrate in anhydrous acetonitrile under an atmosphere of nitrogen at different temperatures and reaction times (Table 1) to yield 4-bromo-1,2-catecholato complex **96** (Scheme 16).

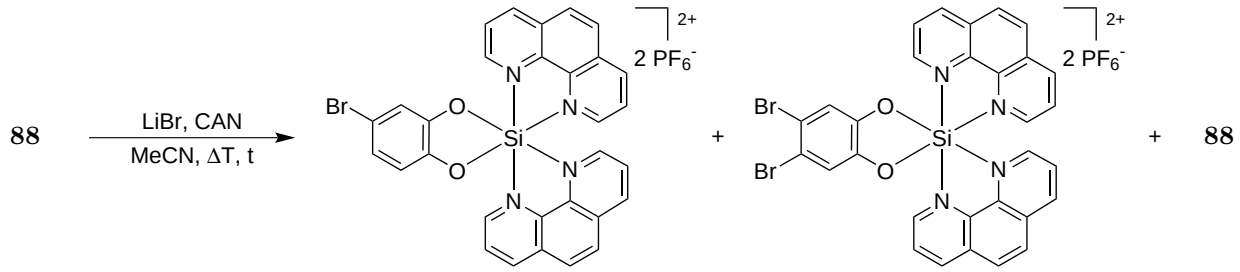

Scheme 16: The attempt to synthesize (4-bromobenzene-1,2-diolato)silicon(IV) complex **96** by an oxidative bromination reaction starting from $[Si(DHB)(phen)_2](PF_6)_2$ (**88**) gave an inseparable mixture of the mono- and dibrominated species (**96** and **108**) together with the unsubstituted complex **88**.

Table 1: Screening of different reaction conditions for the bromination of complex **88** with lithium bromide and ceric ammonium nitrate.

eq. of LiBr/CAN	Temperature / Time	Yield of mixture /%
1.1 / 1.1	rt / 4 h	No conversion[a]
1.1 / 1.1	rt / 18 h	72[a,b]
1.1 / 1.1	55 °C / 18 h	58[a,c]
1.1 / 1.1	55 °C / 72 h	71[a,c]
1.1 / 1.1	85 °C / 18 h	77[a,b]
1.4 / 1.1	50 °C / 18 h	72[c]
3.2 / 2.1	rt / 46 h	70[c]
1.9 / 1.7	rt / 22 h	54[c]

[a] Experiment performed by Philip Hofmann during his bachelor thesis.[224,232] [b] Isolated as a mixture of unsubstituted complex **88** and traces of mono- and dibrominated complexes **96** and **108**, respectively. [c] Isolated as an of inseparable mixture of mono- and dibrominated species (**96** and **108**) together with the unsubstituted (benzene-1,2-diolato)silicon(IV) complex **88**.

Having screened various reaction conditions, it was found that a reaction temperature of 50 °C over 18 hours or an increase of the lithium bromide and ceric ammonium nitrate equivalents is needed to obtain a high conversion of the silicon(IV) complex **88** (Table 1).[224] Unfortunately, every synthetic attempt yielded in an inseparable mixture of mono- and dibrominated species (**96** and **108**) together with the unsubstituted (benzene-1,2-diolato)silicon(IV) complex **88**, as monitored by ^{1}H-NMR spectroscopy (Figure 40).

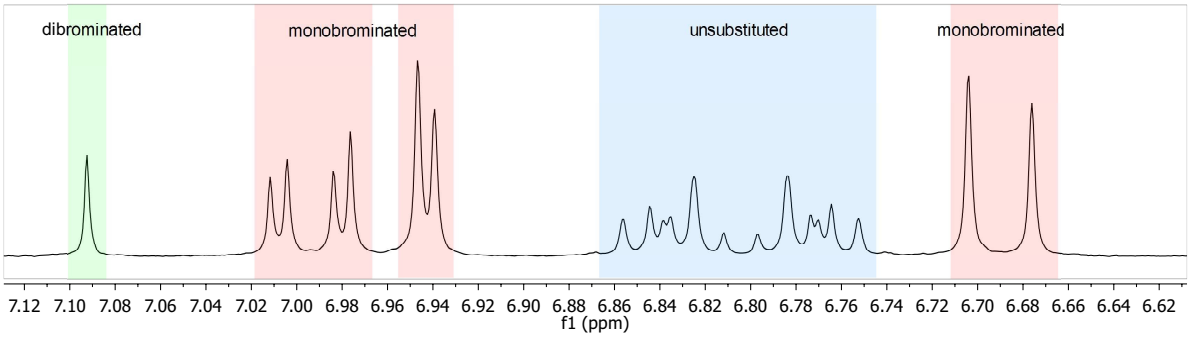

Figure 40: ^{1}H-NMR showing the catechol region of the product mixture of mono- and dibrominated complex **96** and **108** together with the unsubstituted (benzene-1,2-diolato)silicon(IV) complex **88** in acetonitrile-d_3. This mixture was obtained in the synthesis approach shown in Scheme 16.

The inseparable mixtures were finally converted into the dibrominated species **108** using the bromination reagent *N*-bromosuccinimide. Adopting a literature procedure published by García Ruano *et al.* in 1995,[233] the product mixture and *N*-bromosuccinimide (1.1–1.6 eq.) were reacted in anhydrous acetonitrile under an atmosphere of nitrogen at room temperature over three days (Scheme 17). In doing so, pure dibrominated complex **108** was isolated as hexafluorophosphate salt in a yield of 81 % starting from Table 1 entry 6 after purification by silica gel flash column chromatography.

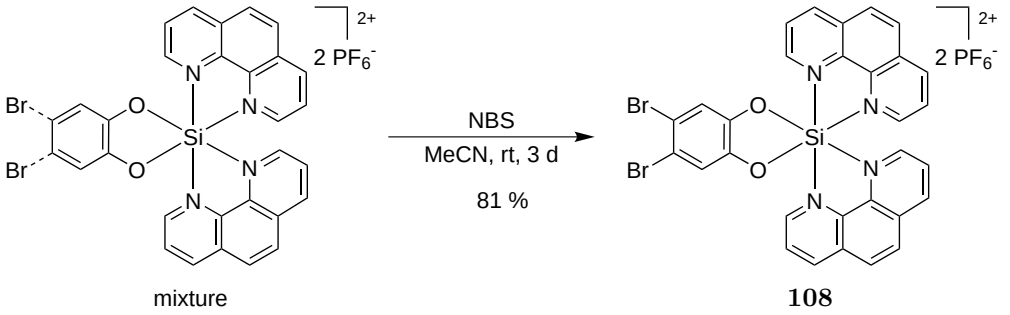

Scheme 17: Synthesis of (4,5-dibromobenzene-1,2-diolato)silicon(IV) complex **108** starting from the inseparable mixture of **88**, **96** and **108** using *N*-bromosuccinimide.

Adopting the reaction with *N*-bromosuccinimide, the dibrominated silicon(IV) complexes **108** and **109** were obtained in good yields starting from $[Si(DHB)(pp)_2](PF_6)_2$ (**87** and **88**, Scheme 18). Therefore, complex **88** was reacted with *N*-bromosuccinimide (2.6 eq.) in anhydrous acetonitrile under an atmosphere of nitrogen at room temperature for three days. After flash column chromatography and precipitation with ammonium hexafluorophosphate, complex **108** was obtained in a yield of 76 %. Using the same reaction conditions for the bipyridine coordinate silicon(IV) complex **87**, a mixture of mono- and dibrominated species was obtained. Addition of more equivalents of *N*-bromosuccinimide

or using a longer reaction time also yielded in a mixture. However, after increasing the reaction temperature to 60 °C over night, complex **109** was isolated as the hexafluorophosphate salt in a yield of 69 % after purification by flash column chromatography on silica gel.

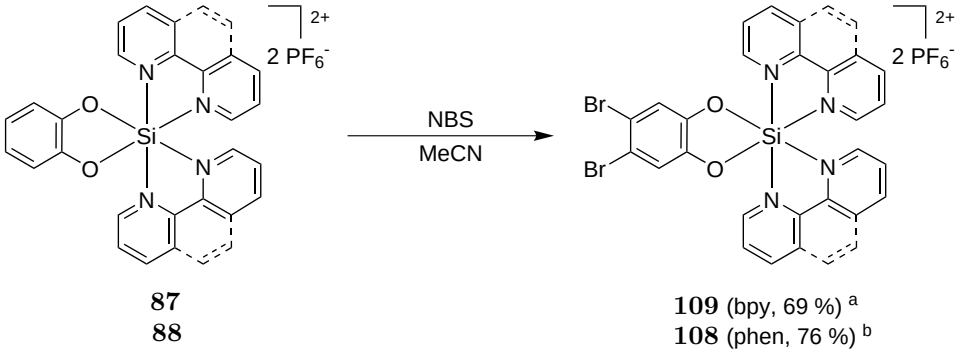

87
88

109 (bpy, 69 %) [a]
108 (phen, 76 %) [b]

Scheme 18: Synthesis of (4,5-dibromobenzene-1,2-diolato)silicon(IV) complex **108** and **109** starting from the unsubstituted (benzene-1,2-diolato)silicon(IV) complexes **87** and **88** using *N*-bromosuccinimide. (Conditions: [a] 1. 2.8 eq. NBS, room temperature, five days, 2. 0.3 eq. NBS, room temperature, over night, 3. 60 °C, over night. After step 1 and 2, a mixture of mono- and dibrominated complexes was obtained as monitored by LC-MS analytic. [b] 2.6 eq. NBS, room temperature, three days.)

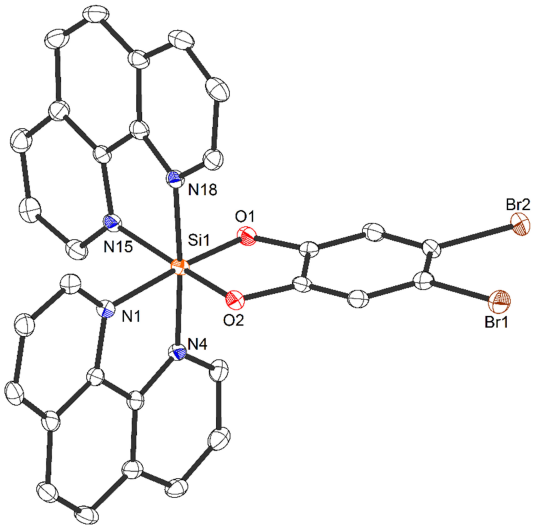

Figure 41: Crystal structure of complex **108**. ORTEP drawing with 50 % probability thermal ellipsoids. The PF_6^- counterions and solvent are omitted for clarity. Selected bond lengths [Å] and angles [°]: N1–Si1 1.923(2), N4–Si1 1.925(2), N15–Si1 1.936(2), N18–Si 1.939(2), O1–Si1 1.7196(18), O2–Si1 1.7137(19); N15–Si1–N18 82.79(10), N1–Si1–N15 89.51(9), N1–Si1–N18 94.80(9), N1–Si–N4 83.57(9), N4–Si1–N15 92.64(9), N4–Si1–N18 175.17(10), O1–Si1–N15 91.05(9), O1–Si1–N18 90.43(9), O1–Si1–N1 174.78(10), O1–Si1–N4 91.22(9), O2–Si1–N15 172.87(10), O2–Si1–N18 91.32(9), O2–Si1–N1 86.96(9), O2–Si1–N4 93.12(9), O2–Si1–O1 93.02(9).

The hexacoordinate structure of silicon(IV) complex **108** was verified by crystal structure analysis showing also the two bromine substituents introduced in *para*-positions to the hydroxy groups of

the 1,2-benzenediolato ligand (Figure 41). Single crystals suitable for crystal structure analysis were obtained upon slow diffusion of diethylether into a concentrated solution of the complex in acetonitrile at 4 °C. Complex **108** crystallized as yellow prism in the triclinic space group P −1 with two formula units per unit cell. Together with the complex, two formula units of the counter ion PF_6^- and 2.5 formula units of acetonitrile as crystal solvent were incorporated in the crystal structure.

Next, the bromination of (4-methylbenzene-1,2-diolato)silicon(IV) **90** was studied (Scheme 19). To obtain a substitution at the methyl side-chain of the benzene ring, a radical substitution reaction was tried. Therefore, **90** was reacted with the the bromine source *N*-bromosuccinimide[234] (1.3 eq.) in the presence of the radical initiator azobis*iso*butyronitrile[234] (0.2 eq.) in anhydrous acetonitrile under an inert gas atmosphere at 90 celsius for one hour (Scheme 19). However, only a bromination at the benzene ring occurred during the reaction. Moreover, only an inseparable mixture of starting material **90** and complex **110** was obtained after flash column chromatography. Even in the presence of a radical initiator, the reaction led only to a nuclear substitution if executed in acetonitrile. These findings support the observations of García Ruano *et al.*, who found out that the reaction of substituted anisoles with *N*-bromosuccinimide in acetonitrile yielded exclusively the ring bromination.[233] A substitution at the methyl group may be possible using another solvent like carbon tetrachloride.[233,234] As the octahedral silicon complexes are not very soluble in this solvent and thus a successful reaction is not very likely, the bromination of the side-chain was not examined any further.

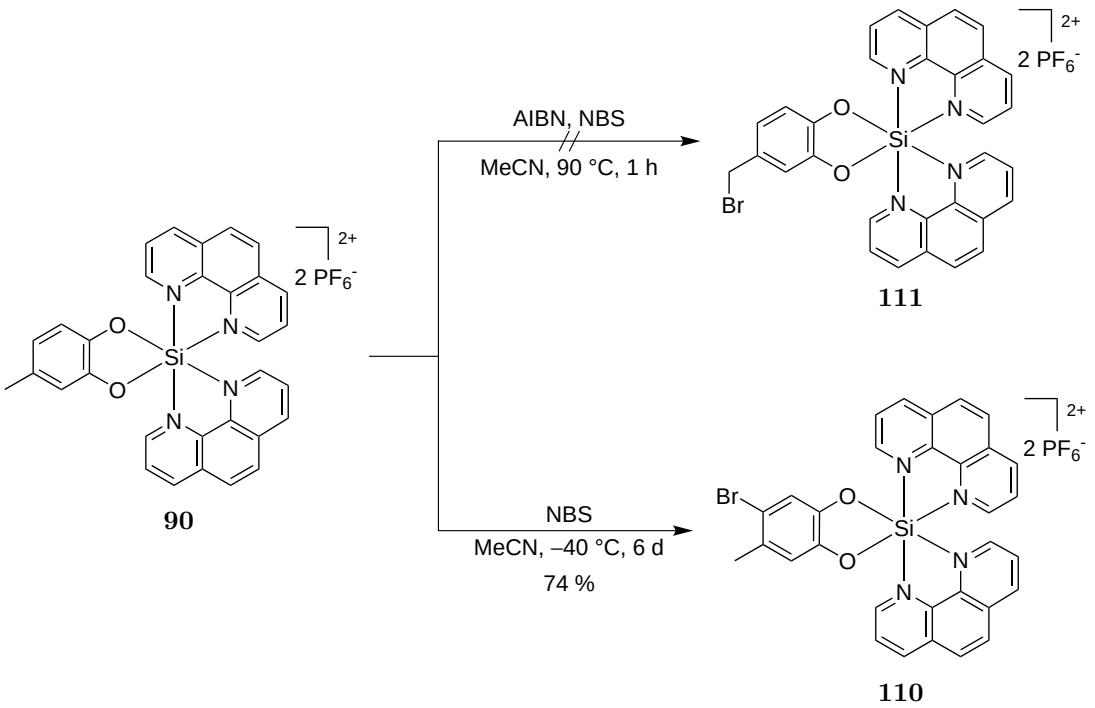

Scheme 19: Bromination reaction of (4-methylbenzene-1,2-diolato)silicon(IV) complex **90**.

Having a method to address only ring bromination in hand, complex **90** was reacted with *N*-bromosuccinimide (2.1 eq.) in acetonitrile at room temperature over three days. Unfortunately, besides the desired product **110**, the ^{1}H-NMR spectra shows two other set of signals which are perhaps due to an unfavored bromination at the methyl group or a further reaction at the benzene core. These further reaction were inhibited by lowering the reaction temperature to −40 °C for

six days (Scheme 19). After flash column chromatography on silica gel and anion exchange to hexafluorophosphate, pure silicon(IV) complex **110** was obtained in a yield of 74 %.

With the bromine substituted ligands in hand, it was then tried to obtained the corresponding diiodine substituted complex **112** utilizing similar conditions. Therefore, complex **88** was reacted with *N*-iodosuccinimide using the previously discussed method (Scheme 20). However, only starting material was recovered after purification using silica gel flash column chromatography. By changing the iodination reagent to a combination of *N*-iodosuccinimide (2.2 eq.) and catalytic amounts of trifluoroacetic acid (0.5 eq.) at a reaction temperature of 60 °C for 18 hours,[235] an inseparable mixture of mono- and diiodinated complex was obtained after purification by column chromatography. The mixture was further reacted with additional *N*-iodosuccinimide (1.0 eq.) and catalytic amounts of trifluoroacetic acid (0.6 eq.) at a reaction temperature of 60 °C for two hours yielding the diiodo substituted complex **112** in a yield of 59 % after silica gel column chromatography and anion metathesis.

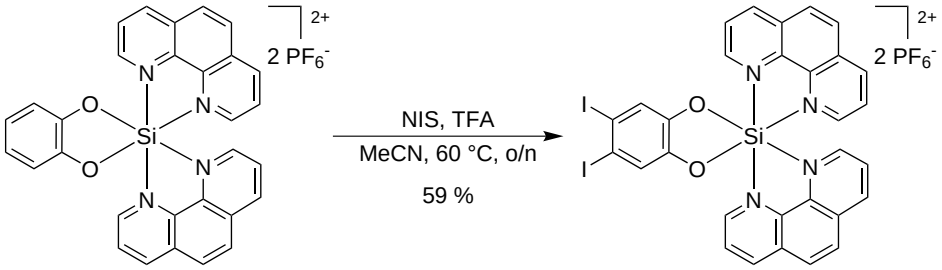

Scheme 20: Attempt to obtain (4,5-diiodobenzene-1,2-diolato)silicon(IV) complex **112** by an iodination with *N*-iodosuccinimide.

A very potent reagent for the oxidative iodination of aromatic substrates is the hypervalent iodine(V) compound potassium 4-iodylbenzenesulfonate (**113**) which was introduced by Zhdankin and coworkers in 2012.[236] **113** was synthesized from iodobenzene (**114**) in a two step synthesis. In the first step, an electrophilic aromatic sulfonation, **114** was reacted in concentrated sulphuric acid at 55 °C for three days yielding the *para*-substituted product (Scheme 21).[236] The obtained intermediate was then oxidized with oxone in water at 60 °C for 16 hours.[236] Finally, the potassium salt **113** was isolated in quantitative yield over two steps by filtration.

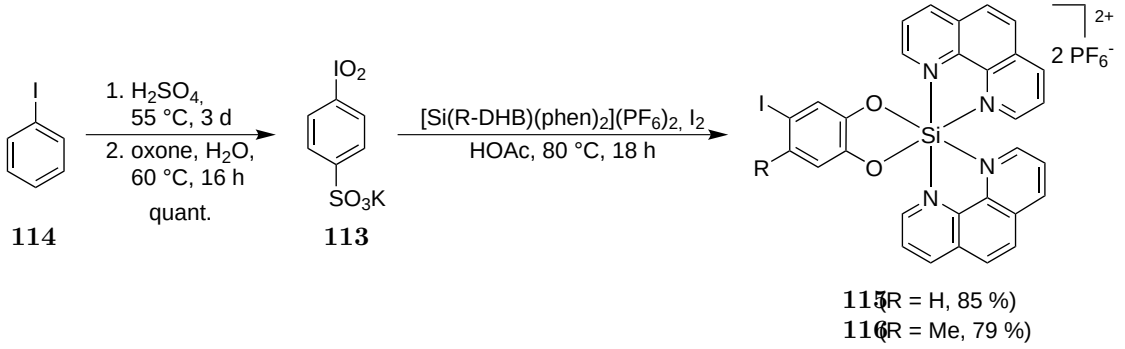

Scheme 21: Synthesis of the iodation reagent potassium 4-iodylbenzenesulfonate (**113**)[236] and the subsequent monoiodination of silicon(IV) complexes **88** and **90**.

Having the iodination reagent **113** in hand, Tom Breiding was able to synthesize the monoiodinated silicon(IV) complex **115** in moderate yields and to confirm its structure by X-ray crystallography.[28,224] Adopting his procedure, both silicon complexes **88** and **90** were reacted with iodine and **113** in glacial acetic acid under an atmosphere of nitrogen at 80 °C for 18 hours. After flash column chromatography on silica gel, monoiodinated complexes **115** and **116** were obtained as hexafluorophosphate salts in yields of 85 % and 83 %, respectively.

In the context of palladium[237–241] or nickel[242] mediated cross-coupling reactions, triflates are also frequently used leaving group.[243] Hence, the triflation of the hydroxy substituted complex **91** was investigated next. Therefore, complex **91** was reacted with various amounts of trifluoromethanesulfonic anhydride in the presence of pyridine in anhydrous acetonitrile under an atmosphere of nitrogen at room temperature for 2–24 hours (Scheme 22). Unfortunately, only a mixture of products (**117**, **118**, **118a**, **119** and **119a**,**b**) could be isolated. For example, using 2.4 equivalents of the trifluoromethanesulfonic anhydride, an additional and unusual electrohilic aromatic substitution introducing a triflyl group in position five (**118**) or three (**118a**) of the benzene-1,2-diolato ligand seemed to occur as monitored by ^{1}H-NMR spectroscopy (Figure 42). By increasing the amounts of trifluoromethanesulfonic anhydride to 4.8 equivalents, three further signals belonging to a double insertion of a triflyl group (**119** and **119a**,**b**) can be observed. This unexpected observation can be explained due to electron rich, double deprotonated benzene-1,2-diolato ligand that can easily attack the strong electrophile trifluoromethanesulfonic anhydride.

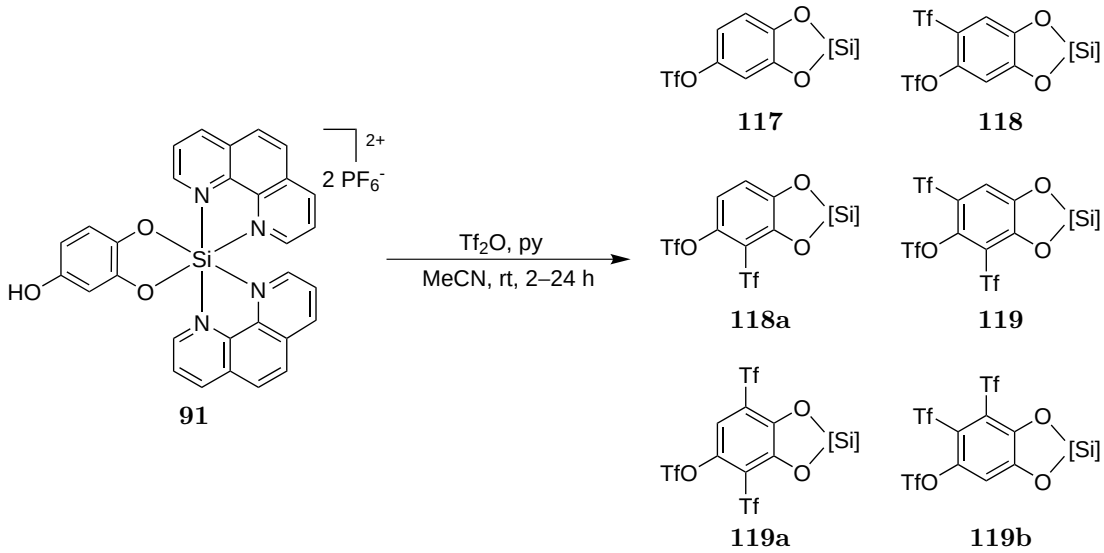

Scheme 22: Attempt to triflate the hydroxy group of silicon(IV) complex **91**.

Palladium catalyzed cross-coupling reactions of higher-coordinate silicon(IV) complexes were studied by Philipp Hofmann[232] during his bachelor thesis and by Sebastian Ullrich[244] during his research internship in the Meggers group. Although different reaction conditions were tested, clean cross-coupling products were not obtained. In nearly all cases, only starting material was recovered or an inseparable mixture of starting material and small amounts of product was obtained.[232,244] Hence, other routs for the modification of silicon(IV) complexes were investigated.

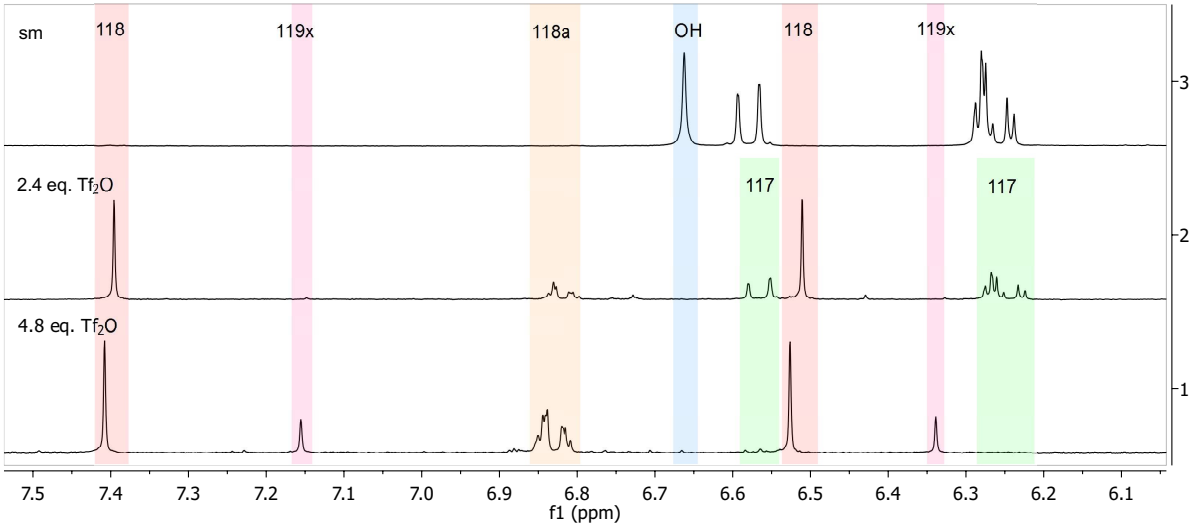

Figure 42: ^{1}H-NMR showing the catechol region of a mixture obtained after the reaction of complex **91** (sm) with trifluoromethanesulfonic anhydride in in acetonitrile-d_3.

Finally, the hydrolytical stability of the halogenated silicon(IV) complexes was studied for complex **108** by way of example. After eight days at room temperature under daylight, complex **108** did not show any sign of decomposition as monitored by ^{1}H-NMR spectroscopy in CD_3CN/D_2O (1:1).

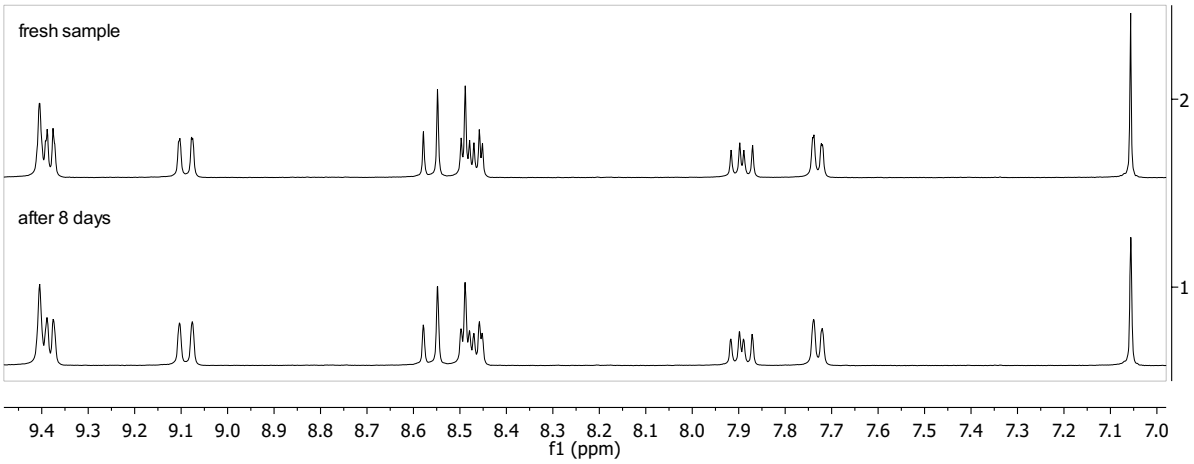

Figure 43: Hydrolytical stability of the hexacoordinate silicon(IV) complex **108** (8 mM) in CD_3CN/D_2O (1:1) at room temperature under daylight. Shown are the aromatic region of the ^{1}H-NMR spectra right after the addition of D_2O and after eight days. No decomposition can be observed.

3.2.2. Oxidation

Besides halogenation, another frequently used synthetic strategy in organic chemistry is the oxidation. It allows the formation of reactive functional groups like carbonyls, carbonic acids or epoxides.[245–258] Therefore, the oxidation of hexacoordinate silicon(IV) complexes was also studied. First, the oxidation of the 1,10-phenanthroline ligands of complex **88** was investigated as it would permit the introduction of various functional groups as well as a possibility of expanding the planar system.

In 2010, Sun and co-workers published a method to oxidize substituted 1,10-phenanthroline derivatives to the corresponding 1,10-phenanthrolin-5,6-diones at room temperature using potassium bromate and 60 % sulfuric acid as the oxidant.[252] These relatively mild reaction conditions were adopted to synthesize the silicon(IV) complexes **120**. In doing so, complex **88** was reacted with sodium bromate in 60 % sulfuric acid at room temperature for one to three days (Scheme 23). The reaction mixture was purified by neutralization with sodium hydroxide until pH 6–7 and isolation of a precipitate obtained upon addition of ammonium hexafluorophosphate. Unfortunately, the desired product **120** was not obtained. Another typical oxidation condition to obtain 1,10-phenanthroline-5,6-dione, a mixture of sulphuric and nitric acid in the presence of potassium/sodium bromide under reflux conditions,[245–247,259] was not investigated as it would also nitrate the benzene-1,2-diolato ligand.

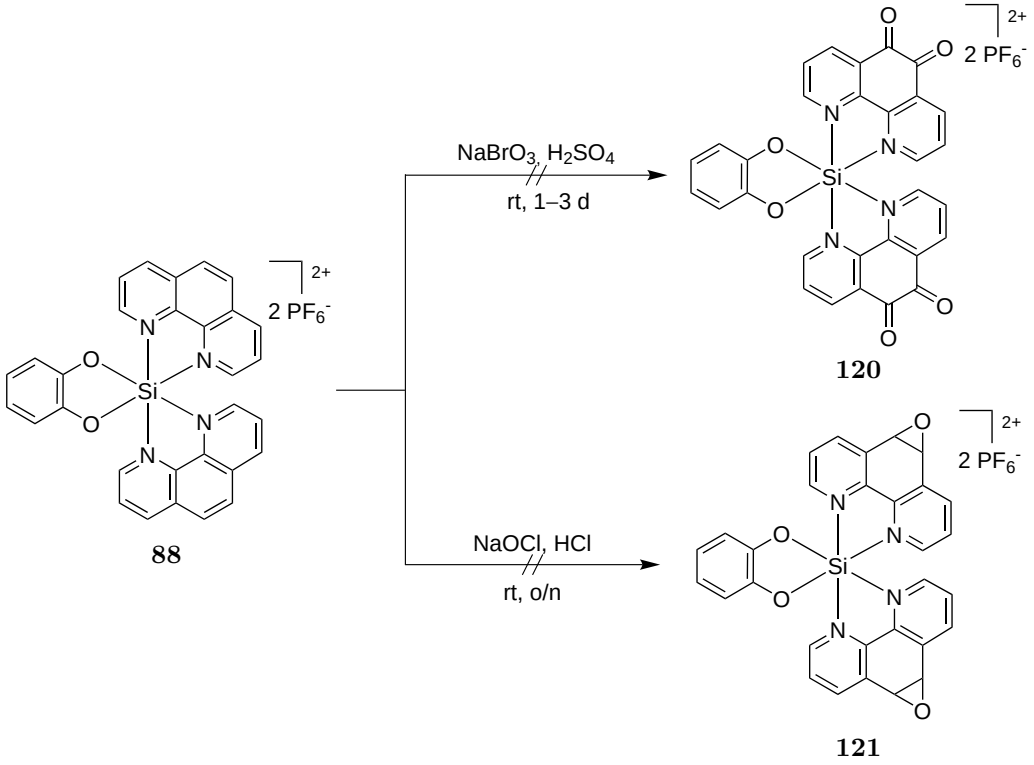

Scheme 23: Attempt to oxidize the 1,10-phenanthroline ligands coordinate to a silicon(IV) center.

It was then tried to generate the epoxide complex **121** using sodium hypochloride in water at a pH of 8–9 at room temperature over night, according to a modified procedure published by Hamilton *et al.* in 1977[254] or Sullivan and co-workers,[255] who used commercial bleach as the oxidant, in 1995. As a result, after purification by silica gel chromatography and exchanging the counter ion to hexaflurophosphate, a mixture of products was isolated. But, the desired epoxide complex **121** could not be identified. Thus, the oxidation of the 1,10-phenanthroline ligands was not very promising and therefore not investigated any further.

In 2005 Paul *et al.* published a interesting method for benzylic oxidations utilizing the inexpensive and non-toxic zinc oxide as the oxidation reagent.[250] In accordance to this procedure, it was tried to oxidize the methyl group of silicon(IV) complex **90** under different conditions (Scheme 24, Table 2).

In doing so, complex **90** was reacted with zinc oxide in *N,N*-dimethylformamide at 90 °C for 18 hours. Observing no conversion of the starting material as monitored by LC-MS, the reaction was performed under µ-wave irradiation. However, also upon µ-wave irradiation of the reaction mixture at 150 °C for 105 minutes, no conversion of the staring material could be monitored by LC-MS. Thus, another oxidation reagent was tried.

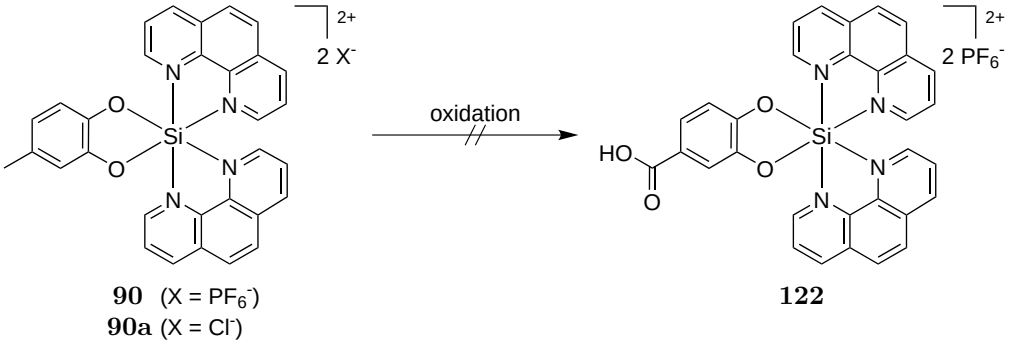

Scheme 24: Attempt to oxidize the methyl group of complex **90** to obtain the carbonic acid **122**. The reaction conditions are given in Table 2.

Table 2: Reaction conditions and reagents used to oxidize the methyl group of complex **90** and **90a** to the carbonic acid **122**. The conversion of the reaction was monitored by LC-MS.

Complex	Oxidant	Solvent	Temperature / Time
90	ZnO [250]	DMF	90 °C / 18 h
90	ZnO [250]	DMF	150 °C / 105 min[a]
90a	$KMnO_4$	HOAc,H_2O	110 °C / 20 h

[a] Reaction was performed under µ-wave irradiation (150 W).

Another possible oxidation reagent for the benzylic oxidation already known since the 19th century is potassium permanganate. For example, Tiemann and Mendelsohn used it in 1875 to oxidize 3,4-dimethoxytoluene to 3,4-dimethoxybenzoic acid.[258] Since the typical solvent for a potassium permanganate oxidation is water,[234,258] the water soluble chloride complex **90a** was synthesized first according to a general procedure (Scheme 25).

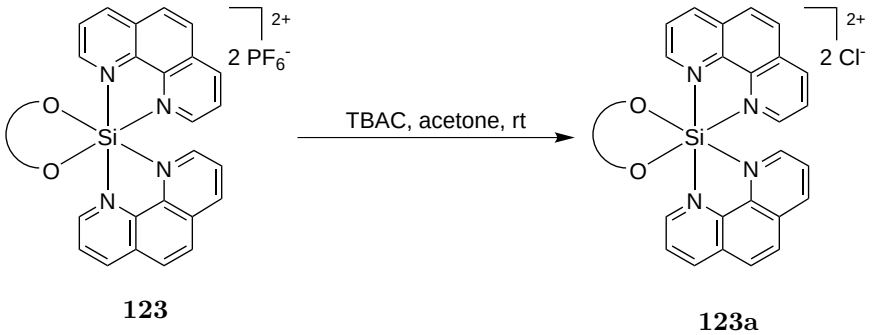

Scheme 25: General procedure for the anion exchange from hexafluorophosphate to chloride.

Therefore, the hexafluorophosphate salts were dissolved in acetone and filtered to remove all insoluble particles. Then the corresponding chloride salts were precipitated upon addition of a concentrated solution of tetra-*n*-butylammonium chloride in acetone. After washing of the precipitate with acetone, the chloride salt **90a** was obtained in a yield of 99 %. Complex **90a** was then reacted with potassium permanganate in a mixture of glacial acetic acid and water at 110 °C over night. However, after purification by column chromatography on silica gel and treatment with ammonium hexafluorophospahte, only unreacted complex **90** was isolated instead of the desired product **122**.

As benzene-1,2-diol is known for its ability to easily oxidize to a benzoquinone structure,[112,251] the oxidation of hexacoordinate silicon(IV) complexes yielding (1,2-benzoquinone-4,5-diolato)silicon(IV) complex **95** was studied next. The direct oxidation of silicon(IV) complex **88** with the oxidizing reagent lead(IV)dioxide in acetic acid at 80 °C for 16 hours, according to a procedure published by Crank *et al.* in 1980,[251] was not successful as only starting material was recovered. This observation is consistent with cyclic voltammetry studies measured by Schmedake and co-workers who found a very positive oxidation potential for the bis(2,2'-bipyridine)silicon(IV) complex **87** due to a badly defined E_{pa} at 1.2 V (versus FC^+/FC) and no distinct E_{pc}.[112]

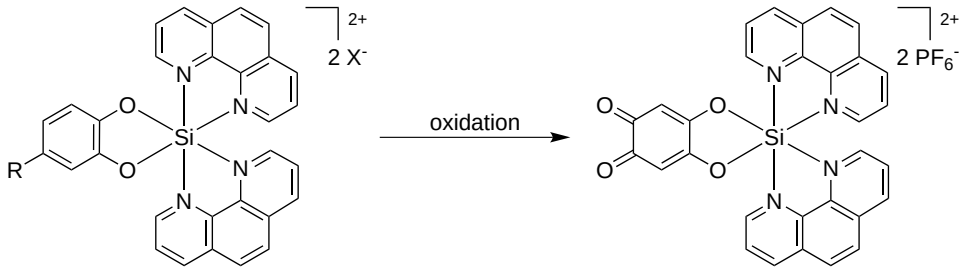

Scheme 26: Synthesis of (1,2-benzoquinone-4,5-diolato)silicon(IV) complex **95**. The reaction conditions are given in Table 3.

Table 3: Reaction conditions and reagents used to obtain (1,2-benzoquinone-4,5-diolato)silicon(IV) complex **95**.

Complex	Oxidant	Conditions	Yield
88	PbO_2 [251]	HOAc, 80 °C, 16 h	–[a]
91	Fremy's salt [249]	MeOH, $KH_2PO_{4aq.}$ (0.9 M), rt, 30 min	83 %[b]
91a	Fremy's salt [249]	MeOH, $KH_2PO_{4aq.}$ (0.9 M), rt, 1–1.5 h	72–74 %

[a] Only starting material **88** was isolated. [b] Isolated as an inseparable mixture of **91** and **95**.

Starting with (4-hydroxy-1,2-catecholato)silicon(IV) complex **91** and utilizing the oxidation agent Fremy's salt that is commonly used for the oxidation of phenols to quinones,[249,260] a very mild oxidation reaction was obtained. According to to procedure of Saa and co-workers,[249] complex **91** was reacted with Fremy's salt in a mixture of methanol and aqueous potassium dihydrogenphosphate buffer at room temperature for 30 minutes. After purification by silica gel column chromatography

and exchanging the counterion to hexafluorophosphate, a mixture of the product **95** and the starting material **91** was obtained in a yield of 83 % with a ratio of 4:1 as determined by ^{1}H-NMR spectroscopy. Using the chloride salt **91a**, which was synthesized in a yield of 94 % according to the general procedure (Scheme 25), instead of the hexafluorophosphate salt **91**, pure (1,2-benzoquinone-4,5-diolato)silicon(IV) complex **95** was obtained in a yield of 72–74 %. In addition, the chloride salt **95a** was obtained in a yield of 76 % according to the general synthesis route (Scheme 25).

Crystal structure analysis of complex **95** showed not only the octahedral coordination of the silicon center but also verified the 1,2-benzoquinone-4,5-diolato structure of the ligand as its bond lengths are consistent with a benzoquinone structure (an average of 1.346 Å and 1.477 Å for the carbon carbon double and single bonds, respectively).[261] The single crystals suitable for the X-ray analysis were obtained upon slow diffusion of diethyl ether into a concentrated solution of the complex in acetonitrile at 4 °C. Complex **95** crystallized as a yellow prism in the monoclinic space group P $2_1/n$ with four formula units per unit cell. Together with the complex, two formula units of the counter ion PF_6^- and three formula units of acetonitrile as crystal solvent were incorporated in the crystal structure.

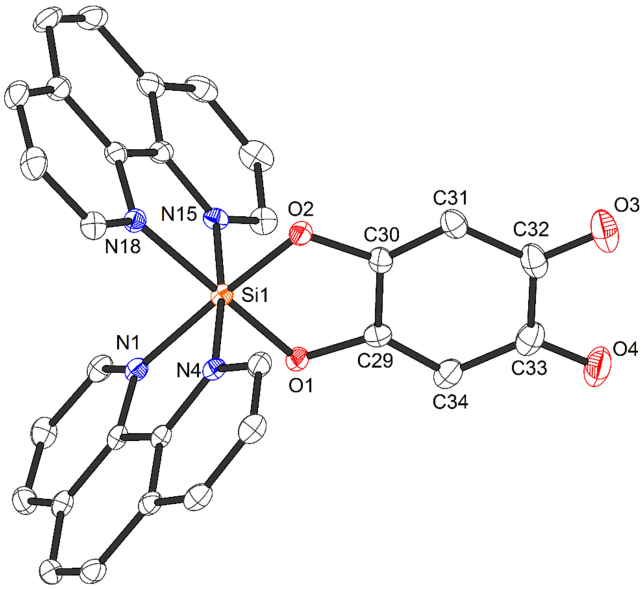

Figure 44: Crystal structure of complex **95**. ORTEP drawing with 50 % probability thermal ellipsoids. The PF_6^- counterions and solvent are omitted for clarity. Selected bond lengths [Å] and angles [°]: N1–Si1 1.921(2), N4–Si1 1.921(2), N15–Si1 1.931(2), N18–Si1 1.927(2), O1–Si1 1.7184(19), O2–Si1 1.7252(19), C29–C34 1.348(4), C29–C30 1.468(4), C30–C31 1.344(4), C31–C32 1.457(4), C32–O3 1.229(3), C32–C33 1.553(5), C33–O4 1.228(3), C33–C34 1.431(4), C30–O2 1.352(3), C29–O1 1.336(3); O1–Si1–O2 91.37(9), O1–Si1–N4 92.33(9), O2–Si1–N4 92.42(9), O1–Si1–N1 87.36(9), O2–Si1–N1 176.25(9), N4–Si1–N1 84.10(9), O1–Si1–N18 175.92(10), O2–Si1–N18 90.41(9), N4–Si1–N18 91.26(9), N1–Si1–N18 91.07(9), O1–Si1–N15 92.75(9), O2–Si1–N15 91.60(9), N4–Si1–N15 173.44(9), N1–Si1–N15 91.99(9), N18–Si1–N15 83.53(9).

Having the dione complex **95** in hand, it was tried to condense it with aromatic amines (Scheme 27). Therefore, complex **95** and **95a** were reacted with *ortho*-phenylenediamine (**124**) or 4,5-dimethoxy-1,2-

phenylenediamine (**106**)[229] using various reaction conditions (Table 4). All reactions were purified by column chromatography in silica gel and isolated as hexafluorophosphate salts. Unfortunately, the desired condensation products **125** or **126** could not be isolated as inseparable mixtures of starting material **95**, product and at least one other compound were obtained. Hence, this reaction was not investigated any further.

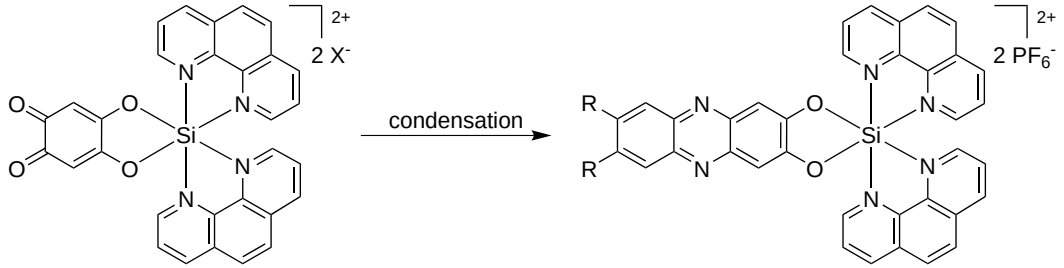

Scheme 27: Attempt to use complex **95** in a condensation reaction. The reaction conditions are given in Table 4.

Table 4: Reaction conditions and reagents used to condense complex **95** with diamines.

Complex	Diamine	Conditions	Isolated
95	**124**	MeCN, rt, 20 h	**95**
95	**124**	MeCN, 90 °C, o/n	**95** + **125**[a]
95	**124**	MeCN, 100 °C, 2 h[b]	mixture[c]
95	**124**	MeCN, HOAc, 90 °C, o/n	mixture[c]
95a	**106**	MeOH, 65 °C, 2 d	no product
95a	**106**	HOAc, 120 °C, 2 d	no product

[a] Isolated as an inseparable mixture with about 20 % of complex **125**. [b] Reaction was performed under μ-wave irradiation (150 W). [c] Isolated as an inseparable mixture of at least three compounds including complex **95**.

3.2.3. Nitration

The nitration of (benzene-1,2-diolato)silicon(IV) complexes **87**, **88** and **89** was achieved in the Meggers group[28,37,149,150,224] by adopting a procedure published by Marquet and co-workers using a 2:1 mixture of nitric acid and glacial acidic acid at room temperature.[262,263] Interestingly, the nitration pattern could be varied by changing the concentration of the nitric acid. Hence, utilizing 65 % nitric acid yielded in the formation of the mononitrated complexes **127** and **128**, whereas fuming nitric acid led to the dinitrated species **129**, **130** and **131** Scheme 28. The purification of complexes **127**, **128**, **129** and **130** was really convenient as it was sufficient to precipitate the complexes with ammonium hexafluorophosphate out of the neutralized, aqueous reaction solution. Complexes **127**, **128**, **129** and **130** were obtained in yield of 77–86 % and can be further purified by silica gel column chromatography if necessary. The reaction conditions for the dinitration of complex **89** yielding **131** were slightly modified to avoid the formation of tri- and tetra-nitrated complexes. Therefore, **89** was

reacted at 0 °C for three hours, whereupon the temperature slowly increased to 10 °C. After column chromatography on silica gel and anion exchange to hexafluorophosphate, silicon complex **131** was obtained in a yield of 68 %.

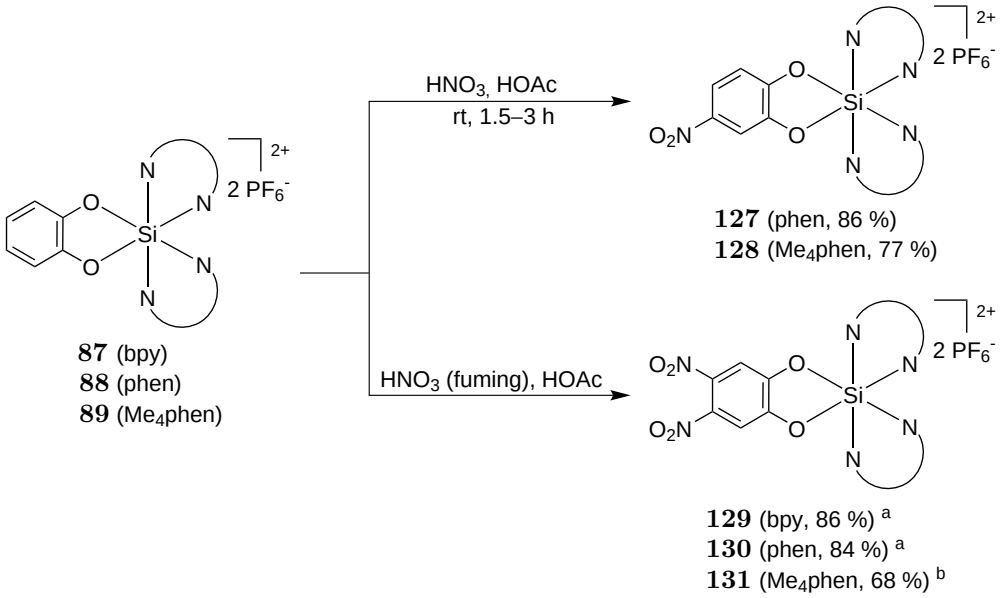

Scheme 28: Nitration of hexacoordinate (benzene-1,2-diolato)silicon(IV) complexes **87**, **88** and **89** using a mixture of nitric acid and glacial acidic acid. (Conditions: [a] rt, 1–2 hours; [b] 0 °C → 10 °C, 3 hours.)

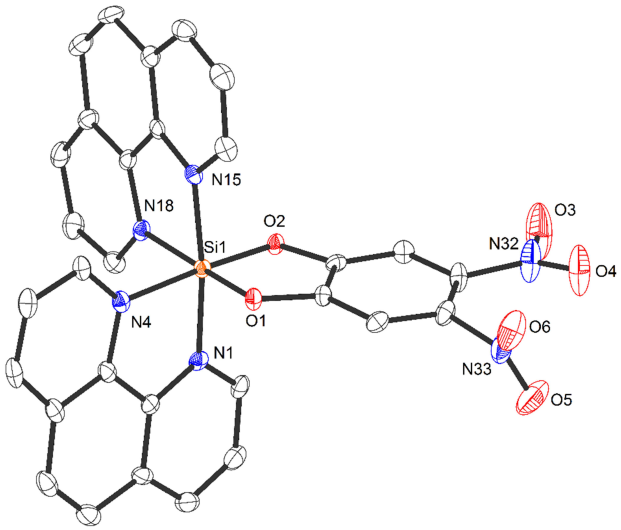

Figure 45: Crystal structure of complex **130**. ORTEP drawing with 50 % probability thermal ellipsoids. The PF_6^- counterions and solvent are omitted for clarity. Selected bond lengths [Å] and angles [°]: N1–Si1 1.924(3), N4–Si1 1.934(3), N15–Si1 1.924(2), N18–Si1 1.935(3), O1–Si1 1.733(2), O2–Si1 1.718(2); O2–Si1–O1 91.87(11), O2–Si1–N1 92.96(12), O1–Si1–N1 91.90(12), O2–Si1–N15 91.31(12), O1–Si1–N15 93.78(12), N1–Si1–N15 172.78(13), O2–Si1–N4 176.39(13), O1–Si1–N4 87.06(11), N1–Si1–N4 83.64(13), N15–Si1–N4 92.20(13), O2–Si1–N18 90.47(12), O1–Si1– N18 176.17(13), N1–Si1–N18 91.01(12), N15–Si1–N18 83.12(12), N4–Si1–N18 90.79(12).

The structure of dinitrated silicon(IV) complexes was verified by crystal structure analysis for **130** by way of example. In Figure 45 the crystal structure is pictured, showing the octahedral coordination sphere of the silicon as well as the two nitro groups introduced in *para*-positions to the hydroxy groups of the catecholato ligand. Single crystals suitable for crystal structure analysis were obtained upon slow diffusion of diethylether into a concentrated solution of the complex in acetonitrile at 4 °C. Complex **130** crystallized as an orange block in the monoclinic space group C 2/c with eight formula units per unit cell. Together with the complex, two formula units of the counter ion PF_6^- and three formula units of acetonitrile as crystal solvent were incorporated in the crystal structure.

The conversion of the methylated silicon(IV) complex **90** with a mixture of 65 % nitric acid and glacial acetic acid at room temperature for two hours afforded the mononitrated complex **132** in a yield of 88 % (Scheme 29) utilizing the isolation described above. Using the same conditions but fuming nitric acid, a dinitration is observed. After purification by silica gel column chromatography and precipitation with ammonium hexafluorophosphate, silicon(IV) complex **133** was obtained in a yield of 51 %. The regioselectivity of the nitration is determined by stability of the Wheland intermediate. As the methyl and the aryloxy groups are *ortho-para* directing and the nitro group is *meta* directing, the substitution at position 3 of the ring is favored over position 6.[234,248]

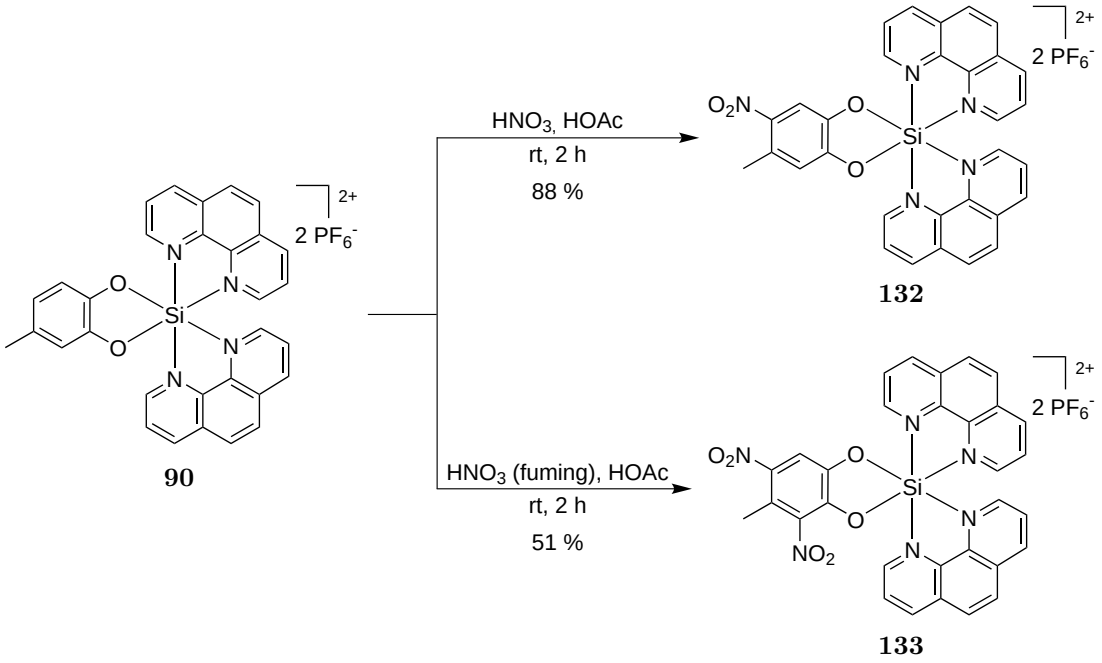

Scheme 29: Nitration of hexacoordinate (4-methylbenzene-1,2-diolato)silicon(IV) complex **90** using a mixture of nitric acid and glacial acidic acid.

3.2.4. Condensation

During his PhD studies in the Meggers group, Yonggang Xiang found a simple way to modify dinitro-substituted silicon(IV) complexes. By reducing the nitro groups to amines using tin in hydrocloric acid followed by a condensation reaction with various diones, silicon(IV) complexes with an expanded aromatic ligand could be synthesized (Scheme 30).[149]

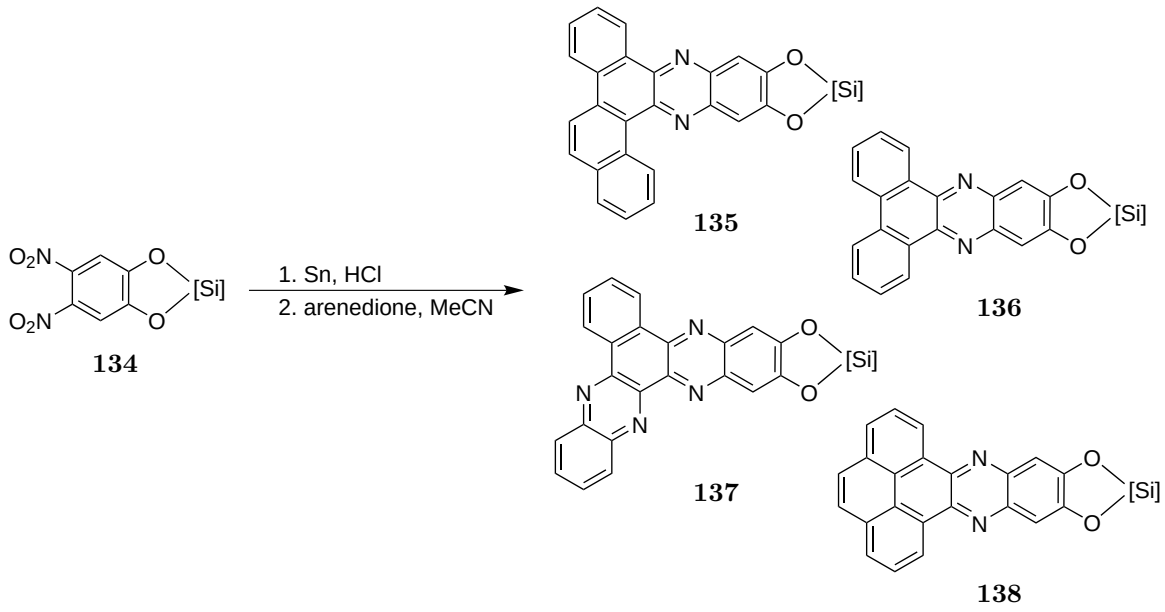

Scheme 30: Examples for hexacoordinate silicon(IV) complexes synthesized by Yonggang Xiang.

This synthesis route seems to be a very nice method building up sophisticated ligand structures and was studied more detailed. Hence, according to the procedure developed by Yonggang Xiang,[149] the nitro groups of complexes **130** were reduced using tin powder in half concentrated hydrochloric acid at 110 °C for three hours (Scheme 31). After adjusting the pH of the yellow reaction mixture to a value of 6–7, extracting the mixture with water, and isolating the hexafluorophosphate salts by addition of ammonium hexafluorophosphate, crude (4,5-diaminobenzene-1,2-diolato)silicon(IV) complexes **140** was obtained as a brown solid in a yield of about 76 %. Unfortunately, the complex could not be further purified as it decomposes during flash column chromatography on silica gel or even when stored at room temperature under nitrogen. In addition, attempts to crystallize complex **140** were not successful. Similar observations were made for the reduction of complexes **129** and **131**. Hence, the intermediates **139**, **140** and **141** were used for the next step without any additional purification or analysis.

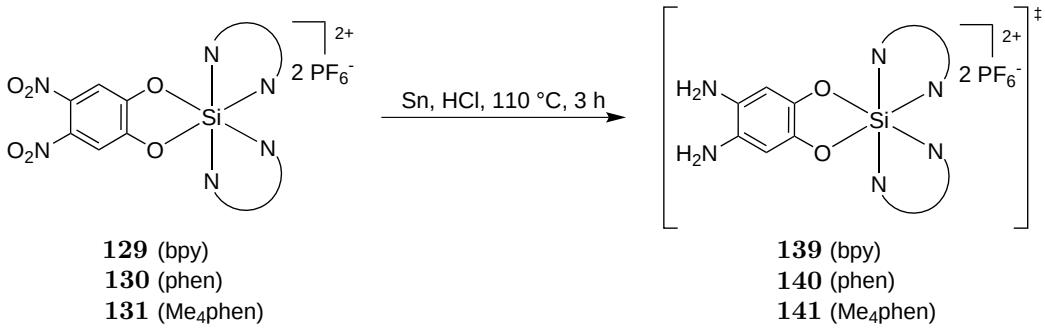

Scheme 31: Reduction of the dinitro substituted silicon(IV) complexes **129**, **130** and **131** to the diamino intermediates **139**, **140** and **141** using tin in hydrochloric acid.

Next, intermediates **139** and **140** were condensed with various substituted oxidized pyrene fragments which were synthesized according to a procedure published by Harris and co-worker using a ruthenium(III) chloride catalyzed oxidation.[264] Due to the low stability of the intermediates and to obtain

a reliable quantification of the yield, all syntheses were performed via a two step route starting from (4,5-dinitro-1,2-catecholato)bis(polypyridyl) silicon(IV) complexes **129** and **130**, respectively. After the reduction using tin in hydrochlorid acid, the intermediates **139** and **140** were reacted with oxidized pyrene fragments in acetonitrile at room temperature overnight (Scheme 32). The corresponding phenazine complexes **143**–**151** were obtained in yields of 12–37 % over two steps after purification by silica gel flash column chromatography and precipitation with ammonium hexafluorophosphate.

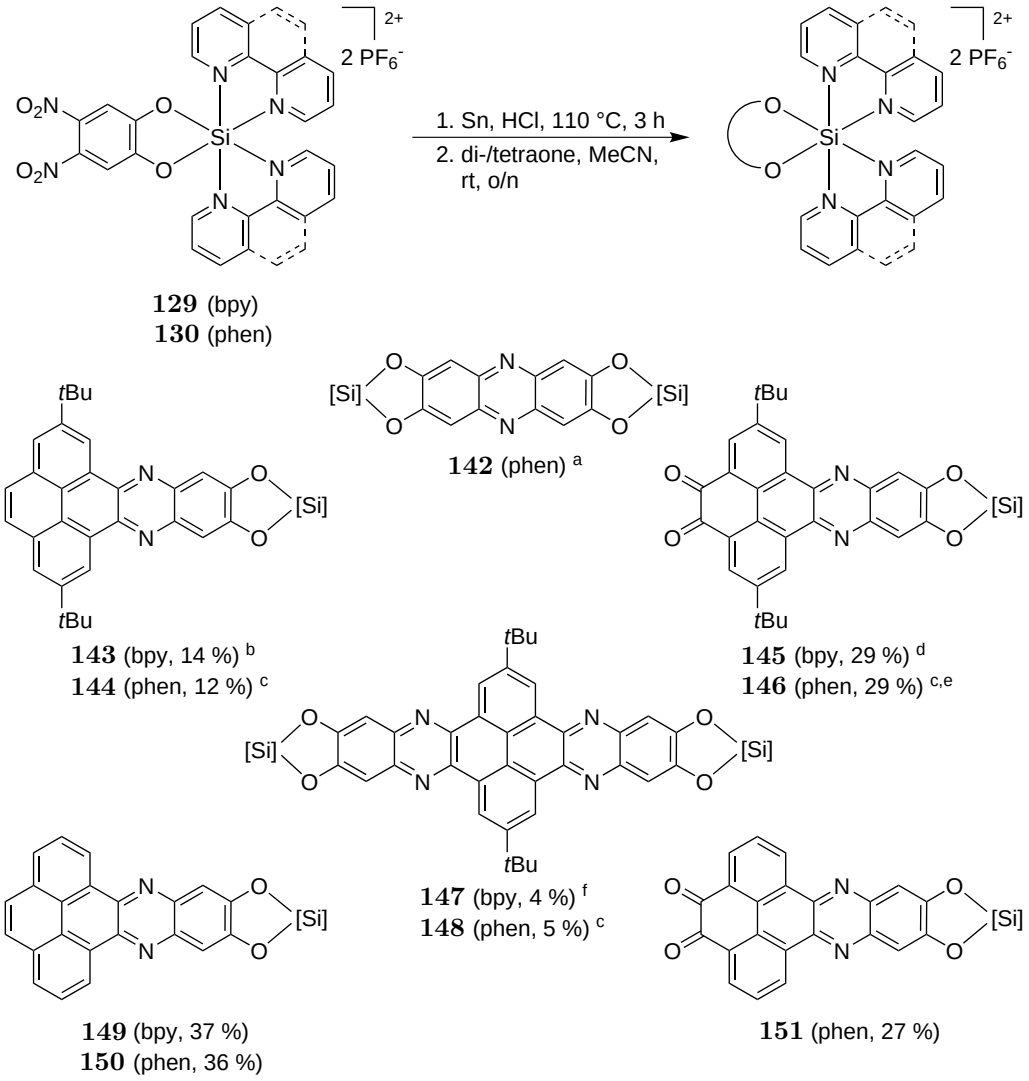

Scheme 32: Two-step condensation reaction starting from (4,5-dinitro-1,2-catecholato)silicon(IV) complexes **129** and **130** to obtain the phenazine derivatives **143**–**151**. The yields are given over two steps. ([a] The dinuclear silicon complex could not be isolated. [b] Starting with a 3:1 mixture of DTBPDO and DTBPTO, **145** was also isolated in a yield of 16 %. [c] Synthesized by Sebastian Weber during a research internship in the Meggers group.[265] Starting with a 3:1 mixture of DTBPDO and DTBPTO, the complexes **144**, **146** and **148** were isolated. [d] Starting with DTBPTO, dinuclear complex **147** was isolated in a yield of 4 %. [e] Due to its low solubility, the complex was isolated as the nitrate salt. [f] Side product of the condensation reaction to obtain **145**.)

Interestingly, the dinuclear silicon complexes **147** and **148**, bearing a charge of +4, could also be isolated in very low yields if 2,7-di-*tert*-butylpyrene-4,5,9,10-tetraone was used as the condensation substrate. The yield might be improved by a condensation reaction of the dione **145** and **146** with the

intermediate **139** and **140** but was not studied any further. Anyhow, the *tert*-butyl groups of **147** and **148** were crucial for the successful isolation of the complexes as similar complexes without them could not be obtained. The reason for this observation may be the purification by column chromatography. The big planar system is capable of forming strong $\pi\pi$ interactions and together with the charge of +4 this may result in a strong affinity to the silica gel. The condensation of the reactive (diamino) intermediate **140** with the (1,2-benzoquinone-4,5-diolato)silicon(IV) complex **95** was also investigated using different reaction temperatures (room temperature, heating to 40 °C). But, the dinuclear silicon(IV) complex **142** could not be isolated. Somehow, dione complex **95** seems to be very unreactive towards a condensation as it may be a poor electrohile due to the high electron density in the ring.

Further enlargement of the planar system of complexes **145** and **146** was achieved by a second, acid catalyzed condensation reaction (Scheme 33). Therefore, both complexes were reacted with ethylenediamine, *ortho*-phenylenediamine or 2,3-diaminonaphthalene in a mixture of acetonitrile and water (2:1) in the presence of catalytic amounts of acetic acid at 75 °C over night. After column chromatography on silica gel and anion metathesis, complexes **152**–**156** were obtained as hexafluorophosphate salts in yields of 45–92 %.

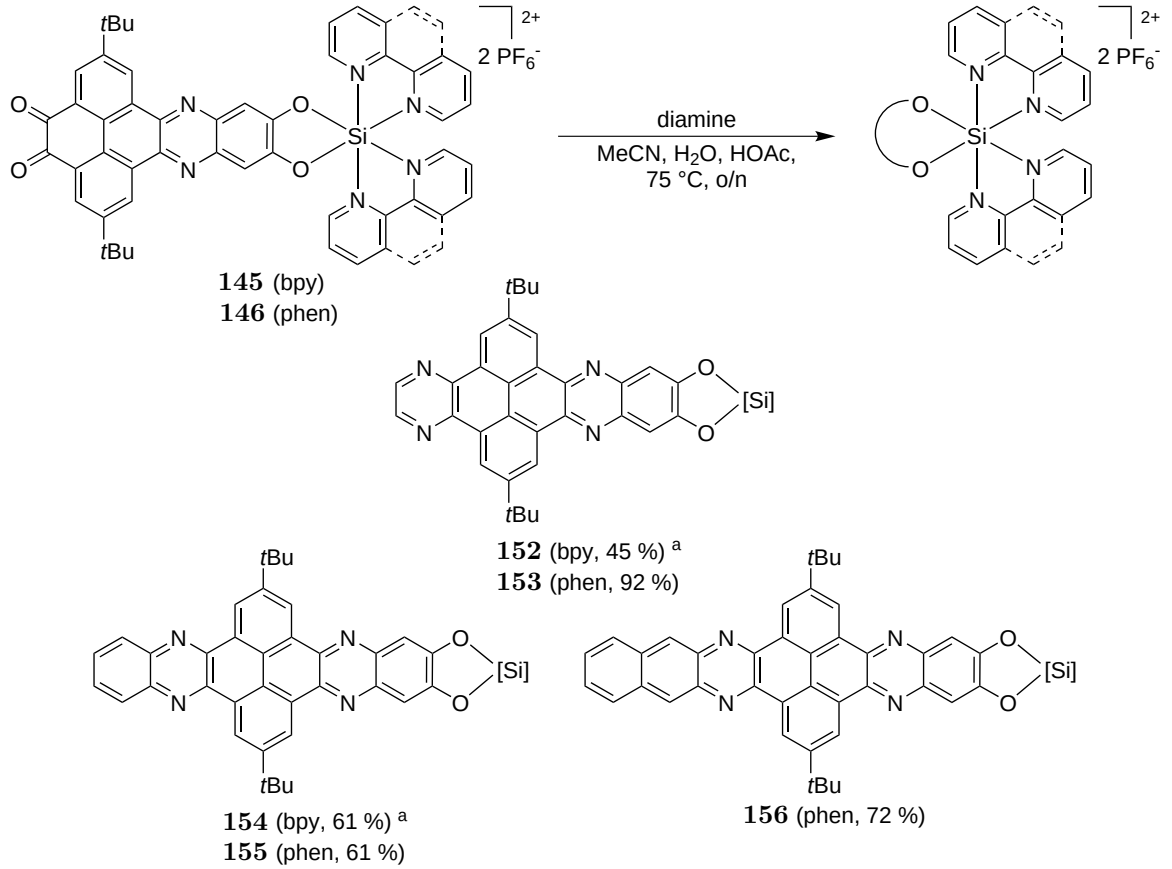

Scheme 33: Condensation of complexes **145** and **146** with different diamines. ([a] Synthesized by Sebastian Weber during a research internship in the Meggers group.[265])

Next, the scope of the condensation was expanded to obtain a simple way to introduce different functional groups that can be useful for further modifications. Therefore, the reaction of diamino intermediate **140** with various aldehydes was studied as a model system. Using the discussed two-

step synthesis with substituted benzylic and aliphatic aldehydes, the (benzimidazolato)silicon(IV) complexes **157**–**169** were obtained in moderate yields (Scheme 34). The reaction turned out to be very mild tolerating various functionalities like nitro groups, alkynes, and halogens. Furthermore, the introduction of even charged functional groups like methyl pyridinium (**159**) or trimetyl ammonium (**160**) was achieved in reasonable yields.

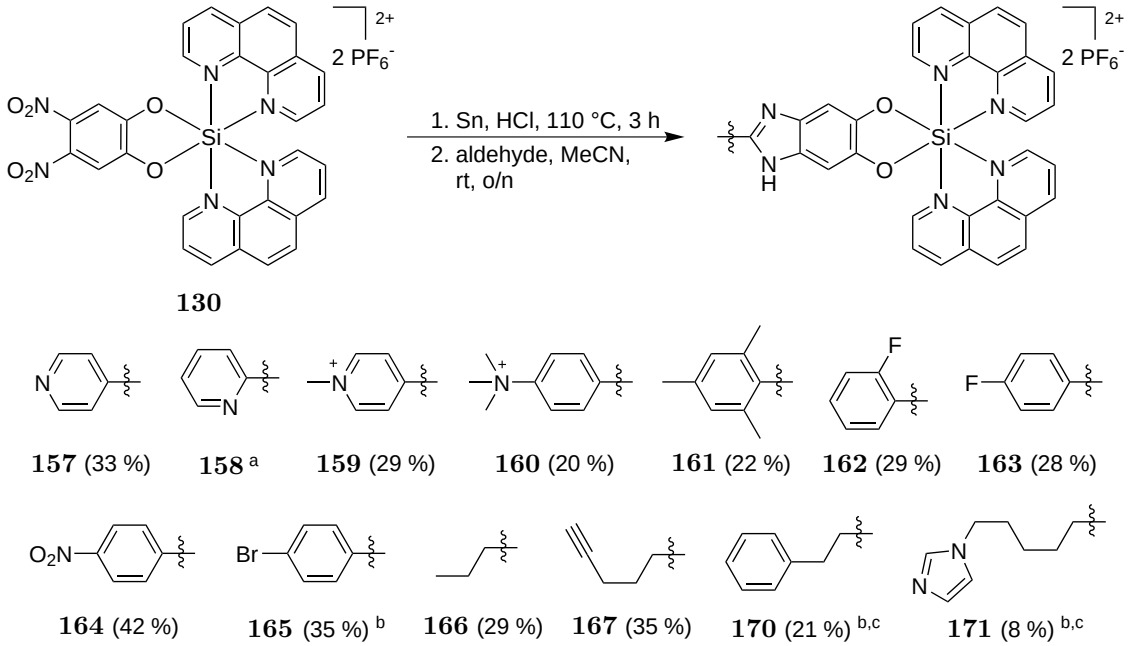

Scheme 34: Condensation of complexes **130** with different substituted benzylic and aliphatic aldehydes. The yields are given over two steps. ([a] Synthesized by Andreas Schrimpf during a research internship in the Meggers group.[230] No yield is given due to the high amount of salt in the product. The condensation was performed at 50 °C. [b] Synthesized by Sebastian Ullrich during a research internship in the Meggers group.[244] The condensation was performed at 60 °C. [c] Isolated as the chloride salt, yield is given over three steps.)

In addition, the two alkyne complexes **172** and **173** (Figure 46) were obtained in yields of 32 % and 60 % starting from complexes **129** and **131**, respectively.

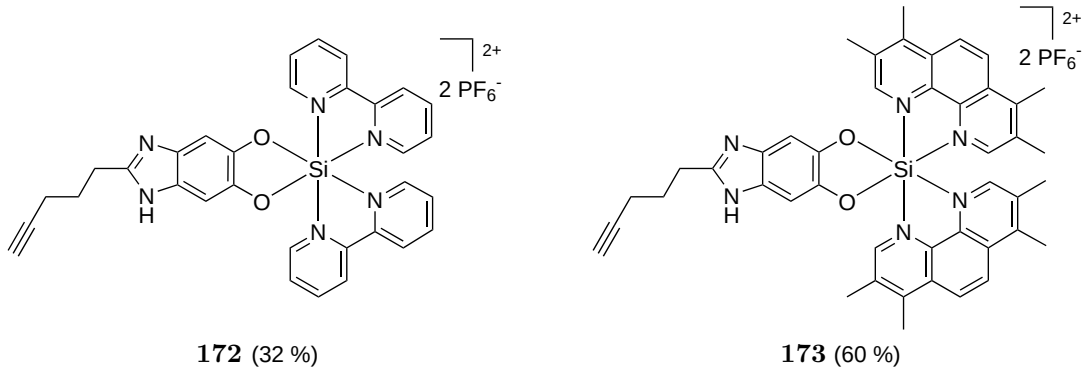

Figure 46: Synthesized alkyne substituted silicon(IV) complexes. The yields are given over two steps starting from **129** and **131**, respectively.

Taken all together, this synthesis strategy of condensing an functionalized aldehyde with a (diamino)silicon(IV) intermediate is a very powerful modification tool for hexacoordinate silicon complexes. Further experiments with the alkyne complexes **167**, **172** and **173** were discussed in chapter 3.5.

Complex **159** was further characterized by crystal structure analysis, confirming the octahedral coordination sphere of the silicon center as well as the 2-(1-methylpyridin-1-ium-4-yl)-1*H*-benzo[*d*]imidazole-5,6-diolato structure of the ligand (Figure 47). Single crystals suitable for this analysis were obtained upon slow solvent evaporation of a solution of complex **159** in acetonitrile at room temperature. Complex **88** crystallized as beige plates in the triclinic space group P −1 with two formula units per unit cell. Interestingly, a structure with two different counterions (1.35 hexafluorophosphate, 1.65 nitrate) was obtained. The counterion coordinated to the imidazole N-H showed a structural disorder (see Appendix). Together with the complex, two formula units of acetonitrile as crystal solvent were incorporated in the crystal structure.

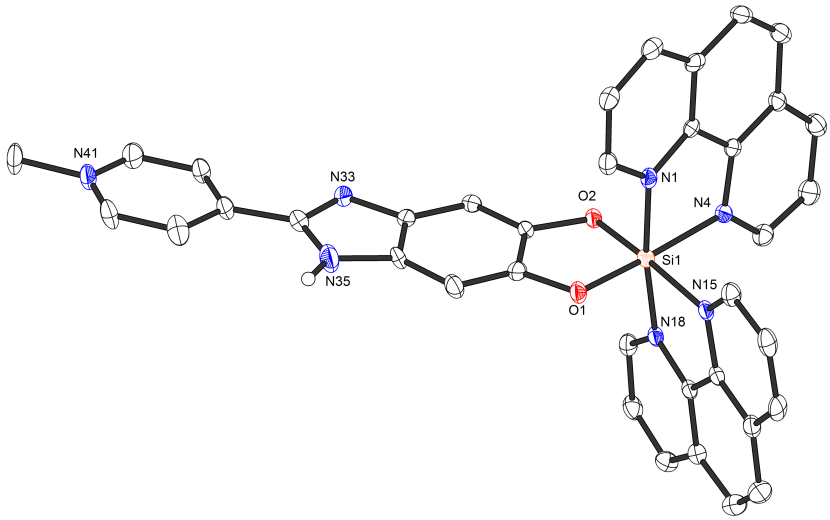

Figure 47: Crystal structure of complex **159**. ORTEP drawing with 50 % probability thermal ellipsoids. The PF_6^- and NO_3^- counterions and solvent are omitted for clarity. Selected bond lengths [Å] and angles [°]: N1–Si1 1.931(3), N4–Si1 1.951(3), N15–Si1 1.938(3), N18–Si1 1.919(3), O1–Si1 1.711(2), O2–Si1 1.707(2), O2–Si1–O1 92.84(10), O2–Si1–N18 91.56(11), O1–Si1–N18 93.97(11), O2–Si1–N1 92.07(10), O1–Si1–N1 92.45(11), N18–Si1–N1 172.46(11), O2–Si1–N15 174.59(11), O1–Si1–N15 87.72(11), N18–Si1–N15 83.04(11), N1–Si1–N15 93.28(11), O2–Si1–N4 88.42(11), O1–Si1–N4 174.99(12), N18–Si1–N4 90.85(11), N1–Si1–N4 82.65(11), N15–Si1–N4 91.49(11).

For some *in-vitro* investigations of the binding of the complexes synthesized to DNA by ^{1}H-NMR experiments, a certain water solubility of the complexes is needed. As the hexafluorophosphate salts are often poorly soluble in water, the counterion was exchange to chloride increasing the water solubility. Using the general strategy for the anion metathesis discussed in chapter 3.2.2 (Scheme 25) the chloride salts in Figure 48 were obtained in yields of 73–93 %.

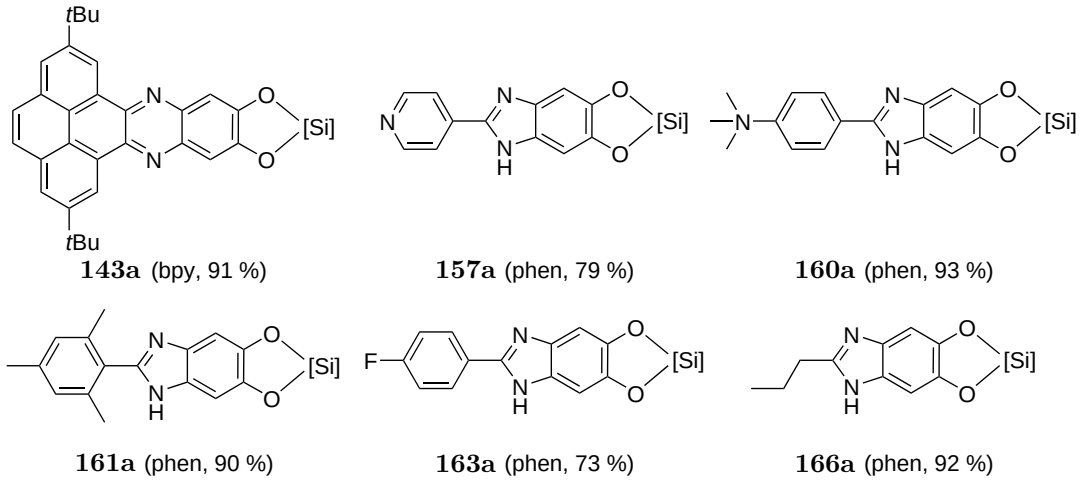

Figure 48: Synthesized chloride salts (with [Si] = $Si(bpy)_2$ or $Si(phen)_2$) according to the method discussed in chapter 3.2.2 (Scheme 25).

3.2.5. Electrophilic Aromatic Substitutions

Besides cross-coupling reactions, the Friedel-Crafts reactions are very fertile tools for building up carbon-carbon bonds.[234,248,266] With regard to the introduced residue, there are two different reactions known. Both have in common that a aromatic system is attacked by a strong Lewis acid, often aluminum trichloride or sulphuric acid, activated electrophile.[234,248] The reaction of the aromatic system with an alkyl halide or an alcohol is called Friedel-Crafts alkylation introducing an alkyl substituent.[234,248] Due to the +I effect of the introduced residues, the product of this Lewis acid catalyzed reaction is more nucleophilic compared to the starting material leading to a higher reactivity and thus to an unwanted overalkylation.[234,248] Preventing this drawback, the Friedel-Crafts acylation, a reaction of an aromatic system with an acyl chloride or anhydride, is affording a ketone substituent.[234,248] Possessing a -I effect of the formed carbonyl group, the product of this reaction is less active than the starting material inhibiting additional alkylations.[234,248]

As the benzene-1,2-diolato ligand of silicon(IV) complex **88** is electron rich, it seemed to be a good substrate for the Friedel-Crafts reactions. First, a double acylation was tried using a procedure published by Danielsen in 1996.[267] Therefore, complex **88** was reacted with phthalic anhydride in the presence of anhydrous aluminium trichloride in acetonitrile at 80 °C for three days (Scheme 35). Unfortunately, only starting material was recovered after purification by column chromatography.

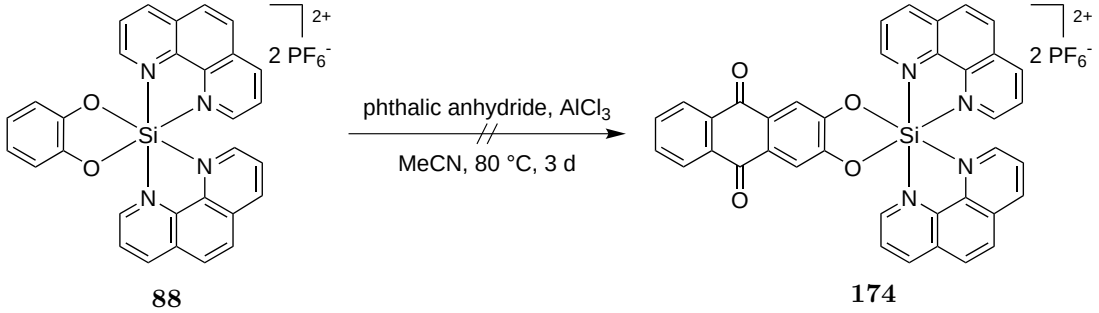

Scheme 35: Attempt to synthesize complex **174** by a Friedel-Crafts acylation.

Next, a bisbromomethylation of complex **88** was tried. To accomplish this, a literature procedure of Tayama *et al.* was adopted.[268] Hence, complex **88** was reacted with *para*-formaldehyde and stoichiometric amount of hydrogen bromide in acetic acid at room temperature for 23 hours (Scheme 36). After purification by silicon gel column chromatography, single crystals suitable for X-ray analysis had formed and were measured. Unfortunately, the structure could not be solved as a mixture of starting material (30 %) and a complex bearing a new ring system was formed. The structure could not be identified and due to the fact that no bromine atom was present in the structure and an inseparable mixture of products was obtained, this synthesis was not investigated any further.

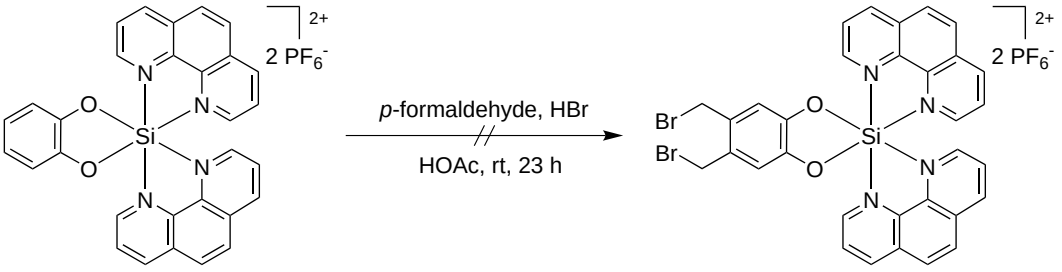

88 **175**

Scheme 36: Attempt to synthesize complex **175** by a bisbromomethylation.

Finally, a Friedel-Crafts alkylation at the hexacoordinate silicon complexes **88** and **90** was studied using various reaction conditions (Scheme 37, Table 5).[234] Therefore, complex **88** or **90** were reacted with *tert*-butyl chloride or *tert*-butanol in the presence of a Lewis acid under an atmosphere of nitrogen. All reaction mixtures were purified by column chromatography on silica gel and the anion was exchanged to hexafluorophosphate. Anyhow, only starting material could be recovered in all cases which was quite surprising as the benzene-1,2-diolato ligand should be a very good nucleophile and other electrophilic aromatic reactions, like for example the nitration, are obtained under very mild conditions (see chapter 3.2.3). Taken all together, the carbon-carbon bond formation at the hexacoordinate silicon(IV) complexes via a Friedel-Crafts reaction does not lead to the desired result, just like cross-coupling reactions.

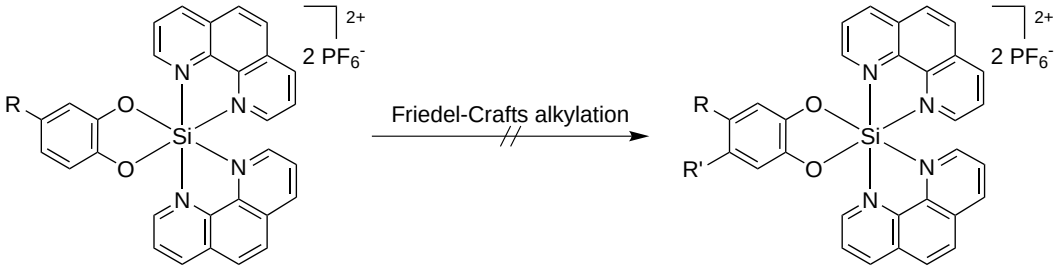

88 (R = H)
90 (R = Me)

176 (R = R' = *t*Bu)
177 (R = Me, R' = *t*Bu)

Scheme 37: Attempt to react complexes **88** and **90** in a Friedel-Crafts alkylation.

Table 5: Screening of different reaction conditions for the FRIEDEL-CRAFTS alkylation of complexes **88** and **90**. All reactions were carried out in anhydrous acetonitrile under an atmosphere of nitrogen.

Complex	Substrate	Acid	Temperature / Time
88	*tert*-butyl chloride	$AlCl_3$	rt / 20 hours
88	*tert*-butanol	H_3PO_4	80 °C / 1.5 hours
88	*tert*-butanol	H_2SO_4	90 °C[a] / 24 hours
90	*tert*-butanol	H_2SO_4	80 °C / 24 hours

[a] Reaction was performed in a pressure vessel.

The direct coordination of 3,4-dihydroxybenzaldehyde to a silicon(IV) complex could only be achieved in very poor yields as discussed in chapter 3.1. Therefore, it was tried to modify the (benzene-1,2-diolato)silicon(IV) complex **88** in a VILSMEIER-HAACK reaction as this reaction allows the introduction of a carbonyl group into activated aromatic systems[269,270] with for example amino substituents[270] or even into an indol structure.[271] Adopting a procedure of LAMBOOY,[269] complex **88** was added under an atmosphere of nitrogen to an ice-cold mixture of phosphoryl chloride in *N,N*-dimethylformamide. After heating to 100 °C over night, the reaction mixture was concentrated and purified by flash column chromatography on silica gel. Unfortunately, only starting material was isolated although different amounts of phosphoryl chloride (1.0–2.9 eq.) were used. The reaction was not investigated any further.

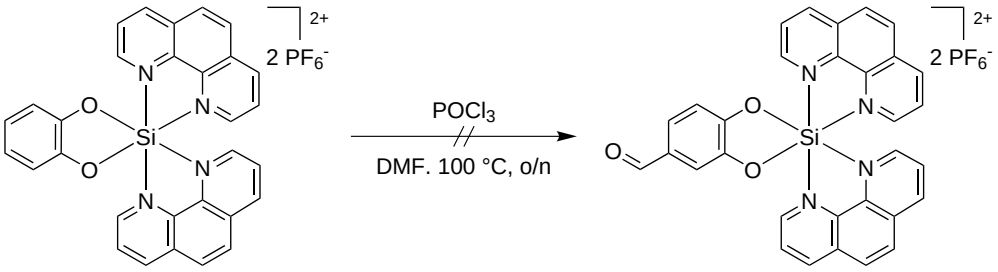

88 **92**

Scheme 38: Attempt to synthesize the aldehyde substituted complex **178** via a VILSMEIER-HAACK reaction.

3.2.6. Biological Activity

Getting an idea of the biological activity of some of the synthesized silicon(IV) complexes, the capability of complexes **87**, **88**, **145** and **157** to interact with duplex DNA was investigated next by utilizing the MCGHEE-VON HIPPEL method.[145,272] Therefore, an UV/Vis-absorption spectrum of the corresponding complex (20 µM) in Tris-buffer (5 mM Tris-HCl, 20 mM NaCl, pH 7.4) at room temperature was measured. The solution was then titrated with *calf thymus* DNA (1.54 mM) monitored by UV/Vis spectroscopy. Upon addition of the DNA, the absorption of the complex decreased. The decrease of absorption at a specific wave length was finally plotted as a function of increasing DNA concentration. Fitting the obtained plot using the MCGHEE-VON HIPPEL equation (1) yielded the

binding constant (k_B) and the binding size s.[145,272] The UV/Vis-absorption titration spectrum of complex **145** including the McGhee-von Hippel plot is shown in Figure 49 by way of example.

$$\frac{\epsilon_a - \epsilon_f}{\epsilon_b - \epsilon_f} = \frac{b - \sqrt{\frac{2k_B^2 C_t [DNA]_t}{s}}}{2k_B C_t} \tag{1}$$

$$b = 1 + k_B C_t + \frac{k_B [DNA]_t}{2s} \tag{2}$$

with C_t and $[DNA]_t$ = total complex and DNA concentrations, s = base pair binding site size and ϵ_a = extinction coefficient of the complex at a given DNA concentration, ϵ_b = extinction coefficient when fully bound to DNA (determined from the plateau of the DNA titration, where addition of DNA did not lead to any further absorbance change), and ϵ_f = extinction coefficient of the complex in the absence of DNA.[145,272]

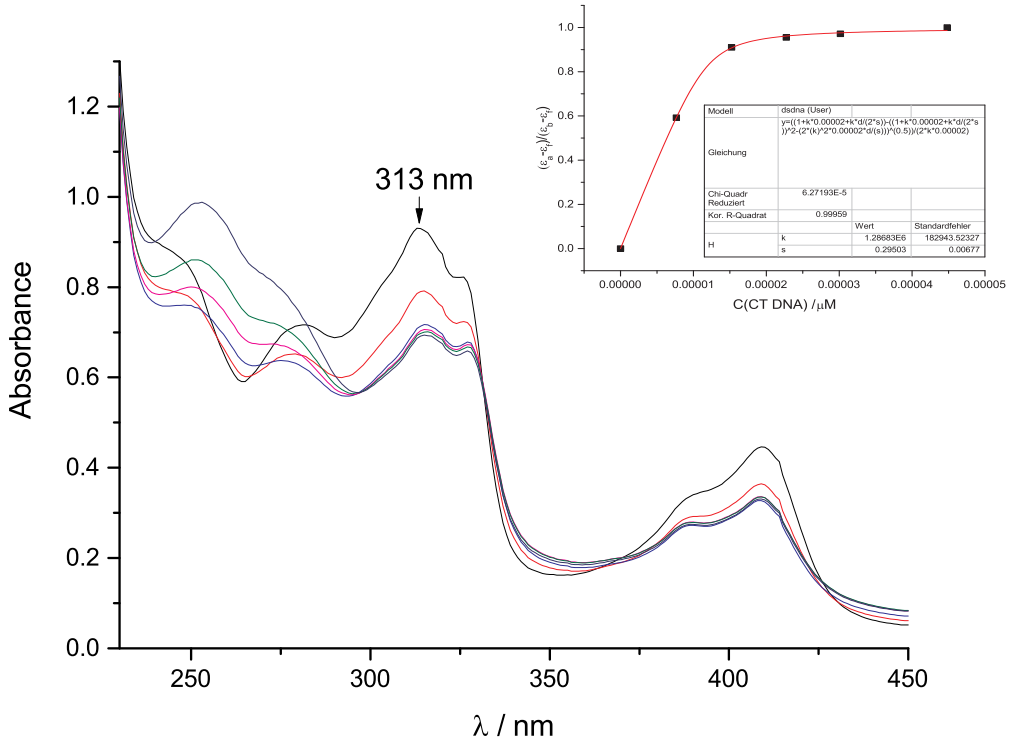

Figure 49: UV/Vis-absorption spectra of complex **145** (20 µM) in Tris-buffer (5 mM Tris-HCl, 20 mM NaCl, pH 7.4) upon titration with *calf thymus* DNA at room temperature. Insert: plot of $(\epsilon_a - \epsilon_f)/(\epsilon_b - \epsilon_f)$ at 357 nm versus DNA concentration, with ϵ_a = extinction coefficient of the complex at a given DNA concentration, ϵ_b = extinction coefficient when fully bound to DNA, and ϵ_f = extinction coefficient of the complex in the absence of DNA.

The obtained binding constants are tabulated in Table 6. Interestingly, complex **88** did not show any decrease of the absorption after addition of increasing amount of *calf thymus* DNA. Hence, a binding constant could not be determined. Similar results were obtained for complex **87**. However, due to a slightly absorption decrease, a binding constant of about $10^5\,\mathrm{M}^{-1}$ was determined. As a matter of fact, the value is not very reliable since the single points of the measurement have a huge variance (see Appendix E).

Table 6: Binding constants k_B and binding site size s of the silicon(IV) complexes **87**, **88**, **145** and **157** to *calf thymus* DNA. The values were obtained by plotting the decrease of the absorption at a specific wavelength λ as a function of increasing DNA concentration using the McGhee-von Hippel equation.[145,272]

Complex	λ /nm	k_B /M^{-1}	**s**
87[a]	325	$(4.4 \pm 3.9) \times 10^5$	1.76 ± 0.37
88[b]	–	–	–
145[a]	313	$(1.3 \pm 0.2) \times 10^6$	0.30 ± 0.01
157[c]	340	$(7.5 \pm 0.3) \times 10^5$	2.23 ± 0.41

[a] Single determination. [b] No absorption decrease upon addition of DNA. [c] Repeat determination.

Complex **145** showed a strong binding to duplx DNA with a k_B $=(1.3 \pm 0.2) \times 10^6\,\text{M}^{-1}$ of similar or higher order of magnitude compared to other DNA binding metal complexes (Table 7). This result was very surprising as it was assumed that the two *tert*-butyl groups of the complex may reduce the affinity to duplex DNA since these big groups should prohibit an intercalation mechanism. The binding site size, the number of DNA bases associated with the complex, of $s < 1$ support these thoughts as such values are obtained for hydrophobic molecules that aggregate on the DNA surface.[138,145] In addition, a hypochromicity of 26 % and a bathochromic shift of 2 nm was observed. Since the results for complex **145** were very promising, the modified complex **179**, **180**, **181** and **182** were also tested by Sebastian Weber during his research internship.[265] Unfortunately, no reliable binding constants were obtained as the absorption intensity of complexes changed irregular during titration. A possible reason for this behavior may be due to the solubility problems of the huge complexes in the buffer solution used, leading to a non-constant concentration of the complex in solution. Similar observations were made for complex **149** by Yonggang Xiang during his Ph.D. Thesis.[149]

Complex **157** showed a lower affinity to duplex DNA compared to **145** but its binding site size of $s > 0$ is indicating an intercalative binding motive.[138,145] Although an intercalation should increase the affinity to ds-DNA (for examples see Chapter 3.3.2 and 3.5.3), the lower binding constant of $(4.4 \pm 3.9) \times 10^5\,\text{M}^{-1}$ can be explained by the free rotatability of the pyridine residue. Furthermore, complex **157** showed a strong hypochromicity of 47 % and a modest bathochromic shift of 5 nm.

Table 7: Examples for reported binding constants of different mono and dinuclear metal complexes to *calf thymus* DNA.

Complex	k_B /M^{-1}
$[Si(phen)_2(pyrenediol)](PF_6)_2$	1.7×10^6 [37]
$[Si(phen)_2(bqp)](PF_6)_2$ (**137**)	2.0×10^7 [149]
$[Ru(bpy)_2(dppz)]^{2+}$	$> 1 \times 10^6$ [142]
$[Ru(dppz)(phen)_2]^{2+}$	$(1–6) \times 10^6$ [135,136,138]
$[Ru(bpy)_2(tpphz)]^{2+}$	1.8×10^6 [137]
$[Os(Me_2dppz)(phen)_2]^{2+}$	$> 1 \times 10^6$ [130]
cis-$[Rh_2(\mu\text{-}O_2CCH_3)_2(dppz)_2]^{2+}$	1.3×10^6 [145]
$[Ru(dppz)(NH_3)_4]^{2+}$	1.2×10^5 [138]
$[Ru(dmphen)_3]^{2+}$	1.6×10^4 [139]
$[Ru(dmphen)_2(phen)]^{2+}$	6.5×10^3 [139]
$[Ru(phen)_3]^{2+}$	5.5×10^3 [139]
cis-$[Rh_2(\mu\text{-}O_2CCH_3)_2(dppz)(\eta^1\text{-}O_2CCH_3)(CH_3OH)]^{2+}$	2.4×10^5 [145]
$[Ru(phen)_2(\mu\text{-tpphz})Ru(phen)_2](NO_3)_4$	1.1×10^7 [140]
$[Ru(bpy)_2(\mu\text{-tpphz})Ru(bpy)_2](NO_3)_4$	3.3×10^8 [140]
$[Ru(bpy)_2(\mu\text{-tpphz})Ru(bpy)_2](PF_6)_4$	5.1×10^7 [144]
$[Ru(phen)_2(\mu\text{-tatpp})Ru(phen)_2](NO_3)_4$	1.1×10^7 [140]
$[Ru(dppz)_2(\mu\text{-TBphen}_2)Ru(dppz)_2](NO_3)_4$	$(8.8 \pm 1.1) \times 10^6$ [151]

3.3. Tris-heteroleptic Silicon(IV) Complexes

3.3.1. Synthesis and Modification

The synthesis of tris-heteroleptic bis(polypyridyl)(benzene-1,2-diolato)silicon(IV) complexes was studied as this structure allows both the introduction of a DNA binding ligand, like dppz,[128–130,135,137,138,141,142,145,223] together with the possibility of modifying the benzene-1,2-diolato ligand. The tris-heteroleptic complex $[Si(DHB)(dppz)(phen)](PF_6)_2$ (**184**) was first synthesized by Chen Fu using the two step synthesis introduced in chapter 3.1 in a yield of 9 %.[150] Adopting and modifying his preparation protocol, each of the two tris-heteroleptic silicon(IV) complexes **183** and **184** were synthesized in a one-pot reaction (Scheme 39). Therefore, dppz (**185**, 1.1 equivalents) and the polypyridine (1 equivalent, 2,2'-bipyridine or 1,10-phenanthroline) were reacted with silicon tetraiodide in anhydrous chlorobenzene under an atmosphere of nitrogen at 110 °C over night. To minimize the formation of the bis-heteroleptic species, it was crucial to first heat the suspension of the ligands to 80 °C before silicon tetraiodide was added at once since the solubility of dppz in the used solvent is much lower compared to 2,2'-bipyridine or 1,10-phenanthroline. The diiodo intermediates were not isolated but reacted *in situ* with 1,2-dihydroxybenzene at 110–120 °C for additional 14–28 hours. Purification via silica gel flash column chromatography and precipitation with ammonium hexafluorophosphate gave the tris-heteroleptic complexes **183** and **184** in a yield of 11 % and 12 %, respectively. In addition, the corresponding bis-heteroleptic complexes $[Si(DHB)(pp)_2](PF_6)_2$ **87** and **88** were isolated in yields of 10–15 %. The ^{1}H-NMR spectra of complex **184** is given in Figure 50 as an example for tris-heteroleptic silicon(IV) complexes.

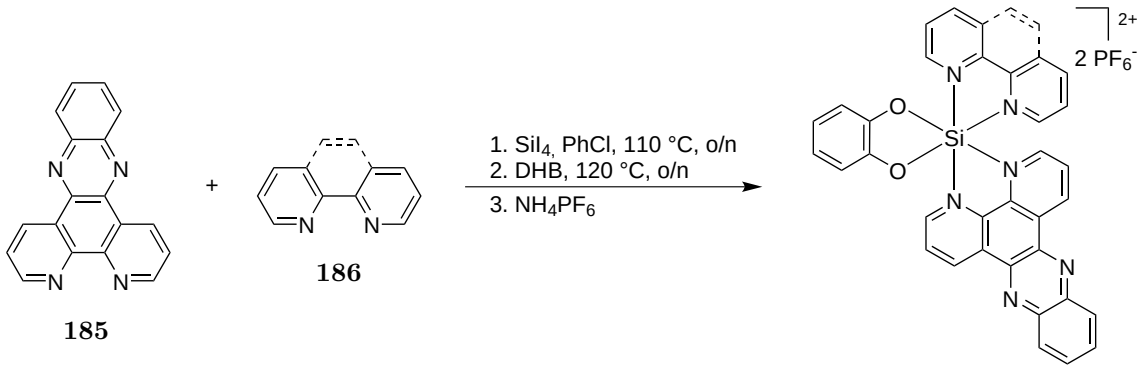

Scheme 39: Synthesis of tris-heteroleptic silicon(IV) complexes **183** and **184**. The yield are given over two steps. As a side product, the bis-heteroleptic complexes **87** and **88** was isolated in 15 %[a)] and 10 %[b)], respectively.

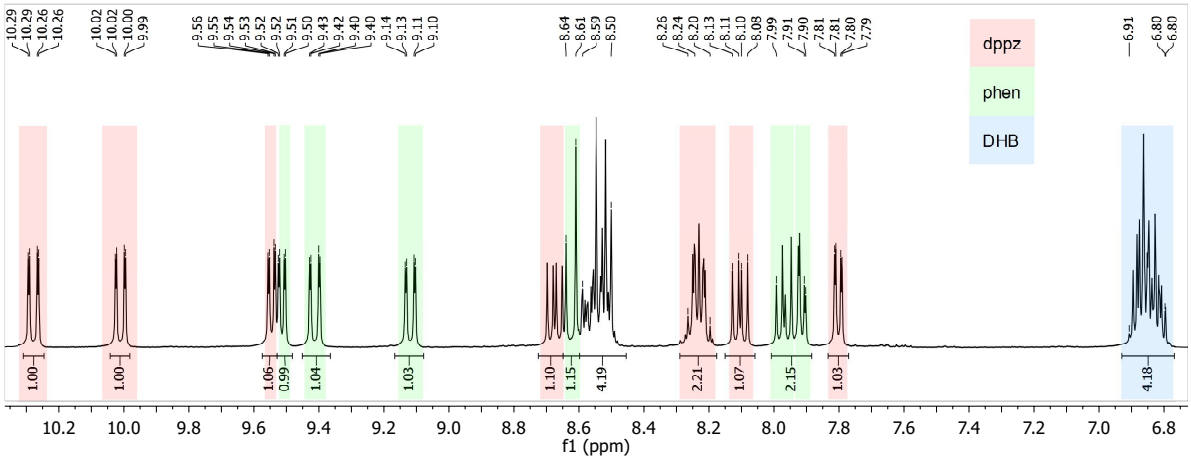

Figure 50: ^{1}H-NMR of complex **184** (29 mM) in acetonitrile-d_3.

The octahedral tris-heteroleptic coordination of the silicon center was verified by X-ray crystallography of complex **184** (Figure 51). Single crystals suitable for crystal structure analysis were obtained upon slow precipitation from a concentrated solution of complex **184** in acetonitrile at room temperature. Complex **184** crystallized as yellow column in the triclinic space group P −1 with two formula units per unit cell. Together with the complex, two formula units of the counter ion PF_6^- and 1.4 formula units of acetonitrile as crystal solvent were incorporated in the crystal structure.

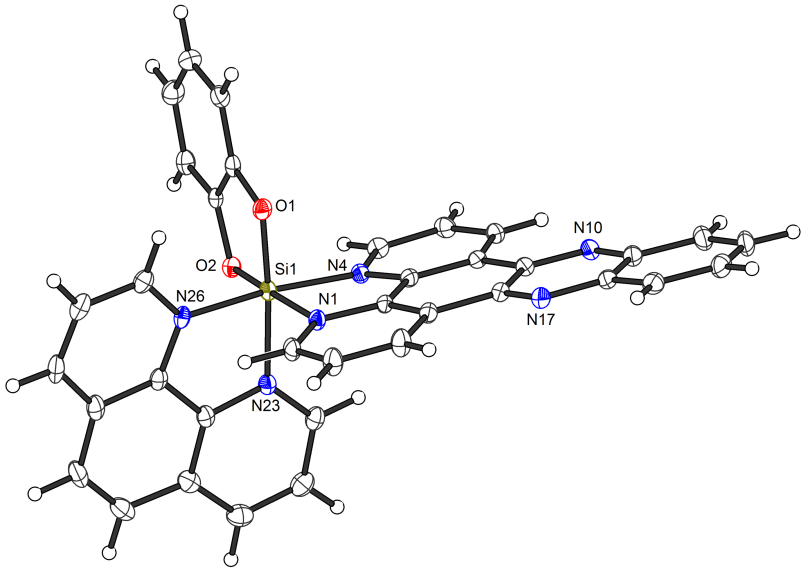

Figure 51: Crystal structure of complex **184**. ORTEP drawing with 50 % probability thermal ellipsoids. The PF_6^- counterions and solvent are omitted for clarity. Selected bond lengths [Å] and angles [°]: Si1–O2 1.7101(12), Si1–O1 1.7107(12), Si1–N26 1.9265(15), Si1–N4 1.9329(15), Si1–N1 1.9402(15), Si1–N23 1.9423(15), O2–Si1–O1 93.20(6), O2–Si1–N26 94.03(6), O1–Si1–N26 92.02(6), O2–Si1–N4 92.86(6), O1–Si1–N4 91.77(6), N26–Si1–N4 171.94(6), O2–Si1–N1 174.64(6), O1–Si1–N1 89.73(6), N26–Si1–N1 90.35(6), N4–Si1–N1 82.56(6), O2–Si1–N23 87.07(6), O1–Si1–N23 175.02(7), N26–Si1–N23 83.00(6), N4–Si1–N23 93.18(6), N1–Si1–N23 90.40(6).

The nitration of the benzene-1,2-diolato ligand of the complexes **183** and **184** was performed using the modified method discussed in chapter 3.2.3 (Scheme 40). Complexes **183** and **184** were reacted with fuming nitric acid in glacial acetic acid at 0 °C. During the reaction time of 3.5–4.5 hours, the temperature increased slowly to 18–20 °C. After purification by flash column chromatography on silicon gel and exchange of the counterion to hexafluorophosphate, both dinitrated silicon(IV) complexes (**187** and **188**) were obtained in a yield of 73 %. Shorter reaction times of less than three hours including a lower end temperature of ≤ 14 °C led to an inseparable mixture of the dinitrated and very little of the mononitrated complex as monitored by ^{1}H-NMR spectroscopy. However, these impurities did not disturb continuing experiments and could be removed during the following work-up.

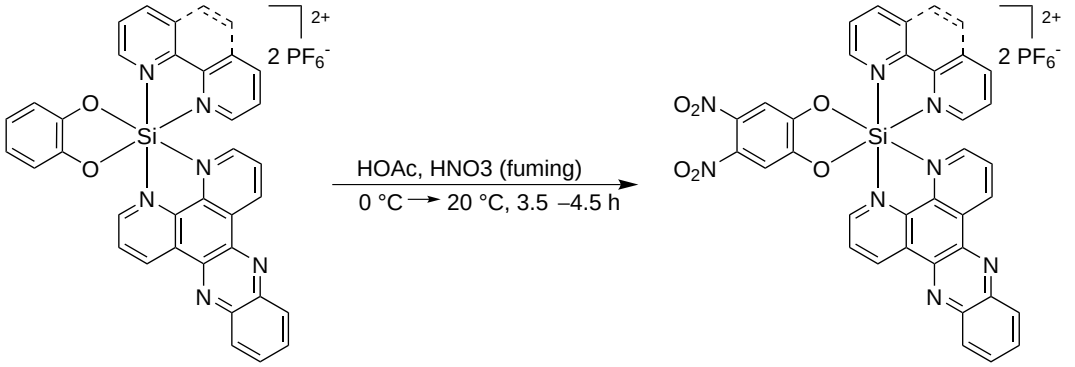

Scheme 40: Nitration of the tris-heteroleptic silicon(IV) complexes **183** and **184** yielding the dinitro complexes **187** and **188**.

The nitro groups of the complexes **187** and **188** were then reduced to amines utilizing tin in half-concentrated hydrochloric acid at 110 °C for three hours. In comparison to the reactions described in chapter 3.2.4, the reaction mixtures turned black after addition of the tin. Nevertheless, the solid obtained upon precipitation with ammonium hexafluorophosphate was further converted with 5-hexynal (**189**) in acetonitrile at room temperature over night. After purification by flash column chromatography on silica gel, the tris-heteroleptic alkyne complex **190** was obtained in a yield of 53 % whereas complex **191** was isolated in 57 %.

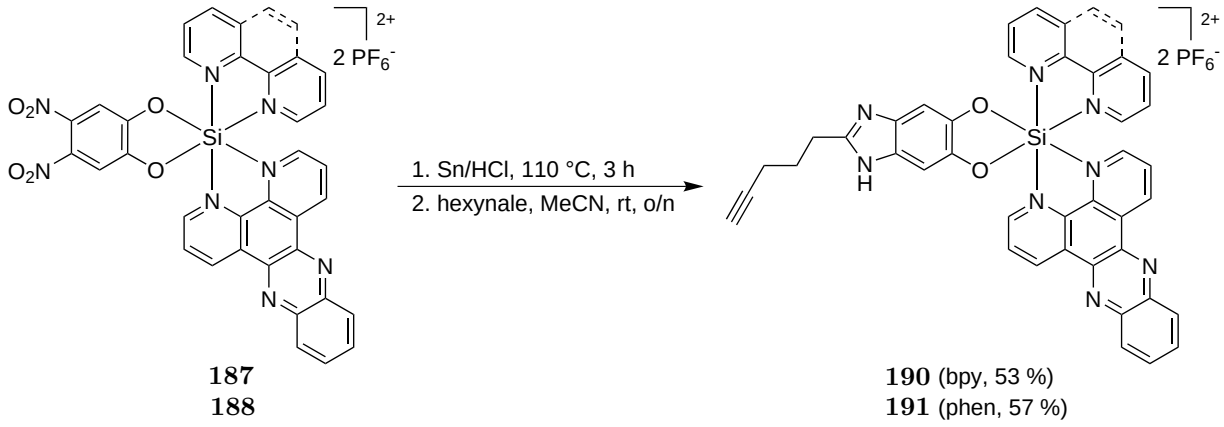

Scheme 41: Synthesis of the tris-heteroleptic silicon(IV) complexes **190** and **191** using the reduction-condensation method described above. The yields are given over two steps.

3.3.2. Biological Activity

Having the tris-heteroleptic silicon(IV) complexes in hand, the binding of complex **184** to *calf thymus* DNA was investigated by way of example. The binding constant k_B was determined by UV-Vis-monitored titration at room temperature in Tris-buffer (5 mM Tris-HCl, 20 mM NaCl, pH 7.4) according to the method discussed in Chapter 3.2.6. Complex **184** (20 µM) exhibited a strong absorption band in the 330–380 nm region with a maximum at 357 nm which arises from a dppz $\pi \rightarrow \pi^*$ ligand-centered charge transfer transition and has been observed in various dppz coordinate transition metal complexes (Figure 52).[130,135,137,138,145]

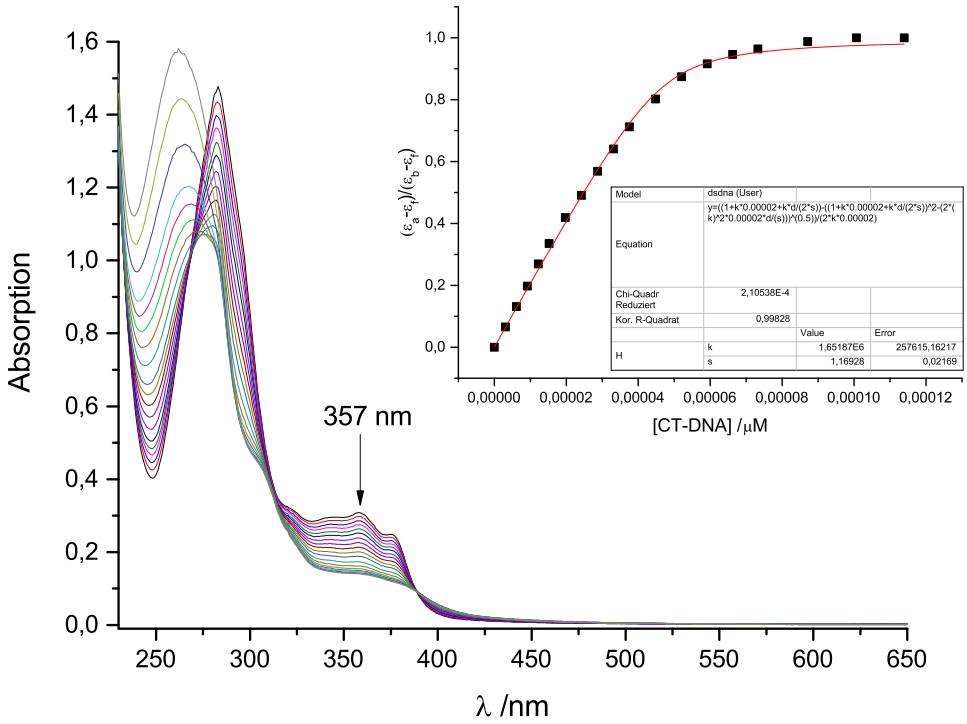

Figure 52: UV/Vis-absorption spectra of complex **184** (20 µM) in Tris-buffer (5 mM Tris-HCl, 20 mM NaCl, pH 7.4) upon titration with *calf thymus* DNA at room temperature. Insert: plot of $(\epsilon_a - \epsilon_f)/(\epsilon_b - \epsilon_f)$ at 357 nm versus DNA concentration, with ϵ_a = extinction coefficient of the complex at a given DNA concentration, ϵ_b = extinction coefficient when fully bound to DNA, and ϵ_f = extinction coefficient of the complex in the absence of DNA. The binding constant was determined to $K_b = (1.6 \pm 0.1) \times 10^6\ \text{M}^{-1}$.

Upon titration with *calf thymus* DNA, the absorption band at 357 nm showed a strong hypochromicity (53 %). Interestingly, no bathochromic shift could be observed. The binding constant was determined to $k_B = (1.6 \pm 0.1) \times 10^6\ \text{M}^{-1}$ and is of similar or higher order of magnitude compared to other DNA binding metal complexes (Table 7). In addition, the binding site size of $s = 1.17 \pm 0.02$ indicates that complex **184** binds ds-DNA by intercalation.[145] This observation is consistent with the literature as the dppz ligand is believed to intercalate between the base pairs of ds-DNA.[130,138,141,145]

3.4. Dinuclear Metal-Silicon(IV) Complexes

3.4.1. Synthesis Strategies

A major aim of this work is the synthesis of multinuclear complexes with at least one silicon(IV) center as these structures would allow new biological applications like for example protein surface recognition or a higher affinity to DNA due to a higher charge. In chapter 3.2.4, the successful synthesis of dinuclear silicon(IV) complexes **147** and **148** was presented. Unfortunately, the complexes were obtained only in very low yields and did not show any fluorescence properties which is crucial for usage as a chemical sensor or as imaging agent. To introduce such luminescence functionality, a transition metal center like ruthenium(II) or iridium(III) should be introduced as these complexes are known to show strong fluorescence properties.[142,144,152,273–280] Hence, the synthesis of dinuclear metal-silicon(IV) complexes and their biological activity was investigated next. As a bridging ligand, dipyrido[3,2-*a*:2',3'-*c*]phenazine-7,8-diol (**195**) was chosen as it provides a coordination site for the silicon as well as for the metal center and is structural similar to the bridging ligand of the known biological active dinuclear transition metal complexes like $[Ru(pp)_2](\mu\text{-tpphz})Ru(pp)_2]^{4+}$.[144,152]

The synthesize of the dinuclear metal-silicon(IV) complexes may be achieved using two different synthetic approaches that were studied more detailed. The first approach is based on a linear synthesis in which the bridging ligand **195** is synthesized primarily (Scheme 42). The ligand can then be reacted with a diiodosilicon(IV) precursor (route A) or with the metal precurser (route B) yielding the mononuclear complexes **193** and **194**, respectively. Further conversion with the corresponding second metal or silicon precursor should yield the dinuclear complex **192**.

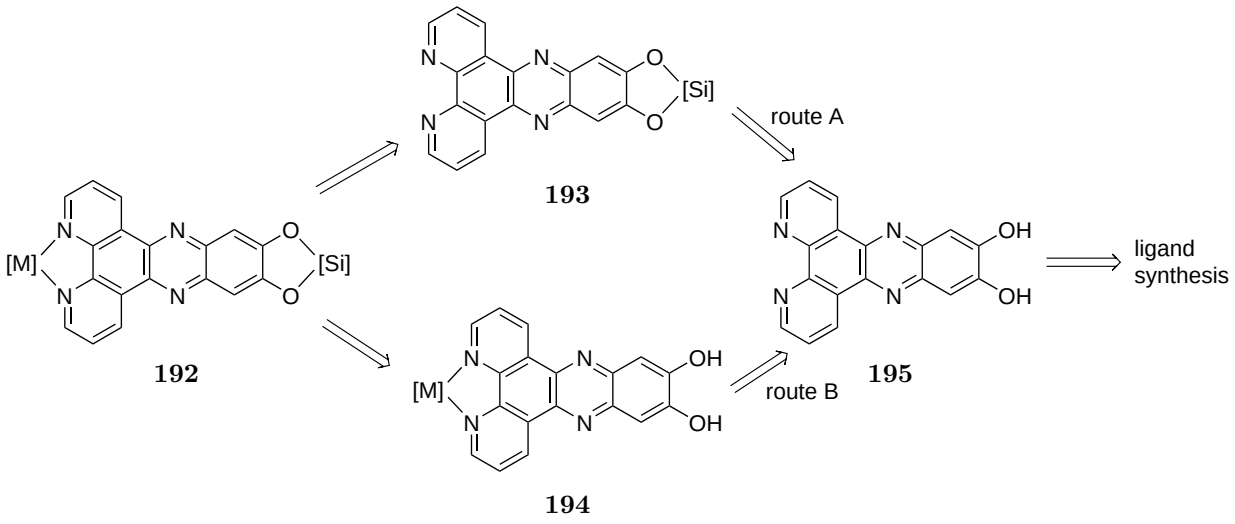

Scheme 42: Retrosynthesis of the linear synthesis approach to obtain dinuclear metal-silicon(IV) complexes.

Otherwise, dinuclear metal-silicon(IV) complexes may be synthesize by a convergent synthesis approach (Scheme 43). Hereby, the key step of the synthesis route is the condensation reaction of a (1,10-phenanthroline-5,6-dione)metal fragment **196** and the (4,5-diaminobenzene-1,2-diolato)silicon(IV) intermediate **197**, in analogy to the condensation reactions discussed in Chapter 3.2.4. The metal fragment should be easily accessible by reaction of the metal precursor with 1,10-phenanthroline-5,6-

dione (**198**). The preparation of the silicon(IV) fragment **197** was discussed previously (Chapter 3.1, 3.2.3 and 3.2.4).

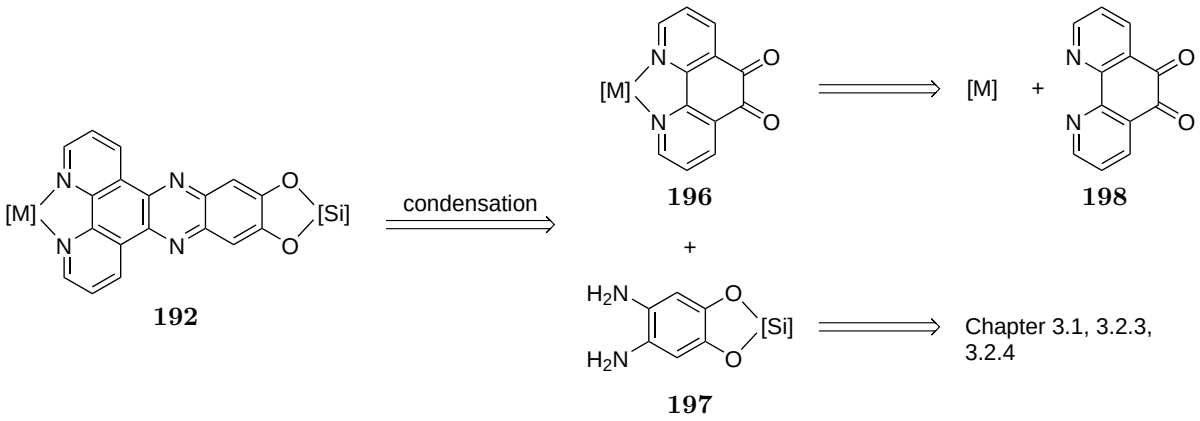

Scheme 43: The condensation reaction of a metal and a silicon(IV) fragment is the key step in the convergent synthesis approach to obtain dinuclear metal-silicon(IV) complexes.

3.4.2. Linear Synthesis

First, route A of the linear synthesis approach was investigated. Therefore, the bridging ligand dipyrido[3,2-*a*:2',3'-*c*]phenazine-7,8-diol (**195**) was prepared first. Using a four step synthesis, ligand **195** was obtained in an overall yield of 22 % (Scheme 44).

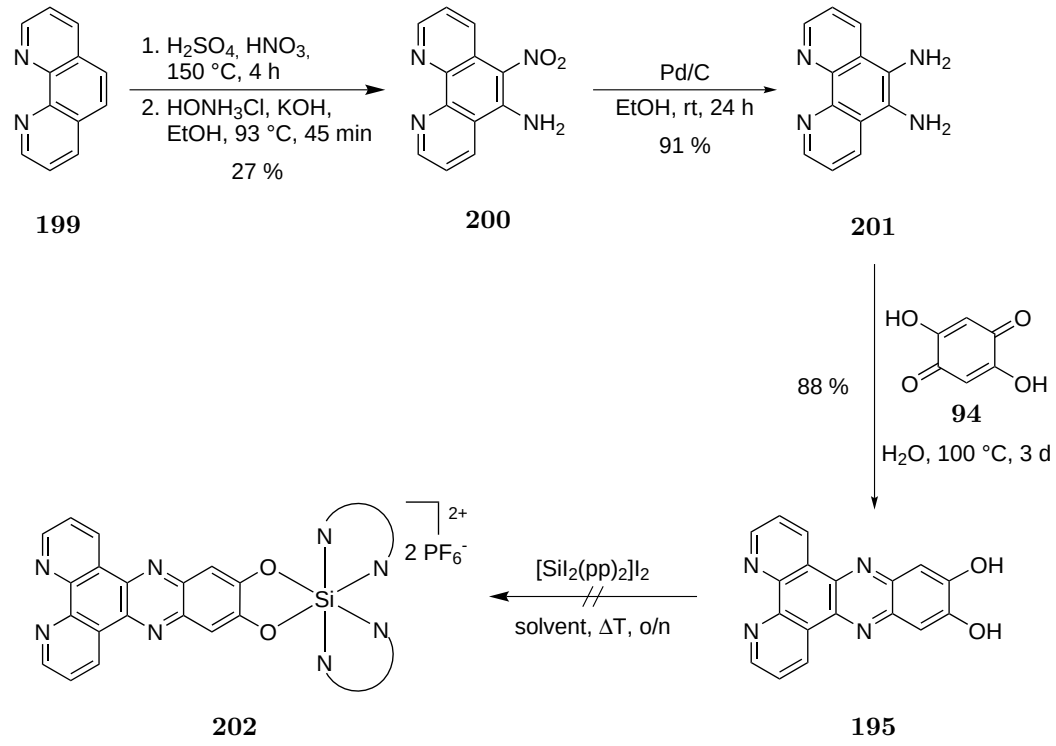

Scheme 44: Synthesis of Dipyrido[3,2-*a*:2',3'-*c*]phenazine-7,8-diol (**195**) and attempt to obtain complexes **202**.

1,10-phenanthroline (**199**) was nitrated in 5-position using a an electrophilic aromatic substitution reaction.[146] Therefore, **199** was reacted with a mixture of nitric and sulphuric acid at 150 °C for three

hours, according to a method of Zhao and co-workers.[146,281] After neutralization of the reaction mixture and isolation of the precipitate by filtration, the obtained solid was reacted in a nucleophilic aromatic substitution yielding 5-amino-6-nitro-1,10-phenanthroline (**200**). Utilizing a procedure published by Gourdon *et al.*, the solid was reacted with hydroxylamine hydrochloride and potassium hydroxide in ethanol at 90 °C for two hours.[146,282] After isolation by filtration, compound **200** was obtained in a yield of 27 % over two steps. Following, the nitro group of compound **200** was reduced to the amine using a palladium on charcoal catalyzed hydrogenation in ethanol at room temperature for 24 hours. Removal of the catalyst by filtration through celite afforded the pure compound **201** in a yield of 91 %. Finally, compound **201** was treated with 2,5-dihydroxy-*p*-benzoquinone (**94**) in water at 105 °C for three days yielding ligand **195** in 88 % after isolation by filtration. The reaction was also performed in ethanol, whereat ligand **195** was isolated in a yield of 84 %. Due to the planar system and the two hydroxy groups that are capable of forming hydrogen bonds, **195** is poorly soluble in all established solvents used in organic or inorganic chemistry. As expected, the poor solubility had a big influence on the complexation of ligand **195** with the silicon precursor $[SiI_2(pp)_2]I_2$ (**85** and **86**). Although different solvents (chloroform, *ortho*-xylene) and reaction conditions (temperature of 90–165 °C, one to three days) were tried, the desired silicon complex **202** could not be isolated. Hence, route B was tried next as it was expected that the solubility of the metal bound complexes **194** in the solvents used would be better compared to the solubility of ligand **195**.

Therefore, ligand **195** was reacted with the iridium precursor $[Ir(\mu\text{-}Cl)(ppy)_2]$[283] in a mixture of anhydrous dichloromethane and methanol (1:1) at 55 °C for two days as well as with the ruthenium precursor $[Ru(bpy)_2Cl_2] \cdot 2\,H_2O$[284] in ethanol under μ-wave irradiation (90 °C, one hour, 150 W) (Scheme 45). In both cases, the desired product was not obtained after column chromatography on silica gel as monitored by LC-MS, HRMS and ^{1}H-NMR spectroscopy. For example, using the ruthenium precursor, an inseparable mixture of products was isolated. The reason for this observation is very likely the low solubility of ligand **195** together with a possible coordination of the metal center to the two hydroxyl groups. Hence, a protecting group approach was investigated next.

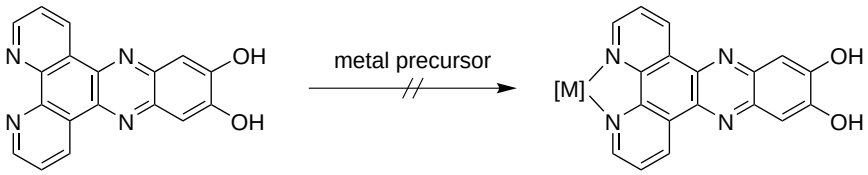

Scheme 45: Attempt to coordinate a metal center (M = $Ir(ppy)_2$ or $Ru(bpy)_2$) to ligand **195**.

The dimethoxy protected ligand **203** was synthesized in a two step synthesis starting from 1,10-phenanthroline (**199**) that was oxidized in position 5 and 6 using potassium bromide in a mixture of concentrated sulphuric and nitric acid at 120 °C for four hours, in accordance with a procedure published by Paw and Eisenberg.[245] After extraction of the neutralized reaction mixture with dichloromethane, 1,10-phenanthroline-5,6-dione (**198**) was obtained in quantitative yield and very good purity. If necessary, **198** could be further purified by recrystallization from ethanol. Next, dione **198** was reacted with 4,5-dimethoxy-1,2-phenylenediamine (**106**, see Chapter 3.1) at 90 °C for six hours. Isolation of the precipitate formed upon cooling to room temperature by simple filtration

afforded ligand **203** in a yield of 70 %. Due to the two methoxy groups, ligand **203** showed a much higher solubility in organic solvents compared to **195**.

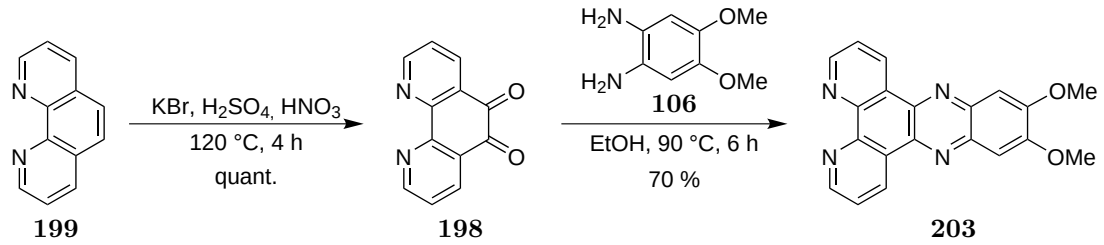

Scheme 46: Synthesis of ligand **203** starting from 1,10-phenanthroline (**199**).

With ligand **203** in hand, the corresponding metal complexes (**204** and **205**) were synthesized next (Scheme 47). In doing so, **203** was reacted with the ruthenium precursor $[Ru(bpy)_2Cl_2] \cdot 2\,H_2O$[284] in ethanol at 90 °C for 60 minutes under μ-wave irradiation. After purification using silica gel column chromatography and precipitation with ammonium hexafluorophosphate, ruthenium(II) complex **204** was obtained in a yield of 93 %. The reaction of ligand **203** with the iridium precursor $[Ir(\mu\text{-}Cl)(ppy)_2]$[283] in a mixture of anhydrous dichloromethane and methanol (1:1) at 50 °C for three days afforded iridium(III) complex **205** as the hexafluorophosphate salt in a yield of 76 % after column chromatography on silica gel.

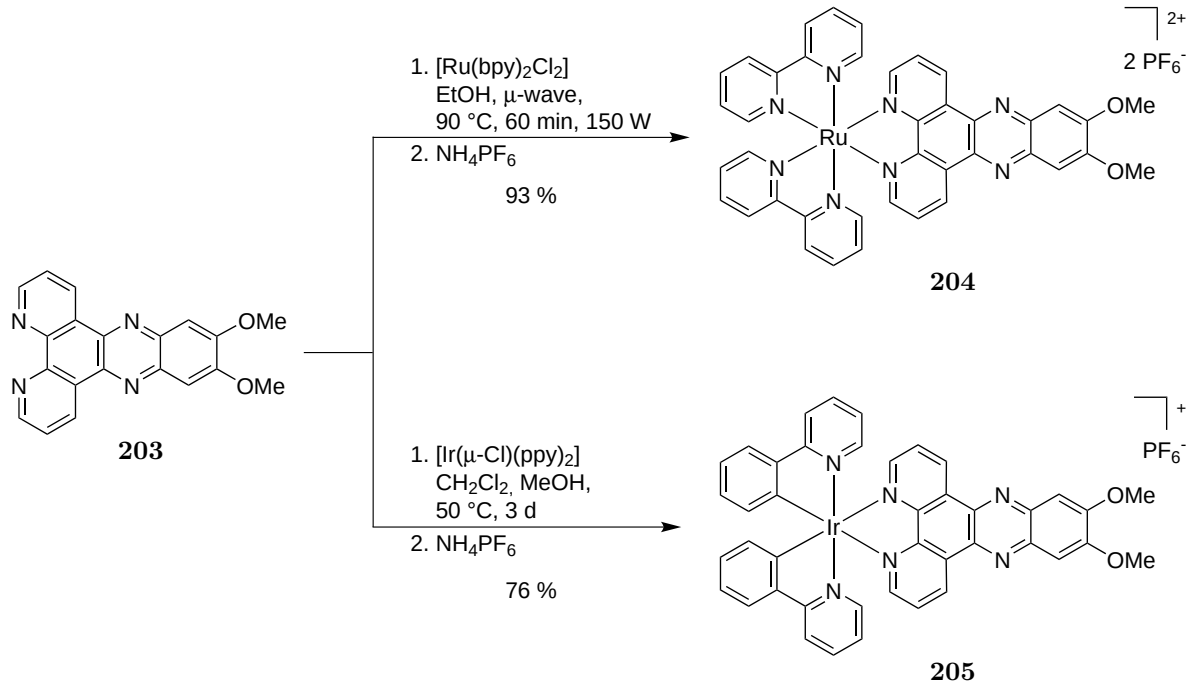

Scheme 47: Synthesis of ruthenium(II) and iridium(III) complexes **204** and **205**, respectively.

The structure of iridium(III) complex **205** could be verified by crystal structure analysis. Measurable single crystals were obtained upon slow diffusion of of diethyl ether into a solution of complex **205** in acetonitrile at 4 °C. Unfortunately, the structure could not be refined but it confirms that the nitrogen atoms of the 2-phenylpyridine ligands are *trans* to each other whereas the carbon atoms are *cis* to each other and in *trans*-position to ligand **203**. This observation is general for most

bis(2-phenylpyridinato)iridium(III) and bis(2-phenylpyridinato)rhodium(III) complexes and can be explained by the *trans*-effect.[285,286]

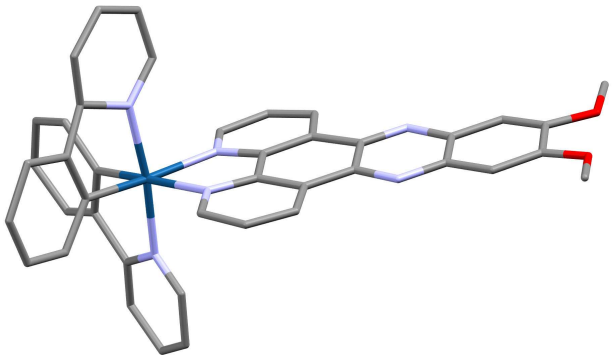

Figure 53: Unrefined crystal structure of complex **205**. The PF_6^- counterion and solvent molecules are omitted for clarity. (Colors: grey = carbon, red = oxygen, light purple = nitrogen, turquoise = iridium)

Next, the deprotection of the methoxy groups of complex **205** was tried using different mild and harsh deprotection conditions (Scheme 48, Table 8). Unfortunately, the desired product **206** could not be isolated. In nearly all attempts, the starting material **205** was recovered besides a mixture of unidentified side products. Only after using BBr_3 in anhydrous chloroform at 120 °C over night, the product **206** was found by HRMS but could not be isolated. Hence, a different approach to obtain **206** was tried next.

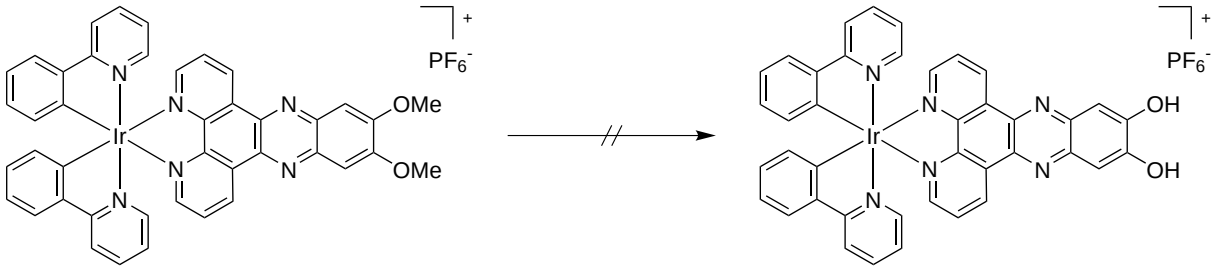

205 **206**

Scheme 48: Attempt to deprotect the methoxy groups of complex **205**. The reaction conditions are given in Table 8

Table 8: Screening of different reaction conditions for the deprotection of complex **205**. All reactions were carried out under an atmosphere of nitrogen.

Reagent	Solvent	Temperature / Time	Isolated
HI	AcOH	85 °C / 22 hours	mainly **205** (>62 %)[a]
BBr_3	CH_2Cl_2	first 0 °C, then rt / over night	mixture of three compounds[b]
BBr_3	$CHCl_3$	90 °C / over night	mixture[c]
HBr (48 % aq.)	HOAc	120 °C / 21 hours	mainly **205**

[a] A mixed fraction (9 %) was also isolated but the desired product or the mono deprotected complex was not found by HRMS and ^{1}H-NMR. [b] A mixture of starting material and two other, unidentified products were obtained as monitored by HRMS and ^{1}H-NMR. [c] Full conversion but **206** could not be isolated.

The last approach using a linear synthesis route to yield dinuclear metal-silicon(IV) complexes was based on a condensation reaction of (diamino)iridium(III) complex **207**[146] with 2,5-dihydroxy-*p*-benzoquinone (**94**). Therefore, ligand **200** was reacted with $[Ir(\mu\text{-}Cl)(ppy)_2]$[283] in a mixture of anhydrous dichloromethane and anhydrous methanol (1:1) at 55 °C for four hours (Scheme 49). After column chromatography on silica gel and exchange of the counterion to hexafluorophosphate, iridium(III) complex **208** was obtained in a yield of 93 %. Subsequent palladium catalyzed reduction of the nitro group with hydrogen in dichloromethane for 26 hours afforded complex **207** in a yield of 98 %. Finally, the condensation reaction was tried using various reaction conditions (Table 9) but the desired product could not be isolated. As the convergent synthesis approach to obtain dinuclear metal-silicon(IV) complexes showed much better results, the linear synthesis route was not pursued any further.

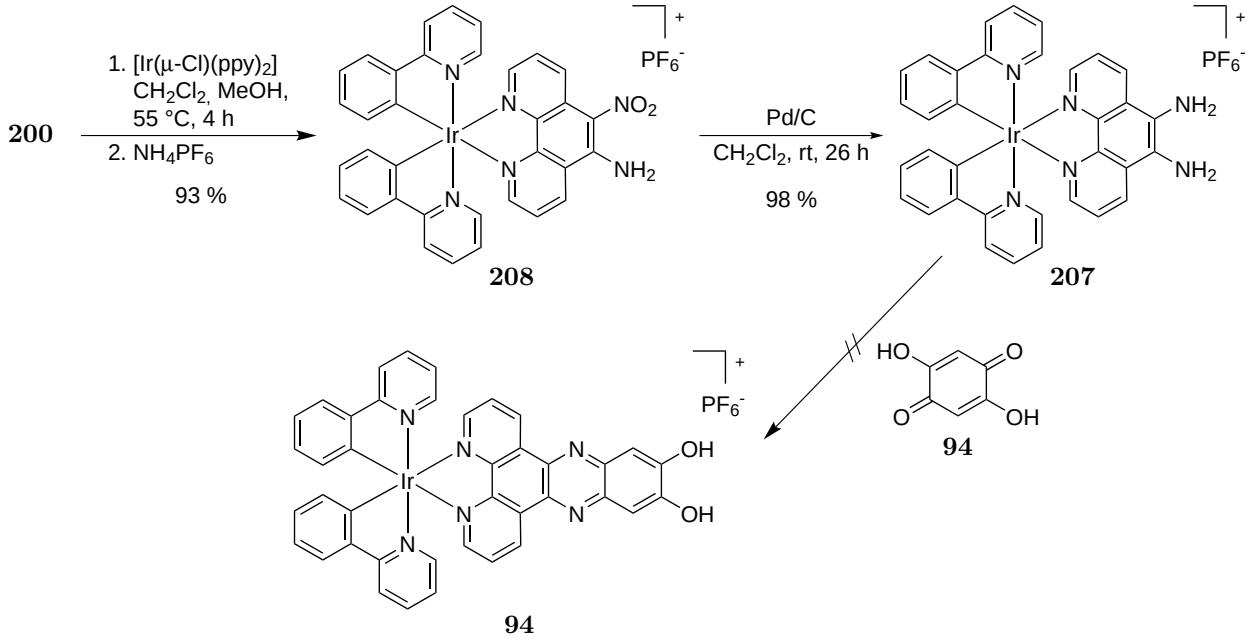

Scheme 49: Synthesis of (diamino)iridium(III) complex **207** and attempt to obtain complex **206** in a condensation reaction. The reaction conditions are given in Table 9

Table 9: Screening of different reaction conditions for the condensation of complex **207** with 2,5-dihydroxy-*p*-benzoquinone (**94**). All reactions were carried out under an atmosphere of nitrogen.

Solvent	Temperature / Time	Isolated
$CHCl_3$	90 °C / 16 hours	complex **207** (87 %
EtOH	90 °C / 2 days	no product[a]
MeCN / H_2O 2:1	75 °C / 24 hours	-[b]

[a] Monitored by ^{1}H-NMR. [b] Product could be found by LCMS control but it could not be isolated by column chromatography.

3.4.3. Convergent Synthesis

The convergent synthesis strategy relied on a condensation reaction of a (4,5-diaminobenzene-1,2-diolato)silicon(IV) and a (1,10-phenanthroline-5,6-dione)metal part (see Scheme 43). The synthesis

of the silicon(IV) intermediate **197** has been discussed in Chapters 3.2.3 and 3.2.4. Following, the synthesis of the metal parts will be discussed.

The synthesis of bis(polypyridyl)metal complexes coordinate to 1,10-phenanthroline-5,6-dione (**198**) was achieved by treatment of the ligand with different metal precursors under various reaction conditions (Scheme 50). After purification by column chromatography on silica gel and treatment with ammonium hexaflurophosphate, the corresponding complexes were isolated as the hexafluorophosphate salts in very good yields. In doing so, ruthenium(II) complexes **209**, **210** and **211** were obtained by reacting ligand **198** and ruthenium precursor $[Ru(pp)_2Cl_2] \cdot 2\,H_2O$ [284] in ethanol for one to four hours in yields of 44–74 %. In contrast to complexes **210** and **211**, complex **209** was synthesized using a μ-wave mediated reaction (150 W). The corresponding iridium(III) complex **212** was obtained in a yield of 82 % by the conversion of ligand **198** with $[Ir(\mu\text{-}Cl)(ppy)_2]$ [283] in a mixture of anhydrous dichloromethane and anhydrous methanol (1:1) at 55 °C for two hours. Finally, the reaction of $[Rh(\mu\text{-}Cl)(pp)_2]_2$ [287,288] with ligand **198** in a mixture of ethanol and dichloromethane (2:1) at 70 °C for 3.5 to four hours afforded the rhodium(III) complexes **213** and **214** [288] in yields of 90 % and 79 %, respectively.

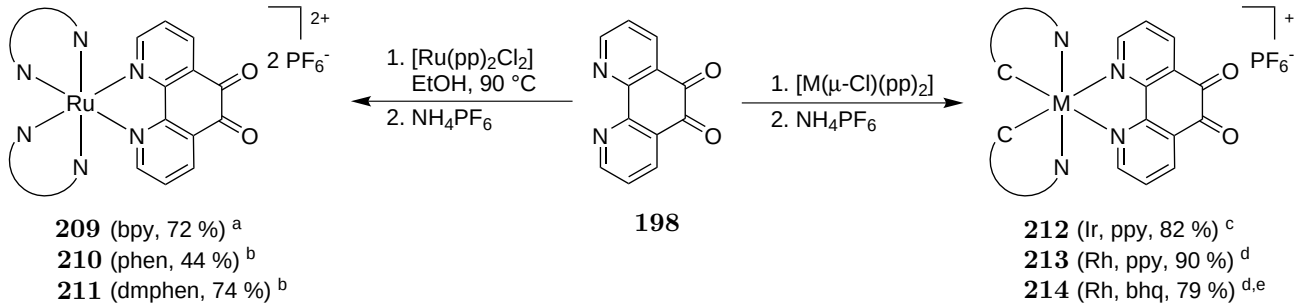

Scheme 50: Synthesis of various (1,10-phenanthroline-5,6-dione)metal complexes. (Conditions: [a] μ-wave irradiation, 150 W, 60 min. [b] 3.5–4 h. [c] $MeOH/CH_2Cl_2$ 1:1, 55 °C, 2 h. [d] $EtOH/CH_2Cl_2$ 2:1, 70 °C, 2–3 h. [e] Synthesized by Alexandra Gruber during her bachelor thesis.[288])

The geometrical structure of complex **210** and **211** were verified by crystal structure analysis. Single crystals suitable for this analysis were obtained upon slow diffusion of diethyl ether into a solution of the corresponding complex in acetonitrile at 4 °C. Complex **210** crystallized as red nuggets in the triclinic space group P −1 with two formula units per unit (Figure 54). Together with the complex, two formula units of the counter ion PF_6^-, two formula units diethyl ether and 1.88 formula units acetonitrile were incorporated in the crystal structure. In comparison, complex **211** crystallized as dark blocks in the monoclinic space group P $2_1/c$ with eight formula units per unit (Figure 55). Together with the complex, two formula units of the counter ion PF_6^-, 0.5 formula units diethyl ether and 1.5 formula units acetonitrile were incorporated in the crystal structure.

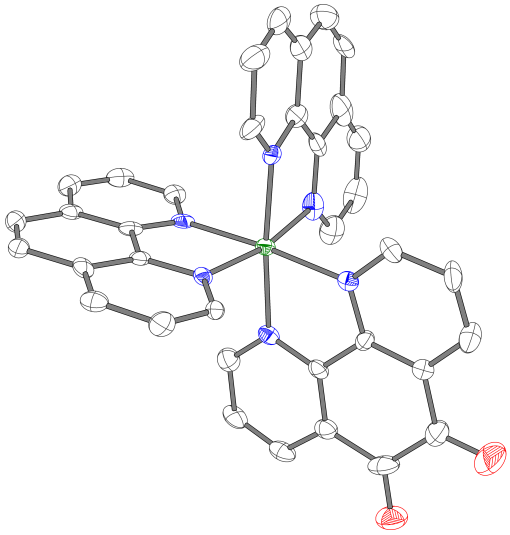

Figure 54: Crystal structure of complex **210**. ORTEP drawing with 50 % probability thermal ellipsoids. The PF_6^- counterions and solvent molecules are omitted for clarity. Selected bond lengths [Å] and angles [°]: N1–Ru1 2.063(7), N4–Ru1 2.041(6), N15–Ru1 2.065(7), N18–Ru1 2.053(8), N31–Ru1 2.055(6), N34–Ru1 2.053(6), N4–Ru1–N34 177.1(2), N4–Ru1–N18 94.2(3), N34–Ru1–N18 88.2(3), N4–Ru1–N31 98.5(2), N34–Ru1–N31 79.5(2), N18–Ru1–N31 95.3(3), N4–Ru1–N1 79.7(3), N34–Ru1–N1 98.0(3), N18–Ru1–N1 173.3(3), N31–Ru1–N1 88.4(3), N4–Ru1–N15 86.5(2), N34–Ru1–N15 95.7(2), N18–Ru1–N15 80.1(3), N31–Ru1–N15 173.5(3), N1–Ru1–N15 96.6(3)..

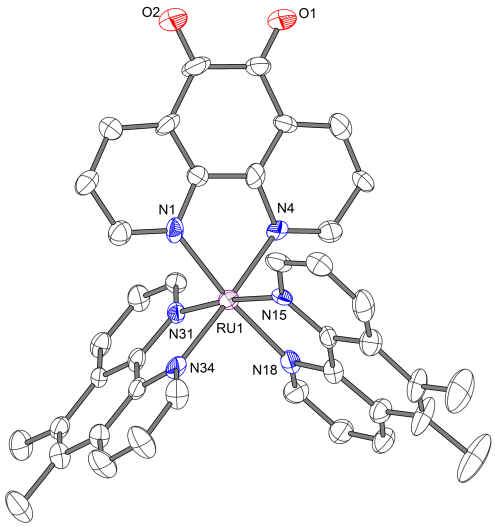

Figure 55: Crystal structure of complex **211**. ORTEP drawing with 50 % probability thermal ellipsoids. The PF_6^- counterions and solvent molecules are omitted for clarity. Selected bond lengths [Å] and angles [°]: N1–Ru1 2.063(7), N4–Ru1 2.041(6), N15–Ru1 2.065(7), N18–Ru1 2.053(8), N31–Ru1 2.055(6), N34–Ru1 2.053(6), N4–Ru1–N34 177.1(2), N4–Ru1–N18 94.2(3), N34–Ru1–N18 88.2(3), N4–Ru1–N31 98.5(2), N34–Ru1–N31 79.5(2), N18–Ru1–N31 95.3(3), N4–Ru1–N1 79.7(3), N34–Ru1–N1 98.0(3), N18–Ru1–N1 173.3(3), N31–Ru1–N1 88.4(3), N4–Ru1–N15 86.5(2), N34–Ru1–N15 95.7(2), N18–Ru1–N15 80.1(3), N31–Ru1–N15 173.5(3), N1–Ru1–N15 96.6(3).

Next, 2,9-dimethyl-1,10-phenanthroline-5,6-done (**215**) was synthesized according to a procedure published by Garas and Vagg.[247] Therefore, 2,9-dimethyl-1,10-phenanthroline (**216**) was oxidized using potassium bromide in a mixture of concentrated sulphuric and nitric acid at 80 °C for four hours (Scheme 51). Neutralization of the reaction mixture, followed by isolation of the crude product with dichloromethane and recrystallization from dioxane gave ligand **215** in a yield of 51 %. Due to the two sterical demanding methyl groups in position 2 and 9, the complexation reaction of of ligand **215** needed harsher conditions compared to complex **209**. In addition, the reaction had to be performed under exclusion of light since complex **217** would be very likely light sensitive, according to studies of Glazer *et al.* dealing with light induced ligand cleavage of strained ruthenium(II) complexes.[289] Hence, after a μ-wave mediated reaction of **215** with $[Ru(bpy)_2Cl_2] \cdot 2\,H_2O$[284] in ethanol at 90 °C for 90 minutes, only the precursor could be isolated. On the other hand, the reaction of both reagents in ethylene glycol at 200 °C for 20 hours[289] gave some conversion and a brown solid was isolated by column chromatography on silica gel. However, complex **217** could not be identified by ^{1}H-NMR and HRMS.

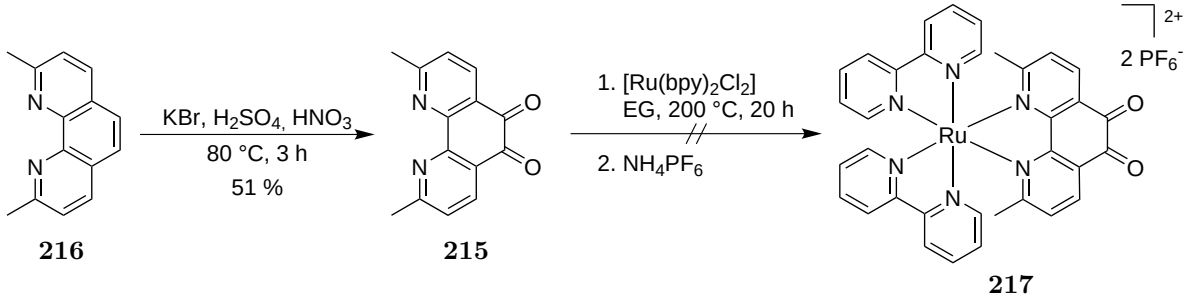

Scheme 51: Synthesis of 2,9-dimethyl-1,10-phenanthroline-5,6-done (**215**) and attempt to obtain complex **217**.

As the complexation of the oxidized ligand was not successful, the oxidation at complex **218** was studied next as similar reactions have been reported.[146,259] Therefore, 2,9-dimethyl-1,10-phenanthroline (**216**) was reacted in the dark with $[Ru(bpy)_2Cl_2] \cdot 2\,H_2O$[284] in ethylene glycol at 200 °C for 20 hours (Scheme 52). After purification by silica gel column chromatography under exclusion of light and exchanging the counterion to hexaflurophosphate, complex **218** was obtained in a yield of 87 %. Next, the oxidation of **218** was studied using different oxidation reagents and conditions (Table 10). In 2005, Bergman and Kol published an oxidation of $[Ru(bpy)_2(phen)]^{2+}$ using similar conditions used for the oxidation of 1,10-phenanthroline.[146,259] According to this procedure, complex **218** was reacted with sodium bromide in a mixture of concentrated sulphuric and nitric acid at 110 °C for two to five hours. These harsh conditions led to the formation of desired product that was isolated in a very low yield of 11–18 % after column chromatography on silica gel as hexaflurophosphate salt. Unfortunately, the ^{1}H-NMR spectrum of complex **217** showed some minor impurities that could not be removed and did not interfere with following reactions. Hence, complex **217** was used for the next step as isolated. Since the low yield of the reaction may be explained by the harsh reaction conditions, other methods were also tried. The reaction of complex **218** with iodine pentoxide in acetic acid at 110 °C for 20 hours led to an inseparable mixture of products and was not studied any further. Adopting the mild oxidation method of Sun *et al.*,[252] complex **217** could be isolated in very good yields of 61–84 %. Therefore, complex **218** was reacted with sodium bromate in 60 % sulfuric acid at room temperature

over night. Conveniently, no column chromatography on silica gel was need as complex **217** could easily be isolated by precipitation with ammonium hexafluorophosphate from the neutralized reaction mixture. The obtained solid showed some minor impurities in the ^{1}H-NMR that could not be removed by column chromatography. Hence, the precipitate was used for the next step without any further purification.

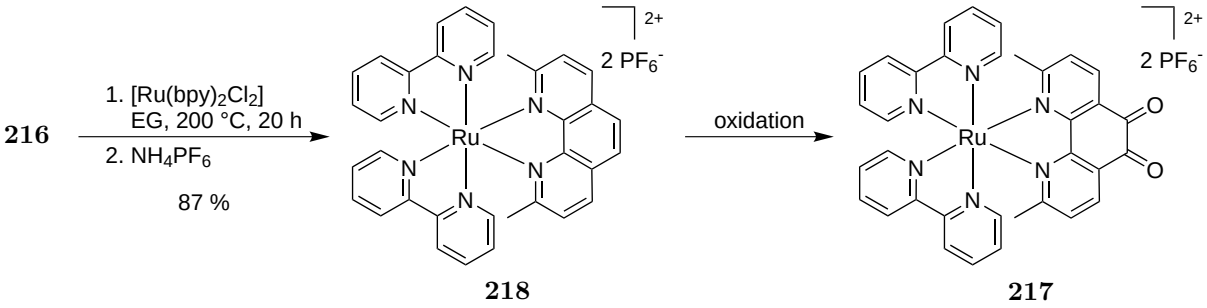

Scheme 52: Synthesis of complex **218** and its oxidation to complex **217**.

Table 10: Screening of different reaction conditions for the oxidation of complex **218**. All reactions including the work-up were performed under exclusion of light.

Reagent	Solvent	Temperature / Time	Isolated
NaBr [146,259]	H_2SO_4/HNO_3	110 °C / 2–5 hours	**217** (11–18 %)[a]
I_2O_5 [158]	HOAc	110 °C / 20 hours	inseparable mixture
$NaBrO_3$ [252]	H_2SO_4 (60 %)	rt / 18–20 hours	**217** (61–84 %)[a]

[a] ^{1}H-NMR showed minor impurities in the aromatic region that could not be removed by column chromatography.

The strained coordination geometry of ruthenium(II) complexes coordinate to a 2,9-dimethylated 1,10-phenanthroline derivative was confirmed by crystal structure analysis of complex **219** by way of example. Single crystals suitable for this analysis were obtained upon slow diffusion of diethyl ether into a solution of complex **218** in acetonitrile at 4 °C. It crystallized as red nuggets in the monoclinic space group C 2/c with eight formula units per unit cell (Figure 56). Together with the complex, two formula units of the counter ion PF_6^- were incorporated in the crystal structure.

Ruthenium(II) complex **221** was synthesized using a similar procedure due to a missing practicable oxidation method for 3,4,7,8-tetramethyl-1,10-phenanthroline (**222**). Hence, ligand **222** was reacted with $[Ru(bpy)_2Cl_2] \cdot 2\,H_2O$ [284] in ethanol at 90 °C for 16 hours (Scheme 53). Purification by column chromatography on silica gel and precipitation with ammonium hexafluorophosphate afforded complex **220** in a yield of 96 %. Subsequent conversion with sodium bromate in 60 % sulfuric acid at room temperature gave complex **210** in a yield of 84 %. Just like discussed for complex **217**, purification by column chromatography did not remove the minor impurities visible in ^{1}H-NMR spectrum. Hence, **210** was used for the next step without any further purification.

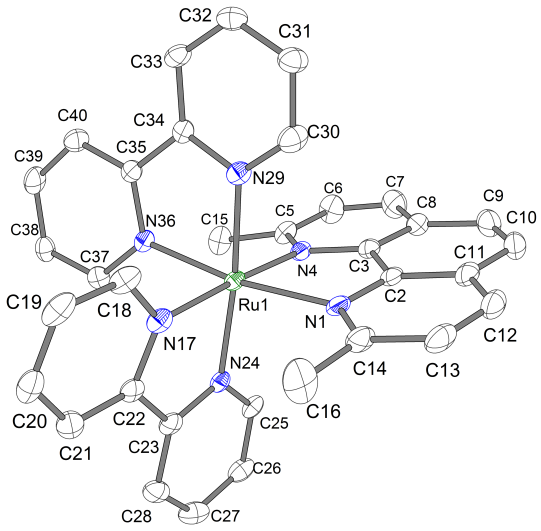

Figure 56: Crystal structure of complex **218**. ORTEP drawing with 50 % probability thermal ellipsoids. The PF_6^- counterions are omitted for clarity. Selected bond lengths [Å] and angles [°]: N1–Ru1 2.117(2), N4–Ru1 2.115(2), N17–Ru1 2.053(2), N24–Ru1 2.053(2), N29–Ru1 2.068(2), N36–Ru1 2.052(2), N36–Ru1–N17 81.00(9), N36–Ru1–N24 96.81(9), N17–Ru1–N24 78.48(9), N36–Ru1–N29 78.60(9), N17–Ru1–N29 97.43(9), N24–Ru1–N29 174.36(9), N36–Ru1–N4 98.29(8), N17–Ru1–N4 175.19(9), N24–Ru1–N4 96.91(9), N29–Ru1–N4 87.07(9), N36–Ru1–N1 170.37(9), N17–Ru1–N1 102.14(9), N24–Ru1–N1 92.75(9), N29–Ru1–N1 91.92(9), N4–Ru1–N1 79.34(9).

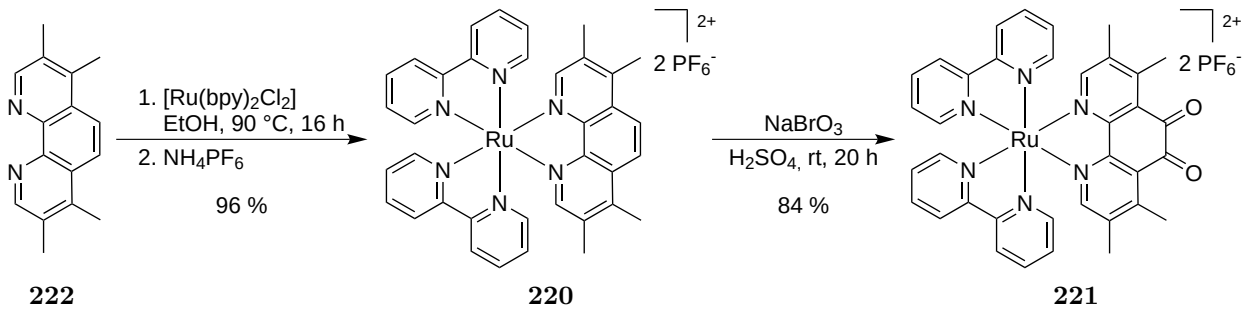

Scheme 53: Synthesis of complex **221** starting from 3,4,7,8-tetramethyl-1,10-phenanthroline (**222**).

Finally, dinuclear metal-silicon(IV) complexes (**192**) were synthesized by a condensation reaction of the (1,10-phenanthroline-5,6-dione)metal fragments and the (4,5-diaminobenzene-1,2-diolato)silicon(IV) parts. In accordance to the two step synthesis discussed in Chapter 3.2.4, the (4,5-dinitrobenzene-1,2-diolato)silicon(IV) fragments **134** were reduced with tin in hydrochlorid acid at 110 °C for three hours (Scheme 54) and the obtained diamino intermediates were then reacted with the metal fragments **196** in acetonitrile at 40 °C over night. After column chromatography and exchanging the counterion to hexafluorophosphate, a small library of dinuclear metal-silicon(IV) complexes was obtained. Surprisingly, all complexes could be purified on normal silica gel with a mixture of MeCN/H_2O/satd. aq. KNO_3 (50:6:2 or 50:12:4, depending on the charge of the complex) as eluent. All complexes were obtained as mixtures of diastereomers eluating with the same retention time. Further attempts to separate the single isomers by normal phase HPLC were not carried out. Due to the distance between

the chiral metal and silicon(IV) center, the difference of the chemical shifts of the single diastereomers in the ^{1}H-NMR spectrum is marginal.

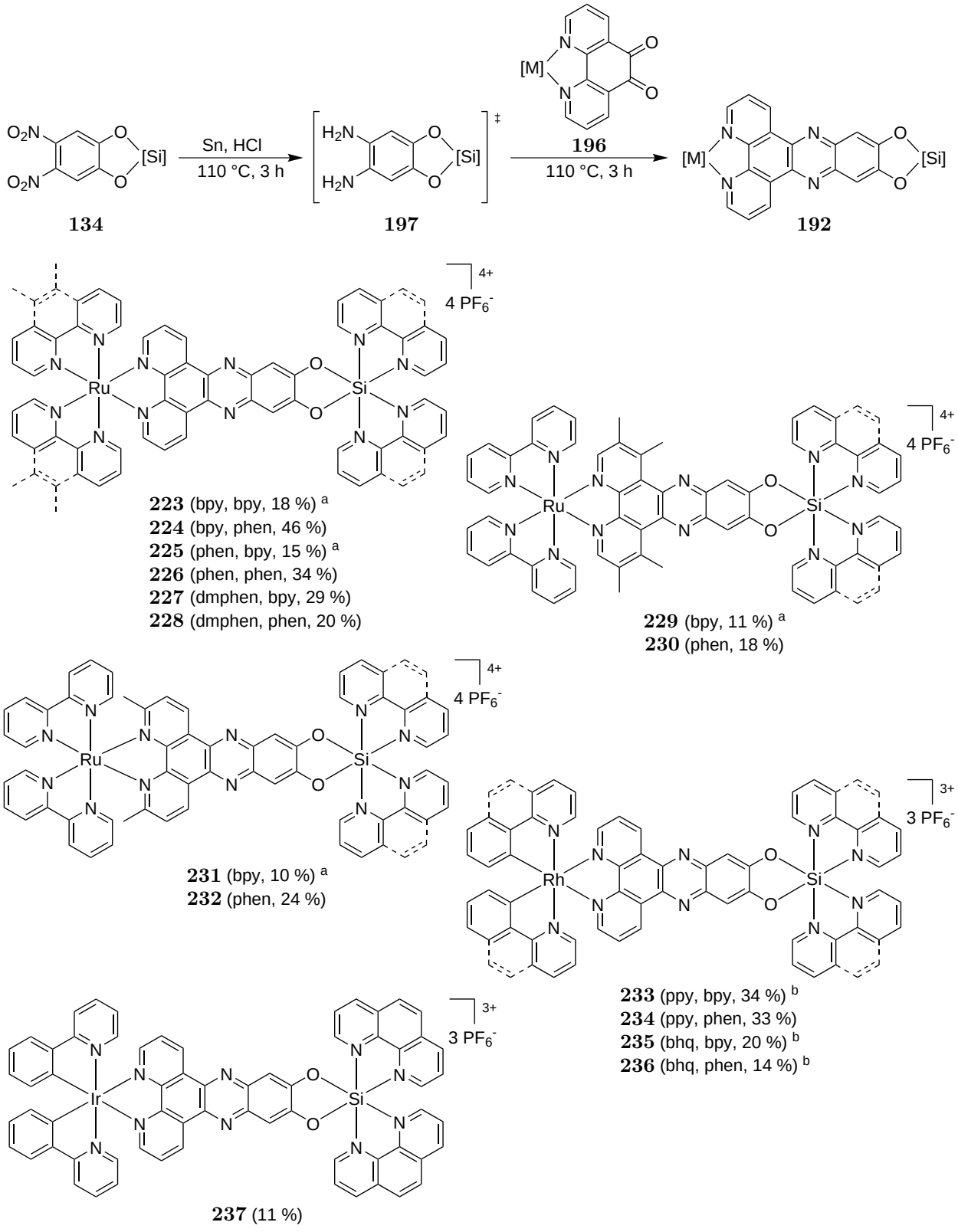

Scheme 54: Synthesis of dinuclear metal-silicon(IV) complexes (**192**). All complexes are obtained as mixtures of diastereomers. Yields are given over two steps. ([a] Synthesized by Steffen Glöckner during his bachelor thesis. [b] Synthesized by Alexandra Gruber during her bachelor thesis.)

Using a compound in biological applications requires a certain stability against hydrolysis as well as against thiols, especially if ruthenium(II) centers are involved. Hence, the stability of the dinuclear complexes under these conditions was studied for complex **227** (2.9 mM in a mixture of CD_3CN/D_2O (3:1) at room temperature under daylight by way of example. The measurement was monitored by ^{1}H-NMR spectroscopy for 62 hours to determine the hydrolytical stability of the complex. Then 2-mercaptoethanol (3.6 mM) was added to study the stability of the complex against thiols. As a result, **227** did not show any sign of decomposition after three months leading to the conclusion that the dinuclear complexes are hydrolytically stable as well as stable against thiols for at least three months. These results are in accordance with previously reported studies.[37,224] In addition, Alexandra Gruber studied the hydrolytical stability of the complexes **233**, **235** and **236** during her bachelor thesis with the result that the complexes are stable for at least five days at room temperature under daylight in a mixture of CD_3CN/D_2O (3:4).[288]

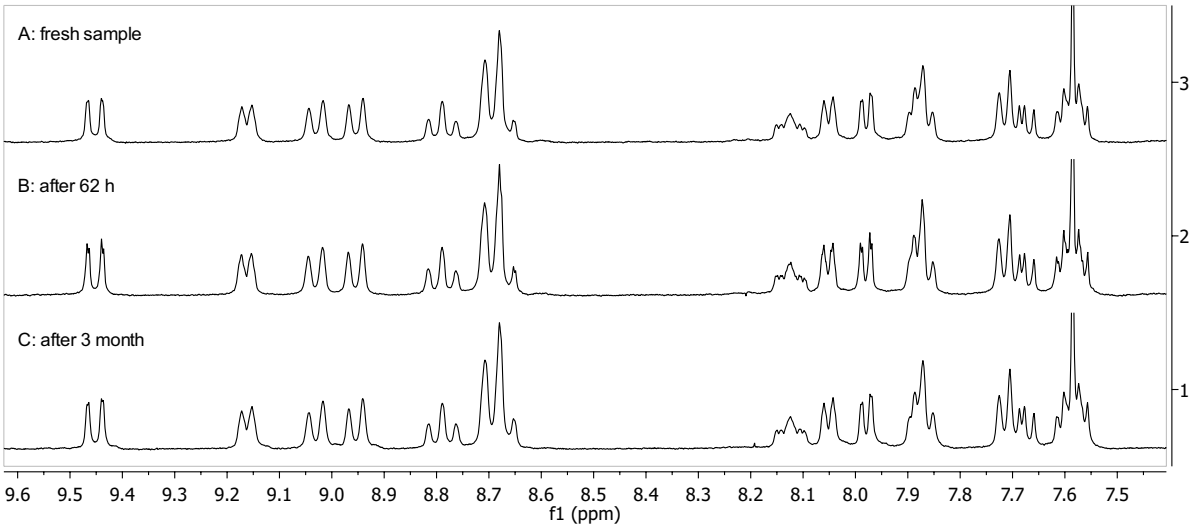

Figure 57: Stability of the dinuclear metal-silicon(IV) complex **227** (2.9 mM) at room temperature in CD_3CN/D_2O (3:1) at room temperature under daylight. Shown are the aromatic region of the ^{1}H-NMR spectra right after the addition of D2O (A), after 62 hours (B) and in the presence of 2-mercaptoethanol (3.6 mM) after three month (C). No decomposition can be observed.

3.4.4. Bifunctional Metal-Silicon(IV) Complexes

In 2012, Glazer and co-workers showed that strained ruthenium(II) complexes can rapidly eject a ligand upon photexcitation leading to active complexes that can be used in the photodynamic therapy as potential anti-cancer agents.[289] Therefore, they synthesized complexes **238** and **239** possessing methyl groups directed towards the coordinated 2,2-bipyridine ligands and studied their photoejection ability. The methyl groups are crucial for this experiment as they provide a distortion of the geometry at the ruthenium(II) center due to steric clashes with the other ligands (for an exemplary crystal structure see Figure 56). While complexes **238** and **239** are completely stable when stored in the dark in aqueous solutions, irradiation with visible light (>450 nm) resulted in a quick and selective cleavage of the methylated ligands with a $t_{1/2}$ of two minutes for **238**.[289] Complex **239** showed slower dissociation kinetics which was explained by a possibly faster rechelating of the ligand interfering the stepwise dissociation bond breaking mechanism.[289] However, the metal fragments were able to cross-

link DNA in a very potent fashion.[289] Hence, both complexes showed very strong cytotoxicity after light activation but non in the dark.

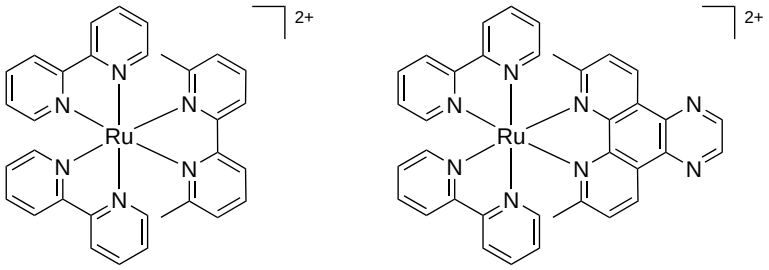

238 **239**

Figure 58: Strained ruthenium(II) complexes studied by Glazer and co-workers.[289]

With the strained dinuclear complexes **231** and **232** in hand, the next step was to investigate their capability for the photodynamic therapy by evaluating their photoejection ability. It was assumed that both complexes would dissociate the ruthenium center upon irradiation with light leading to the formation of an active ruthenium(II) species (**240**) capable of cross-linking DNA[289] and an octahedral silicon(IV) complexes (**241** and **242**) as a possible DNA intercalator (Scheme 55). This bifunctionality of the complex would be very interesting for biological applications as the silicon part could be used as a caging agent for a biological active metal complex, **240** in the case studied. Furthermore, by attaching a fluorophore to the silicon center, a bifunctional complex capable of imaging and cross-link DNA upon light activation could be obtained.

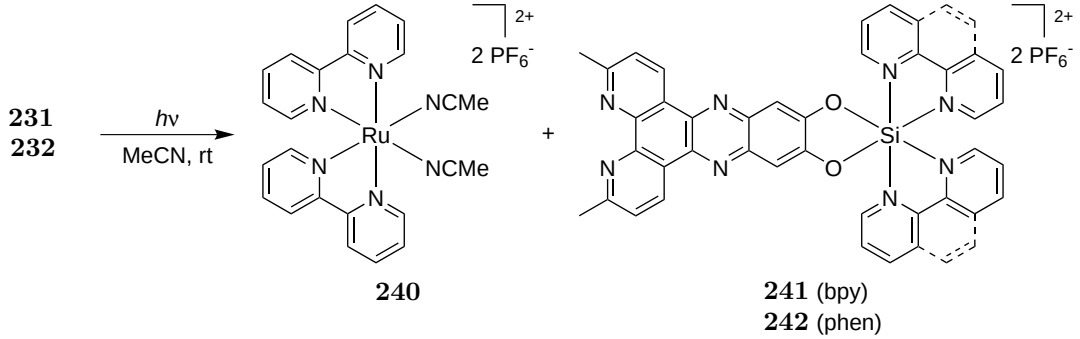

240 **241** (bpy)
242 (phen)

Scheme 55: Biological active metal complexes that could be obtained upon photoinduced cleavage of the dinuclear complexes **231** and **232**.

The photoejection of complexes **231** and **232** were studied by ^{1}H-NMR spectroscopy in acetonitrile. To monitor the formation of the ruthenium fragment, complex **240** was synthesized first. Therefore, ruthenium precursor $[Ru(bpy)_2Cl_2] \cdot 2\,H_2O$[284] was reacted with silver nitrate in acetonitrile at 90 °C for 3.5 hours in the dark (Scheme 56). After purification using column chromatography on silica gel and anion metathesis, complex **240** was obtained as the hexafluorophosphate salt in a yield of 77 %.

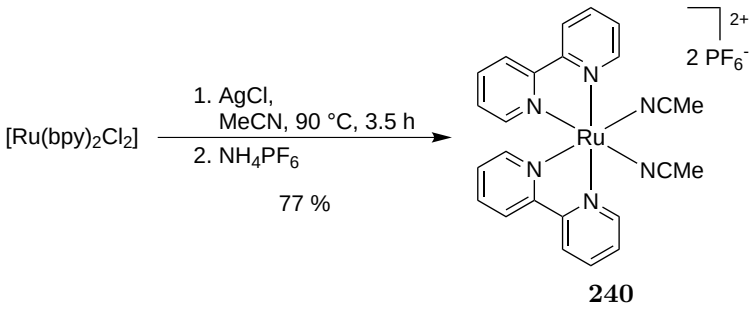

240

Scheme 56: Synthesis of bis(acetonitrile)ruthenium(II) complex **240**.

Next, a solution of complex **232** (3 mM) in acetonitrile-d_3 was irradiated with visible light using a LED lamp (8 W) at room temperature in a NMR tube. The dissociation process was monitored by ^{1}H-NMR spectroscopy over 715 minutes (Figure 59). As a result, a slow dissociation of complex **232** can be observed. In addition, the formation of the ruthenium fragment **240** confirms the postulated cleavage position. Hence, the silicon(IV) fragment **242** had to be formed too. However, its formation could not be visualized as at least three different compounds (**232**, **240** and **242**) are present in the mixture after irradiation with visible light. Anyhow, the experiment supports the results of the kinetic studies made by Glazer *et al.* since the dissociation speed depends of the size of the ligand that should be cleaved, with **241** and **242** being the biggest and slowest.[289]

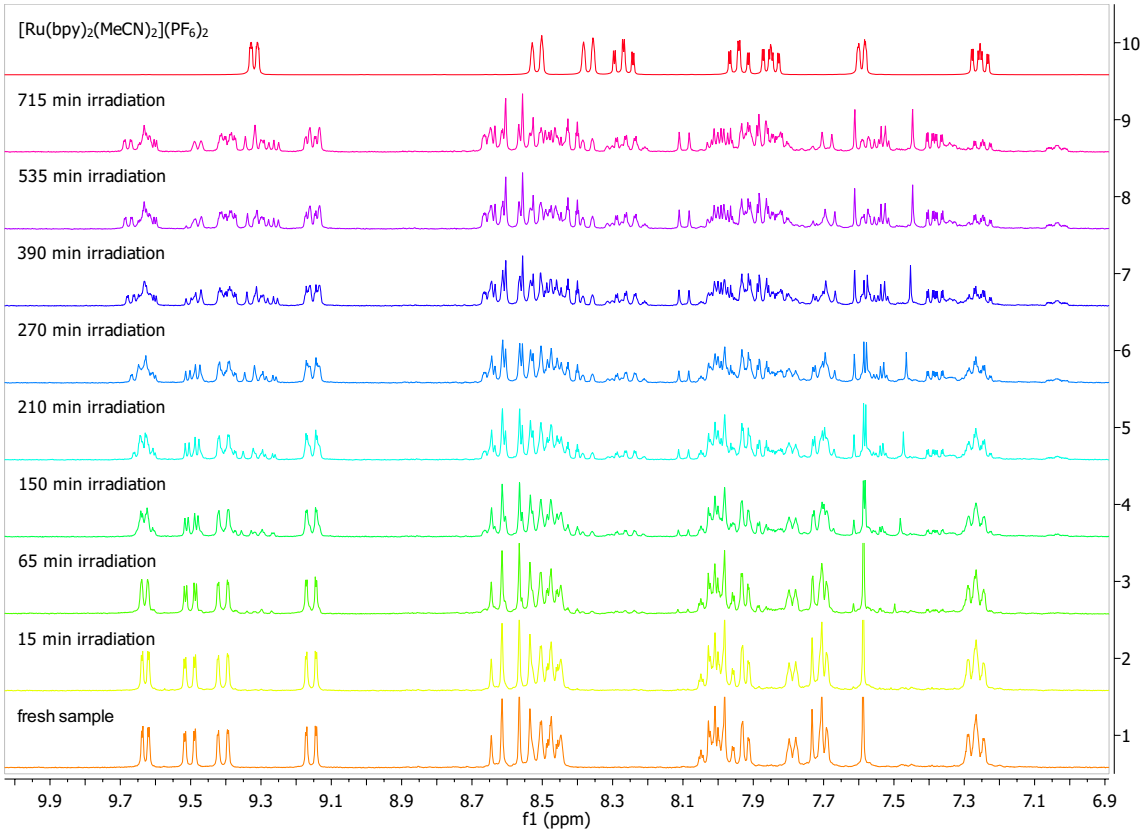

Figure 59: Photoinduced cleavage of complex complex **232** (3 mM) using a LED lamp (8 W, λ =) at room temperature monitored by ^{1}H-NMR spectroscopy in acetonitrile-d_3. As a reference, the ^{1}H-NMR spectrum of complex $[Ru(bpy)_2(MeCN)_2](PF_6)_2$ (**240**) that is formed during the cleavage is also given. It can be seen that upon irradiation with visible light a slow cleavage of complex **232** occurs.

Similar results were obtained by Steffen Glöckner during his bachelor thesis for complex **231**.[225] In addition, changing the solvent of the experiment to dimethyl sulfoxide, no cleavage was observed. Due to the very slow photoinduced dissociation, the discussed dinuclear ruthenium-silicon complexes are not suitable for the photodynamic therapy. Hence, this approach was not studied any further.

3.4.5. Biological Activity

The UV-Vis absorption properties of the dinuclear metal-silicon(IV) **223**–**237** were studied in Tris-buffer (5 mM Tris-HCl, 20 mM NaCl, pH 7.4, $C_{complex}$20 mM) at room temperature. A selected example of the absorption spectrum for each ruthenium, rhodium or iridium complex is given in Figure 60. All complexes showed a strong absorption band at $\lambda = 350$–420 nm with a maximum at around $\lambda = 390$ nm for the ruthenium bound complexes and around $\lambda = 404$ nm with a well defined hypsochromic shoulder for the rhodium and iridium bound. This band arises from a $\pi \rightarrow \pi^*$ ligand centered charge-transfer transition of the bridging ligand dppzO, according to similar metal complexes.[130,135,137,138,144,145] In addition, the ruthenium bound complexes exhibited a metal-to-ligand charge transfer (MLCT) absorption band in the visible region at $\lambda = 420$–480 nm. This absorption band is characteristic for ruthenium bound polypyridyl complexes and arises from $Ru(t_{2g} \rightarrow pp(\pi^*)$ and $Ru(t_{2g} \rightarrow dppzO(\pi^*)$ transitions.[137,144,153]

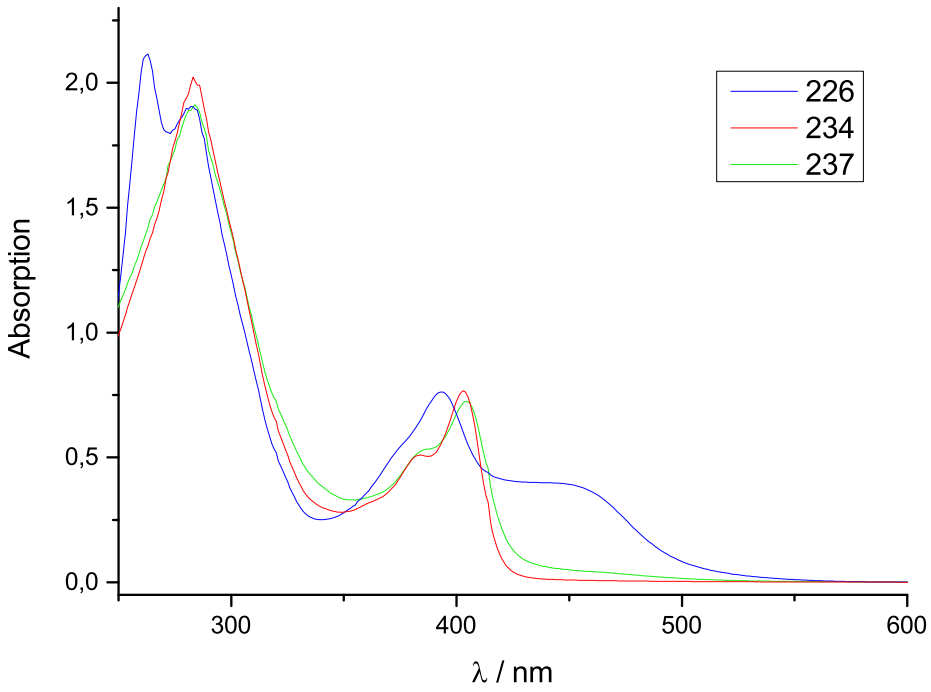

Figure 60: UV/Vis-absorption spectra of complexes **226**, **234** and **237** (20 µM) in Tris-buffer (5 mM Tris-HCl, 20 mM NaCl, pH 7.4) by way of example for dinuclear complexes bound to ruthenium, rhodium and iridium, respectively.

Having the UV-Vis absorption spectra recorded, the binding constants k_B of the dinuclear metal-silicon complexes **223**–**231** and **233**–**237** to *calf thymus* DNA were determined next by UV-Vis-monitored titration at room temperature in Tris-buffer (5 mM Tris-HCl, 20 mM NaCl, pH 7.4), according to the method introduced in Chapter 3.2.6. As an example for the absorption spectra obtained upon the

titration with ds-DNA, Figure 61 shows the spectrum of complex **224**. Depending on the DNA concentration, all complexes studied showed a strong hypochromicity (45–62 %) of the $\pi \rightarrow \pi^*$ LCCT band (λ = 350–420 nm) together with a modest bathocromic shift of its absorption maximum of 3–6 nm. These observations are typical for complexes interacting with DNA.[37,130,135,137,138,140,144,145,151,153]

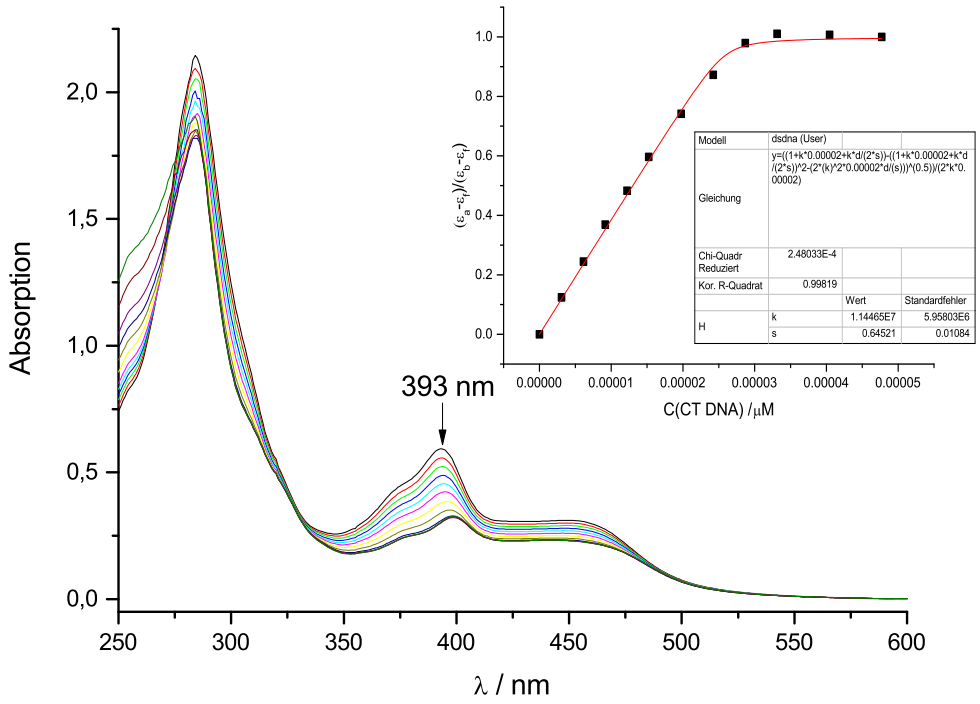

Figure 61: UV/Vis-absorption spectra of complex **224** (20 µM) in Tris-buffer (5 mM Tris-HCl, 20 mM NaCl, pH 7.4) upon titration with *calf thymus* DNA at room temperature. Insert: plot of $(\epsilon_a - \epsilon_f)/(\epsilon_b - \epsilon_f)$ at 393 nm versus DNA concentration, with ϵ_a = extinction coefficient of the complex at a given DNA concentration, ϵ_b = extinction coefficient when fully bound to DNA, and ϵ_f = extinction coefficient of the complex in the absence of DNA.

Plotting the absorption decrease of the $\pi \rightarrow \pi^*$ LCCT maximum as a function of the DNA concentration yielded the binding constants k_B of complexes **223**–**231** and **233**–**237** to *calf thymus* DNA which are listed in Table 11.[145,272] As expected, all complexes tested exhibited a strong affinity to duplex DNA with a binding constant of around 10^5–10^8 M^{-1} and thus within the range of known dinuclear (polypyridyl)ruthenium complexes, for example the structural similar complexes $[Ru(pp)_2(\mu\text{-tpphz})Ru(pp)_2](NO_3)_4$.[140,144] The tetrakis(2,2'-bipyridine) complex **223** showed the strongest binding to ds-DNA with a binding constant of $k_B = (1.1 \pm 0.4) \times 10^8$ M^{-1} whereas the complexes coordinated to 1,10-phenanthroline derivatives bond about one order of magnitude lower. This phenomena has also been observed for the complexes $[Ru(pp)_2(\mu\text{-tpphz})Ru(pp)_2](NO_3)_4$.[140] A possible explanation for this behavior may be a lower sterical hindrance of the small 2,2-bipyridine ligand compared to the 1,10-phenanthroline derivatives. Furthermore, the binding constant is depending on the charge of the complexes as the 4+ charged ruthenium containing complexes bond about one order of magnitude stronger than the 3+ charged rhodium and iridium complexes. Nevertheless, the rhodium and iridium containing complexes bond ds-DNA similar strong or even stronger than the known mononu-

clear metallointercalators, like $[Si(phen)_2(pyrenediol)](PF_6)_2$,[37] $[Ru(dppz)(phen)_2]^{2+}$ [135,136,138] or $[Ru(dppz)(NH_3)_4]^{2+}$ (see Table 7).[138]

Table 11: Binding constants k_B and binding site size s of the dinuclear metal-silicon complexes **223**–**231** and **233**–**237** to *calf thymus* DNA. The values were obtained by plotting the decrease of the absorption at a specific wavelength λ as a function of increasing DNA concentration using the McGhee-von Hippel equation.[145,272]

Complex	λ /nm	k_B /M^{-1}	s
223[a]	393	$(1.1 \pm 0.4) \times 10^8$	1.38 ± 0.10
224	393	$(1.3 \pm 0.2) \times 10^7$	0.87 ± 0.08
225[a]	393	$(2.7 \pm 0.9) \times 10^7$	1.30 ± 0.10
226	393	$(1.7 \pm 0.2) \times 10^7$	1.05 ± 0.07
227	394	$(1.4 \pm 0.5) \times 10^7$	1.21 ± 0.09
228	394	$(1.3 \pm 0.1) \times 10^7$	0.83 ± 0.07
229[a]	382	$(5.7 \pm 1.9) \times 10^7$	1.40 ± 0.04
230	382	$(1.40 \pm 0.03) \times 10^7$	0.92 ± 0.05
231[a]	390	$(2.9 \pm 0.9) \times 10^7$	0.65 ± 0.05
233[b]	403	$(3.7 \pm 0.4) \times 10^6$	0.85 ± 0.04
234	403	$(2.6 \pm 0.3) \times 10^6$	0.94 ± 0.02
235[b]	403	$(7.3 \pm 0.8) \times 10^5$	0.59 ± 0.06
236[b]	403	$(8.7 \pm 0.3) \times 10^5$	0.58 ± 0.02
237	404	$(2.0 \pm 0.1) \times 10^6$	0.86 ± 0.03
$[Ru(phen)_2(\mu\text{-tpphz})Ru(phen)_2](NO_3)_4$		1.1×10^7 [140]	2.6 [140]
		3.1×10^6 [140],[c]	2.0 [140],[c]
$[Ru(bpy)_2(\mu\text{-tpphz})Ru(bpy)_2](NO_3)_4$		3.3×10^8 [140]	2.2 [140]
		6.0×10^6 [140],[c]	1.8 [140],[c]
$[Ru(phen)_2(\mu\text{-tatpp})Ru(phen)_2](NO_3)_4$		1.1×10^7 [140]	1.1 [140]
		3.7×10^5 [140],[c]	1.3 [140],[c]
$[Ru(dppz)_2(\mu\text{-TBphen}_2)Ru(dppz)_2](NO_3)_4$		$(8.8 \pm 1.1) \times 10^6$ [151]	
$[Si(DHB)(dppz)(phen)](PF_6)_2$ (**184**)[d]	357	$(1.6 \pm 0.1) \times 10^6$	1.17 ± 0.02
$[Si(phen)_2(bqp)](PF_6)_2$ (**137**)[e]		2.0×10^7 [149]	

[a] Determined by Steffen Glöckner during his bachelor thesis. [b] Determined by Alexandra Gruber during her bachelor thesis. [c] A 200 mM KCl aqueous buffer was used. [d] For more information see chapter 3.3.2. [e] For more reported binding constants of mono- and dinuclear metal complexes see Table 7 in Chapter 3.3.2.

Interestingly, the rhodium and iridium containing complexes had a lower affinity to ds-DNA than the mononuclear silicon(IV) complex **137** that was synthesized and studied by Yonggang Xiang during his PhD in the Meggers group.[149] Although this complex possesses a lower charge compared to the dinuclear complexes, it showed very strong binding to ds-DNA which is very likely due to intercalation of the huge planar ligand into the base pairs of the DNA. Nevertheless, a similar binding mode can

be discussed for the dinuclear complexes as well as a binding site size s > 1 indicates an intercalative binding mode.[145] However, as also s < 1, an indication for hydrophobic molecules aggregating on the DNA surface,[138,145] was obtained for some dinuclear complexes, the binding mode of the complexes to ds-DNA is not completely understood. In addition, the mode of binding of structural similar dinuclear metal complexes is discussed controversial in the literature.[144,151,152] Hence, additional experiments investigating the interaction of the dinuclear metal-silicon(IV) complexes with double stranded DNA have to be done.

Due to the structure of the dinuclear complexes, it was assumed that they would strongly bind G-quadruplex DNA as demonstrated by Thomas *et al.* in 2006 for structural similar, dinuclear ruthenium complexes.[140] Therefore, the interaction of selected dinuclear metal-silicon(IV) complexes to G4-DNA was studied next. As G-quadruplex target structure, a 24 bases long DNA strand ($[T_2AG_3]_4$, telo24) mimicking the human telomerase G4-DNA was used.[162,290] A similar, only 22 base pair long strand was utilized by Thomas and co-workers.[140] The guanine rich strand is capable of forming a quadruplex structure consisting of three stages and can therefore be used as a model system. The binding constants of the selected dinuclear complexes (10 µM) to the G4-DNA were determined using the UV-Vis monitored DNA binding assay in telo24-buffer (10 mM Tris-HCl, 100 mM NaCl, 1 mM EDTA, pH 7.4) as described above. Upon titration with with G4-DNA, the absorption of the complexes studied decreased (Figure 62) just like observed during titration with ds-DNA.

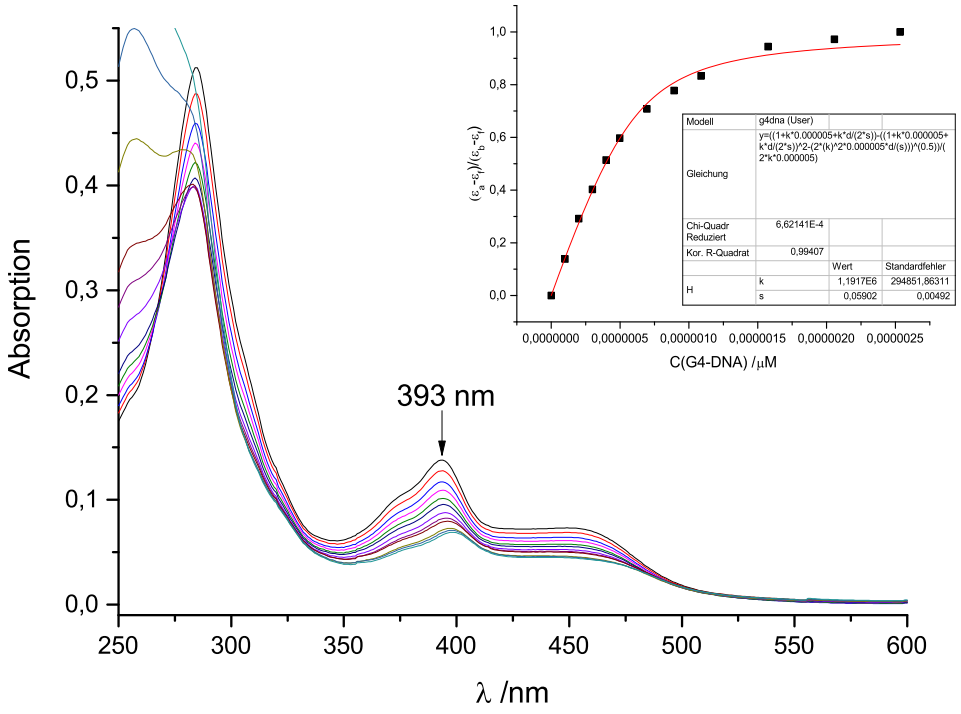

Figure 62: UV/Vis-absorption spectra of complex **224** (10 µM) in Tris-buffer (10 mM Tris-HCl, 100 mM NaCl, 1 mM EDTA, pH 7.4) upon titration with telo24-G4-DNA at room temperature. Insert: plot of $(\epsilon_a - \epsilon_f)/(\epsilon_b - \epsilon_f)$ at 393 nm versus DNA concentration, with ϵ_a = extinction coefficient of the complex at a given DNA concentration, ϵ_b = extinction coefficient when fully bound to DNA, and ϵ_f = extinction coefficient of the complex in the absence of DNA.

Plotting the absorption decrease as a function of increasing G4-DNA concentration using the McGhee-von-Hippel equation,[140,145,272] the binding constants k_B in Table 12 were obtained. Surprisingly, the obtained binding constants are one order of magnitude lower compared to the corresponding binding constants to double stranded *calf-thymus* DNA with a similar charge dependency. However, they are within the same range as the dinuclear ruthenium complexes $[Ru(phen)_2(\mu\text{-}pp)Ru(phen)_2](NO_3)_4$.[140,162] Nevertheless, all dinuclear metal-silicon complexes showed a very strong affinity to quadruplex DNA. Since all complexes had a s value of less than one, a non-intercalative binding mode through interactions with grooves/loops is assumed, according to the literature.[162] To prove this statement, additional experiments have to be done.

Table 12: Binding constants k_B and binding site size s of the dinuclear metal-silicon complexes to telo24 quadruplex DNA ($[T_2AG_3]_4$). The values were obtained by plotting the decrease of the absorption at a specific wavelength λ as a function of increasing DNA concentration using the McGhee-von Hippel equation.[145,272]

Complex	λ /nm	k_B /M^{-1}	s
223	393	$(2.2 \pm 0.1) \times 10^6$	0.160 ± 0.002
224	393	$(2.4 \pm 1.1) \times 10^6$	0.10 ± 0.02
226	393	$(1.8 \pm 0.1) \times 10^6$	0.110 ± 0.003
227	394	$(2.1 \pm 0.4) \times 10^6$	0.100 ± 0.004
228	394	$(1.8 \pm 0.2) \times 10^6$	0.080 ± 0.002
230	382	$(1.4 \pm 0.1) \times 10^6$	0.120 ± 0.003
234	403	$(4.0 \pm 0.1) \times 10^5$	0.060 ± 0.002
237	404	$(3.7 \pm 0.3) \times 10^5$	0.060 ± 0.002
$[Ru(phen)_2(\mu\text{-tpphz})Ru(phen)_2](NO_3)_4$[a]		4.4×10^6 [140]	
$[Ru(bpy)_2(\mu\text{-tpphz})Ru(bpy)_2](NO_3)_4$[a]		9.5×10^6 [140]	

[a] A 200 mM KCl aqueous buffer was used.

Next, the cytotoxicity of the dinuclear metal-silicon(IV) complexes **223**, **224**, **226**, **227**, **228**, **230**, **234** and **237** at a high concentration of 30 µM was investigated using the MTT test. The results are shown in Figure 63. All complexes studied show only weak cytotoxicity with an EC_{50}, the half maximal effective concentration at which 50 % of the cells survive, above 30 µM. However, the charge of the complexes has an influence on its toxicity. Hence, the the ruthenium containing complexes with a charge of 4+ (red bar) led to a cell surviving of > 85 % whereas the iridium and rhodium containing complexes (yellow bar) showed only a cell surviving of 73–75 %. This correlation between charge and cytotoxicity was observed frequently in the Meggers group but is not yet completely understood.[146] Possible explanations for this observation may be the route of cellular uptake as well as different interactions of the complexes with vital proteins. The major routs for molecules to enter cells are the active transport or the facilitated diffusion by a specific carrier protein as well as simple diffusion that can be assisted by certain channel proteins.[182] Especially for the diffusion, a very hydrophobic compound is necessary to cross the lipophilic cell membranes.[182,291] Hence, a lower charge of the complex may facilitate this transport mechanism leading to a higher concentration of the

complex in the cell increasing the cytotoxicity. On the other hand is also imaginable that the carrier proteins differentiate between the charges of the complexes allowing only the lower charged complexes to enter. Nevertheless, all dinuclear complexes synthesized should be able to enter the cell due to their structural similarity to the dinuclear ruthenium complexes $[Ru(pp)_2(\mu\text{-tpphz})Ru(pp)_2](PF_6)_4$ that were used for imaging DNA structure in living cells as demonstrated by Thomas and co-workers in 2009.[152] In addition, the low cytotoxicity of the dinuclear metal-silicon(IV) complexes are in accordance with the low toxicity of similar dinuclear ruthenium(II) complexes.[152]

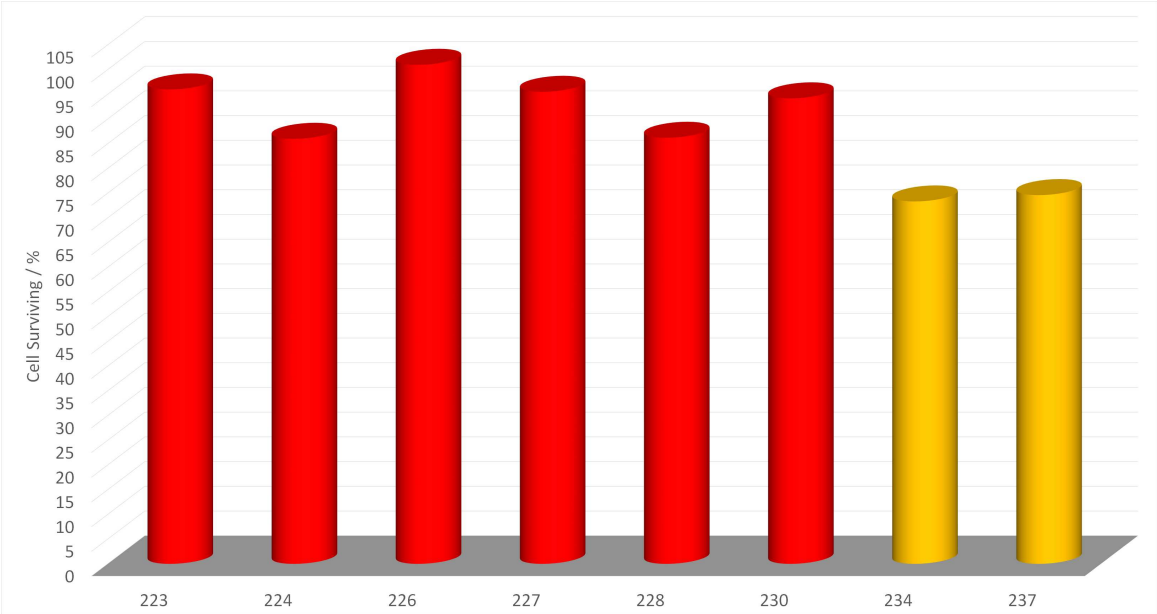

Figure 63: Results of the MTT tests of dinuclear metal-silicon(IV) complexes at a concentration of 30 µM. Complexes with a charge of 3+ or 4+ are colored in yellow and red, respectively.

3.5. Bodipy-modified Octahedral Silicon(IV) Complexes

3.5.1. Synthesis

Unfortunately, all hexacoordinate silicon(IV) complexes discussed so far did not show any fluorescence, which is crucial for their potential use in biological systems, for example as DNA-imaging agents[129,141,142] or to image biomolecules.[292] To obtain such fluorescence, the introduction of a fluorophore was studied next. Due to its well studied fluorescence properties[293–297] and its widely utilization as chemical fluorescent sensors or labeling agents[298,299] including an imaging probe to sensor biomolecules in living cells,[292] a Bodipy dye was used. Having various alkyne substituted silicon(IV) complexes in hand (chapter 3.2.4, 3.3), the idea was to introduce the Bodipy residue using copper catalyzed click chemistry. Hence, Bodipy-N_3 (**243**) bearing a azide group was synthesized in a three step synthesis with an overall yield of 9 % (Scheme 57). According to literature procedures,[300,301] 4-hydroxybenzaldehyde (**244**) was reacted first, in a Williamson ether synthesis, with ethylene dibromide and potassium carbonate in acetonitrile at 60 °C over night obtaining 4-(2-bromoethoxy)benzaldehyde in a yield of 86 %. In a subsequent S_N2 reaction with sodium azide in *N,N*-dimethylformamide at 100 °C for three hours, the bromine residue was substituted with an azide.[298] After purification by column chromatography on silica gel, 4-(2-azidoethoxy)benzaldehyde (**245**) was obtained in a yield of 91 %. Finally, Bodipy-N_3 (**243**) was synthesized in a multistage one-pot synthesis in accordance with a method published by Xiao and co-workers in 2008.[298] Under an atmosphere of nitrogen, compound **245** was reacted with 2,4-dimethylpyrrole in the presence of absolute trifluoroacetic acid in anhydrous dichloromethane at room temperature over night. To ensure a completely oxidized intermediate, the oxidation agent 2,3-dichloro-5,6-dicyano-1,4-benzoquinone was added and the reaction mixture was stirred at room temperature for three hours. After deprotonation with triethylamine, boron trifluoride diethyl etherate was added at 0 °C and the mixture was stirred at room temperature for two days. Having realized several purification steps including silica gel column chromatography, green fluorescent Bodipy-N_3 (**243**) was obtained as a red solid in a yield of 11 %.

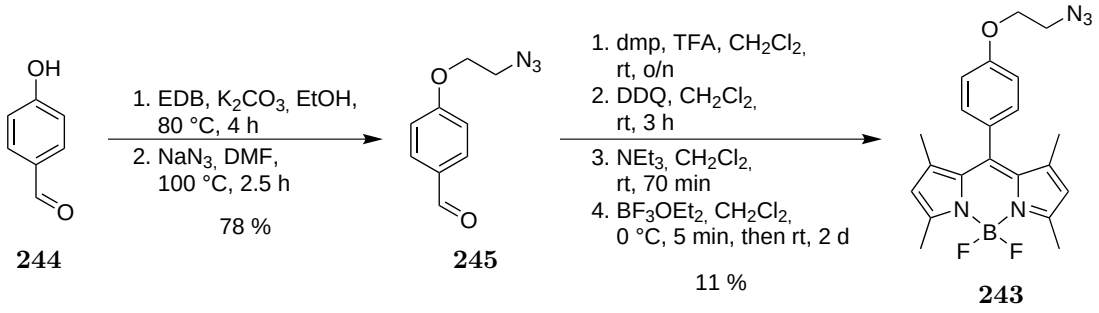

Scheme 57: Synthesis of Bodipy-N_3 (**243**) according to literature procedures.[298,300,301]

A possible reason for the low yield of the final step of the Bodipy-N_3 (**243**) synthesis, which has also been observed by Xiao *et al.*,[298] may be the formation of several side products that are removed during column chromatography. In addition, the compound somehow interact with the silica gel as it got stuck on it leading to a significant yield loss after each column chromatography. Regarding the stability of the starting aldehyde **245** towards oxidation, it is also imaginable that the aldehyde is oxidized to the less electrophilic carbonic acid leading to a slower reaction. This oxidation was

observed by crystal formation in a solution of aldehyde **245** in dichloromethane over a period of two weeks. The obtained crystals were characterized by crystal structure analysis revealing the acid structure (Figure 64). Thus, the aldehyde was oxidized by the air to the carbonic acid that crystallized as colorless prism in the monoclinic space group P $2_1/n$.

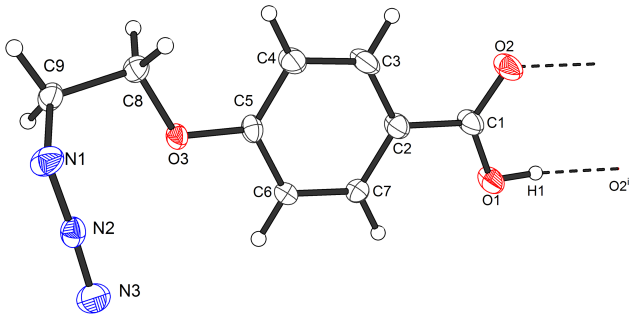

Figure 64: Crystal structure of 4-(2-azidoethoxy)benzoic acid. ORTEP drawing with 50 % probability thermal ellipsoids. In the crystal structure, the compound is forming a dimeric structure connected by hydrogen bonds of the carbonic acid group.

With compound **243** in hand, the click chemistry at the silicon(IV) complexes was studied next. Therefore, complex **167** and Bodipy-N_3 (**243**) were reacted in an acetonitrile/water mixture under an atmosphere of nitrogen in the presence of a freshly prepared mixture of copper sulfate pentahydrate and sodium ascorbate (Scheme 58).

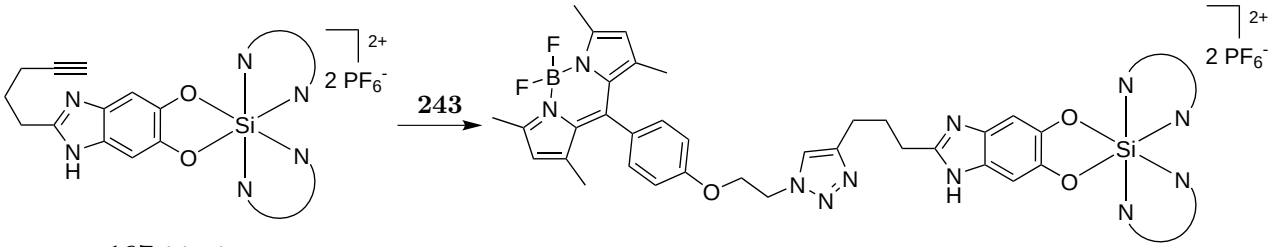

167 (phen)
173 (Me_4phen)
191 (dppz, phen)

246 (phen, 66 %) [a]
247 (Me_4phen, 52 %) [b]
249 (dppz, phen, 18 %) [c]

Scheme 58: Copper catalyzed click chemistry of silicon(IV) complexes **167**, **173** and **191** with Bodipy-N_3 (**243**). ([a] Conditions: 2.7 eq. **243**, 0.6 eq. $Cu(SO_4)$, 0.8 eq. sodium ascorbate, MeCN/H_2O 2:1, 6.7 mM, rt, 2 h → 100 °C, 3 h → 4.0 eq. CuI, 100 °C, 1 h. [b] Conditions: 2.1 eq. **243**, 1.0 eq. $Cu(SO_4)$, 1.3 eq. sodium ascorbate, 0.9 eq. CuI, MeCN/H_2O 2:1, 5.9 mM, 100 °C, 18 h gave an inseparable mixture of starting material **173** and product **247** with a ratio of 1.5:1. [c] Conditions: 2.5 eq. **243**, 0.5 eq. $Cu(SO_4)$, 0.8 eq. sodium ascorbate, MeCN/H_2O 2:1, 5.4 mM, 100 °C, 3 h gave an inseparable mixture of starting material **191** and product **249** with a ratio of 0.7:1 in a yield of 53 %. Further conversion of the obtained mixture led to the pure product. Conditions of the second step: 2.5 eq. **243**, 0.5 eq. $Cu(SO_4)$, 0.8 eq. sodium ascorbate, 1.3 eq. CuI, MeCN/H_2O 2:1, 5.4 mM, 100 °C, 16 h.)

The reaction was monitored by LCMS. After two hours at room temperature, followed by a temperature increase to 100 °C for additional three hours, no conversion was observed. Thus,

copper(I) iodide was added in excess and the mixture was stirred for one additional hour at 100 °C leading to full conversion of the starting material. After silica gel flash column chromatography and exchanging the counter ion to hexafluorophosphate, the green fluorescent silicon(IV) complex **246** was obtained in a yield of 63 %. Unfortunately, similar conditions for complex **173** and **191** gave only an inseparable mixture of starting material and product (**173**) or the desired product (**191**) in a very low yield of 18 %. Unfortunately, complex **190** did not show any sign of conversion.

As the click reaction at the silicon(IV) complexes had a lot of disadvantages, a new synthetic strategy including an introduction of a pre-clicked Bodipy fragment to the hexacoordinate silicon complexes by a condensation reaction was tried. Therefore, the carbonyl substituted Bodipy **250** was synthesized utilizing a modified literature procedure of Xiao and co-workers.[298] Therefore, Bodipy-N_3 (**243**) and 5-hexynal (**189**, 2.0 eq.) were reacted in a mixture of acetonitrile, ethanol and water (12:1:1, 87.1 mM) in the presence of catalytic amount copper sulfate pentahydrate and sodium ascorbate using μ-wave irradiation for 75 minutes, followed by stirring at room temperature for 16 hours (Scheme 59). After purification by flash column chromatography, green fluorescent Bodipy **250** was obtained as a red solid in a moderate yield of 51 %. Besides the product, 21 % of unreacted starting material **243** was recovered.

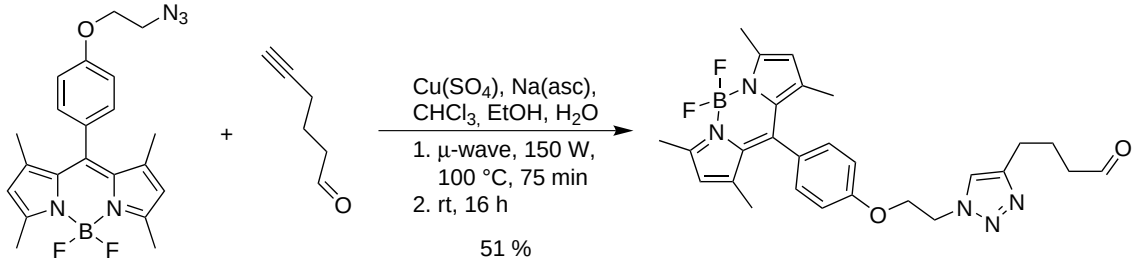

243 **189** **250**

Scheme 59: Synthesis of Bodipy **250** by click chemistry.

Having the aldehyde functionality attached to the Bodipy, the next step was the condensation reaction starting from dinitro substituted silicon(IV) complexes **251**, according to the method discussed above (Scheme 60). After purification by silica gel column chromatography and exchanging the counterion to hexafluorophosphate, the fluorescent, hexacoordinate silicon(IV) complexes **246**–**249** were obtained in moderate yields of 37–63 % over two steps (Figure 65).

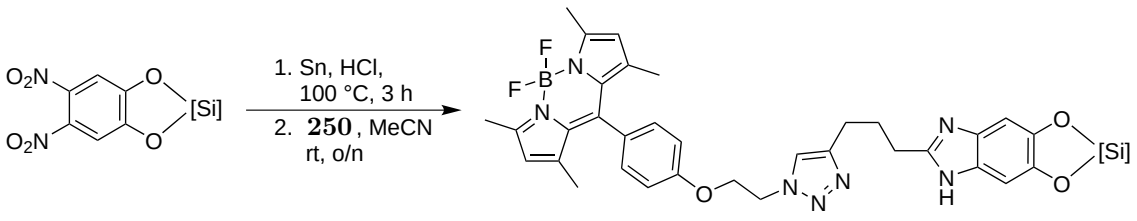

252 **253**

Scheme 60: Scheme of the condensation reaction of hexacoordinate silicon complexes with Bodipy **250**.

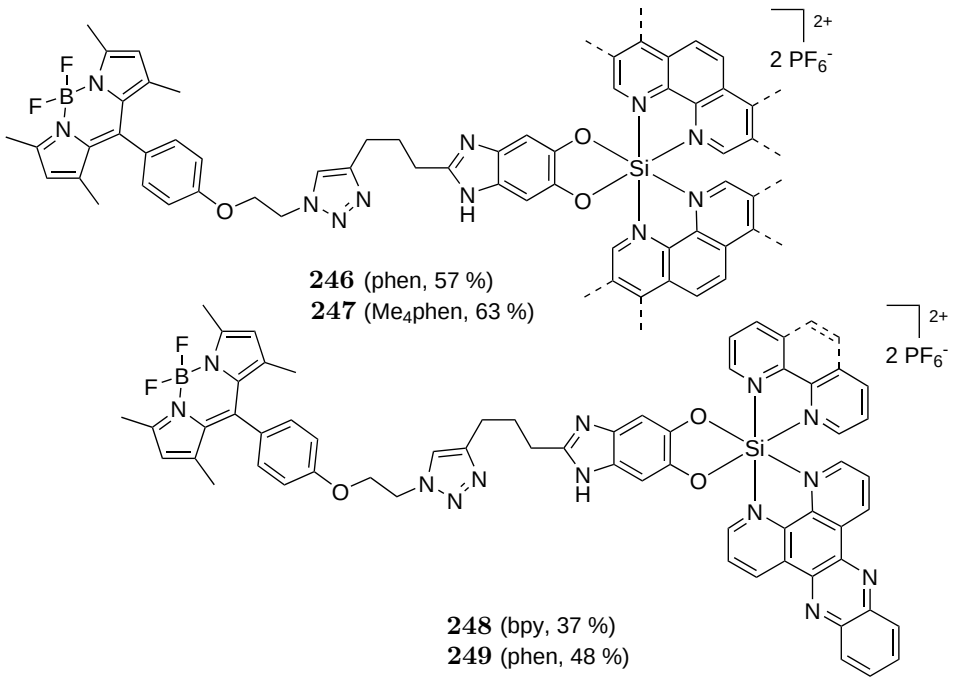

Figure 65: Synthesized hexacoordinate silicon(IV) complexes substituted with a Bodipy moiety.

The ^{1}H-NMR spectrum of complex **249** in acetonitrile-d_3 is shown in Figure 66 demonstrating the purity of the obtained Bodipy-substituted silicon(IV) complexes by way of example. The synthesized complexes **246**–**249** and Bodipy **250** were further characterized by ^{11}B-NMR and ^{19}F-NMR to prove the Bodipy structure. The chemical shifts and the coupling constants are in accordance with various Bodipy structures discussed in the literature.[293,295] Anyhow, complex **248** showed a slightly lower chemical shift of $\delta = -0.45$ ppm, compared to $\delta = -1.2$ to -1.3 ppm for **246**, **247** and **249** in the ^{11}B-NMR.

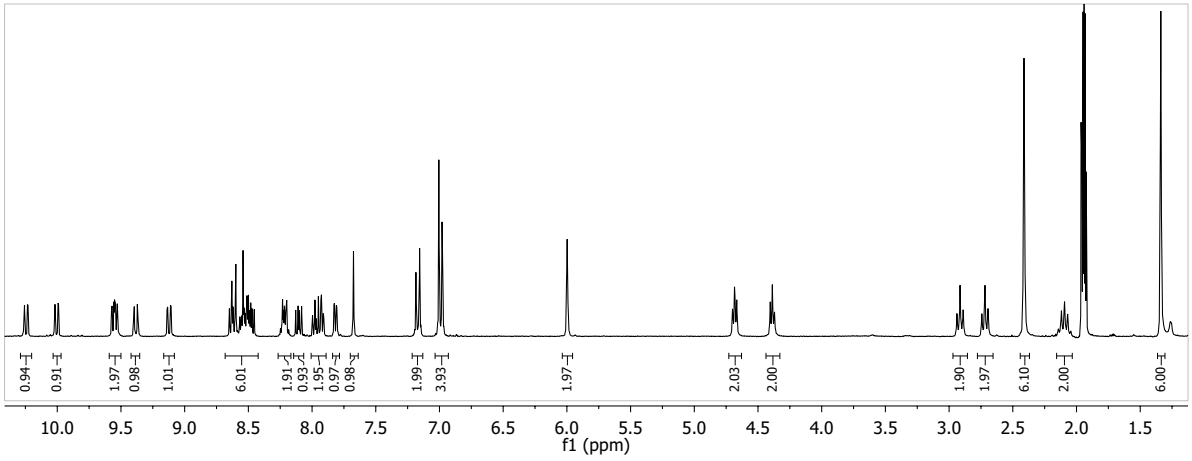

Figure 66: ^{1}H-NMR spectrum of complex **249** (15 mM) in acetonitrile-d_3.

3.5.2. Photochemical Properties

The differences of the absorption and emission properties of the Bodipys **243** and **250** and complex **246** (each 30 μM) were studied in dimethyl sulfoxide (Figure 67). In the absorption spectrum, the characteristic Bodipy band at 501 nm[293–295,297,298] was present for all compounds studied. In addition,

complex **246** showed the silicon centered absorption band below 340 nm with a peak at 281 nm. While Bodipy **243** and **250** exhibited a nearly identical absorption intensity, it was about 18 % lower for complex **246**. Similar results were obtained for the emission spectrum at an excitation at $\lambda = 350$ nm. Interestingly, all three compounds showed a different emission intensity with a peak at 516 nm. In a different way from expected, Bodpiy **250** with the triazole exhibited the strongest fluorescence being 25 % higher compared to Bodipy-N_3 (**243**). On the other hand, silicon(IV) complex **246** offered the weakest fluorescence possessing only 17–21 % of the emission intensity compared to the free Bodipys **243** and **250**. In addition, a hypsochromic shift of 1 nm could be observed. Taken all together, the silicon(IV) center has a big influence on the emission spectra of the Bodipy structure as it quenches fluorescence in a very strong fashion. However, complex **246** still showed some fluorescence and could therefore be used as a fluorescence probe in biological applications.

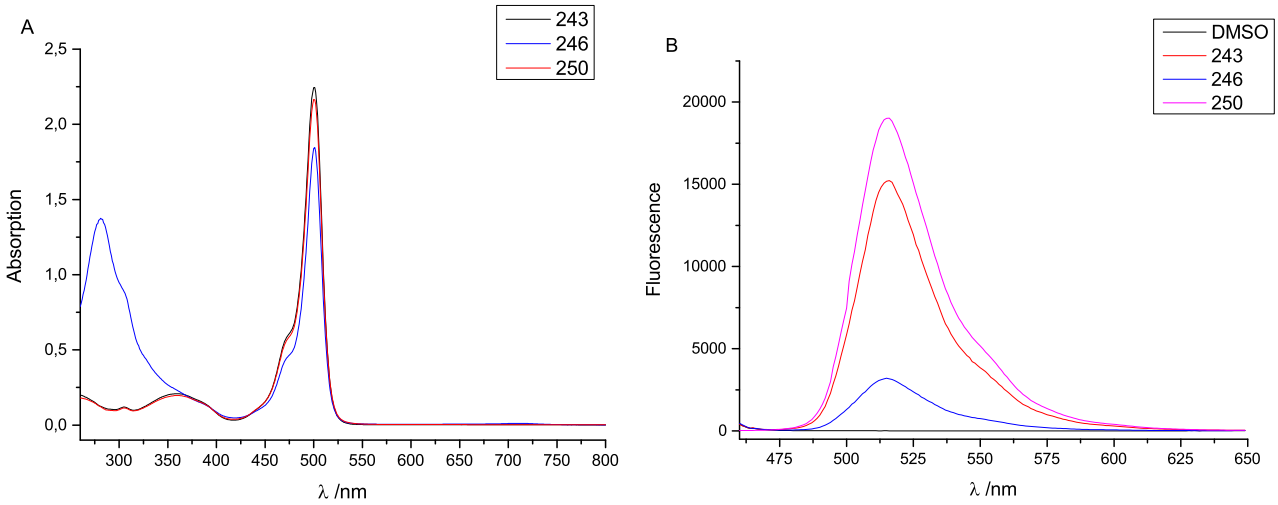

Figure 67: Absorption (A) and emission (B, excitation at $\lambda = 350$ nm) spectra of Bodipy **243** and **250**, as well as of complex **246** (30 µM) in DMSO at room temperature.

The reduction of the Bodipy fluorescence upon coordination to a hexacoordinate silicon(IV) center can be explained by the photoinduced electron transfer (PeT) as the fluorescence intensity is easily altered by an intramolecular electron transfer between nonplanar parts of a fluorescent molecule.[294,302–306] Hence, the fluorescence of a fluorophore can be quenched by an electron donating or accepting residue, depending on their oxidation potential relative to the excited state of the fluorophore, linked to it.[294,302] On the other hand, if there is no such influence, the fluorescence will not be reduced. For example, the Bodipys **243** and **250** combine a very strong fluorophore, the Bodipy core structure (red), and a non or only low fluorescent residue at its *meso*-position (Figure 68, a). Due to the high emission, it is very plausible that there is no electronic interference of the HOMO and LUMO of the residues with the excited state of the fluorophore leading to this high fluorescence.

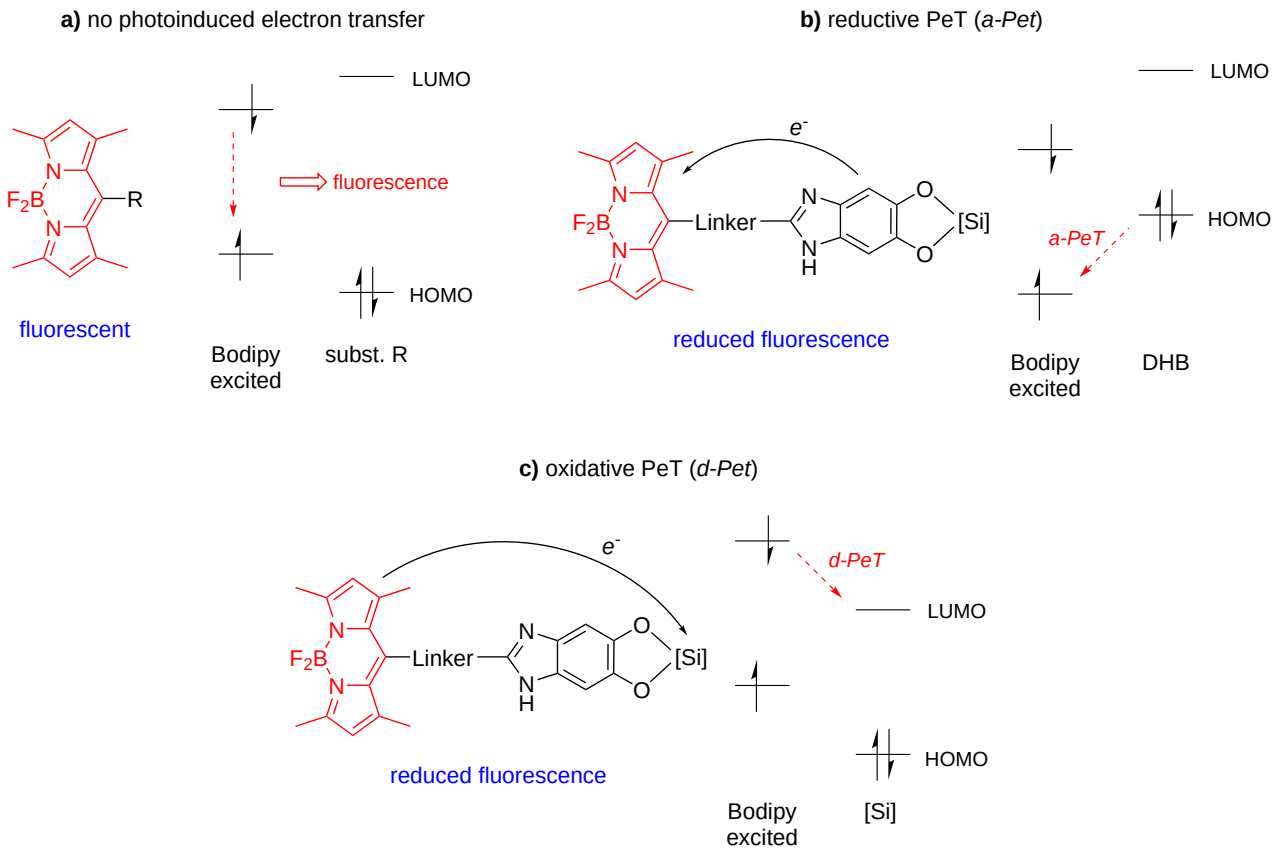

Figure 68: Schematic molecular orbital diagrams of the excited Bodipy core linked to a residue or the silicon(IV) center. If the residue provides no significant electronic perturbation, for example in the Bodipys **89** and **250**, strong fluoresence can be observed (a). If the Bodipy structures are linked to a hexacoordinate silicon(IV) center, for example complex **246**, the benzene-1,2-diolato structure can donate an electron to the Bodipy (b) or the LEWIS acid silicon(IV) can accept with the low lying LUMO an electron of the Bodipy (c) reducing the fluorescence in both cases.

Upon substitution with a hexacoordinate silicon center, for example in complex **246**, two plausible ways for the quenching can be discussed. Firstly, the negatively charged benzimidazolato structure may donate an electron to the excited Bodipy core with the result of reducing it (Figure 68, b). This process is called reductive photoinduced electron transfer or *a-PeT* as the fluorophore acts as an electron acceptor. Otherwise, the strong LEWIS acid silicon(IV) can also accept an electron from the excited state of the Bodipy core in an oxidative photoinduced electron transfer or *d-PeT* (Figure 68, c). Due to the nature of the hexacoordinate silicon(IV) complexes, both effects play an important role quenching the fluorescence of the Bodipy substituted complexes **246**–**249** whereat the *d-PeT* mechanism may be more prominent due to the strong LEWIS acidity of the 4+ charged silicon center.

3.5.3. Biological Activity

The absorption and fluorescence properties of the complexes **246**, **247**, **248** and **249** (20 µM) were studied in Tris-buffer (5 mM Tris-HCl, 20 mM NaCl, pH 7.4) at room temperature. All complexes exhibited a characteristic Bodipy absorption band at 499–502 nm [293–295,297,298] as well as the silicon centered absorption below 340 nm (Figure 69, A). The absorption at around 360 nm of complexes **248** and **249** arises from a dppz $\pi \rightarrow \pi^*$ ligand-centered charge transfer which has been observed

in various transition metal complexes coordinate to a dppz ligand.[130,135,137,138,145] In comparison, complex **184** lacked the Bodipy absorption band and possessed only the dppz $\pi \rightarrow \pi^*$ absorption at 357 nm as well as the silicon centered absorption. These results are in accordance with the color of the complexes as the Bodipy substituted complexes **246**, **247**, **248** and **249** are red, whereas **184** is yellow. Furthermore, upon excitation with a wavelength of 366 nm, all complexes substituted with a Bodipy residue showed a fluorescence band at 510 nm which corresponds to the Bodipy fluorophore (Figure 69, B).[293–295,297,298] The low emission intensity of the dppz complexes **248** and **249** compared to **246** and **247** may be due to possible quenching effects of the dppz ligand itself. Its non-coordinating nitrogen atoms can form hydrogen bonds to the surrounding water molecules which will destroy the excited state and thus inhibit the fluorescence. This so called light-switch behavior is well known and investigated for dppz or tpphz coordinate ruthenium complexes.[128,129,141–144,280]

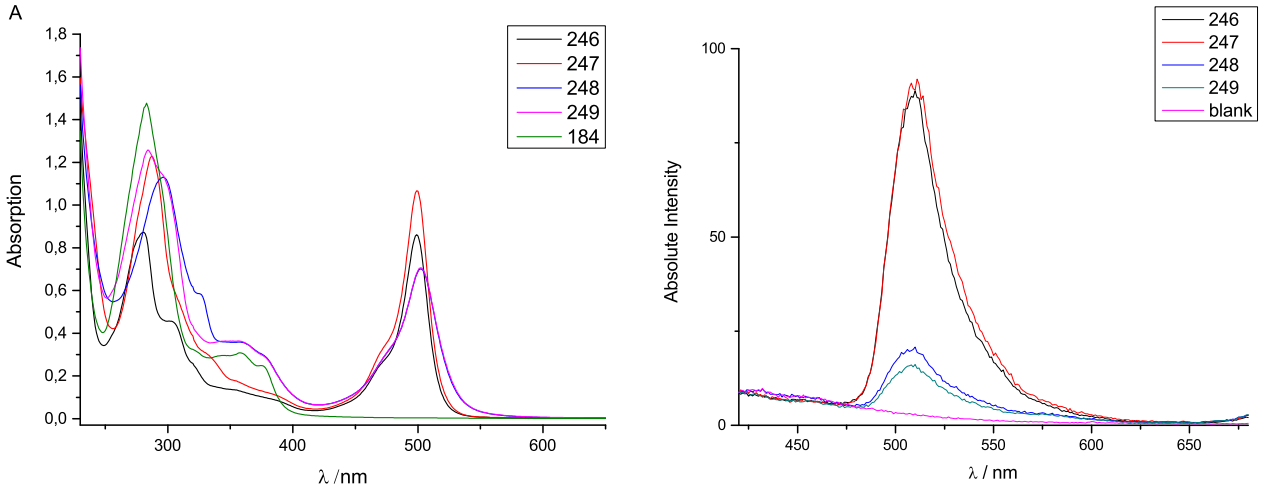

Figure 69: Absorption (A) and emission (B, excitation at $\lambda = 366$ nm) spectra of complexes **184**, **246**, **247**, **248** and **249** (20 µM) in Tris-buffer (5 mM Tris-HCl, 20 mM NaCl, pH 7.4) at room temperature.

Next, the light-switch behavior (excitation at $\lambda = 366$ nm) of the Bodipy substituted complexes **246**, **247**, **248** and **249** in the presence of different equivalents of *calf thymus* DNA was investigated (Figure 70). Interestingly, upon addition of one equivalent DNA, the emission intensity of all complexes decreased and a bathochromic shift could be observed. An explanation for this behavior may be that only a few complexes are bound to DNA and the contribution of the unbound complexes to the emission intensity is much higher than the contribution of the bound ones. After addition of two and more equivalents of *calf thymus* DNA, the emission intensity increased again until it reached a peak after addition of 18 equivalents, indicating that at this DNA concentration the equilibrium bound/unbound was reached. Moreover, a bathochromic shift of 5–6 nm could be observed for all complexes. Anyhow, complex **246** and **247** showed only a weak intensity increase of 480 % and 90 % compared to 1 eq. DNA, respectively. Furthermore, the emission intensities were around the same or even lower compared to the DNA free samples, indicating that the binding to DNA somehow quenched the fluorescence. In comparison, **248** and **249** exhibited a slightly different behavior. Upon addition of *calf thymus* DNA, their emission intensities increased up to around 690 % and 730 % (compared to 1 eq. DNA) and were even around six times higher compared to the DNA free samples indicating

a strong DNA binding as well as a certain light switch behavior as the bound complexes exhibited stronger fluorescence than the unbound ones.

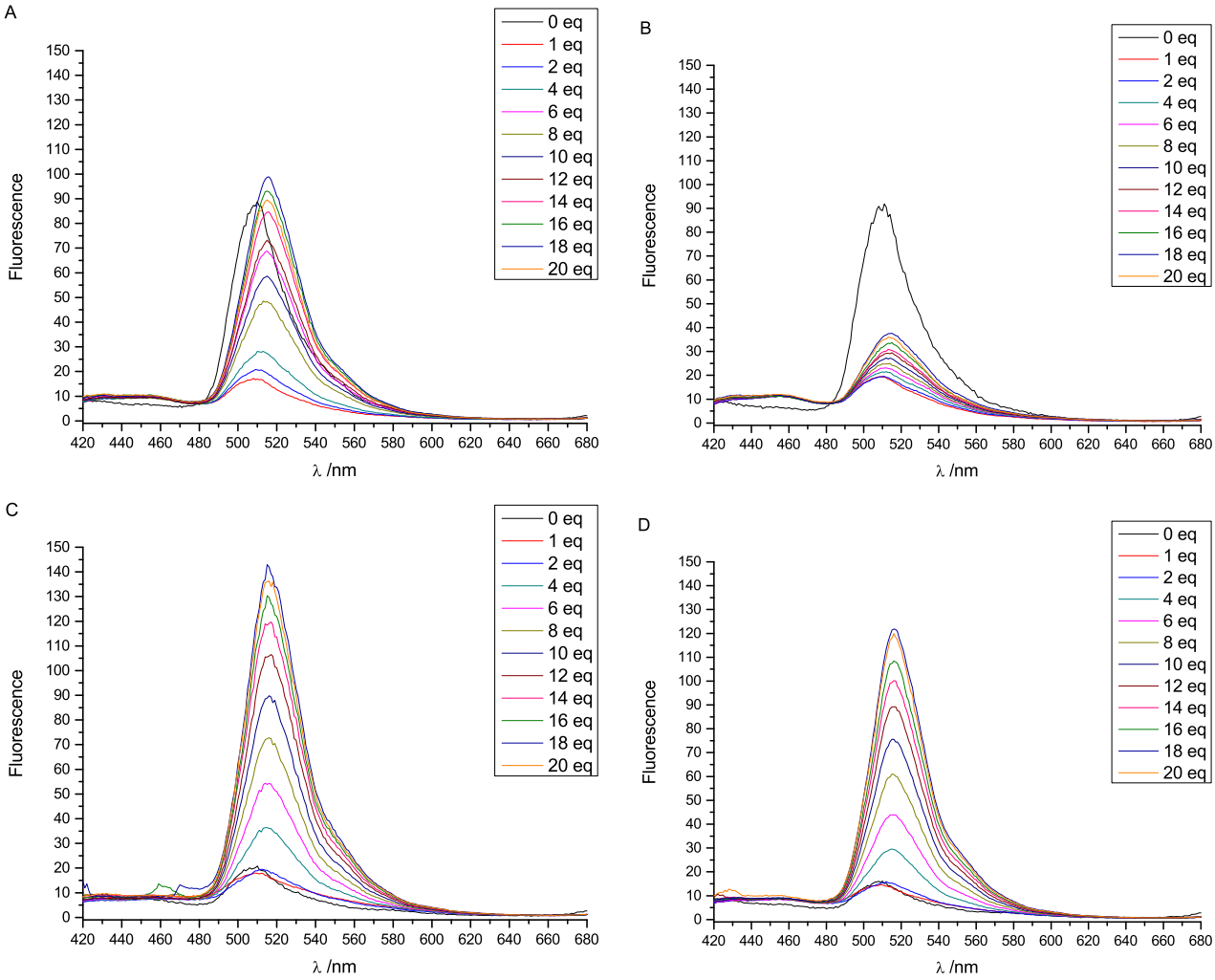

Figure 70: Emission spectra (excitation at $\lambda = 366\,\text{nm}$) of the complexes **246** (A), **247** (B), **248** (C) and **249** (D) (each 20 µM) in Tris-buffer (5 mM Tris-HCl, 20 mM NaCl, pH 7.4) at room temperature and in the presence of various equivalents of *calf thymus* DNA.

The change of the absorption spectrum of complexes **246**, **247**, **248** and **249** (20 µM) in Tris-buffer (5 mM Tris-HCl, 20 mM NaCl, pH 7.4) upon titration with *calf thymus* DNA was studied next. The titration absorption spectrum of complex **249** is shown in Figure 71 by way of example while the spectra for the other complexes can be found in E. All complexes exhibited strong hypochromicity of the bodipy band at 499 nm (70 % decrease for **246** and **247**) or 502 nm (36 % and 40 % decrease for **248** and **249**, respectively). In addition, modest bathochromic shifts of 3–6 nm were observed. Interestingly, the dppz bound complexes showed a lower bathochromic shift compared to the other complexes. Similar behavior was observed for complex **184**, which showed a strong DNA binding but no bathochromic shift.

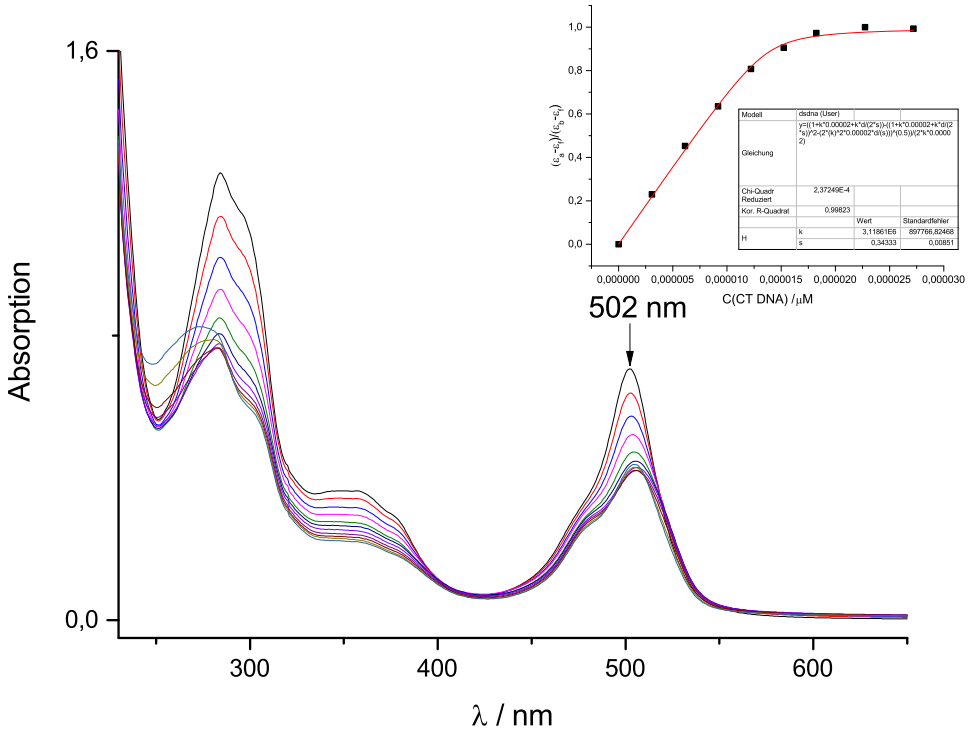

Figure 71: UV/Vis-absorption spectra of complex **249** (20 µM) in Tris-buffer (5 mM Tris-HCl, 20 mM NaCl, pH 7.4) upon titration with *calf thymus* DNA at room temperature. Insert: plot of $(\epsilon_a - \epsilon_f)/(\epsilon_b - \epsilon_f)$ at 357 nm versus DNA concentration, with ϵ_a = extinction coefficient of the complex at a given DNA concentration, ϵ_b = extinction coefficient when fully bound to DNA, and ϵ_f = extinction coefficient of the complex in the absence of DNA.

In Table 13 the binding constants and binding sizes for each complex, determined by plotting the absorption decrease of the Bodipy absorption band as a function of increasing DNA concentration using the McGhee-von Hippel equation,[145,272] are listed. As expected, the dppz bound complexes **248** and **249** exhibited a very strong affinity to double-stranded DNA of about $k_B = 10^6\ \mathrm{M}^{-1}$ and hence were within the range of known DNA binding complexes (see Table 7) and the tris-cationic metal-silicon complexes **234** and **237** (see Chapter 3.4.5). Due to the lower charge of only 2+ compared to 4+ for dinuclear ruthenium or ruthenium-silicon complexes, the binding to *calf thymus* DNA was about one to two orders of magnitude less strong (see Chapter 3.4.5). On the other hand, complexes **246** and **247** showed a binding constant of about $k_B = 10^5\ \mathrm{M}^{-1}$ to CT-DNA which may be explained by the missing dppz ligand leading to a lower intercalation capability compared to **248** and **249** and thus to a loss of affinity. Interestingly, in comparison to complex **184**, the Bodipy substituted complexes had a value for the binding site size, the number of DNA bases associated with the complex, of s < 1, which are obtained for hydrophobic molecules that aggregate on the DNA surface.[138,145] Considering the length of **246**, **247**, **248** and **249** together with the low values for s it is clearly visible that aggregation on the DNA surface and thus an electrostatic interaction with the negatively charged DNA backbone is their most plausible binding mode. In addition, the dppz ligand is nevertheless capable of intercalating between the base pairs of the DNA to increase the binding affinity causing the higher binding constants for **248** and **249** compared to **246** and **247**.

Table 13: Binding constants k_B and binding site size s of the synthesized octahedral silicon(IV) complexes **246**, **247**, **248** and **249** to *calf thymus* DNA. The values were obtained by plotting the decrease of the absorbance at a specific wavelength λ as a function of increasing DNA concentration using the McGhee-von Hippel equation.[145,272]

Complex	λ /nm	k_B /M^{-1}	**s**
246	499	$(2.0 \pm 0.1) \times 10^5$	0.28 ± 0.01
247	499	$(2.6 \pm 0.2) \times 10^5$	0.31 ± 0.02
248	502	$(2.7 \pm 0.3) \times 10^6$	0.330 ± 0.004
249	502	$(3.2 \pm 0.1) \times 10^6$	0.32 ± 0.04
$[Si(DHB)(dppz)(phen)](PF_6)_2$ (**184**)[a]	357	$(1.6 \pm 0.1) \times 10^6$	1.17 ± 0.02
$[Ir(ppy)_2(\mu\text{-dppzO})Si(phen)_2](PF_6)_3$ (**237**)[b]	404	$(3.7 \pm 0.3) \times 10^5$	0.060 ± 0.002
$[Ru(phen)_2(\mu\text{-dppzO})Si(phen)_2](PF_6)_4$ (**226**)[b]	393	$(1.7 \pm 0.2) \times 10^7$	1.05 ± 0.06
$[Ru(dppz)(phen)_2]^{2+c}$		(1–6) $\times 10^6$ [135,136,138]	

[a] For more information see chapter 3.3.2. [b] Examples for dinuclear metal-silicon(IV) complexes. For more information and examples see chapter 3.4.5. [c] Example for a dppz coordinate mononuclear ruthenium complex. For more reported binding constants of mono- and dinuclear metal complexes see Table 7 in Chapter 3.3.2.

Finally, the ability of silicon(IV) complexes **246**, **247**, **249** and **254** to enter the nucleus of a living cells was investigated by Sumaira Ashaf of the group of Wolfgang Parak. Therefore, the internalization of the Bodipy complexes inside Hela cells was studied using a confocal laser scanning microscope. After incubation of Hela cells with the synthesized silicon(IV) complexes for 24 hours, the cells were fixed with paraformaldehyde, and the cell and nucleus membranes were stained with WGA-TMR and Hoechst reagent, respectively. As expected, the silicon complexes were able to enter the cell as can be seen exemplary in Figure 72 for complex **249**. Unfortunately, all complexes remained mainly in the cytoplasm or lysosomes and were unable to enter the nuclei. This indicates that, despite the hydrophobic ligands, the complexes are to hydrophilic to cross the nuclei membrane. Furthermore, it seems that there is no active transport into the nucleus available that tolerates the silicon complexes. On the other hand it is also possible, that the silicon complexes decomposed in the cytoplasm or under the used conditions leading to a free Bodipy residue that is unable to enter the nuclei. Hence, additional experiments ensuring the stability of the silicon(IV) complexes under the used conditions must be made to obtain solid results.

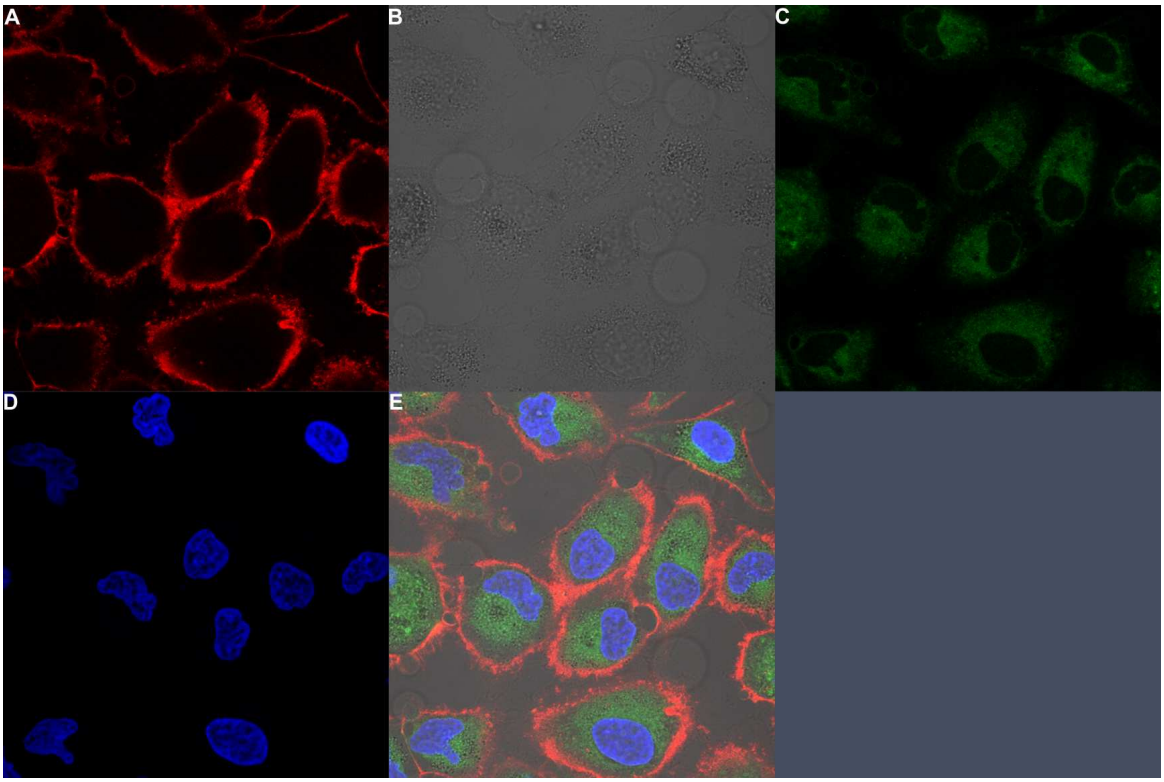

Figure 72: LSM Images of complex **249** internalized inside Hela cells (63× objective). Picture A showing the cell membranes, B showing the Transmission channel, C showing the distribution of the silicon complexes, D showing the nuclei and E showing an overlay channel. The experiment was performed by Sumaira Ashaf.

3.6. ^{29}Si-NMR Spectroscopy

Besides the standard analytic of high resolution mass spectrometry, IR-, ^{1}H-NMR and ^{13}C-NMR spectroscopy, all synthesized hexacoordinate silicon(IV) complexes were characterized by ^{29}Si-NMR spectroscopy to confirm the silicon and its coordination geometry.[307] The spectra were recorded at a reduce temperature of 243 K (1D) or at 300 K using a modified HMQC method (2D, Axis F1 = ^{29}Si, Axis F2 = ^{1}H) to prevent the formation of broad signals that occur due to the long spin-lattice relaxation time (T_1) of the ^{29}Si-nucleus.[307–309] Exemplary spectra for both measurements are shown in Figure 73 and Figure 74, respectively. Since all synthesized silicon(IV) complexes were structural very similar, the ^{29}Si chemical shifts varied only in a small range from $\delta = -152$–147 ppm. These results are in accordance with already reported hexacoordinate silicon complexes containing Si–N- and Si–O-bound ligands and hence confirm the higher coordination sphere of the silicon centers.[68,112–114,224,307]

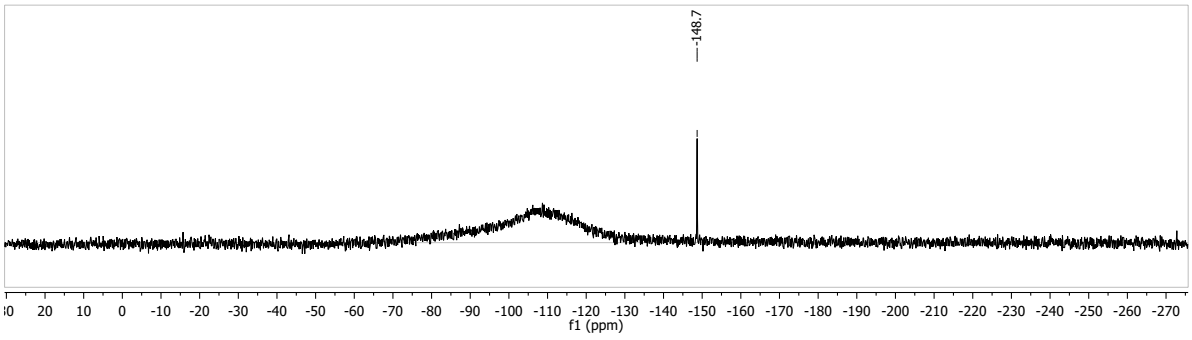

Figure 73: ^{29}Si-NMR (1D) of complex **90** in acetonitrile-d_3, measured at 243 K. The broad signal at around $\delta = -110$ ppm corresponds to the glass of the NMR tube.

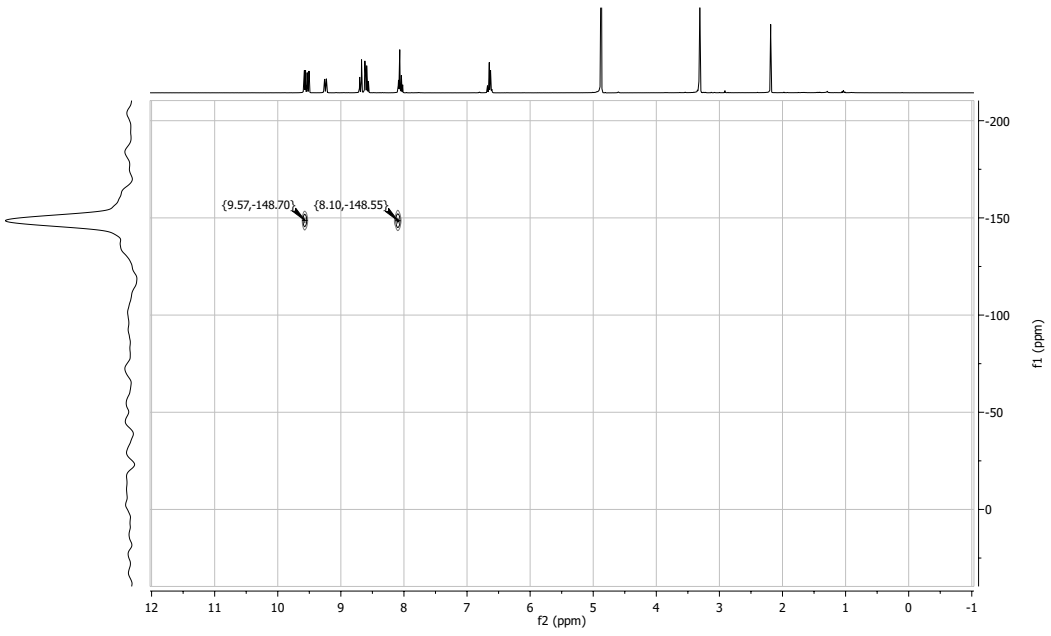

Figure 74: ^{29}Si-NMR (1D) of complex **90a** in methanol-d_4, measured at 300 K using a modified HMQC method (2D, Axis F1 = ^{29}Si, Axis F2 = ^{1}H). Shown are the ^{3}J cross-coupling signals of the polypyridine ligand and the silicon(IV) center.

4. Summary and Outlook

4.1. Synthesis of Octahedral Silicon(IV) Complexes

The synthesis of hexacoordinate silicon(IV) complexes was achieved by the reaction of silicon tetraiodide with various polypyridyl ligands. In this step, intermediate diiodo species (**85**, **86** and **255**) were formed (Scheme 61). Although these intermediates were prone to hydrolysis, they could be easily synthesized in larger amounts and stored for a long period of time under an atmosphere of nitrogen. Further conversion of the diiodo precursors with substituted and unsubstituted arenediols led to the formation of hydrolytically stable (arenediolato)bis(polypyridyl)silicon(IV) complexes in moderate yields over two steps. Surprisingly, also the aldehyde complex **92** could be isolated but only in very low yields. Furthermore, the octahedral geometry of the silicon(IV) center was confirmed by crystal structure analysis.

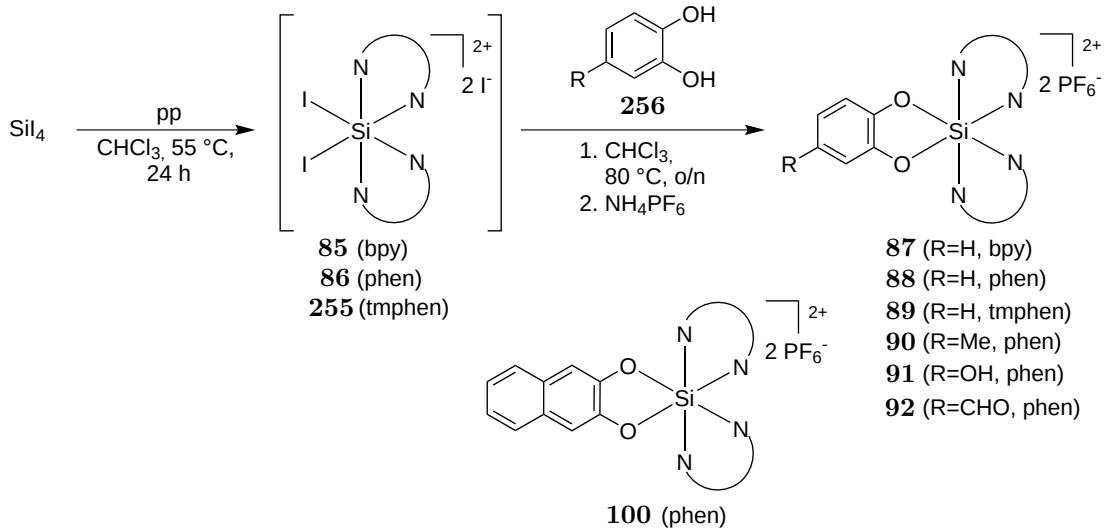

Scheme 61: Synthesis of various hexacoordinate bis(polypyridyl)(arenediolato)silicon(IV) complexes starting from silicon tetraiodide. The intermediate diidod species (**85**, **86** and **255**) could be isolated and stored under nitrogen or converted directly in a one pot synthesis to the desired product.

Although this reaction strategy seems general as it tolerates some functionality, for example hydroxygroups, the vast majority of synthetically attractive functional groups like carbonic acids, halogens, methyl ether, diketones, or large diolpolypyridyl ligands with an extended π-system were not suitable for this reaction. This observations can be explained by an interference of the strong acid hydrogen iodine formed during this reaction, leading for instance to an *ipso*-substitution of an bromine residue at the dihydroxybenzene ring. Since these functionalized silicon(IV) complexes were not accessible by a direct complexation, post-coordination derivatization was investigated next.

4.2. Post-Coordination Modification of Octahedral Silicon(IV) Complexes

Using standard organic reactions, a post-coordination modification of the benzenediolato ligand was realized (Scheme 62). The reaction of complex **257** with *N*-bromosuccinimide or *N*-iodosuccinimide in the presence of trifluoroacetic acid afforded bromine or iodine substituted complexes **258** and **259**, respectively. However, the introduction of only one halogen residue at the unsubstituted 1,2-

benzenediolato ligand proved to be more complicated but could be achieved for iodine (complex **260**) via an oxidative iodination using the reagent potassium 4-iodylbenzenesulfonate. An oxidation of (4-hydroxybenzenediolato)silicon(IV) complex was performed using the mild oxidation agent Fremy's salt. However, further conversion of the obtained dione complex **261** using a condensation reaction could not be realized. The reaction of complexes **257** with a mixture of acetic acid and nitric acid proved to be a very versatile reaction as it allowed the formation of mono- and dinitrated complexes (**134** and **262**, respectively), depending on the concentration of the nitric acid.

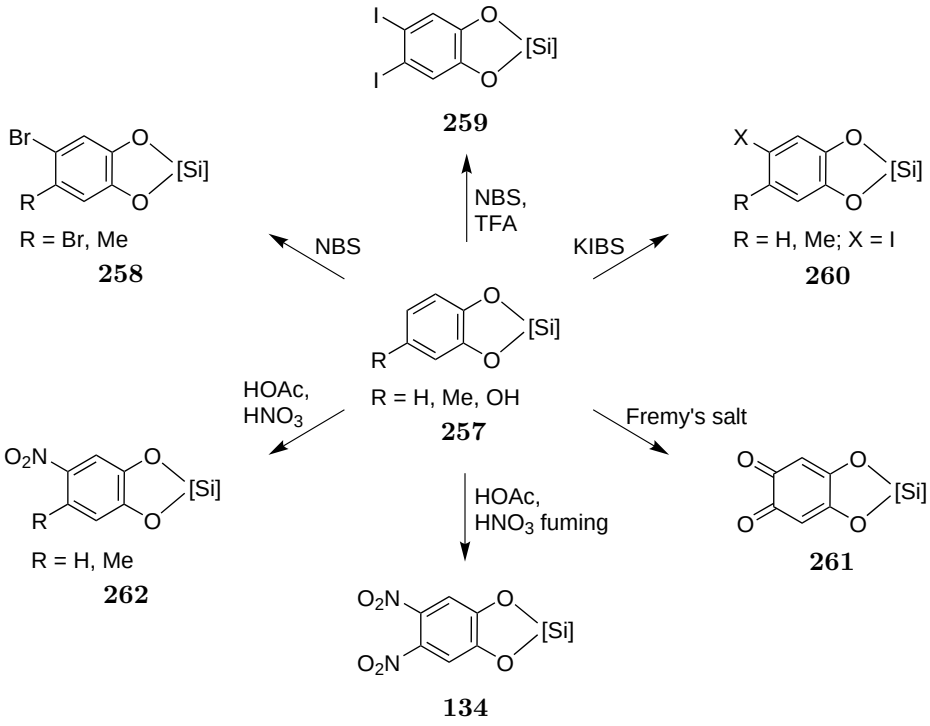

Scheme 62: Post-coordination modification of hexacoordinate (benzene-1,2-diolato)silicon(IV) complexes (with [Si] = $Si(pp)_2$) established within this thesis.

Reduction of the dinitro complex **134** with tin in hydrochloric acid afforded the corresponding diamino complex **197** (Scheme 63) which quickly decomposed if purified on silica gel or even if stored at room temperature under nitrogen for a longer period of time. Nevertheless, complex **197** rapidly reacted with aliphatic and aromatic aldehyds or diones forming imidazole (**263**) or phenazine (**264**) structures, respectively (Scheme 63). This condensation reaction proved to very mild tolerating various functionality at the aldehyde fragment like for example pyridines, halogen substituents or alkynes. Moreover, complexes with an extended aromatic π-system could be realized upon the reaction with oxidized pyrene derivatives. In doing so, dinuclear silicon(IV) complexes (**147** and **148**) could be isolated too. However, the two *tert*-butyl groups at the pyrene fragments, disturbing the formation of strong $\pi\pi$ interactions, were beneficial for the isolation and handling of the complexes.

Complexes **145** and **157** were studied towards their interaction with double stranded *calf thymus* DNA. For complex **157**, a binding constants of about $10^5\,\mathrm{M}^{-1}$ was determined. Surprisingly, a binding constant of about $10^6\,\mathrm{M}^{-1}$ was obtained for complex **145**. Although the *tert*-butyl groups should

prevent an intercalative binding mode as also indicated by the binding site size of s < 1, they somehow supported the hydrophobic aggregation on the DNA surface.

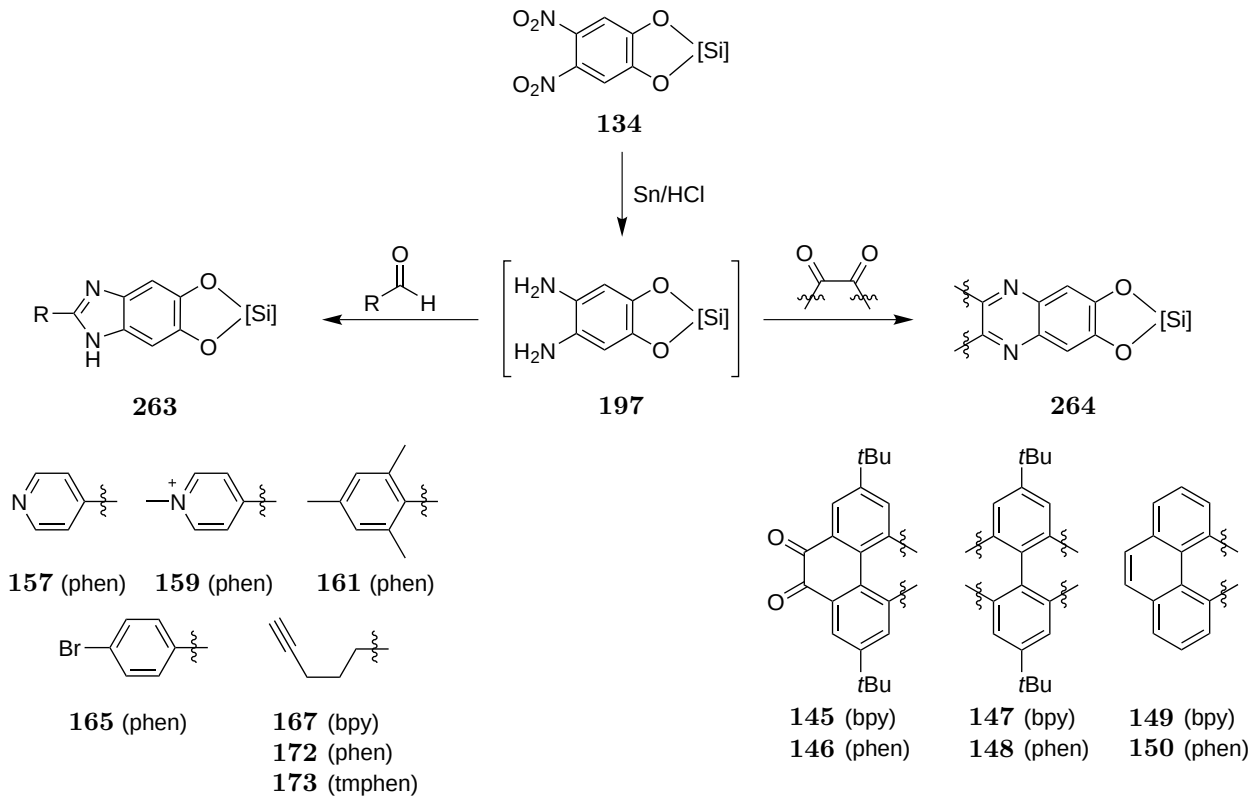

Scheme 63: Reduction of the dinitro complex **265** with tin/HCl and subsequent reaction with an aldehyde or oxidized pyrene fragments afforded various imidazole (**263**) and phenazine (**264**) derivatives, respectively. Some examples of isolated (with [Si] = $Si(pp)_2$) are given.

The planar aromatic system of complexes **266** could further be extended using a second condensation reaction with different diamines (Scheme 64). Some of these complexes were studied towards their interaction with *calf thymus* DNA but reliable results were not obtained. This indicated either a solubility problem of the huge complexes in the buffer solution used or that the complexes were to huge to interact with ds-DNA in a constructive fashion. Binding studies to G-quadruple DNA were not conducted. Hence, it could not be said whether these complexes show a selectivity G4-DNA > ds-DNA.

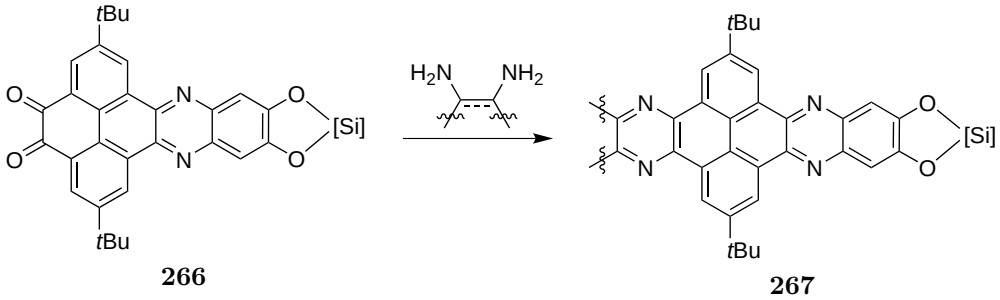

Scheme 64: Silicon(IV) complexes with extended aromatic π-systems (**267**, whereat [Si] = $Si(bpy)_2$ or $Si(phen)_2$) were accessibly by a condensation reaction of the dione complexes **266** with various diamines.

4.3. Tris-heteroleptic Silicon(IV) Complexes

Post-coordination modification could be achieved on the benzene-1,2-diolato ligand. However, building up a bifunctionalized complex, coordinate to an intercalating ligand and accessible for modifications, seemed to be more challenging. Hence, it was tried to build up tris-heteroleptic silicon(IV) complexes coordinate to the ligand dppz, a well-established ligand for DNA intercalation. Modifying the above discussed method, complexes **183** and **184** were obtained (Scheme 65) and could be further characterized by crystal structure analysis proving the tris-heteroleptic structure. Both complexes could further be modified using the nitration and condensation reactions mentioned above. The binding affinity of complex **184** to *calf thymus* DNA was determined to $k_B = (1.55 \pm 0.11) \times 10^6\,\mathrm{M}^{-1}$ with a binding site size of $s = 1.17 \pm 0.02$. Hence, the silicon(IV) complexes bond double stranded DNA similar strong than the well-known DNA binding complexes $[Ru(dppz)(pp)_2]^{2+}$. Moreover, the binding site size indicated an intercalative binding mode.

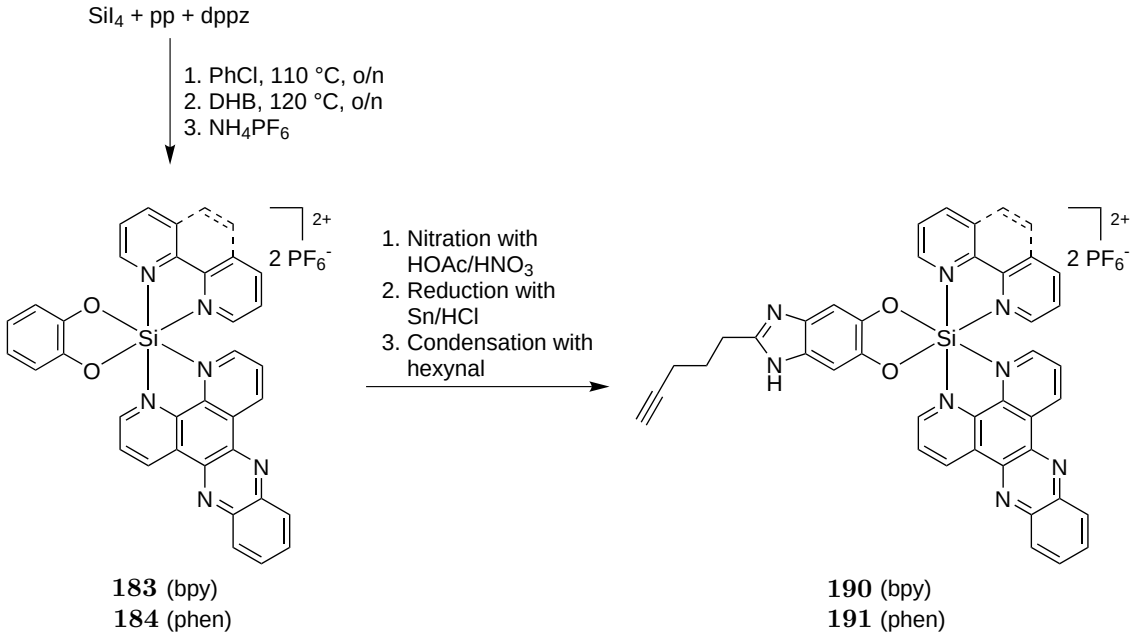

Scheme 65: Synthesis and modification of tris-heteroleptic silicon(IV) complexes.

4.4. Dinuclear Metal-Silicon(IV) Complexes

A major aim of this work was the synthesis of dinuclear silicon(IV) complexes. Unfortunately, such complexes could only be obtained in low yields and the complexes did not show any fluorescence which is crucial for acting as a DNA imaging agent. It was expected that the introduction of a transition metal, such as ruthenium(II) or iridium(III), should overcome these limitations leading to a fluorescent complex. Therefore, dinuclear metal-silicon(IV) complexes bridged by the ligand dipyrido[3,2-*a*:2',3'-*c*]phenazine-7,8-diol (**195**) were investigated. Two different strategies, a linear and a convergent synthesis approach, were tried to synthesize the dinuclear complexes. The linear approach afforded ruthenium(II) and iridium(III) complexes **204** and **205** (Figure 75), respectively. However, dinuclear complexes could not be obtained via further conversions of complexes **204** and **205**.

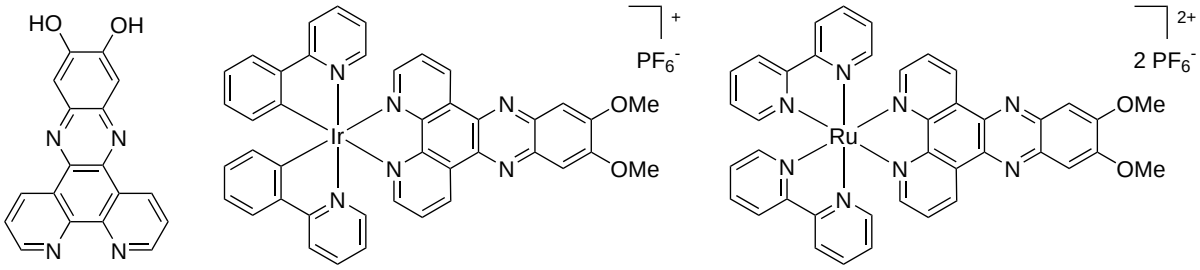

195 **204** **205**

Figure 75: The bridging ligand used for the dinuclear metal-silicon(IV) complexes (**195**) and the ruthenium(II) and iridium(III) complexes (**204** and **205**, respectively) obtained in the linear synthesis approach.

The convergent synthesis approach proved to be more promising. Utilizing the post-coordination modifications of silicon(IV) complexes elaborated in this thesis, the key step of this synthesis approach was a condensation reaction of a (1,10-phenanthroline-5,6-dione)metal fragment (**196**) and a (4,5-diaminobenzene-1,2-diolato)silicon(IV) intermediate (**197**) (Scheme 66). The metal fragments were obtained either by reaction of a metal precursor with 1,10-phenanthroline-4,5-dione or by a post-coordination oxidation of the 1,10-phenathroline ligand using sodium bromate in sulphuric acid.

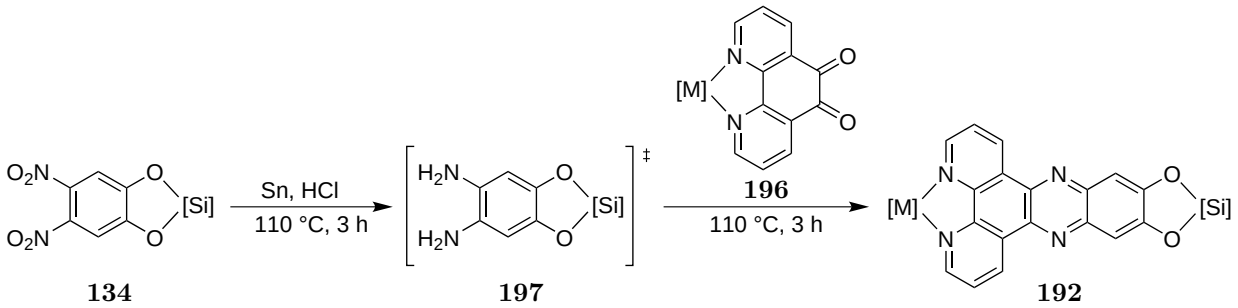

134 **197** **196** **192**

Scheme 66: Key step of the convergent synthesis approach for the synthesis of dinuclear metal-silicon(IV) complexes was a condensation reaction of a (1,10-phenanthroline-5,6-dione)bis(polypyridyl)metal fragment (**196**) and a (4,5-diaminobenzene-1,2-diolato)bis(polypyridyl)silicon(IV) fragment (**197**).

With this method in hand, a small library of dinuclear metal-silicon(IV) complexes was synthesized (Figure 76). All dinuclear complexes were obtained as as mixture of diastereomers in low to moderate yields of 10–34 %. Further attempts to separate the isomers were not conducted. Unfortunately, the dinuclear complexes did not show any sign of fluorescence leading to the assumption that the silicon(IV) center somehow quenched the excited state. Using a compound in biological systems requires a certain stability against hydrolysis or thiols. The dinuclear complexes synthesized fulfill these demands as demonstrated by ^{1}H NMR stability experiments for complexes **227**, **233**, **235** and **236**, by way of example. Moreover, complex **227** did not show any sign of decomposition in the presence of 2-mercaptoethanol, which is a suitable reagent to mimic thiols in biological systems.

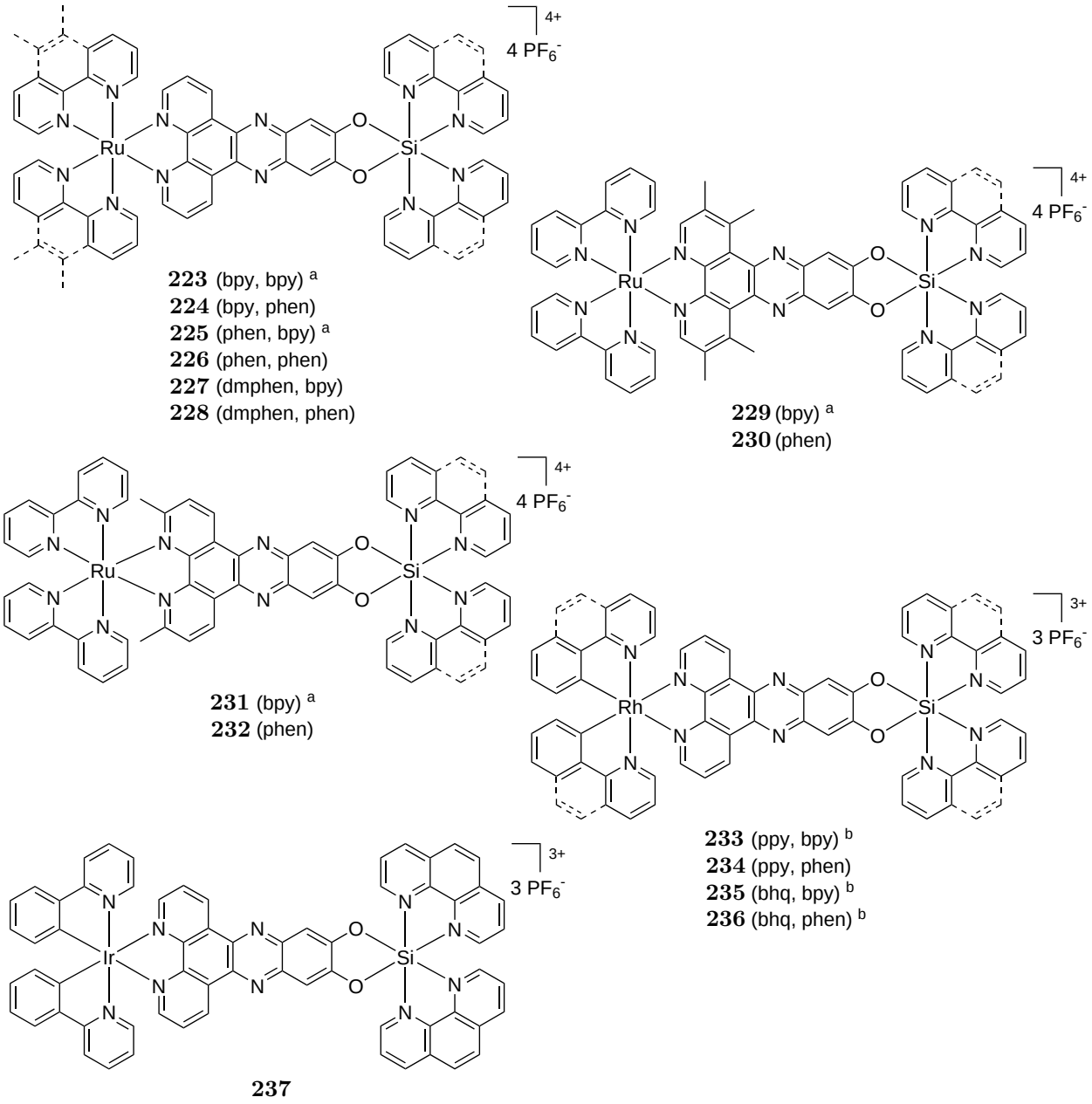

Figure 76: Dinuclear metal-silicon(IV) complexes synthesized in the context of this thesis. All complexes are obtained as mixtures of diastereomers. ([a] Synthesized by Steffen Glöckner during his bachelor thesis. [b] Synthesized by Alexandra Gruber during her bachelor thesis.)

Due to the strained coordination of the ruthenium center, complexes **231** and **232** were expected to easily eject the ruthenium part upon irradiation with visible light leading to an reactive ruthenium(II) center and a DNA intercalating silicon(IV) fragment (Scheme 67). Having a potential novel lead structure for the photodynamic therapy in hand, its photoejection capability was studied more detailed. Although upon irradiation with visible light at room temperature in acetonitrile a slow dissociation was observed, the complexes were not suitable for the photodynamic therapy due to a very slow photoinduced cleavage which may be associated with the size of the fragments **241** and **242**. Moreover, no photoinduced cleavage was observed after changing the solvent to dimethyl sulfoxide.

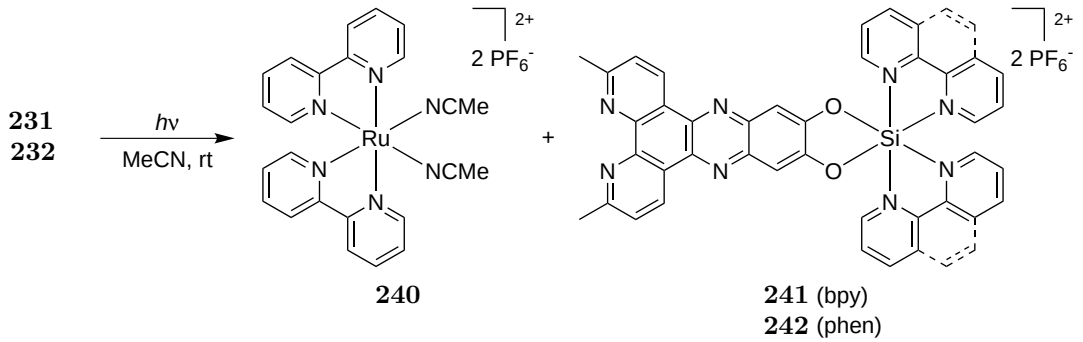

Scheme 67: Biological active metal complexes that could be obtained upon photoinduced cleavage of the dinuclear complexes **231** and **232**.

Having the dinuclear complexes in hand, their binding to duplex-DNA and G-quadruplex DNA was investigated using the McGhee-von-Hippel equation. All complexes showed a strong binding to double stranded *calf thymus* DNA, possessing binding constants of about 10^5–$10^8\,\mathrm{M}^{-1}$. These binding constants are within the range of the well-established mono- and dinuclear ruthenium based DNA binding complexes, for instance $[Ru(dppz)(pp)_2]^{2+}$, $[Ru(dppz)(NH_3)_4]^{2+}$, or $[Ru(pp)_2(\mu\text{-tpphz})Ru(pp)_2](NO_3)_4$. With a k_B of $(1.06 \pm 0.39) \times 10^8$, complex **223** was the strongest binder. In general, the ruthenium(II) coordinate complexes bond ds-DNA about on order of magnitude stronger compared to the ones with an iridium(III) or rhodium(III) metal center. The differences for the binding strength can be explained by stronger electrostatic interactions of the ruthenium(II)-silicon(IV) complexes with the negatively charged DNA backbone due to a higher charge of 4+ compared to 3+. For the binding site size, values between s = 0.1–1.4 were obtained. However, the binding mode is not completely understood and additional experiments have to be done as the data support either an intercalation as well as an aggregation of the complexes on the DNA surface.

Examining the binding of selected dinuclear complexes to G-quadruplex DNA revealed a similar charge dependency as observed for duplex DNA. Nevertheless, the binding constants were about one order of magnitude lower compared to the binding constants to double stranded DNA. However, the binding proved to be similar in strength compared to complex $[Ru(pp)_2(\mu\text{-tpphz})Ru(pp)_2](NO_3)_4$ described in the literature. In regard to the binding site size values of s being approximately 0.1, a non-intercalative binding mode through electrostatic interactions with the grooves/loops of the G-quadruplex structure could be assumed.

Finally, the cytotoxicity of the selected dinuclear complexes coordinate to ruthenium(II) and iridium(III) was investigated using the MTT test. In doing so, only a low cytotoxicity of the complexes studied was observed, exhibiting an $EC_{50} > 30\,\mu\mathrm{M}$. However, the ruthenium(II) containing complexes seemed to be less toxic than the ones coordinate to iridium(III) and rhodium(III), respectively.

4.5. Bodipy-Modified Octahedral Silicon(IV) Complexes

In the absence of luminescent silicon(IV) complexes, it was tried to attach a fluorophor. Due to its well established luminescence properties, the Bodipy was the fluorophor of choice that should be linked to a silicon(IV) complex using click chemistry. Utilizing a post- (route 1) or pre-coordination (route 2)

copper catalyzed click reaction, the four Bodipy bound complexes **246**–**249** were obtained in moderate yields (Scheme 68). However, the click reaction at the silicon(IV) complexes proved to be less effective compared to route 2 and only complexes **246** and **249** could be isolated as pure substances via this method.

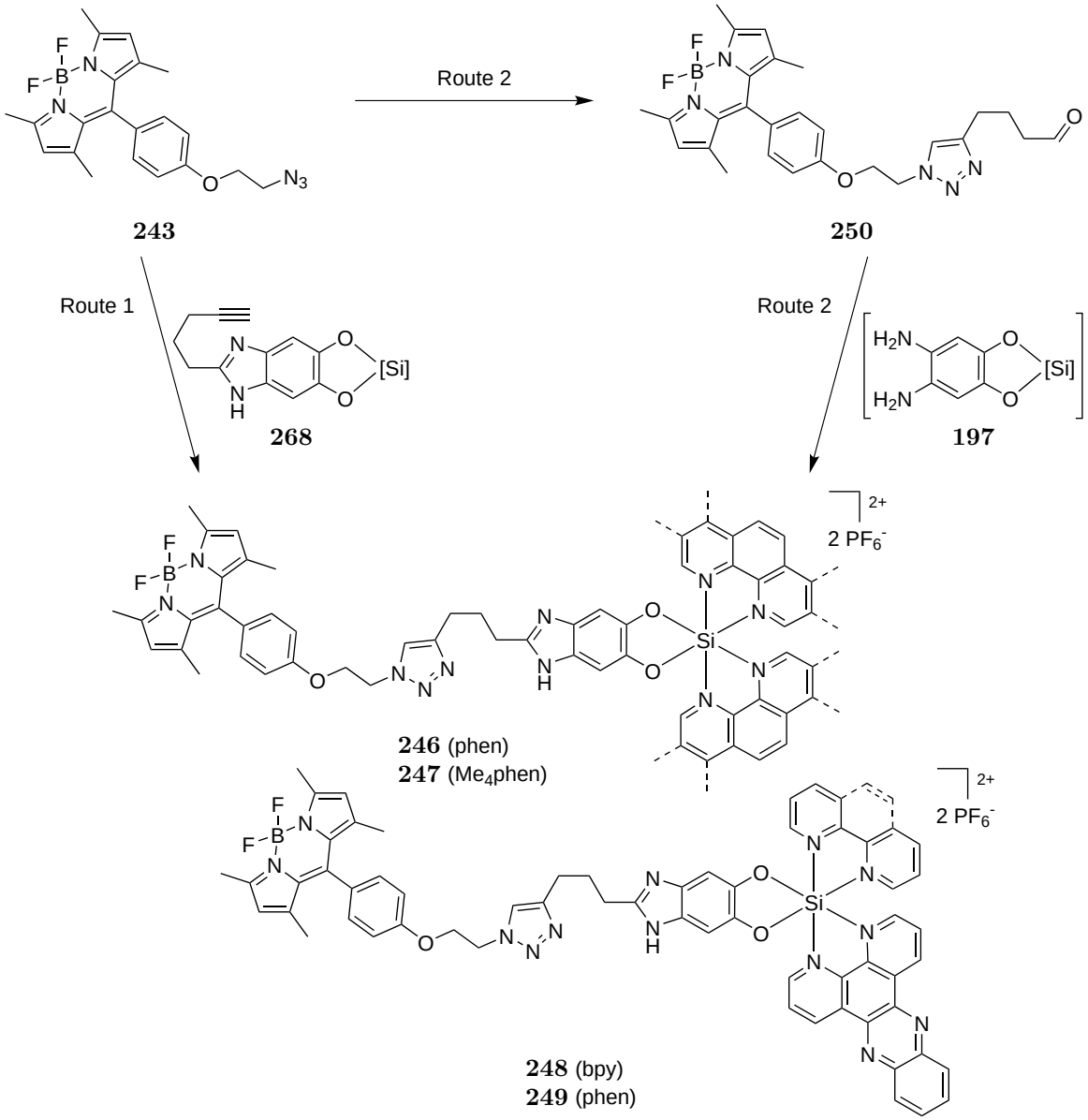

Scheme 68: Synthesis of silicon(IV) complexes **246**–**249** linked to a Bodipy fluorophor. Two synthetic approaches were tried. A post-coordination click reaction (route 1) and a pre-coordination click reaction followed by a condensation reaction (route 2), with [Si] = $Si(bpy)_2$ or $Si(phen)_2$.

All compounds containing the fluorophor were studied towards their absorption and emission properties showing the characteristic Bodipy absorption and emission band at around 501 nm and 510 nm, respectively. In general, the fluorescence of the silicon(IV) complexes was found to be less pronounced compared to the single Bodipys due to the photoinduced electron transfer. Moreover, the dppz coordinate complexes showed a distinct light-switch behavior in the presence of ds-DNA.

The silicon(IV) complexes **246**–**249** strongly bond *calf thymus* DNA with binding constants of $k_B = 10^5$–$10^6\,\text{M}^{-1}$ and thus within the range of ruthenium based DNA intercalators but lower compared to the dinuclear complexes synthesized in this thesis. However, the dppz bound complexes were found to bind with a higher affinity which can be explained by an intercalation of the dppz ligand between the base-pairs of the DNA. Nevertheless, the main binding mode for all complexes seemed to be an aggregation on the DNA surface as indicated by the binding site size of $s < 1$. In cooperation with Sumaira Ashaf of the Parak group, complexes **246**–**249** were studied towards their ability to stain DNA in living cells. Using a confocal laser scanning microscope, it was found that the complexes were able to enter the cells but not the nuclei.

4.6. Outlook

The synthesis route for dicationic octahedral silicon(IV) complexes developed within this thesis is well established. It also allows the introduction of three different ligands. Although the yields were quite low, these concept could be enhanced permitting the synthesis of novel tris-heteroleptic silicon structures. However, the synthesis of stable complexes is restricted to polypyridyl complexes which limits their wider use in biological applications. Therefore, the synthesis should be improved further introducing other ligand systems, for instance a pyridcocarbazole ligand that was found to act as a protein kinase inhibitor. Moreover, other ligand systems would allow the synthesis of less charged or even neutral complexes which would be beneficial for biological applications since a lower charge would permit better cell membrane permeability or protein kinase binding. Although there are a lot of such complexes known, most of them are not very stable towards hydrolysis. Hence, the great challenge in this field would be the synthesis of hydrolytical stable complexes.

The post-coordination modification of the silicon(IV) complexes synthesized proved to be very powerful, especially the nitration-reduction-condensation protocol demonstrated to be highly versatile. However, there have been some major drawbacks as a carbon-carbon bond formation could not be realized. Therefore, electrophilic aromatic substitutions as well as cross-coupling reactions should be studied more detailed. In preliminary investigations[232] several conversions were observed but the products could not be isolated. On this perspective, neutral complexes should be beneficial as they would allow a more efficient purification via column chromatography.

The biological properties of the complexes synthesized were mainly studied towards their binding to double stranded DNA. However, they should be investigated towards their binding to G-quadruplex DNA as these structures are interesting biological targets for novel anticancer therapies. In doing so, the focus should be laid on silicon(IV) complexes with a huge planar ligand as this should increase the selectivity for G-quadruplex DNA over double stranded DNA. As lead structures, the pyrene derivatives synthesized within this thesis could be used. However, their binding to DNA should be studied first. Moreover, it should be tried to isolate the dinuclear complex **269** (Figure 77) using another purification strategy as used in this thesis. Besides, modifying the complexes with additional charges would increase the binding to G-quadruplex DNA as well as the solubility. This could be accomplished by using pyridinium substituents as demonstrated by complexes **270** and **271** in Figure 77.

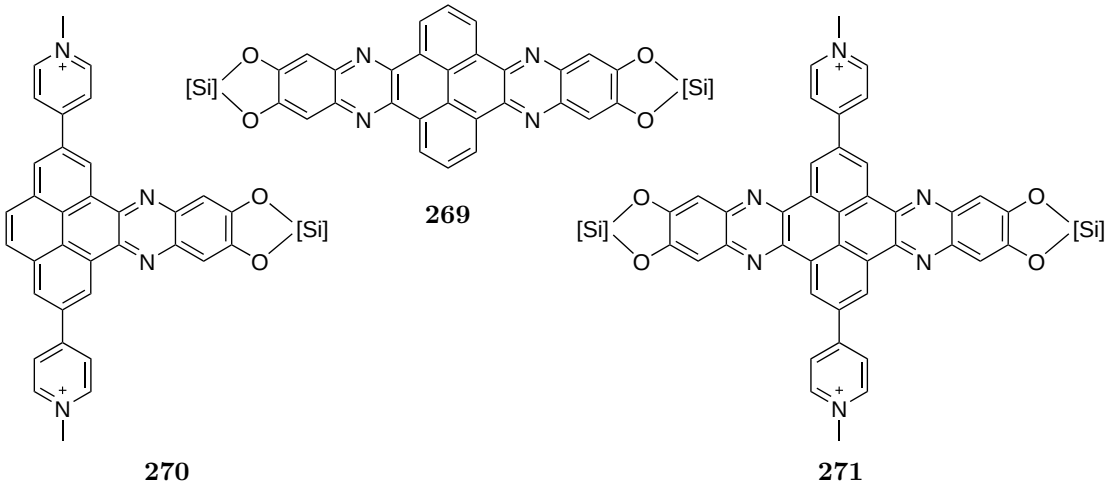

269 **270** **271**

Figure 77: Hexacoordinate silicon(IV) complexes (with [Si] = $Si(pp)_2$) based on a pyrene structure possessing a ligand with a huge planar π-system. The pyridinium substituents should both, increase the solubility as well as the binding to G-quadruplex DNA.

Phthalocyanine structures were shown to be excellent G-quadruplex binders due to their large π-surface. Additionally, they exhibit interesting photochemical properties. These properties could be utilized by attaching such a ring system to a silicon center (Figure 78, **272**) which could increase the binding to or lead to a particular selectivity for a certain G-quadruplex structure. Otherwise, metal structures like **273** and **274** could be synthesized to increase the selectivity in favor of G-quadruplex DNA. By this strategy, the planer ligand would be increased in size and an electrostatic interaction with the central channel of the G-quadruplex structure or a cation-π interaction could be achieved. For the best interaction between the complexes and the G-quadruplex structures, the metal should have a square planar or square pyramidal coordination geometry.

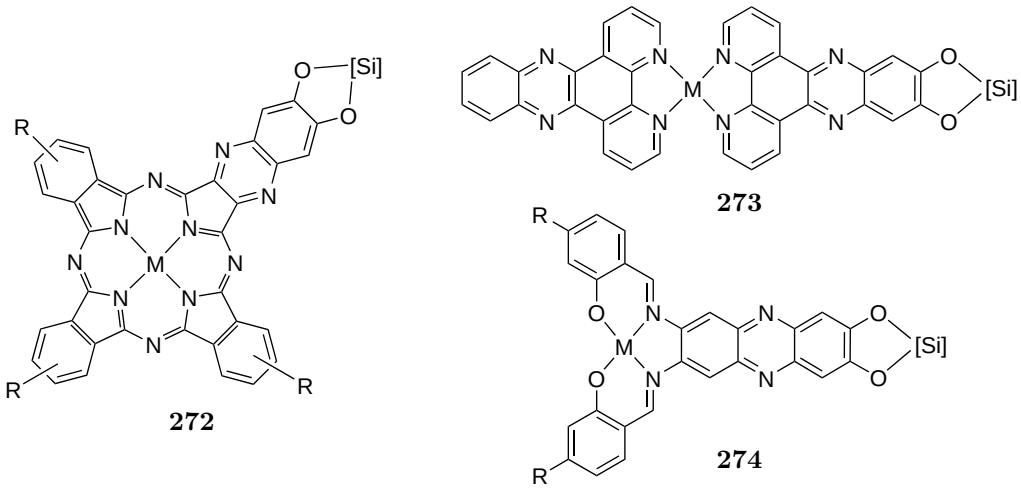

272 **273** **274**

Figure 78: Hexacoordinate silicon(IV) complexes (with [Si] = $Si(pp)_2$) coordinate to a phthalocyanine (**272**) or metal fragments (**273** and **274**). M should be a metal center with a square planar or square pyramidal coordination geometry.

The Bodipy bound complexes **247**–**248** are very inserting complexes whose biological properties should be studied more detailed. For instance, their photochemical properties (singlet oxygen formation,

potential use in the photodynamic therapy) and their binding affinity to G-quadruplex DNA should be surveyed. Moreover, it should be investigated why the complexes are not entering the nuclei of the cells. In doing so, their stability in the medium used and under the conditions in the cell should be analyzed. Moreover, it could be tried to attach the complexes to a small protein capable of transporting the complexes into the nuclei.

5. Experimental Part

5.1. General Information

General Synthetic Methods: All temperatures are given in °C and correspond to the oil-bath temperature. Room temperature is defined as 20–22 °C. Reactions with air- or water-sensitive compounds were carried out under nitrogen using SCHLENK techniques. Therefore, the flask was heated to approximately 600 °C under vacuum and then filled with anhydrous nitrogen. After cooling to room temperature, the procedure was repeated twice. Filtration under inert conditions was performed using a SCHLENK-frit.

Materials: All reagents and reaction solvents (HPLC grade) were purchased from *Acros*, *Sigma Aldrich*, *Strem* or *Alfa Aesar* and used without further purification unless otherwise specified. Solvents for column chromatography were purified by distillation. 1,2-Dihydroxybenzene was sublimated prior to use. Anhydrous acetonitrile and anhydrous dichloromethane were distilled under nitrogen from calcium hydride, whereas anhydrous diethyl ether was distilled under nitrogen from sodium with benzophenone as indicator. Anhydrous methanol was obtained by reaction with magnesia and iodine, followed by distillation under nitrogen. Anhydrous chloroform and anhydrous chlorobenzene were purchased from *Acros* and stored over activated molecular sieve (3 Å). Water was deionized by a cation-anion exchanger. 4,5-Dimethoxy-1,2-phenylenediamine (**106**),[229] 1,10-phenanthroline-5,6-dione (**198**),[245] 2,9-dimethyl-1,10-phenanthroline-5,6-done (**215**),[247] $[Ir(\mu\text{-Cl})(ppy)_2]_2$,[283] $[Rh(\mu\text{-Cl})(ppy)_2]_2$,[287] 5-amino-6-nitro-1,10-phenanthroline (**200**),[281,282] $[Ru(bpy)_2Cl_2] \cdot 2\,H_2O$,[284] $[RuCl_2(phen)_2] \cdot 2\,H_2O$,[284] (5,6-diamino-1,10-phenanthroline)bis(2-phenylpyridinato)iridium(III)-hexafluorophosphate (**207**),[146] potassium 4-iodylbenzenesulfonate,[236] Bodipy-N_3 (**243**),[298,300,301] 5-hexynal (**189**),[310] all oxidized pyrene derivatives (**275**, **276**, **277**, **278**),[264] 1-methylpyridiunium-4-carbaldehyde iodide (**279**),[311] 4-formyl-*N,N,N*-trimethylbenzenaminium iodide (**280**)[312] and 4-bromocatechol (**97**)[226,227] were synthesized according to literature procedures. The ligand dppz (**185**) was synthesized in the group by CHEN FU according to a literature procedure.[245] $[RuCl_2(dmphen)_2] \cdot 2\,H_2O$ and the dinuclear complexes **223**, **225**, **229** and **231** were synthesized by STEFFEN GLÖCKNER during his bachelor thesis.[225] Complex bis(benzo[*h*]qionolinato)(5,6-dimethyl-1,10-phenanthroline-5,6-dione)iridium(III)-hexafluorophosphate (**214**), and the dinuclear complexes **233** and **235** were synthesized by ALAXANDRA GRUBER during her bachelor thesis.[288] Unless otherwise stated, obtained air- or water-sensitive compounds were stored and weighed out in a nitrogen filled glove-box at room temperature.

Thin layer chromatography: TLC was performed on Macherey-Nagel GmbH & Co. KG precoated TLC-sheets ALUGRAM Xtra SIL G/UV254 (silica gel 60 F_{254}, 0.2 mm layer thickness). For aromatic substrates the detection resulted from the irradiation with UV-light ($\lambda = 254$ nm and $\lambda = 366$ nm). Non aromatic compounds were stained using a Cer-Dip (20 g ammonium molybdate and 0.4 g Cer(IV)sulfate in 400 mL 10% sulphuric acid).

Column chromatography: Merck KGaA silica gel (particle size 0.04–0.063 mm) was used as the stationary phase. Compressed air was utilized to build up the pressure for flash column chromatography. The term *salt conditions* means that the eluent mixture contains satd. aq. KNO_3.

Microwave Reactor: Microwave reactions were carried out in a CEM Monomode-microvawe reactor Discover-LabMate using special reaction vessels.

Centrifugation: Centrifugation was carried out on a Eppendorf Centrifuge 5810R

5.2. Analytic Section

Nuclear Magnetic Resonance Spectroscopy: NMR spectra were recorded at 300 Kelvin on a Bruker Avance II 300 spectrometer (^{1}H-NMR: 300 MHz, ^{13}C-NMR: 75.5 MHz) in automation or on a Bruker Avance III HD 300 spectrometer (^{1}H-NMR: 300 MHz, ^{13}C-NMR: 75.5 MHz, ^{29}Si-NMR: 59.7 MHz, ^{19}F-NMR: 283 MHz, ^{11}B-NMR: 96.3 MHz, ^{31}P-NMR: 122 MHz), a Bruker DRX 400 spectrometer (^{1}H-NMR: 400 MHz, ^{13}C-NMR: 101 MHz, ^{29}Si-NMR: 79.5 MHz) or a Bruker Avance III 500 spectrometer (^{1}H-NMR: 500 MHz, ^{13}C-NMR: 126 MHz, ^{29}Si-NMR: 99.4 MHz, ^{11}B-NMR: 160 MHz) by members of the NMR service department of the Philipps-Universität Marburg. Carbon NMR spectra are ^{1}H wide-band decoupled. Chemical shifts are reported on the δ-scale in parts per million (ppm) relative to tetramethylsilane (TMS, $\delta = 0$ ppm) using the residual NMR solvent signal as a reference (Table 14). Coupling constants ^{n}J are given as observed in the spectra in hertz (Hz) with n = number of bonds between the coupled nuclei. If a signal corresponds to two single protons with slightly different chemical shifts, n is left out. The signal multiplicities are described as s = singulet, d = doublet, t = triplet, q = quartet, p = quintet, h = heptet, m = multiplet and combinations thereof. The ^{29}Si-NMR spectra were recorded at 243 K or at 300 K using a modified HMQC method (Axis F1 = ^{29}Si, Axis F2 = ^{1}H).

Table 14: Chemical shifts of the residual proton signals of the NMR solvents used.[313]

Solvent	**^{1}H-NMR**	**^{13}C-NMR**
$CDCl_3$	7.26 ppm	77.16 ppm
DMSO$-d_6$	2.50 ppm	39.52 ppm
CD_3CN	1.94 ppm	1.32 ppm
MeOD	3.31 ppm	49.0 ppm
D_2O	4.79 ppm	

Mass Spectrometry: Mass spectra were recorded on a Thermo Fischer Scientific Finnigan TSQ 700 spectrometer using electrospray ionization (ESI+). The detected ion masses m/z are stated in u and refer to the isotope with the highest natural occurrence. The observed isotopic patterns match the calculated. The measurements were performed by members of the mass spectrometry department of the Philipps-Universität Marburg.

Infrared Spectroscopy: IR-spectra were recorded on a Bruker Alpha series FT-IR spectrometer, ATR-mode (attenuated total reflections). Absorption bands are given as wave numbers $\widetilde{\nu}$ in the unit cm^{-1}. The substances were measured as film. Therefore, a solution of the compound in acetonitrile or dichloromethane was put on the device and after evaporation of the solvent, the absorption spectra was recorded.

UV-Vis Spectroscopy: UV-Vis absorption spectra were measured on a Beckman 800 UV-Vis spectrophotometer in a quartz cuvette with a path length of 10 mm and a volume of 1 mL. UV-Vis fluorescence spectra were recorded on a SpectraMax M5 plate reader.

Single-Crystal X-ray Diffraction Studies: X-ray data were collected with a Stoe IPDS 2, a Stoe IPDS 2T or with a Bruker 3 circuit D8 Quest diffractometer. Measurement and evaluation of the data were conducted by Mr. Riedel, Mr. Marsch or Dr. Harms of the department for crystal structure analysis of the Philipps-Universität Marburg. The obtained crystal structures were resolved and refined by Dr. Harms. Crystallographic data of all published structures (CCDC) (excluding structure factors) have been deposited in the Cambridge Crystallographic Data Center. CIF files can be obtained from the CCDC free of charge via `http://www.ccdc.cam.ac.uk/data_request/cif`.

HPLC-MS: Mass spectrometrical reaction control was performed on a Agilent 1200 Series, 6120 Quadrupol System. As the stationary phase, a CC 8/3 Nucleodor 100-5-column from Macherey-Nagel GmbH & Co. KG was used. The mobile phase contained a mixture of methanol (A) and 0.05 % aqueous formic acid (B). The method used for the runs is shown in Table 15.

Table 15: LCMS method used.

time /min	**% B**	**flow rate** /mL min^{-1}	**maximum pressure** /bar
0.5	80	0.3	200
2.0	5	0.3	200
2.0	5	0.3	200
5.5	80	0.2	200

5.3. General Synthesis Instructions

5.3.1. Anion metathesis from PF_6^- to Cl^-

Method A: The hexafluorophosphate salt was dissolved in acetone (4–10 mL), and the solution was filtered to remove insoluble particles. The filtrate was then treated with an excess of a concentrated solution of tetrabutylammonium chloride in acetone. The precipitate was isolated by filtration, washed extensively with acetone, and rinsed with methanol. After removal of the solvent and drying under vacuum, the chloride salt was obtained.

5.3.2. Condensation Reactions

Method B: A suspension of (4,5-dinitrobenzene-1,2-diolato)bis(polypyridyl)silicon(IV)-bis(hexafluorophosphate) (30–60 µmol) in half concentrated hydrochloric acid (6 M, 2.0 mL) was heated to 80 °C. Tin powder (8.0–8.6 eq.) was added, and the mixture was stirred at 110 °C for three hours. After cooling to 0 °C, the mixture was neutralized with a sodium hydroxide solution (6 M) until pH reached 6–7. The obtained solid was isolated by centrifugation (2000 rpm, 20 °C, 5 min) and extracted

with water (2 × 2 mL). The combined supernatants were treated with NH_4PF_6. The resulting precipitate was isolated by centrifugation (4000 rpm, 4 °C, 5 min) and washed with water to remove the excess amount of salt.
The obtained brown solid was dissolved in acetonitrile (4 mL), and a (1,10-phenanthroline-5,6-dione)bis(polypyridyl)metal complex (1.0 eq.) was added. The reaction mixture was first stirred at 40 °C for 18 hours and then subjected to flash column chromatography (MeCN → MeCN/H_2O/satd. aq. KNO_3 50:3:1 → 50:6:2 → 50:12:4, depending on the charge of the product). The yellow or orange band eluting under salt conditions was collected, and the product eluents were concentrated. Depending on the solubility, the residues were either redissolved in water or in acetonitrile/water 0.5:1. Then NH_4PF_6 was added and the remaining acetonitrile was removed, if applicable. The resulting precipitate was isolated by centrifugation (4000 rpm, 4 °C, 5 min) and washed twice with water to remove the excess amount of salt. The solid was dissolved in acetonitrile, and the gained solution was filtered through cotton before it was concentrated. The obtained solid was dried under vacuum yielding the corresponding dinuclear metal-silicon complex as a mixture of diastereomers (*d.r.* 1:1).

Method C: A suspension of (4,5-dinitrobenzene-1,2-diolato)bis(polypyridyl)silicon(IV)-bis(hexafluorophosphate) (30–120 µmol) in half concentrated hydrochloric acid (6 M, 2.0–6.0 mL) was heated to 80 °C. Tin powder (8.0–9.0 eq.) was added, and the mixture was stirred at 110 °C for three hours. After cooling to 0 °C, the mixture was neutralized with a sodium hydroxide solution (6 M) until pH reached 6–7. The obtained solid was isolated by centrifugation (2000 rpm, 20 °C, 5 min) and extracted with water (3 × 2 mL). The combined supernatants were treated with NH_4PF_6. The resulting precipitate was isolated by centrifugation (4000 rpm, 4 °C, 5 min) and washed with water to remove the excess amount of salt.
The obtained solid was dissolved in acetonitrile (4 mL), and an aldehyde or dione/tetraone (1.1–10 eq.) was added. The reaction mixture was first stirred at room temperature for 18 hours and then subjected to flash column chromatography (MeCN → MeCN/H_2O/satd. aq. KNO_3 50:3:1 → 50:6:2 → 50:12:4, depending on the charge of the product), whereupon the yellow or orange band eluting under salt conditions was collected. The product eluents were concentrated, and the residue was dissolved in water/acetonitrile 1:1. Then NH_4PF_6 was added, and the acetonitrile was removed. The resulting precipitate was isolated by centrifugation (4000 rpm, 4 °C, 5 min) and washed twice with water to remove the excess amount of salt. The solid was dissolved in acetonitrile, and the gained solution was filtered through cotton before it was concentrated. The obtained solid was dried under vacuum yielding either an imidazole or a phenazine silicon(IV) complex.

Method D: Silicon complex **145** or **281** (1.0 eq.) was dissolved in a mixture of acetonitrile (1000 µL), water (500 µL) and glacial acetic acid (20.0 µL). A diamine (6.1–12.6 eq.) was added, and the mixture was stirred at 75 °C for 16 hours. After cooling to room temperature, the reaction mixture was subjected to flash column chromatography (MeCN → MeCN/H_2O/satd. aq. KNO_3 50:3:1 → 50:6:2), whereupon the yellow band eluting under salt conditions was collected. The product eluents were concentrated, and the residue was dissolved in water/acetonitrile 1:1. NH_4PF_6 was added, and the acetonitrile was removed. The resulting precipitate was isolated by centrifugation (4000 rpm, 4 °C, 5 min) and washed twice with water to remove the excess amount of salt. The solid was dissolved

in acetonitrile, and the gained solution was filtered through cotton before it was concentrated. The obtained solid was dried under vacuum yielding the condensation product.

5.4. Synthesis Instructions

5.4.1. Synthesis of Octahedral Silicon(IV) Complexes

4,5-Dinitroveratrole (105)

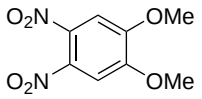

The product was synthesized according to a modified literature procedure of Alcalde *et al.*[228] A solution of veratrole (**98**, 1.00 mL, 7.82 mmol) in concentrated sulphuric acid (20.1 mL) was cooled to 0 °C and treated with potassium nitrate (1.60 g, 15.8 mmol) in small portions. The red solution was stirred at 0 °C for 45 minutes and subsequently at room temperature for three hours. The black reaction mixture was then poured into ice-water (100 mL), and the precipitate was isolated by filtration. The solid was washed with water and diethyl ether before it was subjected to flash column chromatography (dichloromethane/hexane 1:1). The yellow band was collected, concentrated, and the obtained solid was dried under vacuum. Title compound **105** was obtained as a yellow solid (690 mg, 3.02 mmol, 39 %). The analytical data are in accordance with the literature.[228,314] – $\mathbf{C_8H_8N_2O_6}$ (M = 228.16 g mol^{-1}). – ^{1}**H-NMR** (300 MHz, DMSO-d_6): δ = 7.76 (s, 2H, H-3, H-6), 3.96 (s, 6H, H_{Methyl}) ppm. – $\mathbf{R}_f$**:** 0.14 (CH_2Cl_2/hexane 1:1).

7,8-Dimethoxyphenazine-2,3-diol (104)

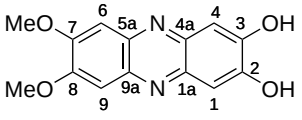

A suspension of 4,5-dimethoxy-1,2-phenylenediamine (**106**, 340 mg, 2.02 mmol) and 2,5-dihydroxy-*p*-benzoquinone (**94**, 321 mg, 2.29 mmol) in water (70 mL) was stirred at 100 °C for 15 hours. After cooling to 8 °C, the precipitate was isolated by filtration, and washed with water (30 mL), ethanol (8 mL) and diethyl ether (3 mL). After drying under vacuum, 7,8-dimethoxyphenazine-2,3-diol (**104**) was obtained as a dark brown solid (481 mg, 1.77 mmol, 88 %). – $\mathbf{C_{14}H_{12}N_2O_4}$ (M = 272.26 g mol^{-1}). – ^{1}**H-NMR** (300 MHz, DMSO-d_6, 47 mM): δ = 10.51 (bs, 2H, OH), 7.32 (s, 2H, H-6, H-9), 7.23 (s, 2H, H-1, H-4), 3.96 (s, 6H, OMe) ppm. – ^{13}**C-NMR** (75.5 MHz, DMSO-d_6, 47 mM): δ = 152.3, 151.3, 139.2, 138.7, 107.5, 105.1, 55.9 ppm. – **FT-IR** (Film) $\tilde{\nu}$ = 3552, 3085, 2943, 2838, 1633, 1556, 1492, 1448, 1429, 1386, 1324, 1305, 1247, 1207, 1159, 1004, 934, 840, 827, 748, 610, 550, 497, 457, 403, 391 cm^{-1}. – **HRMS** (ESI+): calcd. for $C_{14}H_{13}N_2O_4$ $[M+H]^+$: 273.0870 u, found: 273.0668 u.

Bis(2,2'-bipyridine)diiodosilicon(IV)-diiodide (85)

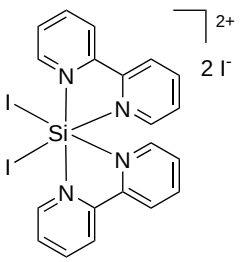

The reaction and the work-up were performed under an atmosphere of nitrogen. A suspension of silicon(IV) iodide (1.64 g, 3.06 mmol) and anhydrous 2,2'-bipyridine (1.10 g, 7.04 mmol) in anhydrous chloroform (41 mL) was purged with nitrogen for five minutes. The mixture was then heated to 55 °C for 24 hours. The resulting brownish-red suspension was cooled to room temperature, and the precipitate was isolated by filtration. The solid was washed with anhydrous chloroform (40 mL),

anhydrous diethyl ether (8 mL) and dried under vacuum. Diiodido-complex **85** was obtained as an auburn solid (2.14 g, 2.52 mmol, 82 %) that was stored under nitrogen. The complex was used for the next step without further purification and analytic. – **$C_{20}H_{16}I_4N_4Si$** (M = 848.07 g mol^{-1}).

Diiodobis(1,10-phenanthroline)silicon(IV)-diiodide (86)

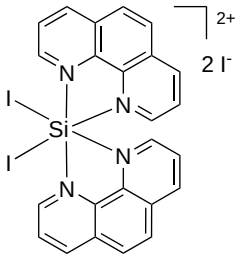

The reaction and the work-up were performed under an atmosphere of nitrogen. A suspension of silicon(IV) iodide (1.92 g, 3.58 mmol) and anhydrous 1,10-phenanthroline (1.45 g, 8.05 mmol) in anhydrous chloroform (41 mL) was purged with nitrogen for 15 minutes. The mixture was then heated to 55 °C for 24 hours. The resulting brownish-red suspension was cooled to room temperature, and the precipitate was isolated by filtration. The solid was washed with anhydrous chloroform (40 mL), anhydrous diethyl ether (20 mL) and dried under vacuum. Diiodido-complex **86** was obtained as an auburn solid (2.48 g, 2.77 mmol, 77 %) that was stored under nitrogen. The complex was used for the next step without further purification and analytic. – **$C_{24}H_{16}I_4N_4Si$** (M = 896.12 g mol^{-1}).

(Benzene-1,2-diolato)bis(2,2'-bipyridine)silicon(IV)-bis(hexafluorophosphate) (87)

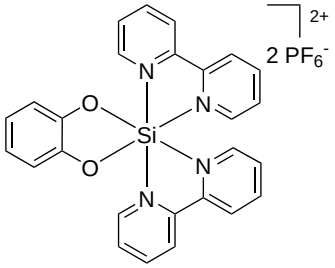

Under an atmosphere of nitrogen, a suspension of $[Si(bpy)_2I_2]I_2$ (**85** 80.0 g, 94.3 µmol) and catechol (42.0 mg, 381 µmol) in anhydrous chloroform (8.0 mL) was purged with nitrogen for ten minutes and then stirred at 80 °C for 18 hours. The resulting orange suspension was cooled to room temperature, and the solvent was removed under vacuum. The residue was subjected to flash column chromatography (MeCN → MeCN/H_2O/satd. aq. KNO_3 50:3:1 → 50:6:2). The yellow band eluting under salt conditions was collected, and the product fractions were concentrated. The residue was dissolved in water, and NH_4PF_6 was added. The resulting precipitate was isolated by centrifugation (4000 rpm, 4 °C, 5 min) and washed twice with water to remove the excess amount of salt. The solid was dissolved in acetonitrile, and the gained solution was filtered through cotton before it was concentrated. After drying under vacuum, complex **87** was obtained as a yellow solid (27.3 mg, 37.0 µmol, 39 %). – **$C_{26}H_{20}F_{12}N_4O_2P_2Si$** (M = 738.49 g mol^{-1}). – **^{1}H-NMR** (300 MHz, CD_3CN): δ = 9.07 (ddd, ^3J = 5.8 Hz, ^4J = 1.3 Hz, ^5J = 0.7 Hz, 2H, H_{bpy}), 8.96–8.88 (m, 2H, H_{bpy}), 8.86–8.73 (m, 4H, H_{bpy}), 8.60 (td, ^3J = 7.9 Hz, ^4J = 1.3 Hz, 2H, H_{bpy}), 8.16 (ddd, ^3J = 7.6, 5.8 Hz, ^4J = 1.2 Hz, 2H, H_{bpy}), 7.85–7.76 (m, 2H, H_{bpy}), 7.59 (ddd, ^3J = 6.0 Hz, ^4J = 1.2 Hz, ^5J = 0.7 Hz, 2H, H_{bpy}), 6.86–6.73 (m, 4H, H_{cat}) ppm. – **^{13}C-NMR** (75.5 MHz, CD_3CN): δ = 147.3, 147.0, 146.7, 145.6, 144.8, 143.5, 142.8, 130.6, 130.0, 124.9, 124.6, 121.7, 113.4 ppm. – **^{29}Si-NMR** (79.5 MHz, CD_3CN): δ = −149.1 ppm. – **FT-IR** (Film) $\tilde{\nu}$ = 3651, 3107, 2243, 2023, 1959, 1617, 1575, 1509, 1482, 1456, 1325, 1243, 1170, 1119, 1101, 1073, 1058, 1044, 1027, 836, 836, 744, 730, 685, 658, 587, 558, 539, 520, 502, 467, 433, 417, 396 cm^{-1}. – **HRMS** (ESI+): calc. for $C_{26}H_{20}N_4O_2SiPF6$ $[M-PF_6]^+$: 593.0992 u, found: 593.0993 u.

(Benzene-1,2-diolato)bis(1,10-phenanthroline)silicon(IV)-bis(hexafluorophosphate) (88)

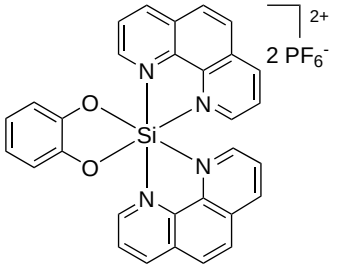

Method 1: Under an atmosphere of nitrogen, a suspension of $[SiI_2(phen)_2]I_2$ **86** (1.10 g, 1.23 mmol) and 1,2-dihydroxybenzene (560 mg, 5.09 mmol) in anhydrous chloroform (40 mL) was purged with nitrogen for 15 minutes and then stirred at 80 °C for 16 hours. The resulting orange suspension was cooled to room temperature, and the solvent was removed under vacuum. The residue was subjected to flash column chromatography (MeCN → MeCN/H_2O/satd. aq. KNO_3 50:3:1 → 50:6:2). The yellow band eluting under salt conditions was collected, and the product fractions were concentrated. The residue was dissolved in water, and NH_4PF_6 was added. The resulting precipitate was isolated by centrifugation (4000 rpm, 4 °C, 5 min) and washed twice with water to remove the excess amount of salt. The solid was dissolved in acetonitrile, and the gained solution was filtered through cotton before it was concentrated. After drying under vacuum, complex **88** was obtained as a dark yellow solid (396 mg, 503 µmol, 41 %).

Method 2: Under an atmosphere of nitrogen, a solution of silicon tetraiodide (2.30 g, 4.29 mmol) in anhydrous chloroform (40 mL) was purged with nitrogen for 10 minutes. Anhydrous 1,10-phenanthroline (1.57 g, 8.71 mmol) was added. The red suspension was purged with nitrogen for additional five minutes and then stirred at 55 °C for 24 hours. After cooling to room temperature, 1,2-dihydroxybenzene (1.89 g, 17.2 mmol) was added, and the red brown suspension was stirred at 80 °C for two days. The resulting orange suspension was cooled to room temperature, and the solvent was removed under vacuum. The residue was subjected to flash column chromatography (MeCN → MeCN/H_2O/satd. aq. KNO_3 50:3:1 → 50:6:2), whereupon the yellow band eluting under salt conditions was collected. The product fractions were concentrated, and the residue was dissolved in water. Then NH_4PF_6 was added, the resulting precipitate was isolated by centrifugation (4000 rpm, 4 °C, 5 min) and washed twice with water to remove the excess amount of salt. The solid was dissolved in acetonitrile, and the gained solution was filtered through cotton before it was concentrated. After drying under vacuum, complex **88** was obtained as a dark yellow solid (1.2 g, 1.52 mmol, 36 % over two steps). – $\mathbf{C_{30}H_{20}F_{12}N_4O_2P_2Si}$ (M = 786.52 g mol^{-1}). – **^{1}H-NMR** (300 MHz, CD_3CN): δ = 9.46 (dd, ^3J = 5.4 Hz, ^4J = 1.2 Hz, 2H, H_{phen}), 9.38 (dd, ^3J = 8.4 Hz, ^4J = 1.2 Hz, 2H, H_{phen}), 9.09 (dd, ^3J = 8.3 Hz, ^4J = 1.0 Hz, 2H, H_{phen}), 8.60 (d, ^3J = 9.2 Hz, 2H, H_{phen}), 8.52–8.47 (m, 4H, H_{phen}), 7.91 (dd, ^3J = 8.4, 5.3 Hz, 2H, H_{phen}), 7.73 (dd, ^3J = 5.6 Hz, ^4J = 1.0 Hz, 2H, H_{phen}), 6.86–6.75 (m, 4H, H_{cat}) ppm. – **^{13}C-NMR** (75.5 MHz, CD_3CN): δ = 149.5, 147.5, 147.2, 147.0, 146.4, 135.7, 134.8, 131.4, 131.0, 129.7, 129.6, 129.3, 128.9, 123.0, 114.6 ppm. – **^{29}Si-NMR** (59.7 MHz, CD_3CN): δ = −149.2 ppm. – **FT-IR** (Film) $\tilde{\nu}$ = 3115, 1626, 1586, 1530, 1484, 1438, 1338, 1248, 1224, 1154, 1117, 1016, 930, 887, 833, 762, 744, 718, 667, 586, 558, 524, 510, 489, 461, 423, 397 cm^{-1}. – **HRMS** (ESI+): calc. for $C_{30}H_{20}N_4O_2SiPF_6$ $[M-PF_6]^+$: 641.0992 u, found: 641.0986 u. – **R_f:** 0.19 (MeCN/H_2O/satd. aq. KNO_3 50:6:2).

(Benzene-1,2-diolato)bis(3,4,7,8-tetramethyl-1,10-phenanthroline)silicon(IV)-bis(hexafluorophosphate) (89)

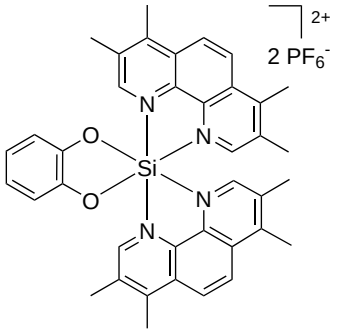

Under an atmosphere of nitrogen, a solution 3,4,7,8-tetramethyl-1,10-phenanthroline (1.00 g, 423 mmol) in anhydrous chloroform (40 mL) was treated with silicon tetraiodide (1.40 g, 2.61 mmol), and the red suspension was stirred at 50 °C for 16 hours. After cooling to room temperature, 1,2-dihydroxybenzene (1.15 g, 10.4 mmol) was added, and the red brown suspension was stirred at 70 °C for six hours. The resulting suspension was cooled to room temperature, and the solvent was removed under vacuum. The residue was subjected to flash column chromatography (MeCN → MeCN/H_2O/satd. aq. KNO_3 50:3:1 → 50:6:2), whereupon the yellow band eluting under salt conditions was collected. The product fractions were concentrated, and the residue was dissolved in water. Then NH_4PF_6 was added, and the resulting precipitate was isolated by centrifugation (4000 rpm, 4 °C, 5 min) and washed twice with water to remove the excess amount of salt. The solid was dissolved in acetonitrile, and the gained solution was filtered through cotton before it was concentrated. After drying under vacuum, complex **89** was obtained as a yellow solid (218 mg, 243 µmol, 11 % over two steps). – **$C_{38}H_{36}F_{12}N_4O_2P_2Si$** (M = 898.75 g mol^{-1}). – **^{1}H-NMR** (300 MHz, CD_3CN): δ = 9.09 (s, 2H, H_{Me_4phen}), 8.64 (d, ^3J = 9.6 Hz, 2H, H_{Me_4phen}), 8.56 (d, ^3J = 9.6 Hz, 2H, H_{Me_4phen}), 7.36 (s, 2H, H_{Me_4phen}), 6.80 (m, 2H, H_{cat}), 6.72 (m, 2H, H_{cat}), 3.03 (s, 6H, H_{Methyl}), 2.84 (s, 6H, H_{Methyl}), 2.68 (s, 6H, H_{Methyl}), 2.30 (s, 6H, H_{Methyl}) ppm. – **^{13}C-NMR** (75.5 MHz, CD_3CN): δ = 157.7, 156.6, 148.5, 147.5, 146.3, 138.8, 138.2, 134.5, 133.6, 129.7, 129.3, 125.9, 125.8, 122.7, 114.4, 18.8, 18.3, 16.7, 16.3 ppm. – **^{29}Si-NMR** (99.4 MHz, CD_3CN): δ = −150.9 ppm. – **FT-IR** (Film) $\tilde{\nu}$ = 3667, 1622, 1545, 1484, 1440, 1391, 1337, 1317, 1243, 1224, 1197, 1099, 1014, 913, 835, 770, 741, 721, 649, 597, 558, 527, 489, 463, 430 cm^{-1}. – **HRMS** (ESI+): calc. for $C_{38}H_{36}F_6N_4O_2PSi$ $[M-PF_6]^+$: 753.2244 u, found: 753.2260 u.

(4-Methylbenzene-1,2-diolato)bis(1,10-phenanthroline)silicon(IV)-bis(hexafluorophosphate) (90)

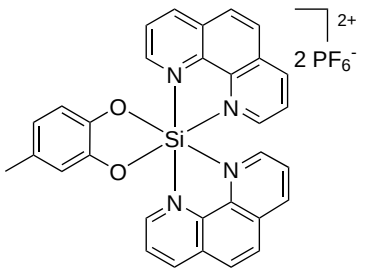

Under an atmosphere of nitrogen, a suspension of $[SiI_2(phen)_2]I_2$ **86** (1.08 g, 1.21 mmol) and 4-methylbenzene-1,2-diol (600 mg, 4.83 mmol) in anhydrous chloroform (40 mL) was purged with nitrogen for 10 minutes and then stirred at 80 °C for 18 hours. The resulting orange-red suspension was cooled to room temperature, and the solvent was removed under vacuum. The residue was subjected to flash column chromatography (MeCN → MeCN/H_2O/satd. aq. KNO_3 50:3:1 → 50:6:2), whereupon the orange band eluting under salt conditions was collected. The product fractions were concentrated, the residue was dissolved in water, and NH_4PF_6 was added. The resulting precipitate was isolated by centrifugation (4000 rpm, 4 °C, 5 min) and washed twice with water to remove the excess amount of salt. The solid was dissolved in acetonitrile, and the gained solution was filtered through cotton before it was concentrated. After drying under vacuum, complex **90** was obtained

as an orange solid (401 mg, 501 µmol, 41 %). – **$C_{31}H_{22}F_{12}N_4O_2P_2Si$** (M = 800.56 g mol^{-1}). – **^{1}H-NMR** (300 MHz, CD_3CN): δ = 9.45 (ddd, J = 5.4, 3.1, 1.2 Hz, 2H, H_{phen}), 9.38 (dd, ^3J = 8.4 Hz, ^4J = 1.2 Hz, 2H, H_{phen}), 9.08 (dt, J = 8.3, 1.0 Hz, 2H, H_{phen}), 8.60 (d, ^3J = 9.1 Hz, 2H, H_{phen}), 8.54–8.44 (m, 4H, H_{phen}), 7.91 (ddd, J = 8.3, 5.6, 1.1 Hz, 2H, H_{phen}), 7.72 (dt, J = 5.5, 1.0 Hz, 2H, H_{phen}), 6.64 (d, ^4J = 1.1 Hz, 2H, H_{cat}), 6.62–6.60 (m, 1H, H_{cat}), 2.20 (s, 3H, H_{Methyl}) ppm. – **^{13}C-NMR** (75.5 MHz, CD_3CN): δ = 149.4, 149.3, 147.4, 146.9, 146.3, 144.7, 135.7, 134.8, 132.6, 131.3, 130.9, 129.6, 129.5, 129.2, 128.8, 123.0, 115.2, 114.0, 21.1 ppm. – **^{29}Si-NMR** (79.5 MHz, CD_3CN): δ = −148.7 ppm. – **FT-IR** (Film) $\tilde{\nu}$ = 3049, 2169, 1584, 1526, 1483, 1429, 1322, 1246, 1150, 1110, 1028, 933, 883, 835, 737, 699, 605, 564, 518, 480, 427 cm^{-1}. – **HRMS** (ESI+): calc. for $C_{31}H_{22}N_4O_2SiPF_6$ $[M-PF_6]^+$: 655.1148 u, found: 655.1137 u.

(4-Methylbenzene-1,2-diolato)bis(1,10-phenanthroline)silicon(IV)-dichloride (90a)

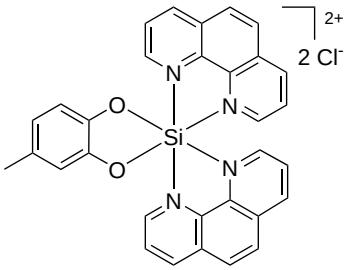

Using method A and silicon complex **90** (98.8 mg, 123 µmol), complex **90a** was obtained as an orange solid (71.1 mg, 122 µmol, 99 %). – **$C_{31}H_{22}Cl_2N_4O_2Si$** (M = 581.53 g mol^{-1}). – **^{1}H-NMR** (300 MHz, MeOD): δ = 9.59 (dd, ^3J = 5.4 Hz, ^4J = 1.2 Hz, 2H, H_{phen}), 9.54 (dd, ^3J = 8.4 Hz, ^4J = 1.1 Hz, 2H, H_{phen}), 9.31–9.21 (m, 2H, H_{phen}), 8.70 (d, ^3J = 9.1 Hz, 2H, H_{phen}), 8.66–8.56 (m, 4H, H_{phen}), 8.15–8.03 (m, 4H, H_{phen}), 6.71–6.58 (m, 3H, H_{cat}), 2.19 (s, 3H, H_{Methyl}) ppm. – **^{13}C-NMR** (75.5 MHz, MeOD): δ = 149.7, 149.6, 147.8, 147.2, 146.5, 145.0, 136.2, 135.3, 133.0, 131.6, 131.4, 129.9, 129.6, 129.5, 129.1, 123.3, 115.4, 114.2, 21.2 ppm. – **^{29}Si-NMR** (59.7 MHz, MeOD): δ = −148.6 ppm. – **FT-IR** (Film) $\tilde{\nu}$ = 3374, 3097, 3055, 2925, 2860, 1639, 1624, 1584, 1528, 1493, 1465, 1434, 1326, 1252, 1233, 1208, 1153, 1116, 1065, 1043, 1003, 943, 929, 887, 852, 837, 761, 746, 716, 667, 623, 598, 573, 563, 525, 508, 489, 477, 462, 449, 424 cm^{-1}. – **HRMS** (ESI+): calc. for $C_{31}H_{22}ClN_4O_2Si$ $[M-Cl]^+$: 545.1195 u, found: 545.1208 u.

(4-Hydroxybenzene-1,2-diolato)bis(1,10-phenanthroline)silicon(IV)-bis(hexafluorophosphate) (91)

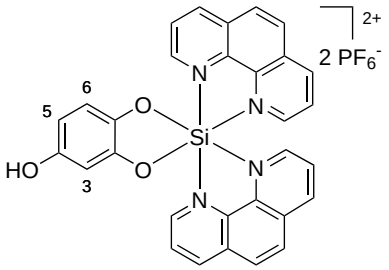

Under an atmosphere of nitrogen, a suspension of $[SiI_2(phen)_2]I_2$ **86** (1.00 g, 1.12 mmol) and 1,2,4-trihydroxybenzene (560 mg, 4.44 mmol) in anhydrous chloroform (40 mL) was purged with nitrogen for 15 minutes and then stirred at 80 °C for 18 hours. The resulting brownish-red suspension was cooled to room temperature, and the solvent was removed under vacuum. The residue was subjected to flash column chromatography (MeCN → MeCN/H_2O/satd. aq. KNO_3 50:3:1 → 50:6:2). The brownish-orange band eluting under salt conditions was collected, and the product fractions were concentrated. The residue was dissolved in water, and NH_4PF_6 was added. The resulting precipitate was isolated by centrifugation (4000 rpm, 4 °C, 5 min) and washed twice with water to remove the excess amount of salt. The solid was dissolved in acetonitrile, and the gained solu-

tion was filtered through cotton before it was concentrated. After drying under vacuum, complex **91** was obtained as a brownish red solid (307 mg, 383 µmol, 34 %). – **$C_{30}H_{20}F_{12}N_4O_3P_2Si$** (M = 802.53 g mol^{-1}). – ^{1}**H-NMR** (300 MHz, CD_3CN): δ = 9.45 (ddd, J = 5.4, 2.9, 1.2 Hz, 2H, H_{phen}), 9.40–9.35 (m, 2H, H_{phen}), 9.07 (dd, ^3J = 8.3 Hz, ^4J = 1.0 Hz, 2H, H_{phen}), 8.59 (d, ^3J = 9.1 Hz, 2H, H_{phen}), 8.54–8.46 (m, 4H, H_{phen}), 7.90 (dd, ^3J = 8.3, 5.6 Hz, 2H, H_{phen}), 7.71 (dt, J = 5.6, 1.1 Hz, 2H, H_{phen}), 6.67 (s, 1H, H_{OH}), 6.58 (d, ^3J = 8.3 Hz, 1H, H-6), 6.30–6.22 (m, 2H, H-3, H-5) ppm. – ^{13}**C-NMR** (75.5 MHz, CD_3CN): δ = 153.0, 149.5, 149.4, 147.6, 147.4, 147.4, 146.9, 146.8, 146.2, 140.0, 135.7, 134.7, 131.3, 130.9, 129.6, 129.2, 128.8, 114.2, 108.3, 103.0 ppm. – ^{29}**Si-NMR** (79.5 MHz, CD_3CN): δ = −148.1 ppm. – **FT-IR** (Film) $\tilde{\nu}$ = 3552, 3112, 2167, 1625, 1586, 1529, 1491, 1435, 1370, 1202, 1151, 1112, 1040, 961, 828, 755, 715, 616, 556, 521, 479 cm^{-1}. – **HRMS** (ESI+): calc. for $C_{30}H_{20}N_4O_3SiPF_6$ $[M-PF_6]^+$: 657.0941 u, found: 657.0993 u.

(4-Hydroxybenzene-1,2-diolato)bis(1,10-phenanthroline)silicon(IV)-dichloride (91a)

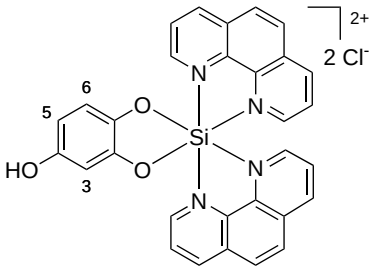

Using method A and silicon complex **91** (21.2 mg, 26.4 µmol), complex **91a** was obtained as an orange solid (14.4 mg, 24.7 µmol, 94 %). – **$C_{30}H_{20}Cl_2N_4O_3Si$** (M = 583.50 g mol^{-1}). – ^{1}**H-NMR** (300 MHz, MeOD): δ = 9.60–9.54 (m, 2H, H_{phen}), 9.54–9.49 (m, 2H, H_{phen}), 9.24 (dd, ^3J = 7.6 Hz, ^4J = 1.6 Hz, 2H, H_{phen}), 8.68 (d, ^3J = 9.1 Hz, 2H, H_{phen}), 8.64–8.56 (m, 4H, H_{phen}), 8.11–7.98 (m, 4H, H_{phen}), 6.59 (d, J = 8.5 Hz, 1H, H-6), 6.30 (d, ^4J = 2.6 Hz, 1H, H-3), 6.23 (dd, ^3J = 8.5 Hz, ^4J = 2.7 Hz, 1H, H-5) ppm. – **FT-IR** (Film) $\tilde{\nu}$ = 3375, 3097, 3064, 1641, 1623, 1584, 1528, 1493, 1467, 1435, 1324, 1281, 1230, 1198, 1146, 1115, 1019, 957, 930, 886, 839, 759, 716, 668, 648, 623, 603, 574, 564, 524, 508, 488, 479, 467, 446, 427, 396, 384 cm^{-1}.

(4-Formylbenzene-1,2-diolato-κ^2O)bis(1,10-phenanthroline)silicon(IV)-bis(hexafluorophosphate) (92)

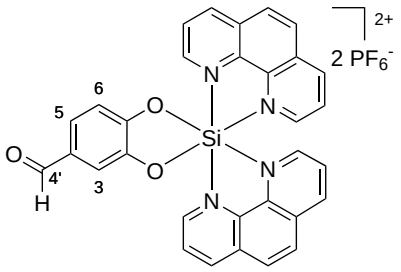

Under an atmosphere of nitrogen, a suspension of $[SiI_2(phen)_2]I_2$ **86** (600 mg, 670 µmol) and 3,4-dihydroxybenzaldehyde (380 mg, 2.75 mmol) in anhydrous chloroform (20 mL) was stirred at 80 °C for 16 hours. The resulting yellow suspension was then cooled to room temperature, and the solvent was removed under vacuum. The residue was subjected to flash column chromatography (MeCN → MeCN/H_2O/satd. aq. KNO_3 50:3:1 → 50:6:2). The yellow band eluting under salt conditions was collected, and the acetonitrile of the product fractions was removed by evaporation. The residue was treated with NH_4PF_6 and stored at 4 °C over night. The resulting precipitate was isolated by centrifugation (4000 rpm, 4 °C, 5 min) and washed twice with water (solid A, impure). As the combined water layers (from precipitation + washing) were still yellow, they were concentrated under vacuum. The residue was suspended in acetonitrile, filtered and rinsed with acetonitrile. Solid A was added to the filtrate, the solvent was removed, and the counterion

was exchanged to PF_6^- by using method A. The chloride salt was then subjected to gravity column chromatography (MeCN → MeCN/H_2O/satd. aq. KNO_3 50:3:1 → 50:6:2). The yellow band eluting under salt conditions was collected, and the acetonitrile of the product fractions was removed by evaporation. The resulting water layer was treated with NH_4PF_6, the formed precipitate was isolated by centrifugation (4000 rpm, 4 °C, 5 min) and washed twice with water to remove the excess amount of salt. The solid was dissolved in acetonitrile, and the gained solution was filtered through cotton before it was concentrated. After drying under vacuum, complex **92** was obtained as a yellow solid (22.9 mg, 28.1 µmol, 4 %). – **$C_{31}H_{20}F_{12}N_4O_3P_2Si$** (M = 814.54 g mol^{-1}). – **^{1}H-NMR** (300 MHz, CD_3CN): δ = 9.77 (s, 1H, H-4'), 9.46 (dd, ^3J = 5.4 Hz, ^4J = 1.2 Hz, 1H, H_{phen}), 9.43 (dd, ^3J = 5.4 Hz, ^4J = 1.2 Hz, 1H, H_{phen}), 9.41–9.36 (m, 2H, H_{phen}), 9.11 (dt, J = 8.3, 1.2 Hz, 2H, H_{phen}), 8.61 (dd, J = 9.1, 0.6 Hz, 2H, H_{phen}), 8.55–8.44 (m, 4H, H_{phen}), 7.93 (ddd, J = 8.3, 5.6, 1.0 Hz, 2H, H_{phen}), 7.75 (dt, J = 5.6, 1.3 Hz, 2H, H_{phen}), 7.46 (dd, ^3J = 8.1 Hz, ^4J = 1.8 Hz, 1H, H-5), 7.25 (d, ^4J = 1.8 Hz, 1H, H-3), 6.94 (d, ^3J = 8.1 Hzz, 1H, H-6) ppm. – **^{13}C-NMR** (101 MHz, CD_3CN): δ = 192.1, 153.3, 149.7, 149.5, 148.1, 147.75, 147.74, 147.3, 147.2, 146.7, 146.6, 135.71, 135.70, 134.8, 132.7, 131.50, 131.47, 131.0, 129.78, 129.75, 129.39, 129.36, 128.9, 128.3, 114.9, 113.0 ppm. – **^{29}Si-NMR** (79.5 MHz, CD_3CN): δ = −148.0 ppm. – **FT-IR** (Film) $\tilde{\nu}$ = 3667, 3113, 1683, 1626, 1587, 1531, 1493, 1439, 1347, 1266, 1235, 1159, 1118, 888, 837, 781, 761, 743, 718, 626, 590, 558, 525, 489, 428, 395 cm^{-1}. – **HRMS** (ESI+): calc. for $C_{31}H_{20}F_6N_4O_3PSi$ $[M-PF_6]^+$: 669.0941 u, found: 669.0959 u.

(Naphthalene-2,3-diolato)bis(1,10-phenanthroline)silicon(IV)-bis(hexafluorophosphate) (100)

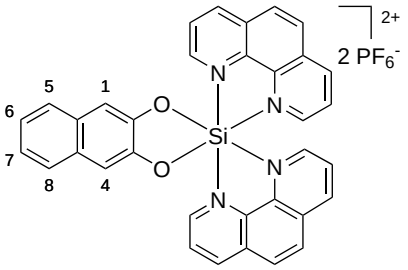

Under an atmosphere of nitrogen, a suspension of $[SiI_2(phen)_2]I_2$ **86** (1.23 g, 1.37 mmol) and 2,3-dihydroxynaphthalene (900 mg, 5.62 mmol) in anhydrous chloroform (40 mL) was purged with nitrogen for 15 minutes and then stirred at 90 °C for 48 hours. The resulting orange suspension was cooled to room temperature, and the solvent was removed under vacuum. The residue was subjected to flash column chromatography (MeCN → MeCN/H_2O/satd. aq. KNO_3 50:3:1 → 50:6:2). The yellow band eluting under salt conditions was collected, the product fractions were concentrated, and the residue was dissolved in water. NH_4PF_6 was added, the resulting precipitate was isolated by centrifugation (4000 rpm, 4 °C, 5 min) and washed twice with water to remove the excess amount of salt. The solid was dissolved in acetonitrile, and the gained solution was filtered through cotton before it was concentrated. After drying under vacuum, complex **100** was obtained as a yellow solid (337 mg, 403 µmol, 29 %). The analytical data are in accordance with the literature.[37] – **$C_{34}H_{22}F_{12}N_4O_2P_2Si$** (M = 836.59 g mol^{-1}). – **^{1}H-NMR** (300 MHz, CD_3CN): δ = 9.52 (dd, ^3J = 5.4 Hz, ^4J = 1.1 Hz, 2H, H_{phen}), 9.37 (dd, ^3J = 8.4 Hz, ^4J = 1.1 Hz, 2H, H_{phen}), 9.11 (dd, ^3J = 8.3 Hz, ^4J = 0.9 Hz, 2H, H_{phen}), 8.61 (d, ^3J = 9.1 Hz, 2H, H_{phen}), 8.52 (d, ^3J = 9.1 Hz, 2H, H_{phen}), 8.45 (dd, ^3J = 8.4, 5.4 Hz, 2H, H_{phen}), 7.95 (dd, ^3J = 8.3, 5.6 Hz, 2H, H_{phen}), 7.77 (dd, ^3J = 5.5 Hz, ^4J = 1.0 Hz, 2H, H_{phen}), 7.69–7.62 (m, 2H, H-5, H-8), 7.32–7.25 (m, 2H, H-6, H-7), 7.16 (s, 2H, H-1, H-4) ppm.

5.4.2. Modification of Octahedral Silicon(IV) Complexes

(4,5-Dibromobenzene-1,2-diolato)bis(1,10-phenanthroline)silicon(IV)-bis(hexafluorophosphate) (108)

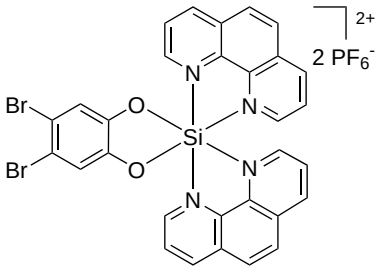

Under an atmosphere of nitrogen, (benzene-1,2-diolato)bis(1,10-phenanthroline)silicon(IV)-bis(hexafluorophosphate) (**88**, 51.8 mg, 65.9 µmol) was dissolved in anhydrous acetonitrile (1.5 mL). *N*-Bromosuccinimide (30.3 mg, 170 µmol) was added, and the yellow solution was stirred at room temperature for three days. The light orange solution was then subjected to flash column chromatography (MeCN → MeCN/H_2O/satd. aq. KNO_3 50:3:1 → 50:6:2), whereupon the yellow band eluting under salt conditions was collected. The product fractions were concentrated, and the residue was dissolved in water. NH_4PF_6 was added, the resulting precipitate was isolated by centrifugation (4000 rpm, 4 °C, 5 min) and washed twice with water to remove the excess amount of salt. The solid was dissolved in acetonitrile, and the gained solution was filtered through cotton before it was concentrated. After drying under vacuum, complex **108** was obtained as a yellow solid (46.9 mg, 49.7 µmol, 75 %). – **$C_{30}H_{18}Br_2F_{12}N_4O_2P_2Si$** (M = 944.32 g mol^{-1}). – **^{1}H-NMR** (300 MHz, CD_3CN): δ = 9.47–9.36 (m, 4H, H_{phen}), 9.10 (dd, ^3J = 8.3 Hz, ^4J = 1.0 Hz, 2H, H_{phen}), 8.61 (d, ^3J = 9.1 Hz, 2H, H_{phen}), 8.55–8.46 (m, 4H, H_{phen}), 7.92 (dd, ^3J = 8.3, 5.6 Hz, 2H, H_{phen}), 7.71 (dd, ^3J = 5.6 Hz, ^4J = 1.0 Hz, 2H, H_{phen}), 7.09 (s, 2H, H_{cat}) ppm. – **^{13}C-NMR** (75.5 MHz, CD_3CN): δ = 149.7, 147.9, 147.7, 147.2, 146.7, 135.7, 134.7, 131.5, 131.0, 129.9, 129.7, 129.4, 128.9, 119.3, 115.9 ppm. – **^{29}Si-NMR** (79.5 MHz, CD_3CN): δ = −149.3 ppm. – **FT-IR** (Film) $\tilde{\nu}$ = 3660, 3112, 1625, 1587, 1531, 1478, 1438, 1365, 1322, 1243, 1177, 1159, 1118, 1082, 888, 837, 761, 746, 717, 658, 578, 558, 527, 510, 494, 474, 424 cm^{-1}. – **HRMS** (ESI+): calc. for $C_{30}H_{18}Br_2N_4O_2SiPF_6$ $[M-PF_6]^+$: 798.9184 u, found: 798.9171 u. – **R_f:** 0.27 (MeCN/H_2O/satd. aq. KNO_3 50:6:2).

Bis(2,2'-bipyridine)(4,5-dibromobenzene-1,2-diolato)silicon(IV)-bis(hexafluorophosphate) (109)

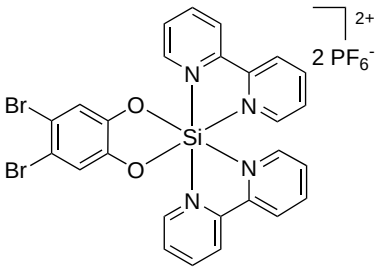

Under an atmosphere of nitrogen, (benzene-1,2-diolato)bis(2,2'-bipyridine)silicon(IV)-bis(hexafluorophosphate) (**87**, 54.0 mg, 73.1 µmol) was dissolved in anhydrous acetonitrile (1.5 mL). *N*-bromosuccinimide (37.0 mg, 208 µmol) was added, and the yellow solution was stirred at room temperature for six days. LCMS control showed no full conversion, thus more *N*-bromosuccinimide (10.0 mg, 56.2 µmol) was added, and mixture was first stirred at room temperature for 14 hours before it was heated to 60 °C for 16 hours. After cooling to room temperature, the yellow solution was subjected to flash column chromatography (MeCN → MeCN/H_2O/satd. aq. KNO_3 50:3:1 → 50:6:2), whereupon the yellow band eluting under salt conditions was collected. The product fractions were concentrated, and the residue was dissolved in water. NH_4PF_6 was added, the resulting precipitate was isolated by centrifugation (4000 rpm, 4 °C, 5 min) and washed twice with water to remove the excess amount of salt. The solid was dissolved in acetonitrile, and the gained

solution was filtered through cotton before it was concentrated. After drying under vacuum, complex **109** was obtained as a yellow solid (45.3 mg, 50.5 µmol, 69 %). – **$C_{26}H_{18}Br_2F_{12}N_4O_2P_2Si$** (M = 896.28 g mol^{-1}). – ^{1}**H-NMR** (300 MHz, CD_3CN): δ = 9.05–9.00 (m, 2H, H_{bpy}), 8.97–8.91 (m, 2H, H_{bpy}), 8.87–8.76 (m, 4H, H_{bpy}), 8.62 (td, ^3J = 7.9 Hz, ^4J = 1.3 Hz, 2H, H_{bpy}), 8.19 (ddd, ^3J = 7.6, 5.8 Hz, ^4J = 1.1 Hz, 2H, H_{bpy}), 7.82 (ddd, ^3J = 7.5, 6.0 Hz, ^4J = 1.2 Hz, 2H, H_{bpy}), 7.62–7.56 (m, 2H, H_{bpy}), 7.07 (s, 2H, H_{cat}) ppm. – ^{13}**C-NMR** (126 MHz, CD_3CN): δ = 148.8, 148.4, 148.3, 147.5, 146.3, 144.8, 144.0, 132.2, 131.4, 126.3, 126.0, 119.3, 115.9 ppm. – ^{29}**Si-NMR** (99.4 MHz, CD_3CN): δ = −149.4 ppm. – **FT-IR** (Film) $\tilde{\nu}$ = 3663, 3110, 1618, 1575, 1509, 1478, 1455, 1325, 1286, 1240, 1180, 1119, 1073, 1058, 1045, 1028, 835, 774, 743, 687, 673, 648, 569, 558, 521, 474, 422 cm^{-1}. – **HRMS** (ESI+): calc. for $C_{26}H_{18}Br_2F_6N_4O_2PSi$ $[M-PF_6]^+$: 750.9184 u, found: 750.9198 u.

(4-Bromo-5-methylbenzene-1,2-diolato)bis(1,10-phenanthroline)silicon(IV)-bis(hexafluorophosphate) (110)

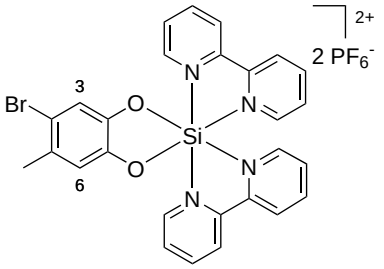

Under an atmosphere of nitrogen, (4-methylbenzene-1,2-diolato)bis(1,10-phenanthroline)silicon(IV)-bis(hexafluorophosphate) (**90**, 88.7 mg, 111 µmol) was dissolved in anhydrous acetonitrile (2.0 mL). *N*-bromosuccinimide (22.0 mg, 124 µmol) was added, and the mixture was stirred at −40 °C for six days. The yellow solution was then subjected to flash column chromatography (MeCN → MeCN/H_2O/satd. aq. KNO_3 50:3:1 → 50:6:2), whereupon the yellow band eluting under salt conditions was collected. The product fractions were concentrated, and the residue was dissolved in water. NH_4PF_6 was added, the resulting precipitate was isolated by centrifugation (4000 rpm, 4 °C, 5 min) and washed twice with water to remove the excess amount of salt. The solid was dissolved in acetonitrile, and the gained solution was filtered through cotton before it was concentrated. After drying under vacuum, complex **110** was obtained as a yellow solid (72.3 mg, 82.2 µmol, 74 %). – **$C_{31}H_{21}BrF_{12}N_4O_2P_2Si$** (M = 879.45 g mol^{-1}). – ^{1}**H-NMR** (300 MHz, CD_3CN): δ = 9.46–9.36 (m, 4H, H_{phen}), 9.08 (d, ^3J = 8.3 Hz, 2H, H_{phen}), 8.60 (d, ^3J = 9.1 Hz, 2H, H_{phen}), 8.54–8.46 (m, 4H, H_{phen}), 7.91 (ddd, J = 8.3, 5.6, 0.9 Hz, 2H, H_{phen}), 7.70 (ddd, J = 5.6, 2.1, 1.1 Hz, 2H, H_{phen}), 6.96 (s, 1H, H-3), 6.73 (s, 1H, H-6), 2.23 (s, 3H, H_{Methyl}) ppm. – ^{13}**C-NMR** (75.5 MHz, CD_3CN): δ = 149.6, 149.5, 147.6, 147.1, 146.8, 146.52, 146.50, 146.2, 135.69, 135.67, 134.8, 131.8, 131.44, 131.44, 131.02, 130.99, 129.73, 129.72, 129.71, 129.4, 128.9, 118.1, 116.6, 115.6, 22.7 ppm. – ^{29}**Si-NMR** (99.4 MHz, CD_3CN): δ = −147.7 ppm. – **FT-IR** (Film) $\tilde{\nu}$ = 3656, 3113, 1625, 1586, 1531, 1487, 1438, 1396, 1327, 1248, 1188, 1159, 1139, 1118, 888, 837, 762, 751, 717, 670, 581, 558, 526, 509, 484, 467, 426, 387 cm^{-1}. – **HRMS** (ESI+): calc. for $C_{31}H_{21}BrF_6N_4O_2PSi$ $[M-PF_6]^+$: 735.0238 u, found: 735.0250 u.

(4,5-Diiodobenzene-1,2-diolato)bis(1,10-phenanthroline)silicon(IV)-bis(hexafluorophosphate) (112)

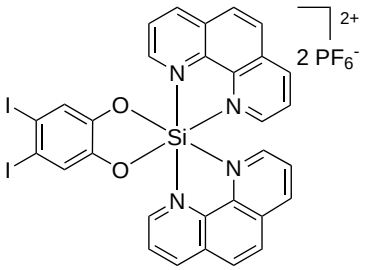

Under an atmosphere of nitrogen, (benzene-1,2-diolato)bis(1,10-phenanthroline)silicon(IV)-bis(hexafluorophosphate) (**88**, 40.0 mg, 50.9 µmol) was dissolved in anhydrous acetonitrile (1.0 mL). *N*-Iodosuccinimide (25.0 mg, 111 µmol) and trifluoroacetic acid (2.0 µL, 26.0 µmol) were added, and the yellow solution was stirred at 60 °C for 18 hours. After cooling to room temperature, the light orange solution was subjected to flash column chromatography (MeCN → MeCN/H_2O/satd. aq. KNO_3 50:3:1 → 50:6:2), whereupon the yellow band eluting under salt conditions was collected. The product fractions were concentrated, and the residue was dissolved in water. NH_4PF_6 was added, the resulting precipitate was isolated by centrifugation (4000 rpm, 4 °C, 5 min) and washed twice with water to remove the excess amount of salt. The solid was dissolved in acetonitrile, and the gained solution was filtered through cotton before it was concentrated. As the ^{1}H-NMR of the product showed some starting material and mono substituted complex, the reaction and work-up procedure was repeated with the mixture (34.1 mg), *N*-iodosuccinimide (10.0 mg, 44.4 µmol) and trifluoroacetic acid (2.0 µL, 26.0 µmol) in acetonitrile (1.0 mL) at 60 °C for 1.5 hours. After drying under vacuum, complex **112** was obtained as a yellow solid (31.3 mg, 30.4 µmol, 59 %). – **$C_{30}H_{18}F_{12}I_2N_4O_2P_2Si$** (M = 1038.32 g mol^{-1}). – **^{1}H-NMR** (500 MHz, CD_3CN): δ = 9.43–9.37 (m, 4H, H_{phen}), 9.09 (dd, ^3J = 8.3 Hz, ^4J = 1.0 Hz, 2H, H_{phen}), 8.61 (d, ^3J = 9.1 Hz, 2H, H_{phen}), 8.54–8.49 (m, 4H, H_{phen}), 7.92 (dd, ^3J = 8.3, 5.6 Hz, 2H, H_{phen}), 7.71 (dd, ^3J = 5.6 Hz, ^3J = 1.0 Hz, 2H, H_{phen}), 7.31 (s, 2H, H_{cat}) ppm. – **^{13}C-NMR** (126 MHz, CD_3CN): δ = 149.6, 148.4, 147.6, 147.2, 146.6, 135.6, 134.6, 131.4, 130.9, 129.8, 129.7, 129.3, 128.9, 124.8, 97.2 ppm. – **^{29}Si-NMR** (59.7 MHz, CD_3CN): δ = −150.0 ppm. – **FT-IR** (Film) $\tilde{\nu}$ = 3112, 1625, 1586, 1531, 1472, 1437, 1420, 1348, 1325, 1304, 1237, 1220, 1173, 1158, 1118, 1067, 1044, 930, 887, 827, 760, 742, 716, 671, 649, 623, 603, 575, 557, 252, 509, 491, 468, 423, 382 cm^{-1}. – **HRMS** (ESI+): calc. for $C_{30}H_{18}Br_2N_4O_2SiPF_6$ $[M-PF_6]^+$: 798.9184 u, found: 798.9171 u.

(4-Iodobenzene-1,2-diolato)bis(1,10-phenanthroline)silicon(IV)-bis(hexafluorophosphate) (115)

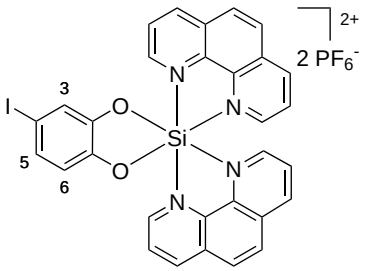

Under an atmosphere of nitrogen, potassium 4-iodylbenzenesulfonate (7.8 mg, 22.0 µmol) and iodine (12.0 mg, 47.3 µmol) were added to a suspension of (benzene-1,2-diolato)bis(1,10-phenanthroline)silicon(IV)-bis(hexafluorophosphate) (**88**, 74.8 mg, 95.1 µmol) in glacial acetic acid (2.5 mL). The orange suspension was stirred at 80 °C for 18 hours. Then the yellow mixture was cooled to room temperature, and the solvent was removed. The residue was subjected to flash column chromatography (MeCN → MeCN/H_2O/satd. aq. KNO_3 50:3:1 → 50:6:2), whereupon the yellow band eluting under salt conditions was collected. The product fractions were concentrated, the residue was dissolved in water, and NH_4PF_6 was added. The resulting precipitate was isolated by centrifugation (4000 rpm,

4 °C, 5 min) and washed twice with water to remove the excess amount of salt. The solid was dissolved in acetonitrile, and the gained solution was filtered through cotton before it was concentrated. After drying under vacuum, complex **115** was obtained as an orange solid (73.7 mg, 80.8 µmol, 85 %). – **$C_{30}H_{19}F_{12}IN_4O_2P_2Si$** (M = 912.43 g mol^{-1}). – **^{1}H-NMR** (300 MHz, CD_3CN): δ = 9.44– 9.38 (m, 4H, H_{phen}), 9.08 (d, ^3J = 8.3 Hz, 2H, H_{phen}), 8.60 (d, ^3J = 9.1 Hz, 2H, H_{phen}), 8.52–8.48 (m, 4H, H_{phen}), 7.93–7.89 (m, 2H, H_{phen}), 7.72 (d, ^3J = 5.5 Hz, 2H, H_{phen}), 7.19 (dd, ^3J = 8.3 Hz, ^4J = 2.0 Hz, 1H, H-5), 7.10 (d, ^4J = 1.9 Hz, 1H, H-3), 6.58 (d, ^3J = 8.2 Hz, 1H, H-6) ppm. – **^{13}C-NMR** (75.5 MHz, CD_3CN): δ = 149.5, 148.5, 147.5, 147.5, 147.1, 146.5, 135.6, 134.7, 131.8, 131.4, 130.9, 129.7, 129.6, 129.3, 128.9, 126.2, 124.8, 123.4, 116.7, 83.3 ppm. – **^{29}Si-NMR** (79.5 MHz, CD_3CN): δ = −149.4 ppm. – **FT-IR** (Film) $\tilde{\nu}$ = 3350, 3046, 2172, 1976, 1624, 1582, 1524, 1471, 1429, 1319, 1233, 1152, 1110, 929, 881, 828, 749, 712,559, 518, 482, 418 cm^{-1}. – **HRMS** (ESI+): calc. for $C_{30}H_{19}IN_4O_2SiPF_6$ $[M-PF_6]^+$: 766.9958 u, found: 766.9958 u.

(4-Iodo-5-methylbenzene-1,2-diolato)bis(1,10-phenanthroline)silicon(IV)-bis(hexafluorophosphate) (116)

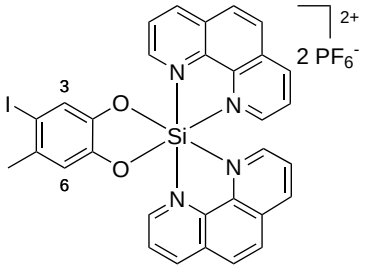

Under an atmosphere of nitrogen, potassium 4-iodylbenzenesulfonate (7.2 mg, 20.3 µmol) and iodine (17.8 mg, 70.1 µmol) were added to a suspension of (4-methylbenzene-1,2-diolato)bis(1,10-phenanthroline)silicon(IV)-bis(hexafluorophosphate) (**90**, 99.6 mg, 124 µmol) in glacial acetic acid (4.5 mL). The orange suspension was stirred at 80 °C for 18 hours. Then the yellow mixture was cooled to room temperature, and the solvent was removed. The residue was subjected to flash column chromatography (MeCN → MeCN/H_2O/satd. aq. KNO_3 50:3:1 → 50:6:2), whereupon the yellow band eluting under salt conditions was collected. The product fractions were concentrated, the residue was dissolved in water, and NH_4PF_6 was added. The resulting precipitate was isolated by centrifugation (4000 rpm, 4 °C, 5 min) and washed twice with water to remove the excess amount of salt. The solid was dissolved in acetonitrile, and the gained solution was filtered through cotton before it was concentrated. After drying under vacuum, complex **116** was obtained as an orange solid (90.3 mg, 97.5 µmol, 79 %). – **$C_{31}H_{21}F_{12}IN_4O_2P_2Si$** (M = 926.45 g mol^{-1}). – **^{1}H-NMR** (300 MHz, CD_3CN): δ = 9.46–9.36 (m, 4H, H_{phen}), 9.08 (dd, ^3J = 8.3 Hz, ^4J = 1.0 Hz, 2H, H_{phen}), 8.60 (d, ^3J = 9.1 Hz, 2H, H_{phen}), 8.54–8.47 (m, 4H, H_{phen}), 7.94–7.87 (m, 2H, H_{phen}), 7.70 (ddd, J = 5.5, 2.3, 1.1 Hz, 2H, H_{phen}), 7.19 (s, 1H, H-3), 6.76 (s, 1H, H-6), 2.27 (s, 3H, H_{Methyl}) ppm. – **^{13}C-NMR** (75.5 MHz, CD_3CN): δ = 149.6, 149.5, 147.7, 147.6, 147.1, 146.5, 146.1, 135.7, 135.6, 134.7, 131.4, 131.4, 130.98, 130.96, 129.71, 129.70, 129.3, 128.8, 124.0, 115.8, 89.6, 28.0 ppm. – **^{29}Si-NMR** (59.7 MHz, CD_3CN): δ = −149.5 ppm. – **FT-IR** (Film) $\tilde{\nu}$ = 3112, 1625, 1586, 1530, 1482, 1437, 1392, 1322, 1244, 1187, 1157, 1139, 1118, 1044, 1003, 929, 887, 826, 760, 749, 715, 668, 621, 579, 556, 536, 524, 509, 496, 483, 466, 447, SI425cm. – **HRMS** (ESI+): calc. for $C_{31}H_{21}IN_4O_2SiPF_6$ $[M-PF_6]^+$: 781.0115 u, found: 781.0132 u.

(4,5-Dioxocyclohexa-2,6-diene-1,2-diolato)bis(1,10-phenanthroline)silicon(IV)-bis(hexafluorophosphate) (95)

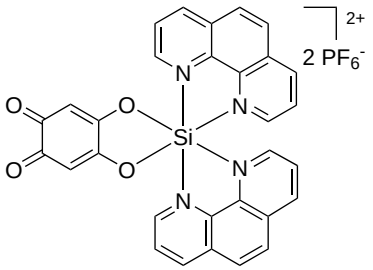

A solution of complex **91a** (101 mg, 172 µmol) in methanol (3.5 mL) was added to a solution of FREMY's salt (105 mg, 391 µmol) in aqueous potassium dihydrogenphosphate buffer (0.9 M, 3.5 mL). To dilute the highly viscous reaction mixture, potassium dihydrogenphosphate buffer (0.9 M, 2.0 mL) was added to the yellow suspension, and the mixture was stirred at room temperature for one hour. The dark reaction suspension was treated with additional FREMY's salt (26.0 mg, 96.6 µmol) and stirred at room temperature for ten minutes. After addition of water (10 mL), NH_4PF_6 was added, and the resulting precipitate was isolated by centrifugation (4000 rpm, 4 °C, 10 min). The solid was washed twice with water before it was subjected to flash column chromatography (MeCN → MeCN/H_2O/satd. aq. KNO_3 50:3:1 → 50:6:2 → 50:12:4), whereupon the yellow band eluting under salt conditions was collected. The product eluents were concentrated, and the residue was dissolved in water. Next, NH_4PF_6 was added, the resulting precipitate was isolated by centrifugation (4000 rpm, 4 °C, 10 min) and washed twice with water to remove the excess amount of salt. After drying under vacuum, complex **95** was obtained as a yellow solid (104 mg, 128 µmol, 74 %). – **$C_{30}H_{18}F_{12}N_4O_4P_2Si$** (M = 816.51 g mol^{-1}). – **^{1}H-NMR** (300 MHz, CD_3CN): δ = 9.48 (dd, ^3J = 8.4 Hz, ^4J = 1.1 Hz, 2H, H_{phen}), 9.44 (dd, ^3J = 5.5 Hz, ^4J = 1.1 Hz, 2H, H_{phen}), 9.14 (dd, ^3J = 8.3 Hz, ^4J = 1.0 Hz, 2H, H_{phen}), 8.69–8.58 (m, 4H, H_{phen}), 8.54 (d, ^3J = 9.1 Hz, 2H, H_{phen}), 7.95 (dd, ^3J = 8.3, 5.6 Hz, 2H, H_{phen}), 7.71 (dd, ^3J = 5.6 Hz, ^4J = 1.0 Hz, 2H, H_{phen}), 5.77 (s, 2H, $H_{benzoq.}$) ppm. – **^{13}C-NMR** (75.5 MHz, CD_3CN): δ = 180.8, 161.7, 149.8, 148.1, 147.9, 147.3, 135.6, 135.4, 131.6, 131.1, 130.3, 130.0, 129.5, 129.1, 107.0 ppm. – **^{29}Si-NMR** (79.5 MHz, CD_3CN): δ = −151.7 ppm. – **FT-IR** (Film) $\tilde{\nu}$ = 3666, 3111, 1664, 1621, 1587, 1531, 1440, 1371, 1327, 1235, 1218, 1161, 1120, 889, 838, 761, 733, 716, 621, 597, 579, 558, 531, 511, 488, 450, 434, 423, 407, 396, 380 cm^{-1}. – **HRMS** (ESI+): calcd. for $C_{30}H_{18}N_4O_4SiPF_6$ $[M-PF_6]^+$: 671.0747 u, found: 671.0734 u.

(4-Nitrobenzene-1,2-diolato)bis(1,10-phenanthroline)silicon(IV)-bis(hexafluorophosphate) (127)

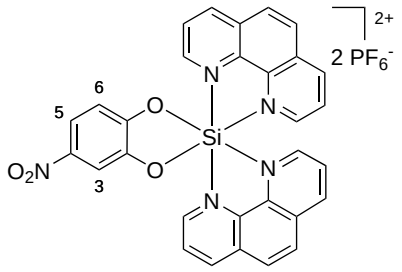

A suspension of (benzene-1,2-diolato)bis(1,10-phenanthroline)silicon(IV)-bis(hexafluorophosphate) (**88**, 202 mg, 257 µmol) in glacial acetic acid (1.5 mL) was treated with nitric acid (65 %, 3.0 mL), and the resulting yellow solution was stirred at room temperature for 1.5 hours. The reaction mixture was then cooled to 0 °C and neutralized with a concentrated sodium hydroxide solution until pH reached 6–7. NH_4PF_6 was added, and the obtained precipitate was isolated by centrifugation (4 °C, 4000 rpm, 10 min). The solid was washed twice with water to remove the excess amount of salt. After drying under vacuum, silicon complex **127** was obtained as a light yellow solid (184 mg, 221 µmol, 86 %). If necessary, the product could be purified by flash column chromatography (MeCN → MeCN/H_2O/satd. aq. KNO_3 50:3:1 → 50:6:2). – **$C_{30}H_{19}F_{12}N_5O_4P_2Si$**

(M = 831.53 g mol^{-1}). – **^{1}H-NMR** (300 MHz, CD_3CN): δ = 9.47–9.39 (m, 4H, H_{phen}), 9.12 (dt, J = 8.4, 1.4 Hz, 2H, H_{phen}), 8.62 (dd, J = 9.1, 1.4 Hz, 2H, H_{phen}), 8.56–8.47 (m, 4H, H_{phen}), 7.95 (ddd, J = 8.3, 5.6, 1.5 Hz, 2H, H_{phen}), 7.84 (dd, ^{3}J = 8.8 Hz, ^{4}J = 2.6 Hz, 1H, H-5), 7.74 (ddd, J = 5.6, 2.6, 1.1 Hz, 2H, H_{phen}), 7.60 (d, ^{3}J = 2.6 Hz, 1H, H-3), 6.90 (d, ^{3}J = 8.8 Hz, 1H, H-6) ppm. – **^{13}C-NMR** (75.5 MHz, CD_3CN): δ = 153.6, 149.6, 149.5, 147.7, 147.5, 147.3, 147.3, 146.8, 146.7, 143.4, 135.6, 134.7, 134.7, 131.4, 131.0, 129.7, 129.7, 129.4, 129.3, 128.9, 119.9, 114.3, 110.1 ppm. – **^{29}Si-NMR** (79.5 MHz, CD_3CN): δ = −149.0 ppm. – **FT-IR** (Film) $\tilde{\nu}$ = 3116, 2158, 1725, 1628, 1588, 1520, 1485, 1437, 1340, 1267, 1229, 1156, 1117, 1070, 945, 884, 827, 743, 715, 591, 553, 526, 485, 419 cm^{-1}. – **HRMS** (ESI+): calc. for $C_{30}H_{19}N_5O_4SiPF_6$ $[M-PF_6]^+$: 686.0843 u, found: 686.0844 u.

(4-Nitrobenzene-1,2-diolato)bis(3,4,7,8-tetramethyl-1,10-phenanthroline)silicon(IV)-bis(hexafluorophosphate) (128)

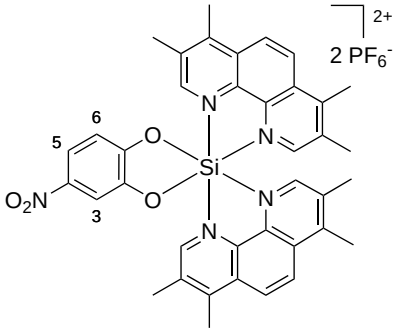

A suspension of complex **89** (22.0 mg, 24.5 µmol) in glacial acetic acid (0.5 mL) was treated with concentrated nitric acid (65 %, 1.0 mL). The yellow solution was stirred at room temperature for three hours. The mixture was then cooled to 0 °C and neutralized with a concentrated potassium hydroxide solution (20 %) until pH reached 6–7. The solvent was removed under vacuum, and the residue was subjected to flash column chromatography (MeCN → MeCN/H_2O/satd. aq. KNO_3 50:3:1 → 50:6:2), whereupon the slightly yellow band eluting under salt conditions was collected. The product fractions were concentrated, and the residue was dissolved in acetonitrile/water 1:1. Then NH_4PF_6 was added, the acetonitrile was removed, and the resulting precipitate was isolated by centrifugation (4000 rpm, 4 °C, 5 min) and washed twice with water to remove the excess amount of salt. The solid was dissolved in acetonitrile, and the gained solution was filtered through cotton before it was concentrated. After drying under vacuum, complex **128** was obtained as a light yellow solid (17.7 mg, 18.8 µmol, 77 %). – **$C_{38}H_{35}F_{12}N_5O_4P_2Si$** (M = 943.74 g mol^{-1}). – **^{1}H-NMR** (300 MHz, CD_3CN): δ = 9.07 (s, 1H, H_{Me_4phen}), 9.01 (s, 1H, H_{Me_4phen}), 8.65 (dd, J = 9.6, 1.4 Hz, 2H, H_{Me_4phen}), 8.58 (dd, J = 9.6, 1.8 Hz, 2H, H_{Me_4phen}), 7.80 (dd, ^{3}J = 8.8 Hz, ^{4}J = 2.6 Hz, 1H, H-5), 7.54 (d, ^{4}J = 2.6 Hz, 1H, H-3), 7.35 (s, 2H, H_{Me_4phen}), 6.84 (d, ^{3}J = 8.8 Hz, 1H, H-6), 3.03 (s, 6H, H_{Methyl}), 2.86 (s, 3H, H_{Methyl}), 2.85 (s, 3H, H_{Methyl}), 2.69 (s, 3H, H_{Methyl}), 2.68 (s, 3H, H_{Methyl}), 2.30 (s, 3H, H_{Methyl}), 2.30 (s, 3H, H_{Methyl}) ppm. – **^{13}C-NMR** (75.5 MHz, CD_3CN): δ = 158.2, 158.1, 157.2, 157.1, 154.1, 148.5, 148.4, 147.8, 146.4, 143.3, 139.2, 139.1, 138.4, 134.5, 133.5, 129.8, 129.3, 126.0, 125.95, 125.94, 119.8, 114.0, 110.0, 18.8, 18.3, 16.8, 16.4 ppm. – **^{29}Si-NMR** (99.4 MHz, CD_3CN): δ = −151.1 ppm. – **FT-IR** (Film) $\tilde{\nu}$ = 3667, 3111, 2933, 1622, 1597, 1544, 1515, 1486, 1439, 1390, 1339, 1269, 1225, 1197, 1183, 1118, 1069, 1027, 945, 914, 875, 828, 769, 735, 721, 649, 636, 599, 572, 557, 535, 526, 462, 446, 430, 383 cm^{-1}. – **HRMS** (ESI+): calc. for $C_{38}H_{35}F_6N_5O_4PSi$ $[M-PF_6]^+$: 798.2095 u, found: 798.2116 u.

Bis(2,2'-bipyridine)(4,5-dinitrobenzene-1,2-diolato)silicon(IV)-bis(hexafluorophosphate) (129)

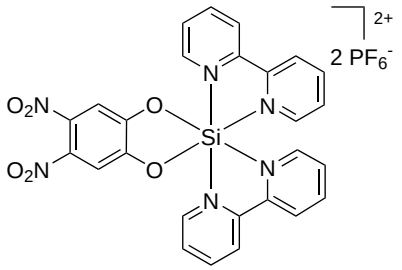

A suspension of (benzene-1,2-diolato)bis(2,2'-bipyridine)silicon(IV)-bis(hexafluorophosphate) (**87**, 13.0 mg, 17.6 µmol) in glacial acetic acid (0.5 mL) was treated with fuming nitric acid (1.0 mL), and the resulting yellow solution was stirred at room temperature for two hours. Then it was cooled to 0 °C and neutralized with a concentrated sodium hydroxide solution until pH reached 6–7. Acetonitrile was added to the mixture until formation of a precipitate ceased. The solid was removed by centrifugation and extracted with acetonitrile (2 × 5 mL). The acetonitrile of the combined solvent layers was removed by distillation, the resulting water layer was treated with NH_4PF_6, and the precipitate was isolated by centrifugation (4 °C, 4000 rpm, 5 min). The solid was washed twice with water to remove the excess amount of salt. After drying under vacuum, silicon complex **129** was obtained as a yellow solid (12.6 mg, 15.2 µmol, 86 %). If necessary, the product can be further purified by flash column chromatography (MeCN → MeCN/H_2O/satd. aq. KNO_3 50:3:1 → 50:6:2). – **$C_{26}H_{18}F_{12}N_6O_6P_2Si$** (M = 828.48 g mol^{-1}). – ^{1}**H-NMR** (300 MHz, CD_3CN): δ = 9.05–8.91 (m, 4H, H_{bpy}), 8.90–8.78 (m, 4H, H_{bpy}), 8.65 (td, ^3J = 8.0 Hz, ^4J = 1.2 Hz, 2H, H_{bpy}), 8.27–8.15 (m, 2H, H_{bpy}), 7.89–7.78 (m, 2H, H_{bpy}), 7.60 (d, ^3J = 5.5 Hz, 2H, H_{bpy}), 7.33 (s, 2H, H_{cat}) ppm. – ^{13}**C-NMR** (75.5 MHz, CD_3CN): δ = 150.9, 149.1, 148.7, 148.6, 146.5, 144.9, 144.0, 138.8, 132.5, 131.6, 126.5, 126.1, 111.5 ppm. – ^{29}**Si-NMR** (79.5 MHz, CD_3CN): δ = −149.1 ppm. – **FT-IR** (Film) $\tilde{\nu}$ = 3663, 3112, 2252, 1619, 1575, 1495, 1480, 1455, 1418, 1374, 1339, 1326, 1293, 1276, 1251, 1227, 1208, 1171, 1120, 1074, 1058, 1046, 1027, 896, 774, 756, 736, 688, 675, 651, 557, 522, 501, 468, 431 cm^{-1}. – **HRMS** (ESI+): calc. for $C_{26}H_{18}N_6O_6Si$ $[M-2PF_6]^{2}$+: 269.0523 u, found: 269.0520 u.

(4,5-Dinitrobenzene-1,2-diolato)bis(1,10-phenanthroline)silicon(IV)-bis(hexafluorophosphate) (130)

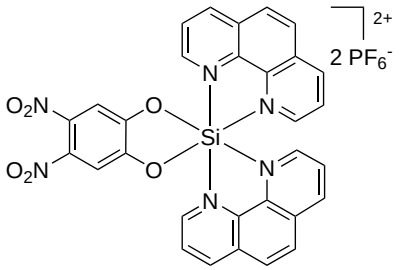

A suspension of (benzene-1,2-diolato)bis(1,10-phenanthroline)silicon(IV)-bis(hexafluorophosphate) (**88**, 460 mg, 585 µmol) in glacial acetic acid (4.0 mL) was treated with fuming nitric acid (8.0 mL), and the resulting orange solution was stirred at room temperature for one hour. Then it was cooled to 0 °C and neutralized with a concentrated sodium hydroxide solution until pH reached 6–7. Acetonitrile was added to the mixture until formation of a precipitate ceased. The solid was removed by centrifugation and extracted with acetonitrile (2 × 10 mL). The acetonitrile of the combined solvent layers was removed by distillation, the resulting water layer was treated with NH_4PF_6, and the precipitate was isolated by centrifugation (4 °C, 4000 rpm, 10 min). The solid was washed twice with water to remove the excess amount of salt. After drying under vacuum, silicon complex **130** was obtained as a yellow solid (430 mg, 491 µmol, 84 %). If necessary, the product can be further purified by flash column chromatography (MeCN → MeCN/H_2O/satd. aq. KNO_3 50:3:1 → 50:6:2). – **$C_{30}H_{18}F_{12}N_6O_6P_2Si$** (M = 876.52 g mol^{-1}). – ^{1}**H-NMR** (300 MHz,

CD_3CN): δ = 9.45–9.41 (m, 4H, H_{phen}), 9.13 (dd, ^3J = 8.3 Hz, ^4J = 0.8 Hz, 2H, H_{phen}), 8.63 (d, ^3J = 9.1 Hz, 2H, H_{phen}), 8.56–8.49 (m, 4H, H_{phen}), 7.95 (dd, ^3J = 8.3, 5.6 Hz, 2H, H_{phen}), 7.75 (dd, ^3J = 5.6 Hz, ^4J = 0.9 Hz, 2H, H_{phen}), 7.35 (s, 2H, H_{cat}) ppm. – **^{13}C-NMR** (75.5 MHz, CD_3CN): δ = 151.3, 150.0, 148.0, 147.5, 147.1, 138.9, 135.6, 134.6, 131.5, 131.0, 130.1, 129.8, 129.5, 129.0, 111.4 ppm. – **^{29}Si-NMR** (79.5 MHz, CD_3CN): δ = −149.4 ppm. – **FT-IR** (Film) $\tilde{\nu}$ = 3656, 3116, 1626, 1587, 1531, 1497, 1439, 1419, 1375, 1341, 1285, 1233, 1206, 1159, 1119, 1025, 890, 837, 780, 760, 739, 717, 659, 558, 529, 510, 490, 421 cm^{-1}. – **HRMS** (ESI+): calc. for $C_{30}H_{18}N_6O_6SiPF_6$ $[M-PF_6]^+$: 731.0693 u, found: 731.0690 u.

(4,5-Dinitrobenzene-1,2-diolato)bis(3,4,7,8-tetramethyl-1,10-phenanthroline)silicon(IV)-bis(hexafluorophosphate) (131)

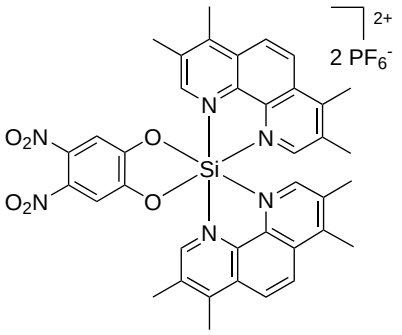

At 0 °C, complex **89** (24.0 mg, 26.7 µmol) was treated with an ice-cold mixture of glacial acetic acid (0.5 mL) and fuming nitric acid (1.0 mL). The yellow solution was stirred at 0 °C for three hours, whereupon the temperature increased slowly to 10 °C. The mixture was then cooled to 0 °C and neutralized with a concentrated potassium hydroxide solution (20 %) until pH reached 6–7. The solvent was removed under vacuum, and the residue was subjected to flash column chromatography (MeCN → MeCN/H_2O/satd. aq. KNO_3 50:3:1), whereupon the slightly yellow band eluting under salt conditions was collected. The product fractions were concentrated, and the residue was dissolved in acetonitrile/water 1:1. Then NH_4PF_6 was added, the acetonitrile was removed, and the resulting precipitate was isolated by centrifugation (4000 rpm, 4 °C, 5 min) and washed twice with water to remove the excess amount of salt. The solid was dissolved in acetonitrile, and the gained solution was filtered through cotton before it was concentrated. After drying under vacuum, complex **131** was obtained as a light yellow solid (18.0 mg, 18.2 µmol, 68 %). – **$C_{38}H_{34}F_{12}N_6O_6P_2Si$** (M = 988.74 g mol^{-1}). – **^{1}H-NMR** (300 MHz, CD_3CN): δ = 9.00 (s, 2H, H_{Me_4phen}), 8.66 (d, ^3J = 9.6 Hz, 2H, H_{Me_4phen}), 8.58 (d, ^3J = 9.6 Hz, 2H, H_{Me_4phen}), 7.32 (s, 2H, H_{Me_4phen}), 7.29 (s, 2H, H_{cat}), 3.05 (s, 6H, H_{Methyl}), 2.85 (s, 6H, H_{Methyl}), 2.72 (s, 6H, H_{Methyl}), 2.29 (s, 6H, H_{Methyl}) ppm. – **^{13}C-NMR** (75.5 MHz, CD_3CN): δ = 158.4, 157.5, 151.6, 148.7, 146.6, 139.5, 138.8, 138.5, 134.4, 133.4, 129.8, 129.3, 126.0, 126.0, 111.2, 18.9, 18.3, 16.8, 16.5 ppm. – **^{29}Si-NMR** (99.4 MHz, CD_3CN): δ = −151.2 ppm. – **FT-IR** (Film) $\tilde{\nu}$ = 3666, 3116, 1623, 1540, 1497, 1440, 1376, 1339, 1284, 1226, 1208, 1182, 1078, 1027, 915, 836, 780, 768, 732, 649, 597, 558, 529, 462, 425 cm^{-1}. – **HRMS** (ESI+): calc. for $C_{38}H_{34}F_6N_6O_6PSi$ $[M-PF_6]^+$: 843.1945 u, found: 843.1957 u.

(5-Methyl-4-nitrobenzene-1,2-diolato)bis(1,10-phenanthroline)silicon(IV)-bis(hexafluorophosphate) (132)

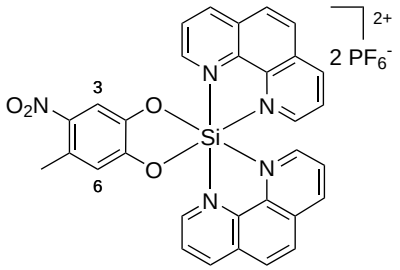

A suspension of (4-methylbenzene-1,2-diolato)bis(1,10-phenanthroline)silicon(IV)-bis(hexafluorophosphate) (**90**, 24.0 mg, 30.0 µmol) in glacial acetic acid (0.3 mL) was treated with nitric acid (65 %, 0.6 mL), and the resulting yellow solution was stirred at room temperature for two hours. The reaction mixture was then cooled to 0 °C and neutralized with a concentrated sodium hydroxide solution until pH reached 6–7. A few drops acetonitrile were added to dissolve everything. Then NH_4PF_6 was added, the obtained precipitate was isolated by centrifugation (4 °C, 4000 rpm, 10 min) and washed twice with water to remove the excess amount of salt. The solid was dissolved in acetonitrile, and the gained solution was filtered through cotton before it was concentrated. After drying under vacuum, silicon complex **132** was obtained as a yellow solid (22.4 mg, 26.5 µmol, 88 %). If necessary, the product could be purified by flash column chromatography (MeCN → MeCN/H_2O/satd. aq. KNO_3 50:3:1 → 50:6:2). – **$C_{31}H_{21}F_{12}N_5O_4P_2Si$** ($M = 845.55\,g\,mol^{-1}$). – **^{1}H-NMR** (300 MHz, CD_3CN): $\delta = 9.46$ (dd, $^3J = 5.4$ Hz, $^4J = 1.0$ Hz, 1H, H_{phen}), 9.43–9.37 (m, 3H, H_{phen}), 9.14–9.07 (m, 2H, H_{phen}), 8.61 (d, $^3J = 9.1$ Hz, 2H, H_{phen}), 8.56–8.46 (m, 4H, H_{phen}), 7.93 (dd, $^3J = 8.3$, 5.6 Hz, 2H, H_{phen}), 7.77–7.70 (m, 2H, H_{phen}), 7.42 (s, 1H, H-3), 6.76 (s, 1H, H-6), 2.46 (s, 3H, H_{Methyl}) ppm. – **^{13}C-NMR** (126 MHz, CD_3CN): δ = 152.0, 149.7, 149.6, 147.78, 147.75, 147.33, 147.30, 146.74, 146.72, 145.5, 143.73, 143.72, 135.68, 135.66, 134.8, 131.51, 131.48, 131.03, 131.02, 130.6, 129.84, 129.81, 129.77, 129.41, 129.39, 128.9, 117.6, 111.2, 20.9 ppm. – **^{29}Si-NMR** (99.4 MHz, CD_3CN): $\delta = -150.7$ ppm. – **FT-IR** (Film) $\tilde{\nu}$ = 3663, 3111, 1626, 1588, 1530, 1491, 1438, 1326, 1267, 1233, 1202, 1153, 1117, 1042, 887, 835, 761, 715, 583, 557, 525, 509, 487, 426, 400, 388 cm^{-1}. – **HRMS** (ESI+): calc. for $C_{31}H_{21}F_6N_5O_4PSi$ $[M-PF_6]^+$: 700.0999 u, found: 700.1019 u.

(4-Methyl-3,5-dinitrobenzene-1,2-diolato)bis(1,10-phenanthroline)silicon(IV)-bis(hexafluorophosphate) (133)

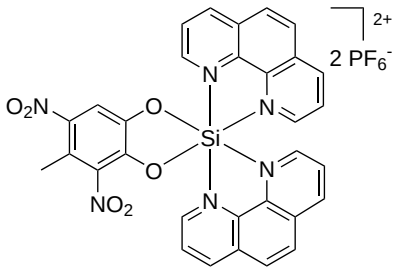

A suspension of (4-methylbenzene-1,2-diolato)bis(1,10-phenanthroline)silicon(IV)-bis(hexafluorophosphate) (**90**, 50.0 mg, 62.5 µmol) in glacial acetic acid (0.5 mL) was treated with fuming nitric acid (1.0 mL), and the resulting yellow solution was stirred at room temperature for two hours. The reaction mixture was then cooled to 0 °C and neutralized with a concentrated sodium hydroxide solution until pH reached 6–7. NH_4PF_6 was added, and the obtained precipitate was isolated by centrifugation (4 °C, 4000 rpm, 10 min). The solid was washed twice with water before it was subjected to flash column chromatography (MeCN → MeCN/H_2O/satd. aq. KNO_3 50:3:1 → 50:6:2). The light yellow band eluting under salt conditions was collected, and the product fractions were concentrated. The residue was dissolved in water, and NH_4PF_6 was added. The resulting precipitate was isolated by centrifugation (4000 rpm, 4 °C, 5 min) and washed twice with water to remove the excess amount of salt. The solid was dissolved in acetonitrile, and the gained

solution was filtered through cotton before it was concentrated. After drying under vacuum, silicon complex **133** was obtained as a light yellow solid (28.2 mg, 31.7 µmol, 51 %). – **$C_{31}H_{20}F_{12}N_6O_6P_2Si$** (M = 890.55 g mol^{-1}). – **^{1}H-NMR** (300 MHz, CD_3CN): δ = 9.49–9.38 (m, 4H, H_{phen}), 9.14 (ddd, J = 8.3, 3.5, 1.1 Hz, 2H, H_{phen}), 8.66–8.50 (m, 6H, H_{phen}), 7.96 (ddd, J = 8.3, 5.6, 1.1 Hz, 2H, H_{phen}), 7.74 (ddd, J = 6.8, 5.6, 1.1 Hz, 2H, H_{phen}), 6.96 (d, ^3J = 0.5 Hz, 1H, H_{cat}), 2.29 (d, ^3J = 0.5 Hz, 3H, H_{Methyl}) ppm. – **^{13}C-NMR** (75.5 MHz, CD_3CN): δ = 151.1, 150.1, 149.8, 148.1, 148.0, 147.62, 147.58, 147.1, 141.3, 138.1, 135.62, 135.60, 134.7, 131.6, 131.5, 131.1, 131.0, 130.5, 130.3, 130.1, 129.94, 129.89, 129.8, 129.51, 129.46, 129.2, 129.10, 129.07, 127.8, 119.4, 18.2 ppm. – **^{29}Si-NMR** (59.7 MHz, CD_3CN): δ = −150.0 ppm. – **FT-IR** (Film) $\tilde{\nu}$ = 3114, 1626, 1586, 1530, 1480, 1438, 1419, 1374, 1342, 1267, 1233, 1160, 1118, 1071, 1045, 976, 934, 888, 825, 790, 777, 759, 738, 717, 679, 663, 623, 596, 557, 528, 510, 490, 466, 448, 425, 406 cm^{-1}. – **HRMS** (ESI+): calc. for $C_{31}H_{20}F_6N_6O_6PSi$ $[M-PF_6]^+$: 745.0850 u, found: 745.0870 u.

(4,5-Diaminobenzene-1,2-diolato-κ^2O)bis(1,10-phenanthroline)silicon(IV)-bis(hexafluorophosphate) (140)

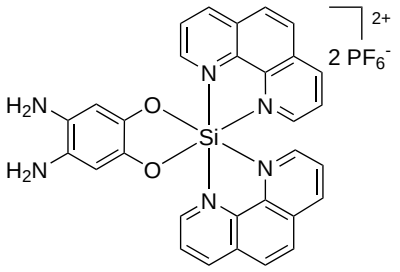

A suspension of (4,5-dinitrobenzene-1,2-diolato)bis(1,10-phenanthroline)silicon(IV)-bis(hexafluorophosphate) (**130**, 25.0 mg, 28.5 µmol) in half concentrated hydrochloric acid (6 M, 2.0 mL) was heated to 80 °C. Tin powder (28.7 mg, 242 µmol) was added, and the yellow mixture was stirred at 110 °C for three hours. Then it was cooled to 0 °C and neutralized with a sodium hydroxide solution (6 M) until pH reached 6–7. The obtained solid was isolated by centrifugation (2000 rpm, 20 °C, 5 min) and extracted with water (3 × 2 mL). The combined supernatants were treated with NH_4PF_6, the formed precipitate was isolated by centrifugation (4000 rpm, 4 °C, 5 min) and washed twice with water to remove the excess amount of salt. After drying under vacuum, crude silicon complex **140** was obtained as a brown solid (17.7 mg, ~76 % of a contaminated product). As the product decomposes during silica gel flash column chromatography or even when stored at room temperature under nitrogen, it was used for the next step without further purification. – **$C_{30}H_{22}F_{12}N_6O_2P_2Si$** (M = 816.56 g mol^{-1}). – **^{1}H-NMR** (300 MHz, CD_3CN): δ = 9.44 (dd, ^3J = 5.3 Hz, ^4J = 0.9 Hz, 2H, H_{phen}), 9.36 (dd, ^3J = 8.4 Hz, ^4J = 0.9 Hz, 2H, H_{phen}), 9.05 (dd, ^3J = 8.3 Hz, ^4J = 0.8 Hz, 2H, H_{phen}), 8.58 (d, ^3J = 9.2 Hz, 2H, H_{phen}), 8.52–8.46 (m, 4H, H_{phen}), 7.88 (dd, ^3J = 8.3, 5.6 Hz, 2H, H_{phen}), 7.68 (dd, ^3J = 5.6 Hz, ^4J = 0.9 Hz, 2H, H_{phen}), 6.24 (s, 2H, H_{cat}) ppm.

Bis(2,2'-bipyridine)(2,7-di-*tert*-butylphenanthro[4,5-*abc*]phenazine-11,12-diolato-κ^2O) silicon(IV)-bis(hexafluorophosphate) (143)

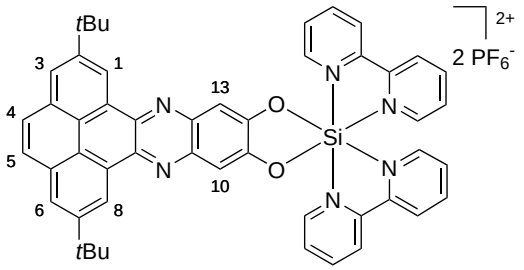

Method 1: Using method C, silicon complex **129** (45.0 mg, 54.3 µmol), tin powder (52.0 mg, 438 µmol) and a mixture of 2,7-di-*tert*-butylpyrene-4,5-dione and 2,7-di-*tert*-butylpyrene-4,5,9,10-tetraone (**277**/**278** 3:1, 20.0 mg, 56.8 µmol) were reacted to yield complex **143** as an orange solid (8.1 mg, 7.52 µmol, 14 % over two steps). In addition, dione complex **145** was obtained as an orange solid (9.4 mg, 8.49 µmol, 16 % over two steps).

Method 2 Using method C, silicon complex **129** (100 mg, 121 µmol), tin powder (116 mg, 977 µmol), half concentrated hydrochloric acid (6 M, 3.0 mL) and a mixture of 2,7-di-*tert*-butylpyrene-4,5-dione and 2,7-di-*tert*-butylpyrene-4,5,9,10-tetraone (**277**/**278** 3:1, 50 mg, 145 µmol) were reacted to yield complex **143** as an orange solid (11.2 mg, 10.4 µmol, 9 % over two steps), dione complex **145** as an orange solid (19.0 mg, 17.2 µmol, 14 % over two steps) and the dinuclear silicon(IV) complex **147** as a yellow solid (5.2 mg, 2.83 µmol, 2 % over two steps). – $\mathbf{C_{50}H_{42}F_{12}N_6O_2P_2Si}$ (M = 1076.94 g mol^{-1}). – ^{1}**H-NMR** (300 MHz, CD_3CN, 13 mM): δ = 9.53 (d, ^4J = 2.0 Hz, 2H, H-1/3, H-6/8), 9.29–9.20 (m, 2H, H_{bpy}), 9.01–8.95 (m, 2H, H_{bpy}), 8.94–8.88 (m, 2H, H_{bpy}), 8.80 (td, ^3J = 7.9 Hz, ^4J = 1.4 Hz, 2H, H_{bpy}), 8.68 (td, ^3J = 7.9 Hz, ^4J = 1.3 Hz, 2H, H_{bpy}), 8.39 (d, ^4J = 2.0 Hz, 2H, H-1/3, H-6/8), 8.16 (ddd, ^3J = 7.5, 5.9 Hz, ^4J = 1.1 Hz, 2H, H_{bpy}), 8.08 (s, 2H, H-4, H-5), 7.89 (ddd, ^3J = 7.6, 6.0 Hz, ^4J = 1.2 Hz, 2H, H_{bpy}), 7.76–7.66 (m, 2H, H_{bpy}), 7.60 (s, 2H, H-10, H-13), 1.61 (s, 18H, H_{tBu}) ppm. – ^{13}**C-NMR** (75.5 MHz, CD_3CN, 13 mM): δ = 151.4, 150.8, 148.9, 148.5, 146.5, 145.0, 144.3, 142.2, 141.7, 132.3, 131.5, 130.1, 128.3, 126.4, 126.3, 126.1, 124.4, 121.2, 110.4, 36.2, 32.0 ppm. – ^{29}**Si-NMR** (79.5 MHz, CD_3CN): δ = −148.1 ppm. – **FT-IR** (Film) $\tilde{\nu}$ = 3658, 3107, 2960, 1675, 1617, 1574, 1509, 1479, 1456, 1366, 1325, 1264, 1219, 1194, 1120, 1073, 1045, 1027, 906, 840, 764, 739, 686, 580, 558, 523, 488, 464, 430, 415, 393 cm^{-1}. – **HRMS** (ESI+): calcd. for $C_{50}H_{42}N_6O_2Si$ $[M-2PF_6]^2$+: 393.1564 u, found: 393.1578 u.

Bis(2,2'-bipyridine)(2,7-di-*tert*-butylphenanthro[4,5-*abc*]phenazine-11,12-diolato-κ^2O) silicon(IV)-dichloride (143a)

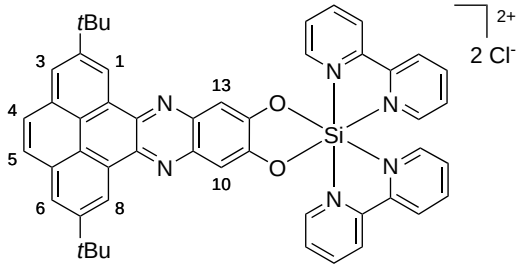

Using method A and silicon complex **143** (8.1 mg, 7.52 µmol), complex **143a** was obtained as an orange solid (5.9 mg, 6.88 µmol, 91 %). – $\mathbf{C_{50}H_{42}Cl_2N_6O_2Si}$ (M = 857.91 g mol^{-1}). – ^{1}**H-NMR** (300 MHz, MeOD, 14 M): δ = 9.52 (d, ^4J = 1.9 Hz, 2H, H-1/3, H-6/8), 9.42–9.36 (m, 2H, 2H, H_{bpy}), 9.27 (d, ^3J = 8.0 Hz, 2H, 2H, H_{bpy}), 9.21 (d, ^3J = 8.1 Hz, 2H, 2H, H_{bpy}), 8.92 (td, ^3J = 7.9 Hz, ^4J = 1.3 Hz, 2H, 2H, H_{bpy}), 8.86–8.78 (m, 2H, 2H, H_{bpy}), 8.33 (d, ^4J = 2.0 Hz, 2H, H-1/3, H-6/8), 8.31–8.24 (m, 2H, 2H, H_{bpy}), 8.08–7.98 (m, 6H, 2H, H_{bpy}, H-4, H-5), 7.67 (s, 2H, H-10, H-13), 1.62 (s, 18H, 2H, H_{tBu}) ppm.

Bis(2,2'-bipyridine)(2,7-di-*tert*-butyl-4,5-dioxo-4,5-dihydrophenanthro[4,5-*abc*]phenazine-11,12-diolato-κ^2O)silicon(IV)-bis(hexafluorophosphate) (145)

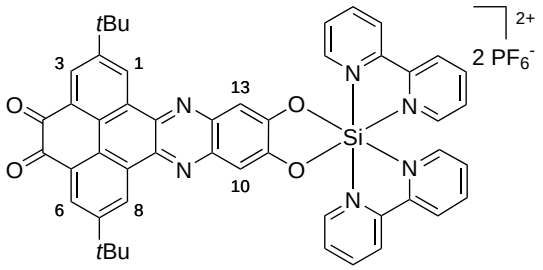

Using method C, silicon complex **129** (100 mg, 121 µmol), tin powder (116 mg, 977 µmol) and 2,7-di-*tert*-butylpyrene-4,5,9,10-tetraone (**278**, 60.0 mg, 160 µmol) were reacted to yield complex **145** as an orange solid (39.3 mg, 35.5 µmol, 29 % over two steps). In addition, the dinuclear complex **147** was obtained as a yellow solid (9.5 mg, 5.16 µmol, 4 % over two steps). – **$C_{50}H_{40}F_{12}N_6O_4P_2Si$** (M = 1106.92 g mol^{-1}). – **^{1}H-NMR** (300 MHz, CD_3CN, 11 mM): δ = 9.40 (d, ^4J = 2.2 Hz, 2H, H-1/3, H-6/8), 9.27 (d, ^3J = 5.3 Hz, 2H, H_{bpy}), 9.00 (d, ^3J = 8.1 Hz, 2H, H_{bpy}), 8.93 (d, ^3J = 8.0 Hz, 2H, H_{bpy}), 8.81 (td, ^3J = 8.0 Hz, ^4J = 1.3 Hz, 2H, H_{bpy}), 8.69 (td, ^3J = 7.9 Hz, ^4J = 1.2 Hz, 2H, H_{bpy}), 8.38 (d, ^4J = 2.2 Hz, 2H, H-1/3, H-6/8), 8.25–8.11 (m, 2H, H_{bpy}), 7.96–7.84 (m, 2H, H_{bpy}), 7.71 (d, ^3J = 5.5 Hz, 2H, H_{bpy}), 7.50 (s, 2H, H-10, H-13), 1.49 (s, 18H, $H_{t\mathrm{Bu}}$) ppm. – **^{13}C-NMR** (125 MHz, CD_3CN, 15 mM): δ = 180.8, 153.1, 152.1, 149.0, 148.6, 148.5, 146.5, 145.0, 144.3, 141.9, 139.9, 132.4, 131.6, 131.33, 131.28, 129.5, 129.1, 128.5, 126.4, 126.1, 110.2, 36.1, 31.4 ppm. – **^{29}Si-NMR** (79.5 MHz, CD_3CN): δ = −148.4 ppm. – **FT-IR** (Film) $\tilde{\nu}$ = 3651, 3107, 2965, 1676, 1618, 1575, 1538, 1510, 1479, 1455, 1368, 1325, 1273, 1250, 1199, 1120, 1073, 1046, 1027, 907, 838, 773, 738, 686, 580, 558, 522, 490, 462, 430, 404 cm^{-1}. – **HRMS** (ESI+): calcd. for $C_{50}H_{40}F_6N_6O_4PSi$ $[M-PF_6]^+$: 961.2517 u, found: 961.2538 u.

Bis(2,2'-bipyridine)(µ-2,11-di-*tert*-butylquinoxalino[2',3':9,10]phenanthro[4,5-*abc*]phenazine-6,7,15,16-tetraolato-κ^4O)disilicon(IV)-tetrakis(hexafluorophosphate) (147)

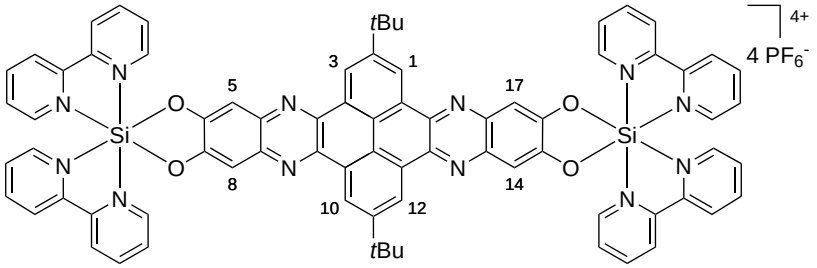

The synthesis is described above. The complex was obtained as a mixture of diastereomers (*d.r.* 1:1). – **$C_{76}H_{58}F_{24}N_{12}O_4P_4Si_2$** (M = 1839.41 g mol^{-1}). – **^{1}H-NMR** (300 MHz, CD_3CN, 6 mM): δ = 9.65 (s, 4H, H-1, H-3, H-10, H-12), 9.25 (d, ^3J = 5.7 Hz, 4H, H_{bpy}), 9.00 (d, ^3J = 8.1 Hz, 4H, H_{bpy}), 8.92 (d, ^3J = 8.0 Hz, 4H, H_{bpy}), 8.80 (td, ^3J = 7.9 Hz, ^4J = 1.3 Hz, 4H, H_{bpy}), 8.69 (td, ^3J = 8.0 Hz, ^4J = 1.2 Hz, 4H, H_{bpy}), 8.22–8.08 (m, 4H, H_{bpy}), 7.95–7.82 (m, 4H, H_{bpy}), 7.71 (d, ^3J = 5.4 Hz, 4H, H_{bpy}), 7.61 (s, 4H, H-5, H-8, H-14, H-17), 1.64 (s, 18H, $H_{t\mathrm{Bu}}$) ppm. – **^{13}C-NMR** (101 MHz, CD_3CN, 6 mM): δ = 151.8, 151.6, 149.0, 148.5, 148.5, 146.5, 145.0, 144.3, 141.9, 141.5, 132.3, 131.6, 130.7, 126.4, 126.1, 125.4, 123.7, 110.3, 36.4, 32.0 ppm. – **^{29}Si-NMR** (79.5 MHz, CD_3CN): δ = −147.8 ppm. – **FT-IR** (Film) $\tilde{\nu}$ = 3659, 2961, 1618, 1576, 1510, 1456, 1417, 1326, 1282, 1249, 1224, 1194, 1073, 1046, 912, 838, 775, 738, 686, 579, 558, 522, 463, 433, 413, 398 cm^{-1}. – **HRMS** (ESI+): calcd. for $C_{76}H_{58}F_{18}N_{12}O_4P_3Si_2$ $[M-PF_6]^+$: 1693.3162 u, found: 1693.3200 u.

Bis(2,2'-bipyridine)(phenanthro[4,5-*abc*]phenazine-11,12-diolato-κ^2O)silicon(IV)-bis(hexafluorophosphate) (149)

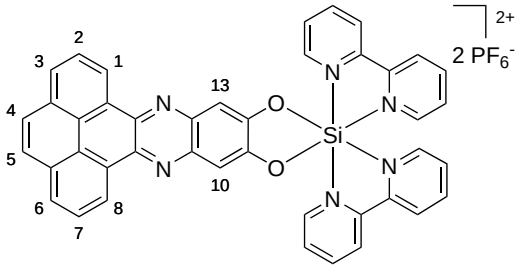

Using method C, silicon complex **129** (35.0 mg, 42.3 µmol), tin powder (44.0 mg, 371 µmol) and pyrene-4,5-dione (**276**, 15.0 mg, 64.6 µmol) were reacted to yield complex **149** as an orange solid (14.9 mg, 15.4 µmol, 37 % over two steps). – **$C_{42}H_{26}F_{12}N_6O_2P_2Si$** (M = 964.72 g mol^{-1}). – **^{1}H-NMR** (300 MHz, CD_3CN, 13 mM): δ = 9.37 (dd, ^3J = 7.7 Hz, ^4J = 1.1 Hz, 2H, H-1/3, H-6/8), 9.29–9.20 (m, 2H, H_{bpy}), 9.01–8.94 (m, 2H, H_{bpy}), 8.94–8.86 (m, 2H, H_{bpy}), 8.80 (td, ^3J = 7.9 Hz, ^4J = 1.4 Hz, 2H, H_{bpy}), 8.68 (td, ^3J = 7.9 Hz, ^4J = 1.3 Hz, 2H, H_{bpy}), 8.31 (dd, ^3J = 7.8 Hz, ^2J = 1.2 Hz, 2H, H-1/3, H-6/8), 8.17 (ddd, ^3J = 7.6, 5.9 Hz, ^4J = 1.1 Hz, 2H, H_{bpy}), 8.12–8.05 (m, 4H, H-2, H-4, H-5, H-7), 7.89 (ddd, ^3J = 7.6, 6.0 Hz, ^4J = 1.2 Hz, 2H, H_{bpy}), 7.73–7.63 (m, 2H, H_{bpy}), 7.55 (s, 2H, H-10, H-13) ppm. – **^{13}C-NMR** (75.5 MHz, CD_3CN, 13 mM): δ = 151.5, 148.9, 148.5, 146.4, 144.9, 144.3, 141.9, 141.7, 132.42, 132.36, 131.6, 130.6, 129.6, 128.2, 128.0, 126.4, 126.2, 126.1, 123.7, 110.4 ppm. – **^{29}Si-NMR** (59.7 MHz, CD_3CN): δ = −149.7 ppm. – **FT-IR** (Film) $\tilde{\nu}$ = 3658, 3110, 2929, 1618, 1573, 1509, 1478, 1455, 1416, 1353, 1325, 1300, 1250, 1217, 1196, 1172, 1119, 1073, 1058, 1045, 1028, 923, 835, 796, 774, 762, 739, 722, 691, 682, 657, 615, 580, 557, 523, 501, 490, 466, 432 cm^{-1}. – **HRMS** (ESI+): calcd. for $C_{42}H_{26}F_6N_6O_2PSi$ [M−PF_6]$^+$: 819.1523 u, found: 819.1535 u.

Bis(2,2'-bipyridine)(phenanthro[4,5-*abc*]phenazine-11,12-diolato-κ^2O)silicon(IV)-dichloride (149a)

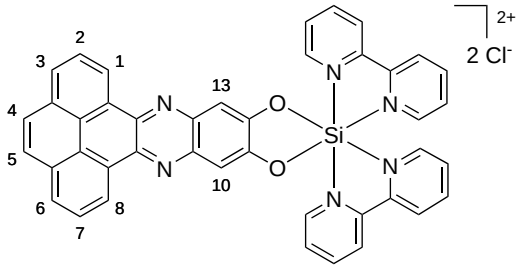

Using method C, silicon complex **149** (44.8 mg, 54.1 µmol), tin powder (52.0 mg, 438 µmol) and pyrene-4,5-dione (**276**, 20.0 mg, 86.1 µmol) were reacted. After the column chromatography, half of the fractions were converted into the hexafluorophosphate salt **149** (6.1 mg, 6.32 µmol, 12 % over two steps) and the other half into the chloride salt using method A starting with the nitrate salt. **149a** was obtained as an orange solid (4.6 mg, 6.17 µmol, 11 % over two steps). – **$C_{42}H_{26}Cl_2N_6O_2Si$** (M = 745.70 g mol^{-1}). – **^{1}H-NMR** (300 MHz, MeOD, 12 mM): δ = 9.40–9.35 (m, 2H, H_{bpy}), 9.31 (dd, ^3J = 7.8 Hz, ^4J = 1.1 Hz, 2H, H-1/3, H-6/8), 9.29–9.24 (m, 2H, H_{bpy}), 9.21–9.16 (m, 2H, H_{bpy}), 8.91 (td, ^3J = 7.9 Hz, ^4J = 1.4 Hz, 2H, H_{bpy}), 8.80 (ddd, ^3J = 8.1, 7.4 Hz, ^4J = 1.8 Hz, 2H, H_{bpy}), 8.31–8.25 (m, 2H, H_{bpy}), 8.23 (dd, ^3J = 7.8 Hz, ^4J = 1.1 Hz, 2H, H-1/3, H-6/8), 8.06–7.95 (m, 8H, H_{bpy}, H-2, H-4, H-5, H-7), 7.59 (s, 2H, H-10, H-13) ppm. – **^{13}C-NMR** (75.5 MHz, MeOD, 12 mM): δ = 151.7, 149.2, 148.6, 148.5, 146.6, 145.7, 145.3, 142.2, 141.8, 132.8, 132.2, 131.6, 130.5, 129.7, 128.2, 127.7, 126.6, 126.5, 126.3, 124.0, 110.5 ppm. – **^{29}Si-NMR** (59.7 MHz, MeOD): δ = −149.6 ppm. – **FT-IR** (Film) $\tilde{\nu}$ = 3396, 3046, 2924, 2854, 1618, 1571, 1546, 1508, 1455, 1352, 1300, 1247, 1197, 1116, 1076, 1047, 981, 923, 870, 842, 736, 685, 618, 581, 555, 523, 493, 438 cm^{-1}. – **HRMS** (ESI+): calcd. for $C_{42}H_{26}ClN_6O_2Si$ [M−Cl]$^+$: 709.1570 u, found: 709.1596 u.

Bis(1,10-phenanthroline)(phenanthro[4,5-*abc*]phenazine-11,12-diolato-κ^2O)silicon(IV)-bis(hexafluorophosphate) (150)

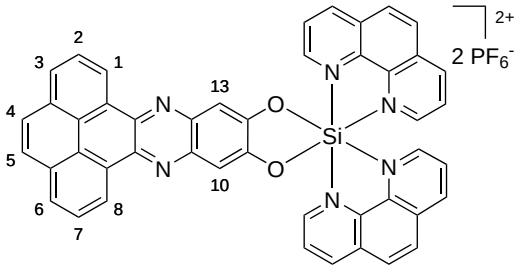

Using method C, silicon complex **130** (36.0 mg, 41.1 µmol), tin powder (42.0 mg, 354 µmol) and pyrene-4,5-dione (**276**, 15.0 mg, 64.6 µmol) were reacted to yield complex **150** as an orange solid (15.1 mg, 14.9 µmol, 36 % over two steps). – **$C_{46}H_{26}F_{12}N_6O_2P_2Si$** (M = 1012.77 g mol^{-1}). – **^{1}H-NMR** (300 MHz, CD_3CN, 21 mM): δ = 9.63 (dd, ^3J = 5.4 Hz, ^4J = 0.9 Hz, 2H, H_{phen}), 9.42–9.35 (m, 4H, H_{phen}, H-1/3, H-6/8), 9.16–9.11 (m, 2H, H_{phen}), 8.62 (d, ^3J = 9.1 Hz, 2H, H_{phen}), 8.54 (d, ^3J = 9.1 Hz, 2H, H_{phen}), 8.47 (dd, ^3J = 8.3, 5.5 Hz, 2H, H_{phen}), 8.32 (dd, ^3J = 7.8 Hz, ^4J = 1.0 Hz, 2H, H-1/3, H-6/8), 8.12–8.05 (m, 4H, H-2, H-4, H-5, H-7), 7.97 (dd, ^3J = 8.3, 5.6 Hz, 2H, H_{phen}), 7.82 (dd, ^3J = 5.5 Hz, ^4J = 0.8 Hz, 2H, H_{phen}), 7.58 (s, 2H, H-10, H-13) ppm. – **^{13}C-NMR** (75.5 MHz, CD_3CN, 21 mM): δ = 151.9, 149.7, 147.8, 147.3, 146.8, 142.0, 141.7, 135.7, 134.9, 132.4, 131.5, 131.0, 130.6, 129.9, 129.8, 129.5, 129.4, 129.0, 128.3, 127.9, 126.3, 123.7, 110.3 ppm. – **^{29}Si-NMR** (99.4 MHz, CD_3CN): δ = −149.8 ppm. – **FT-IR** (Film) $\tilde{\nu}$ = 3651, 3110, 2930, 1722, 1625, 1586, 1531, 1457, 1439, 1416, 1352, 1300, 1195, 1118, 924, 838, 795, 760, 740, 719, 619, 581, 558, 527, 486, 466, 438, 411, 399 cm^{-1}. – **HRMS** (ESI+): calcd. for $C_{46}H_{26}F_6N_6O_2PSi$ [M−PF_6]$^+$: 867.1523 u, found: 867.1527 u.

(4,5-Dioxo-4,5-dihydrophenanthro[4,5-*abc*]phenazine-11,12-diolato-κ^2O)bis(1,10-phenanthroline)silicon(IV)-bis(hexafluorophosphate) (151)

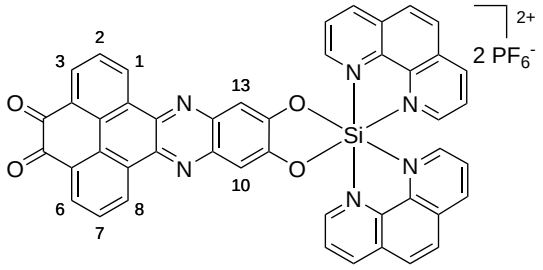

Using method C, silicon complex **130** (31.0 mg, 35.4 µmol), tin powder (36.0 mg, 303 µmol) and pyrene-4,5,9,10-tetraone (**275**, 12.3 mg, 46.9 µmol) were reacted to yield complex **151** as a yellow solid (10.1 mg, 9.69 µmol, 27 % over two steps). – **$C_{46}H_{24}F_{12}N_6O_4P_2Si$** (M = 1042.75 g mol^{-1}). – **^{1}H-NMR** (300 MHz, CD_3CN, 4 mM): δ = 9.76–9.67 (m, 2H, H_{phen}), 9.46–9.36 (m, 2H, H_{phen}), 9.26–9.09 (m, 4H, H_{phen}, H-1/3, H-6/8), 8.65 (d, ^3J = 9.2 Hz, 2H, H_{phen}), 8.58 (d, ^3J = 9.2 Hz, 2H, H_{phen}), 8.52 (dd, ^3J = 8.3, 5.5 Hz, 2H, H_{phen}), 8.37–8.22 (m, 2H, H-1/3, H-6/8), 8.00 (dd, ^3J = 8.3, 5.6 Hz, 2H, H_{phen}), 7.90–7.76 (m, 4H, H_{phen}, H-2, H-7), 7.42 (s, 2H, H-10, H-13) ppm. – **^{29}Si-NMR** (99.4 MHz, CD_3CN): δ = −149.9 ppm. – **FT-IR** (Film) $\tilde{\nu}$ = 3649, 1676, 1585, 1555, 1530, 1452, 1329, 1287, 1199, 1118, 829, 740, 581, 557, 483, 404, 383 cm^{-1}. – **HRMS** (ESI+): calcd. for $C_{46}H_{24}F_6N_6O_4PSi$ [M−PF_6]$^+$: 897.1265 u, found: 897.1270 u.

Bis(2,2'-bipyridine)(2,9-di-*tert*-butylpyrazino[2',3':9,10]phenanthro[4,5-*abc*]phenazine-13,14-diolato-κ^2O)silicon(IV)-bis(hexafluorophosphate) (152)

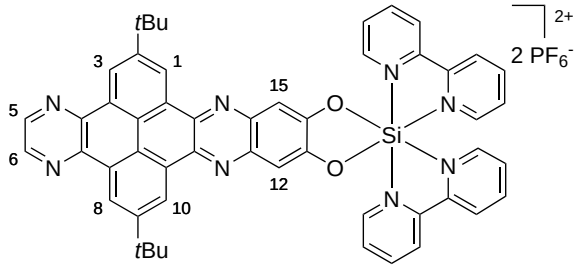

Using method D, silicon complex **145** (14.0 mg, 12.7 µmol) and ethylenediamine (10.0 µL, 150 µmol) were reacted to yield complex **152** as a dark yellow solid (13.2 mg, 11.7 µmol, 92 %). – **$C_{52}H_{42}F_{12}N_8O_2P_2Si$** (M = 1128.98 g mol^{-1}). – ^{1}**H-NMR** (300 MHz, CD_3CN, 21 mM): δ = 9.44 (d, ^4J = 2.1 Hz, 2H, H-1/3, H-8/10), 9.31–9.25 (m, 4H, H_{bpy}, H-1/3, H-8/10), 9.04–8.99 (m, 2H, H_{bpy}), 8.98 (s, 2H, H-5, H-6), 8.97–8.92 (m, 2H, H_{bpy}), 8.82 (td, ^3J = 7.9 Hz, ^4J = 1.4 Hz, 2H, H_{bpy}), 8.71 (td, ^3J = 7.9 Hz, ^4J = 1.3 Hz, 2H, H_{bpy}), 8.20 (ddd, ^3J = 7.5, 5.9 Hz, ^4J = 1.1 Hz, 2H, H_{bpy}), 7.91 (ddd, ^3J = 7.6, 6.0 Hz, ^4J = 1.2 Hz, 2H, H_{bpy}), 7.80–7.68 (m, 2H, H_{bpy}), 7.57 (s, 2H, H-12, H-15), 1.59 (s, 18H, H_{tBu}) ppm. – ^{13}**C-NMR** (126 MHz, CD_3CN, 21 mM): δ = 151.5, 151.3, 149.0, 148.52, 148.45, 146.5, 145.2, 145.0, 144.4, 142.5, 141.8, 141.2, 132.3, 131.6, 130.2, 129.8, 126.4, 126.1, 125.0, 123.7, 123.0, 110.4, 36.4, 32.0 ppm. – ^{29}**Si-NMR** (99.4 MHz, CD_3CN): δ = −149.7 ppm. – **FT-IR** (Film) $\tilde{\nu}$ = 3647, 3100, 2964, 1981, 1618, 1575, 1509, 1478, 1456, 1419, 1366, 1344, 1326, 1274, 1250, 1220, 1200, 1146, 1073, 1046, 1028, 908, 879, 840, 771, 738, 688, 580, 558, 523, 502, 487, 472, 431, 421, 402 cm^{-1}. – **HRMS** (ESI+): calcd. for $C_{52}H_{42}F_6N_8O_2PSi$ [M−PF_6]$^+$: 983.2836 u, found: 983.2852 u.

Bis(2,2'-bipyridine)(2,11-di-*tert*-butylquinoxalino[2',3':9,10]phenanthro[4,5-*abc*]phenazine-6,7-diolato-κ^2O)silicon(IV)-bis(hexafluorophosphate) (154)

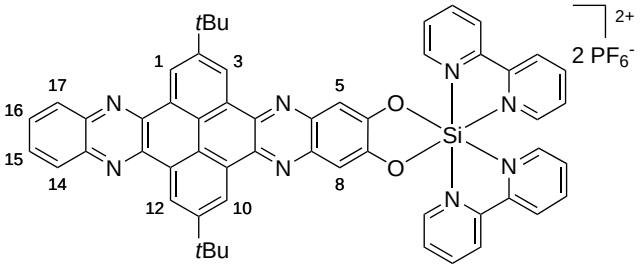

Using method D, silicon complex **145** (14.0 mg, 12.7 µmol) and *ortho*-phenylenediamine (14.3 mg, 132 µmol) were reacted to yield complex **154** as a yellow solid (9.1 mg, 7.72 µmol, 61 %). – **$C_{56}H_{44}F_{12}N_8O_2P_2Si$** (M = 1179.04 g mol^{-1}). – ^{1}**H-NMR** (500 MHz, CD_3CN, 13 mM): δ = 9.36 (d, ^4J = 2.1 Hz, 2H, H-1/3, H-10/12), 9.34 (d, ^4J = 2.1 Hz, 2H, H-1/3, H-10/12), 9.30 (dd, ^3J = 6.0 Hz, ^4J = 0.8 Hz, 2H, H_{bpy}), 9.02 (d, ^3J = 8.1 Hz, 2H, H_{bpy}), 8.95 (d, ^3J = 8.1 Hz, 2H, H_{bpy}), 8.83 (td, ^3J = 8.0 Hz, ^4J = 1.4 Hz, 2H, H_{bpy}), 8.72 (td, ^3J = 8.0 Hz, ^4J = 1.3 Hz, 2H, H_{bpy}), 8.26–8.19 (m, 4H, H_{bpy}, H-14, H-17), 7.92 (ddd, ^3J = 7.7, 5.9 Hz, ^4J = 1.2 Hz, 2H, H_{bpy}), 7.89–7.85 (m, 2H, H-15, H-16), 7.76 (d, ^3J = 5.5 Hz, 2H, H_{bpy}), 7.55 (s, 2H, H-5, H-8), 1.62 (s, 18H, H_{tBu}) ppm. – ^{13}**C-NMR** (126 MHz, CD_3CN, 13 mM): δ = 151.43, 151.40, 149.0, 148.54, 148.45, 146.5, 145.0, 144.4, 143.5, 142.9, 141.7, 141.0, 132.3, 131.6, 131.1, 130.3, 130.2, 130.0, 126.4, 126.2, 125.5, 124.4, 124.0, 110.5, 36.4, 32.0 ppm. – ^{29}**Si-NMR** (99.4 MHz, CD_3CN): δ = −149.0 ppm. – **FT-IR** (Film) $\tilde{\nu}$ = 3669, 3109, 2961, 1617, 1575, 1509, 1478, 1456, 1422, 1366, 1325, 1278, 1249, 1197, 1120, 1073, 1046, 1027, 908, 892, 840, 765, 739, 686, 662, 580, 558, 523, 503, 488, 468, 423 cm^{-1}. – **HRMS** (ESI+): calcd. for $C_{56}H_{44}F_6N_8O_2PSi$ [M−PF_6]$^+$: 1033.2993 u, found: 1033.3012 u.

Bis(2,2'-bipyridine)(2,11-di-*tert*-butylbenzo[*g*]quinoxalino[2',3':9,10]phenanthro[4,5-*abc*]phenazine-6,7-diolato-κ^2O)silicon(IV)-bis(hexafluorophosphate) (156)

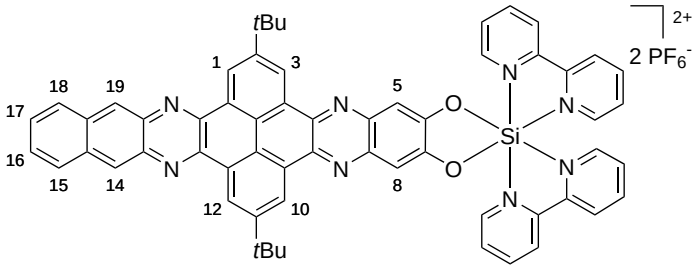

Using method D, silicon complex **145** (11.5 mg, 10.4 µmol) and 2,3-diaminonaphthalene (10.0 mg, 63.2 µmol) were reacted to yield complex **156** as a yellow solid (9.2 mg, 7.49 µmol, 72 %). – **$C_{60}H_{46}F_{12}N_8O_2P_2Si$** (M = 1229.10 g mol^{-1}). – **^{1}H-NMR** (300 MHz, CD_3CN, 13 mM): δ = 9.41–9.30 (m, 6H, H_{bpy}, H-1, H-3, H-10, H-12), 9.02 (d, ^3J = 8.0 Hz, 2H, H_{bpy}), 8.94 (d, ^3J = 8.0 Hz, 2H, H_{bpy}), 8.85 (t, ^3J = 7.7 Hz, 2H, H_{bpy}), 8.70 (t, ^3J = 7.8 Hz, 2H, H_{bpy}), 8.26 (t, ^3J = 6.8 Hz, 2H, H_{bpy}), 7.98–7.85 (m, 4H, H_{bpy}, H-14, H-19), 7.78 (d, ^3J = 5.7 Hz, 2H, H_{bpy}), 7.53–7.41 (m, 4H, H-5, H-8, H-15, H-18), 6.74–6.64 (m, 2H, H-16, H-17), 1.81 (s, 18H, H_{tBu}) ppm. – **^{13}C-NMR** (126 MHz, CD_3CN, 13 mM): δ = 151.5, 151.3, 149.1, 148.6, 148.4, 146.5, 145.0, 144.5, 144.2, 141.6, 140.8, 138.6, 134.1, 132.3, 131.6, 130.1, 129.8, 128.8, 127.2, 126.5, 126.4, 126.2, 125.6, 124.62, 124.56, 110.4, 36.5, 32.3 ppm. – **^{29}Si-NMR** (79.5 MHz, CD_3CN): δ = −147.9 ppm. – **FT-IR** (Film) $\tilde{\nu}$ = 2955, 2868, 1616, 1573, 1508, 1478, 1455, 1421, 1366, 1325, 1279, 1246, 1198, 1119, 1072, 1045, 1026, 910, 841, 736, 686, 672, 580, 558, 522, 503, 487, 474, 466, 446, 434, 418, 403, 392 cm^{-1}. – **HRMS** (ESI+): calcd. for $C_{60}H_{46}F_6N_8O_2PSi$ [M−PF_6]$^+$: 1083.3149 u, found: 1083.3169 u.

Bis(1,10-phenanthroline)(2-(pyridin-4-yl)-1*H*-benzo[*d*]imidazole-5,6-diolato-κ^2O)silicon(IV)-bis(hexafluorophosphate) (157)

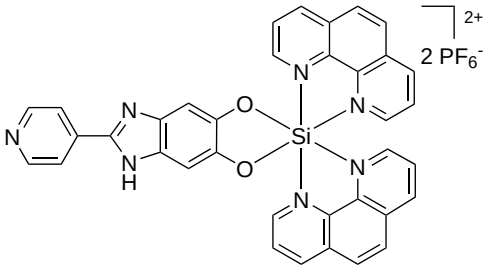

Using method C, silicon complex **130** (22.8 mg, 26.0 µmol), tin powder (27.0 mg, 227 µmol) and pyridine-4-carbaldehyde (**282**, 10.0 µL, 106 µmol) were reacted to yield complex **157** as an orange solid (7.7 mg, 8.52 µmol, 33 % over two steps). – **$C_{36}H_{23}F_{12}N_7O_2P_2Si$** (M = 903.64 g mol^{-1}). – **^{1}H-NMR** (300 MHz, CD_3CN): δ = 9.53 (dd, ^3J = 5.4 Hz, ^4J = 1.2 Hz, 2H, H_{phen}), 9.37 (dd, ^3J = 8.4 Hz, ^4J = 1.2 Hz, 2H, H_{phen}), 9.10 (dd, ^3J = 8.3 Hz, ^4J = 1.1 Hz, 2H, H_{phen}), 8.68–8.63 (m, 2H, H_{py}), 8.60 (d, ^3J = 9.1 Hz, 2H, H_{phen}), 8.51 (d, ^3J = 9.1 Hz, 2H, H_{phen}), 8.46 (dd, ^3J = 8.4, 5.4 Hz, 2H, H_{phen}), 7.93 (dd, ^3J = 8.3, 5.6 Hz, 2H, H_{phen}), 7.90–7.86 (m, 2H, H_{py}), 7.76 (dd, ^3J = 5.5 Hz, ^4J = 1.1 Hz, 2H, H_{phen}), 7.03 (s, 2H, H_{cat}) ppm. – **^{13}C-NMR** (75.5 MHz, CD_3CN): δ = 151.3, 149.6, 148.5, 147.6, 147.0, 146.4, 145.1, 138.4, 135.8, 134.8, 131.4, 131.0, 129.73, 129.71, 129.4, 128.9, 120.8 ppm. – **^{29}Si-NMR** (99.4 MHz, CD_3CN): δ = −148.5 ppm. – **FT-IR** (Film) $\tilde{\nu}$ = 3642, 3411, 3112, 1625, 1605, 1586, 1531, 1482, 1437, 1341, 1265, 1221, 1160, 1118, 1044, 1000, 960, 891, 837, 792, 761, 742, 718, 686, 651, 621, 580, 558, 525, 509, 488, 460, 448, 413 cm^{-1}. – **HRMS** (ESI+): calcd. for $C_{36}H_{23}F_6N_7O_2PSi$ [M−PF_6]$^+$: 758.1319 u, found: 758.1337 u.

Bis(1,10-phenanthroline)(2-(pyridin-4-yl)-1*H*-benzo[*d*]imidazole-5,6-diolato-κ^2O) silicon(IV)-dichloride (157a)

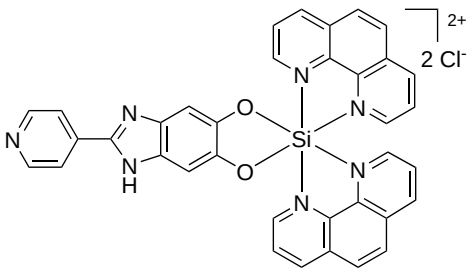

Using method A and silicon complex **157** (4.7 mg, 5.20 µmol), complex **157a** was obtained as an orange solid (2.8 mg, 4.09 µmol, 79 %). – $\mathbf{C_{36}H_{23}Cl_2N_7O_2Si}$ (M = 684.61 g mol^{-1}). – ^{1}**H-NMR** (500 MHz, MeOD): δ = 9.67–9.64 (m, 2H, H_{phen}), 9.51 (dd, ^3J = 8.3 Hz, ^4J = 0.9 Hz, 2H, H_{phen}), 9.27 (dd, ^3J = 8.1 Hz, ^4J = 0.8 Hz, 2H, H_{phen}), 8.69 (d, ^3J = 9.1 Hz, 2H, H_{phen}), 8.66–8.64 (m, 2H, H_{py}), 8.62 (d, ^3J = 9.1 Hz, 2H, H_{phen}), 8.57 (dd, ^3J = 8.3, 5.4 Hz, 2H, H_{phen}), 8.13–8.04 (m, 4H, H_{phen}), 7.97–7.93 (m, 2H, H_{py}), 7.06 (s, 2H, H_{cat}) ppm. – ^{13}**C-NMR** (126 MHz, MeOD): δ = 151.1, 149.7, 148.7, 147.8, 147.3, 146.7, 139.1, 137.3, 136.3, 135.4, 131.73, 131.70, 131.5, 129.9, 129.7, 129.6, 129.1, 121.5 ppm. – ^{29}**Si-NMR** (99.4 MHz, MeOD): δ = −151.6 ppm. – **FT-IR** (Film) $\tilde{\nu}$ = 3393, 3095, 3063, 2956, 2922, 2855, 1626, 1605, 1585, 1528, 1481, 1435, 1344, 1270, 1231, 1163, 1116, 1064, 1043, 1000, 965, 928, 893, 851, 791, 761, 741, 717, 687, 652, 620, 580, 525, 508, 488, 469, 460, 445, 412, 393, 386 cm^{-1}. – **HRMS** (ESI+): calc. for $C_{36}H_{23}ClN_7O_2Si$ [M−Cl]$^+$: 648.1366 u, found: 648.1394 u.

(2-(1-Methylpyridinium-4-yl)-1*H*-benzo[*d*]imidazole-5,6-diolato-κ^2O)bis(1,10-phenanthroline)silicon(IV)-tris(hexafluorophosphate) (159)

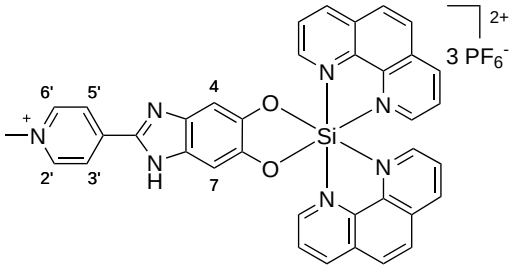

Using method C, silicon complex **130** (42.0 mg, 47.9 µmol), tin powder (49.4 mg, 416 µmol) and 1-methylpyridinium-4-carbaldehyde iodide (**279**, 30.0 mg, 190 µmol) were reacted to yield complex **159** as an orange solid (14.7 mg, 13.8 µmol, 29 % over two steps). Due to the high solubility of the complex in water, the anion exchange was performed as following. The acetonitrile of the product eluents was removed, NH_4PF_6 was added, and the mixture was stored at 4 °C for three weeks. The solid was then isolated by centrifugation (4000 rpm, 4 °C, 5 min) and washed once with water. The product was contaminated with 0.5 eq ammonium hexafluorophosphate. – $\mathbf{C_{37}H_{26}F_{18}N_7O_2P_3Si}$ (M = 1063.64 g mol^{-1}). – ^{1}**H-NMR** (500 MHz, CD_3CN): δ = 9.52 (dd, ^3J = 5.4 Hz, ^4J = 1.2 Hz, 2H, H_{phen}), 9.38 (dd, ^3J = 8.4 Hz, ^4J = 1.2 Hz, 2H, H_{phen}), 9.11 (dd, ^3J = 8.3 Hz, ^4J = 1.0 Hz, 2H, H_{phen}), 8.61 (d, ^3J = 9.1 Hz, 2H, H_{phen}), 8.56–8.54 (m, 2H, H-2', H-6'), 8.52 (d, ^3J = 9.1 Hz, 2H, H_{phen}), 8.47 (dd, ^3J = 8.4, 5.4 Hz, 2H, H_{phen}), 8.45–8.41 (m, 2H, H-3', H-5'), 7.94 (dd, ^3J = 8.3, 5.6 Hz, 2H, H_{phen}), 7.76 (dd, ^3J = 5.6 Hz, ^4J = 1.0 Hz, 2H, H_{phen}), 7.08 (s, 2H, H-4, H-7), 4.23 (s, 3H, H_{Methyl}) ppm. – ^{13}**C-NMR** (126 MHz, CD_3CN): δ = 147.6, 147.1, 146.9, 146.5, 146.3, 145.5, 144.7, 135.7, 134.9, 131.4, 131.0, 129.74, 129.73, 129.3, 128.9, 123.8, 48.6 ppm. – ^{29}**Si-NMR** (99.4 MHz, CD_3CN): δ = −150.9 ppm. – **FT-IR** (Film) $\tilde{\nu}$ = 3652, 3114, 1540, 1585, 1545, 1530, 1488, 1437, 1373, 1339, 1262, 1214, 1191, 1165, 1117, 1042, 889, 835, 778, 759, 739, 716, 672, 621, 578, 557, 525, 509, 487, 476, 445, 427, 409, 399 cm^{-1}. – **HRMS** (ESI+): calcd. for $C_{37}H_{26}F_{12}N_7O_2P_2Si$ [M−PF_6]$^+$: 918.1195 u, found: 918.1233 u.

Bis(1,10-phenanthroline)(2-(4-(trimethylammonio)phenyl)-1*H*-benzo[*d*]imidazole-5,6-diolato-κ^2O)silicon(IV)-tris(hexafluorophosphate) (160)

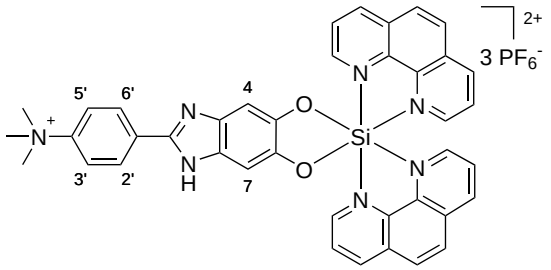

Using method C, silicon complex **130** (52.0 mg, 59.3 µmol), tin powder (60.0 mg, 505 µmol) and 4-formyl-*N,N,N*-trimethylbenzenaminium iodide (**280**, 20.0 mg, 68.7 µmol) were reacted to yield complex **160** as an orange solid (13.2 mg, 11.9 µmol, 20 % over two steps). Due to the high solubility of the complex in water, the anion exchange was performed as following. The acetonitrile of the product eluents was removed, NH_4PF_6 was added, and the mixture was stored at 4 °C for one week. The solid was then isolated by centrifugation (4000 rpm, 4 °C, 5 min) and washed twice with water. – **$C_{40}H_{32}F_{18}N_7O_2P_3Si$** (M = 1105.72 g mol^{-1}). – ^{1}**H-NMR** (500 MHz, CD_3CN): δ = 9.53 (dd, ^3J = 5.4 Hz, ^4J = 1.2 Hz, 2H, H_{phen}), 9.37 (dd, ^3J = 8.4 Hz, ^4J = 1.2 Hz, 2H, H_{phen}), 9.11 (dd, ^3J = 8.3 Hz, ^4J = 1.0 Hz, 2H, H_{phen}), 8.61 (d, ^3J = 9.1 Hz, 2H, H_{phen}), 8.52 (d, ^3J = 9.1 Hz, 2H, H_{phen}), 8.47 (dd, ^3J = 8.4, 5.4 Hz, 2H, H_{phen}), 8.22–8.18 (m, 2H, H-2', H-6'), 7.94 (dd, ^3J = 8.3, 5.6 Hz, 2H, H_{phen}), 7.89–7.85 (m, 2H, H-3', H-5'), 7.77 (dd, ^3J = 5.6 Hz, ^4J = 1.0 Hz, 2H, H_{phen}), 7.04 (s, 2H, H-4, H-7), 3.57 (s, 9H, H_{Methyl}) ppm. – ^{13}**C-NMR** (75.5 MHz, CD_3CN): δ = 149.5, 148.6, 148.0, 147.6, 147.0, 146.4, 145.1, 135.8, 134.9, 132.9, 131.4, 131.0, 129.7, 129.3, 128.9, 128.7, 121.9, 58.1 ppm. – ^{29}**Si-NMR** (99.4 MHz, CD_3CN): δ = −151.4 ppm. – **FT-IR** (Film) $\tilde{\nu}$ = 3652, 3408, 3111, 1626, 1586, 1531, 1493, 1438, 1340, 1262, 1233, 1160, 1118, 1014, 958, 888, 836, 792, 761, 743, 718, 674, 622, 580, 558, 525, 509, 488, 461, 415 cm^{-1}. – **HRMS** (ESI+): calcd. for $C_{40}H_{32}F_{12}N_7O_2P_2Si$ $[M-PF_6]^+$: 960.1665 u, found: 960.1684 u.

Bis(1,10-phenanthroline)(2-(4-(trimethylammonio)phenyl)-1*H*-benzo[*d*]imidazole-5,6-diolato-κ^2O)silicon(IV)-trichloride (160a)

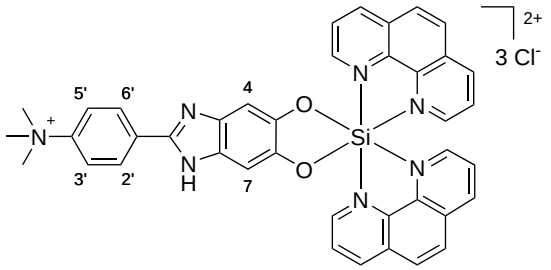

Using method A and silicon complex **160** (8.6 mg, 7.78 µmol), complex **160a** was obtained as an orange solid (5.6 mg, 7.21 µmol, 93 %). – **$C_{40}H_{32}Cl_3N_7O_2Si$** (M = 777.18 g mol^{-1}). – ^{1}**H-NMR** (500 MHz, MeOD): δ = 9.66 (dd, ^3J = 5.4 Hz, ^4J = 1.1 Hz, 2H, H_{phen}), 9.52 (dd, ^3J = 8.4 Hz, ^4J = 1.1 Hz, 2H, H_{phen}), 9.27 (dd, ^3J = 8.2 Hz, ^4J = 1.1 Hz, 2H, H_{phen}), 8.70 (d, ^3J = 9.1 Hz, 2H, H_{phen}), 8.63 (d, ^3J = 9.1 Hz, 2H, H_{phen}), 8.57 (dd, ^3J = 8.3, 5.4 Hz, 2H, H_{phen}), 8.26–8.21 (m, 2H, H-2', H-6'), 8.13 (dd, ^3J = 5.6 Hz, ^4J = 1.1 Hz, 2H, H_{phen}), 8.10–8.06 (m, 4H, H_{phen}, H-3', H-5'), 7.05 (s, 2H, H-4, H-7), 3.72 (s, 9H, H_{phen}) ppm. – ^{13}**C-NMR** (126 MHz, MeOD): δ = 149.7, 149.4, 148.9, 147.8, 147.3, 146.6, 136.3, 135.4, 133.2, 131.7, 131.5, 130.0, 129.9, 129.7, 129.6, 129.2, 128.9, 122.2, 57.8 ppm. – ^{29}**Si-NMR** (99.4 MHz, MeOD): δ = −151.6 ppm. – **FT-IR** (Film) $\tilde{\nu}$ = 3381, 3098, 3057, 1624, 1584, 1528, 1490, 1435, 1343, 1297, 1271, 1233, 1161, 1116, 1043, 1013, 957, 940, 888, 849, 791, 760, 743, 733, 717, 672, 651, 622, 579, 567, 525, 508, 487, 460, 414, 400, 384 cm^{-1}.

(2-Mesityl-1*H*-benzo[*d*]imidazole-5,6-diolato-κ^2O)bis(1,10-phenanthroline)silicon(IV)-bis(hexafluorophosphate) (161)

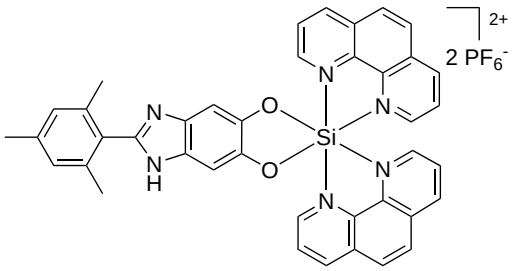

Using method C, silicon complex **130** (70.8 mg, 80.8 µmol), tin powder (83.0 mg, 699 µmol) and mesitaldehyde (**283**, 24.0 µL, 163 µmol) were reacted to yield complex **161** as a yellow solid (17.0 mg, 18.0 µmol, 22 % over two steps). – **$C_{40}H_{30}F_{12}N_6O_2P_2Si$** ($M = 944.73\,g\,mol^{-1}$). – **^{1}H-NMR** (500 MHz, CD_3CN): $\delta = 9.55$ (dd, $^3J = 5.4$ Hz, $^4J = 1.1$ Hz, 2H, H_{phen}), 9.38 (dd, $^3J = 8.4$ Hz, $^4J = 1.2$ Hz, 2H, H_{phen}), 9.10 (dd, $^3J = 8.3$ Hz, $^4J = 1.0$ Hz, 2H, H_{phen}), 8.61 (d, $^3J = 9.1$ Hz, 2H, H_{phen}), 8.52 (d, $^3J = 9.2$ Hz, 2H, H_{phen}), 8.49 (dd, $^3J = 8.4$, 5.5 Hz, 2H, H_{phen}), 7.93 (dd, $^3J = 8.3$, 5.6 Hz, 2H, H_{phen}), 7.75 (dd, $^3J = 5.6$ Hz, $^4J = 1.1$ Hz, 2H, H_{phen}), 6.99 (s, 2H, $H_{mesityl/cat}$), 6.97 (s, 2H, $H_{mesityl/cat}$), 2.30 (s, 3H, $H_{para-Methyl}$), 2.04 (s, 6H, $H_{ortho-Methyl}$) ppm. – **^{13}C-NMR** (126 MHz, CD_3CN): δ = 149.5, 147.5, 147.0, 146.4, 138.8, 135.8, 134.9, 131.4, 131.0, 129.7, 129.7, 129.3, 129.1, 128.9, 21.2, 20.1 ppm. – **^{29}Si-NMR** (99.4 MHz, CD_3CN): $\delta = -148.3$ ppm. – **FT-IR** (Film) $\tilde{\nu}$ = 3650, 3109, 1625, 1586, 1530, 1456, 1438, 1339, 1233, 1158, 1117, 890, 839, 786, 767, 718, 623, 580, 558, 524, 485, 456, 441, 406, 389 cm^{-1}. – **HRMS** (ESI+): calcd. for $C_{40}H_{30}F_6N_6O_2PSi$ $[M-PF_6]^+$: 799.1836 u, found: 799.1857 u.

(2-Mesityl-1*H*-benzo[*d*]imidazole-5,6-diolato-κ^2O)bis(1,10-phenanthroline)silicon(IV)-dichloride (161a)

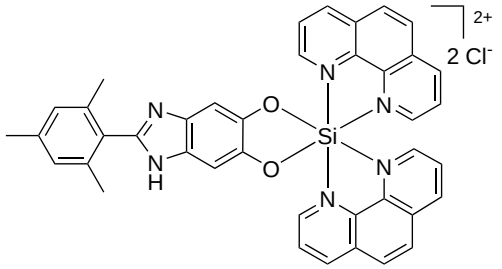

Using method A and silicon complex **161** (13.6 mg, 14.4 µmol), complex **161a** was obtained as an orange solid (9.4 mg, 13.0 µmol, 90 %). – **$C_{40}H_{30}Cl_2N_6O_2Si$** ($M = 725.71\,g\,mol^{-1}$). – **^{1}H-NMR** (500 MHz, MeOD): δ = 9.66 (dd, $^3J = 5.3$ Hz, $^4J = 1.1$ Hz, 2H, H_{phen}), 9.51 (dd, $^3J = 8.4$ Hz, $^4J = 1.1$ Hz, 2H, H_{phen}), 9.26 (dd, $^3J = 8.2$ Hz, $^4J = 1.0$ Hz, 2H, H_{phen}), 8.69 (d, $^3J = 9.1$ Hz, 2H, H_{phen}), 8.62 (d, $^3J = 9.1$ Hz, 2H, H_{phen}), 8.58 (dd, $^3J = 8.4$, 5.4 Hz, 2H, H_{phen}), 8.11 (dd, $^3J = 5.5$ Hz, $^4J = 1.1$ Hz, 2H, H_{phen}), 8.07 (dd, $^3J = 8.1$, 5.6 Hz, 2H, H_{phen}), 7.01 (s, 2H, $H_{mesityl/cat}$), 6.96 (s, 2H, $H_{mesityl/cat}$), 2.30 (s, 3H, $H_{para-Methyl}$), 2.06 (s, 6H, $H_{ortho-Methyl}$) ppm. – **^{13}C-NMR** (126 MHz, MeOD): δ = 152.1, 149.8, 148.8, 147.7, 147.2, 146.6, 144.4, 140.7, 138.9, 136.3, 135.3, 131.71, 131.68, 131.5, 129.9, 129.7, 129.6, 129.19, 129.17, 129.1, 21.2, 19.9 ppm. – **^{29}Si-NMR** (99.4 MHz, MeOD): $\delta = -151.8$ ppm. – **FT-IR** (Film) $\tilde{\nu}$ = 3394, 3097, 3055, 2924, 2856, 1625, 1584, 1529, 1470, 1456, 1435, 1339, 1265, 1232, 1157, 1116, 1042, 1014, 928, 889, 853, 784, 760, 740, 717, 648, 622, 580, 567, 525, 508, 488, 442, 422, 398, 383 cm^{-1}. – **HRMS** (ESI+): calc. for $C_{40}H_{30}ClN_6O_2Si$ $[M-Cl]^+$: u, found: 689.1988 u.

(2-(2-Fluorophenyl)-1*H*-benzo[*d*]imidazole-5,6-diolato-κ^2O)bis(1,10-phenanthroline)silicon(IV)-bis(hexafluorophosphate) (162)

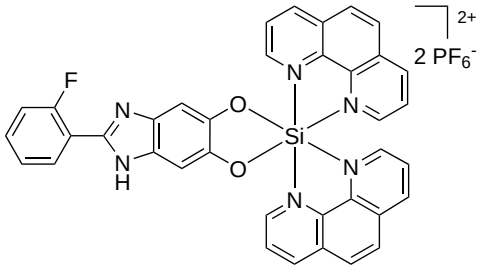

Using method C, silicon complex **130** (70.3 mg, 80.2 µmol), tin powder (83.0 mg, 699 µmol) and 2-fluorobenzaldehyde (**284**, 20.0 µL, 190 µmol) were reacted to yield complex **162** as an orange solid (21.7 mg, 23.6 µmol, 29 % over two steps). – **$C_{37}H_{23}F_{13}N_6O_2P_2Si$** (M = 920.64 g mol^{-1}). – **^{1}H-NMR** (500 MHz, CD_3CN): δ = 9.58 (dd, ^3J = 5.4 Hz, ^4J = 1.1 Hz, 2H, H_{phen}), 9.40 (dd, ^3J = 8.4 Hz, ^4J = 1.1 Hz, 2H, H_{phen}), 9.14 (dd, ^3J = 8.3 Hz, ^4J = 1.0 Hz, 2H, H_{phen}), 8.64 (d, ^3J = 9.1 Hz, 2H, H_{phen}), 8.55 (d, ^3J = 9.1 Hz, 2H, H_{phen}), 8.50 (dd, ^3J = 8.4, 5.4 Hz, 2H, H_{phen}), 8.25 (td, ^3J = 7.8 Hz, ^4J = 1.8 Hz, 1H, H_{phenyl}), 7.98 (dd, ^3J = 8.3, 5.6 Hz, 2H, H_{phen}), 7.80 (dd, ^3J = 5.6 Hz, ^4J = 1.0 Hz, 2H, H_{phen}), 7.53–7.43 (m, 1H, H_{phenyl}), 7.37–7.22 (m, 2H, H_{phenyl}), 7.07 (s, 2H, H_{cat}) ppm. – **^{13}C-NMR** (126 MHz, CD_3CN): δ = 161.8, 159.8, 149.5, 147.5, 146.9, 146.4, 146.3, 144.7, 135.8, 134.8, 132.34, 132.27, 131.4, 131.0, 130.5, 130.48, 129.7, 129.3, 128.9, 126.1, 126.0, 118.8, 118.7, 117.3, 117.1, 100.6 ppm. – **^{29}Si-NMR** (99.4 MHz, CD_3CN): δ = −148.4 ppm. – **FT-IR** (Film) $\tilde{\nu}$ = 3659, 3426, 3110, 1625, 1585, 1530, 1493, 1467, 1438, 1338, 1270, 1242, 1158, 1118, 1044, 958, 929, 888, 828, 783, 761, 743, 717, 674, 653, 622, 581, 557, 524, 509, 487, 461, 423, 398 cm^{-1}. – **HRMS** (ESI+): calcd. for $C_{37}H_{23}F_7N_6O_2PSi$ $[M-PF_6]^+$: 775.1272 u, found: 775.1290 u.

(2-(4-Fluorophenyl)-1*H*-benzo[*d*]imidazole-5,6-diolato-κ^2O)bis(1,10-phenanthroline)silicon(IV)-bis(hexafluorophosphate) (163)

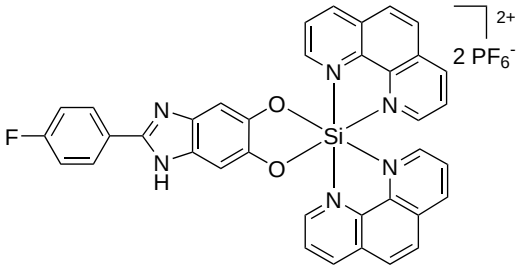

Using method C, silicon complex **130** (70.0 mg, 79.9 µmol), tin powder (82.5 mg, 695 µmol) and 4-fluorobenzaldehyde (**285**, 20.0 µL, 186 µmol) were reacted to yield complex **163** as an orange brown solid (20.4 mg, 22.2 µmol, 28 % over two steps). – **$C_{37}H_{23}F_{13}N_6O_2P_2Si$** (M = 920.64 g mol^{-1}). – **^{1}H-NMR** (500 MHz, CD_3CN): δ = 9.53 (dd, ^3J = 5.4 Hz, ^4J = 1.1 Hz, 2H, H_{phen}), 9.37 (dd, ^3J = 8.4 Hz, ^4J = 1.1 Hz, 2H, H_{phen}), 9.10 (dd, ^3J = 8.3 Hz, ^4J = 1.0 Hz, 2H, H_{phen}), 8.60 (d, ^3J = 9.1 Hz, 2H, H_{phen}), 8.52 (d, ^3J = 9.1 Hz, 2H, H_{phen}), 8.47 (dd, ^3J = 8.4, 5.4 Hz, 2H, H_{phen}), 8.03–7.98 (m, 2H, H_{phenyl}), 7.92 (dd, ^3J = 8.3, 5.6 Hz, 2H, H_{phen}), 7.75 (dd, ^3J = 5.6 Hz, ^4J = 1.0 Hz, 2H, H_{phen}), 7.28–7.22 (m, 2H, H_{phenyl}), 7.01 (s, 2H, H_{cat}) ppm. – **^{13}C-NMR** (126 MHz, CD_3CN): δ = 163.7, 150.0, 149.6, 147.6, 146.9, 146.4, 144.7, 135.8, 134.8, 131.4, 131.0, 129.72, 129.69, 129.5, 129.4, 129.3, 128.9, 117.1, 116.9 ppm. – **^{29}Si-NMR** (99.4 MHz, CD_3CN): δ = −148.4 ppm. – **FT-IR** (Film) $\tilde{\nu}$ = 3650, 3428, 3108, 1626, 1586, 1531, 1499, 1456, 1438, 1342, 1261, 1233, 1162, 1118, 894, 838, 784, 761, 742, 718, 673, 653, 617, 579, 558, 526, 488, 459, 419, 389 cm^{-1}. – **HRMS** (ESI+): calcd. for $C_{37}H_{23}F_7N_6O_2PSi$ $[M-PF_6]^+$: 775.1272 u, found: 775.1294 u.

(2-(4-Fluorophenyl)-1*H*-benzo[*d*]imidazole-5,6-diolato-κ^2O)bis(1,10-phenanthroline)silicon(IV)-dichloride (163a)

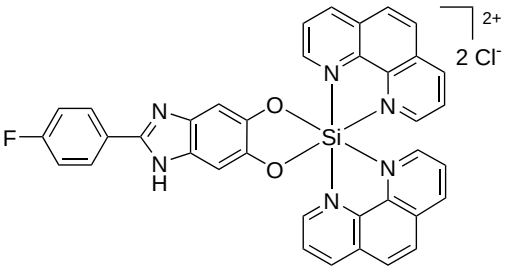

Using method A and silicon complex **163** (10.3 mg, 11.2 µmol), complex **163a** was obtained as an orange solid (5.7 mg, 8.12 µmol, 73 %). – **$C_{37}H_{23}Cl_2FN_6O_2Si$** (M = 701.61 g mol^{-1}). – **^{1}H-NMR** (500 MHz, MeOD): δ = 9.65 (dd, ^3J = 5.4 Hz, ^4J = 1.1 Hz, 2H, H_{phen}), 9.51 (dd, ^3J = 8.4 Hz, ^4J = 1.1 Hz, 2H, H_{phen}), 9.26 (dd, ^3J = 8.2 Hz, ^4J = 1.1 Hz, 2H, H_{phen}), 8.69 (d, ^3J = 9.1 Hz, 2H, H_{phen}), 8.62 (d, ^3J = 9.1 Hz, 2H, H_{phen}), 8.57 (dd, ^3J = 8.3, 5.4 Hz, 2H, H_{phen}), 8.11 (dd, ^3J = 5.5 Hz, ^4J = 1.1 Hz, 2H, H_{phen}), 8.07 (dd, ^3J = 8.2, 5.6 Hz, 2H, H_{phen}), 8.02–7.97 (m, 2H, H_{phenyl}), 7.27–7.20 (m, 2H, H_{phenyl}), 7.01 (s, 2H, H_{cat}) ppm. – **^{13}C-NMR** (126 MHz, MeOD): δ = 168.6, 151.2, 149.7, 147.8, 147.2, 146.6, 136.3, 135.4, 131.7, 131.5, 129.9, 129.7, 129.6, 129.5, 129.4, 129.1, 127.6, 117.1, 117.0, 114.2 ppm. – **^{29}Si-NMR** (99.4 MHz, MeOD): δ = −151.7 ppm. – **FT-IR** (Film) $\tilde{\nu}$ = 3386, 3105, 3059, 1625, 1584, 1528, 1501, 1475, 1438, 1362, 1346, 1306, 1273, 1227, 1163, 1116, 1043, 1013, 962, 927, 895, 849, 830, 814, 785, 761, 743, 716, 654, 616, 578, 525, 486, 459, 444, 412, 391 cm^{-1}. – **HRMS** (ESI+): calc. for $C_{37}H_{23}ClFN_6O_2Si$ [M−Cl]$^+$: 665.1319 u, found: 665.1344 u.

Bis(1,10-phenanthroline)(2-(4-nitrophenyl)-1*H*-benzo[*d*]imidazole-5,6-diolato-κ^2O) silicon(IV)-bis(hexafluorophosphate) (164)

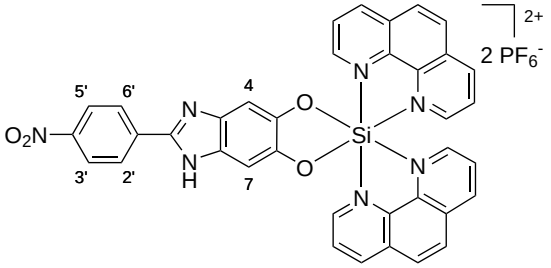

Using method C, silicon complex **130** (42.5 mg, 48.5 µmol), tin powder (48.0 mg, 404 µmol) and 4-nitrobenzaldehyde (**286**, 15.0 mg, 99.3 µmol) were reacted to yield complex **164** as an orange solid (19.3 mg, 20.4 µmol, 42 % over two steps). – **$C_{37}H_{23}F_{12}N_7O_4P_2Si$** (M = 947.65 g mol^{-1}). – **^{1}H-NMR** (500 MHz, CD_3CN): δ = 9.53 (dd, ^3J = 5.4 Hz, ^4J = 1.2 Hz, 2H, H_{phen}), 9.37 (dd, ^3J = 8.4 Hz, ^4J = 1.2 Hz, 2H, H_{phen}), 9.10 (dd, ^3J = 8.3 Hz, ^4J = 1.1 Hz, 2H, H_{phen}), 8.60 (d, ^3J = 9.1 Hz, 2H, H_{phen}), 8.52 (d, ^3J = 9.2 Hz, 2H, H_{phen}), 8.47 (dd, ^3J = 8.4, 5.4 Hz, 2H, H_{phen}), 8.32–8.28 (m, 2H, H-3', H-5'), 8.19–8.15 (m, 2H, H-2', H-6'), 7.93 (dd, ^3J = 8.3, 5.6 Hz, 2H, H_{phen}), 7.75 (dd, ^3J = 5.6 Hz, ^4J = 1.1 Hz, 2H, H_{phen}), 7.02 (s, 2H, H-4, H-7) ppm. – **^{13}C-NMR** (126 MHz, CD_3CN): δ = 149.6, 149.0, 148.9, 147.6, 147.0, 146.4, 143.6, 140.7, 137.1, 135.7, 134.8, 131.4, 131.0, 129.7, 129.3, 128.9, 127.6, 125.2 ppm. – **^{29}Si-NMR** (99.4 MHz, CD_3CN): δ = −148.6 ppm. – **FT-IR** (Film) $\tilde{\nu}$ = 3632, 3107, 2925, 1625, 1601, 1586, 1529, 1481, 1439, 1339, 1269, 1161, 1117, 1044, 952, 927, 890, 842, 789, 761, 742, 717, 703, 622, 582, 558, 525, 508, 485, 445, 423, 407, 397, 389 cm^{-1}. – **HRMS** (ESI+): calcd. for $C_{37}H_{23}F_6N_7O_4PSi$ [M−PF_6]$^+$: 802.1217 u, found: 802.1230 u.

Bis(1,10-phenanthroline)(2-propyl-1*H*-benzo[*d*]imidazole-5,6-diolato-κ^2O)silicon(IV)-bis(hexafluorophosphate) (166)

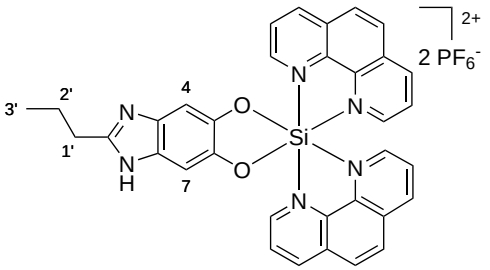

Using method C, silicon complex **130** (70.0 mg, 79.9 µmol), tin powder (83.1 mg, 700 µmol) and butanal (**287**, 25.0 µL, 161 µmol) were reacted to yield complex **166** as a yellow brown solid (19.8 mg, 22.8 µmol, 29 % over two steps). – **$C_{34}H_{26}F_{12}N_6O_2P_2Si$** (M = 868.64 g mol^{-1}). – **^{1}H-NMR** (500 MHz, CD_3CN): δ = 9.46 (dd, ^3J = 5.4 Hz, ^4J = 1.2 Hz, 2H, H_{phen}), 9.39 (dd, ^3J = 8.4 Hz, ^4J = 1.2 Hz, 2H, H_{phen}), 9.12 (dd, ^3J = 8.3 Hz, ^4J = 1.0 Hz, 2H, H_{phen}), 8.61 (d, ^3J = 9.1 Hz, 2H, H_{phen}), 8.53 (d, ^3J = 9.1 Hz, 2H, H_{phen}), 8.47 (dd, ^3J = 8.4, 5.4 Hz, 2H, H_{phen}), 7.95 (dd, ^3J = 8.3, 5.6 Hz, 2H, H_{phen}), 7.75 (dd, ^3J = 5.6 Hz, ^4J = 1.1 Hz, 2H, H_{phen}), 7.05 (s, 2H, H-4, H-7), 2.99 (t, ^3J = 7.5 Hz, 2H, H-1'), 1.82 (h, ^3J = 7.4 Hz, 2H, H-2'), 0.98 (t, ^3J = 7.4 Hz, 3H, H-3') ppm. – **^{13}C-NMR** (126 MHz, CD_3CN): δ = 153.3, 149.5, 147.7, 147.3, 147.0, 146.7, 135.7, 134.8, 131.5, 131.1, 129.8, 129.7, 129.4, 129.0, 126.6, 99.3, 29.0, 21.3, 13.6 ppm. – **^{29}Si-NMR** (99.4 MHz, CD_3CN): δ = −149.0 ppm. – **FT-IR** (Film) $\tilde{\nu}$ = 3664, 3375, 3118, 1626, 1586, 1531, 1475, 1438, 1323, 1234, 1163, 1119, 887, 833, 762, 742, 717, 581, 558, 526, 510, 486, 422, 398 cm^{-1}. – **HRMS** (ESI+): calcd. for $C_{34}H_{26}F_6N_6O_2PSi$ $[M-PF_6]^+$: 723.1523 u, found: 723.1544 u.

Bis(1,10-phenanthroline)(2-propyl-1*H*-benzo[*d*]imidazole-5,6-diolato-κ^2O)silicon(IV)-dichloride (166a)

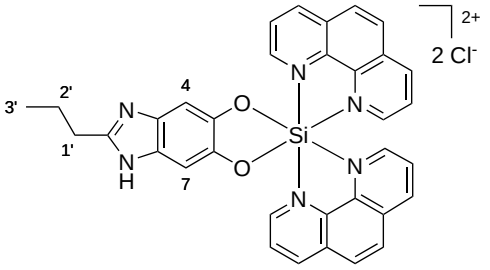

Using method A and silicon complex **166** (11.8 mg, 13.6 µmol), complex **166a** was obtained as a yellow solid (8.1 mg, 12.5 µmol, 92 %). – **$C_{34}H_{26}Cl_2N_6O_2Si$** (M = 649.61 g mol^{-1}). – **^{1}H-NMR** (500 MHz, MeOD): δ = 9.64 (dd, ^3J = 5.4 Hz, ^4J = 1.1 Hz, 2H), 9.53 (dd, ^3J = 8.4 Hz, ^4J = 1.1 Hz, 2H), 9.28 (dd, ^3J = 8.2 Hz, ^4J = 1.1 Hz, 2H), 8.70 (d, ^3J = 9.1 Hz, 2H), 8.63 (d, ^3J = 9.1 Hz, 2H), 8.57 (dd, ^3J = 8.3, 5.4 Hz, 2H), 8.13 (dd, ^3J = 5.6 Hz, ^4J = 1.1 Hz, 2H), 8.09 (dd, ^3J = 8.2, 5.6 Hz, 2H), 7.09 (s, 2H), 3.00 (t, ^3J = 7.5 Hz, 2H), 1.87 (h, ^3J = 7.4 Hz, 2H), 1.01 (t, ^3J = 7.4 Hz, 3H) ppm. – **^{13}C-NMR** (126 MHz, MeOD): δ = 153.5, 149.8, 148.0, 147.5, 146.9, 146.8, 136.2, 135.3, 131.7, 131.5, 130.0, 129.8, 129.6, 129.2, 128.2, 99.4, 29.5, 22.0, 13.7 ppm. – **^{29}Si-NMR** (99.4 MHz, MeOD): δ = −151.2 ppm. – **FT-IR** (Film) $\tilde{\nu}$ = 3393, 3095, 3065, 2965, 2931, 2874, 2709, 2601, 1625, 1584, 1528, 1492, 1472, 1434, 1322, 1281, 1232, 1216, 1164, 1116, 1043, 1008, 930, 888, 854, 807, 786, 760, 738, 716, 671, 645, 621, 581, 568, 525, 509, 488, 447, 421, 403 cm^{-1}. – **HRMS** (ESI+): calc. for $C_{34}H_{26}ClN_6O_2Si$ $[M-Cl]^+$: 613.1570 u, found: 613.1591 u.

Bis(2,2'-bipyridine)(2-(pent-4-yn-1-yl)-1*H*-benzo[*d*]imidazole-5,6-diolato-κ^2O) silicon(IV)-bis(hexafluorophosphate) (172)

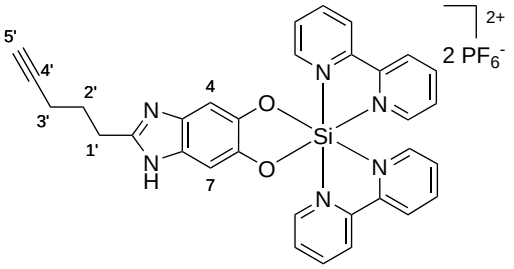

Using method C, silicon complex **129** (40.0 mg, 48.3 µmol), tin powder (48.7 mg, 410 µmol) and 5-hexynal (**189**, 20.0 mg, 208 µmol) were reacted to yield complex **172** as an orange solid (14.1 mg, 16.7 µmol, 35 % over two steps). – **$C_{32}H_{26}F_{12}N_6O_2P_2Si$** (M = 844.61 g mol^{-1}). – ^{1}**H-NMR** (300 MHz, CD_3CN): δ = 9.06 (ddd, ^3J = 5.8 Hz, ^4J = 1.4 Hz, ^5J = 0.7 Hz, 2H, H_{bpy}), 8.93 (dt, ^3J = 8.1 Hz, ^4J = 0.9 Hz, 2H, H_{bpy}), 8.87–8.82 (m, 2H, H_{bpy}), 8.77 (td, ^3J = 7.9 Hz, ^4J = 1.5 Hz, 2H, H_{bpy}), 8.62 (td, ^3J = 7.9 Hz, ^4J = 1.4 Hz, 2H, H_{bpy}), 8.13 (ddd, ^3J = 7.7, 5.8 Hz, ^4J = 1.2 Hz, 2H, H_{bpy}), 7.83 (ddd, ^3J = 7.6, 5.9 Hz, ^4J = 1.3 Hz, 2H, H_{bpy}), 7.61 (ddd, ^3J = 6.0 Hz, ^4J = 1.3 Hz, ^5J = 0.7 Hz, 2H, H_{bpy}), 7.01 (s, 2H, H-4, H-7), 3.13–3.05 (m, 2H, H-1'), 2.29 (td, ^3J = 6.9 Hz, ^4J = 2.6 Hz, 2H, H-3'), 2.18 (t, ^4J = 2.7 Hz, 1H, H-5'), 2.03–1.97 (m, 2H, H-2') ppm. – ^{13}**C-NMR** (75.5 MHz, CD_3CN): δ = 152.7, 148.9, 148.4, 148.3, 146.5, 146.3, 145.0, 144.2, 132.1, 131.5, 127.3, 126.3, 126.0, 99.4, 83.6, 71.1, 26.7, 26.6, 18.3 ppm. – ^{29}**Si-NMR** (59.7 MHz, CD_3CN): δ = −149.1 ppm. – **FT-IR** (Film) $\tilde{\nu}$ = 3654, 3365, 3111, 1618, 1573, 1509, 1476, 1455, 1325, 1246, 1166, 1117, 1073, 1045, 827, 740, 687, 578, 556, 520, 503, 471, 427, 397 cm^{-1}. – **HRMS** (ESI+): calcd. for $C_{32}H_{26}F_6N_6O_2PSi$ $[M-PF_6]^+$: 699.1523 u, found: 699.1538 u.

(2-(Pent-4-yn-1-yl)-1*H*-benzo[*d*]imidazole-5,6-diolato-κ^2O)bis(1,10-phenanthroline) silicon(IV)-bis(hexafluorophosphate) (167)

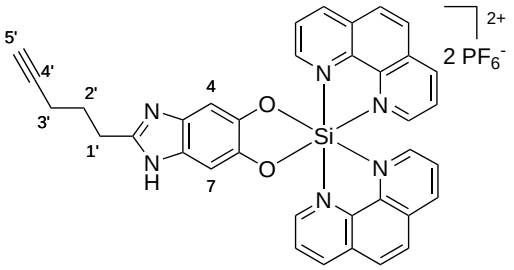

Using method C, silicon complex **130** (41.0 mg, 46.8 µmol), tin powder (48.0 mg, 404 µmol) and 5-hexynal (**189**, 10.0 mg, 104 µmol) were reacted to yield complex **167** as an orange solid (13.5 mg, 15.1 µmol, 32 % over two steps). – **$C_{36}H_{26}F_{12}N_6O_2P_2Si$** (M = 892.66 g mol^{-1}). – ^{1}**H-NMR** (500 MHz, CD_3CN): δ = 9.48 (dd, ^3J = 5.4 Hz, ^4J = 1.2 Hz, 2H, H_{phen}), 9.37 (dd, ^3J = 8.4 Hz, ^4J = 1.2 Hz, 2H, H_{phen}), 9.10 (dd, ^3J = 8.3 Hz, ^4J = 1.1 Hz, 2H, H_{phen}), 8.60 (d, ^3J = 9.1 Hz, 2H, H_{phen}), 8.51 (d, ^3J = 9.1 Hz, 2H, H_{phen}), 8.46 (dd, ^3J = 8.4, 5.4 Hz, 2H, H_{phen}), 7.93 (dd, ^3J = 8.3, 5.6 Hz, 2H, H_{phen}), 7.74 (dd, ^3J = 5.6 Hz, ^4J = 1.1 Hz, 2H, H_{phen}), 6.95 (s, 2H, H-4, H-7), 2.97–2.93 (m, 2H, H-1'), 2.26 (td, ^3J = 7.0 Hz, ^4J = 2.7 Hz, 2H, H-3'), 2.18 (t, ^4J = 2.7 Hz, 1H, H-5'), 1.97–1.95 (m, 2H, H-2') ppm. – ^{13}**C-NMR** (126 MHz, CD_3CN): δ = 153.4, 149.5, 147.5, 147.0, 146.5, 144.8, 135.7, 134.8, 131.4, 131.0, 129.70, 129.67, 129.3, 128.9, 99.9, 84.2, 70.6, 27.6, 27.3, 18.3 ppm. – ^{29}**Si-NMR** (99.4 MHz, CD_3CN): δ = −148.6 ppm. – **FT-IR** (Film) $\tilde{\nu}$ = 3660, 3293, 3114, 1626, 1587, 1531, 1465, 1438, 1323, 1234, 1160, 1118, 832, 761, 742, 718, 671, 580, 558, 525, 488, 400 cm^{-1}. – **HRMS** (ESI+): calcd. for $C_{36}H_{26}F_6N_6O_2PSi$ $[M-PF_6]^+$: 747.1523 u, found: 747.1537 u.

(2-(Pent-4-yn-1-yl)-1*H*-benzo[*d*]imidazole-5,6-diolato-κ^2O)bis(3,4,7,8-tetramethyl-1,10-phenanthroline)silicon(IV)-bis(hexafluorophosphate) (173)

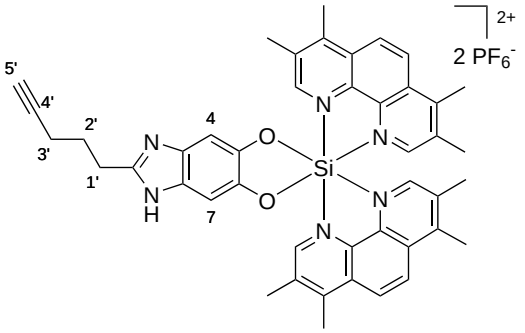

Using method C, silicon complex **131** (20.0 mg, 20.2 µmol), tin powder (21.0 mg, 177 µmol) and 5-hexynal (**189**, 10.0 mg, 104 µmol) were reacted to yield complex **173** as an orange solid (12.3 mg, 12.2 µmol, 60 % over two steps). – **$C_{44}H_{42}F_{12}N_6O_2P_2Si$** (M = 1004.87 g mol^{-1}). – **^{1}H-NMR** (300 MHz, CD_3CN): δ = 9.08 (s, 2H, H_{Me_4phen}), 8.64 (d, ^3J = 9.6 Hz, 2H, H_{Me_4phen}), 8.57 (d, ^3J = 9.6 Hz, 2H, H_{Me_4phen}), 7.35 (s, 2H, H_{Me_4phen}), 6.94 (s, 2H, H-4, H-7), 3.08–2.99 (m, 8H, H_{Methyl}, H-1'), 2.85 (s, 6H, H_{Methyl}), 2.65 (s, 6H, H_{Methyl}), 2.33–2.25 (m, 8H, H_{Methyl}, H-3'), 2.18 (t, ^4J = 2.7 Hz, 1H, H-5'), 2.03–1.96 (m, 2H, H-2') ppm. – **^{13}C-NMR** (126 MHz, CD_3CN): δ = 157.8, 156.8, 152.6, 148.4, 146.3, 146.2, 138.9, 138.2, 134.5, 133.5, 129.7, 129.2, 128.8, 125.9, 125.8, 99.2, 83.8, 70.8, 27.0, 26.9, 18.8, 18.3, 18.2, 16.7, 16.3 ppm. – **^{29}Si-NMR** (99.4 MHz, CD_3CN): δ = −150.6 ppm. – **FT-IR** (Film) $\tilde{\nu}$ = 3658, 3289, 2933, 1633, 1545, 1475, 1440, 1390, 1316, 1255, 1225, 1197, 1162, 1027, 913, 901, 835, 768, 738, 721, 649, 633, 597, 557, 526, 489, 459, 444, 414 cm^{-1}. – **HRMS** (ESI+): calcd. for $C_{44}H_{42}F_6N_6O_2PSi$ [M−PF_6]$^+$: 859.2775 u, found: 859.2791 u.

5.4.3. Synthesis of Tris-heteroleptic Silicon(IV) Complexes

(Benzene-1,2-diolato)(dipyrido[3,2-*a*:2',3'-*c*]phenazine-κ^2N', N'')(2,2'-bipyridine)silicon(IV)-bis(hexafluorophosphate) (183)

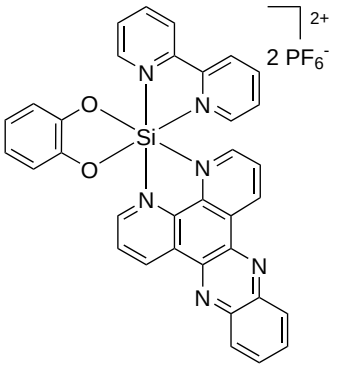

Under an atmosphere of nitrogen, a suspension of anhydrous 2,2'-bipyridine (127 mg, 813 µmol) and dipyrido[3,2-*a*:2',3'-*c*]phenazine (**185**, 246 mg, 871 µmol) in anhydrous chlorobenzene (15 mL) was purged with nitrogen for 15 min and then heated to 80 °C, whereupon the solid dissolved. Then silicon tetraiodide (440 mg, 821 µmol) was added, and the brown suspension was stirred at 110 °C for 16 hours. The mixture was cooled to room temperature, catechol (361 mg, 3.28 mmol) was added, and the mixture was stirred at 120 °C for 28 hours. After cooling to room temperature, the solvent was removed under vacuum. The brownish orange residue was subjected to flash column chromatography (MeCN → MeCN/H_2O/satd. aq. KNO_3 150:3:1 → 100:3:1 → 80:3:1), whereupon the first yellow band eluting under salt conditions was collected. The product fractions were concentrated, the residue was dissolved in acetonitrile/water 1:1 and treated with NH_4PF_6 before the acetonitrile was removed. The resulting precipitate was isolated by centrifugation (4000 rpm, 4 °C, 5 min) and washed twice with water to remove the excess amount of salt. The solid was dissolved in acetonitrile, and the gained solution was filtered through cotton before it was concentrated. After drying under vacuum, the tris-heteroleptic complex **183** was obtained as a yellow solid (79.4 mg, 91.8 µmol, 11 % over two steps). In addition, by collecting the second yellow band eluting under salt conditions during flash column chromatography and exchanging the counter-ion to PF_6^-, the bis-heteroleptic silicon complex [Si(bpy)$_2$(cat)](PF_6)$_2$ (**87**) was obtained as a yellow solid (87.3 mg, 118 µmol, 15 %). – **$C_{34}H_{22}F_{12}N_6O_2P_2Si$** (M = 864.60 g mol^{-1}). – **^{1}H-**

NMR (300 MHz, CD_3CN, 17 mM): δ = 10.23 (dd, ^3J = 8.3 Hz, ^4J = 1.3 Hz, 1H, H_{dppz}), 10.06 (dd, ^3J = 8.3 Hz, ^4J = 1.1 Hz, 1H, H_{dppz}), 9.43 (dd, ^3J = 5.5 Hz, ^4J = 1.3 Hz, 1H, H_{dppz}), 9.27–9.21 (m, 1H, H_{bpy}), 9.04–8.96 (m, 1H, H_{bpy}), 8.92–8.84 (m, 2H, H_{bpy}), 8.68–8.46 (m, 4H, 3 × H_{dppz}, H_{bpy}), 8.33–8.17 (m, 4H, 3 × H_{dppz}, H_{bpy}), 7.93 (dd, ^3J = 5.7 Hz, ^4J = 1.1 Hz, 1H, H_{dppz}), 7.76–7.69 (m, 1H, H_{bpy}), 7.68–7.61 (m, 1H, H_{bpy}), 6.94–6.79 (m, 3H, H_{cat}), 6.79–6.70 (m, 1H, H_{cat}) ppm. – **^{13}C-NMR** (75.5 MHz, CD_3CN, 17 mM): δ = 149.94, 149.90, 149.0, 148.7, 148.2, 148.0, 147.3, 146.8, 146.5, 144.9, 144.3, 144.2, 143.6, 143.1, 134.7, 132.2, 132.1, 131.9, 131.5, 131.3, 130.9, 130.9, 130.9, 130.8, 126.3, 126.1, 123.3, 123.2, 114.9, 114.8 ppm. – **^{29}Si-NMR** (59.7 MHz, CD_3CN): δ = −148.4 ppm. – **FT-IR** (Film) $\tilde{\nu}$ = 3659, 3110, 1618, 1583, 1510, 1482, 1456, 1429, 1336, 1325, 1283, 1243, 1196, 1148, 1100, 1083, 1058, 1046, 1027, 1014, 831, 772, 749, 729, 682, 659, 645, 621, 595, 558, 531, 515, 498, 465, 451, 433, 392 cm^{-1}. – **HRMS** (ESI+): calc. for $C_{34}H_{22}F_6N_6O_2PSi$ $[M-PF_6]^+$: 719.1210 u, found: 719.1226 u.

(Benzene-1,2-diolato)(dipyrido[3,2-*a*:2',3'-*c*]phenazine-κ^2N', N'')(1,10-phenanthroline)silicon(IV)-bis(hexafluorophosphate) (184)

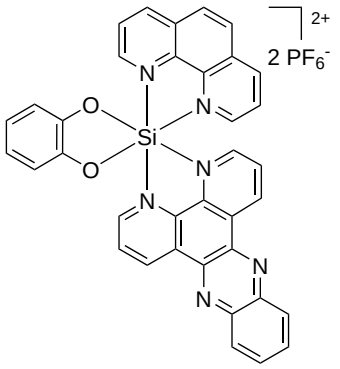

Under an atmosphere of nitrogen, a suspension of anhydrous 1,10-phenanthroline (235 mg, 1.30 mmol) and dipyrido[3,2-*a*:2',3'-*c*]phenazine (**185**, 410 mg, 1.45 mmol) in anhydrous chlorobenzene (30 mL) was purged with nitrogen for 15 min and then heated to 80 °C, whereupon the solid dissolved. Then silicon tetraiodide (701 mg, 1.31 mmol) was added, and the red suspension was stirred at 110 °C for 14 hours. The mixture was cooled to room temperature, catechol (576 mg, 5.23 mmol) was added, and the mixture was stirred at 120 °C for 24 hours. After cooling to room temperature, the solvent was removed under vacuum. The orange-brown residue was subjected to flash column chromatography (MeCN → MeCN/H_2O/satd. aq. KNO_3 150:3:1 → 100:3:1), whereupon the first yellow band eluting under salt conditions was collected. The product fractions were concentrated, the residue was dissolved in acetonitrile/water 1:1 and treated with NH_4PF_6 before the acetonitrile was removed. The resulting precipitate was isolated by centrifugation (4000 rpm, 4 °C, 5 min) and washed twice with water to remove the excess amount of salt. The solid was dissolved in acetonitrile, and the gained solution was filtered through cotton before it was concentrated. After drying under vacuum, the tris-heteroleptic complex **184** was obtained as a yellow solid (134 mg, 151 µmol, 12 % over two steps). In addition, by collecting the second yellow band eluting under salt conditions during flash column chromatography and exchanging the counter-ion to PF_6^-, the bis-heteroleptic silicon complex $[Si(cat)(phen)_2](PF_6)_2$ (**88**) was obtained as a yellow solid (103 mg, 131 µmol, 10 %). – **$C_{36}H_{22}F_{12}N_6O_2P_2Si$** (M = 888.63 g mol^{-1}). – **^{1}H-NMR** (300 MHz, CD_3CN, 29 mM): δ = 10.28 (dd, ^3J = 8.3 Hz, ^4J = 1.3 Hz, 1H, H_{dppz}), 10.01 (dd, ^3J = 8.3 Hz, ^4J = 1.2 Hz, 1H, H_{dppz}), 9.54 (dd, ^3J = 5.5 Hz, ^4J = 1.3 Hz, 1H, H_{dppz}), 9.51 (dd, ^3J = 5.4 Hz, ^4J = 1.2 Hz, 1H, H_{phen}), 9.41 (dd, ^3J = 8.4 Hz, ^4J = 1.3 Hz, 1H, H_{phen}), 9.12 (dd, ^3J = 8.1 Hz, ^4J = 1.3 Hz, 1H, H_{phen}), 8.68 (dd, ^3J = 8.3, 5.5 Hz, 1H, H_{dppz}), 8.63 (d, ^3J = 9.1 Hz, 1H, H_{phen}), 8.60–8.48 (m, 4H, 2 × H_{dppz}, 2 × H_{phen}), 8.30–8.18 (m, 2H, H_{dppz}), 8.10 (dd, ^3J = 8.3, 5.7 Hz, 1H, H_{dppz}), 7.97 (dd, ^3J = 8.1, 5.6 Hz, 1H, H_{phen}), 7.91 (dd, ^3J = 5.6 Hz, ^4J = 1.3 Hz, 1H, H_{phen}), 7.80 (dd, ^3J = 5.7 Hz,

^4J = 1.2 Hz, 1H, H_{dppz}), 6.94–6.75 (m, 4H, H_{cat}) ppm. – **^{13}C-NMR** (75.5 MHz, CD_3CN, 36 mM): δ = 150.2, 149.6, 148.3, 147.6, 147.4, 147.3, 147.2, 146.6, 144.1, 143.7, 143.0, 139.9, 139.8, 138.4, 137.6, 135.9, 134.9, 134.6, 132.1, 131.8, 131.6, 131.5, 131.2, 130.9, 130.9, 130.8, 129.8, 129.4, 129.0, 123.2, 114.9, 114.8 ppm. – **^{29}Si-NMR** (99.4 MHz, CD_3CN): δ = −148.6 ppm. – **FT-IR** (Film) $\tilde{\nu}$ = 3664, 3113, 1626, 1585, 1530, 1510, 1482, 1437, 1335, 1245, 1196, 1151, 1119, 1100, 1086, 1058, 1014, 887, 836, 764, 726, 717, 667, 645, 621, 595, 583, 558, 541, 511, 489, 461, 430 cm^{-1}. – **HRMS** (ESI+): calc. for $C_{36}H_{22}F_6N_6O_2PSi$ $[M-PF_6]^+$: 743.1210 u, found: 743.1225 u.

(2,2'-Bipyridine)(4,5-dinitrobenzene-1,2-diolato)(dipyrido[3,2-*a*:2',3'-*c*]phenazine-κ^2N', N'')silicon(IV)-bis(hexafluorophosphate) (187)

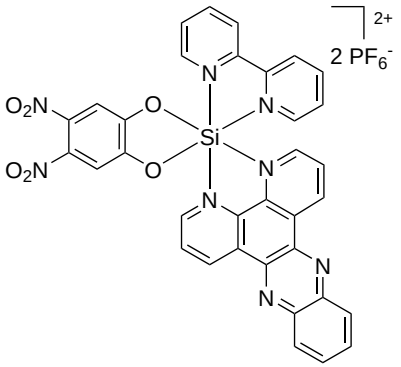

At 0 °C, (2,2'-bipyridine)(benzene-1,2-diolato)(dipyrido[3,2-*a*:2',3'-*c*]phenazine-κ^2N', N'')silicon(IV)-bis(hexafluorophosphate) (**183**, 51.3 mg, 59.3 µmol) was treated with an ice-cold mixture of glacial acetic acid (1.0 mL) and fuming nitric acid (2.0 mL). The yellow solution was stirred at 0 °C for 4.5 hours, whereupon the temperature increased slowly to 20 °C. The mixture was then cooled to 0 °C and neutralized with a concentrated potassium hydroxide solution (20 %) until pH reached 6–7. The solid was isolated by centrifugation (4000 rpm, 4 °C, 5 min), suspended in acetonitrile and filtered. The aqueous supernatant was treated with NH_4PF_6, the precipitate was isolated by centrifugation (4000 rpm, 4 °C, 5 min), washed twice with water and dissolved in acetonitrile. The combined acetonitrile layers were subjected to flash column chromatography (MeCN → MeCN/H_2O/satd. aq. KNO_3 80:3:1 → 50:3:1), whereupon the slightly yellow band eluting under salt conditions was collected. The product fractions were concentrated, and the residue was dissolved in acetonitrile/water 1:1. Then NH_4PF_6 was added, and the acetonitrile was removed. The resulting precipitate was isolated by centrifugation (4000 rpm, 4 °C, 5 min) and washed twice with water to remove the excess amount of salt. The solid was dissolved in acetonitrile, and the gained solution was filtered through cotton before it was concentrated. After drying under vacuum, complex **187** was obtained as an orange solid (41.2 mg, 43.2 µmol, 73 %). – **$C_{34}H_{20}F_{12}N_8O_6P_2Si$** (M = 954.60 g mol^{-1}). – **^{1}H-NMR** (300 MHz, CD_3CN, 8 mM): δ = 10.29 (dd, ^3J = 8.3 Hz, ^4J = 1.2 Hz, 1H, H_{dppz}), 10.12 (dd, ^3J = 8.3 Hz, ^4J = 1.1 Hz, 1H, H_{dppz}), 9.38 (dd, ^3J = 5.6 Hz, ^4J = 1.2 Hz, 1H, H_{dppz}), 9.18–9.13 (m, 1H, H_{bpy}), 9.05–8.98 (m, 1H, H_{bpy}), 8.96–8.84 (m, 2H, H_{bpy}), 8.70–8.49 (m, 4H, 3 × H_{dppz}, H_{bpy}), 8.35–8.21 (m, 4H, 3 × H_{dppz}, H_{bpy}), 7.95 (dd, ^3J = 5.7 Hz, ^4J = 1.1 Hz, 1H, H_{dppz}), 7.75 (ddd, ^3J = 7.5, 6.1 Hz, ^4J = 1.2 Hz, 1H, H_{bpy}), 7.67–7.58 (m, 1H, H_{bpy}), 7.47 (s, 1H, H_{cat}), 7.31 (s, 1H, H_{cat}) ppm. – **^{13}C-NMR** (126 MHz, CD_3CN, 19 mM): δ = 151.2, 150.8, 150.3, 149.4, 148.9, 148.8, 148.4, 146.7, 144.9, 144.2, 144.1, 144.0, 143.7, 139.7, 139.6, 138.9, 138.3, 137.2, 134.8, 134.7, 132.6, 132.3, 132.0, 131.9, 131.5, 131.0, 130.9, 130.9, 126.6, 126.2, 111.6, 111.5 ppm. – **^{29}Si-NMR** (99.4 MHz, CD_3CN): δ = −148.9 ppm. – **FT-IR** (Film) $\tilde{\nu}$ = 3665, 3114, 1618, 1584, 1537, 1511, 1496, 1456, 1429, 1375, 1343, 1288, 1277, 1251, 1205, 1173, 1150, 1120, 1087, 1059, 1048, 1026, 896, 836, 774, 757, 741, 728, 684, 656, 621, 595, 557, 518, 498, 465, 432 cm^{-1}. – **HRMS** (ESI+): calc. for $C_{34}H_{20}F_6N_8O_6PSi$ $[M-PF_6]^+$: 809.0911 u, found: 809.0931 u.

(4,5-Dinitrobenzene-1,2-diolato)(dipyrido[3,2-*a*:2',3'-*c*]phenazine-κ^2N', N'')(1,10-phenanthroline)silicon(IV)-bis(hexafluorophosphate) (188)

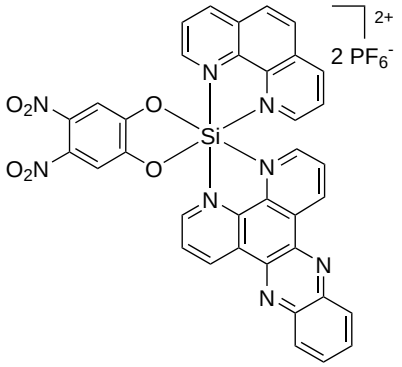

At 0 °C, (benzene-1,2-diolato)(dipyrido[3,2-*a*:2',3'-*c*]phenazine)(1,10-phenanthroline-κ^2N', N'')silicon(IV)-bis(hexafluorophosphate) (**184**, 45.0 mg, 50.6 µmol) was treated with an ice-cold mixture of glacial acetic acid (0.5 mL) and fuming nitric acid (1.0 mL). The yellow solution was stirred at 0 °C for 3.5 hours, whereupon the temperature increased slowly to 18 °C. The mixture was then cooled to 0 °C and neutralized with a concentrated potassium hydroxide solution (20 %) until pH reached 6–7. The solid was isolated by centrifugation (4000 rpm, 4 °C, 5 min), suspended in acetonitrile and filtered. The aqueous supernatant was treated with NH_4PF_6, the precipitate was isolated by centrifugation (4000 rpm, 4 °C, 5 min), washed twice with water and dissolved in acetonitrile. The combined acetonitrile layers were subjected to flash column chromatography (MeCN → MeCN/H_2O/satd. aq. KNO_3 150:3:1 → 80:3:1 → 50:3:1), whereupon the slightly yellow band eluting under salt conditions was collected. The product fractions were concentrated, and the residue was dissolved in acetonitrile/water 1:1. Then NH_4PF_6 was added, and the acetonitrile was removed. The resulting precipitate was isolated by centrifugation (4000 rpm, 4 °C, 5 min) and washed twice with water to remove the excess amount of salt. The solid was dissolved in acetonitrile, and the gained solution was filtered through cotton before it was concentrated. After drying under vacuum, complex **188** was obtained as a yellow solid (36.3 mg, 37.1 µmol, 73 %). – **$C_{36}H_{20}F_{12}N_8O_6P_2Si$** (M = 978.62 g mol^{-1}). – **^{1}H-NMR** (300 MHz, CD_3CN, 27 mM): δ = 10.34 (dd, ^3J = 8.3 Hz, ^4J = 1.2 Hz, 1H, H_{dppz}), 10.06 (dd, ^3J = 8.3 Hz, ^4J = 1.1 Hz, 1H, H_{dppz}), 9.50 (dd, ^3J = 5.6 Hz, ^4J = 1.2 Hz, 1H, H_{dppz}), 9.48–9.43 (m, 2H, H_{phen}), 9.17 (dd, ^3J = 8.2 Hz, ^4J = 1.1 Hz, 1H, H_{phen}), 8.72 (dd, ^3J = 8.3, 5.6 Hz, 1H, H_{dppz}), 8.65 (d, ^3J = 9.1 Hz, 1H, H_{phen}), 8.63–8.51 (m, 4H, 2 × H_{dppz}, 2 × H_{phen}), 8.29–8.23 (m, 2H, H_{dppz}), 8.14 (dd, ^3J = 8.3, 5.7 Hz, 1H, H_{dppz}), 8.00 (dd, ^3J = 8.2, 5.6 Hz, 1H, H_{phen}), 7.91 (dd, ^3J = 5.6 Hz, ^4J = 1.1 Hz, 1H, H_{phen}), 7.81 (dd, ^3J = 5.7 Hz, ^4J = 1.1 Hz, 1H, H_{dppz}), 7.41 (s, 1H, H_{cat}), 7.39 (s, 1H, H_{cat}) ppm. – **^{13}C-NMR** (126 MHz, CD_3CN, 27 mM): δ = 151.3, 151.1, 150.6, 150.1, 148.7, 148.0, 147.7, 147.3, 144.27, 144.25, 144.2, 143.7, 139.75, 139.69, 139.0, 138.9, 138.2, 137.3, 135.7, 134.8, 134.6, 132.4, 132.0, 131.9, 131.6, 131.1, 130.95, 130.89, 130.87, 130.2, 129.9, 129.6, 129.0, 111.6, 111.4 ppm. – **^{29}Si-NMR** (99.4 MHz, CD_3CN): δ = −149.1 ppm. – **FT-IR** (Film) $\tilde{\nu}$ = 3664, 3114, 1641, 1626, 1586, 1532, 1512, 1496, 1458, 1437, 1374, 1342, 1282, 1236, 1204, 1151, 1119, 1088, 1059, 1025, 889, 831, 779, 759, 745, 727, 718, 659, 645, 622, 596, 557, 523, 497, 462, 430, 395 cm^{-1}. – **HRMS** (ESI+): calc. for $C_{36}H_{20}F_6N_8O_6PSi$ $[M-PF_6]^+$: 833.0911 u, found: 833.0928 u.

(2,2'-Bipyridine)(dipyrido[3,2-*a*:2',3'-*c*]phenazine-κ^2N', N'')(2-(pent-4-yn-1-yl)-1*H*-benzo[*d*]imidazole-5,6-diolato-κ^2O)silicon(IV)-bis(hexafluorophosphate) (190)

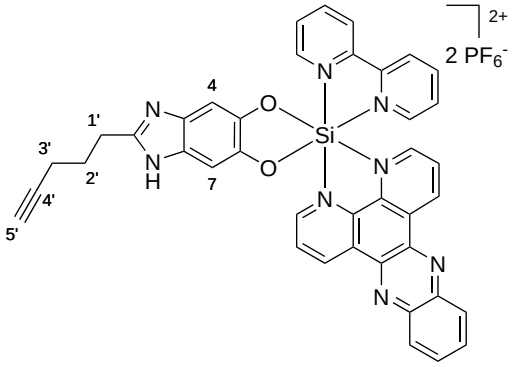

Using method C, silicon complex **187** (16.0 mg, 16.8 µmol), tin powder (17.5 mg, 147 µmol) and 5-hexynal (**189**, 10.0 mg, 104 µmol) were reacted to yield complex **190** as an orange solid (8.7 mg, 8.96 µmol, 53 % over two steps). – **$C_{40}H_{28}F_{12}N_8O_2P_2Si$** (M = 970.73 g mol^{-1}). – **^{1}H-NMR** (300 MHz, CD_3CN, 15 mM): δ = 10.20 (dd, ^3J = 8.3 Hz, ^4J = 1.3 Hz, 1H, H_{dppz}), 10.07 (dd, ^3J = 8.3 Hz, ^4J = 1.1 Hz, 1H, H_{dppz}), 9.46 (dd, ^3J = 5.5 Hz, ^4J = 1.3 Hz, 1H, H_{dppz}), 9.31–9.20 (m, 1H, H_{bpy}), 9.05–8.94 (m, 1H, H_{bpy}), 8.93–8.80 (m, 2H, H_{bpy}), 8.65–8.47 (m, 4H, 3 × H_{dppz}, H_{bpy}), 8.29–8.18 (m, 4H, 3 × H_{dppz}, H_{bpy}), 7.96 (dd, ^3J = 5.7 Hz, ^4J = 1.1 Hz, 1H, H_{dppz}), 7.77–7.70 (m, 1H, H_{bpy}), 7.69–7.63 (m, 1H, H_{bpy}), 7.10 (s, 1H, H-4/7), 6.96 (s, 1H, H-4/7), 3.04–2.95 (m, 2H, H-1'), 2.28 (td, ^3J = 7.0 Hz, ^4J = 2.7 Hz, 2H, H-3'), 2.18 (t, ^4J = 2.6 Hz, 1H, H-5'), 2.03–1.95 (m, 2H, H-2') ppm. – **^{13}C-NMR** (126 MHz, CD_3CN, 15 mM): δ = 153.4, 149.9, 148.9, 148.7, 148.2, 148.1, 146.5, 145.2, 144.9, 144.7, 144.21, 144.15, 144.1, 143.5, 143.1, 139.9, 139.8, 138.5, 137.5, 134.6, 132.1, 131.8, 131.5, 131.3, 130.88, 130.86, 126.3, 126.1, 100.1, 99.9, 84.1, 70.6, 27.4, 27.2, 18.3 ppm. – **^{29}Si-NMR** (99.4 MHz, CD_3CN): δ = −148.0 ppm. – **FT-IR** (Film) $\tilde{\nu}$ = 3650, 3407, 3288, 3109, 2935, 1618, 1577, 1511, 1457, 1430, 1358, 1324, 1251, 1161, 1085, 1058, 1046, 1027, 900, 838, 764, 747, 682, 644, 621, 595, 558, 515, 500, 428, 417, 401, 387 cm^{-1}. – **HRMS** (ESI+): calcd. for $C_{40}H_{28}F_6N_8O_2PSi$ [M−PF_6]$^+$: 825.1741 u, found: 825.1760 u.

(Dipyrido[3,2-*a*:2',3'-*c*]phenazine-κ^2N', N'')(2-(pent-4-yn-1-yl)-1*H*-benzo[*d*]imidazole-5,6-diolato-κ^2O)(1,10-phenanthroline)silicon(IV)-bis(hexafluorophosphate) (191)

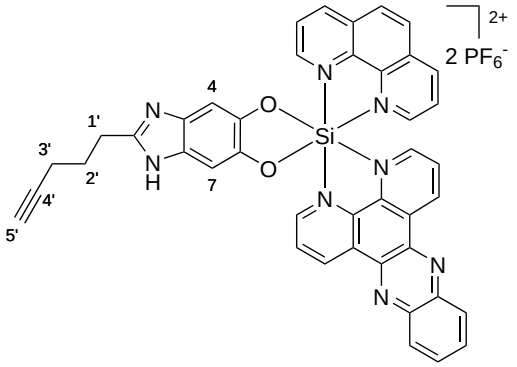

Using method C, silicon complex **188** (15.0 mg, 15.3 µmol), tin powder (16.0 mg, 135 µmol) and 5-hexynal (**189**, 10.0 mg, 104 µmol) were reacted to yield complex **191** as a brownish orange solid (8.7 mg, 8.75 µmol, 57 % over two steps). – **$C_{42}H_{28}F_{12}N_8O_2P_2Si$** (M = 994.75 g mol^{-1}). – **^{1}H-NMR** (300 MHz, CD_3CN, 18 mM): δ = 10.28 (dd, ^3J = 8.3 Hz, ^4J = 1.2 Hz, 1H, H_{dppz}), 10.04 (dd, ^3J = 8.2 Hz, ^4J = 1.1 Hz, 1H, H_{dppz}), 9.56 (dd, ^3J = 5.5 Hz, ^4J = 1.2 Hz, 1H, H_{dppz}), 9.52 (dd, ^3J = 5.4 Hz, ^4J = 1.1 Hz, 1H, H_{phen}), 9.40 (dd, ^3J = 8.4 Hz, ^4J = 1.1 Hz, 1H, H_{phen}), 9.14 (dd, ^3J = 8.1 Hz, ^4J = 1.3 Hz, 1H, H_{phen}), 8.68–8.52 (m, 5H, 3 × H_{dppz}, 2 × H_{phen}), 8.49 (dd, ^3J = 8.4, 5.4 Hz, 1H, H_{phen}), 8.29–8.20 (m, 2H, H_{dppz}), 8.12 (dd, ^3J = 8.3, 5.7 Hz, 1H, H_{dppz}), 8.01–7.91 (m, 2H, H_{phen}), 7.82 (dd, ^3J = 5.7 Hz, ^4J = 1.1 Hz, 1H, H_{dppz}), 7.09 (s, 1H, H-4/7), 7.07 (s, 1H, H-4/7), 3.13–3.00 (m, 2H, H-1'), 2.29 (td, ^3J = 6.9 Hz, ^4J = 2.6 Hz, 2H, H-3'), 2.18 (t, ^3J = 2.7 Hz, 1H, H-5'), 2.06–1.97 (m, 2H, H-2') ppm. – **^{13}C-NMR** (126 MHz, CD_3CN, 18 mM): δ = 153.2, 150.1, 149.6, 148.4, 147.7, 147.3, 146.8, 145.7, 145.6, 144.2, 143.8, 143.1, 139.9, 139.8, 138.4, 137.6, 135.8, 134.8, 134.7, 132.2, 131.9, 131.6, 131.5,

131.1, 130.9, 130.87, 130.8, 129.82, 129.80, 129.4, 128.9, 99.8, 99.7, 83.9, 70.8, 27.1, 27.0, 18.3 ppm. – ^{29}**Si-NMR** (99.4 MHz, CD_3CN): $\delta = -148.4$ ppm. – **FT-IR** (Film) $\tilde{\nu}$ = 3658, 3290, 3111, 2928, 1626, 1585, 1531, 1511, 1473, 1437, 1345, 1323, 1235, 1161, 1119, 1087, 1058, 901, 836, 764, 746, 726, 717, 645, 621, 595, 558, 522, 509, 498, 430, 405 cm^{-1}. – **HRMS** (ESI+): calcd. for $C_{42}H_{28}F_6N_8O_2PSi$ $[M-PF_6]^+$: 849.1741 u, found: 849.1749 u.

5.4.4. Synthesis of Dinuclear Metal-Silicon(IV) Complexes

5,6-Diamino-1,10-phenanthroline (201)

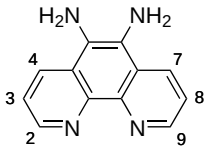

Under an atmosphere of nitrogen, a suspension of 5-amino-6-nitro-1,10-phenanthroline (**200**, 388 mg, 1.62 mmol) in degassed ethanol (80 mL) was treated with palladium on charcoal (10 % palladium, dry, 127 mg, 120 µmol). The nitrogen gas in the flask was slowly exchanged with hydrogen gas by slowly evacuation and refilling several times. The reaction mixture was stirred vigorously under an atmosphere of hydrogen (1 bar) at room temperature for two days. The flask was then purged with nitrogen to remove excess hydrogen gas. The reaction mixture was then filtered through celite and rinsed with ethanol. The solvent was removed (to prevent the formation of unwanted side products the temperature shall not be higher than 35 °C), and the product was dried under vacuum. Compound **201** was obtained as a yellow-orange solid (310 mg, 1.48 mmol, 91 %). The analytical data are in accordance with the literature.[282,315] – $\mathbf{C_{12}H_{10}N_4}$ (M = 210.24 g mol^{-1}). – ^{1}**H-NMR** (300 MHz, DMSO-d_6): δ = 8.77 (dd, ^3J = 4.2 Hz, ^4J = 1.5 Hz, 2H, H-2, H-9), 8.48 (dd, ^3J = 8.5 Hz, ^4J = 1.6 Hz, 2H, H-4, H-7), 7.61 (dd, ^3J = 4.2, 8.4 Hz, 2H, H-3, H-8), 5.23 (s, 4H, NH) ppm. – **HRMS** (ESI+): calcd. for $C_{12}H_{10}N_4Na$ $[M+Na]^+$: 233.0798 u, found: 233.0798 u.

Dipyrido[3,2-*a*:2',3'-*c*]phenazine-7,8-diol (195)

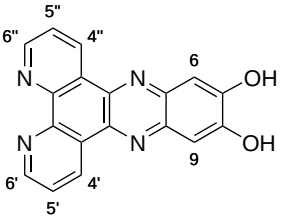

Method 1: A suspension of 5,6-diamino-1,10-phenanthroline (**201**, 179 mg, 851 µmol) and 2,5-dihydroxy-*p*-benzoquinone (**94**, 142 mg, 1.01 mmol) in water (30 mL) was stirred at 105 °C for three days. The reaction mixture was then cooled to −8 °C, the precipitate was isolated by filtration and washed with water, ethanol and diethyl ether until the filtrate was colorless. After drying under vacuum, compound **195** was obtained as a beige, poorly soluble solid (236 mg, 752 µmol, 88 %).

Method 2: 5,6-Diamino-1,10-phenanthroline (**201**, 130 mg, 0.618 µmol) and 2,5-dihydroxy-*p*-benzoquinone (**94**, 100 mg, 714 µmol) were suspended in ethanol (10 mL), and the mixture was stirred at 90 °C for 20 hours. After cooling to room temperature, the solid was isolated by filtration, washed with ethanol until the filtrate was colorless and dried under vacuum. Title compound **195** was obtained as a beige solid (163 mg, 519 µmol, 84 %). – $\mathbf{C_{18}H_{10}N_4O_2}$ (M = 314.30 g mol^{-1}). – ^{1}**H-NMR** (300 MHz, DMSO-d_6, 9 mM): δ = 11.00 (bs, 2H, OH), 9.49 (dd, ^3J = 8.1 Hz, ^4J = 1.7 Hz, 2H, H-4', H-4"), 9.15 (dd, ^3J = 4.4 Hz, ^4J = 1.7 Hz, 2H, H-6', H-6"), 7.90 (dd, ^3J = 8.2, 4.4 Hz, 2H, H-5', H-5"), 7.50 (s, 2H, H-6, H-9) ppm. – **HRMS** (ESI+): calcd. for $C_{18}H_{10}N_4O_2Na$ $[M+Na]^+$: 337.0696 u, found: 337.0697 u.

11,12-Dimethoxydipyrido[3,2-*a*:2',3'-*c*]phenazine (203)

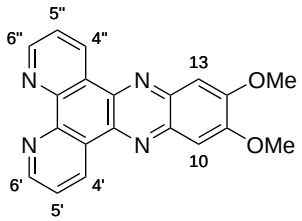

Under an atmosphere of nitrogen, 1,10-phenanthroline-5,6-dione (**198**, 400 mg, 1.90 mmol) and 4,5-dimethoxy-1,2-phenylenediamine (**106**, 350 mg, 2.08 mmol) were dissolved in degassed ethanol (20.0 mL). The solution was heated to 90 °C for six hours. Then it was cooled to room temperature, and the precipitate was isolated by filtration, washed with ethanol and dried under vacuum. 11,12-Dimethoxydipyrido[3,2-*a*:2',3'-*c*]phenazine (**203**) was obtained as a bright beige solid (455 mg, 1.33 mmol, 70 %). – $\mathbf{C_{20}H_{14}N_4O_2}$ (M = 342.35 g mol^{-1}). – ^{1}**H-NMR** (300 MHz, $CDCl_3$): δ = 9.40 (dd, ^3J = 8.1 Hz, ^4J = 1.7 Hz, 2H, H-4', H-4"), 9.22 (dd, ^3J = 4.4 Hz, ^4J = 1.7 Hz, 2H, H-6', H-6"), 7.71 (dd, ^3J = 8.1, 4.4 Hz, 2H, H-5', H-5"), 7.37 (s, 2H, H-10, H-13), 4.13 (s, 6H, OMe) ppm. – ^{13}**C-NMR** (75.0 MHz, $CDCl_3$): δ = 154.1, 151.8, 147.5, 140.4, 138.1, 133.2, 127.7, 123.9, 56.7 ppm. – **FT-IR** (Film) $\tilde{\nu}$ = 3013, 2938, 2833, 2202, 1622, 1575, 1543, 1492, 1460, 1427, 1402, 1354, 1325, 1255, 1221, 1160, 1073, 1010, 938, 911, 885, 839, 810, 725, 689, 641, 538, 406 cm^{-1}. – **HRMS** (ESI+): calcd. for $C_{20}H_{14}N_4O_2Na$ $[M+Na]^+$: 365.1009 u, found: 365.1001 u.

Bis(2,2'-bipyridine)(11,12-dimethoxydipyrido[3,2-*a*:2',3'-*c*]phenazine-κ^2N', N'') ruthenium(II)-bis(hexafluorophosphate) (204)

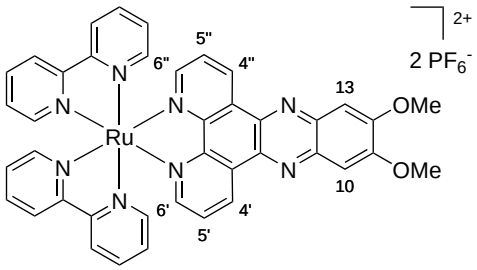

11,12-Dimethoxydipyrido[3,2-*a*:2',3'-*c*]phenazine (**203**, 59.6 mg, 174 μmol) and $[Ru(bpy)_2Cl_2] \cdot 2\,H_2O$ (98.2 mg, 189 μmol) were suspended in ethanol (3.0 mL) and reacted in a micro wave reactor (150 W) at 90 °C for 60 minutes. Afterward, the solvent was removed, and the residue was subjected to flash column chromatography (MeCN → MeCN/H_2O/satd. aq. KNO_3 50:3:1 → 50:6:2), whereupon the red band eluting under salt conditions was collected. The product fractions were concentrated, and the residue was dissolved in acetonitrile/water 0.5:1. Then NH_4PF_6 and some water were added. The resulting precipitate was isolated by centrifugation (4000 rpm, 4 °C, 10 min) and washed twice with water to remove the excess amount of salt. Then it was dissolved in acetonitrile, and the gained solution was filtered through cotton before it was concentrated. After drying under vacuum, ruthenium complex **204** was obtained as a red solid (170 mg, 163 μmol, 93 %). – $\mathbf{C_{40}H_{30}F_{12}N_8O_2P_2Ru}$ (M = 1045.72 g mol^{-1}). – ^{1}**H-NMR** (300 MHz, CD_3CN, 14 mM): δ = 9.57 (dd, ^3J = 8.3 Hz, ^4J = 1.3 Hz, 2H, H-4', H-4"), 8.57–8.51 (m, 4H, H_{bpy}), 8.15–9.09 (m, 4H, H-6', H-6", H_{bpy}), 8.02 (td, ^3J = 7.9 Hz, ^4J = 1.5 Hz, 2H, H_{bpy}), 7.88–7.84 (m, 4H, H-5', H-5", H_{bpy}), 7.73–7.70 (m, 2H, H_{bpy}), 7.60 (s, 2H, H-10, H-13), 7.45 (ddd, ^3J = 7.6, 5.7 Hz, ^4J = 1.3 Hz, 2H, H_{bpy}), 7.26 (ddd, ^3J = 7.6, 5.7 Hz, ^4J = 1.3 Hz, 2H, H_{bpy}), 4.08 (s, 6H, OMe) ppm. – ^{13}**C-NMR** (75.5 MHz, CD_3CN, 14 mM): δ = 158.3, 158.1, 156.8, 153.9, 153.1, 153.0, 150.4, 142.3, 139.0, 138.9, 138.5, 134.0, 131.9, 128.6, 128.5, 128.1, 125.4, 125.3, 107.0, 57.5 ppm. – **FT-IR** (Film) $\tilde{\nu}$ = 3659, 3086, 2944, 1624, 1604, 1548, 1493, 1466, 1447, 1426, 1353, 1315, 1270, 1223, 1178, 1162, 1124, 1004, 836, 764, 731, 661, 592, 558, 541, 492, 422 cm^{-1}. – **HRMS** (ESI+): calcd. for $C_{40}H_{30}N_8O_2RuPF_6$ $[M-PF_6]^+$: 901.1182 u,

found: 901.1173 u. – **R_f:** 0.22 (MeCN/H_2O/satd. aq. KNO_3 50:6:2).

(11,12-Dimethoxydipyrido[3,2-*a*:2',3'-*c*]phenazine-κ^2N', N'')bis(2-phenylpyridinato)iridium(III)-hexafluorophosphate (205)

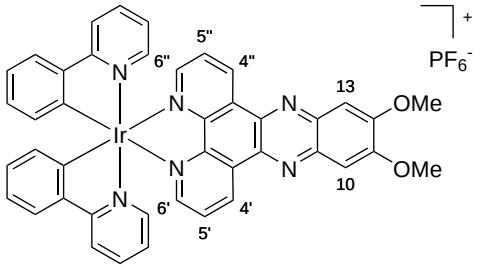

Under an atmosphere of nitrogen, 11,12-dimethoxydipyrido[3,2-*a*:2',3'-*c*]phenazine (**203**, 42.3 mg, 124 µmol) was dissolved in a mixture of anhydrous methanol (5.0 mL) and anhydrous dichloromethane (5.0 mL). The orange-brwon solution was treated with $[Ir(\mu\text{-Cl})(ppy)_2]_2$ (61.8 mg, 57.6 µmol) and stirred at 50 °C for three days. After cooling to room temperature, the solvent was removed. The orange residue was subjected to flash column chromatography (MeCN → MeCN/H_2O/satd. aq. KNO_3 150:3:1 → 100:3:1). The yellow band eluting under salt conditions was collected, and the product fractions were concentrated. The obtained residue was dissolved in water/acetonitrile 1:1. Then NH_4PF_6 was added, and complex **205** was precipitated upon addition of water. The resulting precipitate was isolated by centrifugation (4000 rpm, 4 °C, 10 min) and washed twice with water to remove the excess amount of salt. The solid was dissolved in acetonitrile, and the gained solution was filtered through cotton before it was concentrated. After drying under vacuum, complex **205** was obtained as an orange solid (86.8 mg, 87.9 µmol, 76 %). – **$C_{42}H_{30}F_6IrN_6O_2P$** ($M = 987.91\,g\,mol^{-1}$). – **^{1}H-NMR** (300 MHz, CD_3CN, 28 mM): δ = 9.42 (dd, ^3J = 8.3 Hz, ^4J = 1.3 Hz, 2H, H-4', H-4"), 8.36 (dd, ^3J = 5.1 Hz, ^4J = 1.4 Hz, 2H, H-6', H-6"), 8.10 (d, ^3J = 8.0 Hz, 2H, H_{ppy}), 7.88–7.80 (m, 6H, H-5', H-5", H_{ppy}), 7.64 (dd, ^3J = 5.8 Hz, ^4J = 0.7 Hz, 2H, H_{ppy}), 7.33 (s, 2H, H-10, H-13), 7.11 (dd, ^3J = 7.6 Hz, ^4J = 1.2 Hz, 2H, H_{ppy}), 7.02–6.93 (m, 4H, H_{ppy}), 6.42 (dd, ^3J = 7.5 Hz, ^4J = 0.9 Hz, 2H, H_{ppy}), 3.94 (s, 6H, OMe) ppm. – **^{13}C-NMR** (75.5 MHz, CD_3CN, 28 mM): δ = 168.6, 156.6, 152.8, 150.7, 150.6, 149.5, 145.3, 142.0, 139.6, 138.1, 135.4, 132.7, 132.0, 131.5, 128.8, 126.0, 124.5, 123.8, 120.9, 106.8, 57.4 ppm. – **FT-IR** (Film) $\tilde{\nu}$ = 3046, 1605, 1583, 1551, 1487, 1424, 1360, 1315, 1270, 1223, 1162, 1083, 1005, 839, 759, 733, 557, 421 cm^{-1}. – **HRMS** (ESI+): calcd. for $C_{42}H_{30}IrN_6O_2$ $[M-PF_6]^+$: 843.2056 u, found: 843.2042 u. – **R_f:** 0.21 (MeCN/H_2O/satd. aq. KNO_3 100:3:1).

Bis(2,2'-bipyridine)(1,10-phenanthroline-5,6-dione-κ^2N)ruthenium(II)-bis(hexafluorophosphate) (209)

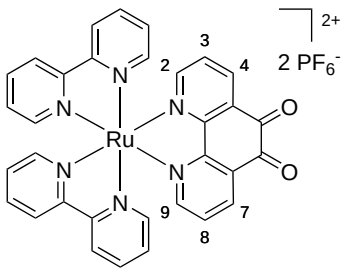

A suspension of 1,10-phenanthroline-5,6-dione (**198**, 25.0 mg, 119 µmol) and $[Ru(bpy)_2Cl_2] \cdot 2\,H_2O$ (60.0 mg, 115 µmol) in ethanol (3.0 mL) was reacted in a micro wave reactor (150 W) at 90 °C for 60 minutes. The solvent was removed, and the residue was subjected to flash column chromatography (MeCN → MeCN/H_2O/satd. aq. KNO_3 50:3:1 → 50:6:2). The black band eluting under salt conditions was collected, and the product fractions were concentrated. The residue was redissolved in acetonitrile/water 0.5:1. Then NH_4PF_6 and some water were added. The resulting precipitate was isolated

by centrifugation (4000 rpm, 4 °C, 10 min) and washed twice with water to remove the excess amount of salt. The solid was dissolved in acetonitrile, and the gained solution was filtered through cotton before it was concentrated. After drying under vacuum, ruthenium complex **204** was obtained as a black solid (75.8 mg, 83.0 μmol, 72 %). The analytical data are in accordance with the literature.[259] – **$C_{32}H_{22}F_{12}N_6O_2P_2Ru$** (M = 913.56 g mol^{-1}). – **^{1}H-NMR** (300 MHz, CD_3CN): δ = 8.55–8.48 (m, 6H, H-4, H-7, H_{bpy}), 8.13–8.05 (m, 4H, H_{bpy}), 7.98 (dd, ^3J = 5.6 Hz, ^3J = 1.4 Hz, 2H, H-2, H-9), 7.84 (ddd, ^3J = 5.6 Hz, ^4J = 1.4 Hz, ^5J = 0.7 Hz, 2H, H_{bpy}), 7.75 (ddd, ^3J = 5.6 Hz, ^4J = 1.3 Hz, ^5J = 0.7 Hz, 2H, H_{bpy}), 7.61 (dd, ^3J = 8.0, 5.6 Hz, 2H, H-3, H-8), 7.42 (ddt, ^3J = 7.1, 5.6 Hz, ^4J = 2.1 Hz, 4H, H_{bpy}) ppm. – **^{13}C-NMR** (75.5 MHz, CD_3CN): δ = 176.3, 158.01, 157.97, 157.5, 157.3, 153.2, 152.9, 152.7, 139.4, 139.3, 137.0, 131.8, 129.8, 128.8, 128.7, 125.51, 125.48, 125.3 ppm. – **FT-IR** (Film) $\tilde{\nu}$ = 3650, 3090, 2358, 1702, 1604, 1567, 1467, 1447, 1428, 1296, 1244, 1188, 1162, 1127, 1106, 1070, 1038, 940, 834, 763, 730, 557, 420, 395 percm. – **HRMS** (ESI+): calcd. for $C_{32}H_{22}N_6O_2RuPF_6$ $[M-PF_6]^+$: 769.0493 u, found: 769.0477 u. – **R_f:** 0.26 ($MeCN/H_2O$/satd. aq. KNO_3 50:6:2).

Bis(1,10-phenanthroline)(1,10-phenanthroline-5,6-dione-κ^2N)ruthenium(II)-bis(hexafluorophosphate) (210)

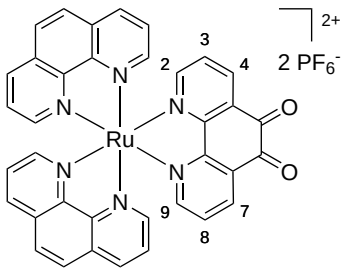

A suspension of 1,10-phenanthroline-5,6-dione (**198**, 49.8 mg, 209 μmol) and $[RuCl_2(phen)_2] \cdot 2\,H_2O$ (116 mg, 205 μmol) in ethanol (20 mL) was stirred at 90 °C for four hours. After cooling to room temperature, the solvent was removed, and the residue was subjected to flash column chromatography ($MeCN \rightarrow MeCN/H_2O$/satd. aq. KNO_3 50:3:1 → 50:6:2). The brown band eluting under salt conditions was collected, and the product fractions were concentrated. The residue was redissolved in acetonitrile/water 0.5:1. Then NH_4PF_6 and some water were added. The resulting precipitate was isolated by centrifugation (4000 rpm, 4 °C, 10 min) and washed twice with water to remove the excess amount of salt. The solid was dissolved in acetonitrile, and the gained solution was filtered through cotton before it was concentrated. After drying under vacuum, ruthenium complex **210** was obtained as a black solid (86.2 mg, 89.6 μmol, 44 %). The analytical data are in accordance with the literature.[157] – **$C_{36}H_{22}F_{12}N_6O_2P_2Ru$** (M = 961.61 g mol^{-1}). – **^{1}H-NMR** (300 MHz, CD_3CN): δ = 8.70 (dd, ^3J = 8.3 Hz, ^4J = 1.2 Hz, 2H, H_{phen}), 8.59 (dd, ^3J = 8.3 Hz, ^4J = 1.2 Hz, 2H, H_{phen}), 8.49 (dd, ^3J = 8.0 Hz, ^4J = 1.4 Hz, 2H, H-4, H-7), 8.33 (dd, ^3J = 5.2 Hz, ^4J = 1.2 Hz, 2H, H_{phen}), 8.29 (d, ^3J = 8.9 Hz, 2H, H_{phen}), 8.25 (d, ^3J = 8.9 Hz, 2H, H_{phen}), 7.93–7.88 (m, 4H, H_{phen}, H-2, H-9), 7.82 (dd, ^3J = 8.3, 5.3 Hz, 2H, H_{phen}), 7.59 (dd, ^3J = 8.3, 5.3 Hz, 2H, H_{phen}), 7.49 (dd, ^3J = 8.0, 5.6 Hz, 2H, H-3, H-8) ppm. – **^{13}C-NMR** (75.5 MHz, CD_3CN): δ = 176.4, 158.1, 157.7, 154.3, 153.9, 148.8, 148.6, 138.4, 138.2, 136.9, 132.20, 132.16, 131.7, 129.6, 129.2, 127.0 ppm. – **FT-IR** (Film) $\tilde{\nu}$ = 3649, 3320, 3093, 1701, 1567, 1429, 1299, 1208, 1148, 1071, 1025, 944, 836, 722, 558, 408, 398 percm. – **HRMS** (ESI+): calcd. for $C_{36}H_{22}N_6O_2Ru$ $[M-2PF_6]^{2+}$: 336.0423 u, found: 336.0413 u. – **R_f:** 0.37 ($MeCN/H_2O$/satd. aq. KNO_3 50:6:2).

Bis(5,6-dimethyl-1,10-phenanthroline)(1,10-phenanthroline-5,6-dione-κ^2N) ruthenium(II)-bis(hexafluorophosphate) (211)

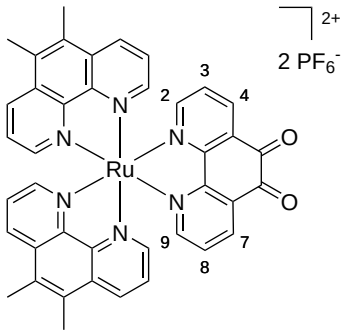

A suspension of 1,10-phenanthrolin-5,6-dione (**198**, 23.3 mg, 111 μmol) and $[RuCl_2(dmphen)] \cdot 2\,H_2O$ (68.0 mg, 109 μmol) in ethanol was stirred at 90 °C) for 3.5 hours. After cooling to room temperature, the solvent was removed and the black residue was subjected to gravity column chromatography (MeCN → MeCN/H_2O/satd. aq. KNO_3 50:3:1 → 50:6:2), whereupon the black band eluting under salt conditions was collected. The product fractions were concentrated, and the residue was dissolved in water. NH_4PF_6 was added, and the solution was extracted with dichloromethane until the water layer was colorless. The combined organic layers were dried over anhydrous sodium sulfate and concentrated. After drying under vacuum, ruthenium complex **211** was obtained as a black solid (81.9 mg, 80.5 μmol, 74 %). – $\mathbf{C_{40}H_{30}F_{12}N_6O_2P_2Ru}$ (M = 1017.72 g mol^{-1}). – **^{1}H-NMR** (300 MHz, CD_3CN): δ = 8.82 (dd, ^3J = 8.6 Hz, ^4J = 1.0 Hz, 2H, H_{phen}), 8.70 (dd, ^3J = 8.6 Hz, ^4J = 1.0 Hz, 2H, 2H, H_{phen}), 8.48 (dd, ^3J = 8.0 Hz, ^4J = 1.3 Hz, 2H, H-4, H-7), 8.26 (dd, ^3J = 5.1 Hz, ^4J = 0.9 Hz, 2H, 2H, H_{phen}), 7.87 (dd, ^3J = 5.6 Hz, ^4J = 1.3 Hz, 2H, H-2, H-9), 7.84–7.76 (m, 4H, 2H, H_{phen}), 7.58 (dd, ^3J = 8.6, 5.2 Hz, 2H, 2H, H_{phen}), 7.48 (dd, ^3J = 8.0, 5.6 Hz, 2H, H-3, H-8), 2.86 (s, 6H, 2H, H_{Methyl}), 2.83 (s, 6H, 2H, H_{Methyl}) ppm. – **^{13}C-NMR** (75.5 MHz, CD_3CN): δ = 176.5, 157.8, 157.6, 152.8, 152.3, 147.8, 147.7, 136.8, 135.3, 135.1, 133.8, 133.7, 132.6, 132.5, 131.7, 129.5, 126.7, 126.6, 15.67, 15.65 ppm. – **FT-IR** (Film) $\tilde{\nu}$ = 3656, 1704, 1615, 1568, 1483, 1428, 1296, 1108, 1070, 942, 840, 805, 725, 557, 455, 424, 397 percm. – **HRMS** (ESI+): calcd. for $C_{40}H_{30}N_6O_2RuPF_6$ $[M-PF_6]^+$: 873.1121 u, found: 873.1102 u. – **R_f:** 0.42 (MeCN/H_2O/satd. aq. KNO_3 50:6:2).

(1,10-Phenanthroline-5,6-dione-κ^2N)bis(2-phenylpyridinato)iridium(III)-hexafluorophosphate (212)

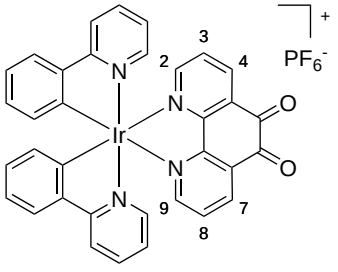

Under an atmosphere of nitrogen, 1,10-phenanthroline-5,6-dione (**198**, 40.5 mg, 193 μmol) and $[Ir(\mu\text{-}Cl)(ppy)_2]_2$ (103 mg, 95.6 μmol) were dissolved in a mixture of anhydrous methanol (5.0 mL) and anhydrous dichloromethane (5.0 mL). The solution was stirred at 55 °C for two hours. After cooling to room temperature, the solvent was removed and the residue was subjected to flash column chromatography (MeCN → MeCN/H_2O/satd. aq. KNO_3 100:3:1), whereupon the dark brown band eluting under salt conditions was collected. The product fractions were concentrated, and the residue was dissolved in acetonitrile/water 2:1. Then NH_4PF_6 was added, and complex **212** was precipitated upon addition of excess water. The resulting solid was isolated by centrifugation (4000 rpm, 4 °C, 10 min) and washed twice with water to remove the excess amount of salt. The solid was dissolved in acetonitrile, and the gained solution was filtered through cotton before it was concentrated. After drying under vacuum, iridium complex **212** was obtained as a black solid (136 mg, 159 μmol, 82 %). – $\mathbf{C_{34}H_{22}F_6IrN_4O_2P}$ (M = 855.75 g mol^{-1}). – **^{1}H-NMR** (300 MHz, CD_3CN): δ = 8.62 (dd,

^3J = 8.1 Hz, ^4J = 1.5 Hz, 2H, H-4, H-7), 8.20 (dd, ^3J = 5.4 Hz, ^4J = 1.5 Hz, 2H, H-2, H-9), 8.13–8.06 (m, 2H, H_{ppy}), 7.91–7.81 (m, 4H, H_{ppy}), 7.75–7.68 (m, 4H, H-3, H-8, H_{ppy}), 7.10–7.03 (m, 4H, H_{ppy}), 6.95 (td, ^3J = 7.5 Hz, ^4J = 1.3 Hz, 2H, H_{ppy}), 6.30 (dd, ^3J = 7.5 Hz, ^4J = 0.9 Hz, 2H, H_{ppy}) ppm. – **^{13}C-NMR** (75.5 MHz, CD_3CN): δ = 176.3, 156.0, 150.6, 149.4, 145.1, 139.9, 138.6, 132.6, 132.0, 131.5, 131.0, 126.0, 124.6, 124.0, 123.5, 121.1 ppm. – **FT-IR** (Film) $\tilde{\nu}$ = 3062, 1701, 1608, 1583, 1572, 1479, 1428, 1299, 1270, 1228, 1207, 1165, 1127, 1066, 1031, 939, 840, 759, 730, 716, 670, 631, 557, 418, 387 cm^{-1}. – **HRMS** (ESI+): calcd. for $C_{34}H_{22}IrN_4O_2$ $[M-PF_6]^+$: 711.1368 u, found: 711.1370 u. – **R_f:** 0.21 ($MeCN/H_2O$/satd. aq. KNO_3 100:3:1).

(1,10-Phenanthroline-5,6-dione-κ^2N)bis(2-phenylpyridinato)rhodium(III)-hexafluorophosphate (213)

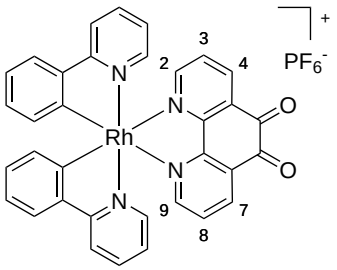

Under an atmosphere of nitrogen, 1,10-phenanthroline-5,6-dione (**198**, 44.0 mg, 209 μmol) and $[Rh(\mu\text{-Cl})(ppy)_2]_2$ (90.0 mg, 101 μmol) were dissolved in a mixture of ethanol (10.0 mL) and anhydrous dichloromethane (5.0 mL). The solution was stirred at 70 °C for three hours. After cooling to room temperature, the solvent was removed and the residue was subjected to flash column chromatography (MeCN → $MeCN/H_2O$/satd. aq. KNO_3 100:3:1), whereupon the brown band eluting under salt conditions was collected. The product fractions were concentrated, and the residue was dissolved in acetonitrile/water 2:1. Then NH_4PF_6 was added, and complex **213** was precipitated upon addition of excess water. The resulting solid was isolated by centrifugation (4000 rpm, 4 °C, 5 min) and washed twice with water to remove the excess amount of salt. The solid was dissolved in acetonitrile, and the gained solution was filtered through cotton before it was concentrated. After drying under vacuum, iridium complex **213** was obtained as a brownish yellow solid (139 mg, 181 μmol, 90 %). – **$C_{34}H_{22}F_6N_4O_2PRh$** (M = 766.45 g mol^{-1}). – **^{1}H-NMR** (300 MHz, CD_3CN): δ = 8.64 (d, ^3J = 7.7 Hz, 2H, H-4, H-7), 8.27–8.17 (m, 2H, H-2, H-9), 8.13–8.08 (m, 2H, H_{ppy}), 8.00–7.91 (m, 2H, H_{ppy}), 7.88 (dd, ^3J = 7.8 Hz, ^4J = 1.3 Hz, 2H, H_{ppy}), 7.74 (dd, ^3J = 8.0, 5.3 Hz, 2H, H-3, H-8), 7.69–7.62 (m, 2H, H_{ppy}), 7.20–7.06 (m, 4H, H_{ppy}), 7.01 (td, ^3J = 7.5 Hz, ^4J = 1.4 Hz, 2H, H_{ppy}), 6.33 (d, ^3J = 7.7 Hz, 2H, H_{ppy}) ppm. – **^{13}C-NMR** (75.5 MHz, CD_3CN): δ = 176.9, 167.0, 166.5, 165.6, 155.7, 154.4, 150.5, 145.0, 139.9, 139.1, 133.6, 131.2, 130.3, 125.8, 124.8, 124.6, 121.2 ppm. – **FT-IR** (Film) $\tilde{\nu}$ = 3651, 3047, 1698, 1606, 1574, 1480, 1426, 1374, 1300, 1271, 1251, 1227, 1208, 1165, 1126, 1106, 1067, 1025, 937, 876, 831, 757, 732, 712, 704, 668, 651, 630, 556, 488, 416, 387 cm^{-1}. – **HRMS** (ESI+): calcd. for $C_{34}H_{22}N_4O_2Rh$ $[M-PF_6]^+$: 621.0792 u, found: 621.0795 u. – **R_f:** 0.49 ($MeCN/H_2O$/satd. aq. KNO_3 50:3:1).

Bis(2,2'-bipyridine)(2,9-dimethyl-1,10-phenanthroline)ruthenium(II)-bis(hexafluorophosphate) (218)

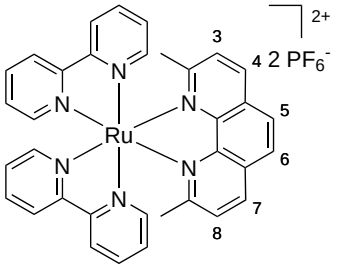

The reaction and the work-up were performed under exclusion of light to avoid decomposition of the product. In a brown glass vial, a mixture of 2,9-dimethyl-1,10-phenanthroline (**288**, 36.0 mg, 173 µmol) and $[Ru(bpy)_2Cl_2] \cdot 2\,H_2O$ (53.0 mg, 102 μmol) in anhydrous ethylene glycol (2 mL) was purged with nitrogen for five minutes before it was stirred at 200 °C for 20 hours. After cooling to room temperature, the red solution was poured into water (12 mL). NH_4PF_6 was added, the precipitate was isolated by centrifugation (4000 rpm, 4 °C, 10 min) and washed once with water. The red solid was subjected to flash column chromatography (MeCN → MeCN/H_2O/satd. aq. KNO_3 50:3:1 → 50:6:2), whereupon the red band eluting under salt conditions was collected. The product fractions were concentrated, and the solid was dissolved in acetonitrile/water 0.5:1. Then excess NH_4PF_6 and some water were added, and the resulting precipitate was isolated by centrifugation (4000 rpm, 4 °C, 10 min). The precipitate was washed twice with water to remove the excess amount of salt. The solid was dissolved in acetonitrile, and the gained solution was filtered through cotton before it was concentrated. After drying under vacuum, ruthenium complex **218** was obtained as an orange red solid (81.3 mg, 89.2 μmol, 87 %). – **$C_{34}H_{28}F_{12}N_6P_2Ru$** (M = 911.64 g mol^{-1}). – **^{1}H-NMR** (300 MHz, CD_3CN): δ = 8.53–8.40 (m, 6H, H_{bpy}, H-4, H-7), 8.10 (s, 2H, H-5, H-6), 8.00 (dtd, ^3J = 12.9, 8.1 Hz, ^4J = 1.5 Hz, 4H, H_{bpy}), 7.74–7.65 (m, 2H, H_{bpy}), 7.65–7.57 (m, 4H, H_{bpy}, H-3, H-8), 7.30–7.21 (m, 4H, H_{bpy}), 1.91 (s, 6H, H_{Methyl}) ppm. – **^{13}C-NMR** (75.5 MHz, CD_3CN): δ = 168.1, 158.6, 158.5, 153.9, 152.9, 149.6, 138.8, 138.6, 130.5, 128.6, 128.4, 128.2, 128.1, 125.4, 125.4, 26.2 ppm. – **FT-IR** (Film) $\tilde{\nu}$ = 3671, 3086, 1629, 1604, 1510, 1467, 1447, 1425, 1379, 1349, 1313, 1272, 1242, 1162, 1034, 833, 765, 732, 660, 557, 428 percm. – **HRMS** (ESI+): calcd. for $C_{34}H_{28}N_6Ru$ $[M-2PF_6]^{2+}$: 311.0708 u, found: 311.0700 u. – **R_f:** 0.29 (MeCN/H_2O/satd. aq. KNO_3 50:6:2)

Bis(2,2'-bipyridine)(2,9-dimethyl-1,10-phenanthroline-5,6-dione-κ^2N)ruthenium(II)-bis(hexafluorophosphate) (217)

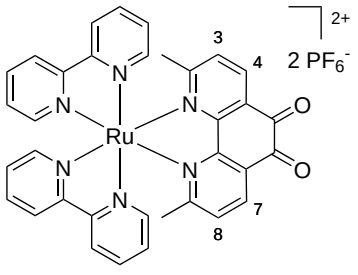

The reaction and the work-up were performed under exclusion of light to avoid decomposition of the product. Sodium bromate (26.7 mg, 177 µmol) was added to a suspension of bis(2,2'-bipyridine)(2,9-dimethyl-1,10-phenanthroline)ruthenium(II)-bis (hexafluorophosphate) (**218**, 114 mg, 125 µmol) in sulfuric acid (60 %, 1.5 mL). The resulting green solution was stirred at room temperature for 20 hours before it was poured on ice. The mixture was neutralized with a concentrated sodium hydroxide solution until pH reached 6–7. The dark solution was treated with NH_4PF_6, the precipitate was isolated by centrifugation (4000 rpm, 4 °C, 10 min) and washed twice with water to remove the excess amount of salt. The solid was dissolved in acetonitrile, and the gained solution was filtered through cotton before it was concentrated. After drying under vacuum, ruthenium complex **217** was obtained as a dark brown solid (99.1 mg, 105 µmol, 84 %). As the ^{1}H-NMR spectra showed

some impurities that could not be remove by flash column chromatography, the complex was used for the next step without further purification. – **$C_{34}H_{26}F_{12}N_6O_2P_2Ru$** (M = 941.62 g mol^{-1}). – **^{1}H-NMR** (300 MHz, CD_3CN): δ = 8.56–8.50 (m, 2H, H_{bpy}), 8.48–8.40 (m, 4H, H_{bpy}, H-4, H-7), 8.14 (td, ^3J = 8.0 Hz, ^4J = 1.5 Hz, 2H, H_{bpy}), 8.01–7.94 (m, 4H, H_{bpy}), 7.64–7.59 (m, 2H, H_{bpy}), 7.54–7.46 (m, 4H, H_{bpy}, H-3, H-8), 7.26 (ddd, ^3J = 7.2, 5.7 Hz, ^4J = 1.3 Hz, 2H, H_{bpy}), 1.79 (s, 6H, H_{Methyl}) ppm. – **^{13}C-NMR** (75.5 MHz, CD_3CN): δ = 173.1, 158.6, 158.4, 158.3, 154.2, 152.8, 139.3, 139.2, 137.9, 130.5, 129.6, 129.0, 128.5, 125.8, 125.6, 26.8 ppm. – **FT-IR** (Film) $\tilde{\nu}$ = 3664, 3087, 1698, 1605, 1589, 1569, 1467, 1447, 1378, 1362, 1319, 1243, 1162, 1141, 1127, 1036, 941, 835, 766, 733, 660, 557, 427 cm^{-1}. – **HRMS** (ESI+): calcd. for $C_{34}H_{26}N_6O_2Ru$ $[M-2PF_6]^{2+}$: 326.0579 u, found: 326.0569 u. – **R_f:** 0.29 ($MeCN/H_2O$/satd. aq. KNO_3 50:6:2)

Bis(2,2'-bipyridine)(3,4,7,8-tetramethyl-1,10-phenanthroline)ruthenium(II)-bis(hexafluorophosphate) (220)

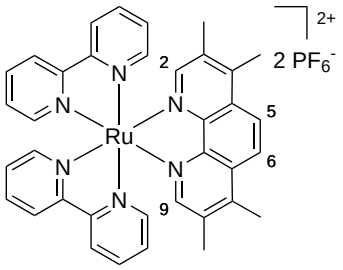

A suspension of 3,4,7,8-tetramethyl-1,10-phenanthroline (29.3 mg, 124 µmol) and $[Ru(bpy)_2Cl_2] \cdot 2\,H_2O$ (62.4 mg, 120 µmol) in ethanol (10.0 mL) was stirred at 90 °C for 16 hours. After cooling to room temperature, the solvent was removed, and the residue was subjected to flash column chromatography ($MeCN \rightarrow MeCN/H_2O$/satd. aq. KNO_3 50:3:1 $\rightarrow$ 50:6:2), whereupon the red band eluting under salt conditions was collected. The product fractions were concentrated, and the residue was redissolved in acetonitrile/water 0.5:1. Then NH_4PF_6 and some water were added. The resulting precipitate was isolated by centrifugation (4000 rpm, 4 °C, 5 min) and washed twice with water to remove the excess amount of salt. The solid was dissolved in acetonitrile, and the gained solution was filtered through cotton before it was concentrated. After drying under vacuum, ruthenium complex **220** was obtained as a red solid (112 mg, 119 μmol, 96 %). – **$C_{36}H_{32}F_{12}N_6P_2Ru$** (M = 939.69 g mol^{-1}). – **^{1}H-NMR** (300 MHz, CD_3CN): δ = 8.55–8.45 (m, 4H, H_{bpy}), 8.37 (s, 2H, H-2, H-9), 8.07 (td, ^3J = 8.1 Hz, ^4J = 1.5 Hz, 2H, H_{bpy}), 7.98 (td, ^3J = 8.1 Hz, ^4J = 1.5 Hz, 2H, H_{bpy}), 7.82 (ddd, ^3J = 5.6 Hz, ^4J = 1.3 Hz, ^5J = 0.7 Hz, 2H, H_{bpy}), 7.77 (s, 2H, H-5, H-6), 7.58–7.49 (m, 2H, H_{bpy}), 7.42 (ddd, ^3J = 7.5, 5.6 Hz, ^4J = 1.3 Hz, 2H, H_{bpy}), 7.21 (ddd, ^3J = 7.5, 5.7 Hz, ^4J = 1.3 Hz, 2H, H_{bpy}), 2.79 (s, 6H, H_{Methyl}), 2.33 (s, 6H, H_{Methyl}) ppm. – **^{13}C-NMR** (75.5 MHz, CD_3CN): δ = 158.4, 158.3, 153.5, 152.9, 152.6, 147.0, 146.0, 138.5, 138.4, 136.0, 130.5, 128.5, 128.1, 125.2, 18.0, 15.1 ppm. – **FT-IR** (Film) $\tilde{\nu}$ = 2931, 1750, 1604, 1466, 1447, 1426, 1352, 1271, 1112, 838, 764, 732, 558, 475, 419 percm. – **HRMS** (ESI+): calcd. for $C_{36}H_{32}N_6RuPF_6$ $[M-PF_6]^+$: 795.1377 u, found: 795.1377 u. – **R_f:** 0.35 ($MeCN/H_2O$/satd. aq. KNO_3 50:6:2).

Bis(2,2'-bipyridine)3,4,7,8-tetramethyl-1,10-phenanthroline-5,6-dione-κ^2N) ruthenium(II)-bis(hexafluorophosphate) (221)

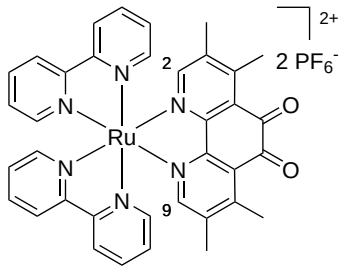

Sodium bromate (9.8 mg, 64.9 µmol) was added to a suspension of bis(2,2'-bipyridine)(3,4,7,8-dimethyl-1,10-phenanthroline)ruthenium(II)-bis(hexafluorophosphate) (**220**, 34.8 mg, 37.0 µmol) in sulfuric acid (60 %, 1.0 mL). The resulting green solution was stirred at room temperature for 20 hours before it was poured on ice. The mixture was neutralized with a concentrated sodium hydroxide solution until pH reached 6–7. The dark solution was treated with NH_4PF_6, the precipitate was isolated by centrifugation (4000 rpm, 4 °C, 10 min) and washed twice with water to remove the excess amount of salt. The solid was dissolved in acetonitrile, and the gained solution was filtered through cotton before it was concentrated. After drying under vacuum, ruthenium complex **221** was obtained as a dark brown solid (30.3 mg, 31.2 µmol, 84 %). As the ^{1}H-NMR spectra showed some minor impurities that could not be remove by flash column chromatography, the complex was used for the next step without further purification. – **$C_{36}H_{30}F_{12}N_6O_2P_2Ru$** (M = 969.67 g mol^{-1}). – **^{1}H-NMR** (300 MHz, CD_3CN): δ = 8.54–8.47 (m, 4H, H_{bpy}), 8.13–8.02 (m, 4H, H_{bpy}), 7.87–7.82 (m, 2H, H_{bpy}), 7.71–7.67 (m, 2H, H_{bpy}), 7.61 (s, 2H, H-2, H-9), 7.46–7.36 (m, 4H, H_{bpy}), 2.72 (s, 6H, H_{Methyl}), 2.19 (s, 6H, H_{Methyl}) ppm. – **FT-IR** (Film) $\tilde{\nu}$ = 3660, 3084, 1697, 1604, 1537, 1465, 1445, 1425, 1375, 1313, 1287, 1272, 1243, 1220, 1162, 1101, 1026, 964, 876, 830, 762, 732, 661, 648, 556, 470, 422, 395 cm^{-1}. – **HRMS** (ESI+): calcd. for $C_{36}H_{30}N_6O_2RuPF_6$ $[M-PF_6]^+$: 825.1120 u, found: 825.1130 u.

Bis(acetonitrile)bis(2,2'-bipyridine)ruthenium(II)-bis(hexafluorophosphate) (240)

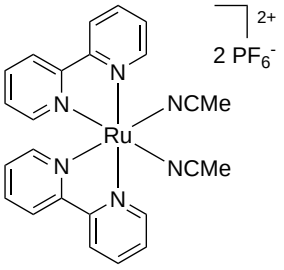

Under exclusion of light, a suspension of $[Ru(bpy)_2Cl_2] \cdot 2\,H_2O$ (31.8 mg, 61.1 µmol) and silver nitrate (61.8 mg, 364 µmol) in acetonitrile (5.0 mL) was stirred at 90 °C for 3.5 hours. The yellow solution was cooled to room temperature and subjected to flash column chromatography (MeCN → MeCN/H_2O/satd. aq. KNO_3 50:3:1 → 50:6:2), whereupon the yellow band eluting under salt conditions was collected. The product fractions were concentrated, and the residue was redissolved in acetonitrile/water 0.5:1. Then NH_4PF_6 and some water were added. The resulting precipitate was isolated by centrifugation (4000 rpm, 4 °C, 10 min) and washed twice with water to remove the excess amount of salt. The solid was dissolved in acetonitrile, and the gained solution was filtered through cotton before it was concentrated. After drying under vacuum, ruthenium complex **240** was obtained as a bright yellow solid (37.1 mg, 47.2 µmol, 77 %). – **$C_{24}H_{22}F_{12}N_6P_2Ru$** (M = 785.48 g mol^{-1}). – **^{1}H-NMR** (300 MHz, CD_3CN): δ = 9.32 (ddd, ^3J = 5.6 Hz, ^4J = 1.4 Hz, ^5J = 0.7 Hz, 2H, H_{bpy}), 8.55–8.48 (m, 2H, H_{bpy}), 8.43–8.33 (m, 2H, H_{bpy}), 8.27 (td, ^3J = 7.9 Hz, ^4J = 1.5 Hz, 2H, H_{bpy}), 7.94 (td, ^3J = 7.9 Hz, ^4J = 1.5 Hz, 2H, H_{bpy}), 7.85 (ddd, ^3J = 7.6, 5.6 Hz, ^4J = 1.3 Hz, 2H, H_{bpy}), 7.59 (ddd, ^3J = 5.7 Hz, ^4J = 1.4 Hz, ^5J = 0.7 Hz, 2H, H_{bpy}), 7.26 (ddd, ^3J = 7.2, 5.7 Hz, ^4J = 1.3 Hz, 2H, H_{bpy}), 2.27 (s, 6H, H_{MeCN}) ppm. – **^{13}C-NMR** (75.5 MHz, CD_3CN): δ = 159.0, 158.2, 154.4, 153.2, 139.4, 139.0, 128.5, 127.7, 126.8, 124.9, 124.6, 4.5 ppm. – **FT-IR** (Film) $\tilde{\nu}$ = 3121, 3088, 2944, 1606, 1570,

1467, 1447, 1427, 1315, 1275, 1243, 1162, 1125, 1070, 1039, 876, 829, 762, 732, 663, 648, 556, 425, 405 percm. – **HRMS** (ESI+): calcd. for $C_{24}H_{22}F_6N_6PRu$ $[M-PF_6]^+$: 641.0592 u, found: 641.0606 u. – **R_f:** 0.33 ($MeCN/H_2O$/satd. aq. KNO_3 50:6:2).

Bis(2,2'-bipyridine-1κ^4N)(μ-dipyrido[3,2-*a*:2',3'-*c*]phenazine-11,12-diolato-1κ^2N',N'':2κ^2O)bis(1,10-phenanthroline-2κ^4N)ruthenium(II)silicon(IV)-tetrakis(hexafluorophosphate) (224)

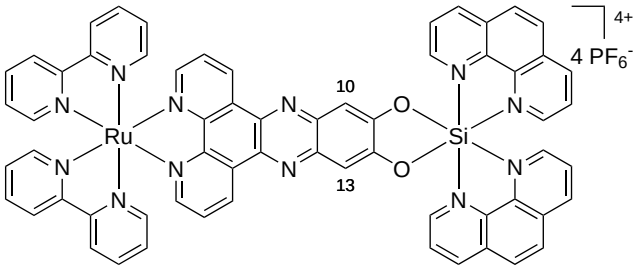

Using method B, silicon complex **130** (52.0 mg, 59.3 µmol), tin powder (61.0 mg, 514 µmol) and ruthenium complex **209** (54.5 mg, 59.7 µmol) were reacted to yield complex **224** as an orange red solid (46.1 mg, 27.2 µmol, 46 % over two steps) as a mixture of diastereomers. – **$C_{62}H_{40}F_{24}N_{12}O_2P_4RuSi$** (M = 1694.10 g mol^{-1}). – **^{1}H-NMR** (300 MHz, CD_3CN, 17 mM): δ = 9.61 (d, J = 5.3 Hz, 4H, H_{arom}), 9.53 (d, J = 8.1 Hz, 4H, H_{arom}), 9.42 (d, J = 8.2 Hz, 4H, H_{arom}), 9.18 (d, J = 8.1 Hz, 4H, H_{arom}), 8.65 (d, J = 9.1 Hz, 4H, $H_{phen,Dia.a/b}$), 8.61–8.43 (m, 16H, H_{arom}, $H_{phen,Dia.a/b}$), 8.16–8.07 (m, 8H, H_{arom}), 8.06–7.96 (m, 8H, H_{arom}), 7.90–7.78 (m, 12H, H_{arom}), 7.69 (d, J = 5.4 Hz, 4H, H_{arom}), 7.63 (s, 2H, H-$10_{Dia.a}$, H-$13_{Dia.a}$), 7.62 (s, 2H, H-$10_{Dia.b}$, H-$13_{Dia.b}$), 7.50–7.38 (m, 4H, H_{arom}), 7.30–7.15 (m, 4H, H_{arom}) ppm. – **^{13}C-NMR** (75.5 MHz, CD_3CN, 17 mM): δ = 158.2, 158.1, 154.0, 153.9, 153.1, 153.0, 150.6, 149.8, 148.0, 147.5, 147.0, 143.1, 139.0, 138.9, 138.6, 135.7, 135.0, 134.0, 131.9, 131.5, 131.1, 130.0, 129.9, 129.5, 129.1, 128.6, 128.5, 128.1, 125.4, 125.3, 110.3 ppm. – **^{29}Si-NMR** (99.4 MHz, CD_3CN): δ = −150.0 ppm. – **FT-IR** (Film) $\tilde{\nu}$ = 3659, 3329, 3114, 1626, 1604, 1586, 1532, 1454, 1362, 1316, 1270, 1203, 1179, 1161, 1120, 889, 836, 762, 739, 720, 582, 558, 528, 489 cm^{-1}. – **HRMS** (ESI+): calcd. for $C_{62}H_{40}N_{12}O_2RuSiPF_6$ $[M-3PF_6]^{3+}$: 419.7284 u, found: 419.7269 u. – **R_f:** 0.19 ($MeCN/H_2O$/satd. aq. KNO_3 50:12:4).

(μ-Dipyrido[3,2-*a*:2',3'-*c*]phenazine-11,12-diolato-1κ^2N',N'':2κ^2O)tetrakis(1,10-phenanthroline-1κ^4N,2κ^4N)ruthenium(II)silicon(IV)-tetrakis(hexafluorophosphate) (226)

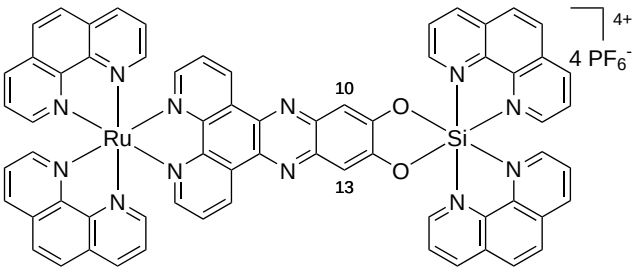

Using method B, silicon complex **130** (29.0 mg, 33.1 µmol), tin powder (32.0 mg, 270 µmol) and ruthenium complex **210** (30.3 mg, 31.5 µmol) were reacted to yield complex **226** as an orange red solid (19.8 mg, 11.4 µmol, 34 % over two steps) as a mixture of diastereomers. – **$C_{66}H_{40}F_{24}N_{12}O_2P_4RuSi$** (M = 1742.14 g mol^{-1}). – **^{1}H-NMR** (300 MHz, CD_3CN, 19 mM): δ = 9.61 (dd, J = 5.4, 1.1 Hz, 4H, H_{arom}), 9.50 (dd, J = 8.3, 1.2 Hz, 4H, H_{arom}), 9.46–9.38 (m, 4H, H_{arom}), 9.18 (dd, J = 8.3, 1.0 Hz, 4H,

H_{arom}), 8.70–8.54 (m, 16H, H_{arom}), 8.48 (ddd, J = 8.3, 5.4, 1.6 Hz, 4H, H_{arom}), 8.26 (d, J = 1.2 Hz, 8H, H_{arom}), 8.18 (dt, J = 5.2, 1.3 Hz, 4H, H_{arom}), 8.08–7.97 (m, 12H, H_{arom}), 7.85 (dt, J = 5.6, 1.1 Hz, 4H, H_{arom}), 7.71 (dd, J = 8.3, 5.4 Hz, 4H, H_{arom}), 7.68–7.59 (m, 12H, H_{arom}, H-10$_{Dia.a/b}$, H-13$_{Dia.a/b}$) ppm. – **^{13}C-NMR** (75.5 MHz, CD_3CN, 19 mM): δ = 154.5, 154.2, 154.0, 153.8, 151.0, 149.8, 148.93, 148.86, 148.0, 147.5, 147.0, 143.1, 138.7, 137.9, 137.9, 135.8, 135.0, 133.9, 132.09, 132.06, 131.8, 131.6, 131.1, 130.0, 129.9, 129.5, 129.11, 129.08, 127.9, 126.95, 126.90, 110.3 ppm. – **^{29}Si-NMR** (99.4 MHz, CD_3CN): δ = −150.1 ppm. – **FT-IR** (Film) $\tilde{\nu}$ = 3651, 3109, 2259, 1626, 1585, 1531, 1492, 1453, 1438, 1414, 1361, 1316, 1269, 1201, 1178, 1159, 1119, 1044, 890, 827, 761, 738, 720, 669, 635, 622, 602, 582, 557, 527, 510, 488, 460, 432, 412 cm^{-1}. – **HRMS** (ESI+): calcd. for $C_{66}H_{40}N_{12}O_2RuSi$ $[M-4PF_6]^{4+}$: 290.5551 u, found: 290.5540 u. – **R_f:** 0.13 ($MeCN/H_2O$/satd. aq. KNO_3 50:12:4).

Bis(2,2'-bipyridine-2κ^4N)bis(5,6-dimethyl-1,10-phenanthroline-1κ^4N)(μ-dipyrido[3,2-*a*:2',3'-*c*]phenazine-11,12-diolato-1κ^2N',N'':2κ^2O)ruthenium(II)silicon(IV)-tetrakis(hexafluorophosphate) (227)

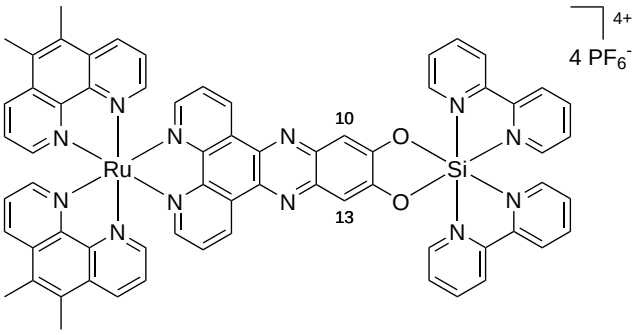

Using method B, silicon complex **129** (45.0 mg, 54.3 µmol), tin powder (52.0 mg, 438 µmol) and ruthenium complex **211** (53.0 mg, 52.1 µmol) were reacted to yield complex **227** as an orange red solid (27.9 mg, 15.9 µmol, 29 % over two steps) as a mixture of diastereomers. – **$C_{66}H_{48}F_{24}N_{12}O_2P_4RuSi$** (M = 1750.20 g mol^{-1}). – **^{1}H-NMR** (300 MHz, CD_3CN, 25 mM): δ = 9.53–9.43 (m, 4H, H_{arom}), 9.25–9.17 (m, 4H, H_{arom}), 9.02 (d, J = 8.1 Hz, 4H, H_{arom}), 8.94 (d, J = 8.0 Hz, 4H, H_{arom}), 8.86–8.78 (m, 4H, H_{arom}), 8.77–8.66 (m, 12H, H_{arom}), 8.21–8.08 (m, 8H, H_{arom}), 8.01 (dt, J = 5.4, 1.3 Hz, 4H, H_{arom}), 7.96–7.87 (m, 8H, H_{arom}), 7.76–7.57 (m, 20H, H_{arom}, H-10$_{Dia.a/b}$, H-13$_{Dia.a/b}$), 2.84 (s, 24H, H_{Methyl}) ppm. – **^{13}C-NMR** (75.5 MHz, CD_3CN, 25 mM): δ = 154.3, 153.4, 152.7, 152.4, 151.0, 149.1, 148.7, 148.4, 148.0, 146.6, 145.0, 144.4, 143.0, 138.7, 134.8, 133.8, 133.7, 132.5, 132.4, 131.8, 131.6, 127.9, 126.6, 126.5, 126.2, 110.4, 15.7 ppm. – **^{29}Si-NMR** (99.4 MHz, CD_3CN): δ = −150.3 ppm. – **FT-IR** (Film) $\tilde{\nu}$ = 3647, 3423, 3083, 2918, 1617, 1598, 1575, 1510, 1479, 1454, 1353, 1316, 1268, 1251, 1205, 1178, 1120, 1073, 1045, 1028, 953, 895, 876, 834, 809, 779, 754, 737, 725, 713, 686, 664, 634, 621, 580, 557, 525, 492, 467, 432, 385 cm^{-1}. – **HRMS** (ESI+): calcd. for $C_{66}H_{48}N_{12}O_2RuSiP_2F_{12}$ $[M-2PF_6]^{2+}$: 730.1063 u, found: 730.1053 u. – **R_f:** 0.26 ($MeCN/H_2O$/satd. aq. KNO_3 50:12:4).

Bis(5,6-dimethyl-1,10-phenanthroline-1κ^4N)(μ-dipyrido[3,2-*a*:2',3'-*c*]phenazine-11,12-diolato-1κ^2N',N'':2κ^2O)bis(1,10-phenanthroline-2κ^4N)ruthenium(II)silicon(IV)-tetrakis(hexafluorophosphate) (228)

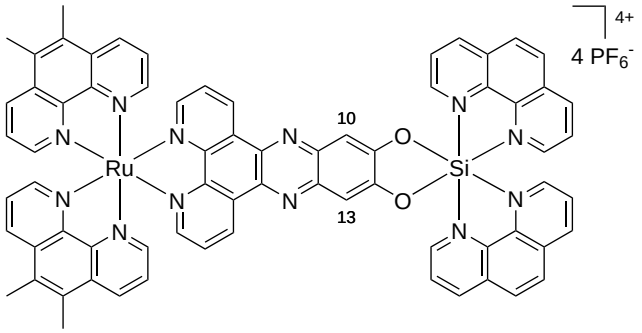

Using method B, silicon complex **130** (40.0 mg, 45.6 µmol), tin powder (42.8 mg, 361 µmol) and ruthenium complex **211** (48.4 mg, 47.6 µmol) were reacted to yield complex **228** as an orange red solid (16.7 mg, 9.29 µmol, 20 % over two steps) as a mixture of diastereomers. – $\mathbf{C_{70}H_{48}F_{24}N_{12}O_2P_4RuSi}$ (M = 1798.25 g mol^{-1}). – ^{1}**H-NMR** (300 MHz, CD_3CN, 11 mM): δ = 9.61 (dd, J = 5.3, 0.8 Hz, 4H, H_{arom}), 9.49 (d, J = 7.8 Hz, 4H, H_{arom}), 9.42 (d, J = 8.3 Hz, 4H, H_{arom}), 9.23–9.13 (m, 4H, H_{arom}), 8.73 (dd, J = 8.5, 2.8 Hz, 8H, H_{arom}), 8.65 (dd, J = 9.1, 0.8 Hz, 4H, $H_{phen,Dia.a/b}$), 8.57 (d, J = 9.1 Hz, 4H, $H_{phen,Dia.a/b}$), 8.54–8.42 (m, 4H, H_{arom}), 8.13–8.06 (m, 4H, H_{arom}), 8.06–7.97 (m, 8H, H_{arom}), 7.92 (d, J = 5.1 Hz, 4H, H_{arom}), 7.89–7.84 (m, 4H, H_{arom}), 7.74–7.67 (m, 4H, H_{arom}), 7.67–7.57 (m, 12H, H_{arom}, H-10$_{Dia.a/b}$, H-13$_{Dia.a/b}$), 2.84 (s, 24H, H_{Methyl}) ppm. – ^{13}**C-NMR** (75.5 MHz, CD_3CN, 11 mM): δ = 154.3, 153.9, 152.6, 152.4, 151.0, 149.8, 148.1, 148.03, 148.01, 147.5, 147.0, 143.1, 138.7, 135.8, 135.0, 134.79, 134.77, 133.8, 133.7, 133.6, 132.5, 132.4, 131.8, 131.6, 131.1, 130.0, 129.9, 129.5, 129.1, 127.9, 126.6, 110.3, 15.7 ppm. – ^{29}**Si-NMR** (59.7 MHz, CD_3CN): δ = −150.2 ppm. – **FT-IR** (Film) $\tilde{\nu}$ = 3651, 3110, 1625, 1586, 1531, 1455, 1439, 1353, 1316, 1268, 1203, 1178, 1160, 1119, 892, 839, 761, 738, 723, 622, 582, 558, 525, 488, 461, 428, 391 cm^{-1}. – **HRMS** (ESI+): calcd. for $C_{70}H_{48}N_{12}O_2RuSiP_2F_{12}$ [M−2PF_6]$^{2+}$: 754.1062 u, found: 754.1052 u. – $\mathbf{R_f}$**:** 0.31 ($MeCN/H_2O$/satd. aq. KNO_3 50:12:4).

Bis(2,2'-bipyridine-1κ^4N)bis(1,10-phenanthroline-2κ^4N)(μ-1,2,7,8-tetramethyldipyrido[3,2-*a*:2',3'-*c*]phenazine-11,12-diolato-1κ^2N',N'':2κ^2O)ruthenium(II)silicon(IV)-tetrakis(hexafluorophosphate) (230)

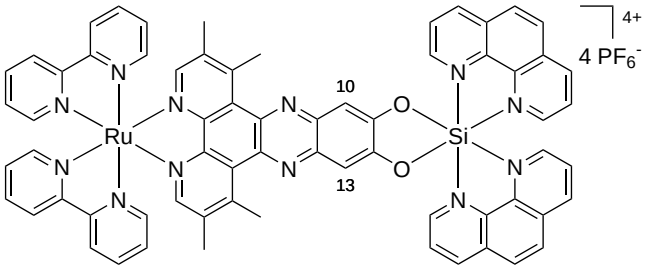

Using method B, silicon complex **130** (28.0 mg, 31.9 µmol), tin powder (30.2 mg, 254 µmol) and ruthenium complex **221** (30.3 mg, 31.2 µmol) were reacted to yield complex **230** as an orange red solid (10.1 mg, 5.77 µmol, 18 % over two steps) as a mixture of diastereomers. – $\mathbf{C_{66}H_{48}F_{24}N_{12}O_2P_4RuSi}$ (M = 1750.20 g mol^{-1}). – ^{1}**H-NMR** (300 MHz, CD_3CN, 10 mM): δ = 9.60 (dt, J = 5.4, 1.4 Hz, 4H, H_{arom}), 9.41 (d, J = 8.3 Hz, 4H, H_{arom}), 9.16 (dd, J = 8.3, 0.9 Hz, 4H, H_{arom}), 8.64 (dd, J = 9.1, 0.3 Hz, 4H, $H_{phen,Dia.a/b}$), 8.56 (d, J = 9.4 Hz, 4H, $H_{phen,Dia.a/b}$), 8.54–8.45 (m, 12H, H_{arom}), 8.07 (td, J = 8.0, 1.3 Hz, 4H, H_{arom}), 8.03–7.95 (m, 8H, H_{arom}), 7.87 (d, J = 5.3 Hz, 4H, H_{arom}), 7.80–7.75 (m, 8H, H_{arom}, H-3$_{Dia.a/b}$, H-6$_{Dia.a/b}$), 7.68–7.63 (m, 4H, H_{arom}), 7.609 (s, 2H, H-10$_{Dia.a}$, H-13$_{Dia.a}$), 7.607 (s, 2H, H-10$_{Dia.b}$, H-13$_{Dia.b}$), 7.46–7.37 (m, 4H, H_{arom}), 7.27–7.19 (m, 4H, H_{arom}), 3.32 (s, 12H,

H_{Methyl}), 2.34 (s, 12H, H_{Methyl}) ppm. – ^{13}**C-NMR** (75.5 MHz, CD_3CN, 10 mM): δ = 178.7, 158.2, 153.3, 152.83, 152.77, 152.7, 150.4, 149.7, 148.0, 147.5, 146.9, 139.6, 138.7, 138.6, 138.5, 135.8, 131.5, 131.1, 130.0, 129.9, 129.5, 129.1, 128.6, 128.2, 125.31, 125.25, 110.1, 20.8, 18.7 ppm. – ^{29}**Si-NMR** (99.4 MHz, CD_3CN): δ = −150.1 ppm. – **FT-IR** (Film) $\tilde{\nu}$ = 3649, 3113, 1626, 1604, 1586, 1531, 1456, 1347, 1270, 1256, 1200, 1159, 1118, 1043, 890, 835, 762, 736, 718, 636, 622, 579, 558, 527, 485, 434 cm^{-1}. – **HRMS** (ESI+): calcd. for $C_{66}H_{48}N_{12}O_2RuSiP_2F_{12}$ $[M-2PF_6]^{2+}$: 730.1063 u, found: 730.1053 u. – **R**$_f$**:** 0.29 (MeCN/H_2O/satd. aq. KNO_3 50:12:4).

Bis(2,2'-bipyridine-1κ^4N)(μ-3,6-dimethyldipyrido[3,2-*a*:2',3'-*c*]phenazine-11,12-diolato-1κ^2N',N'':2κ^2O)bis(1,10-phenanthroline-2κ^4N)ruthenium(II)silicon(IV)-tetrakis(hexafluorophosphate) (232)

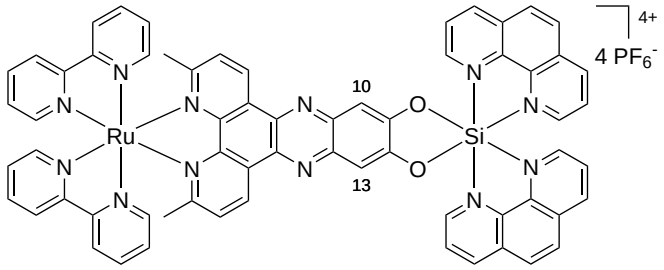

The reaction and the work-up were performed under exclusion of light to avoid decomposition of the product. Using method B, silicon complex **130** (51.2 mg, 58.4 µmol), tin powder (62.1 mg, 523 µmol) and ruthenium complex **217** (24.1 mg, 25.6 µmol) were reacted to yield complex **232** as an orange red solid (24.6 mg, 14.3 µmol, 24 % over two steps, 56 % starting from **217**) as a mixture of diastereomers. To avoid decomposition of the product, the complex was stored in the dark at −20 °C. – **$C_{64}H_{44}F_{24}N_{12}O_2P_4RuSi$** (M = 1722.15 g mol^{-1}). – ^{1}**H-NMR** (300 MHz, CD_3CN, 13 mM): δ = 9.62 (dd, J = 5.4, 0.8 Hz, 4H, H_{arom}), 9.50 (dd, J = 8.4, 2.3 Hz, 4H, H_{arom}), 9.41 (dd, J = 8.4, 1.0 Hz, 4H, H_{arom}), 9.19–9.11 (m, 4H, H_{arom}), 8.63 (d, J = 9.1 Hz, 4H, $H_{phen,Dia.a/b}$), 8.58–8.42 (m, 16H, H_{arom}, $_{phen,Dia.a/b}$), 8.07–7.94 (m, 12H, H_{arom}), 7.91–7.86 (m, 4H, H_{arom}), 7.82–7.77 (m, 4H, H_{arom}), 7.75–7.68 (m, 8H, H_{arom}), 7.591 (s, 2H, H-10$_{Dia.a}$, H-13$_{Dia.a}$), 7.587 (s, 2H, H-10$_{Dia.b}$, H-13$_{Dia.b}$), 7.32–7.22 (m, 8H, H_{arom}), 1.92 (s, 12H, H_{Methyl}) ppm. – ^{13}**C-NMR** (126 MHz, CD_3CN, 13 mM): δ = 168.8, 158.6, 158.4, 154.0, 153.6, 152.9, 151.8, 149.8, 148.1, 147.5, 146.9, 143.3, 139.0, 138.8, 137.9, 135.7, 135.0, 134.8, 131.5, 131.1, 130.0, 129.9, 129.5, 129.4, 129.3, 129.1, 128.44, 128.40, 125.55, 125.48, 110.1, 26.3 ppm. – ^{29}**Si-NMR** (99.4 MHz, CD_3CN): δ = −147.2 ppm. – **FT-IR** (Film) $\tilde{\nu}$ = 3113, 2931, 2856, 1738, 1626, 1586, 1531, 1453, 1360, 1247, 1200, 1119, 1044, 887, 838, 766, 738, 581, 558, 526, 487, 425, 385 cm^{-1}. – **HRMS** (ESI+): calcd. for $C_{64}H_{44}N_{12}O_2RuSiP_2F_{12}$ $[M-2PF_6]^{2+}$: 716.0906 u, found: 716.0895 u. – **R**$_f$**:** 0.19 (MeCN/H_2O/satd. aq. KNO_3 50:12:4).

(μ-Dipyrido[3,2-*a*:2',3'-*c*]phenazine-11,12-diolato-1κ²*N*′,*N*″:2κ²*O*)bis(1,10-phenanthroline-2κ⁴*N*)bis(2-phenylpyridinato-1κ²*C*,1κ²*N*)rhodium(III)silicon(IV)-tris(hexafluorophosphate) (234)

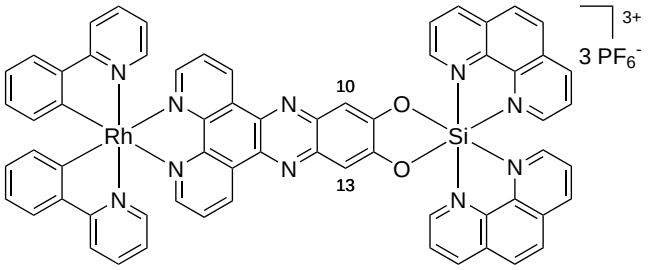

Using method B, silicon complex **130** (45.3 mg, 51.7 µmol), tin powder (49.5 mg, 417 µmol) and rhodium complex **213** (40.0 mg, 52.2 µmol) were reacted to yield complex **234** as a yellow solid (26.1 mg, 16.9 µmol, 33 % over two steps) as a mixture of diastereomers. – **$C_{64}H_{40}F_{18}N_{10}O_2P_3RhSi$** (M = 1546.98 g mol^{-1}). – **^{1}H-NMR** (300 MHz, CD_3CN, 22 mM): δ = 9.66 (ddd, J = 8.3, 5.3, 1.5 Hz, 4H, H_{arom}), 9.61 (d, J = 5.1 Hz, 4H, H_{arom}), 9.42 (dd, J = 8.4, 1.0 Hz, 4H, H_{arom}), 9.18 (dd, J = 8.3, 0.9 Hz, 4H, H_{arom}), 8.65 (d, J = 9.2 Hz, 4H, $H_{phen,Dia.a/b}$), 8.57 (d, J = 9.1 Hz, 4H, $H_{phen,Dia.a/b}$), 8.48 (ddd, J = 8.4, 5.4, 0.4 Hz, 4H, H_{arom}), 8.40–8.35 (m, 4H, H_{arom}), 8.12–8.06 (m, 4H, H_{arom}), 8.02 (dd, J = 8.3, 5.6 Hz, 4H, H_{arom}), 7.97–7.82 (m, 16H, H_{arom}), 7.62 (s, 2H, H-10$_{Dia.a}$, H-13$_{Dia.a}$), 7.61 (s, 2H, H-10$_{Dia.b}$, H-13$_{Dia.b}$), 7.58–7.50 (m, 4H, H_{arom}), 7.16 (td, J = 7.6, 1.1 Hz, 4H, H_{arom}), 7.03 (td, J = 7.5, 1.2 Hz, 4H, H_{arom}), 6.98–6.90 (m, 4H, H_{arom}, 6.45–6.36 (m, 4H, H_{arom}) ppm. – **^{13}C-NMR** (75.5 MHz, CD_3CN, 22 mM): δ = 168.1, 167.8, 165.8, 153.7, 152.3, 150.5, 149.8, 148.38, 148.36, 148.0, 147.5, 147.0, 145.2, 143.0, 139.7, 138.6, 135.9, 135.8, 135.0, 133.7, 131.7, 131.5, 131.2, 131.1, 130.0, 129.9, 129.5, 129.1, 128.5, 125.8, 124.6, 124.5, 121.1, 110.3 ppm. – **^{29}Si-NMR** (99.4 MHz, CD_3CN): δ = −149.4 ppm. – **FT-IR** (Film) $\tilde{\nu}$ = 3653, 3109, 1626, 1606, 1583, 1566, 1531, 1481, 1455, 1439, 1363, 1325, 1270, 1203, 1160, 1119, 890, 840, 760, 737, 719, 622, 582, 558, 529, 505, 486, 471, 425, 411, 402, 390, 382 cm^{-1}. – **HRMS** (ESI+): calcd. for $C_{64}H_{40}RhN_{10}O_2SiP_2F_{12}$ $[M-PF_6]^+$: 1401.1438 u, found: 1401.1468 u. – **R_f:** 0.15 ($MeCN/H_2O$/satd. aq. KNO_3 50:6:2).

(μ-Dipyrido[3,2-*a*:2',3'-*c*]phenazine-11,12-diolato-1κ²*N*′,*N*″:2κ²*O*)bis(1,10-phenanthroline-2κ⁴*N*)bis(2-phenylpyridinato-1κ²*C*,1κ²*N*)iridium(III)silicon(IV)-tris(hexafluorophosphate) (237)

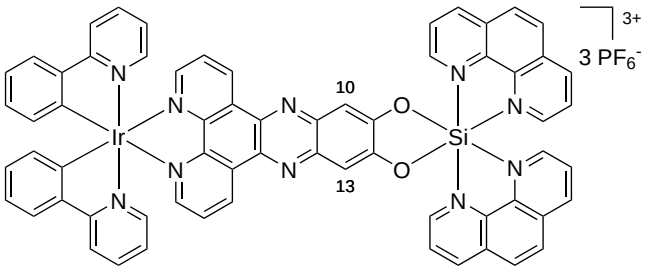

Using method B, silicon complex **130** (40.0 mg, 45.6 µmol), tin powder (44.3 mg, 373 µmol) and iridium complex **212** (40.0 mg, 46.7 µmol) were reacted to yield complex **237** as an orange solid (10.0 mg, 6.11 µmol, 13 % over two steps) as a mixture of diastereomers. – **$C_{64}H_{40}F_{18}IrN_{10}O_2P_3Si$** (M = 1636.29 g mol^{-1}). – **^{1}H-NMR** (300 MHz, CD_3CN, 8 mM): δ = 9.66–9.56 (m, 8H, H_{arom}), 9.45–9.37 (m, 4H, H_{arom}), 9.18 (dd, J = 8.3, 0.7 Hz, 4H, H_{arom}), 8.65 (d, J = 9.1 Hz, 4H, $H_{phen,Dia.a/b}$), 8.57 (d, J = 9.1 Hz, 4H, $H_{phen,Dia.a/b}$), 8.47 (dd, J = 8.3, 5.5 Hz, 4H, H_{arom}), 8.34 (dd, J = 5.2, 1.4 Hz, 4H, H_{arom}), 8.08 (d, J = 8.0 Hz, 4H, H_{arom}), 8.01 (dd, J = 8.3, 5.6 Hz, 4H, H_{arom}), 7.94 (ddd, J = 8.3, 5.3, 0.5 Hz, 4H, H_{arom}), 7.89–7.77 (m, 12H, H_{arom}), 7.621 (s, 2H, H-10$_{Dia.a}$, H-13$_{Dia.a}$), 7.616 (s,

2H, H-10$_{Dia.b}$, H-13$_{Dia.b}$), 7.59–7.52 (m, 4H, H$_{arom}$), 7.10 (td, J = 7.6, 0.9 Hz, 4H, H$_{arom}$), 6.98 (td, J = 7.4, 0.9 Hz, 4H, H$_{arom}$), 6.92–6.85 (m, 4H, H$_{arom}$), 6.38 (d, J = 7.5 Hz, 4H, H$_{arom}$) ppm. – **^{13}C-NMR** (75.5 MHz, CD_3CN, 8 mM): δ = 168.6, 153.9, 152.9, 150.7, 150.5, 149.9, 149.8, 148.0, 147.5, 147.0, 145.3, 143.2, 139.6, 138.6, 135.8, 135.6, 135.0, 132.7, 132.3, 131.6, 131.5, 131.2, 130.0, 129.9, 129.5, 129.1, 129.0, 126.0, 124.4, 123.8, 120.9, 110.3 ppm. – **^{29}Si-NMR** (59.7 MHz, CD_3CN): δ = −150.2 ppm. – **FT-IR** (Film) $\tilde{\nu}$ = 3650, 3106, 1626, 1608, 1585, 1531, 1479, 1454, 1439, 1363, 1270, 1203, 1161, 1119, 1033, 890, 839, 760, 737, 718, 622, 582, 558, 526, 510, 488, 456, 444, 432, 397 cm^{-1}. – **HRMS** (ESI+): calcd. for $C_{64}H_{40}IrN_{10}O_2SiP_2F_{12}$ [M−PF_6]$^+$: 1491.2016 u, found: 1491.2014 u. – **R$_f$:** 0.13 (MeCN/H_2O/satd. aq. KNO_3 50:6:2).

5.4.5. Synthesis of Bodipy-Modified Silicon Complexes

(2-(3-(1-(2-(4-(5,5-Difluoro-1,3,7,9-tetramethyl-5*H*-4λ^4,5λ^4-dipyrrolo[1,2-*c*:2',1'-*f*][1,3,2]diazaborinin-10-yl)phenoxy)ethyl)-1*H*-1,2,3-triazol-4-yl)propyl)-1*H*-benzo[*d*]imidazole-5,6-diolato-κ^2*O*)bis(1,10-phenanthroline)silicon(IV)-bis(hexafluorophosphate) (246)

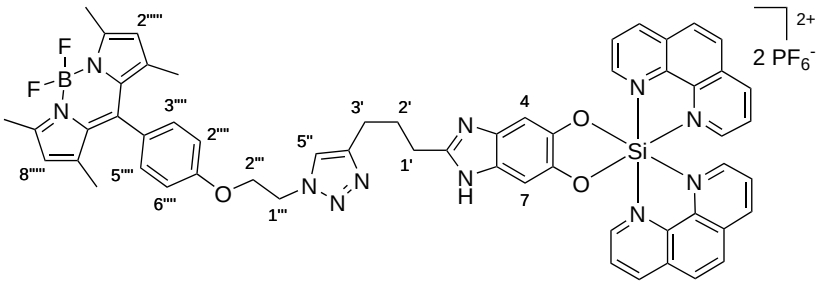

Method 1: Using method C, silicon complex **130** (19.0 mg, 21.7 µmol), tin powder (22.0 mg, 185 µmol) and Bodipy **250** (16.2 mg, 32.1 µmol) were reacted to yield complex **246** as a red solid (16.1 mg, 12.4 µmol, 57 % over two steps).

Method 2: Under an atmosphere of nitrogen, complex **167** (9.0 mg, 10.1 µmol), Bodipy-N_3 (**243**, 11.0 mg, 26.9 µmol), copper(II)sulfate pentahydrate (1.5 mg, 6.01 µmol) and sodium ascorbate (1.5 mg, 7.57 µmol) were suspended in a solution of acetonitrile (1000 µL) and water (500 µL). The reaction was stirred at room temperature for two hours before it was heated to 100 °C for three hours. Then copper(I)iodide (8 mg, 42 µmol) was added, and the mixture was stirred at 100 °C for an additional hour. The brown mixture was cooled to room temperature, and the solvent was removed under vacuum. The residue was subjected to flash column chromatography (MeCN → MeCN/H_2O/satd. aq. KNO_3 50:3:1 → 50:6:2). The yellow, green fluorescent band eluting under salt conditions was collected. The product fractions were concentrated, the residue was dissolved in water and treated with NH_4PF_6. The resulting precipitate was isolated by centrifugation (4000 rpm, 4 °C, 5 min) and washed twice with water to remove the excess amount of salt. The solid was dissolved in acetonitrile, and the gained solution was filtered through cotton before it was concentrated. After drying under vacuum, complex **246** was obtained as a red solid (8.3 mg, 6.38 µmol, 63 %). – **$C_{57}H_{48}BF_{14}N_{11}O_3P_2Si$** (M = 1301.91 g mol^{-1}). – **^{1}H-NMR** (300 MHz, CD_3CN): δ = 9.47 (dd, ^3J = 5.4 Hz, ^4J = 1.2 Hz, 2H, H$_{phen}$), 9.37 (dd, ^3J = 8.4 Hz, ^4J = 1.2 Hz, 2H, H$_{phen}$), 9.10 (dd, ^3J = 8.3 Hz, ^4J = 1.1 Hz, 2H, H$_{phen}$), 8.65–8.55 (m, 2H, H$_{phen}$), 8.54–8.49 (m, 2H, H$_{phen}$), 8.46 (dd, ^3J = 8.4, 5.4 Hz, 2H, H$_{phen}$), 7.93 (dd, ^3J = 8.3, 5.6 Hz, 2H, H$_{phen}$), 7.74 (dd, ^3J = 5.6 Hz, ^4J = 1.1 Hz, 2H, H$_{phen}$), 7.71 (s, 1H, H-5"), 7.21–7.13 (m, 2H, H-3"", H-5""), 7.05 (s, 2H, H-4, H-7),

7.04–6.95 (m, 2H, H-2"", H-6""), 6.05 (s, 2H, H-2""', H-8""'), 4.73–4.63 (m, 2H, H-2"'), 4.44–4.33 (m, 2H, H-1"'), 3.04 (t, ^3J = 7.3 Hz, 2H, H-1'), 2.74 (t, ^3J = 7.3 Hz, 2H, H-3'), 2.46 (s, 6H, H_{Methyl}), 2.18–2.11 (m, 2H, H-2'), 1.37 (s, 6H, H_{Methyl}) ppm. – **^{13}C-NMR** (126 MHz, CD_3CN): δ = 159.9, 156.2, 153.1, 149.5, 147.7, 147.2, 147.1, 146.6, 146.4, 144.5, 143.3, 135.7, 134.8, 132.5, 131.4, 131.0, 130.4, 129.74, 129.69, 129.3, 128.9, 128.3, 127.8, 123.8, 122.20, 122.18, 116.3, 99.5, 67.6, 50.4, 27.7, 26.6, 24.8, 14.8, 14.7 ppm. – **^{29}Si-NMR** (99.4 MHz, CD_3CN): δ = −148.9 ppm. – **^{19}F-NMR** (283 MHz, CD_3CN): δ = −72.1 (d, J_{FP} = 706.4 Hz, PF_6), −144.9 (q, J_{FB} = 32.7 Hz, BF_2) ppm. – **^{11}B-NMR** (160 MHz, CD_3CN): δ = 1.27 (t, J_{BF} = 33.6 Hz) ppm. – **^{31}P-NMR** (122 MHz, CD_3CN): δ = −143.2 (h, J_{PF} = 706.5 Hz) ppm. – **FT-IR** (Film) $\tilde{\nu}$ = 3111, 2926, 1626, 1609, 1586, 1544, 1531, 1509, 1472, 1438, 1409, 1365, 1307, 1244, 1196, 1159, 1118, 1086, 1045, 983, 901, 888, 836, 762, 741, 717, 673, 622, 581, 558, 525, 509, 488, 420, 399 cm^{-1}. – **HRMS** (ESI+): calcd. for $C_{57}H_{48}BF_8N_{11}O_3PSi$ $[M-PF_6]^+$: 1156.3418 u, found: 1156.3436 u.

(2-(3-(1-(2-(4-(5,5-Difluoro-1,3,7,9-tetramethyl-5*H*-4λ^4,5λ^4-dipyrrolo[1,2-*c*:2',1'-*f*][1,3,2]diazaborinin-10-yl)phenoxy)ethyl)-1*H*-1,2,3-triazol-4-yl)propyl)-1*H*-benzo[*d*]imidazole-5,6-diolato-κ^2O)bis(3,4,7,8-tetramethyl-1,10-phenanthroline)silicon(IV)-bis(hexafluorophosphate) (247)

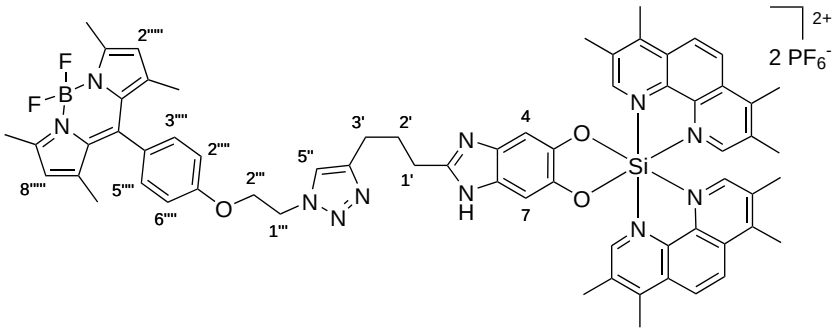

Using method C, silicon complex **130** (12.8 mg, 12.9 µmol), tin powder (13.0 mg, 110 µmol) and Bodipy **250** (12.0 mg, 23.7 µmol) were reacted to yield complex **247** as a red solid (11.5 mg, 8.14 µmol, 63 % over two steps). – **$C_{65}H_{64}BF_{14}N_{11}O_3P_2Si$** (M = 1414.12 g mol^{-1}). – **^{1}H-NMR** (300 MHz, CD_3CN): δ = 9.09 (s, 2H, H_{phen}), 8.63 (d, ^3J = 9.6 Hz, 2H, H_{phen}), 8.56 (d, ^3J = 9.6 Hz, 2H, H_{phen}), 7.69 (s, 1H, H-5"), 7.35 (s, 2H, H_{phen}), 7.22–7.14 (m, 2H, H-3"", H-5""), 7.03–6.97 (m, 2H, H-2"", H-6""), 6.91 (s, 2H, H-4, H-7), 6.04 (s, 2H, H-2""', H-8""'), 4.76–4.60 (m, 2H, H-2"'), 4.44–4.34 (m, 2H, H-1"'), 3.00 (s, 6H, $H_{Methyl,phen}$), 2.93 (t, ^3J = 7.2 Hz, 2H, H-1'), 2.84 (s, 6H, $H_{Methyl,phen}$), 2.73 (t, ^3J = 7.2 Hz, 2H, H-3'), 2.64 (s, 6H, $H_{Methyl,phen}$), 2.44 (s, 6H, $H_{Methyl,pyrrole}$), 2.29 (s, 6H, $H_{Methyl,phen}$), 2.09 (p, ^3J = 7.1 Hz, 2H, H-2'), 1.37 (s, 6H, $H_{Methyl,pyrrole}$) ppm. – **^{13}C-NMR** (75.5 MHz, CD_3CN): δ = 159.9, 157.7, 156.7, 156.2, 153.3, 148.4, 147.4, 146.3, 145.5, 144.5, 143.3, 138.8, 138.2, 134.5, 133.5, 132.5, 130.4, 130.1, 129.6, 129.2, 128.3, 125.9, 125.8, 123.7, 122.2, 116.3, 99.5, 67.7, 50.4, 28.2, 27.4, 25.0, 18.8, 18.3, 16.7, 16.3, 14.8, 14.7 ppm. – **^{29}Si-NMR** (59.7 MHz, CD_3CN): δ = −150.5 ppm. – **^{19}F-NMR** (283 MHz, CD_3CN): δ = −72.2 (d, J_{FP} = 706.5 Hz, PF_6), −145.0 (q, J_{FB} = 32.5 Hz, BF_2) ppm. – **^{11}B-NMR** (96.3 MHz, CD_3CN): δ = 1.22 (t, J_{BF} = 33.0 Hz) ppm. – **^{31}P-NMR** (122 MHz, CD_3CN): δ = −143.3 (h, J_{PF} = 706.8 Hz) ppm. – **FT-IR** (Film) $\tilde{\nu}$ = 3651, 3416, 2931, 1622, 1544, 1509, 1464, 1440, 1409, 1307, 1246, 1196, 1158, 1122, 1086, 1046, 984, 913, 898, 839, 767, 739, 720, 706, 649, 633, 596, 558, 525, 478, 459, 445, 421 cm^{-1}. – **HRMS** (ESI+): calcd. for $C_{65}H_{64}BF_8N_{11}O_3PSi$ $[M-PF_6]^+$: 11 268.4671 u, found: 1268.4689 u.

(2,2'-Bipyridine)(2-(3-(1-(2-(4-(5,5-difluoro-1,3,7,9-tetramethyl-5*H*-4λ^4,5λ^4-dipyrrolo[1,2-*c*:2',1'-*f*][1,3,2]diazaborinin-10-yl)phenoxy)ethyl)-1*H*-1,2,3-triazol-4-yl)propyl)-1*H*-benzo[*d*]imidazole-5,6-diolato-κ^2O)(dipyrido[3,2-*a*:2',3'-*c*]phenazine-κ^2N', N'') silicon(IV)-bis(hexafluorophosphate) (248)

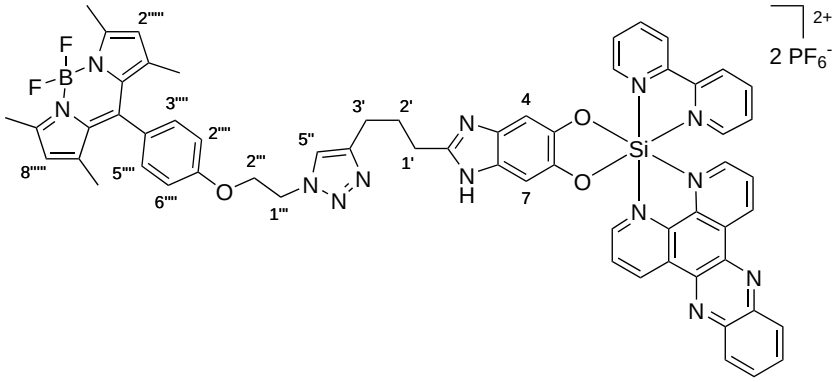

Using method C, silicon complex **187** (14.5 mg, 15.2 µmol), tin powder (16.0 mg, 135 µmol) and Bodipy **250** (10.0 mg, 19.8 µmol) were reacted to yield complex **248** as a red solid (7.8 mg, 5.65 µmol, 37 % over two steps). – **$C_{61}H_{50}BF_{14}N_{13}O_3P_2Si$** (M = 1379.98 g mol^{-1}). – ^{1}**H-NMR** (300 MHz, CD_3CN, 11 mM): δ = 10.20 (dd, ^3J = 8.3 Hz, ^4J = 1.2 Hz, 1H, H_{dppz}), 10.07 (dd, ^3J = 8.3 Hz, ^4J = 1.1 Hz, 1H, H_{dppz}), 9.46 (dd, ^3J = 5.5 Hz, ^4J = 1.2 Hz, 1H, H_{dppz}), 9.29–9.23 (m, 1H, H_{bpy}), 9.02–8.96 (m, 1H, H_{bpy}), 8.90–8.80 (m, 2H, H_{bpy}), 8.63–8.49 (m, 4H, 3 × H_{dppz}, H_{bpy}), 8.28–8.18 (m, 4H, 3 × H_{dppz}, H_{bpy}), 7.94 (dd, ^3J = 5.7 Hz, ^4J = 1.1 Hz, 1H, H_{dppz}), 7.76–7.63 (m, 3H, 2 × H_{bpy}, H-5"), 7.23–7.16 (m, 2H, H-3"", H-5""), 7.04 (s, 1H, H-4/7), 7.03–6.98 (m, 2H, H-2"", H-6""), 6.88 (s, 1H, H-4/7), 6.02 (s, 2H, H-2"'', H-8"''), 4.69 (t, ^3J = 5.0 Hz, 2H, H-2"'), 4.40 (t, ^3J = 4.9 Hz, 2H, H-1"'), 2.88 (t, ^3J = 7.4 Hz, 2H, H-1'), 2.72 (t, ^3J = 7.4 Hz, 2H, H-3'), 2.44 (s, 6H, H_{Methyl}), 2.12–2.05 (m, 2H, H-2'), 1.36 (s, 6H, H_{Methyl}) ppm. – ^{13}**C-NMR** (75.5 MHz, CD_3CN, 11 mM): δ = 159.9, 156.2, 154.2, 149.9, 148.9, 148.7, 148.2, 148.0, 147.7, 146.5, 145.9, 144.8, 144.5, 144.3, 144.1, 143.7, 143.4, 143.2, 143.0, 139.8, 139.7, 138.4, 137.4, 134.7, 134.6, 134.3, 132.5, 132.1, 131.8, 131.5, 131.3, 130.9, 130.8, 130.4, 128.4, 128.2, 126.2, 126.0, 123.5, 122.2, 122.14, 122.12, 116.3, 115.3, 67.7, 50.3, 28.4, 28.1, 25.2, 14.8, 14.7 ppm. – ^{29}**Si-NMR** (59.7 MHz, CD_3CN): δ = −147.7 ppm. – ^{19}**F-NMR** (283 MHz, CD_3CN): δ = −72.2 (d, J_{FP} = 707.0 Hz, PF_6), −145.0 (q, J_{FB} = 32.7 Hz, BF_2) ppm. – ^{11}**B-NMR** (96.3 MHz, CD_3CN): δ = 0.45 (t, J_{BF} = 33.1 Hz) ppm. – ^{31}**P-NMR** (122 MHz, CD_3CN): δ = −143.3 (h, J_{PF} = 706.7 Hz) ppm. – **FT-IR** (Film) $\tilde{\nu}$ = 3649, 3412, 3108, 2925, 1616, 1575, 1544, 1510, 1456, 1409, 1361, 1306, 1245, 1196, 1158, 1085, 1058, 1046, 983, 897, 837, 764, 748, 729, 706, 682, 644, 621, 594, 558, 515, 499, 478, 430 cm^{-1}. – **HRMS** (ESI+): calcd. for $C_{61}H_{50}BF_8N_{13}O_3PSi$ $[M-PF_6]^+$: 1234.3636 u, found: 1234.3657 u.

(2-(3-(1-(2-(4-(5,5-Difluoro-1,3,7,9-tetramethyl-5*H*-4λ^4,5λ^4-dipyrrolo[1,2-*c*:2',1'-*f*][1,3,2]diazaborinin-10-yl)phenoxy)ethyl)-1*H*-1,2,3-triazol-4-yl)propyl)-1*H*-benzo[*d*]imidazole-5,6-diolato-κ^2O)(dipyrido[3,2-*a*:2',3'-*c*]phenazine-κ^2N', N'')(1,10-phenanthroline) silicon(IV)-bis(hexafluorophosphate) (249)

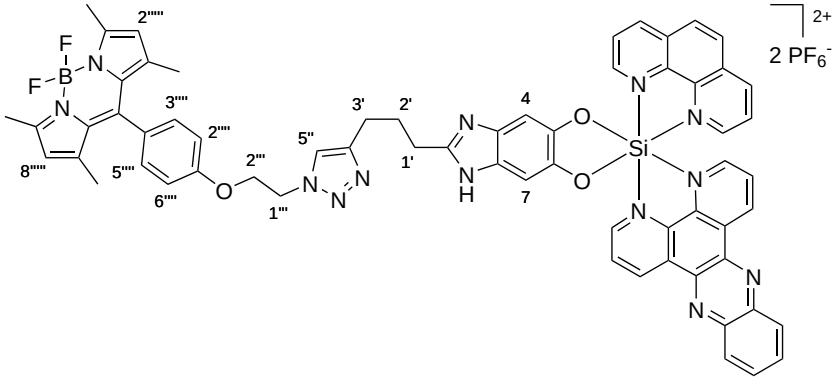

Method 1: Using method C, silicon complex **188** (18.3 mg, 18.7 µmol), tin powder (19.0 mg, 160 µmol) and Bodipy **250** (12.0 mg, 23.7 µmol) were reacted to yield complex **249** as a red solid (12.6 mg, 8.97 µmol, 48 % over two steps).

Method 2: Under an atmosphere of nitrogen, complex **191** (8.0 mg, 8.04 µmol), Bodipy-N_3 (**243**, 8.1 mg, 19.8 µmol), copper(II)sulfate pentahydrate (1.0 mg, 4.00 µmol) and sodium ascorbate (1.2 mg, 6.06 µmol) were suspended in a solution of acetonitrile (1000 µL) and water (500 µL). The reaction was stirred at 100 °C for three hours. The brown mixture was cooled to room temperature, and the solvent was removed under vacuum. The residue was subjected to flash column chromatography (MeCN → MeCN/H_2O/satd. aq. KNO_3 50:3:1 → 50:6:2). The yellow, green fluorescent band eluting under salt conditions was collected. The product fractions were concentrated, the residue was dissolved in water and treated with NH_4PF_6. The resulting precipitate was isolated by centrifugation (4000 rpm, 4 °C, 5 min) and washed twice with water to remove the excess amount of salt. The solid was dissolved in acetonitrile, and the gained solution was filtered through cotton before it was concentrated. After drying under vacuum, a inseparable mixture of starting material **191** and product **249** with a ratio of 0.7:1 was obtained as a red solid (6.0 mg, ∼53 %).

Under an atmosphere of nitrogen, the mixture (6.0 mg), Bodipy-N_3 (**243**, 8.1 mg, 19.8 µmol), copper(II)sulfate pentahydrate (1.0 mg, 4.00 µmol), sodium ascorbate (1.2 mg, 6.06 µmol) and copper(I)iodide (2.0 mg, 10.5 µmol) were suspended in a solution of acetonitrile (800 µL) and water (400 µL). The reaction was stirred at 100 °C for 16 hours. The brown mixture was then cooled to room temperature, and the solvent was removed under vacuum. The residue was subjected to flash column chromatography (MeCN → MeCN/H_2O/satd. aq. KNO_3 50:3:1 → 50:6:2). The yellow, green fluorescent band eluting under salt conditions was collected. The product fractions were concentrated, the residue was dissolved in water and treated with NH_4PF_6. The resulting precipitate was isolated by centrifugation (4000 rpm, 4 °C, 5 min) and washed twice with water to remove the excess amount of salt. The solid was dissolved in acetonitrile, and the gained solution was filtered through cotton before it was concentrated. After drying under vacuum, complex **249** was obtained as a red solid (2.0 mg, 1.42 µmol, 18 % over two steps). – $\mathbf{C_{63}H_{50}BF_{14}N_{13}O_3P_2Si}$ (M = 1404.00 g mol^{-1}). – **^{1}H-NMR** (300 MHz, CD_3CN, 15 mM): δ = 10.25 (dd, ^3J = 8.3 Hz, ^4J = 1.2 Hz, 1H, H_{dppz}), 10.01 (dd, ^3J = 8.3 Hz, ^4J = 1.1 Hz, 1H, H_{dppz}), 9.56 (dd, ^3J = 5.5 Hz, ^4J = 1.3 Hz, 1H, H_{dppz}), 9.54 (dd, ^3J = 5.4 Hz, ^4J = 1.2 Hz, 1H, H_{phen}), 9.38 (dd, ^3J = 8.4 Hz, ^4J = 1.1 Hz, 1H, H_{phen}), 9.12 (dd, ^3J = 8.1 Hz, ^4J = 1.3 Hz, 1H, H_{phen}), 8.66–8.44 (m, 6H, 3 × H_{dppz}, 3 × H_{phen}), 8.27–8.17 (m, 2H, H_{dppz}), 8.11 (dd, ^3J = 8.3, 5.7 Hz, 1H, H_{dppz}), 8.01–7.90 (m, 2H, H_{phen}), 7.82 (dd, ^3J = 5.7 Hz,

^4J = 1.1 Hz, 1H, H_{dppz}), 7.68 (s, 1H, H-5"), 7.21–7.12 (m, 2H, H-3"", H-5""), 7.05–6.94 (m, 4H, H-4, H-7, H-2"", H-6""), 6.00 (s, 2H, H-2""', H-8""'), 4.68 (t, ^3J = 5.0 Hz, 2H, H-2"'), 4.39 (t, ^3J = 5.0 Hz, 2H, H-1"'), 2.91 (t, ^3J = 7.4 Hz, 2H, H-1'), 2.72 (t, ^3J = 7.3 Hz, 2H, H-3'), 2.41 (s, 6H, H_{Methyl}), 2.09 (p, ^3J = 7.3 Hz, 2H, H-2'), 1.34 (s, 6H, H_{Methyl}) ppm. – **^{13}C-NMR** (126 MHz, CD_3CN, 15 mM): δ = 159.9, 156.2, 154.0, 150.1, 149.6, 148.3, 147.62, 147.57, 147.2, 146.7, 144.8, 144.6, 144.4, 144.1, 143.6, 143.2, 143.0, 139.84, 139.76, 138.3, 137.5, 135.8, 134.8, 134.6, 132.5, 132.1, 131.8, 131.5, 131.4, 131.1, 130.87, 130.86, 130.7, 130.4, 129.8, 129.4, 128.9, 128.3, 123.6, 122.18, 122.17, 116.3, 100.0, 67.7, 50.3, 28.3, 27.8, 25.1, 14.8, 14.7 ppm. – **^{29}Si-NMR** (59.7 MHz, CD_3CN): δ = −147.9 ppm. – **^{19}F-NMR** (283 MHz, CD_3CN): δ = −72.1 (d, J_{FP} = 706.9 Hz, PF_6), −144.9 (q, J_{FB} = 32.6 Hz, BF_2) ppm. – **^{11}B-NMR** (96.3 MHz, CD_3CN): δ = 1.16 (t, J_{BF} = 33.0 Hz) ppm. – **^{31}P-NMR** (122 MHz, CD_3CN): δ = −143.3 (h, J_{PF} = 706.8 Hz) ppm. – **FT-IR** (Film) $\tilde{\nu}$ = 3107, 2929, 1609, 1584, 1543, 1509, 1460, 1436, 1360, 1305, 1241, 1194, 1156, 1118, 1084, 1057, 982, 898, 824, 761, 725, 716, 673, 644, 620, 594, 556, 521, 509, 497, 478, 430 cm^{-1}. – **HRMS** (ESI+): calcd. for $C_{63}H_{50}BF_8N_{13}O_3PSi$ $[M-PF_6]^+$: 1258.3637 u, found: 1258.3648 u.

4-(1-(2-(4-(5,5-Difluoro-1,3,7,9-tetramethyl-5*H*-4λ^4,5λ^4-dipyrrolo[1,2-*c*:2',1'-*f*][1,3,2]diazaborinin-10-yl)phenoxy)ethyl)-1*H*-1,2,3-triazol-4-yl)butanal (250)

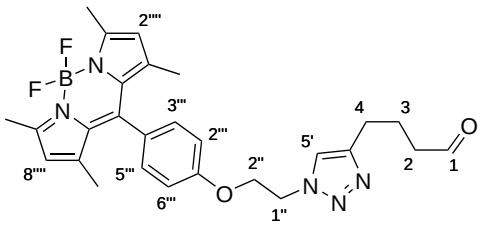

A mixture of 5-hexynal (**189**, 24.0 mg, 250 µmol), Bodipy-N_3 (**243**, 50 mg, 122 µmol), copper(II)sulfate pentahydrate (1.6 mg, 6.41 µmol) and sodium ascorbate (3.2 mg, 16.2 µmol) was suspended in a mixture of chloroform (1200 µL), ethanol (100 µL) and water (100 µL). The mixture was first reacted in a micro wave reactor (150 W) at 100 °C for 75 minutes and then stirred at room temperature for 16 hours. The solvents were removed and the residue was purified by flash column chromatography (CH_2Cl_2/EtOAc 10:1). After drying under vacuum, Bodipy **250** was obtained as a red sold (31.2 mg, 61.7 µmol, 51 %). Besides the product, not reacted Bodipy-N_3 (**243**) was isolated as a red solid (10.3 mg). – **$C_{27}H_{30}BF_2N_5O_2$** (M = 505.38 g mol^{-1}). – **^{1}H-NMR** (300 MHz, CD_3CN): δ = 9.72–9.64 (m, 1H, H-1), 7.66 (s, 1H, H-5'), 7.28–7.15 (m, 2H, H-3"', H-5"'), 7.08–6.94 (m, 2H, H-2"', H-6"'), 6.07 (s, 2H, H-2"", H-8""), 4.71 (t, ^3J = 5.0 Hz, 2H, H-2"), 4.41 (t, ^3J = 5.0 Hz, 2H, H-1"), 2.70 (t, ^3J = 7.6 Hz, 2H, H-4), 2.55–2.38 (m, 8H, H-2, H_{Methyl}), 1.99–1.86 (m, 2H, H-3), 1.40 (s, 6H, H_{Methyl}) ppm. – **^{13}C-NMR** (75.5 MHz, CD_3CN): δ = 203.6, 159.9, 156.2, 148.0, 144.5, 143.3, 132.6, 130.4, 128.3, 123.4, 122.2, 116.3, 67.7, 50.2, 43.7, 25.5, 22.7, 14.8, 14.7 ppm. – **^{19}F-NMR** (283 MHz, CD_3CN): δ = −145.0 (q, J_{FB} = 32.7 Hz, BF_2) ppm. – **^{11}B-NMR** (96.3 MHz, CD_3CN): δ = 1.29 (t, J_{BF} = 33.0 Hz) ppm. – **FT-IR** (Film) $\tilde{\nu}$ = 3144, 2928, 2729, 1720, 1669, 1609, 1543, 1509, 1470, 1438, 1409, 1371, 1306, 1287, 1243, 1194, 1157, 1120, 1085, 1047, 1013, 982, 907, 887, 843, 764, 705, 665, 640, 621, 602, 581, 558, 525, 478, 426 cm^{-1}. – **HRMS** (ESI+): calcd. for $C_{27}H_{31}BF_2N_5O_2$ $[M^+H]^+$: 506.2538 u, found: 506.2544 u.

5.4.6. Octahedral Silicon(IV) Complexes synthesized by Vertiefungsstudents

Synthesized by Andreas Schrimpf [230]

Bis(1,10-phenanthroline)(2-(pyridin-2-yl)-1*H*-benzo[*d*]imidazole-5,6-diolato-κ^2O) silicon(IV)-bis(hexafluorophosphate) (158)

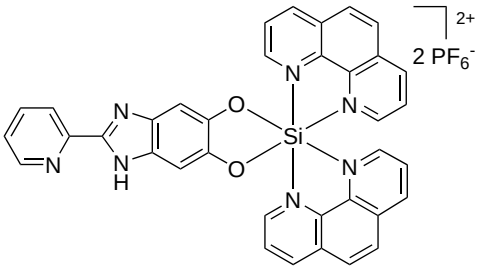

Using method C, silicon complex **130** (40.6 mg, 46.3 µmol), tin powder (43.7 mg, 368 µmol) and pyridine-2-carbaldehyde (10.0 µL, 106 µmol) were reacted to yield complex **158** as a red solid. The yield could not be determined due to the high amount of salt in the product. – **$C_{36}H_{23}F_{12}N_7O_2P_2Si$** (M = 903.64 g mol^{-1}). – **^{1}H-NMR** (300 MHz, CD_3CN): δ = 9.52 (dd, ^3J = 5.6 Hz, ^4J = 1.0 Hz, 2H, H_{phen}), 9.36 (dd, ^3J = 8.4 Hz, ^4J = 1.1 Hz, 2H, H_{phen}), 9.09 (dd, ^3J = 8.3 Hz, ^4J = 1.1 Hz, 2H, H_{phen}), 8.62–8.56 (m, 3H, H_{phen}, H_{py}), 8.54–8.44 (m, 4H, H_{phen}), 8.14 (dt, ^3J = 7.9 Hz, ^4J = 1.0 Hz, 1H, H_{py}), 7.93 (ddd, ^3J = 8.3 Hz, ^4J = 2.7, 1.5 Hz, 2H, H_{phen}), 7.85 (td, ^3J = 7.9 Hz, ^4J = 1.8 Hz, 1H, H_{py}), 7.75 (dd, ^3J = 5.7 Hz, ^4J = 1.1 Hz, 2H, H_{phen}), 7.37 (ddd, ^3J = 7.6 Hz, ^4J = 2.7, 1.0 Hz, H_{py}), 7.02 (s, 2H, H_{cat}) ppm. – **^{13}C-NMR** (75.5 MHz, CD_3CN): δ = 150.5, 149.5, 149.0, 147.5, 146.9, 146.4, 145.0, 138.3, 135.7, 134.8, 131.3, 131.0, 129.6, 129.3, 128.9, 125.3, 121.7 ppm. – **FT-IR** (Film) $\tilde{\nu}$ = 3611, 3092, 2261, 1632, 1437, 1192, 1097, 1037, 844, 759, 688, 558 cm^{-1}. – **HRMS** (ESI+): calcd. for $C_{36}H_{23}N_7O_2SiPF_6$ $[M-PF_6]^+$: 758.1319 u, found: 758.1316 u.

Synthesized by Sebastian Ullrich [244]

(2-(4-Bromophenyl)-1*H*-benzo[*d*]imidazole-5,6-diolato-κ^2O)bis(1,10-phenanthroline)silicon(IV)-bis(hexafluorophosphate) (165)

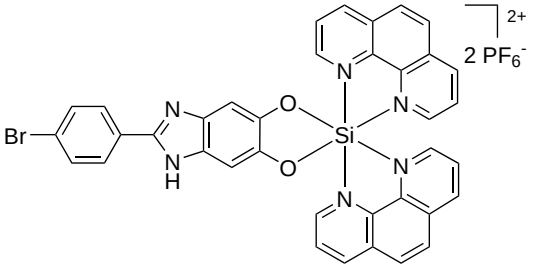

Using method C, silicon complex **130** (42.0 mg, 48.0 µmol), tin powder (48.0 mg, 406 µmol) and 4-bromobenzaldehyde (19.0 mg, 102 µmol) were reacted to yield complex **165** as an orange brown solid (16.6 mg, 16.9 µmol, 35 % over two steps). – **$C_{37}H_{23}BrF_{12}N_6O_2P_2Si$** (M = 981.55 g mol^{-1}). – **^{1}H-NMR** (300 MHz, CD_3CN): δ = 9.53 (dd, ^3J = 5.4 Hz, ^4J = 1.2 Hz, 2H, H_{phen}), 9.36 (dd, ^3J = 8.4 Hz, ^4J = 1.2 Hz, 2H, H_{phen}), 9.09 (dd, ^3J = 8.3 Hz, ^4J = 1.1 Hz, 2H, H_{phen}), 8.60 (d, ^3J = 9.1 Hz, 2H, H_{phen}), 8.51 (d, ^3J = 9.1 Hz, 2H, H_{phen}), 8.46 (dd, ^3J = 8.4, 5.4 Hz Hz, 2H, H_{phen}), 7.91–7.89 (m, 4H, 2 × H_{phenyl}, 2 × H_{phen}), 7.77 (dd, ^3J = 5.6 Hz, ^3J = 1.1 Hz, 2H, H_{phen}), 7.64 (dt, ^3J = 9.1 Hz, ^3J = 2.2 Hz, 2H, H_{phenyl}), 7.01 (s, 2H, H-4, H-7) ppm. – **FT-IR** (Film) $\tilde{\nu}$ = 3634, 3406, 3111, 1629, 1585, 1530, 1488, 1439, 1332, 1256, 1158, 1117, 1069, 1007, 958, 888, 827, 755, 713, 579, 554, 520, 484, 407 cm^{-1}. – **HRMS** (ESI+): calcd. for $C_{37}BrF_6H_{23}N_6O_2PSi$ $[M-PF_6]^+$: 837.0458 u, found: 837.0471 u. – **R_f:** 0.13 (MeCN/H_2O/satd. aq. KNO_3 50:6:2).

Bis(1,10-phenanthroline)(2-phenethyl-1*H*-benzo[*d*]imidazole-5,6-diolato-κ^2O)silicon(IV)-bis(hexafluorophosphate) (168a)

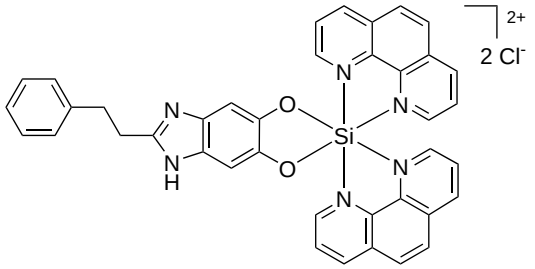

Using method C followed by method A, silicon complex **130** (105 mg, 120 µmol), tin powder (117 mg, 986 µmol) and 3-phenylpropionaldehyde (9.2 mg, 69 µmol) were reacted to yield complex **168a** as an orange brown solid (8.9 mg, 12.0 µmol, 10 % over three steps). – **$C_{39}H_{28}Cl_2N_6O_2Si$** (M = 711.68 g mol^{-1}). – **^{1}H-NMR** (300 MHz, MeOD): δ = 9.62 (d, ^3J = 4.8 Hz, 2H, H_{phen}), 9.50 (d, ^3J = 8.1 Hz, 2H, H_{phen}), 9.24 (dd, ^3J = 8.8 Hz, ^4J = 0.8 Hz, 2H, H_{phen}), 8.67 (d, ^3J = 9.1 Hz, 2H, H_{phen}), 8.61 (d, ^3J = 9.2 Hz, 2H, H_{phen}), 8.55 (dd, ^3J = 8.3, 5.4 Hz, 2H, H_{phen}), 8.09–9.02 (m, 4H, 2 × H_{phenyl}, 2 × H_{phen}), 7.25–7.15 (m, 5H, 3 × H_{phenyl}, 2 × H_{phen}), 6.91 (s, 2H, H-4, H-7), 3.11–3.07 (m, 4H, $H_{aliphatic}$) ppm. – **HRMS** (ESI+): calcd. for $C_{39}H_{27}N_6O_2Si$ $[M-2PF_6-H]^+$: 639.1959 u, found: 639.1957 u.

(2-(5-(1*H*-Imidazol-1-yl)pentyl)-1*H*-benzo[*d*]imidazole-5,6-diolato-κ^2O)bis(1,10-phenanthroline)silicon(IV)-bis(hexafluorophosphate) (169a)

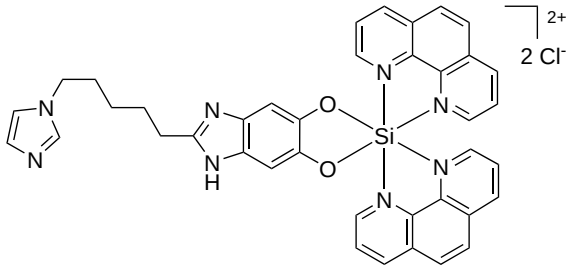

Using method C followed by method A, silicon complex **130** (49.8 mg, 56.9 µmol), tin powder (69.1 mg, 582 µmol) and 6-(1*H*-imidazol-1-yl)hexanal (14.1 mg, 84.8 µmol) were reacted to yield complex **169a** as a purple brown solid (3.4 mg, 4.8 µmol, 8 % over three steps). – **$C_{39}H_{32}Cl_2N_8O_2Si$** (M = 743.72 g mol^{-1}). – **^{1}H-NMR** (300 MHz, MeOD): δ = 9.74–9.71 (m, 2H, H_{arom}), 9.57 (d, ^3J = 8.3 Hz, 2H, H_{arom}), 9.37 (dd, ^3J = 8.2 Hz, ^4J = 1.7 Hz, 1H, H_{arom}), 9.32 (dt, ^3J = 8.1 Hz, ^4J = 1.1 Hz, 2H, H_{arom}), 9.08 (dd, ^3J = 4.5 Hz, ^4J = 1.7 Hz, 1H, H_{arom}), 8.73 (d, ^3J = 9.1 Hz, 2H, H_{arom}), 8.66 (d, ^3J = 9.2 Hz, 2H, H_{arom}), 8.63–8.57 (m, 2H, H_{arom}), 8.17 (tt, ^3J = 5.5 Hz, ^4J = 1.2 Hz, 2H, H_{arom}), 8.12 (dd, ^3J = 8.2, 5.5 Hz, 2H, H_{arom}), 7.90 (dd, ^3J = 8.2, 4.5 Hz, 1H, H_{arom}), 7.64 (d, ^3J = 4.7 Hz, 2H, H_{arom}), 3.74 (t, ^3J = 5.6 Hz, 2H, $H_{aliphatic}$), 3.07 (t, ^3J = 6.3 Hz, 2H, $H_{aliphatic}$), 2.22 (p, ^3J = 5.6 Hz, 2H, $H_{aliphatic}$), 2.05 (m, 2H, $H_{aliphatic}$), 1.29 (s, br, 2H, $H_{aliphatic}$) ppm. – **HRMS** (ESI+): calcd. for $C_{39}H_{31}N_8O_2Si$ $[M-2PF_6-H]^+$: 671.2334 u, found: 671.2224 u.

Synthesized by Sebastian Weber[265]

(2,7-Di-*tert*-butylphenanthro[4,5-*abc*]phenazine-11,12-diolato-κ^2O)bis(1,10-phenanthroline)silicon(IV)-bis(hexafluorophosphate) (144)

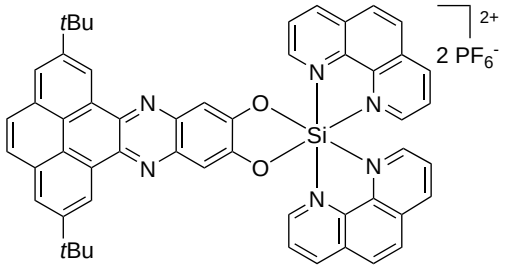

Using method C, silicon complex **130** (100 mg, 114 µmol), tin powder (115 mg, 970 µmol) and a mixture of 2,7-di-*tert*-butylpyrene-4,5-dione and 2,7-di-*tert*-butylpyrene-4,5,9,10-tetraone (3:1, 53.3 mg, 137 µmol) were reacted to yield complex **144** as an yellow solid (14.4 mg, 13.0 µmol, 12 % over two steps). In addition, the nitrate salt of dione complex **146** and dinuclear silicon(IV) complex **148** were obtained as yellow solids (31.9 mg, 32.3 µmol, 29 % and 10.0 mg, 5.17 µmol, 5 % over two steps). The product contained salt. – $\mathbf{C_{54}H_{42}F_{12}N_6O_2P_2Si}$ (M = 1124.98 g mol^{-1}). – **^{1}H-NMR** (300 MHz, CD_3CN): δ = 9.57 (dd, ^3J = 5.5 Hz, ^4J = 1.2 Hz, 2H, H_{phen}), 9.44 (d, ^4J = 2.0 Hz, 2H, H-1/3, H-6/8), 9.32 (dd, ^3J = 8.4 Hz, ^4J = 1.2 Hz, 2H, H_{phen}), 9.09 (dd, ^3J = 8.3 Hz, ^4J = 1.2 Hz, 2H, H_{phen}), 8.63–8.45 (m, 4H, H_{phen}), 8.40 (dd, ^3J = 8.4, 5.4 Hz, 2H, H_{phen}), 8.30 (d, ^4J = 2.0 Hz, 2H, H-1/3, H-6/8), 8.00 (s, 2H, H-4, H-5), 7.92 (dd, ^3J = 8.4, 5.6 Hz, 2H, H_{phen}), 7.76 (dd, ^3J = 5.6 Hz, ^4J = 1.1 Hz, 2H, H_{phen}), 7.54 (s, 2H, H-10, H-13), 1.52 (s, 18H, H_{tBu}) ppm. – **^{29}Si-NMR** (79.5 MHz, CD_3CN): δ = −149.9 ppm. – **FT-IR** (Film) $\tilde{\nu}$ = 3642, 3329,2960, 1625, 1583, 1531, 1452, 1365, 1263, 1194, 1159, 117, 834, 763, 736, 619, 559, 529, 487 cm^{-1}.

(2,7-Di-*tert*-butyl-4,5-dioxo-4,5-dihydrophenanthro[4,5-*abc*]phenazine-11,12-diolato-κ^2O)bis(1,10-phenanthroline)silicon(IV)-bis(nitrate) (146a)

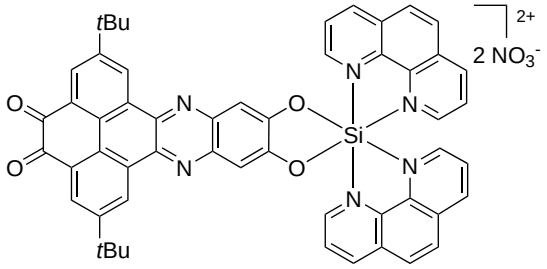

The synthesis is described above (see synthesis for complex **144**). – $\mathbf{C_{54}H_{40}N_8O_{10}Si}$ (M = 989.05 g mol^{-1}). – **^{1}H-NMR** (300 MHz, DMSO-d_6): δ = 9.73 (d, ^3J = 5.5 Hz, 2H, H_{phen}), 9.63 (d, ^3J = 8.2 Hz, 2H, H_{phen}), 9.39 (d, ^3J = 8.2 Hz, 2H, H_{phen}), 9.29 (d, ^4J = 2.2 Hz, 2H, 2H, H-1/3, H-6/8), 8.85–8.69 (m, 4H, H_{phen}), 8.63 (dd, ^3J = 8.4, 5.5 Hz, 2H, H_{phen}), 8.36 (d, ^4J = 2.2 Hz, 2H, 2H, H-1/3, H-6/8), 8.22 (d, ^3J = 5.4 Hz, 2H, H_{phen}), 8.14 (dd, ^3J = 8.2, 5.6 Hz, 2H, H_{phen}), 7.51 (s, 2H, H-10, H-13), 1.46 (s, 18H, H_{tBu}) ppm. – **^{13}C-NMR** (101 MHz, DMSO-d_6): δ = 183.4, 178.6, 151.4, 151.1, 148.8, 147.6, 146.3, 145.6, 140.3, 138.0, 134.2, 133.4, 130.5, 129.7, 129.4, 129.1, 128.9, 128.6, 128.2, 128.2, 127.8, 127.7, 127.0, 126.6, 108.8, 107.9, 35.0, 30.9 ppm. – **^{29}Si-NMR** (79.5 MHz, DMSO-d_6): δ = −147.0 ppm. – **FT-IR** (Film) $\tilde{\nu}$ = 3069, 2962, 1990, 1677, 1634, 1584, 1531, 1452, 1355, 1276, 1198, 1154, 1114, 889, 727, 619, 581,529,490, 452 cm^{-1}.

(μ-2,11-Di-*tert*-butylquinoxalino[2',3':9,10]phenanthro[4,5-*abc*]phenazine-6,7,15,16-tetraolato-κ^4O)bis(1,10-phenanthroline)disilicon(IV)-tetrakis(hexafluorophosphate) (148)

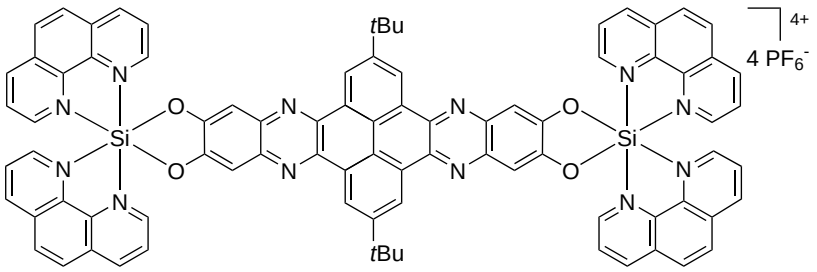

The synthesis is described above (see synthesis for complex **144**). The complex was obtained as a mixture of diastereomers (*d.r.* 1:1). – **$C_{84}H_{58}F_{24}N_{12}O_4P_4Si_2$** (M = 1935.50 g mol^{-1}). – **^{1}H-NMR** (300 MHz, CD_3CN): δ = 9.70–9.60 (m, 8H, 4H, H-1, H-3, H-10, H-12, H_{phen}), 9.41 (dd, ^3J = 8.4 Hz, ^4J = 1.2 Hz, 4H, H_{phen}), 9.18 (dd, ^3J = 8.4 Hz, ^4J = 1.1 Hz, 4H, H_{phen}), 8.67–8.55 (m, 8H, H_{phen}), 8.48 (dd, ^3J = 8.4, 5.4 Hz, 4H, H_{phen}), 8.00 (dd, ^3J = 8.3, 5.6 Hz, 4H, H_{phen}), 7.86 (dd, ^3J = 5.6 Hz, ^4J = 1.1 Hz, 4H, H_{phen}), 7.63 (s, 4H, H-5, H-8, H-14, H-17), 1.63 (s, 18H, H_{tBu}) ppm. – **^{29}Si-NMR** (79.5 MHz, CD_3CN): δ = −149.7 ppm. – **FT-IR** (Film) $\tilde{\nu}$ = 3644, 3330, 2963, 1628, 1584, 1531, 1450, 1366, 1285, 1193, 1159, 1117, 834, 763, 736, 619, 559, 528, 486 cm^{-1}.

(2,9-Di-*tert*-butylpyrazino[2',3':9,10]phenanthro[4,5-*abc*] phenazine-13,14-diolato-κ^2O)bis(1,10-phenanthroline)silicon(IV)-bis(hexafluorophosphate) (153)

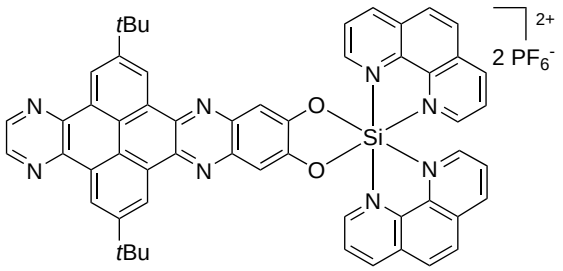

Using method D, silicon complex **146** (14.0 mg, 14.2 µmol) and ethylenediamine (10.6 µL, 158 µmol) were reacted to yield complex **153** as a yellow solid (7.6 mg, 6.45 µmol, 45 %). The product contained salt. – **$C_{56}H_{42}F_{12}N_8O_2P_2Si$** (M = 1177.02 g mol^{-1}). – **^{1}H-NMR** (300 MHz, CD_3CN): δ = 9.66 (dd, ^3J = 5.5 Hz, ^4J = 1.2 Hz, 2H, H_{phen}), 9.62 (d, ^4J = 2.1 Hz, 2H, H-1/3, H-8/10), 9.50 (d, ^4J = 2.1 Hz, 2H, H-1/3, H-8/10), 9.41 (dd, ^3J = 8.4 Hz, ^4J = 1.2 Hz, 2H, H_{phen}), 9.18 (dd, ^3J = 8.3 Hz, ^4J = 1.1 Hz, 2H, H_{phen}), 9.03 (s, 2H, H-5, H-6), 8.68–8.55 (m, 4H, H_{phen}), 8.49 (dd, ^3J = 8.3, 5.5 Hz, 2H, H_{phen}), 8.01 (dd, ^3J = 8.3, 5.6 Hz, 2H, H_{phen}), 7.85 (dd, ^3J = 5.6 Hz, ^4J = 1.2 Hz, 2H, H_{phen}), 7.63 (s, 2H, H-12, H-15), 1.62 (s, 18H, H_{tBu}) ppm. – **^{29}Si-NMR** (79.5 MHz, CD_3CN): δ = −150.2 ppm. – **FT-IR** (Film) $\tilde{\nu}$ = 3648, 2963, 1626, 1586, 1531, 1457, 1438, 1420, 1367, 1344, 1275, 1198, 1158, 1118, 1045, 908, 830, 759, 739, 718, 621, 581, 559, 528, 509, 485, 425, 412, 389 cm^{-1}.

(2,11-Di-*tert*-butylquinoxalino[2',3':9,10]phenanthro[4,5-*abc*] phenazine-6,7-diolato-κ^2O)bis(1,10-phenanthroline)silicon(IV)-bis(hexafluorophosphate) (155)

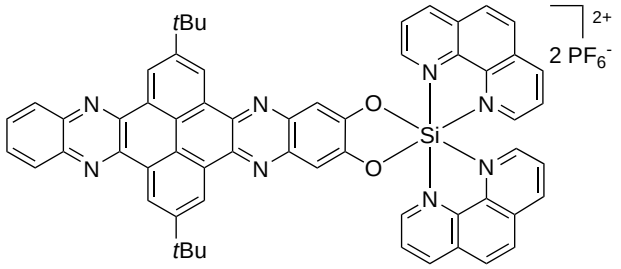

Using method D, silicon complex **146** (13.0 mg, 13.1 µmol) and *ortho*-phenylenediamine (15.0 mg, 138 µmol) were reacted to yield complex **155** as an orange solid (9.8 mg, 7.99 µmol, 61 %). The product contained salt. – $\mathbf{C_{60}H_{44}F_{12}N_8O_2P_2Si}$ (M = 1227.08 g mol^{-1}). – **^{1}H-NMR** (500 MHz, CD_3CN): δ = 9.67 (dd, ^3J = 5.5 Hz, ^4J = 1.2 Hz, 2H, H_{phen}), 9.60 (d, ^4J = 2.1 Hz, 2H, H-1/3, H-10/12), 9.48 (d, ^4J = 2.1 Hz, 2H, H-1/3, H-10/12), 9.42 (dd, ^3J = 8.4 Hz, ^4J = 1.2 Hz, 2H, H_{phen}), 9.18 (dd, ^3J = 8.3 Hz, ^4J = 1.1 Hz, 2H, H_{phen}), 8.69–8.55 (m, 4H, H_{phen}), 8.51 (dd, ^3J = 8.3, 5.5 Hz, 2H, H_{phen}), 8.32 (dd, ^3J = 6.5 Hz, ^4J = 3.4 Hz, 2H, H-14, H-17), 8.01 (dd, ^3J = 8.4, 5.6 Hz, 2H, H_{phen}), 7.91 (dd, ^3J = 6.5 Hz, ^4J = 3.4 Hz, 2H, H-15, H-16), 7.86 (dd, ^3J = 5.5 Hz, ^4J = 1.2 Hz, 2H, H_{phen}), 7.61 (s, 2H, H-5, H-8), 1.64 (s, 18H, H_{tBu}) ppm. – **^{29}Si-NMR** (79.5 MHz, CD_3CN): δ = −149.7 ppm. – **FT-IR** (Film) $\tilde{\nu}$ = 3331, 2961, 2759, 1716, 1633, 1593, 1534, 1446, 1328, 1279, 1195, 1120, 834, 764, 739, 613, 560, 530, 489, 412 cm^{-1}.

5.5. Biological Studies

5.5.1. General Information

Materials *Calf thymus* DNA (CT-DNA, c = 15.4 mM) was purchased from *Invitrogen* and human telomerase quadruplex DNA ($[TTAGGG]_4$, telo24, c = 100 µM) was purchased from *Sigma Aldrich*. For the DNA assays, CT-DNA-buffer (5 mM Tris-HCl, 20 mM NaCl, pH 7.4) and telo24-buffer (10 mM Tris-HCl, 100 mM NaCl, 1 mM EDTA, pH 7.4) were prepared. *Dolbecco's Modified Eagle's Medium* (DMEM) *low glucose* and PBS buffer, used for the cultivation of HeLa cells, were purchased from *Sigma Aldrich*. 10 mM stock solution of the investigated silicon complexes in dimethyl sulfoxide were prepared and used for all biological assays.

Biological Work: Living cell cultures like HeLa-cells were handled in a Thermo Scientific MSC-Advantage Class II biological safety cabinet. The working place was cleaned with 75% ethanol before and after usage.

5.5.2. Measurement of DNA and G4-DNA binding constants

The binding constants of the dinuclear complexes to *calf thymus* DNA and *human telomerase* quadruplex DNA ($[TTAGGG]_4$) were measured using UV-monitored titration at room temperature in buffer. A solution of the complexes in Tris-buffer (CT-DNA: 20 µM; 2 µL stock + 998 µL CT-DNA-buffer; telo24: 10 µM, 1 µL stock + 999 µL telo24-buffer) was titrated with a concentrated DNA solution (CT-DNA: 15.4 mM, diluted with buffer to a concentration of 1.54 mM; telo24: 100 µM). The dilution of the complex concentration and the remaining DMSO amount occurring during the titration was negligible. During addition of the DNA solution, a large hypochromicity and a modest bathochromic shift of the $\pi \rightarrow \pi^*$ ligand-centered charge transfer absorption band[130,135,137,138,145] or the Bodipy absorption band[293–295,297,298] was observed. The binding constants k_B and the binding volumes s

were obtained by plotting the absorption decrease of the $\pi \rightarrow \pi^*$ or of the Bodipy band as a function of increasing DNA concentration using the McGhee-von-Hippel equation (3).

$$\frac{\epsilon_a - \epsilon_f}{\epsilon_b - \epsilon_f} = \frac{b - \sqrt{\frac{2k_B^2 C_t [\mathrm{DNA}]_t}{s}}}{2k_B C_t} \tag{3}$$

$$b = 1 + k_B C_t + \frac{k_B [\mathrm{DNA}]_t}{2s} \tag{4}$$

with C_t and $[DNA]_t$ = total complex and DNA concentrations, s = base pair binding site size and ϵ_a = extinction coefficient of the complex at a given DNA concentration, ϵ_b = extinction coefficient when fully bound to DNA (determined from the plateau of the DNA titration, where addition of DNA did not lead to any further absorption change), and ϵ_f = extinction coefficient of the complex in the absence of DNA.[145,272] Each determination was performed several times. The single determinations including the mean values ± standard deviations are given in Appendix D. The corresponding spectra can be found in Appendix E.

5.5.3. Fluorescence Assay

The fluorescence assay was performed in a 96 well plate (Table 16). Each of the blue marked wells was filled with 150 µL CT-DNA-buffer (row B) or with 150 µL of a 20 µM solution of the complex in CT-DNA-buffer (row C–F). The fluorescence was measured in a range from 420–680 nm at a fixed excitation wavelength of 366 nm and a wavelength cut-off at 420 nm (5 seconds mixing before reading, 100 reads per well) to obtain the blank runs. Then, CT-DNA was added to each well (line B shows how much µL of a 1.54 mM DNA-solution was added) so that the concentration of DNA was increased by the equivalents given in line F. Then the fluorescence was measured again using the same conditions as for the blank runs.

Table 16: Figure of the 96 well plate for the measurement of the fluorescence assay. The data in the cells marked in cyan correspond to the complete column. The values in each row correspond to the units given in column 12.

		1	2	3	4	5	6	7	8	9	10	11	12
Cmp.	A												
Tris	B	1.95	3.9	7.8	11.7	15.6	19.5	23.4	27.3	31.2	35.1	39	ad. DNA /µL
246	C	152	154	158	162	166	170	173	177	181	185	189	final vol. /µL
247	D	19.8	39.0	76.1	111	145	177	208	237	265	292	318	[DNA] /µM
249	E	19.7	19.5	19	18.6	18.1	17.7	17.3	16.9	16.6	16.2	15.9	[Si] /µM
248	F	**1**	**2**	**4**	**6**	**8**	**10**	**12**	**14**	**16**	**18**	**20**	eq. DNA/Si
	G												
	H												

5.5.4. Hela Cells

The HeLa cell line is the first continuous cancer cell line extracted from human cells.[146,316] In 1951, the cells were taken from the cervix cancer of the 30-year-old black lady named Henrietta Lacks at the Johns Hopkins Hospital and were cultivated first by George Gey.[146,316] Although the growth of cervix cancer is relatively slow, the cells extracted from Ms. Lacks showed an astonishing accelerated growth together with a high resistance towards radiation therapy.[146,316] Surprisingly, further investigations exhibit that HeLa cells consists of very uncommon adenocarcinoma cells which are capable of infinite cell division due to an infection of the carcinoma cells with the human papilloma virus 18 (HPV18) leading to a deactivation of the p53 tumor-suppressor protein.[146,316–319] In addition, HeLa cells showed an unusual mutation of the human leukocyte antigen (HLA) supporting the effect of the viral infection.[316] Nowadays, HeLa cells are by far the most utilized cancer cell line in the world still possessing a relatively stable genome although cross-contaminations with other cell lines were already observed.[146,316]

5.5.5. Determination of the Cell Survival using the MTT Assay

MTT assay:[146,158,320] The survival rate of cells exposed to potential cytotoxic substances can be determined using the colorimetric MTT assay. The assay is based on a reduction of the water soluble, yellow dye 3-(4,5-dimethylthiazol-2-yl)-2,5-diphenyltetrazolium bromide (**289**, MTT) to its water insoluble form formazan (**290**) which is purple in color (Scheme 69). During the assay, the reduction is mediated by NADH or NADPH. As the biosynthesis of these reducing agents occurs in the context of vital metabolic processes like the phosphogluconate pathway or the glycolysis,[182] their presence is a direct indicator of the cell viability. Hence, the assay can be evaluated spectroscopically by measuring the absorption of the purple formazan (**290**) at 535 nm since it is proportional to the number of metabolic active cells.

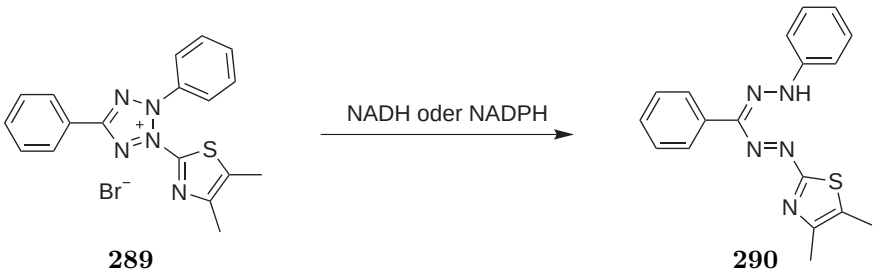

289 **290**

Scheme 69: Reduction of MTT (**289**) to formazan (**290**) using NADH or NADPH.

Cell Subcultivation: To ensure an ideal growth of the HeLa cells, a cell subcultivation of the used cell lines had to be performed every second day. This means, the cell density was diluted to provide the cells with fresh nutrient and to remove toxic metabolites of the cellular metabolism. Therefore, the medium of the culture vessel was first removed with a serological pipette. The cell culture was washed with PBS buffer (6 mL) to remove remaining medium. Then a solution of *trypsin* (4 mL, 0.05 %) was added, and the culture vessel was incubated (37 °C, 5 min, 5 % CO_2). At this step, the HeLa cells were digested and detached from the surface. Medium (4 mL) was added to cut the digestion off, and the suspension was transferred into a falcon tube. The cells were isolated by centrifugation (1000 rpm,

20 °C, 5 min), resuspended in medium (5 mL), transferred into a new culture vessel (14 drops), treated with medium (28 mL) and incubated (37 °C, 48 hours, 5 % CO_2).

Cultivation in microtiter plates: The amount of HeLa cells in the suspension gained during the cell subcultivation was calculated using a Neubauer hemocytometer (1:10 dilution of the suspension). Then the cell suspension was diluted with medium to obtain a concentration of 90 cells per microL. The MTT assay was performed in a 96 well plate in which the the outer wells were filled with medium (each with 200 µL). The inner wells were charged with the diluted cell suspension (each with 100 µL, which is equal to 9000 cells per well). The plate was finally incubated (37 °C, 24 hours, 5 % CO_2) to assure the accretion of the cells at the ground.

Execution of the assay: The stock solutions of the investigated complexes were diluted with medium and dimethyl sulfoxide to a concentration of 60 µM in medium containing 2 % dimethyl sulfoxide. The diluted solutions (100 µL) were then added to the HeLa cells in the 96 well plate (for each complex four wells were filled to gain four determinations) yielding a final concentration of 30 µM. 12 wells of the 98 well plate were treated with medium (98 µL) and dimethyl sulfoxide (2 µL) to serve as a reference. The plate was then incubated (37 °C, 24 hours, 5 % CO_2). Then the medium of all inner wells and the first six outer wells (column A) was removed and replaced by a MTT solution in medium (each with 200 µL, final concentration: 1.09 mM MTT {12 mM MTT in PBS}). After incubation (37 °C, 3 hours, 5 % CO_2) of the plate, medium (155 µL) was removed and replaced with dimethyl sulfoxide (90 µL). The plate was incubated (37 °C, 10 min, 150 rpm) again, and the absorption of the wells at 535 nm was measured on a SpectraMax M5 plate reader (2 seconds mixing before reading). To get a independent repeat determination, the assay was repeated once.

Table 17: Schematic figure of the 96 well plate that was used for the MTT assay, whereas cyan = background, violet = reference, yellow and orange = the investigated complexes. The numbers correspond to the particular silicon complexes.

	1	2	3	4	5	6	7	8	9	10	11	12
A												
B		**291**	**291**	**291**	**291**			**227**	**227**	**227**	**227**	
C		**237**	**237**	**237**	**237**			**234**	**234**	**234**	**234**	
D		**226**	**226**	**226**	**226**							
E		**224**	**224**	**224**	**224**							
F		**230**	**230**	**230**	**230**							
G		**228**	**228**	**228**	**228**							
H												

The cell surviving rate per well in percent (x) was determined using equation 5, with $\overline{OD}_{535\,\mathrm{nm},background}$ = the average of the cell free wells, $\overline{OD}_{535\,\mathrm{nm},reference}$ = average of the cell

containing but complex free wells (corresponds to a cell surviving rate of 100 % by definition) and $\overline{OD}_{535\,\mathrm{nm},wells}$ = average of the wells containing the investigated complex.

$$x = \frac{\overline{OD}_{535\,\mathrm{nm},wells} - \overline{OD}_{535\,\mathrm{nm},background}}{\overline{OD}_{535\,\mathrm{nm},reference} - \overline{OD}_{535\,\mathrm{nm},background}} \cdot 100 \tag{5}$$

6. References

[1] A. G. W. Cameron, *Space Science Reviews* **1970**, *15*, 121–146.

[2] C. Allègre, G. Manhès, E. Lewin, *Earth and Planetary Science Letters* **2001**, *185*, 49–69.

[3] E. Riedel, *Anorganische Chemie*, 6. Edition, Walter de Gruyter GmbH & Co. KG, Berlin, **2004**.

[4] R. Tacke, *Chemie in unserer Zeit* **1980**, *6*, 197–207.

[5] J. A. Duffy, D. E. Macphee, *J. Phys. Chem. B* **2007**, *111*, 8740–8745.

[6] S. D. Jacobsen, J. R. Smyth, R. J. Swope, *Phys. Chem. Minerals* **2003**, *30*, 321–329.

[7] R. Tacke, *Angew. Chem.* **1999**, *111*, 3197–3200.

[8] R. Jugdaohsingh, *J. Nutr. Health Aging* **2007**, *11*, 99–110.

[9] S. K. Wason, *J. Soc. Cosmet. Chem.* **1978**, *29*, 497–521.

[10] J. L. Gurav, I.-K. Jung, H.-H. Park, E. S. Kang, D. Y. Nadargi, *Journal of Nanomaterials* **2010**, 1–11.

[11] C.-A. Chen, S. M. Sieburth, A. Glekas, G. W. Hewitt, G. L. Trainor, S. Erickson-Viitanen, S. S. Garber, B. Cordova, S. Jeffry, R. M. Klabe, *Chemistry & Biology* **2001**, *8*, 1161–1166.

[12] R. Tacke, T. Schmid, M. Penka, C. Burschka, W. Bains, J. Warneck, *Organometallics* **2004**, *23*, 4915–4923.

[13] M. Geyer, J. A. Baus, O. Fjellström, E. Wellner, L. Gustafsson, R. Tacke, *ChemMedChem* **2015**, *10*, 2063–2070.

[14] R. Emanuelsson, H. Löfås, A. Wallner, D. Nauroozi, J. Baumgartner, C. Marschner, R. Ahuja, S. Ott, A. Grigoriev, H. Ottosson, *Chem. Eur. J.* **2014**, *20*, 9304–9311.

[15] A. Schäfer, M. Reißmann, A. Schäfer, M. Schmidtmann, T. Müller, *Chem. Eur. J.* **2014**, *20*, 9387–9393.

[16] G. Tan, B. Blom, D. Gallego, E. Irran, M. Driess, *Chem. Eur. J.* **2014**, *20*, 9400–9408.

[17] M.-D. Su, *Chem. Eur. J.* **2014**, *20*, 9419–9423.

[18] N. Hurkes, H. M. A. Ehmann, M. List, S. Spirk, M. Bussiek, F. Belaj, R. Pietschnig, *Chem. Eur. J.* **2014**, *20*, 9330–9335.

[19] K. Taira, M. Ichinohe, P. A. Sekiguchi, *Chem. Eur. J.* **2014**, *20*, 9342–9348.

[20] J. Hermeke, H. F. T. Klare, P. M. Oestreich, *Chem. Eur. J.* **2014**, *20*, 9250–9254.

[21] K. Igawa, Y. Kawasaki, K. Nishino, N. Mitsuda, K. Tomooka, *Chem. Eur. J.* **2014**, *20*, 9255–9258.

[22] M. Zhao, W. Xie, C. Cui, *Chem. Eur. J.* **2014**, *20*, 9259–9262.

[23] E. Riedel, R. Alsfasser, C. Janiak, T. M. Klapötke, H.-J. Meyer, *Moderne Anorganische Chemie*, 3. Edition, Walter de Gruyter GmbH & Co. KG, Berlin, **2007**.

[24] F. S. Kipping, L. L. Lloyd, *J. Chem. Soc., Trans.* **1901**, *79*, 449–459.

[25] R. D. Dickerson, I. Geis, *Chemie - eine lebendige und anschauliche Einführung*, 1. Edition, WILEY-VCH Verlag GmbH, Weinheim, **1999**.

[26] B. G. Gribov, K. V. Zinov'ev, *Inorg. Mat.* **2003**, *39*, 653–662.

[27] A. Müller, M. Ghosh, R. Sonnenschein, P. Woditsch, *Mat. Sci. Eng. B* **2006**, *134*, 257–262.

[28] T. Breiding, *Oktaedrische Silicium(IV)komplexe: Methodenentwicklung und Anwendung als Enzyminhibitoren*, PhD Thesis, Philipps-Universität Marburg, **2015**.

[29] G. Cook, L. Billman, R. Adcock, *Photovoltaic Fundamentals*, 1. revised Edition, U.S. Department of Energy, Washington, **1995**.

[30] S. Rendler, M. Oestreich, *Synthesis* **2005**, *11*, 1727–1747.

[31] R. R. Holmes, *Chem. Rev.* **1990**, *90*, 17–31.

[32] R. R. Holmes, *Chem. Rev.* **1996**, *96*, 927–950.

[33] C. Chuit, R. J. P. Corriu, C. Reye, J. C. Young, *Chem. Rev.* **1993**, *93*, 1371–1448.

[34] D. Schöne, D. Gerlach, C. Wiltzsch, E. Brendler, T. Heine, E. Kroke, J. Wagler, *Eur. J. Inorg. Chem.* **2010**, *93*, 461–467.

[35] N. Auner, R. Probst, F. Hahn, E. Herdtweck, *J. Organomet. Chem.* **1993**, *459*, 25–41.

[36] C. Brelière, F. Carré, R. J. P. Corriu, G. Royo, M. Wong Chi Man, *Organometallics* **1994**, *13*, 307–314.

[37] Y. Xiang, C. Fu, T. Breiding, P. K. Sasmal, H. Liu, Q. Shen, K. Harms, L. Zhang, E. Meggers, *Chem. Commun.* **2012**, *48*, 7331–7133.

[38] J. Henker, S. Glöckner, E. Meggers, *J. Biol. Inorg. Chem.* **2014**, *19 (Suppl. 1)*, S367.

[39] R. J. P. Corriu, C. Guérin, B. Henner, Q. Wang, *Organometallics* **1991**, *10*, 2297–2303.

[40] R. J. P. Corriu, C. Guérin, B. J. L. Henner, Q. Wang, *Organometallics* **1991**, *10*, 3574–3581.

[41] B. Becker, R. Corriu, C. Guérin, B. Henner, Q. Wang, *J. Organomet. Chem.* **1989**, *368*, C25–C28.

[42] W. B. Jensen, *J. Chem. Edu.* **2006**, *83*, 1751–1752.

[43] O. J. Curnow, *J. Chem. Edu.* **1998**, *75*, 910–915.

[44] D. W. Smith, *J. Chem. Edu.* **2005**, *82*, 1202–1204.

[45] R. J. Gillespie, B. Silvi, *Coord. Chem. Rev.* **2002**, *233-234*, 53–62.

[46] G. N. Lewis, *J. Am. Chem. Soc.* **1916**, *38*, 762–785.

[47] I. Langmuir, *J. Am. Chem. Soc.* **1919**, *41*, 868–934.

[48] J. L. Musher, *Angew. Chem. Int. Ed. Engl.* **1969**, *8*, 54–68.

[49] A. E. Reed, F. Weinhold, *J. Am. Chem. Soc.* **1986**, *108*, 3586–3593.

[50] E. Magnusson, *J. Am. Chem. Soc.* **1990**, *112*, 7940–7951.

[51] D. G. Gilheany, *Chem. Rev.* **1994**, *94*, 1339–1374.

[52] A. E. Reed, P. von Ragué Schleyer, *J. Am. Chem. Soc.* **1990**, *112*, 1434–1445.

[53] S. C. A. H. Pierrefixe, *Hypervalence and Aromaticity*, PhD Thesis, Vrije Universitetit Amsterdam, **2008**.

[54] I. Storer, *Hypervalent Silicon: Bonding, Properties and Synthetic Utility*, MacMillan Group Meeting, Princeton University, **20th July, 2005**.

[55] G. C. Pimentel, *J. Chem. Phys.* **1951**, *19*, 446–448.

[56] R. J. Hach, R. Rundle, *J. Am. Chem. Soc.* **1951**, *73*, 4321–4324.

[57] R. Rundle, *J. Am. Chem. Soc.* **1963**, *85*, 112–113.

[58] D. Schomburg, *Z. Naturforsch.* **1982**, *37B*, 195–197.

[59] J. L. Gay-Lussac, L. J. Thenard, *Mémoires de Physique et de Chimie de la Société d'Arcueil* **1809**, *2*, 317–331.

[60] J. Davy, *Phil. Trans. R. Soc. Lond.* **1812**, *102*, 352–369.

[61] J. J. Berzelius, *Philosophical Magazine* **1825**, *65*, 254–267.

[62] J. J. Berzelius, *Annalen der Physik* **1824**, *77*, 169–230.

[63] U. Wannagat, *Angew. Chem.* **1957**, *69*, 516.

[64] R. M. Pike, R. R. Luongo, *J. Am. Chem. Soc.* **1966**, *88*, 2972–2976.

[65] W. B. Farnham, J. F. Whitney, *J. Am. Chem. Soc.* **1984**, *106*, 3992–3994.

[66] C. Brelière, R. J. P. Corriu, G. Royo, W. W. C. Wong Chi Man, J. Zwecker, *Organometallics* **1990**, *9*, 2633–2635.

[67] C. Brelière, F. Carré, R. J. P. Corriu, M. Poirier, G. Royo, J. Zwecker, *Organometallics* **1989**, *8*, 1831–1833.

[68] K. Junold, C. Burschka, R.Bertermann, R. Tacke, *Dalton Trans.* **2011**, *40*, 9844–9857.

[69] K. Junold, C. Burschka, R. Bertermann, R. Tacke, *Dalton Trans.* **2010**, *39*, 9401–9413.

[70] O. Seiler, C. Burschka, M. Fischer, M. Penka, R. Tacke, *Inorg. Chem.* **2005**, *44*, 2337–2346.

[71] F. M. Mück, J. A. Baus, R. Bertermann, R. Tacke, *Eur. J. Inorg. Chem.* **2016**, 3240–3245.

[72] K. Junold, M. Nutz, J. A. Baus, C. Burschka, C. Fonseca Guerra, F. M. Bickelhaupt, R. Tacke, *Chem. Eur. J.* **2014**, *20*, 9319–9329.

[73] K. Junold, F. M. Mück, C. Kupper, J. A. Baus, C. Burschka, R. Tacke, *Chem. Eur. J.* **2014**, *20*, 12781–12785.

[74] J. Weiß, J. A. Baus, C. Burschka, R. Tacke, *Eur. J. Inorg. Chem.* **2014**, 2449–2455.

[75] S. Cota, M. Beyer, R. Bertermann, C. Burschka, K. Götz, M. Kaupp, R. Tacke, *Chem. Eur. J.* **2010**, *16*, 6582–6589.

[76] O. Seiler, C. Burschka, S. Metz, M. Penka, R. Tacke, *Chem. Eur. J.* **2005**, *11*, 7379–7386.

[77] J. Wagler, U. Böhme, E. Kroke, *Struct. Bond.* **2014**, *155*, 29–106.

[78] A. Kämpfe, E. Brendler, E. Kroke, , J. Wagler, *Chem. Eur. J.* **2014**, *20*, 9409–9418.

[79] D. Gerlach, E. Brendler, J. Wagler, *Inorganics* **2016**, *4*, 8.

[80] S. Karamouzi, A. Maniadaki, D. A. Nasiopoulou, E. Kotali, A. Kotali, P. A. Harris, J. Raftery, J. A. Joule, *Synthesis* **2013**, *45*, 2150–2154.

[81] K. Singh, D. Pal, *J. Serb. Chem. Soc.* **2010**, *75*, 917–927.

[82] K. Singh, P. Puri, Y. Kumar, C. Sharma, *ISRN Inorg. Chem.* **2013**, *Article ID 356802*.

[83] P.-C. Lo, C. M. H. Chan, J.-Y. Liu, W.-P. Fong, D. K. P. Ng, *J. Med. Chem.* **2007**, *50*, 2100–2107.

[84] N. L. Oleinick, A. R. Antunez, M. E. Clay, B. D. Rihter, M. E. Kenney, *Photochem. Photobiol.* **1993**, *57*, 242–247.

[85] J.-D. Huang, S. Wang, P.-C. Lo, W.-P. Fong, W.-H. Ko, D. K. P. Ng, *New. J. Chem.* **2004**, *28*, 348–354.

[86] M. Kumada, K. Tamao, J. Yoshida, *J. Organomet. Chem.* **1982**, *239*, 115–132.

[87] R. Müller, *Organometal. Chem. Rev.* **1966**, *1*, 359–377.

[88] A. Boudin, G. Cerveau, C. Chuit, R. J. P. Corriu, C. Reye, *Organometallics* **1988**, *7*, 1165–1171.

[89] A. Boudin, G. Cerveau, C. Chuit, R. J. P. Corriu, C. Reye, *Angew. Chem. Int. Ed. Engl.* **1986**, *25*, 474–476.

[90] R. Tacke, M. Penka, F. Popp, I. Richter, *Eur. J. Inorg. Chem.* **2002**, 1025–1028.

[91] O. Seiler, C. Burschka, M. Penka, R. Tacke, *Z. Anorg. Allg. Chem.* **2002**, *628*, 2427–2434.

[92] X. Kästele, P. Klüfers, F. Kopp, J. Schuhmacher, M. Vogt, *Chem. Eur. J.* **2005**, *11*, 6326–6346.

[93] K. Benner, P. K. und Martin Vogt, *Angew. Chem.* **2003**, *115*, 1088–1093.

[94] S. D. Kinrade, A.-M. E. Gillson, C. T. G. Knight, *J. Chem. Soc., Dalton Trans.* **2002**, 307–309.

[95] T. Schmiederer, S. Rausch, M. Valdebenito, Y. Mantri, E. Mösker, T. Baramov, K. Stelmaszyk, P. Schmieder, D. Butz, S. I. Müller, K. Schneider, M.-H. Baik, K. Hantke, R. D. Süssmuth, *Angew. Chem. Int. Ed.* **2011**, *50*, 4230–4233.

[96] T. J. N. Kenla, M. D. Kongue Tatong, F. M. Talontsi, B. Dittrich, H. Frauendorf, H. Laatsch, *Chem. Commun.* **2013**, *49*, 7641–7643.

[97] F. Peuckert, *Identifizierung und Charakterisierung von Siderophorbindungsproteinen aus Bacillus subtilis*, PhD Thesis, Philipps-Universität Marburg, **2011**.

[98] W. Dilthey, *Chem. Ber.* **1903**, *36*, 923–929.

[99] W. Dilthey, F. Eduardoff, F. J. Schumacher, *Liebigs Ann. Chem.* **1903**, *344*, 300–313.

[100] R. WEST, *J. Am. Chem. Soc.* **1958**, *80*, 3246–3249.

[101] V. D. S. K. Dhar, S. Kirschner, *J. Am. Chem. Soc.* **1958**, *80*, 753–754.

[102] V. D. S. K. Dhar, S. Kirschner, *J. Am. Chem. Soc.* **1959**, *81*, 6372–6375.

[103] F. Pietra, *Chem. Rev.* **1973**, *73*, 239–364.

[104] E. L. Muetterties, C. M. Wright, *J. Am. Chem. Soc.* **1964**, *86*, 5132–5137.

[105] D. Kummer, K. Gaißer, T. Seshadri, *Chem. Ber.* **1977**, *110*, 1950–1962.

[106] D. Kummer, T. Seshadri, *Chem. Ber.* **1977**, *110*, 2355–2367.

[107] D. Kummer, H. Köster, *Z. Anorg. Allg. Chem.* **1973**, *398*, 279–292.

[108] D. Kummer, H. Köster, *Z. Anorg. Allg. Chem.* **1973**, *402*, 297–304.

[109] D. Kummer, T. Seshadri, *Z. Anorg. Allg. Chem.* **1976**, *425*, 236–248.

[110] D. Kummer, T. Seshadri, *Z. Anorg. Allg. Chem.* **1977**, *432*, 153–159.

[111] Y. Ohmori, M. Kojima, S. Kashino, Y. Yoshikawa, *J. Coord. Chem.* **1996**, *39*, 219–230.

[112] C. Maguylo, C. Chukwu, M. Aun, T. B. Monroe, C. Ceccarelli, D. S. Jones, J. W. Merkert, B. T. Donovan-Merkert, T. A. Schmedake, *Polyhedron* **2015**, *94*, 52–58.

[113] D. A. Lee, S. K. Moon, A. N. Sizeland, N. W. Gould, E. M. Gbarbea, D. Owusu, D. S. Jones, T. A. Schmedake, *Inorg. Chem. Commun.* **2013**, *33*, 125–128.

[114] B. Suthar, A. Aldongarov, I. S. Irgibaeva, M. Moazzen, B. T. Donovan-Merkert, J. W. Merkert, T. A. Schmedake, *Polyhedron* **2012**, *31*, 754–758.

[115] M. J. Cleare, J. D. Hoeschele, *Bioinorg. Chem.* **1973**, *2*, 187–210.

[116] M. J. Cleare, J. D. Hoeschele, *Platin. Met. Rev.* **1973**, *17*, 2–13.

[117] J. C. Dabrowiak, *Metals in Medcine*, 1. Edition, John Wiley & Sons Ltd, West Sussex, **2009**.

[118] E. R. Jamieson, S. J. Lippard, *Chem. Rev.* **1999**, *99*, 2467–2498.

[119] A. M. J. Fichtinger-Schepman, J. L. van der Veer, J. H. J. den Hartog, P. H. M. Lohman, J. Reedijk, *Biochemistry* **1984**, *24*, 707–713.

[120] B. Rosenberg, *Platin. Met. Rev.* **1971**, *15*, 42–51.

[121] F. A. Blommaert, H. C. M. van Dijk-Knijnenburg, F. J. Dijt, L. den Engelse, R. A. Baan, F. Berends, A. M. J. Fichtinger-Schepman, *Biochemistry* **1995**, *34*, 8474–8480.

[122] P. Takahara, A. C. Rosenzweig, C. A. Frederick, S. Lippard, *Nature* **1995**, *377*, 649–652.

[123] Y. Maeda, K. Nunomura, E. Ohtsubo, *J. Mol. Biol.* **1990**, *215*, 321–239.

[124] H. Köpf, P. Köpf-Maier, *Angew Chem. Int. Ed. Engl.* **1979**, *19*, 477–478.

[125] E. Meléndez, *Crit. Rev. in Oncology/Hematology* **2002**, *42*, 309–315.

[126] M. Guo, H. Sun, H. J. McArdle, L. Gambling, P. J. Sadler, *Biochemistry* **2000**, *39*, 10023–10033.

[127] P. Yang, M. Guo, *Coord. Chem. Rev.* **1999**, *189*, 185–186.

[128] B. M. Zeglis, V. C. Pierre, J. K. Barton, *Chem. Commun.* **2007**, 4565–4579.

[129] K. E. Erkilla, D. T. Odom, J. K. Barton, *Chem. Rev.* **1999**, *99*, 2777–2795.

[130] R. E. Holmlin, J. A. Yao, J. K. Barton, *Inorg. Chem.* **1999**, *38*, 174–189.

[131] J. K. Barton, *Science* **1986**, *233*, 727–734.

[132] J. K. Barton, A. D. LENA A. Basile, A. Alexandrescu, *Proc. Natl. Acad. Sci. USA* **1984**, *81*, 1961–1965.

[133] T. E. Goyne, D. S. Sigman, *J. Am. Chem. Soc.* **1987**, *109*, 2846–2848.

[134] T. B. Thederahn, M. D. Kuwabara, T. A. Larsen, D. S. Sigman, *J. Am. Chem. Soc.* **1989**, *111*, 4941–4946.

[135] C. Hiort, P. Lincoln, B. Norden, *J. Am. Chem. Soc.* **1993**, *115*, 3448–3454.

[136] I. Haq, P. Lincoln, D. Suh, B. Norden, B. Z. Chowdhry, J. B. Chaires, *J. Am. Chem. Soc.* **1995**, *117*, 4788–4796.

[137] Y. Sun, D. A. Lutterman, C. Turro, *Inorg. Chem.* **2008**, *47*, 6427–6434.

[138] R. B. Nair, E. S. Teng, S. L. Kirkland, C. J. Murphy, *Inorg. Chem.* **1998**, *37*, 139–141.

[139] P. U. Maheswari, V. Rajendiran, M. Palaniandavar, R. Thomas, G. Kulkarni, *Inorg. Chim. Acta* **2006**, *359*, 4601–4612.

[140] C. Rajput, R. Rutkaite, L. Swanson, I. Haq, , J. A. Thomas, *Chem. Eur. J* **2006**, *12*, 4611–4619.

[141] Y. Jenkins, A. E. Friedman, N. J. Turro, J. K. Barton, *Biochemistry* **1992**, *31*, 10809–10816.

[142] A. E. Friedman, J.-C. Chambron, J.-P. Sauvage, N. J. Turro, J. K. Barton, *J. Am. Chem. Soc.* **1990**, *112*, 4960–4962.

[143] Y. Liu, A. Chouai, N. N. Degtyareva, D. A. Lutterman, K. R. Dunbar, C. Turro, *J. Am. Chem. Soc.* **2005**, *127*, 10796–10797.

[144] D. A. Lutterman, A. Chouai, Y. Liu, Y. Sun, C. D. Stewart, K. R. Dunbar, C. Turro, *J. Am. Chem. Soc.* **2008**, *130*, 1163–1170.

[145] A. M. Angeles-Boza, P. M.Bradley, P. K. Fu, S. E. Wicke, J. Bacsa, K. R. Dunbar, C. Turro, *Inorg. Chem.* **2004**, *43*, 8510–8519.

[146] J. Henker, *Darstellung mehrkerniger Metallkomplexe als neue strukturelle Gerüste für die chemische Biologie*, Master Thesis, Philipps-Universität Marburg, **2011**.

[147] H. Murner, B. A. Jackson, J. K. Barton, *Inorg. Chem.* **1998**, *37*, 3007–3012.

[148] H. Junicke, J. R. Hart, J. Kisko, O. Glebov, I. R. Kirsch, J. K. Barton, *Proc. Natl. Acad. Sci. USA* **2003**, *100*, 3737–3742.

[149] Y. Xiang, *GNA as a scaffold for chromophores aggregates and design of silicon-based DNA binders*, PhD Thesis, Philipps-Universität Marburg, **2013**.

[150] C. Fu, *Contributions to the Asymmetric Synthesis of Octahedral Ruthenium(II) Complexes and to Bioactive Hexacoordinate Silicon Complexes*, PhD Thesis, Philipps-Universität Marburg, **2014**.

[151] S. A. Ezadyar, A. S. Kumbhar, A. A. Kumbhar, A. Khan, *Polyhedron* **2012**, *36*, 45–55.

[152] M. R. Gill, J. Garcia-Lara, S. J. Foster, C. Smythe, G. Battaglia, J. A. Thomas, *Nat. Chem.* **2009**, *1*, 662–667.

[153] C.-C. Ju, A.-G. Zhang, C.-L. Yuan, X.-L. Zhao, K.-Z. Wang, *J. Inorg. Biochem.* **2011**, *105*, 435–443.

[154] E. Craver, A. McCrate, M. Nielsen, S. Swavey, *Inorg. Chim. Acta* **2010**, *363*, 453 – 456.

[155] Y.-G. Fang, J. Zhang, S.-Y. Chen, N. Jiang, H.-H. Lin, Y. Zhang, X.-Q. Yu, *Bioorg. Med. Chem.* **2007**, *15*, 696 – 701.

[156] M. G. Mendoza-Ferri, C. G. Hartinger, M. A. Mendoza, M. Groessl, A. E. Egger, R. E. Eichinger, J. B. Mangrum, N. P. Farrell, M. Maruszak, P. J. Bednarski, F. Klein, M. A. Jakupec, A. A. Nazarov, K. Severin, B. K. Keppler, *J. Med. Chem.* **2009**, *52*, 916 – 925.

[157] R. M. Hartshorn, J. K. Barton, *J. Am. Chem. Soc.* **1992**, *114*, 5919–5925.

[158] E. K. Martin, *Dimetallische molekulare Verbindungen auf Basis von Benzo[h]tripyrido[3,2-a:2',3'-c:2",3"-j]phenazin und 2,2':5',2"-Terpyridin als potentielle neue Gerüste in der chemischen Biologie.*, Master Thesis, Philipps-Universität Marburg, **2011**.

[159] M. K. Brennaman, T. J. Meyer, J. M. Papanikolas, *J. Phys. Chem. A* **2004**, *108*, 9938–9944.

[160] M. K. Brennaman, J. H. Alstrum-Acevedo, C. N. Fleming, P. Jang, T. J. Meyer, J. M. Papanikolas, *J. Am. Chem. Soc.* **2002**, *124*, 15094–15098.

[161] J. D. Watson, F. H. C. Crick, *Nature* **1953**, *171*, 737–738.

[162] P. Murat, Y. Singh, E. Defrancq, *Chem. Soc. Rev.* **2011**, *40*, 5293–5307.

[163] J. L. Huppert, *Chem. Soc. Rev.* **2008**, *37*, 1375–1384.

[164] S. N. Georgiades, N. H. A. Karim, K. Suntharalingam, R. Vilar, *Angew. Chem. Int. Ed.* **2010**, *49*, 4020–4034.

[165] E. Gavathiotis, M. S. Searle, *Org. Biomol. Chem.* **2003**, *1*, 1650–1656.

[166] M. Gellert, M. N. Lipsett, D. R. Davies, *Proc. Natl. Acad. Sci. USA* **1962**, *48*, 2013–2018.

[167] S. T. Madariaga, J. G. Contreras, *J. Chil. Chem. Soc.* **2010**, *55*, 50–52.

[168] G. N. Parkinson, M. P. H. Lee, S. Neidle, *Nature* **2002**, *417*, 876–880.

[169] Y. Wang, D. J. Patel, *Structure* **1993**, *1*, 263–282.

[170] J. T. Davis, *Angew. Chem.* **2004**, *116*, 684–716.

[171] D. J. Patel, A. T. Phan, V. Kuryavyi, *Nucl. Acids Res.* **2007**, *35*, 7429–7455.

[172] A. T. Phan, K. N. Luu, D. J. Patel, *Nucl. Acids Res.* **2006**, *34*, 5715–5719.

[173] S. Burge, G. N. Parkinson, P. Hazel, A. K. Todd, S. Neidle, *Nucl. Acids Res.* **2006**, *34*, 5402–5415.

[174] N. H. Campbell, G. N. Parkinson, *Methods* **2007**, *43*, 252–263.

[175] J. Dai, C. Punchihewa, A. Ambrus, D. Chen, R. A. Jones, D. Yang, *Nucl. Acids Res.* **2007**, *35*, 2440–2450.

[176] A. Siddiqui-Jain, C. L. Grand, D. J. Bearss, L. H. Hurley, *Proc. Natl. Acad. Sci. USA* **2002**, *99*, 11593–11598.

[177] C. L. Grand, H. Han, R. M. Muñoz, S. Weitman, D. D. Von Hoff, L. H. Hurley, D. J. Bearss, *Mol. Cancer Ther.* **2002**, *1*, 565–573.

[178] A. M. Zahler, J. R. Williamson, T. R. Cech, D. M. Prescott, *Nature* **1991**, *350*, 718–720.

[179] V. L. Makarov, Y. Hirose, J. P. Langmore, *Cell* **1997**, *88*, 657–666.

[180] E. H. Blackburn, *Nature* **1991**, *350*, 657–573.

[181] J. Y. Lee, B. Okumus, D. S. Kim, T. Ha, *Proc. Natl. Acad. Sci. USA* **2005**, *102*, 18938–18943.

[182] J. M. Berg, J. L. Tymoczko, L. Stryer, *Biochemie*, 6. Edition, Elsevier GmbH, München, **2007**.

[183] C. W. Greider, E. H. Blackburn, *Cell* **1985**, *43*, 405–413.

[184] K. A. Olaussen, K. Dubrana, J. Domont, J.-P. Spano, L. Sabatier, J.-C. Soria, *Crit. Rev. Oncol. Hematol.* **2006**, *57*, 191–214.

[185] M.-Y. Kim, H. Vankayalapati, K. Shin-ya, K. Wierzba, L. H. Hurley, *J. Am. Chem. Soc.* **2006**, *124*, 2098–2099.

[186] H. Han, D. R. Langley, A. Rangan, L. H. Hurley, *J. Am. Chem. Soc.* **2001**, *123*, 8902–8913.

[187] A. D. Moorhouse, A. M. Santos, M. Gunaratnam, M. Moore, S. Neidle, J. E. Moses, *J. Am. Chem. Soc.* **2006**, *128*, 15972–15973.

[188] S. Balasubramanian, L. H. Hurley, S. Neidle, *Nat. Rev. Drug. Discov.* **2011**, *10*, 261–275.

[189] S. Rankin, A. P. Reszka, J. Huppert, M. Zloh, G. N. Parkinson, A. K. Todd, S. Ladame, S. Balasubramanian, , S. Neidle, *J. Am. Chem. Soc.* **2005**, *127*, 10584–10589.

[190] J. Dash, P. S. Shirude, S.-T. D. Hsu, S. Balasubramanian, *J. Am. Chem. Soc.* **2008**, *130*, 15950–15956.

[191] I. Ourliac-Garnier, M.-A. Elizondo-Riojas, S. Redon, N. P. Farrell, S. Bombard, *Biochemistry* **2005**, *44*, 10620–10634.

[192] H. Bertrand, S. Bombard, D. Monchaud, E. Talbot, A. Guédin, J.-L. Mergny, R. Grünert, P. J. Bednarski, M.-P. Teulade-Fichou, *Org. Biomol. Chem.* **2009**, *7*, 2864–2871.

[193] R. Rodriguez, G. Dan Pantos, D. P. N. Goncalves, J. K. M. Sanders, S. Balasubramanian, *Angew. Chem. Int. Ed.* **2007**, *46*, 5405–5407.

[194] G. N. Parkinson, R. Ghosh, S. Neidle, *Biochemistry* **2007**, *46*, 2390–2397.

[195] D.-F. Shi, R. T. Wheelhouse, D. Sun, L. H. Hurley, *J. Med Chem.* **2001**, *44*, 4509–4523.

[196] M. A. Read, S. Neidle, *Biochemistry* **2000**, *39*, 13422–13432.

[197] L. R. Keating, V. A. Szalai, *Biochemistry* **2004**, *43*, 15891–15900.

[198] J. Pan, S. Zhang, *J. Biol. Inorg. Chem.* **2007**, *14*, 401–407.

[199] S. E. Evans, M. A. Mendez, K. B. Turner, L. R. Keating, R. T. Grimes, S. Melchoir, V. A. Szalai, *J. Biol. Inorg. Chem.* **2007**, *12*, 1235–1249.

[200] I. M. Dixon, F. Lopez, A. M. Tejera, J.-P. Estève, M. A. Blasco, G. Pratviel, B. Meunier, *J. Am. Chem. Soc.* **2007**, *129*, 1502–1503.

[201] J. Alzeer, B. R. Vummidi, P. J. C. R. und Nathan W. Luedtke, *Angew. Chem.* **2009**, *121*, 9526–9529.

[202] L. Zhang, J. Huang, L. Ren, M. Bai, L. Wu, B. Zhai, X. Zhou, *Bioorg. Med. Chem.* **2008**, *16*, 303–312.

[203] L. Ren, A. Zhang, J. Huang, P. Wang, X. Weng, L. Zhang, F. Liang, Z. Tan, X. Zhou, *ChemBioChem* **2007**, *8*, 775–780.

[204] J. E. Reed, A. A. Arnal, S. Neidle, R. Vilar, *J. Am. Chem. Soc.* **2006**, *128*, 5992–5993.

[205] A. Arola-Arnal, J. Benet-Buchholz, S. Neidle, R. Vilar, *Inorg. Chem.* **2008**, *47*, 11910–11919.

[206] P. Wu, D.-L. Ma, C.-H. Leung, S.-C. Yan, N. Zhu, R. Abagyan, C.-M. Che, *Chem. Eur. J.* **2009**, *15*, 13008–13021.

[207] D. Monchaud, P. Yang, L. Lacroix, M.-P. Teulade-Fichou, J.-L. Mergny, *Angew. Chem.* **2008**, *120*, 4936–4939.

[208] K. Suntharalingam, A. J. P. White, R. Vilar, *Inorg. Chem.* **2009**, *48*, 9427–9435.

[209] H. Bertrand, D. Monchaud, A. De Cian, R. Guillot, J.-L. Mergny, M.-P. Teulade-Fichou, *Org. Biomol. Chem.* **2007**, *5*, 2555–2559.

[210] J. Talib, C. Green, K. J. Davis, T. Urathamakul, J. L. Beck, J. R. Aldrich-Wright, S. F. Ralph, *Dalton Trans.* **2008**, 1018–1026.

[211] J. E. Reed, S. Neidle, R. Vilar, *Chem. Commun.* **2007**, 4366–4368.

[212] D.-L. Ma, C.-M. Che, S.-C. Yan, *J. Am. Chem. Soc.* **2009**, *131*, 1835–1846.

[213] R. Kieltyka, P. Englebienne, J. Fakhoury, C. Autexier, N. Moitessier, H. F. Sleiman, *J. Am. Chem. Soc.* **2008**, *130*, 10040–10041.

[214] W.-J. Mei, X.-Y. Wei, Y.-J. Liu, B. Wang, *Transition Met. Chem.* **2008**, *33*, 907–910.

[215] S. Shi, J. Liu, T. Yao, X. Geng, L. Jiang, Q. Yang, L. Cheng, L. Ji, *Inorg. Chem.* **2008**, *47*, 2910–2912.

[216] L. Feng, Y. Geisselbrecht, S. Blanck, A. Wilbuer, G. E. Atilla-Gokcumen, P. Filippakopoulos, K. Kräling, M. A. Celik, K. Harms, J. Maksimoska, R. Marmorstein, G. Frenking, S. Knapp, L.-O. Essen, E. Meggers, *J. Am. Chem. Soc.* **2011**, *133*, 5976–5986.

[217] S. Blanck, T. Cruchter, A. Vultur, R. Riedel, K. Harms, M. Herlyn, E. Meggers, *Organometallics* **2011**, *30*, 4598–4606.

[218] A. Wilbuer, D. H. Vlecken, D. J. Schmitz, K. Kräling, K. Harms, C. P. Bagowski, E. Meggers, *Angew. Chem. Int. Ed.* **2010**, *49*, 3839–3842.

[219] J. Qin, R. Rajaratnam, L. Feng, J. Salami, J. S. Barber-Rotenberg, J. Domsic, P. Reyes-Uribe, H. Liu, D. Dang, S. L. Berger, J. Villanueva, E. Meggers, R. Marmorstein, *J. Med. Chem.* **2015**, *58*, 305–314.

[220] M. Streib, K. Kräling, K. Richter, X. Xie, H. Steuber, E. Meggers, *Angew. Chem. Int. Ed.* **2014**, *53*, 305–309.

[221] K. Wähler, A. Ludewig, P. Szabo, K. Harms, E. Meggers, *Eur. J. Inorg. Chem.* **2014**, 807–811.

[222] P. Göbel, F. Ritterbusch, M. Helms, M. Bischof, K. Harms, M. Jung, *Eur. J. Inorg. Chem.* **2015**, 1654–1659.

[223] F. Shao, J. K. Barton, *J. Am. Chem. Soc.* **2007**, *129*, 14733–14738.

[224] T. Breiding, J. Henker, C. Fu, Y. Xiang, S. Glöckner, P. Hofmann, K. Harms, E. Meggers, *Eur. J. Inorg. Chem.* **2014**, 2924–2933.

[225] S. Glöckner, *Darstellung zweikerniger Ruthenium-Silicium-Komplexe als DNA-bindende Moleküle*, Bachelor Thesis, Philipps-Universität Marburg, **2013**.

[226] Z. Yang, F. Tan, H. Wong, *Process for production of hydroxytyrosol using organometallic compounds,* **2012**, Patent: WO 2012/006783 A1, Page 12–13.

[227] P. K. Sharma, M. He, L. J. Romanczyk Jr, H. Schroeter, *J. Label Compd. Radiopharm* **2010**, *53*, 605–612.

[228] E. Alcalde, I. Dinarés, J. Frigola, *Eur. J. Med. Chem.* **1991**, *26*, 633–642.

[229] R. B. Baudy, L. P. Greenblatt, I. L. Jirkovsky, M. Conklin, R. J. Russo, D. R. Bramlett, T. A. Emrey, J. T. Simmonds, D. M. Kowal, *J. Med. Chem.* **1993**, *36*, 331–342.

[230] A. Schrimpf, *Modifikation hyperkoordinierter oktaedrischer Siliciumkomplexe*, Research Project, Philipps-Universität Marburg, **2013**.

[231] S. C. Roy, C. Guin, K. K. Rana, G. Maiti, *Tetrahedron Lett.* **2001**, *42*, 6941–6942.

[232] P. E. Hofmann, *Untersuchungen zur Halogenierung und Kreuzkupplung an oktaedrischen Silicium-Komplexen*, Bachelor Thesis, Philipps-Universität Marburg, **2013**.

[233] M. C. Carreño, J. L. García Ruano, G. Sanz, M. A. Toledo, A. Urbano, *J. Org. Chem.* **1995**, *60*, 5328–5331.

[234] H. G. O. Becker, R. Beckert, W. Berger, G. Domschke, E. Fanghänel, J. Faust, M. Fischer, F. Gentz, K. Gewald, R. Gluch, W. D. Habicher, R. Mayer, P. Metz, K. Müller, D. Pavel, H. Schmidt, K. Schollberg, K. Schwetlick, E. Seiler, G. Zeppenfeld, *Organikum - Organisch-chemisches Grundpraktikum*, 21. Edition, WILEY-VCH Verlag GmbH, Weinheim, **2001**.

[235] A.-S. Castanet, F. Colobert, P.-E. Broutin, *Tetrahedron Lett.* **2002**, *43*, 5047–5048.

[236] M. S. Yusubov, R. Y. Yusubova, V. N. Nemykin, A. V. Maskaev, M. R. Geraskina, A. Kirschning, V. V. Zhdankin, *Eur. J. Org. Chem.* **2012**, 5935–5942.

[237] S. Hesse, G. Kirsch, *Tetrahedron Lett.* **2003**, *44*, 97–99.

[238] K. R. Roh, J. Y. Kim, Y. H. Kim, *Tetrahedron Lett.* **1999**, *40*, 1903–1906.

[239] G. Espino, A. Kurbangalieva, J. M. Brown, *Chem. Commun.* **2007**, 1742–1744.

[240] M. Bonaterra, R. A. Rossi, S. E. Martín, *Organometallics* **2009**, *28*, 933–936.

[241] R. R. Tykwinski, Y. Zhao, *Synlett* **2002**, *12*, 1939–1953.

[242] A. Pitchaiah, I. T. Hwang, J.-S. Hwang, H. Kim, K.-I. Lee, *Synthesis* **2012**, *44*, 1631–1636.

[243] K. Ritter, *Synthesis* **1993**, *8*, 735–762.

[244] S. Ullrich, *Modifizierung hyperkoordinierter, oktaedrischer Siliziumkomplexe*, Research Project, Philipps-Universität Marburg, **2013**.

[245] W. Paw, R. Eisenberg, *Inorg. Chem.* **1997**, *36*, 2287–2293.

[246] A. S. Denisova, M. B. Degtyareva, E. M. Dem'yanchuk, A. A. Simanova, *Russ. J. Org. Chem.* **2005**, *41*, 1690–1693.

[247] A. M. S. Garas, R. S. Vagg, *J. Heterocyclic Chem.* **2000**, *37*, 151–158.

[248] K. P. C. Vollhardt, N. E. Schore, *Organische Chemie*, 4. Edition, WILEY-VCH Verlag GmbH, Weinheim, **2005**.

[249] P. M. Deya, M. Dopico, A. G. Raso, J. Morey, J. M. Saa, *Tetrahedron* **1987**, *43*, 3523–3532.

[250] M. Gupta, S. Paul, R. Gupta, A. Loupy, *Tetrahedron Lett.* **2005**, *46*, 4957–4960.

[251] E. R. Cole, A. G. Crank, H. T. H. Minh, *Aust. J. Chem.* **1980**, *33*, 527–543.

[252] R. H. Zheng, H. C. Guo, H. J. Jiang, K. H. Xu, B. B. Liu, W. L. Sun, Z. Q. Shen, *Chin. Chem. Lett.* **2010**, *21*, 1270–1272.

[253] D. S. Beaudoin, S. O. Obare, *Tetrahedron Lett.* **2008**, *49*, 6054–6057.

[254] S. Krishnan, D. G. Kuhn, G. A. Hamilton, *J. Am. Chem. Soc.* **1977**, *24*, 8121–8123.

[255] Y. Shen, B. P. Sullivan, *Inorg. Chem.* **1995**, *34*, 6235–6236.

[256] K. K. S. Gupta, S. C. Kumar, P. K. Sen, A. Banerjee, *React. Kinet. Catal. Lett.* **1988**, *36*, 423–428.

[257] CH. Sanjeeva Reddy, E. V. Sundaram, *Tetrahedron* **1989**, *45*, 2109–2126.

[258] F. Tiemann, B. Mendelsohn, *Chem. Ber.* **1875**, *8*, 1136–1139.

[259] S. D. Bergman, M. Kol, *Inorg. Chem.* **2005**, *44*, 1647–1654.

[260] Hans-J. Teuber, S. Benz, *Chem. Ber.* **1967**, *100*, 2918–2929.

[261] F. H. Allen, O. Kennard, D. G. Watson, L. Brammer, A. G. Orpen, R. Taylor, *J. Chem. Soc. Perkin Trans. 2* **1987**, S1–S19.

[262] J. Marquet, M. Moreno-Mañas, A. Vallribera, A. Virgili, J. Bertran, A. Gonzalez-Lafont, J. M. Lluch, *Tetrahedron* **1987**, *43*, 351–360.

[263] R. Judele, S. Laschat, A. Baroa, M. Nimtz, *Tetrahedron* **2006**, *62*, 9681–9687.

[264] J. Hu, D. Zhang, F. W. Harris, *J. Org. Chem.* **2005**, *70*, 707–708.

[265] S. Weber, *Synthese von einkernigen und mehrkernigen hexakoor- dinierten Siliciumkomplexen als potentielle G4-DNA Inhibitoren*, Research Project, Philipps-Universität Marburg, **2015**.

[266] J. A. Joule, K. Mills, *Heterocyclic Chemistry*, 5. Edition, John Wiley & Sons Ltd, West Sussex, **2010**.

[267] K. Danielsen, *Acta Chem. Scand.* **1996**, *50*, 954–957.

[268] E. Tayama, K. Takedachi, H. Iwamoto, E. Hasegawa, *Tetrahedron Lett.* **2012**, *53*, 1373–1375.

[269] J. P. Lambooy, *J. Am. Chem. Soc.* **1956**, *78*, 771–774.

[270] A. Vilsmeier, A. Haack, *Chem. Ber.* **1927**, *60*, 119–122.

[271] P. N. James, H. R. Snyder, *Org. Synth.* **1959**, *39*, 30.

[272] J. D. McGhee, P. H. von Hippel, *J. Mol. Biol.* **1974**, *86*, 469–489.

[273] M. S. Lowry, W. R. Hudson, R. A. Pascal, Jr., S. Bernhard, *J. Am. Chem. Soc.* **2004**, *126*, 14129–14135.

[274] A. Juris, V. Balzani, F. Barigelletti, S. Campagna, P. Belser, A. von Zelewsky, *Coord. Chem. Rev.* **1988**, *84*, 85–277.

[275] B.-S. Du, C.-H. Lin, Y. Chi, J.-Y. Hung, M.-W. Chung, T.-Y. Lin, G.-H. Lee, K.-T. Wong, P.-T. Chou, W.-Y. Hung, H.-C. Chiu, *Inorg. Chem.* **2010**, *49*, 8713–8723.

[276] M. Bandini, M. Bianchi, G. Valenti, F. Piccinelli, F. Paolucci, M. Monari, A. Umani-Ronchi, M. Marcaccio, *Inorg. Chem.* **2010**, *49*, 1439–1448.

[277] K. K.-W. Lo, C.-K. Chung, N. Zhu, *Chem. Eur. J.* **2006**, *12*, 1500–1512.

[278] J. Li, P. I. Djurovich, B. D. Alleyne, M. Yousufuddin, N. N. Ho, J. C. Thomas, J. C. Peters, R. Bau, M. E. Thompson, *Inorg. Chem.* **2005**, *44*, 1713–1727.

[279] E. Baranoff, B. F. E. Curchod, J. Frey, R. Scopelliti, F. Kessler, I. Tavernelli, U. Rothlisberger, M. Grätzel, Md. K. Nazeeruddin, *Inorg. Chem.* **2012**, *51*, 215–224.

[280] Y.-M. Chen, Y.-J. Liu, Q. Li, K.-Z. Wang, *J. Inorg. Biochem.* **2009**, *103*, 1395–1404.

[281] S. Ji, H. Guo, X. Yuan, X. Li, H. Ding, P. Gao, C. Zhao, W. Wu, W. Wu, J. Zhao, *Org. Lett.* **2010**, *12*, 2876–2879.

[282] J. Bolger, A. Gourdon, E. Ishow, J.-P. Launay, *Inorg. Chem.* **1996**, *35*, 2937–2944.

[283] V. Marin, E. Holder, R. Hoggenboom, U. S. Schubert, *J. Polym. Sci. Part A* **2004**, *42*, 4153–4160.

[284] B. P. Sullivan, D. J. Salmon, T. J. Meyer, *Inorg. Chem.* **1978**, *17*, 3334–3341.

[285] Y. You, W. Nam, *Chem. Soc. Rev.* **2011**, *41*, 7061–7084.

[286] S. Sprouse, K. A. King, P. J. Spellane, R. J. Watts, *J. Am. Chem. Soc.* **1984**, *106*, 6647–6653.

[287] J. H. Van Diemen, J. G. Haasnoot, R. Hage, J. Reedijk, J. G. Vos, R. Wang, *Inorg. Chem.* **1992**, *30*, 4038–4043.

[288] A. Gruber, *Darstellung zweikerniger Rhodium-Silicium-Komplexe als DNA-bindende Moleküle*, Bachelor Thesis, Philipps-Universität Marburg, **2014**.

[289] B. S. Howerton, D. K. Heidary, E. C. Glazer, *J. Am. Chem. Soc.* **2012**, *134*, 8324–8327.

[290] M. Tera, H. Ishizuka, M. Takagi, M. Suganuma, K. Shin-ya, K. Nagasawa, *Angew. Chem.* **2008**, *120*, 5639–5642.

[291] L. P. Graham, *Medicinal Chemistry*, 4. Edition, Oxford University Press Inc., New York, **2009**.

[292] T. Kowada, H. Maeda, K. Kikuchi, *Chem. Soc. Rev.* **2015**, *44*, 4953–4972.

[293] E. Ganapathi, S. Madhu, M. Ravikanth, *Tetrahedron* **2014**, *70*, 664–671.

[294] A. Loudet, K. Burgess, *Chem. Rev.* **2007**, *107*, 4891–4932.

[295] L. Yang, R. Simionescu, A. Lough, H. Yan, *Dyes and Pigments* **2011**, *91*, 264–267.

[296] A. Coskun, E. U. Akkaya, *J. Am. Chem. Soc.* **2005**, *127*, 10464–10465.

[297] R. Ziessel, G. Ulrich, A. Harriman, *New J. Chem.* **2007**, *31*, 496–501.

[298] X. Zhang, Y. Xiao, X. Qian, *Org. Lett.* **2008**, *10*, 29–32.

[299] I. Johnson, M. T. Spence, *Molecular Probes Handbook, A Guide to Fluorescent Probes and Labeling Technologies*, 11th Edition, Molecular Probes: Eugene, OR, USA, Chapter 1, **2010**.

[300] M. Prat Quinones, S. Fonquerna Pou, C. Puig Duran, W. Lumeras Amador, J. Aiguade Bosch, J. F. Caturla Javaloyes, *New cyclohexylamine derivatives having beta2 adrenergic agonist and m3 muscarinic antagonist activities,* **2011**, Patent: EP 2 386 555 A1, Page 20.

[301] L.-F. Pan, X.-B. Wang, S.-S. Xie, S.-Y. Li, L.-Y. Kong, *Med. Chem. Commun.* **2014**, *5*, 609–616.

[302] T. Ueno, Y. Urano, K. ichi Setsukinai, H. Takakusa, H. Kojima, K. Kikuchi, K. Ohkubo, S. Fukuzumi, T. Nagano, *J. Am. Chem. Soc.* **2004**, *126*, 14079–14085.

[303] A. P. de Silva, H. Q. N. Gunaratne, T. Gunnlaugsson, A. J. M. Huxley, C. P. McCoy, J. T. Rademacher, T. E. Rice, *Chem. Rev.* **1997**, *97*, 1515–1566.

[304] H. Sunahara, Y. Urano, H. Kojima, T. Nagano, *J. Am. Chem. Soc.* **2007**, *129*, 5597–5604.

[305] T. Miura, Y. Urano, K. Tanaka, T. Nagano, K. Ohkubo, S. Fukuzumi, *J. Am. Chem. Soc.* **2003**, *125*, 8666–8671.

[306] K. Tanaka, T. Miura, N. Umezawa, Y. Urano, K. Kikuchi, T. Higuchi, T. Nagano, *J. Am. Chem. Soc.* **2001**, *123*, 2530–2536.

[307] E. Williams, *Annual Reports on NMR Spectroscopy* **1984**, *15*, 235–289.

[308] M. Hesse, H. Meier, B. Zeeh, S. Bienz, L. Bigler, T. Fox, *Spektroskopische Methoden in der organischen Chemie*, 8. Edition, Thieme Verlagsgruppe, Stuttgart, **2012**.

[309] K. M. Delak, T. C. Farrar, N. Sahai, *J. Non-Cryst. Solids* **2005**, *351*, 2244–2250.

[310] R. W. Hoffmann, G. Niel, *Liebigs Ann. Chem.* **1991**, 1195–1201.

[311] V. Maraval, D. Prévôté–Pinet, R. Laurent, A.-M. Caminade, J.-P. Majoral, *New J. Chem.* **2000**, *24*, 561–566.

[312] H. Yuan, Z. Zhou, J. Xiao, L. Liang, L. Dai, *Tetrahedron: Asymmetry* **2010**, *21*, 1874–1884.

[313] H. E. Gottlieb, V. Kotlyar, A. Nudelman, *J. Org. Chem.* **1997**, *62*, 7512–7515.

[314] R. Judele, S. Laschat, A. Baro, M. Nimtz, *Tetrahedron* **2006**, *62*, 9681–9687.

[315] H. Camren, M.-Y. Chang, L. Zeng, M. E. McGuire, *Synth. Commun.* **1996**, *26*, 1247–1252.

[316] J. R. Masters, *Nat. Rev. Cancer* **2002**, *2*, 315–319.

[317] M. Boshart, L. Gissmann, H. Ikenberg, A. Kleinheinzl, W. Scheurlen, H. zur Hausen, *The EMBO Journal* **1984**, *3*, 1151–1157.

[318] M. M. Pater, A. Pater, *Virology* **1985**, *145*, 313–318.

[319] M. Scheffner, K. Munger, J. C. Byrne, P. M. Howley, *Proc. Natl. Acad. Sci. USA* **1991**, *88*, 5523–5527.

[320] A. Kastl, *Photoreaktive organometallische Verbindungen als mögliche Chemotherapeutika in der Krebstherapie*, Master Thesis, Philipps-Universität Marburg, **2009**.

A. List of Abbreviations

2c-2e bond	2-center-2-electron bond
3c-4e bond	3-center-4-electron bond
4c-6e bond	4-center-6-electron bond
A	adenine, adenosine, deoxyadenosine
ad.	added
AIBN	azobis*iso*butyronitrile
arom	aromatic
bhq	benzo[*h*]quinoline
bpy	2,2'-bipyridine
bqp	benzo[*a*]quinoxalino[2,3-*c*]phenazine-2,3-bis(olate)
Br-DHB	4-bromo-1,2-dihydroxybenzene
c	centi
C	cytosine, cytidine, deoxycytidine
CAN	ceric ammonium nitrate
cat	1,2-dihydroxybenzene, catechol
Cmp.	complex
CO_2	carbon dioxide
Cp	cyclopentadienyl
CT-DNA	*calf thymus* DNA
$\Delta\lambda$	bathochromic shift
δ	chemical shift
ΔT	heating to undefined temperature
d	days; NMR = duplet
DDQ	2,3-dichloro-5,6-dicyano-1,4-benzoquinone
DHB	1,2-dihydroxybenzene, catechol
DHBNO22	4,5-dinitrobenzene-1,2-diol
DHBA	3,4-dihydroxybenzaldehyde or 3,4-dihydroxybenzoic acid
DHBQ, DHpBQ	2,5-dihydroxy-*p*-benzoquinone
Dia	diastereomer
DIPEA	*N,N*-diisopropylethylamine
DMEM	*Dolbecco's Modified Eagle's Medium*
DMF	*N,N*-dimethylformamide
dmp	2,4-dimethylpyrrole
dmphen	5,6-dimethyl-1,10-phenanthroline
DMSO	dimethyl sulfoxide
[DNA]	Concentration of DNA
DNA	deoxyribonucleic acid

dppz	dipyrido[3,2-*a*:2',3'-*c*]phenazine
dppzO	dipyrido[3,2-*a*:2',3'-*c*]phenazine-11,12-diolato
ds-DNA	double stranded DNA, duplex DNA
DTBPDO	2,7-di-*tert*-butylpyrene-4,5-dione
DTBPTO	2,7-di-*tert*-butylpyrene-4,5,9,10-tetraone
EC_{50}	half maximal effective concentration
EDB	1,2-Dibromoethane (ethylene dibromide)
EDTA	ethylenediaminetetraacetic acid
EG	ethylene glycol
eq.	equivalents
ESI	electrospray ionization
EtOH	ethanol
G	guanine, guanosine, deoxyguanosine
G4-DNA	G-quadruplex DNA
GS	ground state
h	NMR = heptet
H-telo	human telomeric G-quadruplex DNA
HOMO	highest occupied molecular orbital
HPLC	high-performance liquid chromatography
Hz	hertz
IC_{50}	half maximal inhibitory concentration
IR	infrared
J	coupling constant
K	Kelvin
k_B	binding constant
KIBS	potassium 4-iodylbenzenesulfonate
λ	wavelength
LCCT	ligand centered charge transfer
LSM	confocal laser scanning microscope
LUMO	lowest unoccupied molecular orbital
m	milli; meter; NMR = multiplet
Molar	molar, molar
M	mega; molecular weight
m/z	mass per ionization
Me2dppz	7,8-dimetyldipyrido[3,2-*a*:2',3'-*c*]phenazine
min	minute(s)
MLCT	metal-to-ligand charge transfer
MS	mass spectrometry
MTT	3-(4,5-dimethylthiazol-2-yl)-2,5-diphenyltetrazolium bromide

n	nano
Na(asc)	sodium ascorbate
NBS	*N*-bromosuccinimide
NEt_3	triethylamine
NH_4PF_6	ammonium hexafluorophosphate
NIS	*N*-iodosuccinimide
NMR	nuclear magnetic resonance
No.	number
[M]	bis(polypyridyl)metal fragment
o/n	over night
p	NMR = quintet
PBS	phosphate buffered saline
PDT	photodynamic therapy
PeT	photoinduced electron transfer
phen	1,10-phenanthroline
PNA	peptide nucleic acid
pp	polypyridyl
ppm	parts per million
ppy	2-phenylpyridine
q	NMR = quartet
R-DHB	4-substituted-1,2-dihydroxybenzene
RNA	ribonucleic acid
rpm	rounds per minute
rt	room temperature
s	NMR = singulet; DNA assay = binding site
[Si]	bis(polypyridyl)silicon(IV) fragment, concentration of silicon complex
t	time; NMR = triplet
T	thymin, thymidine
tatpp	tetraazatetrapyrido[3,2-*a*:2'3'-*c*:3",2"-*l*:2"',3"'-*n*]pentacene
TBAC	tetra-*n*-butylammonium chloride
TBAF	tetra-*n*-butylammonium fluoride
$TBphen_2$	*bis*-1,10-phenanthroline analogue of TRÖGER's base
*t*Bu	*tert*-butyl
TFA	trifluoroacetic acid
TLC	thin layer chromatography
tmphen	3,4,7,8-tetramethyl-1,10-phenanthroline
tpphz	tetrapyrido[3,2-*a*:2',3'-*c*:3",2"-*h*:2",3"-*j*]phenazine
u	atomic mass
UV	ultraviolet

$\widetilde{\nu}$	wave number
Vis	visible light
vol.	volume

B. List of Compounds Synthesized

Synthesis of Octahedral Silicon(IV) Complexes

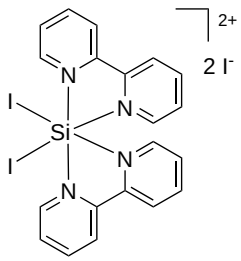

85

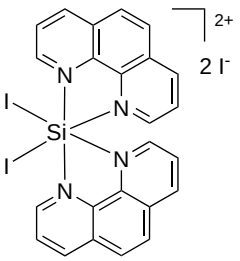

86

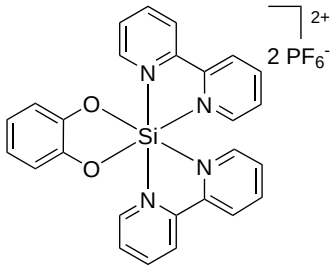

87

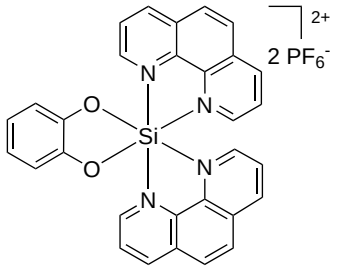

88

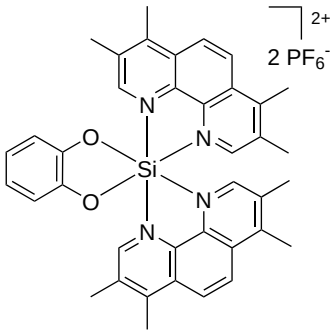

89

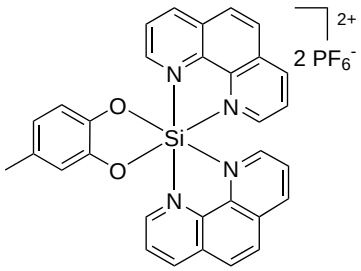

90

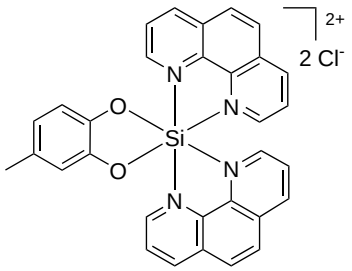

90a

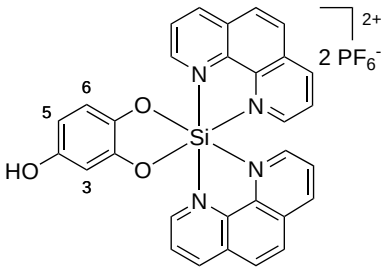

91

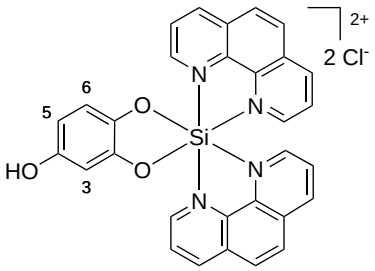

91a

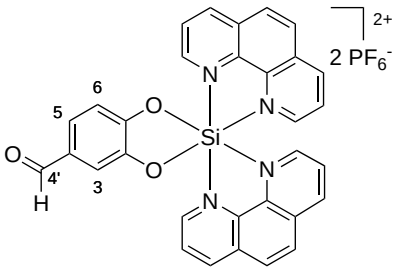

92

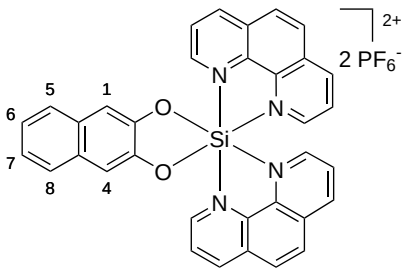

100

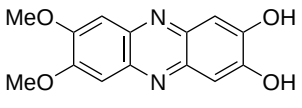

104

Post-Coordination Modification of Ocahedral Silicon(IV) Complexes

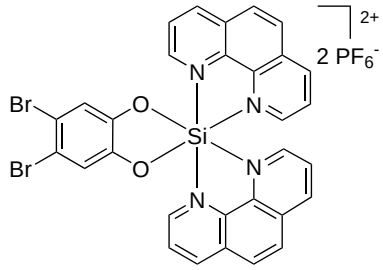

108

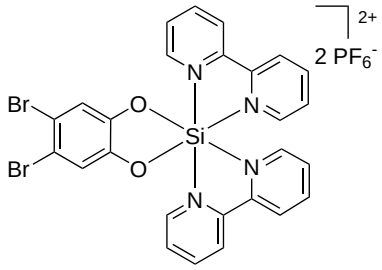

109

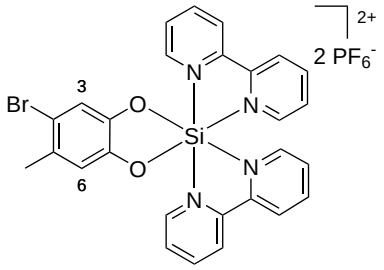

110

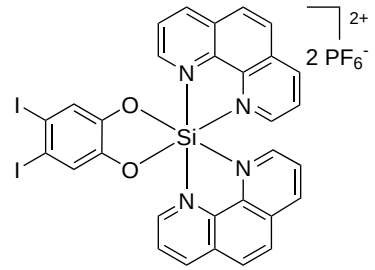

112

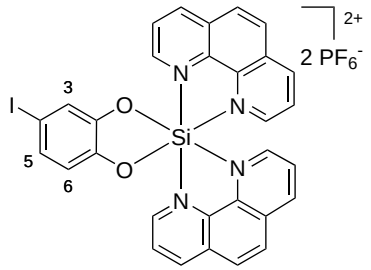

115

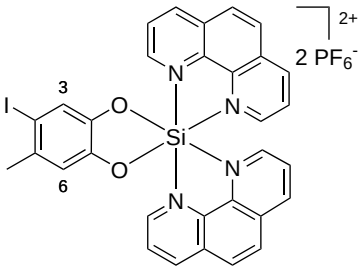

292

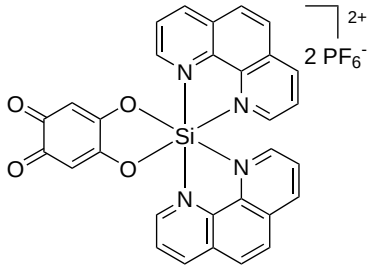

95

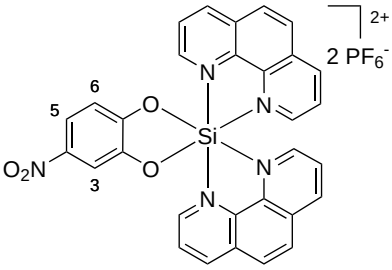

127

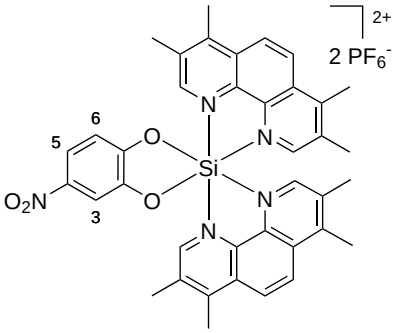

128

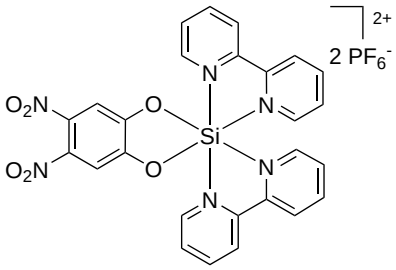

129

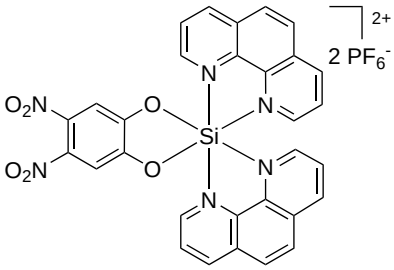

130

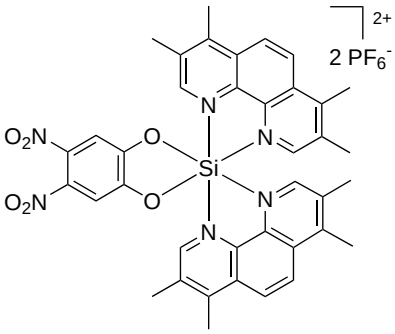

131

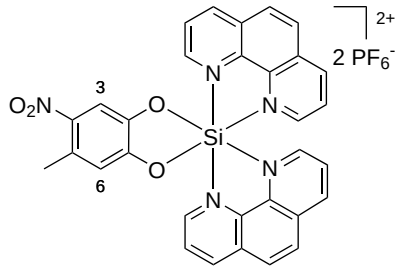

132

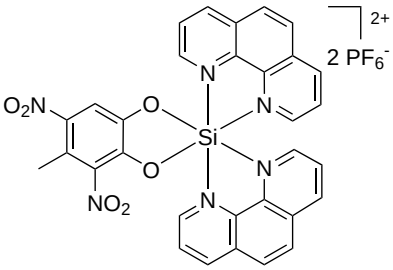

132

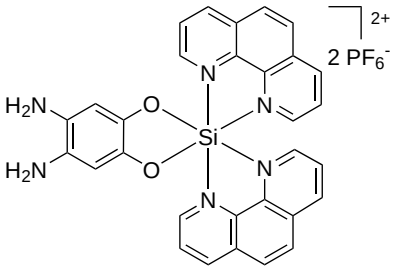

133

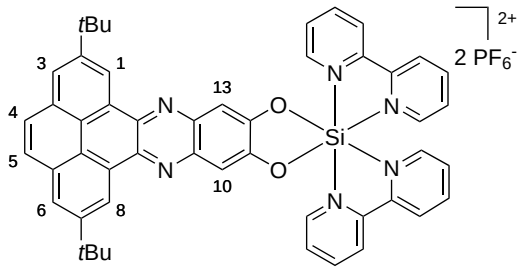

143

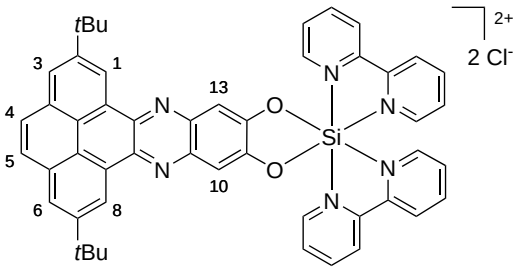

143a

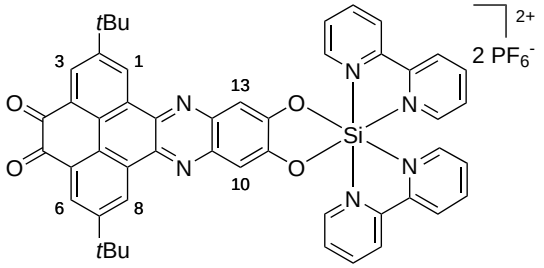

145

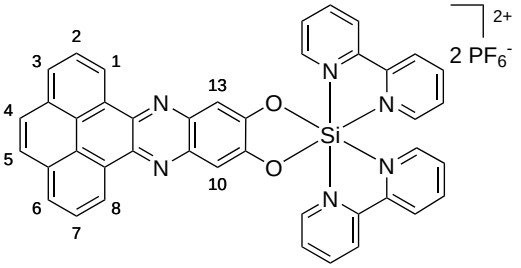

149

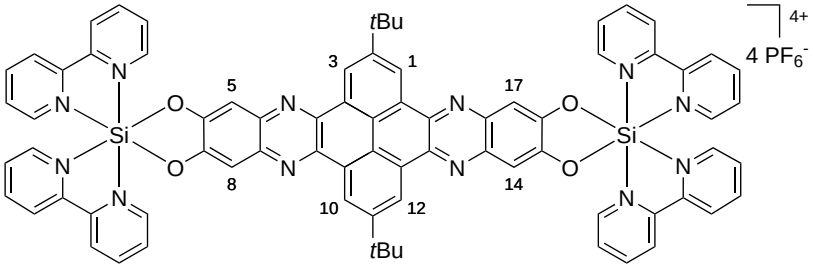

147

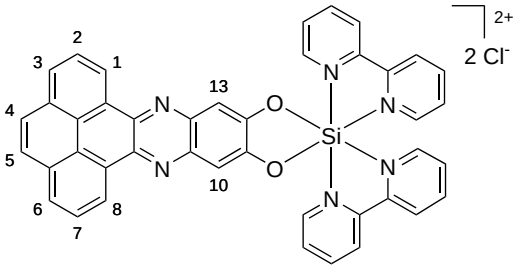

149a

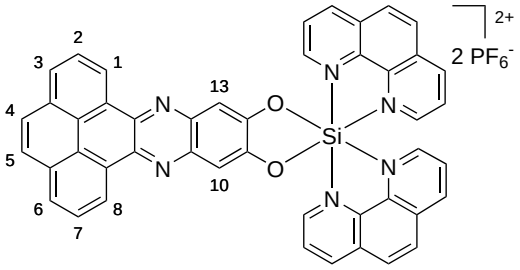

150

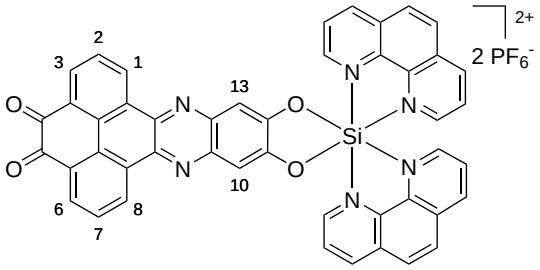

151

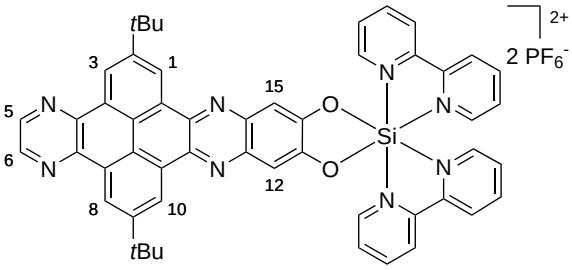

152

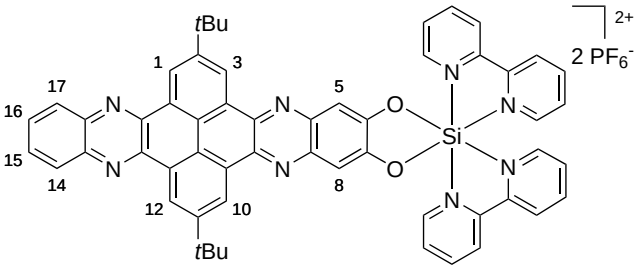

154

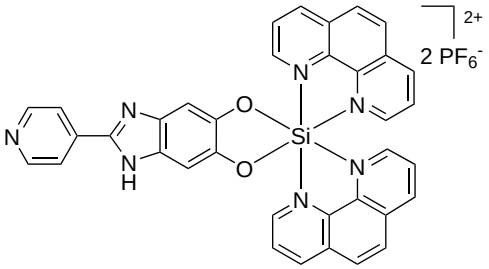

157

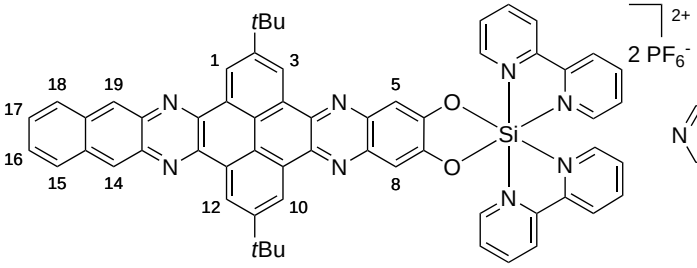

156

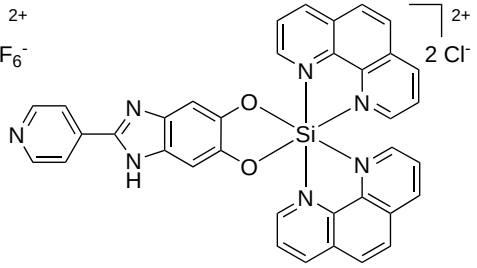

157a

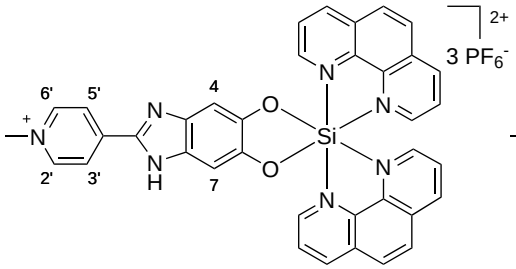

159

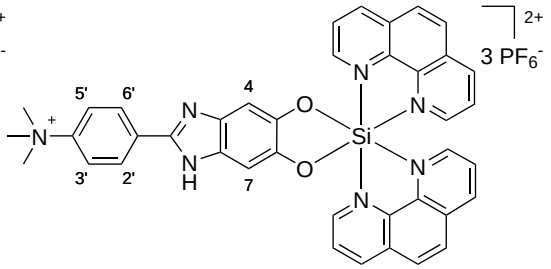

160

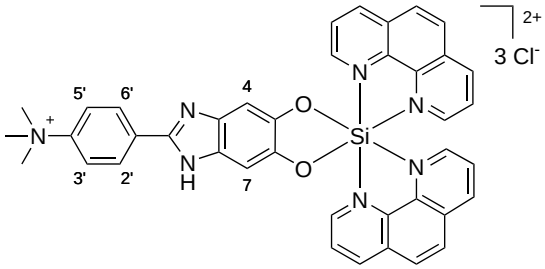

160a

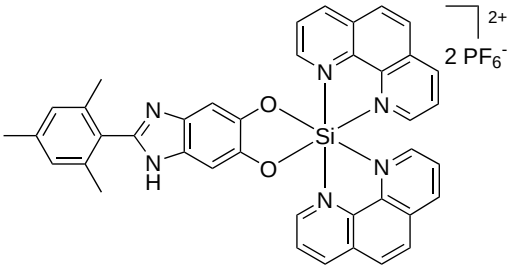

161

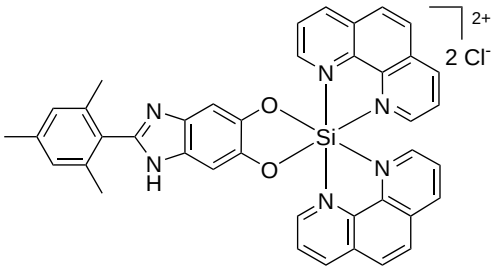

161a

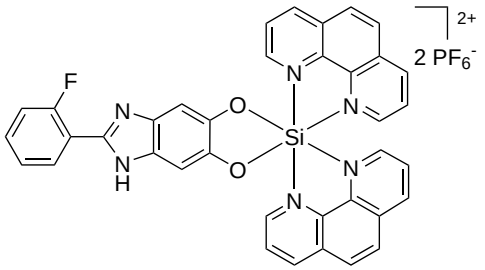

162

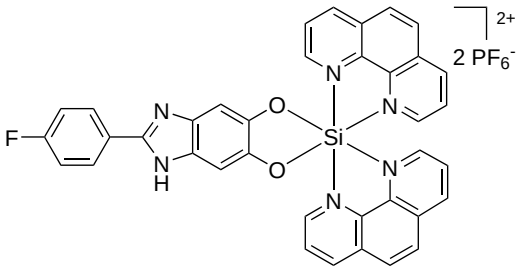

163

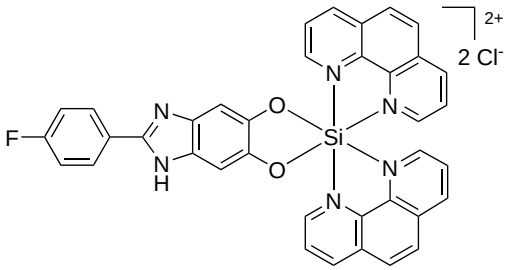

163a

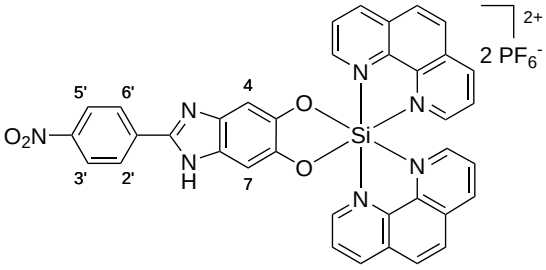

164

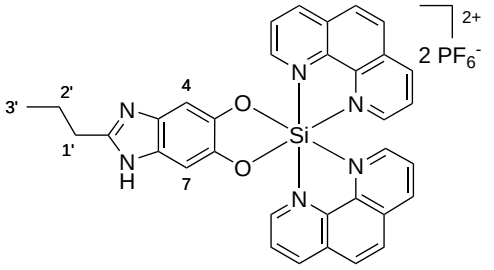

166

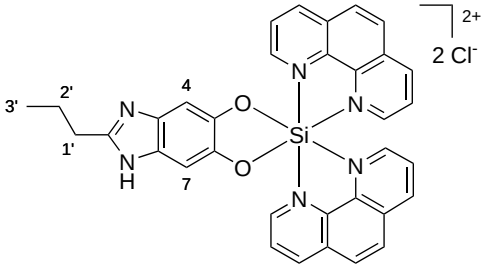

166a

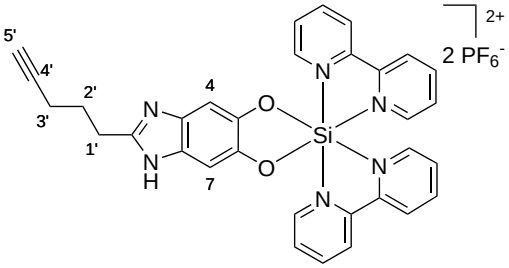

172

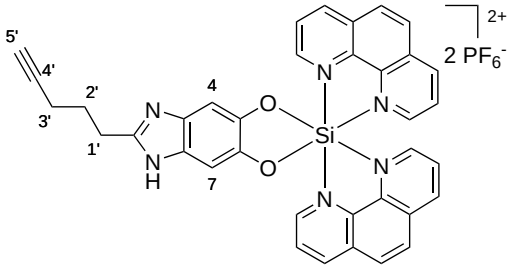

167

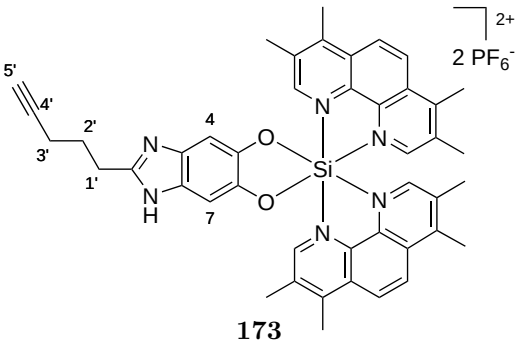

173

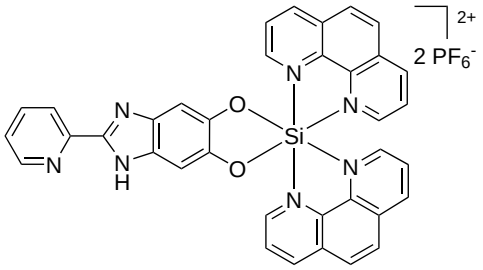

158

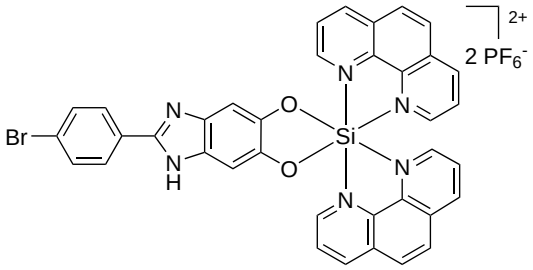

165

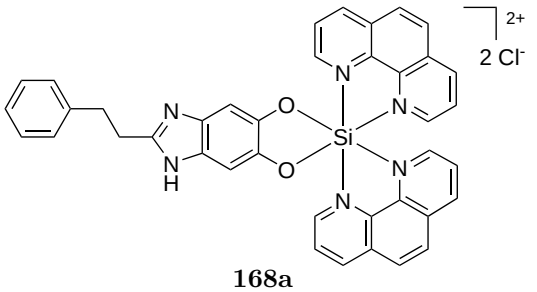

168a

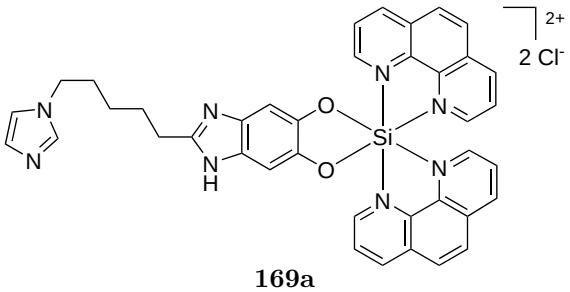

169a

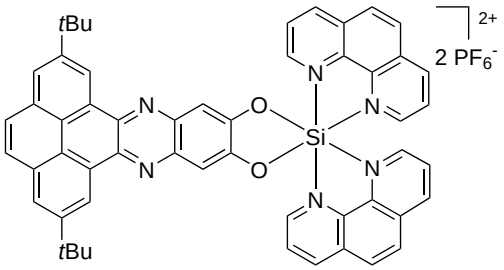

144

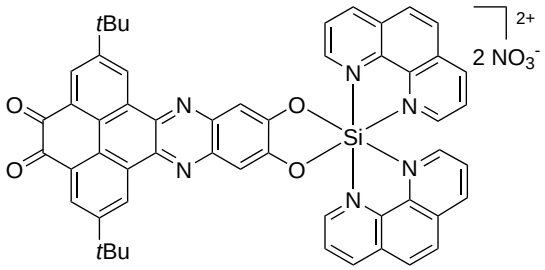

146a

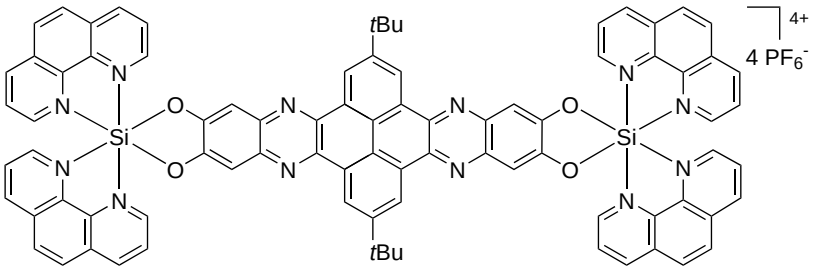

148

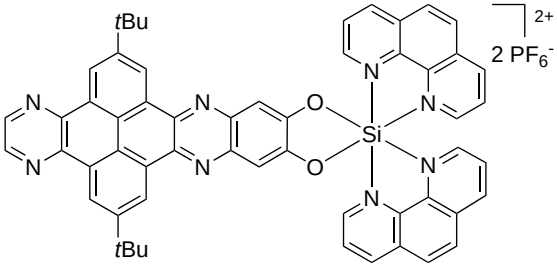

153

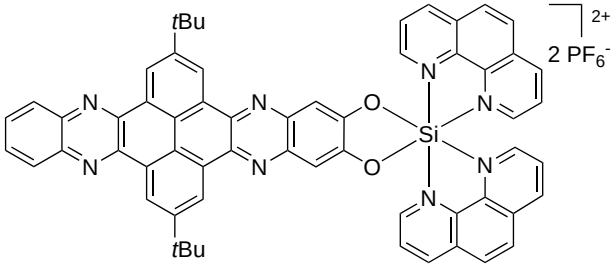

155

Tris-heteroleptic Silicon(IV) Complexes

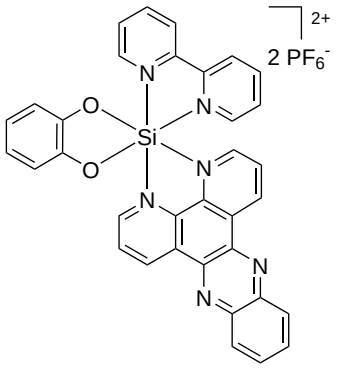

183

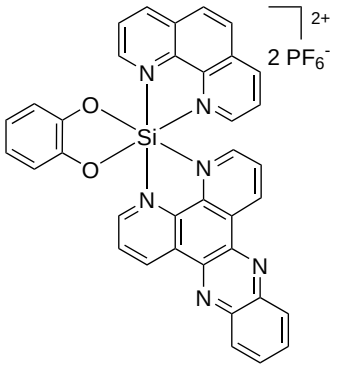

184

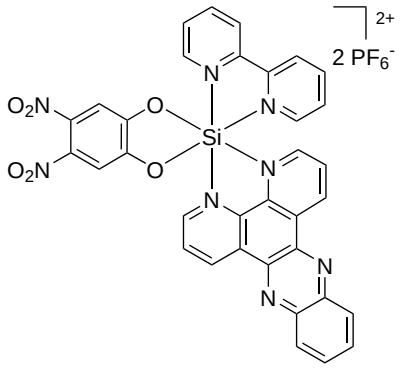

187

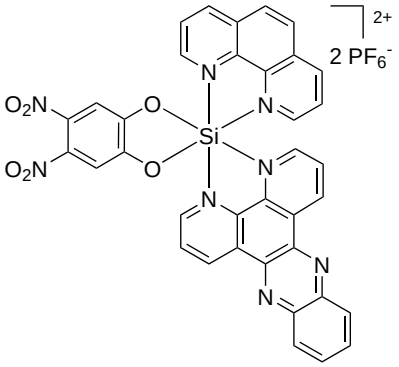

188

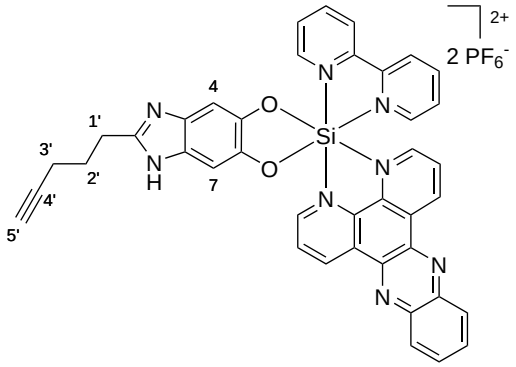

190

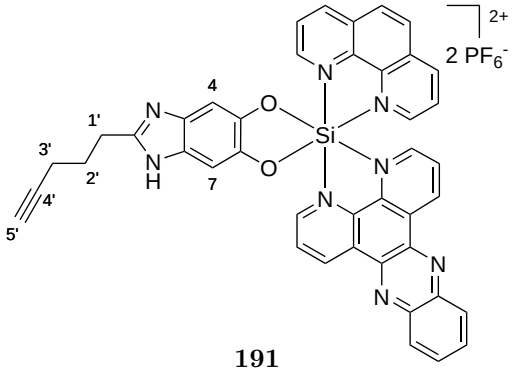

191

Dinuclear Metal-Silicon(IV) Complexes

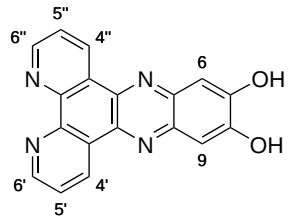

195

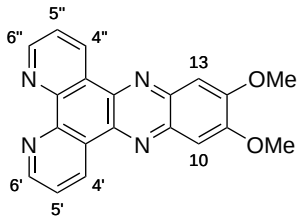

203

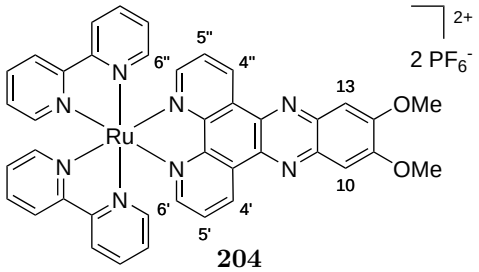

204

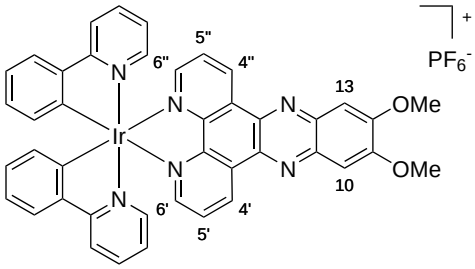

205

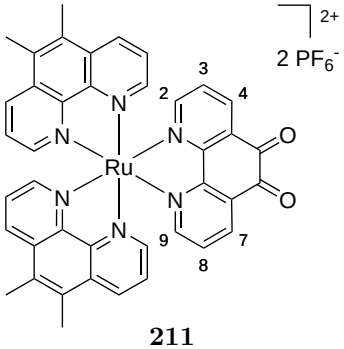

211

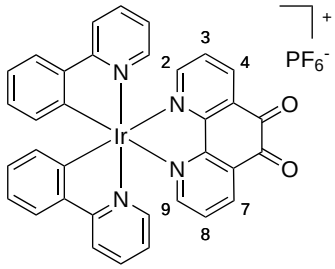

212

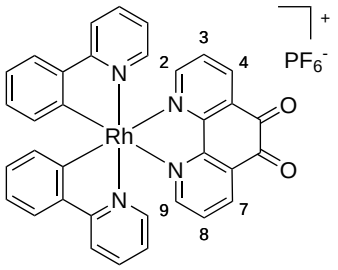

213

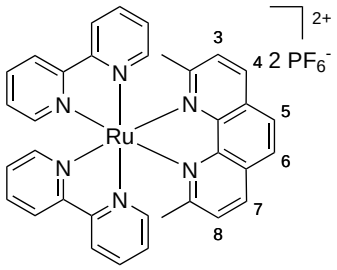

218

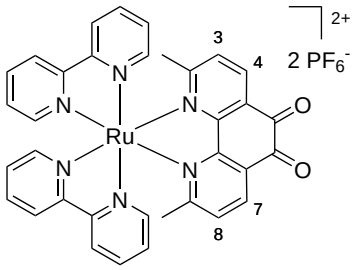

217

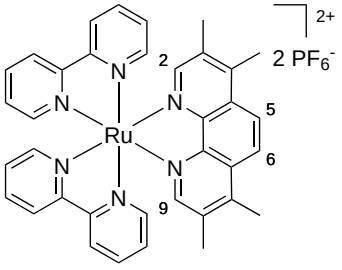

220

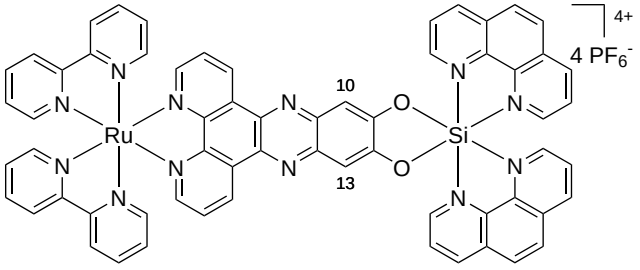

224

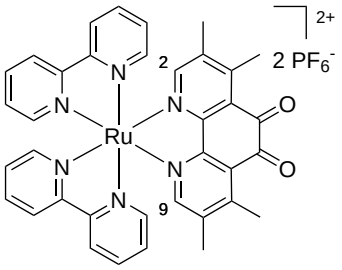

221

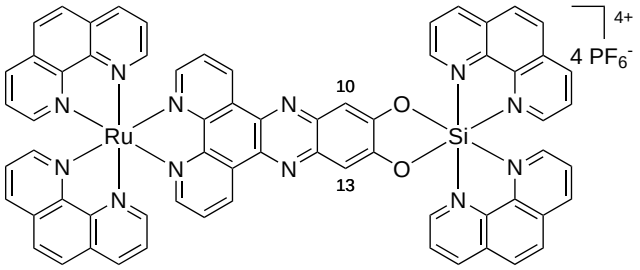

226

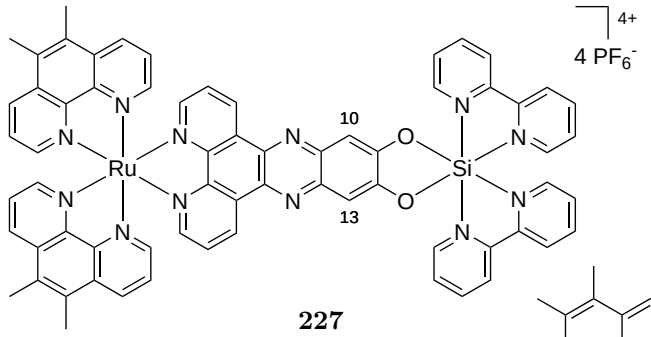

227

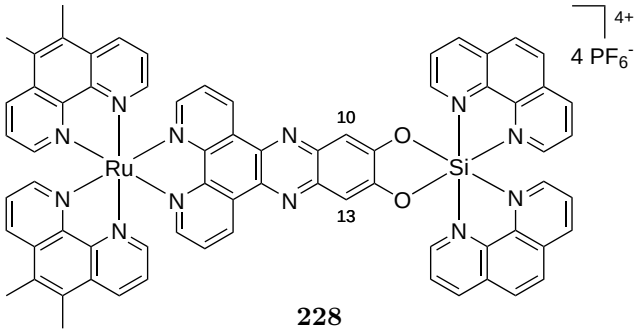

228

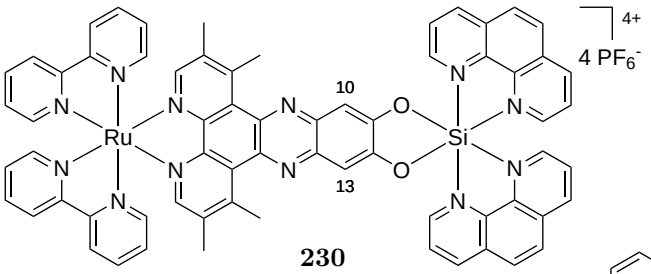

230

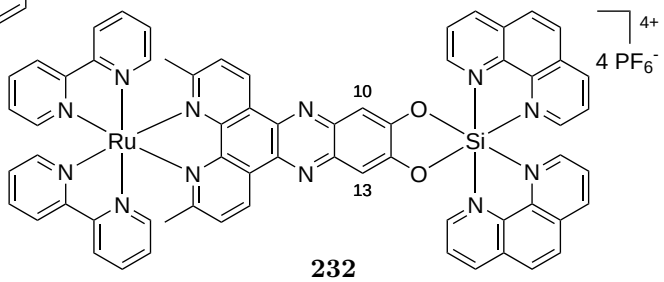

232

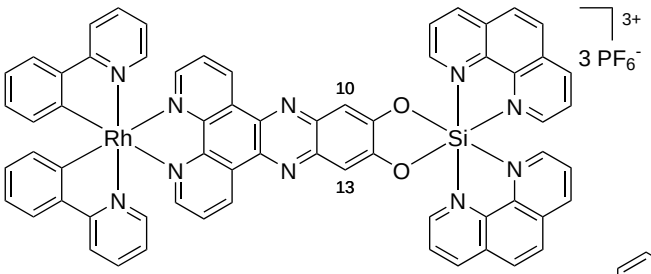

234

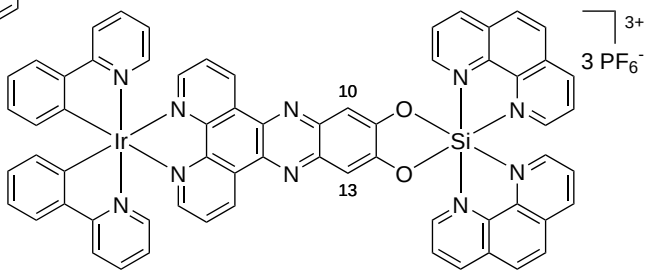

237

Bodipy-modified Octahedral Silicon(IV) Complexes

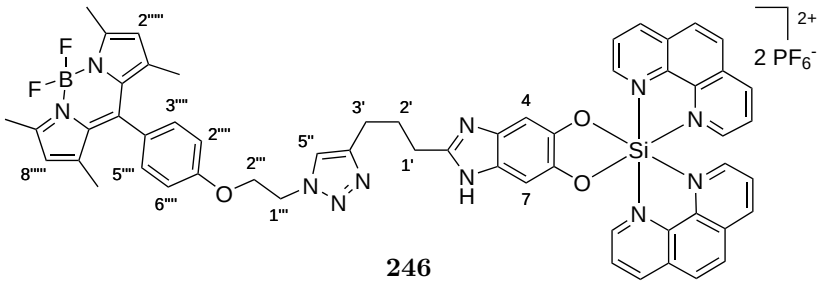

246

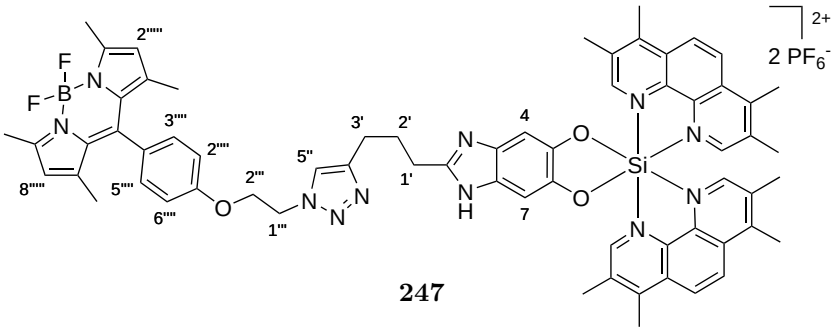

247

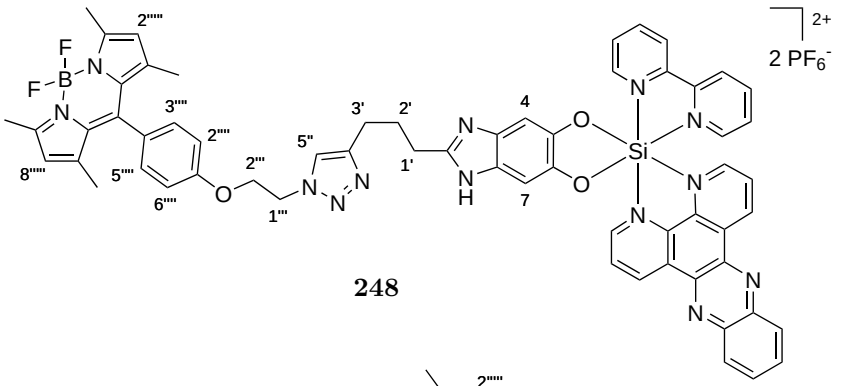

248

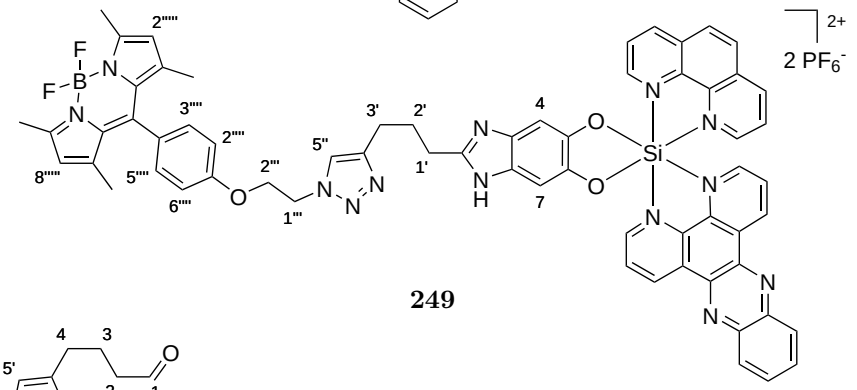

249

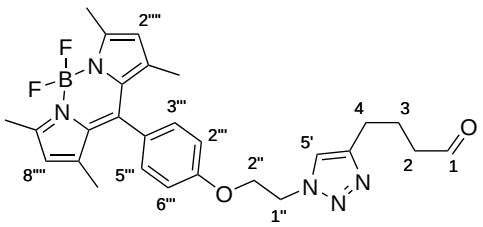

250

C. Crystallographic Appendix

(4,5-Dioxocyclohexa-2,6-diene-1,2-diolato)bis(1,10-phenanthroline)silicon(IV)-bis(hexafluorophosphate) (95)

Single crystals suitable for crystal structure analysis were obtained upon slow diffusion of diethyl ether into a solution of complex **95** in acetonitrile at 4 °C.

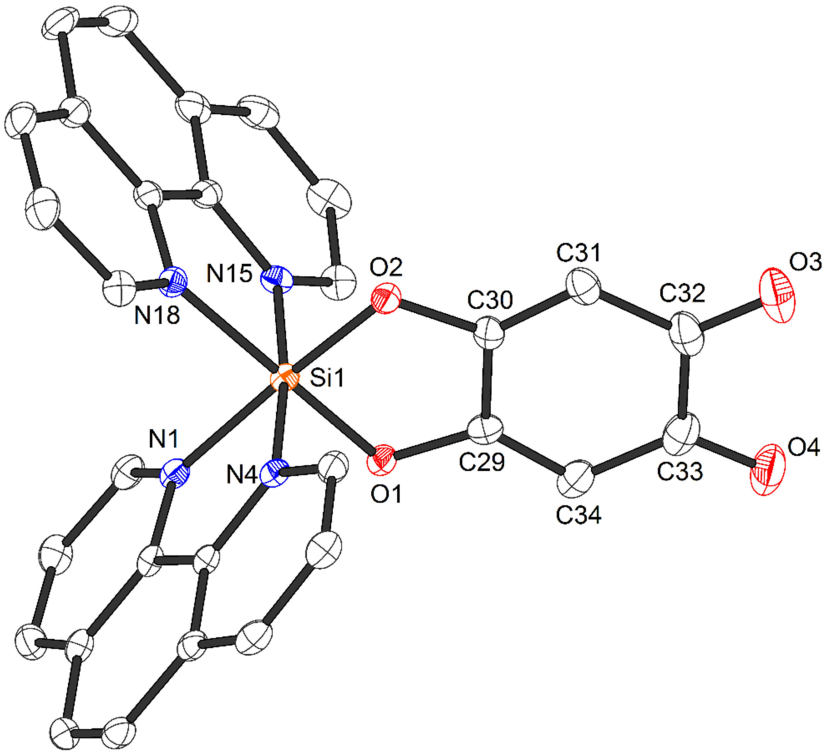

Figure 79: Crystal structure of complex **95**. ORTEP drawing with 50 % probability thermal ellipsoids. The PF_6 counterions and solvent are omitted for clarity.

Table 19: Crystal data and structure refinement for complex **95**.

Crystal data		
Identification code	JWKA019c_0m	
Habitus, colour	prism, yellow	
Crystal size	$0.550 \times 0.180 \times 0.030\,\mathrm{mm}^3$	
Crystal system	Monoclinic	
Space group	P $2_1/n$	Z = 4
Unit cell dimensions	a = 10.5434(6) Å	$\alpha = 90°$
	b = 22.3096(9) Å	$\beta = 106.3281(16)°$
	c = 17.0798(7) Å	$\gamma = 90°$

Volume	3855.5(3) $Å^3$
Cell determination	7469 peaks with Θ = 2.6–27.3°
Empirical formula	$C_{36}H_{27}F_{12}N_7O_4P_2Si$
Formula weight	939.67 u
Density (calculated)	1.619 $Mg\,m^{-3}$
Absorption coefficient	0.254 mm^{-1}
F(000)	1904

Data collection

Diffractometer type	Bruker D8 QUEST area detector
Wavelength	0.710 73 Å
Temperature	100(2) K
Theta range for data collection	2.208–25.498°
Index ranges	$-10 \leq h \leq 12, -27 \leq k \leq 27, -20 \leq l \leq 20$
Data collection software	BRUKER APEX II
Cell refinement software	SAINT V8.34A (Bruker AXS Inc., 2013)
Data reduction software	SAINT V8.34A (Bruker AXS Inc., 2013)

Solution and refinement

Reflections collected	34797
Independent reflections	7149 [R(int) = 0.0723]
Completeness to theta = 25.242°	99.8 %
Observed reflections	5006[II > 2(I)]
Reflections used for refinement	7149
Absorption correction	Semi-empirical from equivalents
Max. and min. transmission	0.99 and 0.91
Largest diff. peak and hole	0.523 and −0.361 $e.Å^{-3}$
Solution	Direct methods
Refinement	Full-matrix least-squares on F^2
Treatment of hydrogen atoms	Calculated positions, constr. ref.
Programs used	SHELXS-97 (Sheldrick, 2008)
	SHELXL-2013 (Sheldrick, 2013)
	DIAMOND (Crystal Impact)
Data / restraints / parameters	7149 / 180 / 599
Goodness-of-fit on F^2	1.027
R index (all data)	wR2 = 0.1231
R index conventional [I>2sigma(I)]	R1 = 0.0476
CCDC no.	985476

(Benzene-1,2-diolato)bis(1,10-phenanthroline)silicon(IV)-bis(hexafluorophosphate) (88)

Single crystals suitable for crystal structure analysis were obtained upon slow diffusion of diethyl ether into a solution of complex **88** in acetonitrile at 4 °C.

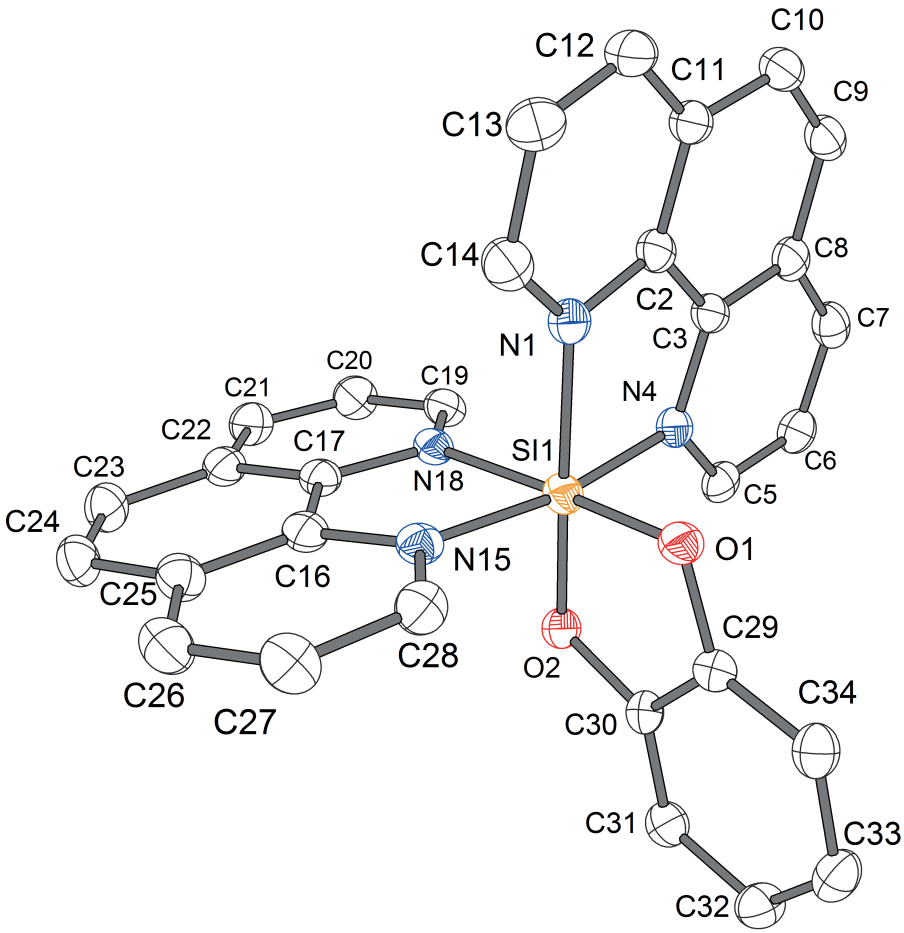

Figure 80: Crystal structure of complex **88**. ORTEP drawing with 50 % probability thermal ellipsoids. The PF_6 counterions and solvent are omitted for clarity.

Table 20: Crystal data and structure refinement for complex **88**.

Crystal data		
Identification code	jwka024	
Habitus, colour	block, orange	
Crystal size	$0.270 \times 0.260 \times 0.210\,mm^3$	
Crystal system	Monoclinic	
Space group	C 2/c	Z = 8
Unit cell dimensions	a = 32.2770(10) Å	$\alpha = 90°$
	b = 11.9801(5) Å	$\beta = 105.979(2)°$

	c = 22.1543(7) Å $\gamma = 90°$
Volume	8235.7(5) $Å^3$
Cell determination	20515 peaks with Θ = 1.3–27.0°
Empirical formula	$C_{34}H_{26}F_{12}N_6O_2P_2Si$
Formula weight	868.64 u
Density (calculated)	1.401 $Mg\,m^{-3}$
Absorption coefficient	0.227 mm^{-1}
F(000)	3520

Data collection

Diffractometer type	STOE IPDS 2
Wavelength	0.710 73 Å
Temperature	100(2) K
Theta range for data collection	1.312–25.500°
Index ranges	$-40 \leq h \leq 40, -15 \leq k \leq 15, -28 \leq l \leq 27$
Data collection software	STOE X-AREA
Cell refinement software	STOE X-AREA
Data reduction software	STOE X-RED

Solution and refinement

Reflections collected	40900
Independent reflections	7678 [R(int) = 6.36 %]
Completeness to theta = 25.242°	100 %
Observed reflections	4834[II > 2(I)]
Reflections used for refinement	7678
Absorption correction	Integration
Max. and min. transmission	0.9665 and 0.9375
Largest diff. peak and hole	0.422 and −0.270 $e.Å^{-3}$
Solution	Direct methods
Refinement	Full-matrix least-squares on F^2
Treatment of hydrogen atoms	Calculated positions, constr. ref.
Programs used	SIR2011
	SHELXL-2012 (Sheldrick, 2012)
	DIAMOND
	STOE IPDS2 software
Data / restraints / parameters	7678 / 0 / 516
Goodness-of-fit on F^2	0.807
R index (all data)	wR2 = 0.0826
R index conventional [I>2sigma(I)]	R1 = 0.0363
CCDC no.	

(4,5-Dinitrobenzene-1,2-diolato)bis(1,10-phenanthroline)silicon(IV)-bis(hexafluorophosphate) (130)

Single crystals suitable for crystal structure analysis were obtained upon slow diffusion of diethyl ether into a solution of complex **130** in acetonitrile at 4 °C.

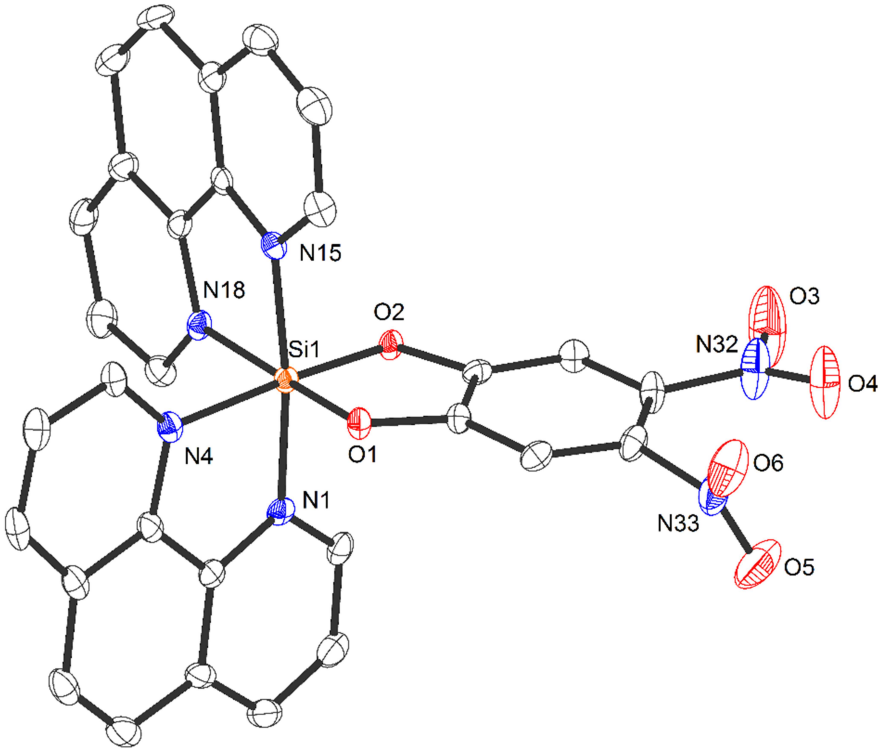

Figure 81: Crystal structure of complex **130**. ORTEP drawing with 50 % probability thermal ellipsoids. The PF_6 counterions and solvent are omitted for clarity.

Table 21: Crystal data and structure refinement for complex **130**.

Crystal data		
Identification code	jwka047d_0m	
Habitus, colour	block, orange	
Crystal size	$0.580 \times 0.260 \times 0.160\,mm^3$	
Crystal system	Monoclinic	
Space group	C 2/c	Z = 8
Unit cell dimensions	a = 31.140(2) Å	$\alpha = 90°$
	b = 13.7141(11) Å	$\beta = 128.9074(19)°$
	c = 24.1283(16) Å	$\gamma = 90°$
Volume	8018.3(10) $Å^3$	
Cell determination	4780 peaks with Θ = 2.3–26.9°	

Empirical formula	$C_{36}H_{27}F_{12}N_9O_6P_2Si$
Formula weight	999.69 u
Density (calculated)	$1.656\,Mg\,m^{-3}$
Absorption coefficient	$0.254\,mm^{-1}$
F(000)	4048

Data collection

Diffractometer type	Bruker D8 QUEST area detector
Wavelength	0.710 73 Å
Temperature	100(2) K
Theta range for data collection	2.288–25.499°
Index ranges	$-37 \leq h \leq 32, -16 \leq k \leq 16, -29 \leq l \leq 29$
Data collection software	BRUKER APEX II
Cell refinement software	SAINT V8.27B (Bruker AXS Inc., 2012)
Data reduction software	SAINT V8.27B (Bruker AXS Inc., 2012)

Solution and refinement

Reflections collected	23070
Independent reflections	7467 [R(int) = 0.0672]
Completeness to theta = 25.242°	99.8 %
Observed reflections	5078[II > 2(I)]
Reflections used for refinement	7467
Absorption correction	Semi-empirical from equivalents
Max. and min. transmission	0.96 and 0.87
Largest diff. peak and hole	0.754 and -0.438 e.Å^{-3}
Solution	Direct methods
Refinement	Full-matrix least-squares on F^2
Treatment of hydrogen atoms	Calculated positions, riding model
Programs used	SIR2011
	SHELXL-2012 (Sheldrick, 2012)
	DIAMOND (Crystal Impact)
Data / restraints / parameters	7467 / 9 / 599
Goodness-of-fit on F^2	1.033
R index (all data)	wR2 = 0.1596
R index conventional [I>2sigma(I)]	R1 = 0.0571
CCDC no.	985475

Bis(2,2'-bipyridine)(2,9-dimethyl-1,10-phenanthroline)ruthenium(II)-bis(hexafluorophosphate) (218)

Single crystals suitable for crystal structure analysis were obtained upon slow diffusion of diethyl ether into a solution of complex **218** in acetonitrile at 4 °C.

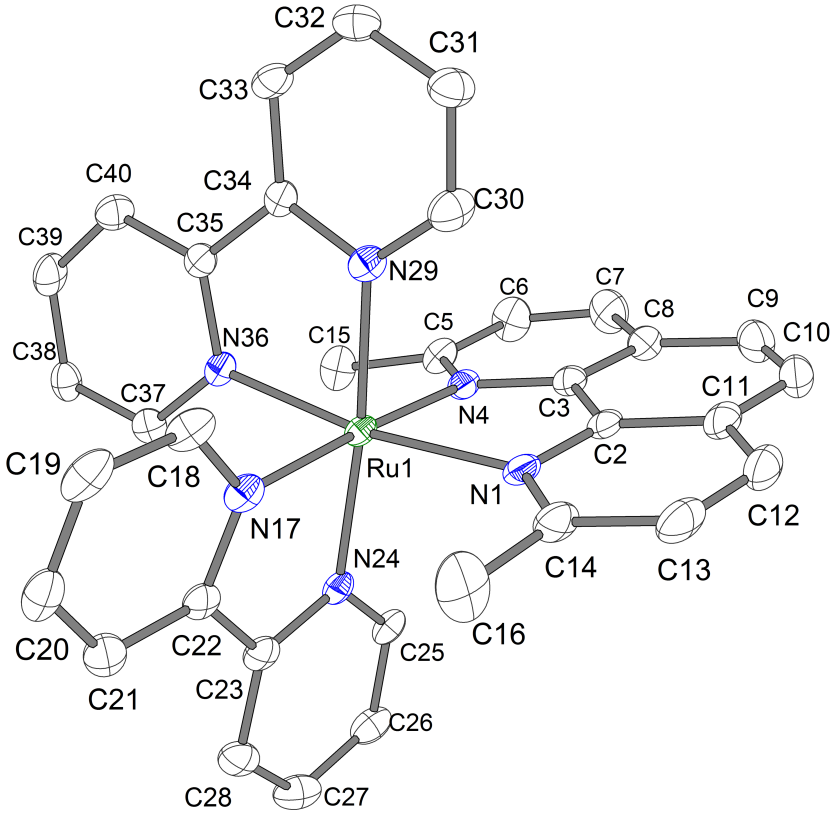

Figure 82: Crystal structure of complex **218**. ORTEP drawing with 50 % probability thermal ellipsoids. The PF_6 counterions and solvent are omitted for clarity.

Table 22: Crystal data and structure refinement for complex **218**.

Crystal data		
Identification code	jwka060_0m	
Habitus, colour	nugget, red	
Crystal size	$0.460 \times 0.220 \times 0.170\,mm^3$	
Crystal system	Monoclinic	
Space group	C 2/c	Z = 8
Unit cell dimensions	a = 26.2772(13) Å	$\alpha = 90°$
	b = 9.8283(5) Å	$\beta = 91.0319(16)°$
	c = 26.6559(11) Å	$\gamma = 90°$
Volume	6883.0(6) $Å^3$	

Cell determination	8223 peaks with Θ = 2.3–27.5°
Empirical formula	$C_{34}H_{28}F_{12}N_6P_2Ru$
Formula weight	911.63 u
Density (calculated)	1.759 $Mg\,m^{-3}$
Absorption coefficient	0.651 mm^{-1}
F(000)	3648

Data collection

Diffractometer type	Bruker D8 QUEST area detector
Wavelength	0.710 73 Å
Temperature	100(2) K
Theta range for data collection	2.212–25.499°
Index ranges	$-26 \leq h \leq 31, -11 \leq k \leq 11, -32 \leq l \leq 32$
Data collection software	BRUKER APEX II
Cell refinement software	SAINT V8.27B (Bruker AXS Inc., 2012)
Data reduction software	SAINT V8.27B (Bruker AXS Inc., 2012)

Solution and refinement

Reflections collected	19716
Independent reflections	6382 [R(int) = 0.0434]
Completeness to theta = 25.242°	99.8 %
Observed reflections	5288[II > 2(I)]
Reflections used for refinement	6382
Absorption correction	Integration
Max. and min. transmission	0.90 and 0.74
Largest diff. peak and hole	0.484 and −0.577 e.$Å^{-3}$
Solution	Direct methods
Refinement	Full-matrix least-squares on F^2
Treatment of hydrogen atoms	Calculated positions, riding model
Programs used	SHELXS-97 (Sheldrick, 2008)
	SHELXL-2012 (Sheldrick, 2012)
	DIAMOND
Data / restraints / parameters	6382 / 96 / 535
Goodness-of-fit on F^2	1.041
R index (all data)	wR2 = 0.0799
R index conventional [I>2sigma(I)]	R1 = 0.0345
CCDC no.	

Bis(1,10-phenanthroline)(1,10-phenanthroline-5,6-dione-$\kappa^2 N$)ruthenium(II)-bis(hexafluorophosphate) (210)

Single crystals suitable for crystal structure analysis were obtained upon slow diffusion of diethyl ether into a solution of complex **210** in acetonitrile at 4 °C.

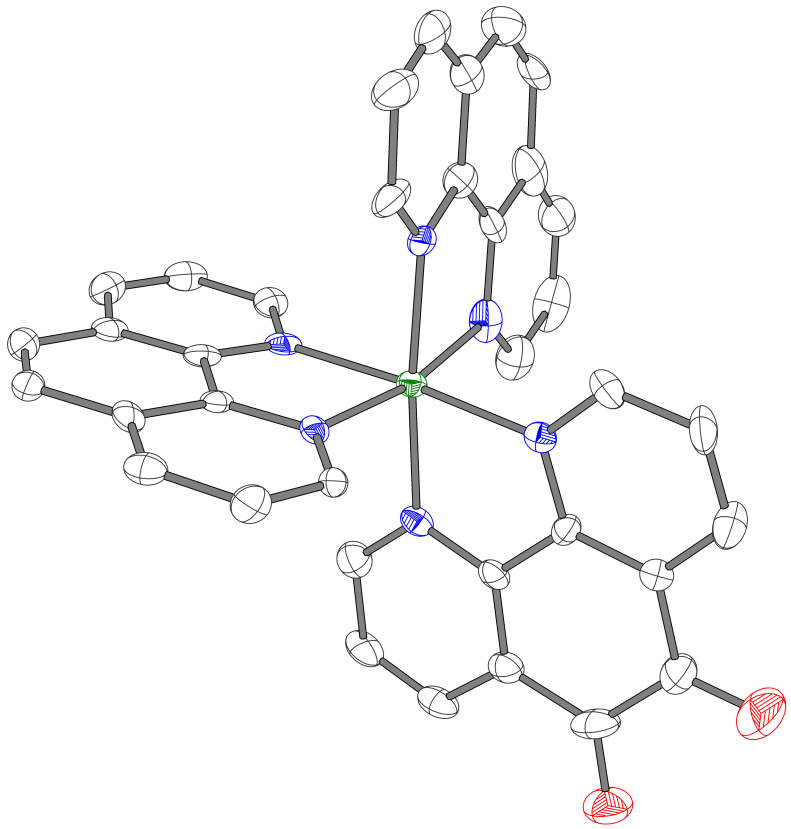

Figure 83: Crystal structure of complex **210**. ORTEP drawing with 50 % probability thermal ellipsoids. The PF_6 counterions and solvent are omitted for clarity.

Table 23: Crystal data and structure refinement for complex **210**.

Crystal data		
Identification code	jwka063_0m	
Habitus, colour	nugget, red	
Crystal size	$0.430 \times 0.140 \times 0.090\,mm^3$	
Crystal system	Triclinic	
Space group	P −1	Z = 2
Unit cell dimensions	a = 13.6775(9) Å	$\alpha = 90.424(2)°$
	b = 21.0045(15) Å	$\beta = 105.3799(19)°$
	c = 23.4389(14) Å	$\gamma = 107.4667(19)°$
Volume	6165.5(7) $Å^3$	

Cell determination	7134 peaks with Θ = 2.2–24.0°
Empirical formula	$C_{119.77}H_{91.65}F_{36}N_{19.88}O_8P_6Ru_3$
Formula weight	3110.41 u
Density (calculated)	1.675 $Mg\,m^{-3}$
Absorption coefficient	0.562 mm^{-1}
F(000)	3119

Data collection

Diffractometer type	Bruker D8 QUEST area detector
Wavelength	0.710 73 Å
Temperature	100(2) K
Theta range for data collection	2.042–24.999°
Index ranges	$-16 \leq h \leq 16, -24 \leq k \leq 24, -27 \leq l \leq 27$
Data collection software	BRUKER APEX II
Cell refinement software	SAINT V8.27B (Bruker AXS Inc., 2012)
Data reduction software	SAINT V8.27B (Bruker AXS Inc., 2012)

Solution and refinement

Reflections collected	58382
Independent reflections	21682 [R(int) = 0.1178]
Completeness to theta = 25.242°	97.1 %
Observed reflections	12594[II > 2(I)]
Reflections used for refinement	21682
Absorption correction	Semi-empirical from equivalents
Max. and min. transmission	0.95 and 0.86
Largest diff. peak and hole	1.299 and −0.673 e.$Å^{-3}$
Solution	Direct methods
Refinement	Full-matrix least-squares on F^2
Treatment of hydrogen atoms	Calculated positions, constr ref
Programs used	SHELXS-97 (Sheldrick, 2008)
	SHELXL-2012 (Sheldrick, 2012)
	DIAMOND
Data / restraints / parameters	21682 / 619 / 1860
Goodness-of-fit on F^2	0.967
R index (all data)	wR2 = 0.1485
R index conventional [I>2sigma(I)]	R1 = 0.0616
CCDC no.	

(4,5-Dibromobenzene-1,2-diolato)bis(1,10-phenanthroline)silicon(IV)-bis(hexafluorophosphate) (108)

Single crystals suitable for crystal structure analysis were obtained upon slow diffusion of diethyl ether into a solution of complex **108** in acetonitrile at 4 °C.

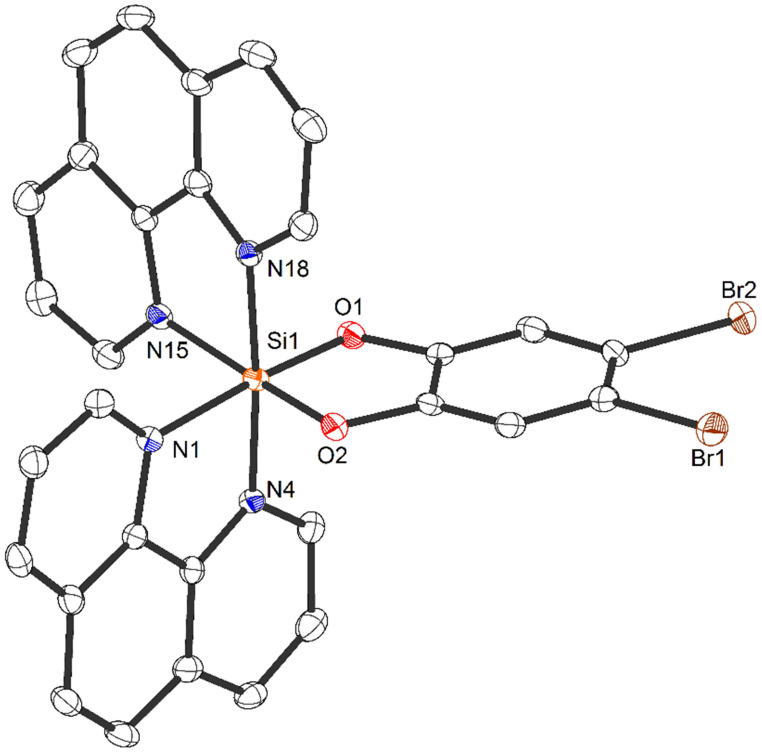

Figure 84: Crystal structure of complex **108**. ORTEP drawing with 50 % probability thermal ellipsoids. The PF_6 counterions and solvent are omitted for clarity.

Table 24: Crystal data and structure refinement for complex **108**.

Crystal data		
Identification code	jwka098_0m	
Habitus, colour	prism, yellow	
Crystal size	$0.120 \times 0.19 \times 0.08\,mm^3$	
Crystal system	Triclinic	
Space group	P −1	Z = 2
Unit cell dimensions	a = 11.5630(17) Å	α = 97.650(6)°
	b = 11.725(2) Å	β = 95.422(6)°
	c = 15.931(2) Å	γ = 117.067(10)°
Volume	1876.5(5) $Å^3$	
Cell determination	9965 peaks with Θ = 2.5–27.5°	

Empirical formula	$C_{35}H_{25.50}Br_2F_{12}N_{6.50}O_2P_2Si$
Formula weight	1046.97 u
Density (calculated)	$1.853\,Mg\,m^{-3}$
Absorption coefficient	$2.383\,mm^{-1}$
F(000)	1038

Data collection

Diffractometer type	Bruker D8 QUEST area detector
Wavelength	0.710 73 Å
Temperature	100(2) K
Theta range for data collection	2.154–26.000°
Index ranges	$-14 \leq h \leq 14, -14 \leq k \leq 13, -19 \leq l \leq 19$
Data collection software	BRUKER APEX II
Cell refinement software	SAINT V8.27B (Bruker AXS Inc., 2012)
Data reduction software	SAINT V8.27B (Bruker AXS Inc., 2012)

Solution and refinement

Reflections collected	44047
Independent reflections	7360 [R(int) = 0.0607]
Completeness to theta = 25.242°	99.9 %
Observed reflections	5902[II > 2(I)]
Reflections used for refinement	7360
Absorption correction	Semi-empirical from equivalents
Max. and min. transmission	0.7456 and 0.6274
Largest diff. peak and hole	0.481 and −0.450 e.$Å^{-3}$
Solution	Direct methods
Refinement	Full-matrix least-squares on F^2
Treatment of hydrogen atoms	Calculated positions, constr. ref.
Programs used	SHELXS (Sheldrick, 2008)
	SHELXL-2013 (Sheldrick, 2013)
	DIAMOND
Data / restraints / parameters	7360 / 243 / 660
Goodness-of-fit on F^2	1.031
R index (all data)	wR2 = 0.0759
R index conventional [I>2sigma(I)]	R1 = 0.0303
CCDC no.	985474

Bis(5,6-dimethyl-1,10-phenanthroline)(1,10-phenanthroline-5,6-dione-$\kappa^2 N$) ruthenium(II)-bis(hexafluorophosphate) (211)

Single crystals suitable for crystal structure analysis were obtained upon slow diffusion of diethyl ether into a solution of complex **211** in acetonitrile at 4 °C.

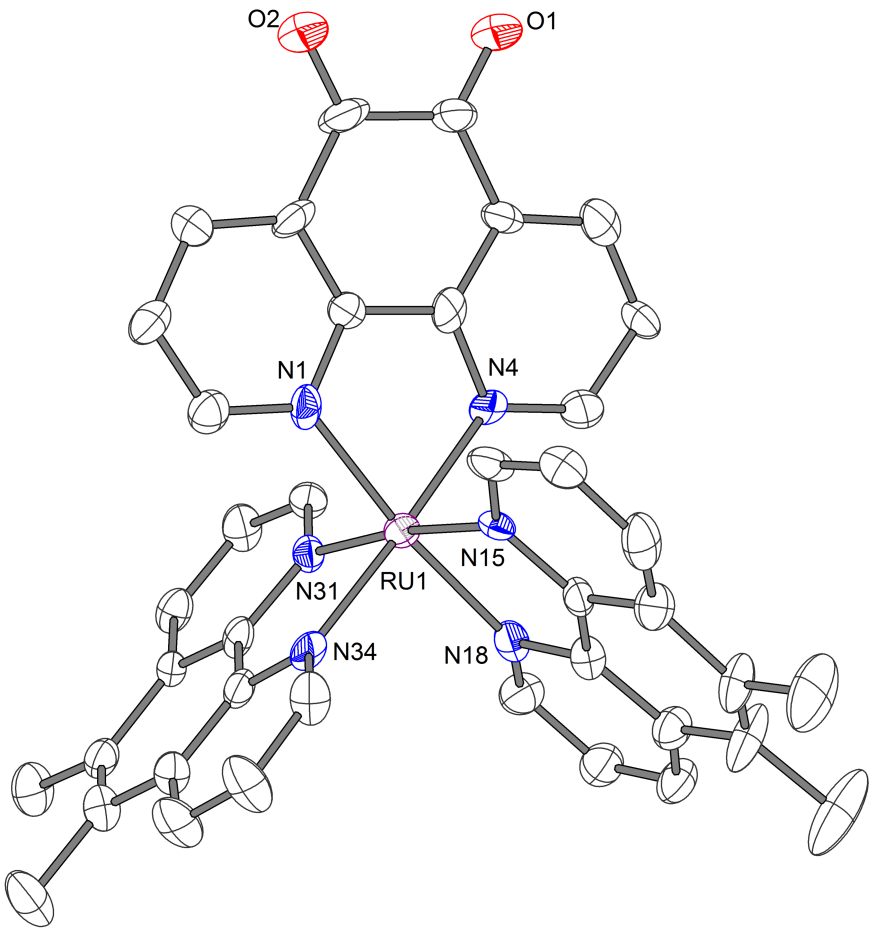

Figure 85: Crystal structure of complex **211**. ORTEP drawing with 50 % probability thermal ellipsoids. The PF_6 counterions and solvent are omitted for clarity.

Table 25: Crystal data and structure refinement for complex **211**.

Crystal data		
Identification code	JWKA133_0m	
Habitus, colour	block, dark	
Crystal size	$0.310 \times 0.220 \times 0.140\,mm^3$	
Crystal system	Monoclinic	
Space group	P $2_1/c$	Z = 8
Unit cell dimensions	a = 13.7302(7) Å	$\alpha = 90°$

	b = 23.2969(12) Å	$\beta = 90.131(3)°$
	c = 27.9128(15) Å	$\gamma = 90°$
Volume	8928.5(8) $Å^3$	
Cell determination	9854 peaks with Θ = 2.4–27.3°	
Empirical formula	$C_{45}H_{39.50}F_{12}N_{7.50}O_2.50P_2Ru$	
Formula weight	1116.35 u	
Density (calculated)	1.661 $Mg\,m^{-3}$	
Absorption coefficient	0.524 mm^{-1}	
F(000)	4512	

Data collection

Diffractometer type	Bruker D8 QUEST area detector
Wavelength	0.710 73 Å
Temperature	100(2) K
Theta range for data collection	2.277–25.000°
Index ranges	$-13 \leq h \leq 15, -27 \leq k \leq 27, -33 \leq l \leq 33$
Data collection software	BRUKER APEX II
Cell refinement software	SAINT V8.27B (Bruker AXS Inc., 2012)
Data reduction software	SAINT V8.27B (Bruker AXS Inc., 2012)

Solution and refinement

Reflections collected	74508
Independent reflections	13555 [R(int) = 0.0956]
Completeness to theta = 25.000°	95.3 %
Observed reflections	9795[II > 2(I)]
Reflections used for refinement	13555
Absorption correction	Semi-empirical from equivalents
Max. and min. transmission	0.93 and 0.81
Largest diff. peak and hole	0.762 and −0.658 e.$Å^{-3}$
Solution	direct/ difmap
Refinement	Full-matrix least-squares on F^2
Treatment of hydrogen atoms	geom, constr.
Programs used	SHELXS-97 (Sheldrick, 2008)
	SHELXL-2013 (Sheldrick, 2013)
	DIAMOND (Crystal Impact)
Data / restraints / parameters	13555 / 101 / 1364
Goodness-of-fit on F^2	1.160
R index (all data)	wR2 = 0.1840
R index conventional [I>2sigma(I)]	R1 = 0.0839
CCDC no.	

Chlorido(2,2':6',2"-terpyridine)palladium(II)-chloride (293)

Single crystals suitable for crystal structure analysis were obtained upon slow precipitation from a concentrated solution of complex **293** in dimethyl sulfoxide at room temperature.

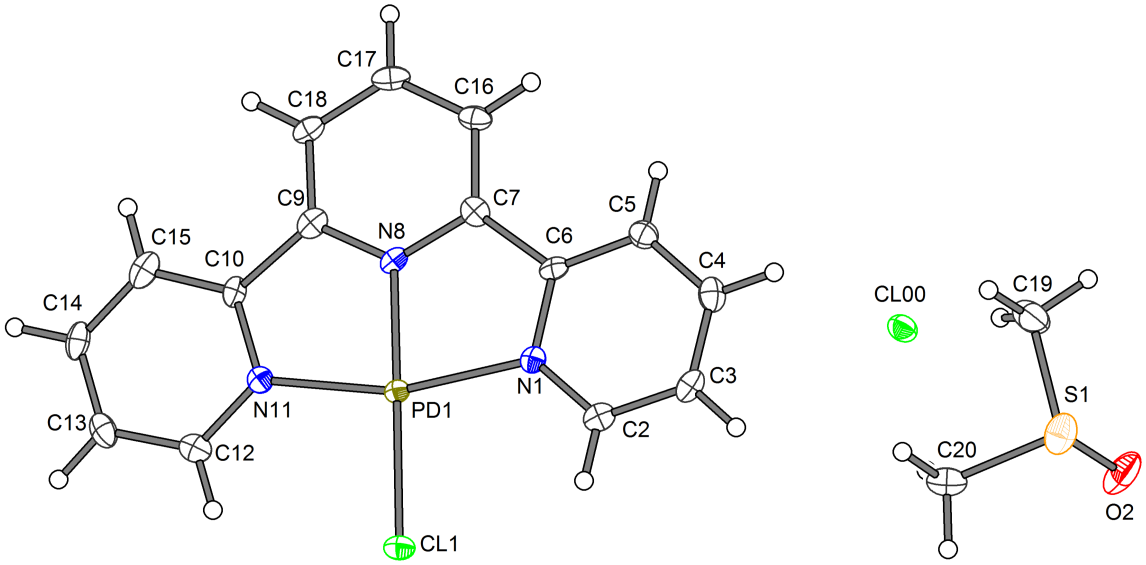

Figure 86: Crystal structure of complex **293**. ORTEP drawing with 50 % probability thermal ellipsoids.

Table 26: Crystal data and structure refinement for complex **293**.

Crystal data		
Identification code	JWKA151a_0m	
Habitus, colour	needle, colorless	
Crystal size	$0.33 \times 0.07 \times 0.03\,mm^3$	
Crystal system	Monoclinic	
Space group	P $2_1/n$	Z = 4
Unit cell dimensions	a = 6.7500(6) Å	$\alpha = 90°$
	b = 13.2638(12) Å	$\beta = 90.452(3)°$
	c = 20.8969(18) Å	$\gamma = 90°$
Volume	1870.9(3) $Å^3$	

Cell determination	6905 peaks with Θ = 2.5–27.1°
Empirical formula	$C_{17}H_{17}Cl_2N_3OPdS$
Formula weight	488.69 u
Density (calculated)	1.735 $Mg\,m^{-3}$
Absorption coefficient	1.399 mm^{-1}
F(000)	976

Data collection

Diffractometer type	Bruker D8 QUEST area detector
Wavelength	0.710 73 Å
Temperature	100(2) K
Theta range for data collection	2.482–25.496°
Index ranges	$-8 \leq h \leq 8, -16 \leq k \leq 16, -25 \leq l \leq 25$
Data collection software	BRUKER APEX II
Cell refinement software	SAINT V8.34A (Bruker AXS Inc., 2013)
Data reduction software	SAINT V8.34A (Bruker AXS Inc., 2013)

Solution and refinement

Reflections collected	24590
Independent reflections	3471 [R(int) = 0.0792]
Completeness to theta = 25.242°	99.9 %
Observed reflections	2690[II > 2(I)]
Reflections used for refinement	3471
Absorption correction	Semi-empirical from equivalents
Max. and min. transmission	0.96 and 0.77
Largest diff. peak and hole	0.479 and −0.597 e.$Å^{-3}$
Solution	direct/ difmap
Refinement	Full-matrix least-squares on F^2
Treatment of hydrogen atoms	geom, constr.
Programs used	SHELXS-97 (Sheldrick, 2008)
	SHELXL-2013 (Sheldrick, 2013)
	DIAMOND (Crystal Impact)
Data / restraints / parameters	3471 / 0 / 228
Goodness-of-fit on F^2	1.093
R index (all data)	wR2 = 0.0690
R index conventional [I>2sigma(I)]	R1 = 0.0394
CCDC no.	

(2-(1-Methylpyridinium-4-yl)-1*H*-benzo[*d*]imidazole-5,6-diolato-κ^2O)bis(1,10-phenanthroline)silicon(IV)-tris(hexafluorophosphate) (159)

Single crystals suitable for crystal structure analysis were obtained upon slow solvent evaporation of a solution of complex **159** in acetonitrile at room temperature.

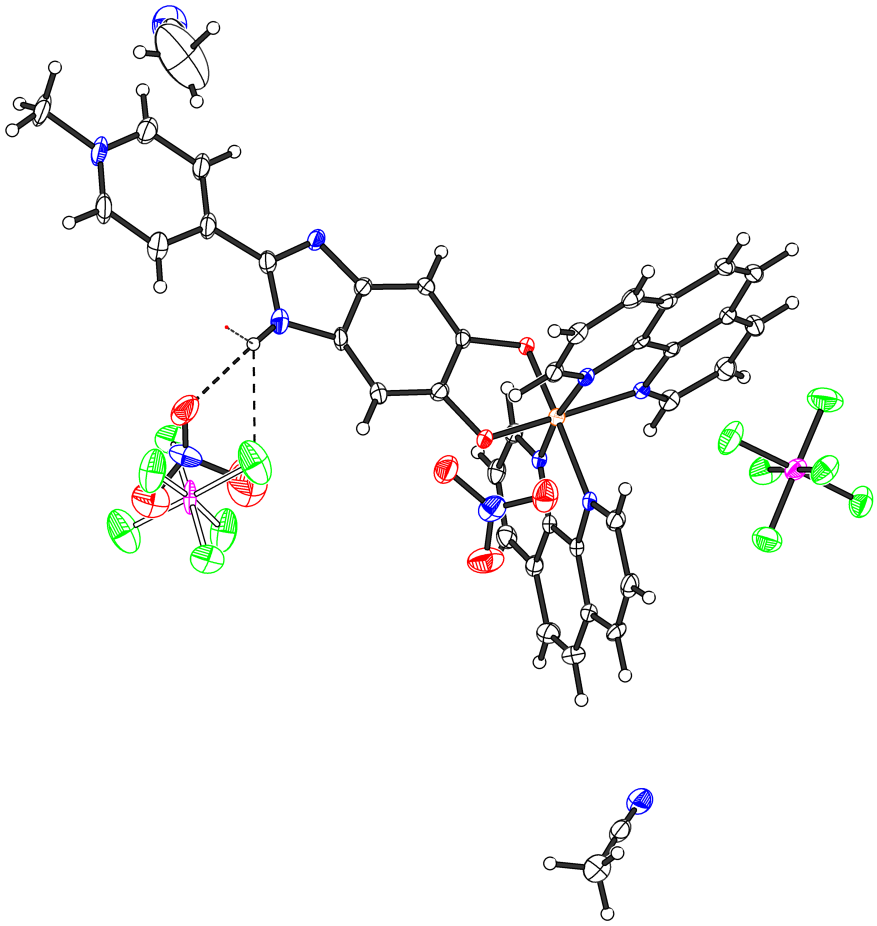

Figure 87: Crystal structure of complex **159**. ORTEP drawing with 50 % probability thermal ellipsoids.

Table 27: Crystal data and structure refinement for complex **159**.

Crystal data		
Identification code	JWKA192_0m	
Habitus, colour	plate, beige	
Crystal size	$0.26 \times 0.05 \times 0.05\,\mathrm{mm}^3$	
Crystal system	Triclinic	
Space group	P −1	Z = 2
Unit cell dimensions	a = 9.1209(9) Å	$\alpha = 75.922(3)°$

	b = 12.5044(11) Å	β = 79.162(3)°
	c = 19.3837(18) Å	γ = 79.813(3)°
Volume	2086.0(3) Å^3	
Cell determination	9650 peaks with Θ = 2.2–25.3°	
Empirical formula	$C_{41}H_{32}F_{8.09}N_{10.65}O_{6.95}P_{1.35}Si$	
Moiety formula	$C_{37}H_{26}N_7O_2Si$,1.35 (F_6P), 1.65 (NO_3), 2 (C_2H_3N)	
Formula weight	1008.70 u	
Density (calculated)	1.606 Mg m^{-3}	
Absorption coefficient	0.211 mm^{-1}	
F(000)	1030	

Data collection

Diffractometer type	Bruker D8 QUEST area detector
Wavelength	0.710 73 Å
Temperature	100(2) K
Theta range for data collection	2.192–25.324°
Index ranges	$-10 \leq h \leq 10, -15 \leq k \leq 15, -23 \leq l \leq 22$
Data collection software	BRUKER APEX2 2014.9-0
Cell refinement software	BRUKER SAINT
Data reduction software	SAINT V8.34A (Bruker AXS Inc., 2013)

Solution and refinement

Reflections collected	27834
Independent reflections	7539 [R(int) = 0.0551]
Completeness to theta = 25.242°	99.7 %
Observed reflections	5670[I>2sigma(I)]
Reflections used for refinement	7539
Absorption correction	Numerical
Max. and min. transmission	0.99 and 0.87
Largest diff. peak and hole	1.031 and −0.833 e.Å^{-3}
Solution	Direct methods
Refinement	Full-matrix least-squares on F^2
Treatment of hydrogen atoms	Calculated positions, constr. ref.
Programs used	XT V2014/1 (Bruker AXS Inc., 2014)
	SHELXL-2014/7 (Sheldrick, 2014)
	DIAMOND (Crystal Impact)
Data / restraints / parameters	7539 / 46 / 662
Goodness-of-fit on F^2	1.028
R index (all data)	wR2 = 0.1435
R index conventional [I>2sigma(I)]	R1 = 0.0581
CCDC no.	1490975

4-(2-Azidoethoxy)benzoic acid (294)

Single crystals suitable for crystal structure analysis were obtained upon slow oxidation using air in a solution of compound **245** in dichloromethane at room temperature.

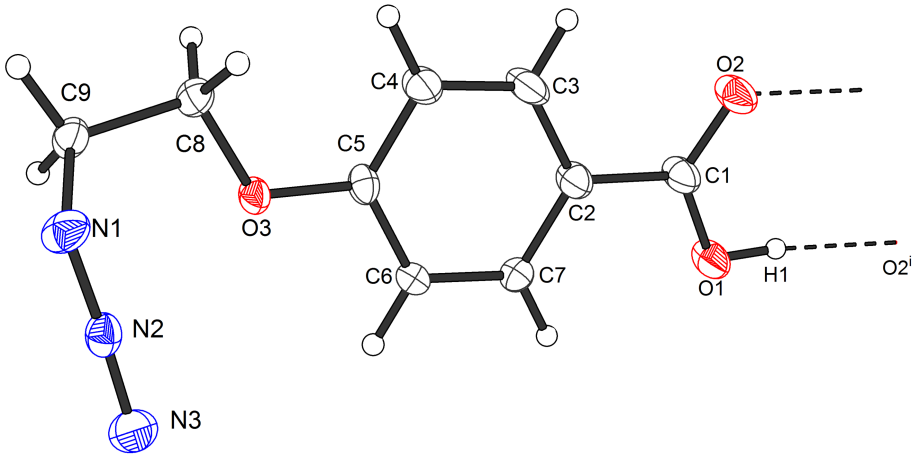

Figure 88: Crystal structure of complex **294**. ORTEP drawing with 50 % probability thermal ellipsoids. The PF_6 counterions and solvent are omitted for clarity.

Table 28: Crystal data and structure refinement for complex **294**.

Crystal data		
Identification code	JWKA242_0m	
Habitus, colour	prism, colorless	
Crystal size	$0.27 \times 0.13 \times 0.08\,mm^3$	
Crystal system	Monoclinic	
Space group	P $2_1/n$	Z = 4
Unit cell dimensions	a = 4.9759(4) Å	$\alpha = 90°$
	b = 27.254(2) Å	$\beta = 110.210(3)°$
	c = 7.2032(5) Å	$\gamma = 90°$
Volume	916.71(12) $Å^3$	
Cell determination	1753 peaks with Θ = 3.0–25.2°	
Empirical formula	$C_9H_9N_3O_3$	
Formula weight	207.19 u	
Density (calculated)	$1.501\,Mg\,m^{-3}$	

Absorption coefficient	$0.116\,\mathrm{mm}^{-1}$
F(000)	432

Data collection

Diffractometer type	Bruker D8 QUEST area detector
Wavelength	0.710 73 Å
Temperature	100(2) K
Theta range for data collection	2.990–25.249°
Index ranges	$-5 \leq h \leq 4, -27 \leq k \leq 32, -8 \leq l \leq 8$
Data collection software	BRUKER APEX2 2014.9-0
Cell refinement software	BRUKER SAINT
Data reduction software	SAINT V8.34A (Bruker AXS Inc., 2013)

Solution and refinement

Reflections collected	3878
Independent reflections	1650 [R(int) = 0.0191]
Completeness to theta = 25.242°	99.9 %
Observed reflections	1391[I>2sigma(I)]
Reflections used for refinement	1650
Absorption correction	Semi-empirical from equivalents
Max. and min. transmission	0.99 and 0.88
Largest diff. peak and hole	0.198 and −0.196 e.Å^{-3}
Solution	Direct methods
Refinement	Full-matrix least-squares on F^2
Treatment of hydrogen atoms	CH calc., constr., OH located, isotr.
Programs used	XT V2014/1 (Bruker AXS Inc., 2014)
	SHELXL-2014/7 (Sheldrick, 2014)
	DIAMOND (Crystal Impact)
Data / restraints / parameters	1650 / 0 / 139
Goodness-of-fit on F^2	1.045
R index (all data)	wR2 = 0.0877
R index conventional [I>2sigma(I)]	R1 = 0.0348
CCDC no.	

(Benzene-1,2-diolato)(dipyrido[3,2-*a*:2',3'-*c*]phenazine-$\kappa^2 N', N''$)(1,10-phenanthroline)silicon(IV)-bis(hexafluorophosphate) (184)

Single crystals suitable for crystal structure analysis were obtained upon slow precipitation from a concentrated solution of complex **184** in acetonitrile at room temperature.

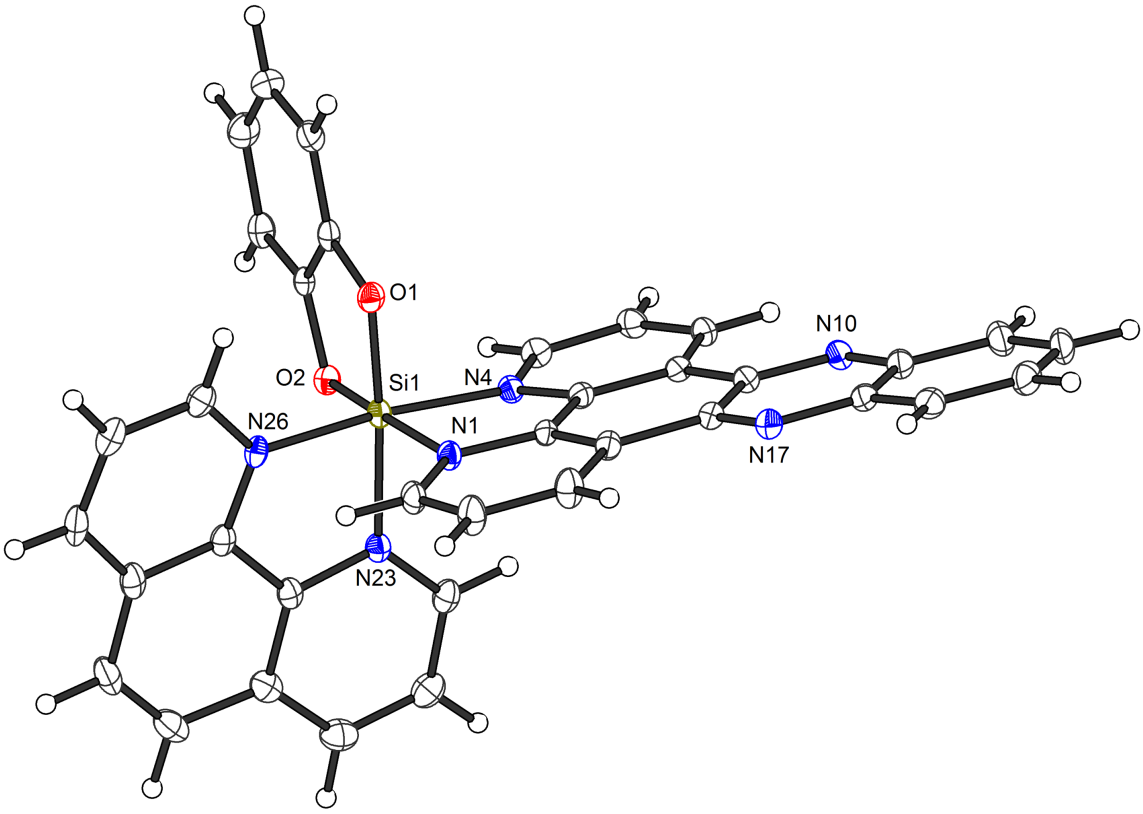

Figure 89: Crystal structure of complex **184**. ORTEP drawing with 50 % probability thermal ellipsoids. The PF_6 counterions and solvent are omitted for clarity.

Table 29: Crystal data and structure refinement for complex **184**.

Crystal data		
Identification code	JWKA253_0m	
Habitus, colour	column, yellow	
Crystal size	$0.34 \times 0.12 \times 0.09\,mm^3$	
Crystal system	Triclinic	
Space group	P −1	Z = 2
Unit cell dimensions	a = 10.8373(5) Å	α = 88.089(2)°
	b = 13.3990(5) Å	β = 83.876(2)°
	c = 13.5169(6) Å	γ = 77.962(2)°

Volume	1908.53(14) $Å^3$
Cell determination	9893 peaks with Θ = 2.3–25.3°
Empirical formula	$C_{38.76}H_{26.15}F_{12}N_{7.38}O_2P_2Si$
Moiety formula	$C_{36}H_{22}N_6O_2Si$,2 (F_6P), 1.383(C_2H_3N)
Formula weight	945.42 u
Density (calculated)	1.645 Mg m^{-3}
Absorption coefficient	0.254 mm^{-1}
F(000)	957

Data collection

Diffractometer type	Bruker D8 QUEST area detector
Wavelength	0.710 73 Å
Temperature	100(2) K
Theta range for data collection	2.215–25.307°
Index ranges	$-13 \leq h \leq 12, -16 \leq k \leq 16, -16 \leq l \leq 16$
Data collection software	BRUKER APEX2 2014.9-0
Cell refinement software	BRUKER SAINT
Data reduction software	SAINT V8.34A (Bruker AXS Inc., 2013)

Solution and refinement

Reflections collected	29160
Independent reflections	6939 [R(int) = 0.0305]
Completeness to theta = 25.242°	99.9 %
Observed reflections	5838[I>2sigma(I)]
Reflections used for refinement	6939
Absorption correction	Numerical
Max. and min. transmission	0.98 and 0.92
Largest diff. peak and hole	0.355 and −0.262 e.$Å^{-3}$
Solution	Direct methods
Refinement	Full-matrix least-squares on F^2
Treatment of hydrogen atoms	Calculated positions, constr. ref.
Programs used	SHELXT V2014/1 (Bruker AXS Inc., 2014)
	SHELXL-2014/7 (Sheldrick, 2014)
	DIAMOND (Crystal Impact)
Data / restraints / parameters	6939 / 165 / 653
Goodness-of-fit on F^2	1.024
R index (all data)	wR2 = 0.0854
R index conventional [I>2sigma(I)]	R1 = 0.0329
CCDC no.	

(Benzene-1,2-diolato)bis(3,4,7,8-tetramethyl-1,10-phenanthroline)silicon(IV)-bis(hexafluorophosphate) (89)

Single crystals suitable for crystal structure analysis were obtained upon slow diffusion of diethyl ether into a solution of complex **89** in acetonitrile at 4 °C.

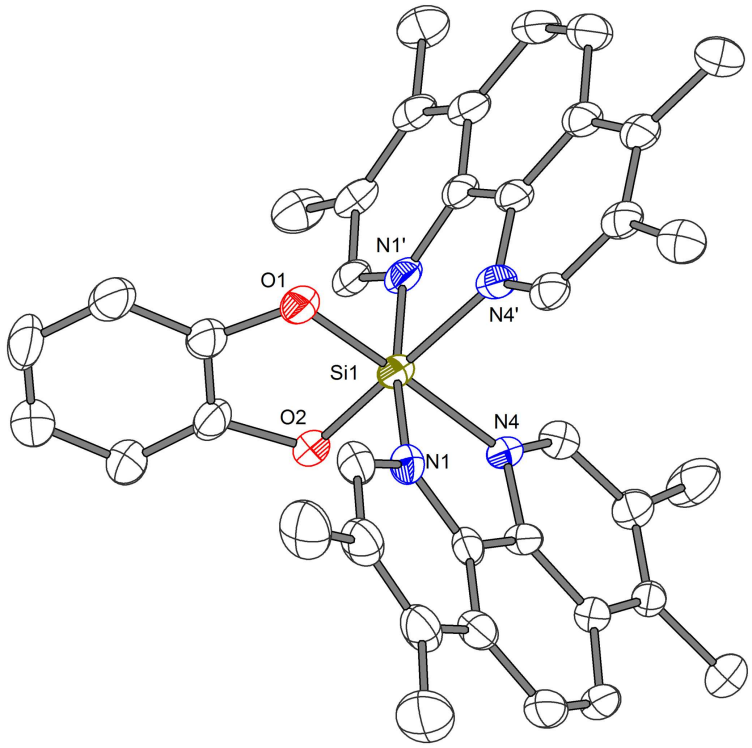

Figure 90: Crystal structure of complex **89**. ORTEP drawing with 50 % probability thermal ellipsoids. The PF_6 counterions and solvent are omitted for clarity.

Table 30: Crystal data and structure refinement for complex **89**.

Crystal data		
Identification code	JWKA254_0m_sq	
Habitus, colour	block, yellow	
Crystal size	$0.28 \times 0.13 \times 0.09\,mm^3$	
Crystal system	Triclinic	
Space group	P −1	Z = 4
Unit cell dimensions	a = 15.3697(7) Å	α = 74.708(2)°
	b = 16.6665(7) Å	β = 88.523(2)°
	c = 19.3271(9) Å	γ = 82.145(2)°
Volume	4730.4(4) $Å^3$	
Cell determination	9863 peaks with Θ = 2.4–24.9°	

Empirical formula	$C_{38}H_{36}F_{12}N_4O_2P_2Si$
Moiety formula	$C_{38}H_{36}N_4O_2Si$,2 (F_6P)
Formula weight	898.74 u
Density (calculated)	1.262 $Mg\,m^{-3}$
Absorption coefficient	0.199 mm^{-1}
F(000)	1840

Data collection

Diffractometer type	Bruker D8 QUEST area detector
Wavelength	0.710 73 Å
Temperature	100(2) K
Theta range for data collection	2.185–25.320°
Index ranges	$-18 \leq h \leq 18, -20 \leq k \leq 20, -23 \leq l \leq 23$
Data collection software	BRUKER APEX2 2014.9-0
Cell refinement software	BRUKER SAINT
Data reduction software	SAINT V8.34A (Bruker AXS Inc., 2013)

Solution and refinement

Reflections collected	103966
Independent reflections	17238 [R(int) = 0.1012]
Completeness to theta = 25.242°	99.9 %
Observed reflections	10999[I>2sigma(I)]
Reflections used for refinement	17238
Absorption correction	Semi-empirical from equivalents
Max. and min. transmission	0.98 and 0.94
Largest diff. peak and hole	1.198 and −0.393 e.$Å^{-3}$
Solution	Direct methods
Refinement	Full-matrix least-squares on F^2
Treatment of hydrogen atoms	Calculated positions, riding model
Programs used	SHELXS-97 (Sheldrick, 2008) XT V2014/1 (Bruker AXS Inc., 2014) SHELXL-2014/7 (Sheldrick, 2014) DIAMOND (Crystal Impact)
Data / restraints / parameters	17238 / 919 / 1398
Goodness-of-fit on F^2	1.018
R index (all data)	wR2 = 0.1990
R index conventional [I>2sigma(I)]	R1 = 0.0677
CCDC no.	

D. Tables of the DNA Binding Assays

Table 31: Single determination of the binding constant to *calf thymus* DNA and the mean value ± standard deviation (Ø) for complex **224**. k_B = binding constant, s = binding site, $\Delta\lambda$ = bathochromic shift, λ = wavelength used for the determination.

No.	λ /nm	k_B /M^{-1}	s	$\Delta\lambda$ /nm	Hyp. /%
1	393	$(1.14 \pm 0.60) \times 10^7$	0.645 ± 0.011	+6	49
2	393	$(1.06 \pm 0.46) \times 10^7$	0.966 ± 0.013	+6	49
3	393	$(1.88 \pm 0.89) \times 10^7$	0.884 ± 0.008	+6	48
4	393	$(1.20 \pm 0.40) \times 10^7$	0.984 ± 0.009	+6	50
Ø	393	$(1.32 \pm 0.19) \times 10^7$	0.870 ± 0.078	+6	49

Table 32: Single determination of the binding constant to telo24 quadruplex DNA ($[T_2AG_3]_4$) and the mean value ± standard deviation (Ø) for complex **224**. k_B = binding constant, s = binding site, $\Delta\lambda$ = bathochromic shift, λ = wavelength used for the determination.

No.	λ /nm	k_B /M^{-1}	s	$\Delta\lambda$ /nm	Hyp. /%
1	393	$(1.19 \pm 0.30) \times 10^6$	0.059 ± 0.005	+6	52
2	393	$(1.34 \pm 0.34) \times 10^6$	0.107 ± 0.006	+5	46
3	393	$(4.65 \pm 1.17) \times 10^6$	0.142 ± 0.004	+6	46
Ø	393	$(2.39 \pm 1.13) \times 10^6$	0.103 ± 0.024	+6	48

Table 33: Single determination of the binding constant to *calf thymus* DNA and the mean value ± standard deviation (Ø) for complex **226**. k_B = binding constant, s = binding site, $\Delta\lambda$ = bathochromic shift, λ = wavelength used for the determination.

No.	λ /nm	k_B /M^{-1}	s	$\Delta\lambda$ /nm	Hyp. /%
1	393	$(1.50 \pm 0.48) \times 10^7$	1.004 ± 0.008	+5	46
2	393	$(1.96 \pm 0.35) \times 10^7$	0.915 ± 0.004	+5	45
3	393	$(2.03 \pm 0.63) \times 10^7$	1.078 ± 0.006	+5	48
4	393	$(1.14 \pm 0.50) \times 10^7$	1.22 ± 0.02	+5	48
Ø	393	$(1.66 \pm 0.21) \times 10^7$	1.05 ± 0.06	+5	47

Table 34: Single determination of the binding constant to telo24 quadruplex DNA ($[T_2AG_3]_4$) and the mean value ± standard deviation (Ø) for complex **226**. k_B = binding constant, s = binding site, $\Delta\lambda$ = bathochromic shift, λ = wavelength used for the determination.

No.	λ /nm	k_B /M^{-1}	s	$\Delta\lambda$ /nm	Hyp. /%
1	393	$(1.53 \pm 0.38) \times 10^6$	0.099 ± 0.005	+5	47
2	393	$(1.81 \pm 0.40) \times 10^6$	0.107 ± 0.004	+5	47
3	393	$(1.93 \pm 0.42) \times 10^6$	0.108 ± 0.004	+5	47
Ø	393	$(1.76 \pm 0.12) \times 10^6$	0.105 ± 0.003	+5	47

Table 35: Single determination of the binding constant to *calf thymus* DNA and the mean value ± standard deviation (Ø) for complex **230**. k_B = binding constant, s = binding site, $\Delta\lambda$ = bathochromic shift, λ = wavelength used for the determination.

No.	λ /nm	k_B /M^{-1}	s	$\Delta\lambda$ /nm	Hyp. /%
1	382	$(1.33 \pm 0.41) \times 10^7$	0.838 ± 0.008	+3	44
2	382	$(1.45 \pm 0.51) \times 10^7$	0.856 ± 0.008	+3	44
3	382	$(1.31 \pm 0.49) \times 10^7$	1.01 ± 0.01	+3	46
4	382	$(1.40 \pm 0.44) \times 10^7$	0.991 ± 0.008	+3	44
Ø	382	$(1.37 \pm 0.03) \times 10^7$	0.924 ± 0.045	+3	45

Table 36: Single determination of the binding constant to telo24 quadruplex DNA ($[T_2AG_3]_4$) and the mean value ± standard deviation (Ø) for complex **230**. k_B = binding constant, s = binding site, $\Delta\lambda$ = bathochromic shift, λ = wavelength used for the determination.

No.	λ /nm	k_B /M^{-1}	s	$\Delta\lambda$ /nm	Hyp. /%
1	382	$(1.51 \pm 0.41) \times 10^6$	0.120 ± 0.007	+4	44
2	382	$(1.44 \pm 0.37) \times 10^6$	0.122 ± 0.007	+4	44
3	382	$(1.32 \pm 0.32) \times 10^6$	0.112 ± 0.006	+5	43
Ø	382	$(1.42 \pm 0.06) \times 10^6$	0.118 ± 0.003	+4	44

Table 37: Single determination of the binding constant to *calf thymus* DNA and the mean value ± standard deviation (Ø) for complex **228**. k_B = binding constant, s = binding site, $\Delta\lambda$ = bathochromic shift, λ = wavelength used for the determination.

No.	λ /nm	k_B /M^{-1}	s	$\Delta\lambda$ /nm	Hyp. /%
1	394	$(1.22 \pm 0.43) \times 10^7$	0.668 ± 0.007	+4	47
2	394	$(1.01 \pm 0.29) \times 10^7$	0.790 ± 0.008	+4	48
3	394	$(1.48 \pm 0.42) \times 10^7$	0.984 ± 0.007	+4	49
4	394	$(1.58 \pm 0.52) \times 10^7$	0.894 ± 0.006	+4	49
Ø	394	$(1.32 \pm 0.13) \times 10^7$	0.833 ± 0.068	+4	48

Table 38: Single determination of the binding constant to telo24 quadruplex DNA ($[T_2AG_3]_4$) and the mean value ± standard deviation (Ø) for complex **228**. k_B = binding constant, s = binding site, $\Delta\lambda$ = bathochromic shift, λ = wavelength used for the determination.

No.	λ /nm	k_B /M^{-1}	s	$\Delta\lambda$ /nm	Hyp. /%
1	394	$(2.02 \pm 0.26) \times 10^6$	0.0778 ± 0.0017	+5	58
2	394	$(1.81 \pm 0.21) \times 10^6$	0.0790 ± 0.0017	+5	59
3	394	$(1.49 \pm 0.22) \times 10^6$	0.0740 ± 0.0022	+5	58
Ø	394	$(1.77 \pm 0.15) \times 10^6$	0.0769 ± 0.0015	+5	58

Table 39: Single determination of the binding constant to *calf thymus* DNA and the mean value ± standard deviation (Ø) for complex **227**. k_B = binding constant, s = binding site, $\Delta\lambda$ = bathochromic shift, λ = wavelength used for the determination.

No.	λ /nm	k_B /M^{-1}	s	$\Delta\lambda$ /nm	Hyp. /%
1	394	$(2.14 \pm 0.58) \times 10^7$	0.942 ± 0.005	+5	48
2	394	$(1.86 \pm 0.53) \times 10^7$	1.340 ± 0.008	+5	51
3	394	$(1.52 \pm 0.38) \times 10^7$	1.27 ± 0.08	+5	52
4	394	$(2.07 \pm 0.47) \times 10^7$	1.300 ± 0.006	+5	52
Ø	394	$(1.38 \pm 0.48) \times 10^7$	1.21 ± 0.09	+5	51

Table 40: Single determination of the binding constant to telo24 quadruplex DNA ($[T_2AG_3]_4$) and the mean value ± standard deviation (Ø) for complex **227**. k_B = binding constant, s = binding site, $\Delta\lambda$ = bathochromic shift, λ = wavelength used for the determination.

No.	**λ /nm**	**k_B /M^{-1}**	**s**	**$\Delta\lambda$ /nm**	**Hyp. /%**
1	394	$(1.45 \pm 0.23) \times 10^6$	0.0920 ± 0.0031	+5	61
2	394	$(2.84 \pm 0.54) \times 10^6$	0.106 ± 0.003	+5	58
3	394	$(1.89 \pm 0.25) \times 10^6$	0.102 ± 0.002	+5	56
Ø	394	$(2.06 \pm 0.41) \times 10^6$	0.100 ± 0.004	+5	58

Table 41: Single determination of the binding constant to *calf thymus* DNA and the mean value ± standard deviation (Ø) for complex **237**. k_B = binding constant, s = binding site, $\Delta\lambda$ = bathochromic shift, λ = wavelength used for the determination.

No.	**λ /nm**	**k_B /M^{-1}**	**s**	**$\Delta\lambda$ /nm**	**Hyp. /%**
1	404	$(1.85 \pm 0.39) \times 10^6$	0.825 ± 0.020	+5	59
2	404	$(1.96 \pm 0.44) \times 10^6$	0.847 ± 0.021	+5	59
3	404	$(1.80 \pm 0.38) \times 10^6$	0.826 ± 0.020	+5	60
4	404	$(2.21 \pm 0.54) \times 10^6$	0.938 ± 0.023	+5	55
Ø	404	$(1.96 \pm 0.09) \times 10^6$	0.859 ± 0.027	+5	57

Table 42: Single determination of the binding constant to telo24 quadruplex DNA ($[T_2AG_3]_4$) and the mean value ± standard deviation (Ø) for complex **237**. k_B = binding constant, s = binding site, $\Delta\lambda$ = bathochromic shift, λ = wavelength used for the determination.

No.	**λ /nm**	**k_B /M^{-1}**	**s**	**$\Delta\lambda$ /nm**	**Hyp. /%**
1	404	$(3.40 \pm 0.77) \times 10^5$	0.0575 ± 0.0062	+6	65
2	404	$(4.34 \pm 1.08) \times 10^5$	0.0633 ± 0.0067	+6	62
3	404	$(3.25 \pm 0.88) \times 10^5$	0.0552 ± 0.0072	+6	66
Ø	404	$(3.66 \pm 0.34) \times 10^5$	0.0587 ± 0.0024	+6	64

Table 43: Single determination of the binding constant to *calf thymus* DNA and the mean value ± standard deviation (Ø) for complex **234**. k_B = binding constant, s = binding site, $\Delta\lambda$ = bathochromic shift, λ = wavelength used for the determination.

No.	λ /nm	k_B /M^{-1}	s	$\Delta\lambda$ /nm	Hyp. /%
1	403	$(3.07 \pm 0.89) \times 10^6$	0.948 ± 0.022	+5	62
2	403	$(2.91 \pm 0.87) \times 10^6$	0.977 ± 0.024	+5	62
3	403	$(2.68 \pm 0.79) \times 10^6$	0.974 ± 0.025	+5	62
4	403	$(1.87 \pm 0.56) \times 10^6$	0.876 ± 0.031	+5	62
Ø	403	$(2.63 \pm 0.27) \times 10^6$	0.944 ± 0.024	+5	62

Table 44: Single determination of the binding constant to telo24 quadruplex DNA ($[T_2AG_3]_4$) and the mean value ± standard deviation (Ø) for complex **234**. k_B = binding constant, s = binding site, $\Delta\lambda$ = bathochromic shift, λ = wavelength used for the determination.

No.	λ /nm	k_B /M^{-1}	s	$\Delta\lambda$ /nm	Hyp. /%
1	403	$(4.09 \pm 0.75) \times 10^5$	0.0589 ± 0.0047	+5	69
2	403	$(4.18 \pm 0.74) \times 10^5$	0.0648 ± 0.0049	+5	68
3	403	$(3.72 \pm 0.75) \times 10^5$	0.0601 ± 0.0055	+5	70
Ø	403	$(4.00 \pm 0.14) \times 10^5$	0.0613 ± 0.0018	+5	69

Table 45: Single determination of the binding constant to telo24 quadruplex DNA ($[T_2AG_3]_4$) and the mean value ± standard deviation (Ø) for complex **223**. k_B = binding constant, s = binding site, $\Delta\lambda$ = bathochromic shift, λ = wavelength used for the determination.

No.	λ /nm	k_B /M^{-1}	s	$\Delta\lambda$ /nm	Hyp. /%
1	393	$(2.40 \pm 0.55) \times 10^6$	0.180 ± 0.005	+5	45
2	393	$(2.07 \pm 0.61) \times 10^6$	0.153 ± 0.007	+5	43
3	393	$(2.02 \pm 0.58) \times 10^6$	0.159 ± 0.007	+5	44
Ø	393	$(2.16 \pm 0.12) \times 10^6$	0.157 ± 0.002	+5	44

Table 46: Single determination of the binding constant to *calf thymus* DNA and the mean value ± standard deviation (Ø) for complex **157**. k_B = binding constant, s = binding site, $\Delta\lambda$ = bathochromic shift, λ = wavelength used for the determination.

No.	λ /nm	k_B /M^{-1}	s	$\Delta\lambda$ /nm	Hyp. /%
1	340	$(7.78 \pm 1.78) \times 10^5$	1.82 ± 0.08	+3	45
2	340	$(7.26 \pm 1.40) \times 10^5$	2.64 ± 0.10	+7	49
Ø	340	$(7.52 \pm 0.26) \times 10^5$	2.23 ± 0.41	+5	47

Table 47: Single determination of the binding constant to *calf thymus* DNA and the mean value ± standard deviation (Ø) for complex **145**. k_B = binding constant, s = binding site, $\Delta\lambda$ = bathochromic shift, λ = wavelength used for the determination.

No.	λ /nm	k_B /M^{-1}	s	$\Delta\lambda$ /nm	Hyp. /%
1	313	$(1.29 \pm 0.18) \times 10^6$	0.295 ± 0.007	+2	26

Table 48: Single determination of the binding constant to *calf thymus* DNA and the mean value ± standard deviation (Ø) for complex **87**. k_B = binding constant, s = binding site, $\Delta\lambda$ = bathochromic shift, λ = wavelength used for the determination.

No.	λ /nm	k_B /M^{-1}	s	$\Delta\lambda$ /nm	Hyp. /%
1	325	$(4.43 \pm 3.88) \times 10^5$	1.761 ± 0.374	–	7

Table 49: Single determination of the binding constant to *calf thymus* DNA and the mean value ± standard deviation (Ø) for complex **184**. k_B = binding constant, s = binding site, $\Delta\lambda$ = bathochromic shift, λ = wavelength used for the determination.

No.	λ /nm	k_B /M $^{-1}$	s	$\Delta\lambda$ /nm	Hyp. /%
1	357	$(1.65 \pm 0.26) \times 10^6$	1.17 ± 0.02	–	54
2	357	$(1.68 \pm 0.32) \times 10^6$	1.14 ± 0.03	–	54
3	357	$(1.33 \pm 0.17) \times 10^6$	1.21 ± 0.02	–	52
Ø	357	$(1.55 \pm 0.11) \times 10^6$	1.17 ± 0.02	–	53

Table 50: Single determination of the binding constant to *calf thymus* DNA and the mean value ± standard deviation (Ø) for complex **246**. k_B = binding constant, s = binding site, $\Delta\lambda$ = bathochromic shift, λ = wavelength used for the determination.

No.	λ /nm	k_B /M $^{-1}$	s	$\Delta\lambda$ /nm	Hyp. /%
1	499	$(1.84 \pm 0.25) \times 10^5$	0.261 ± 0.016	+6	70
2	499	$(1.87 \pm 0.31) \times 10^5$	0.277 ± 0.021	+6	67
3	499	$(2.26 \pm 0.38) \times 10^5$	0.301 ± 0.021	+6	69
Ø	499	$(1.99 \pm 0.14) \times 10^5$	0.280 ± 0.012	+6	69

Table 51: Single determination of the binding constant to *calf thymus* DNA and the mean value ± standard deviation (Ø) for complex **248**. k_B = binding constant, s = binding site, $\Delta\lambda$ = bathochromic shift, λ = wavelength used for the determination.

No.	**λ /nm**	$\boldsymbol{k_B}$ **/M** $^{\mathbf{-1}}$	**s**	**Δλ /nm**	**Hyp. /%**
1	502	$(2.13 \pm 0.81) \times 10^6$	0.325 ± 0.013	+3	33
2	502	$(2.82 \pm 0.70) \times 10^6$	0.335 ± 0.008	+3	37
3	502	$(3.09 \pm 1.05) \times 10^6$	0.338 ± 0.010	+3	37
Ø	502	$(2.68 \pm 0.29) \times 10^6$	0.333 ± 0.004	+3	36

Table 52: Single determination of the binding constant to *calf thymus* DNA and the mean value ± standard deviation (Ø) for complex **249**. k_B = binding constant, s = binding site, $\Delta\lambda$ = bathochromic shift, λ = wavelength used for the determination.

No.	**λ /nm**	$\boldsymbol{k_B}$ **/M** $^{\mathbf{-1}}$	**s**	**Δλ /nm**	**Hyp. /%**
1	502	$(3.12 \pm 0.90) \times 10^6$	0.343 ± 0.009	+3	39
2	502	$(3.47 \pm 0.91) \times 10^6$	0.372 ± 0.008	+3	41
3	502	$(3.37 \pm 0.92) \times 10^6$	0.354 ± 0.008	+3	41
Ø	502	$(3.23 \pm 0.12) \times 10^6$	0.318 ± 0.039	+3	40

Table 53: Single determination of the binding constant to *calf thymus* DNA and the mean value ± standard deviation (Ø) for complex **247**. k_B = binding constant, s = binding site, $\Delta\lambda$ = bathochromic shift, λ = wavelength used for the determination.

No.	**λ /nm**	$\boldsymbol{k_B}$ **/M** $^{\mathbf{-1}}$	**s**	**Δλ /nm**	**Hyp. /%**
1	499	$(2.40 \pm 0.28) \times 10^5$	0.286 ± 0.014	+6	69
2	499	$(2.45 \pm 0.28) \times 10^5$	0.308 ± 0.014	+6	69
3	499	$(3.08 \pm 0.33) \times 10^5$	0.348 ± 0.013	+6	72
Ø	499	$(2.64 \pm 0.22) \times 10^5$	0.314 ± 0.018	+5	70

E. UV/Vis-Spectra of the DNA Binding Assays

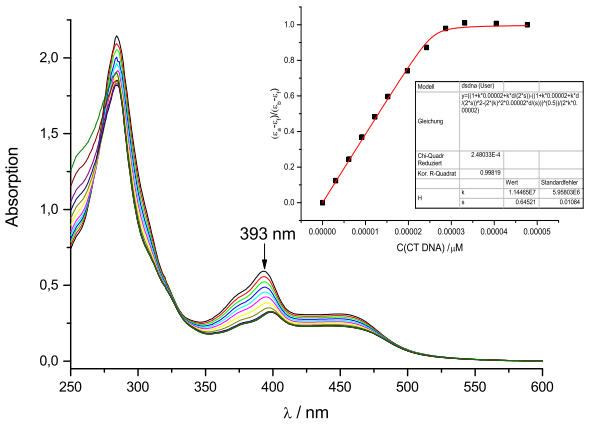

Figure 91: Exemplary UV/Vis-absorption spectra of complex **224** (20 µM) in CT-DNA-buffer upon titration with *calf thymus* DNA at room temperature. Insert: McGhee-von-Hippel Plot.

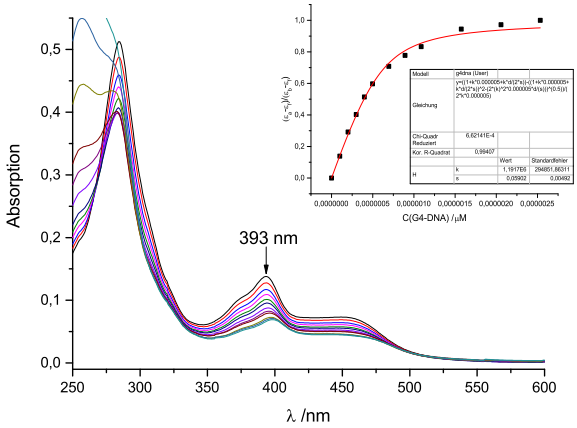

Figure 92: Exemplary UV/Vis-absorption spectra of complex **224** (10 µM) in telo-24-buffer upon titration with telo24-G4-DNA at room temperature. Insert: McGhee-von-Hippel Plot.

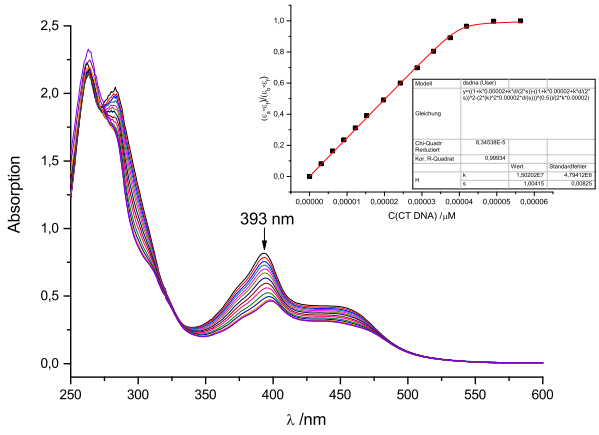

Figure 93: Exemplary UV/Vis-absorption spectra of complex **226** (20 µM) in CT-DNA-buffer upon titration with *calf thymus* DNA at room temperature. Insert: McGhee-von-Hippel Plot.

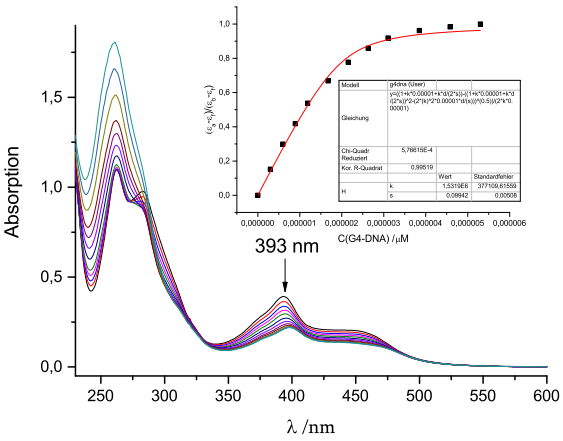

Figure 94: Exemplary UV/Vis-absorption spectra of complex **226** (10 µM) in telo-24-buffer upon titration with telo24-G4-DNA at room temperature. Insert: McGhee-von-Hippel Plot.

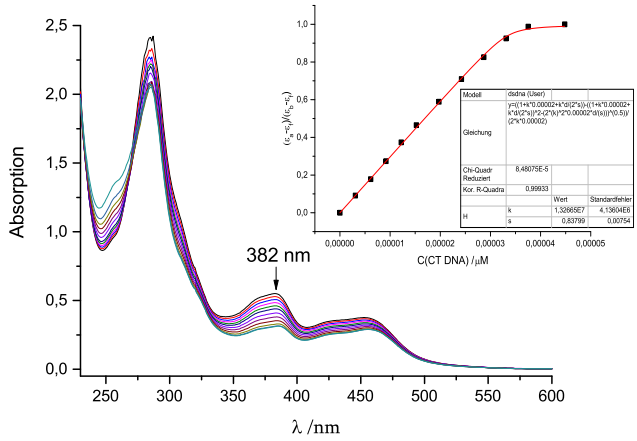

Figure 95: Exemplary UV/Vis-absorption spectra of complex **230** (20 µM) in CT-DNA-buffer upon titration with *calf thymus* DNA at room temperature. Insert: McGhee-von-Hippel Plot.

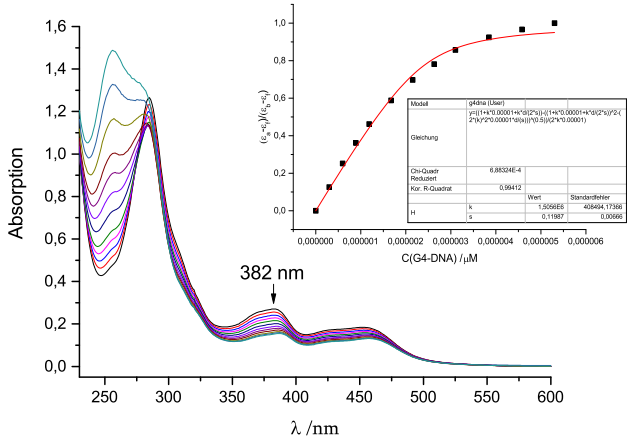

Figure 96: Exemplary UV/Vis-absorption spectra of complex **230** (10 µM) in telo-24-buffer upon titration with telo24-G4-DNA at room temperature. Insert: McGhee-von-Hippel Plot.

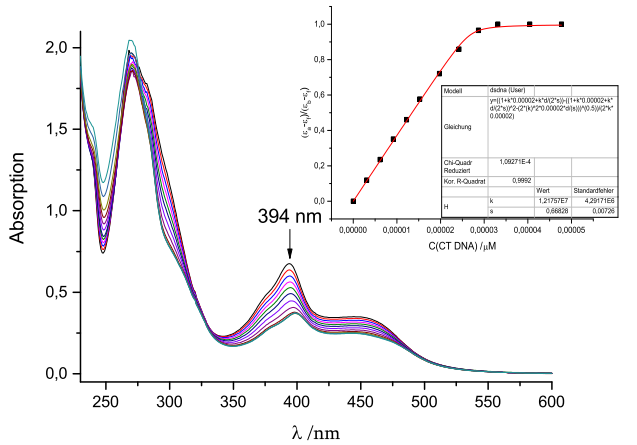

Figure 97: Exemplary UV/Vis-absorption spectra of complex **228** (20 µM) in CT-DNA-buffer upon titration with *calf thymus* DNA at room temperature. Insert: McGhee-von-Hippel Plot.

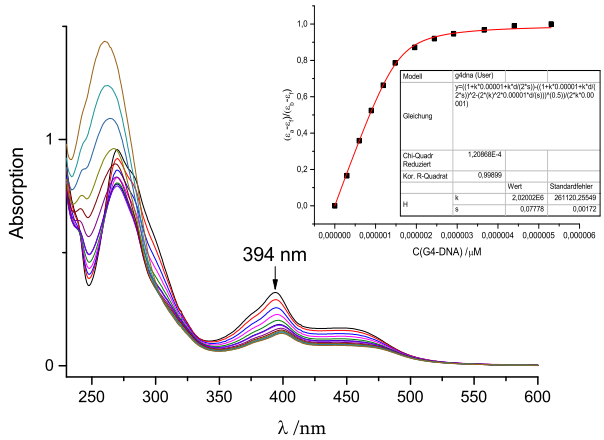

Figure 98: Exemplary UV/Vis-absorption spectra of complex **228** (10 µM) in telo-24-buffer upon titration with telo24-G4-DNA at room temperature. Insert: McGhee-von-Hippel Plot.

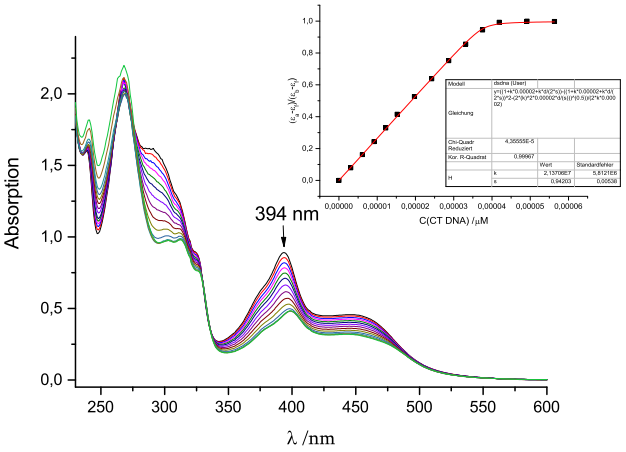

Figure 99: Exemplary UV/Vis-absorption spectra of complex **227** (20 µM) in CT-DNA-buffer upon titration with *calf thymus* DNA at room temperature. Insert: McGhee-von-Hippel Plot.

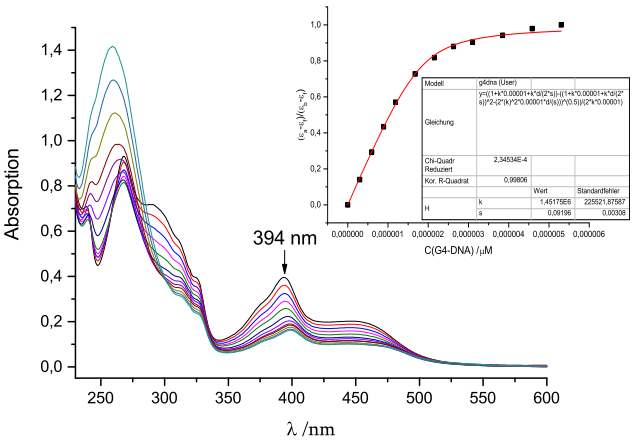

Figure 100: Exemplary UV/Vis-absorption spectra of complex **227** (10 µM) in telo-24-buffer upon titration with telo24-G4-DNA at room temperature. Insert: McGhee-von-Hippel Plot.

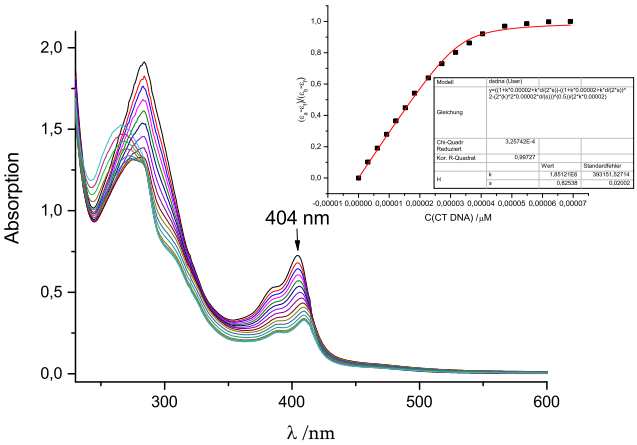

Figure 101: Exemplary UV/Vis-absorption spectra of complex **237** (20 µM) in CT-DNA-buffer upon titration with *calf thymus* DNA at room temperature. Insert: McGhee-von-Hippel Plot.

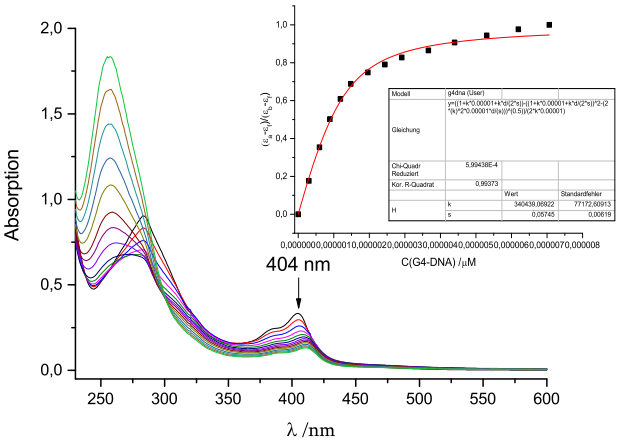

Figure 102: Exemplary UV/Vis-absorption spectra of complex **237** (10 µM) in telo-24-buffer upon titration with telo24-G4-DNA at room temperature. Insert: McGhee-von-Hippel Plot.

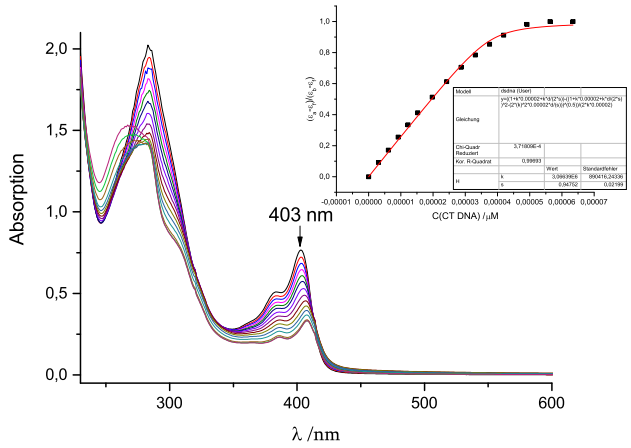

Figure 103: Exemplary UV/Vis-absorption spectra of complex **234** (20 µM) in CT-DNA-buffer upon titration with *calf thymus* DNA at room temperature. Insert: McGhee-von-Hippel Plot.

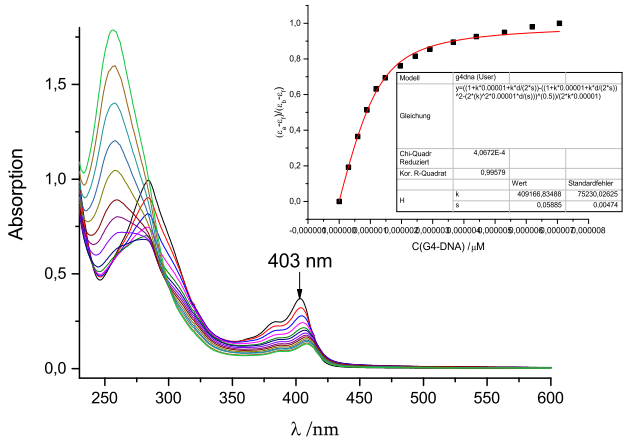

Figure 104: Exemplary UV/Vis-absorption spectra of complex **234** (10 µM) in telo-24-buffer upon titration with telo24-G4-DNA at room temperature. Insert: McGhee-von-Hippel Plot.

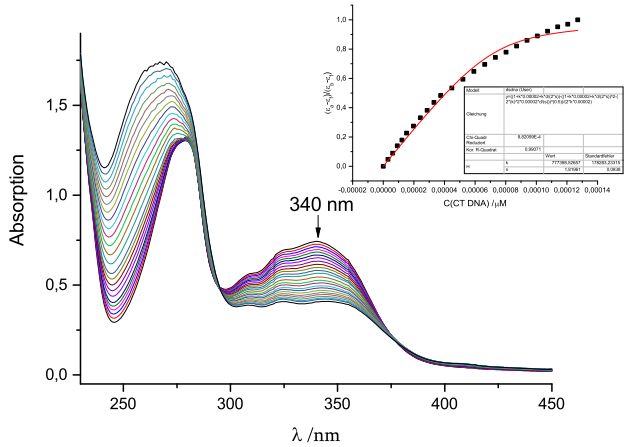

Figure 105: Exemplary UV/Vis-absorption spectra of complex **157** (20 µM) in CT-DNA-buffer upon titration with *calf thymus* DNA at room temperature. Insert: McGhee-von-Hippel Plot.

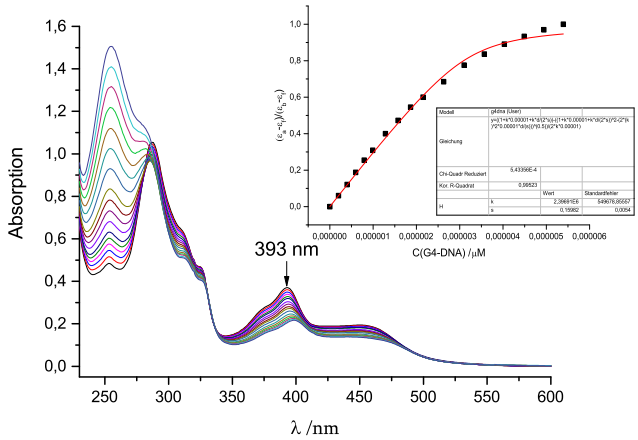

Figure 106: Exemplary UV/Vis-absorption spectra of complex **223** (10 µM) in telo-24-buffer upon titration with telo24-G4-DNA at room temperature. Insert: McGhee-von-Hippel Plot.

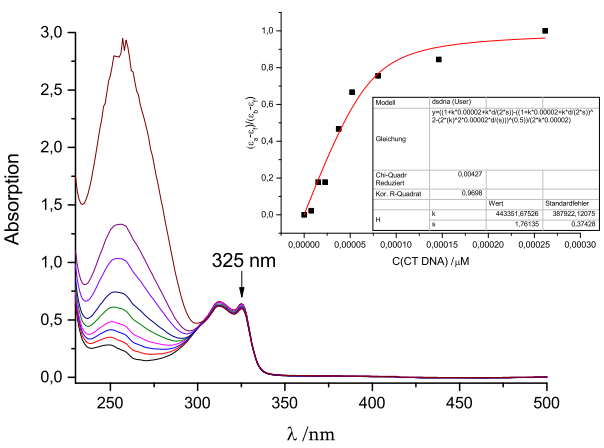

Figure 107: Exemplary UV/Vis-absorption spectra of complex **87** (20 µM) in CT-DNA-buffer upon titration with *calf thymus* DNA at room temperature. Insert: McGhee-von-Hippel Plot.

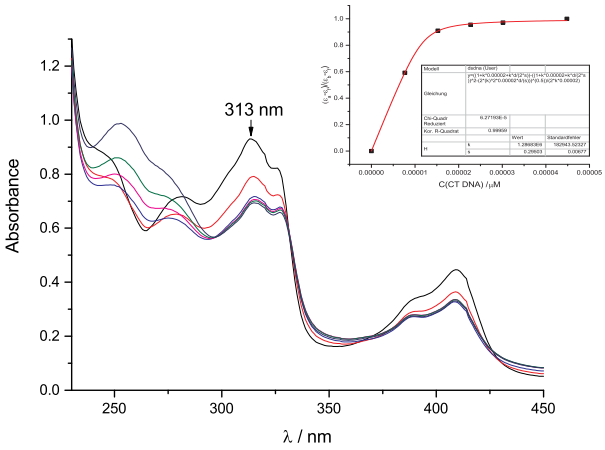

Figure 108: Exemplary UV/Vis-absorption spectra of complex **145** (20 µM) in CT-DNA-buffer upon titration with *calf thymus* DNA at room temperature. Insert: McGhee-von-Hippel Plot.

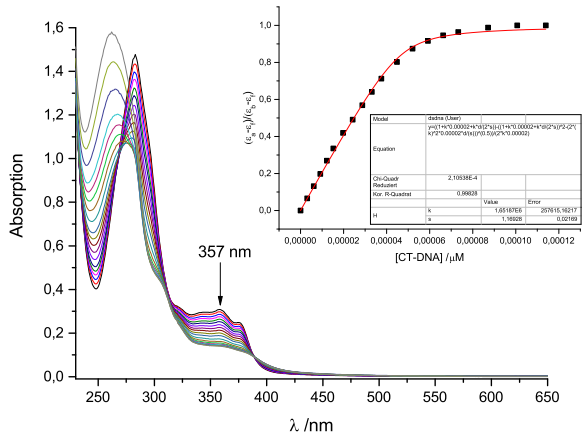

Figure 109: Exemplary UV/Vis-absorption spectra of complex **184** (20 µM) in CT-DNA-buffer upon titration with *calf thymus* DNA at room temperature. Insert: McGhee-von-Hippel Plot.

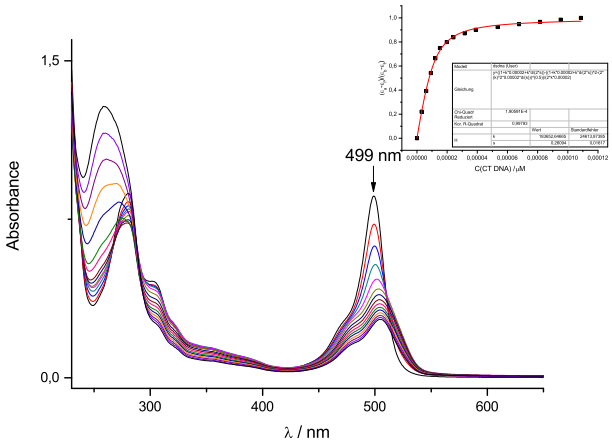

Figure 110: Exemplary UV/Vis-absorption spectra of complex **246** (20 µM) in CT-DNA-buffer upon titration with *calf thymus* DNA at room temperature. Insert: McGhee-von-Hippel Plot.

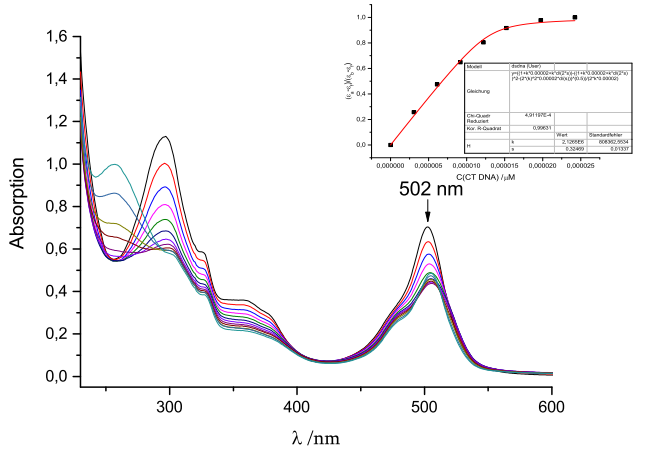

Figure 111: Exemplary UV/Vis-absorption spectra of complex **248** (20 µM) in CT-DNA-buffer upon titration with *calf thymus* DNA at room temperature. Insert: McGhee-von-Hippel Plot.

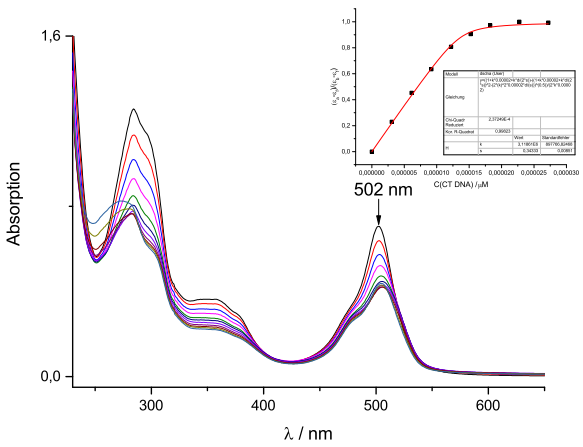

Figure 112: Exemplary UV/Vis-absorption spectra of complex **249** (20 µM) in CT-DNA-buffer upon titration with *calf thymus* DNA at room temperature. Insert: McGhee-von-Hippel Plot.

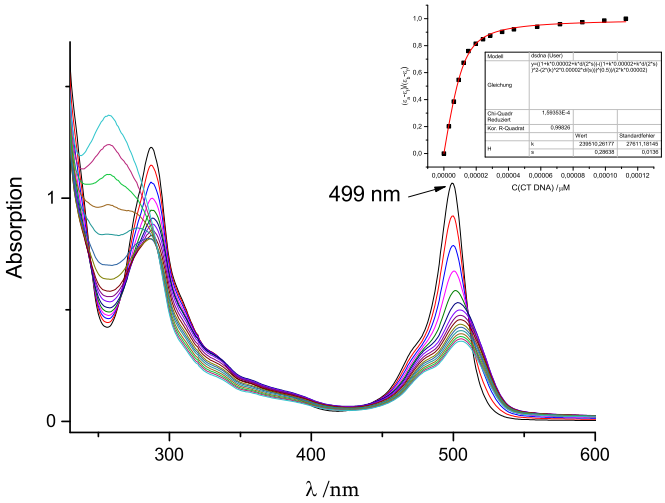

Figure 113: Exemplary UV/Vis-absorption spectra of complex **247** (20 µM) in CT-DNA-buffer upon titration with *calf thymus* DNA at room temperature. Insert: McGhee-von-Hippel Plot.

F. ^{1}H-NMR Spectra of Selected Silicon(IV) Complexes

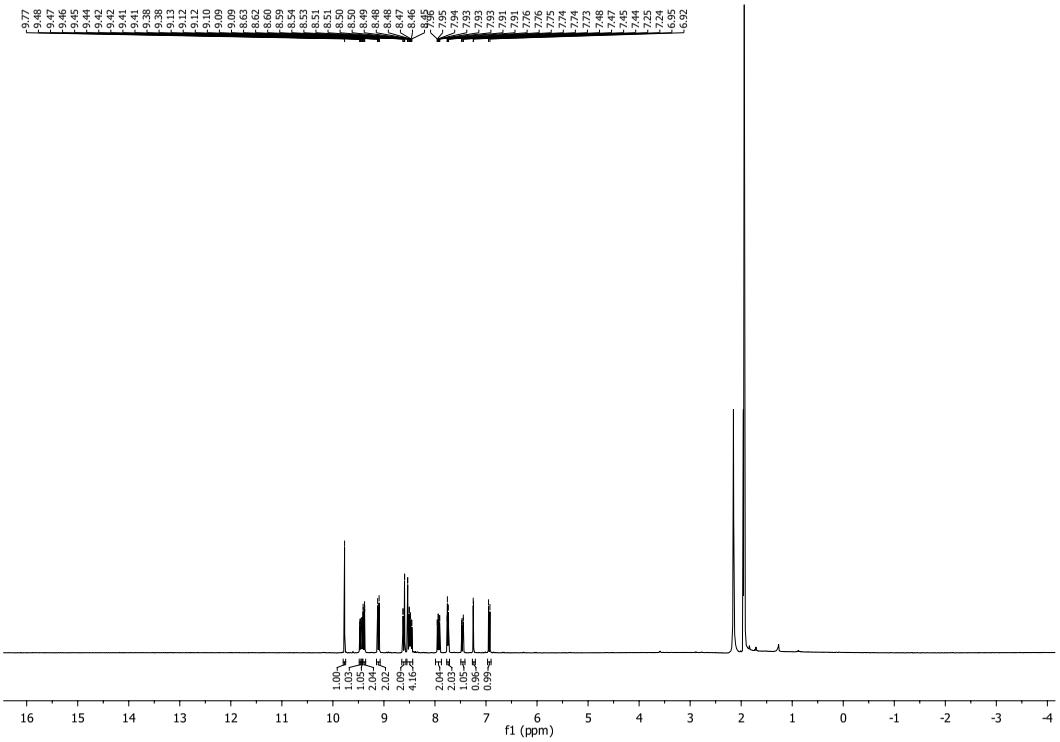

Figure 114: ^{1}H-NMR spectrum of complex **92** in acetonitrile-d_3.

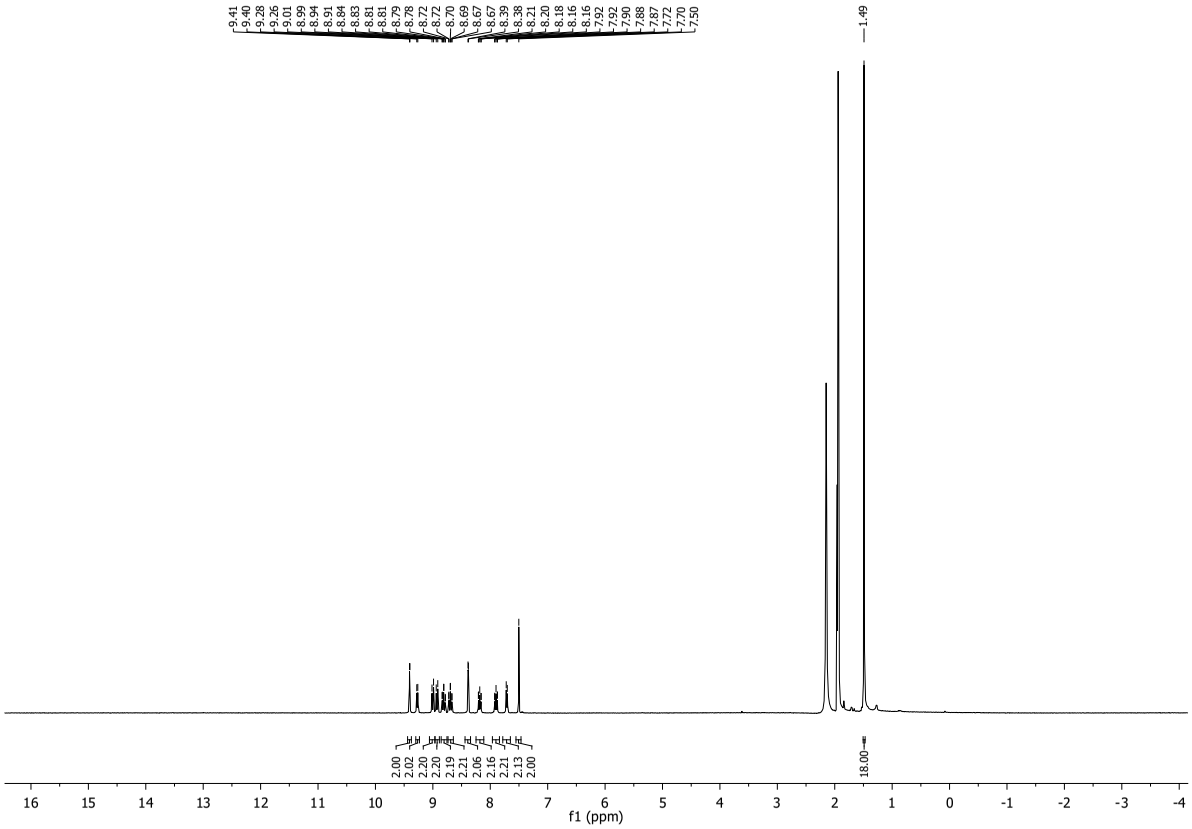

Figure 115: ^{1}H-NMR spectrum of complex **145** (11 mM) in acetonitrile-d_3.

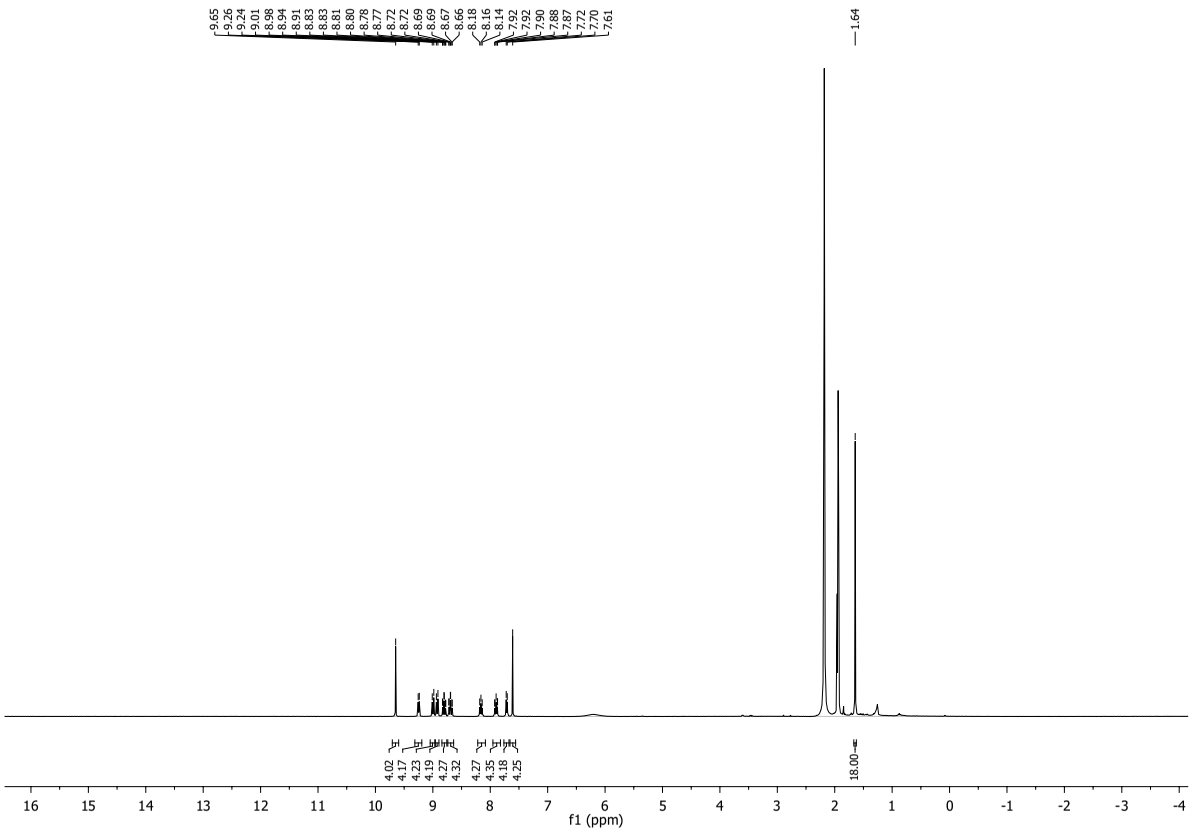

Figure 116: ^{1}H-NMR spectrum of complex **147** (6 mM) in acetonitrile-d_3.

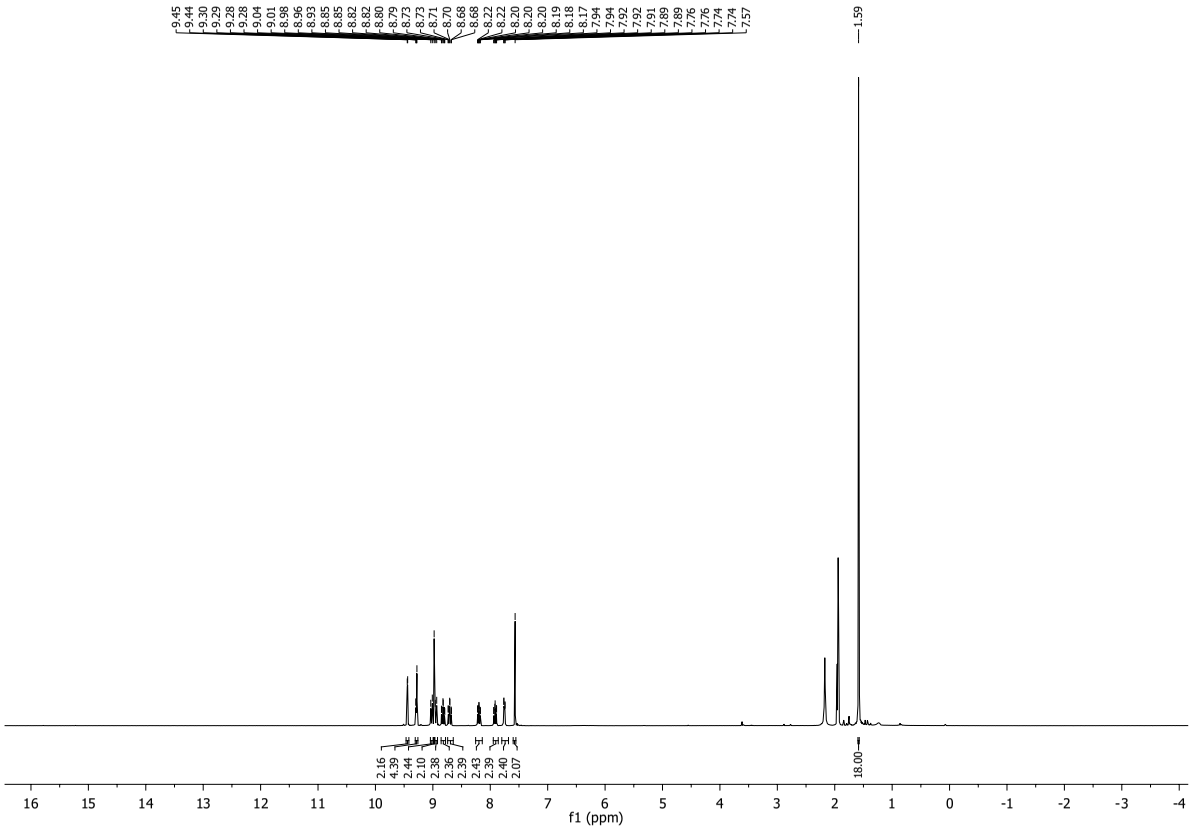

Figure 117: ^{1}H-NMR spectrum of complex **152** (21 mM) in acetonitrile-d_3.

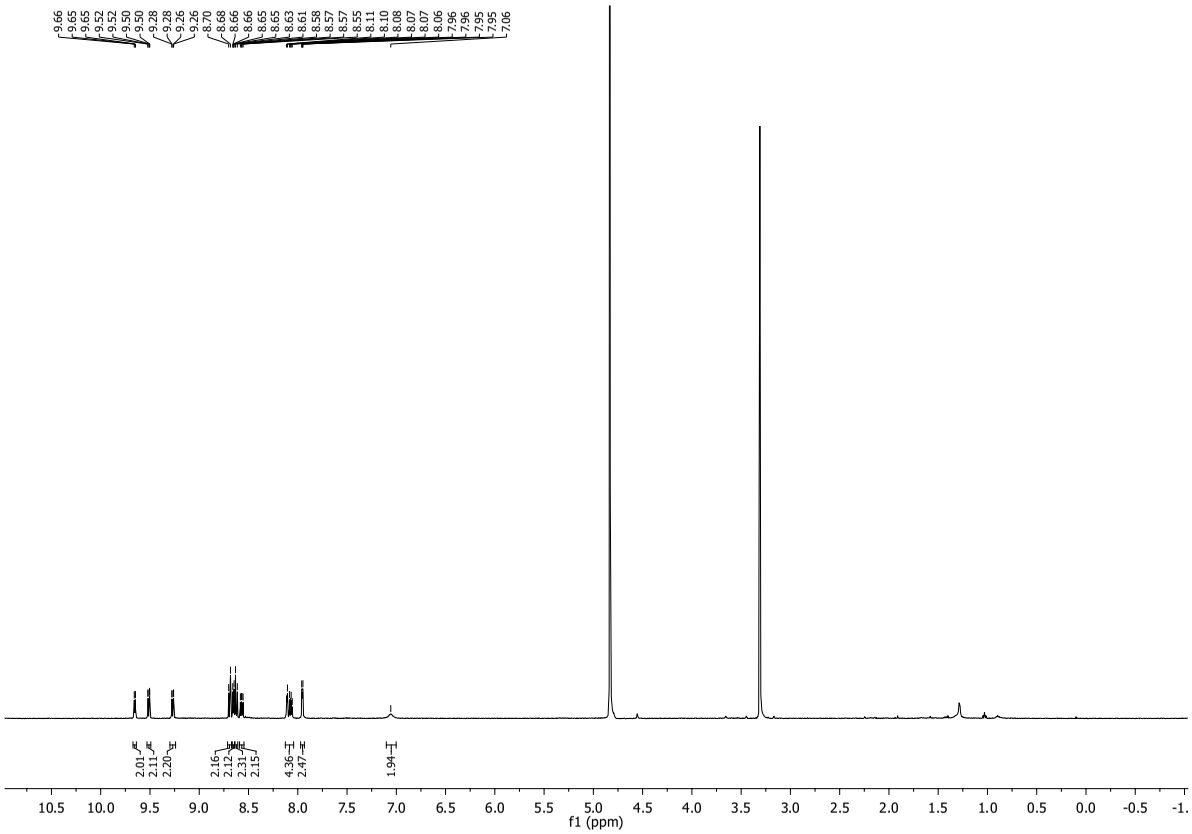

Figure 118: ^{1}H-NMR spectrum of complex **157a** in methanol-d_4.

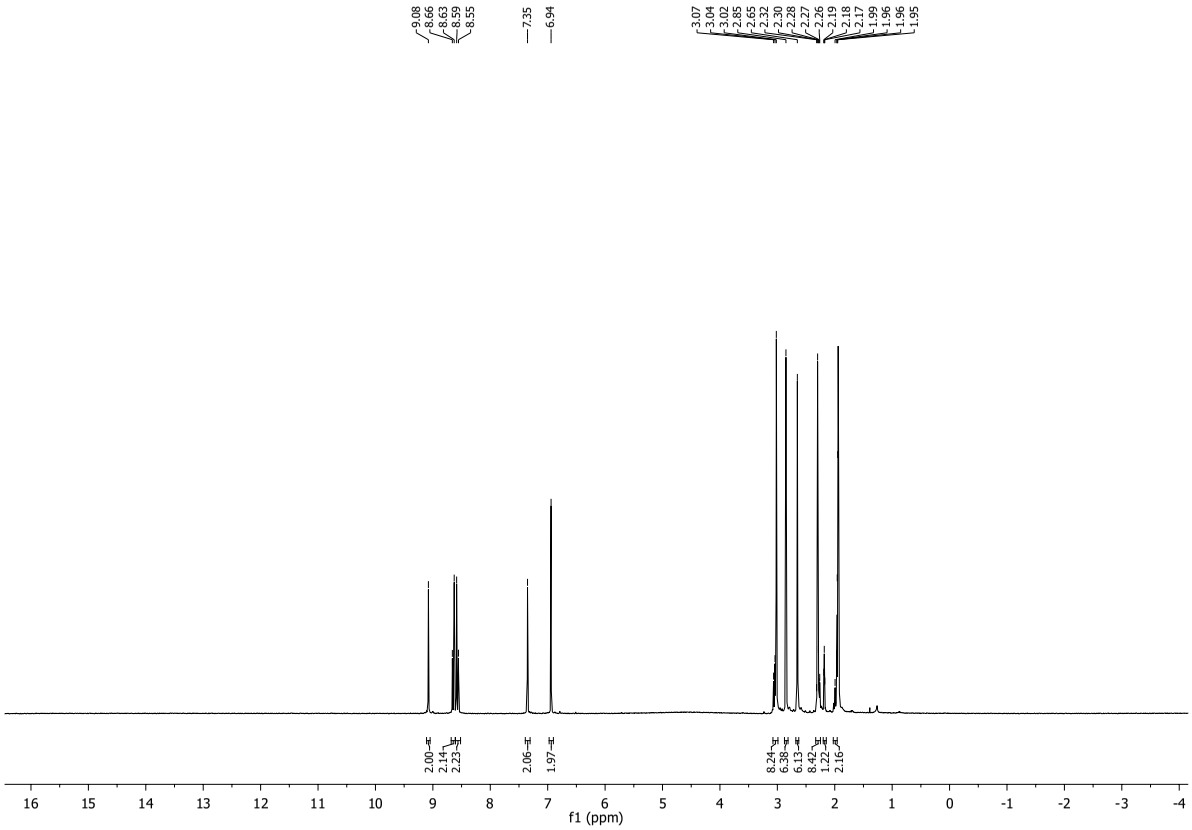

Figure 119: ^{1}H-NMR spectrum of complex **173** in acetonitrile-d_3.

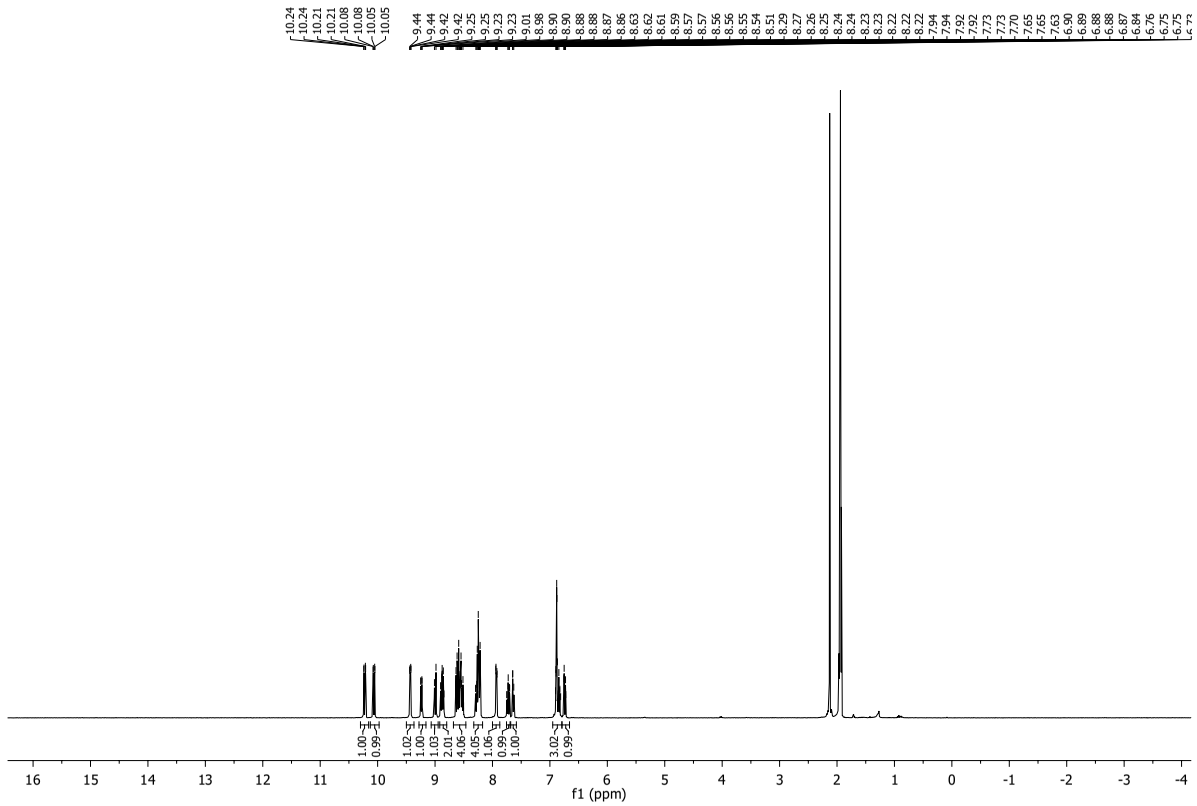

Figure 120: ^{1}H-NMR spectrum of complex **183** (17 mM) in acetonitrile-d_3.

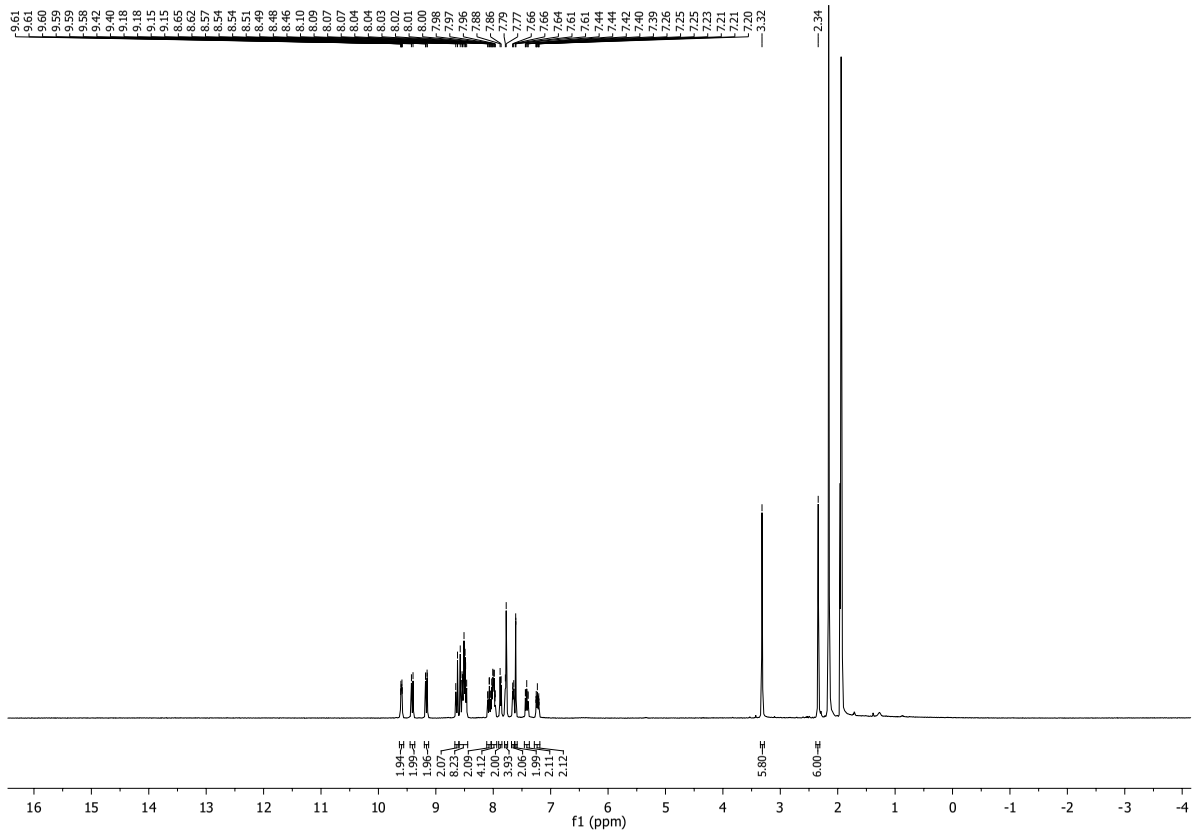

Figure 121: ^{1}H-NMR spectrum of complex **230** (10 mM) in acetonitrile-d_3.

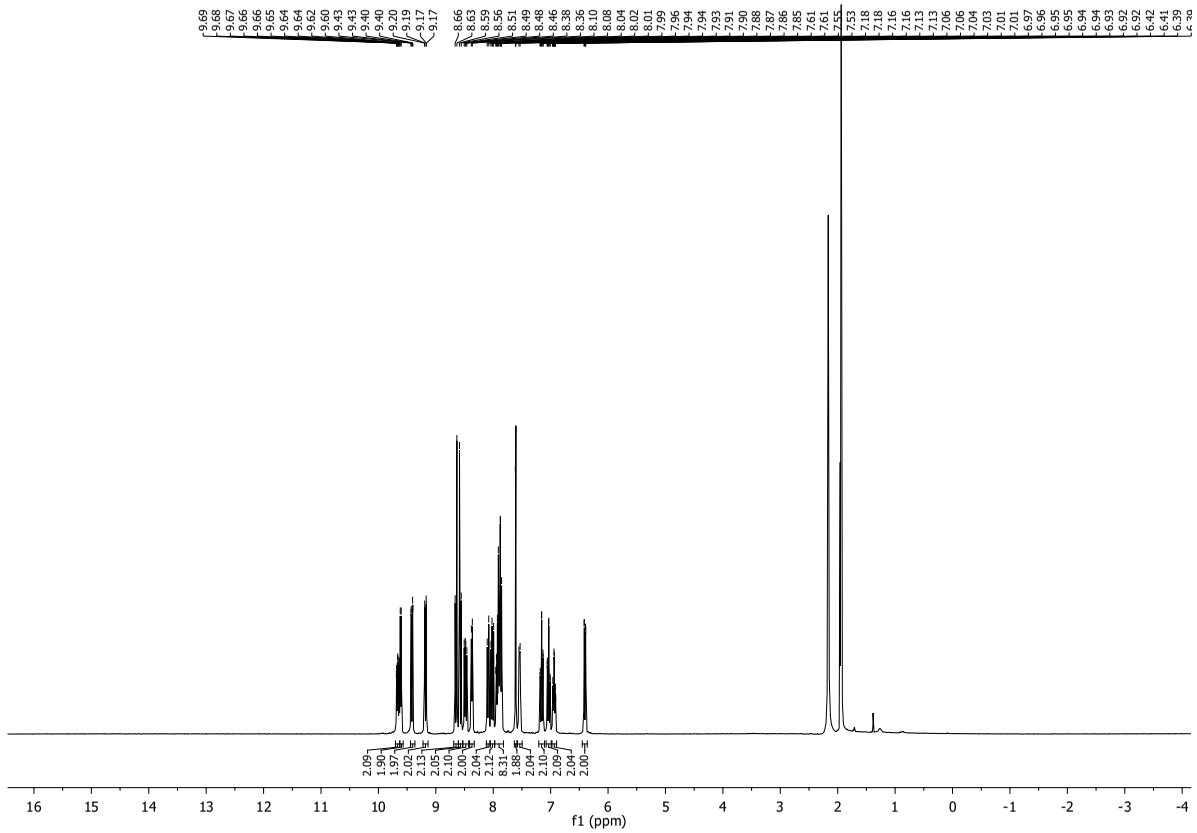

Figure 122: ^{1}H-NMR spectrum of complex **234** (22 mM) in acetonitrile-d_3.

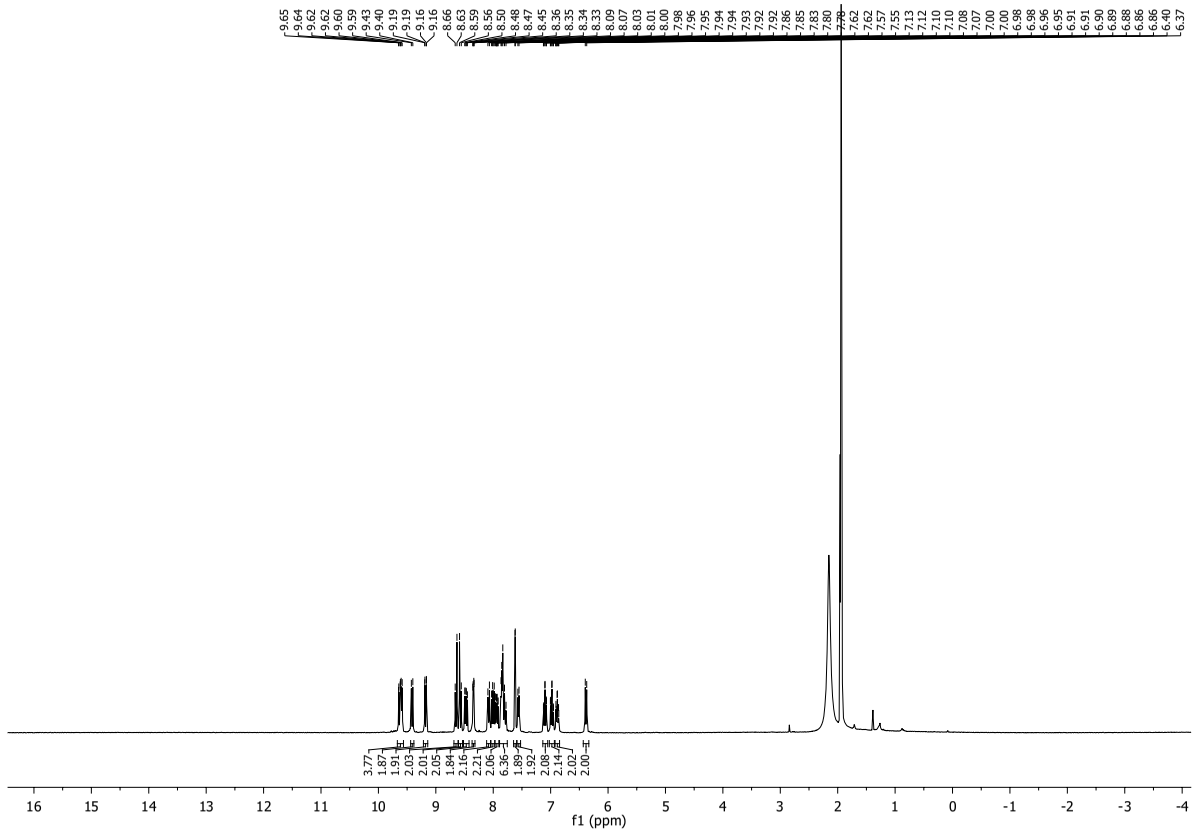

Figure 123: ^{1}H-NMR spectrum of complex **237** (8 mM) in acetonitrile-d_3.

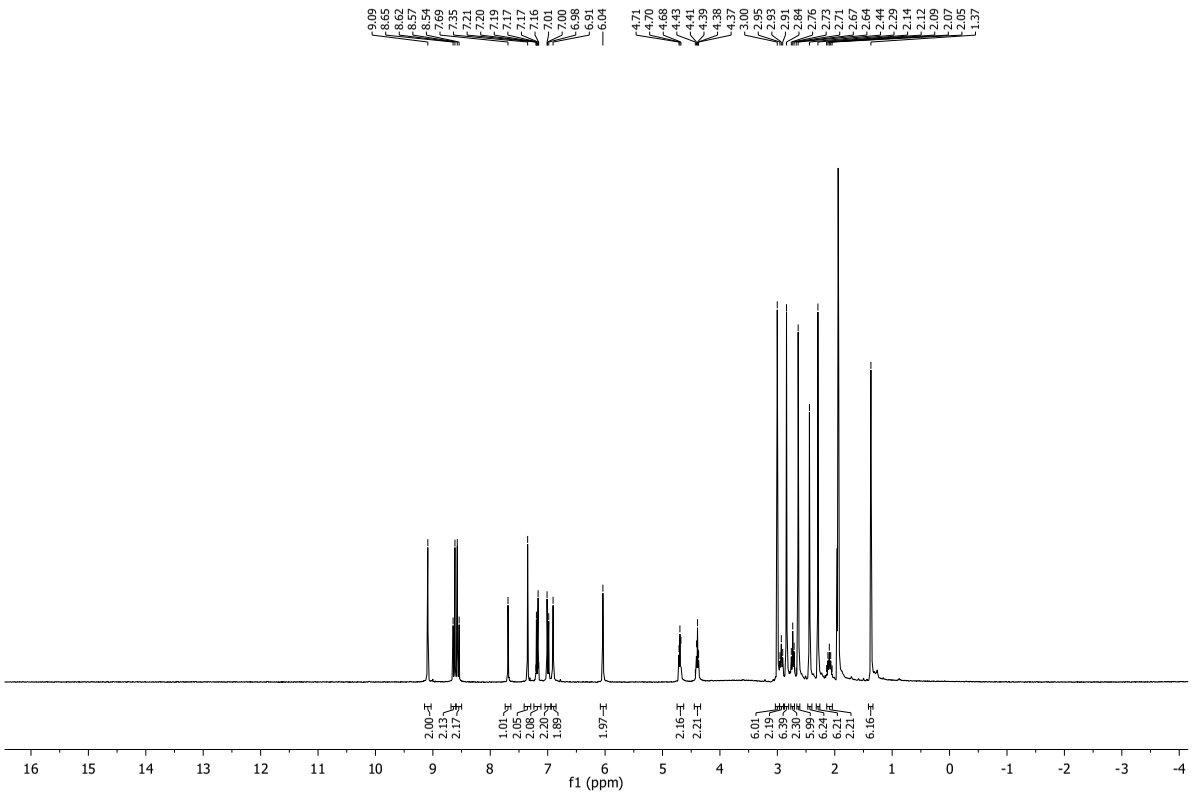

Figure 124: ^{1}H-NMR spectrum of complex **247** in acetonitrile-d_3.

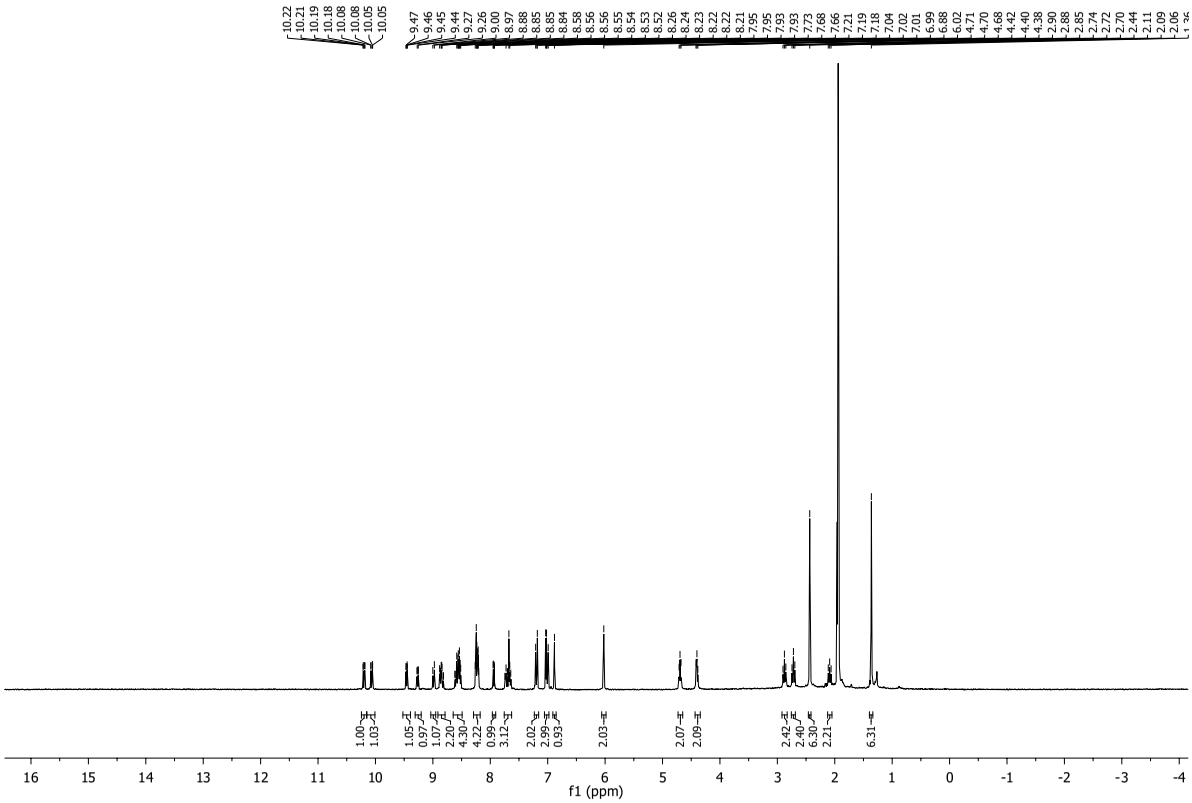

Figure 125: ^{1}H-NMR spectrum of complex **248** (11 mM) in acetonitrile-d_3.

G. Statement

An den
Vorsitzenden des Prüfungsausschusses in Chemie
Fachbereich Chemie der Philipps-Universität Marburg
Hans-Meerwein-Straße
D-35032 Marburg

E r k l ä r u n g

gemäß §10, Abs. 1 der Promotionsordnung der Mathematisch-Naturwissenschaftlichen Fachbereiche und des Medizinischen Fachbereichs für seine mathematisch-naturwissenschaftlichen Fächer der Philipps-Universität Marburg vom 15.07.2009

Ich erkläre, dass eine Promotion noch an keiner anderen Hochschule als der Philipps-Universität Marburg, Fachbereich Chemie, versucht wurde und versichere, dass ich meine vorgelegte Dissertation

Synthesis, Modification and Biological Activity of Hexacoordinate Silicon(IV) Complexes

selbst und ohne fremde Hilfe verfasst, nicht andere als die in ihr angegebenen Quellen oder Hilfsmittel benutzt, alle vollständig oder sinngemäß übernommenen Zitate als solche gekennzeichnet sowie die Dissertation in der vorliegenden oder ähnlichen Form noch bei keiner anderen in- oder ausländischen Hochschule anlässlich eines Promotionsgesuches oder zu anderen Prüfungszwecken eingereicht habe.

Marburg, den November 30, 2016

(Jens Henker)